T. Mark Harrison

Hadean Earth

Springer

Hadean Earth

T. Mark Harrison

Hadean Earth

Springer

T. Mark Harrison
Department of Earth, Planetary and Space
Sciences
University of California
Los Angeles, CA, USA

ISBN 978-3-030-46686-2 ISBN 978-3-030-46687-9 (eBook)
https://doi.org/10.1007/978-3-030-46687-9

This Springer imprint is published by the registered company Springer Nature Switzerland AG
The registered company address is: Gewerbestrasse 11, 6330 Cham, Switzerland

In memory of Richard Lee "Dick" Armstong

Preface

The seed for this book was sown in 2011 when a scientific publisher approached me with a request to encapsulate what was known about the earliest eon of Earth history—the Hadean—in monograph form. As the offer coincided with a partial sabbatical leave, I was able to cobble together an outline of what such a book should cover. I had to put the project aside in light of research exigencies and returned to UCLA with little more than a publication proposal. Eight years later, I'm glad I did so as the structure of this book is significantly different than what that outline embodied. Of course, this will be broadly true of any review of an active scientific discipline after an eight year interregnum but here the reasons went beyond linear progress in the field—the intellectual goalposts had moved as well. Not only had our knowledge of Hadean zircon geochemistry advanced but thinking about other concepts related to Hadean Earth (Late Heavy Bombardment, lunar origin, crustal growth, etc.) had become far more elastic than was the case in 2011. This evolution led me to see complementary patterns in the way these various paradigms had shifted and became a second organizing principle for this book. As well as describing the present status of investigations of the Hadean lithic record, this work also documents how ideas about early Earth have changed over the past half century and attempts to identify the resistive elements to change. By better understanding where we may have gone off the rails in the past, we can strive toward better scientific practices in the future.

This book was destined to be relatively compact. Not only is there a finite amount of geologic knowledge about an eon for which we have no macroscopic rock record, but my writing style has been described by some as "terse". Furthermore, the intended audience for this book is largely professional academic geoscientists and graduate students interested in understanding debates surrounding the nature of early Earth. Thus, I've assumed that the reader has a contemporary understanding of plate tectonics, geologic time, and the principles of radiometric dating so no primer is included to introduce those concepts. I have also not provided a glossary as I presume most are reading this as an e-book and thus have online access to virtually unlimited information close by. Nonetheless, numerous footnotes offer rudimentary explanations of some of the more obscure issues. I have of course sought to present knowledge of early Earth in a balanced and scholarly fashion but caution that some issues, for example biblical interpretations, lie well outside my area of expertise and may not prove to be the last word.

My sincere thanks to Chuck Bailey and his staff at the Department of Geology, The College of William and Mary, for hosting my sabbatical during which time this book was largely written. Their southern hospitality was greatly appreciated as were the undergraduate teaching tips I picked up eavesdropping on the classroom adjacent to my office nook. The poor soundproofing proved a pedagogic bounty. William and Mary was an idyllic setting to come up to speed with the spectrum of literature about early Earth and solar system science and was a convenient jumping off point to pester Bill Moore at nearby Hampton University about mantle dynamics.

Given the range in topics covered in the book—geodynamics, astrobiology, impact studies, mantle geochemistry—I sought out experts across this range of disciplines as mentor/consultants. Many were kind enough to read draft chapters and provide critical feedback which I largely, but not completely, adopted so any remaining errors likely reflect my intransigence. In particular, I thank Bill Moore (Hampton) and Jun Korenaga (Yale) for their critical evaluations of Chap. 2, Rich Walker (Maryland), Patrick Boehnke (Chicago) and Rick Carlson (DTM) for critiques of Chap. 3, Kip Hodges, Bill Hartmann and Alessandro Morbidelli for suggested improvements to Chap. 4, Bob Stern (UT Dallas) for a penetrating analysis of Chap. 6 (and, later, the entire manuscript), Steve Mojzsis (Colorado) and Charley Lineweaver (Australian National University) for helpful comments on Chaps. 10 and 11, and Ellen Alexander for her provocative views that influenced Chap. 12. I thank the National Science Foundation for longterm support of our ion microprobe facility in which many of the discoveries described herein were enabled. I thank my UCLA colleagues, in particular Beth Ann Bell and Kevin McKeegan, for teaching me about early Earth and solar system and the students of ESS 298, the graduate seminar course I taught upon my return to UCLA based on the draft manuscript, for numerous improvements to the prose and aggressive typo spotting. The one dollar per typo bounty I offered both incentivized that quest and provided supplemental nutrition for those with the keenest eye. Chapters 7–9 are updated versions of parts of a recent review paper (Harrison et al. 2017).

Ancient or obscure works I was unable to access through the College of William and Mary and the University of California library systems were all found on the shelves of the atheneum that lies in the bowels of Celâl Şengör's Istanbul home. My sincere thanks to Celâl for making his remarkable collection available and groveling apology for causing him to send de Buffon (1778) back to the book bindery.

I thank Annett Buettner at the Springer Nature for shepherding the manuscript through review, Axel Schmitt for connecting us, and Amanda Hunt and Casey Yamamoto for assistance obtaining figure permissions.

As the draft manuscript was growing during my sabbatical year in Williamsburg, so was our first grandchild, Ingrid, who was born in nearby Richmond as my leave began. While watching both mature was a sublime experience, writing the book did evoke a melancholy moment when I pondered what Dick Armstrong, my undergraduate thesis mentor at the University of British Columbia, might make of it.

Dick was a pioneering proponent of the idea that earliest Earth must have almost immediately differentiated into concentric shells of core, mantle and sialic crust. Although I was then baffled by his unconventional views, which remained unpopular when he passed away in his scientific prime in 1991, he was years ahead of his time. As his ideas gain traction today in light of recent discoveries about early silicate Earth differentiation and mantle dynamics, I'm saddened that he's not here to see his prescient ideas adopted and to help guide the discussion. The latter has been left in my and others less capable hands.

Los Angeles, CA, USA T. Mark Harrison
November 2019

References

de Buffon, G. L. L. "Count" (1778). *Histoire Naturelle, Générale et Particulière. Supplément, Tome Cinquième*. L'Imprimerie Royale, Paris, *615*, 8–23.

Harrison, T. M., Bell, E. A., & Boehnke, P. (2017). Hadean zircon petrochronology. *Reviews in Mineralogy and Geochemistry*, *83*, 329–363.

Contents

Why Hadean?

1

Abstract

The development of the geologic timescale arose from early nineteenth century fossil correlations and thus firmly rooted in the rock record. The thinking of that time included the possibility that our planet had forever existed in a quasi-steady state. By the later part of that century, it was broadly understood that Earth must have experienced a discrete origin but that details of that event might never be discerned. The advent of radiometric dating shortly thereafter catapulted this discussion from considering upper bounds of tens of millions of years to several billions. But it was the return of lunar highland rocks in the early 1970s that revolutionized thinking about the early inner solar system, including a hypothesized impact bombardment at ca. 3.9 billion years that was thought to have obliterated planetary surfaces. It was in this context that the term "Hadean" was proposed as the earliest division of geologic time. Since then, the meaning of Hadean evolved to describe the first roughly 500 million years of Earth history, which currently coincides with the period for which we have no macroscopic rock record. The premise of this book is that there are four avenues available to seek the nature of this eon of Earth history: (1) the presumption that physical laws are time dependent, and thus limits can be placed on early Earth's behavior using mathematical calculations; (2) that isotopic variations resulting from long-lived and extinct radioactivities preserved in mantle rocks can constrain the timing of early, planetary-scale differentiation; (3) that as much as half the rocks on the lunar surface are likely between 4.4 and 3.9 billion years in age and thus can attest to conditions then extant in the inner solar system; and (4) that detrital zircons between 4.0 and nearly 4.4 billion years preserve a lithic record of terrestrial activity in that period. Although the initial choice of the word Hadean was meant in infer that this phase of Earth history was characterized by hellish surface conditions, in classic mythology it was a cool and watery realm. Studies of these ancient zircons over the past 20 years appear to reveal an early history more akin to the latter myth than the former.

T. M. Harrison, *Hadean Earth*, https://doi.org/10.1007/978-3-030-46687-9_1

Keywords

Hadean · Priscoan · Geochronology · Zircon · U-Pb dating · Solar system formation · Origin myths · Geodynamic modelling · Isotope geochemistry · Continental crust evolution · Origin of plate tectonics · Origin of life · Planetary habitability · History of science · Chemofossil · Ion microprobe

1.1 Introduction

All societies have origin myths.[1] They are so common in human culture that our species surely has an innate need to create fables in the face of an otherwise unfathomable past (e.g., Hume 1738; Dawkins 2007; Leeming 2010). As long as our species has roamed the planet, we've surely speculated on the when and how of the creation of Earth and its lifeforms. A brief internet search of 'creation myths' reveals numerous sites summarizing narratives across a range of societies. Read a few dozen and you'll start to see common themes; for instance, an egg-like feature emerging from a vegetable form. Read on and it's tempting to speculate what the controls on creation myth fabrication are. My sense is they principally reflect the limitations of a society's historical record (say, disruptions in oral lore due to an ice age), physiography (Arizonan aboriginal creation myths don't involve oceans), technological state (you need to know what a boat is to build an ark), and the available range of vegetables. One recurrent theme is variants of the water-diver-flood myth that the Judaeo-Christian tradition shares with numerous others (Rooth 1957; Dundes 1962; Leeming 2010).

Some societies support diverse cosmogonies. Take mine, for example. About half[2] the adult population of the United States believes that our planet is about 6000 years old and arose in the watery fashion described in the Book of Genesis I, verses 1 through 9 (Berkman and Plutzer 2010). Despite our impressive technology and a western cultural bias to hydraulic origins, when the scientific community encountered the limits of its own historical record—there are no known rocks older than about 4 billion years (or Ga = 10^9 years)—it chose the following paradigm: the first many hundreds of millions of years (Ma = 10^6 years) of Earth history saw a desiccated, lifeless, molten wasteland (Cloud 1972; Wetherill 1972; Fyfe 1978; Solomon 1980; Smith 1981; Ernst 1983; Maher and Stevenson 1988; Abe 1993; Hamilton 1998; Lunine 1999; Ward and Brownlee 2000; Gradstein et al. 2004; Moorbath 2005; Waltham 2014). Although the timescales of these two coexisting models differ by nearly six orders of magnitude, I see them as intellectual cousins as there is not one shred of empirical evidence that requires either of them to be true.

[1] Possibly excepting the Pirahã (Nevins et al. 2009).
[2] http://news.gallup.com/poll/1942/substantial-numbers-americans-continue-doubt-evolution-explan.aspx; http://news.gallup.com/poll/21814/evolution-creationism-intelligent-design.aspx.

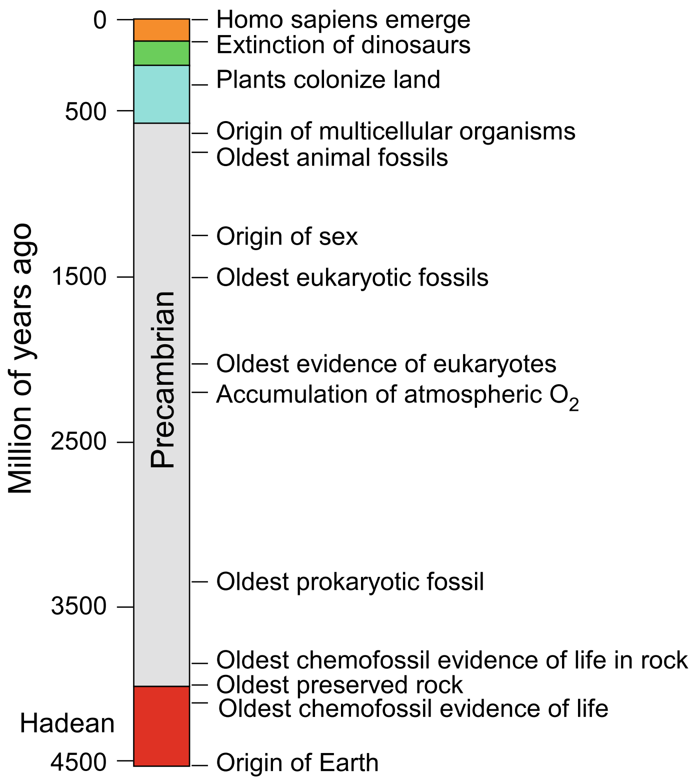

Fig. 1.1 Timeline showing major events in the co-evolution of Earth and life. The Hadean eon is defined as the period of Earth history prior to the oldest known rock, which is presently 4.02 Ga

The take away message, and this should have gone without saying, is that efforts to understand the first half billion years of Earth history—informally called the Hadean eon—should be based on tangible evidence alone (Fig. 1.1). What constitutes tangible evidence? The premise of this book is that there are four avenues available to seek the nature of Hadean Earth. They are:

(1) The presumption that physical laws are time invariant and thus limits can be placed on early Earth's behavior using mathematical models;
(2) That isotopic variations resulting from long-lived and extinct radioactivities preserved in accessible mantle rocks can constrain the timing of early, planetary-scale differentiation;
(3) That as much as half the rocks on the lunar surface are likely between 4.4 and 3.9 billion years in age and thus observations of, and samples from, Moon can attest to conditions then extant in the inner solar system;

(4) That ancient detrital zircons[3] preserve a lithic record of terrestrial activity between 4.0 and nearly 4.4 billion years.

1.2 Organization of This Book

1.2.1 A Brief Overview

Chapters 2–4 lay out evidence gleaned from the first three of the abovementioned research avenues. The structure of this book reflects my view that to appreciate the range of arguments marshalled for and against any proposed early Earth history, one must be familiar with longstanding debates regarding the origin and evolution of planetary differentiation, continental crust, and plate tectonics. Thus before discussing the fourth abovementioned avenue (i.e., ancient zircons), evidence for the growth history of continental crust (Chap. 5) and the origin of plate tectonics (Chap. 6) are presented with which to place information gleaned from >4 billion year Jack Hills zircons (Chap. 7) in context. Because these various issues are interrelated, and despite efforts to cross reference discussions, the reader may as a result encounter some unavoidable duplication. Chapter 8 reviews Hadean zircon data acquired from other locations on Earth and elsewhere in the Solar System from which >4 billion year zircons have been identified. Chapter 9 reviews the variety of published petrogenetic models for the origin of >4 billion year zircons, Chap. 10 surveys current thought on what made Earth (or indeed any planet) habitable, and Chap. 11 reviews the morpho- and chemo-fossil evidence for the appearance of life. Chapter 12 summarizes the main themes of the book and offers directions for future research.

1.2.2 Chapter Themes

The intellectual vacuum that existed prior to the discovery of lithic fragments of Hadean Earth left the narrative of early planetary evolution almost entirely in the hands of geodynamic modelers. From the early 1980s onward, that community coalesced around the view that plate-tectonic-like behavior was unlikely on Hadean Earth, in part because it was assumed that plate velocities were a geometric function of radiogenic heat production (e.g., Davies 1980). This episode provides a counter example to the conventional view that science is the study of the structure and behavior of the natural world through observation. Ordinarily, the role of modeling is to place observations in a physical framework, but speculations about early Earth have long included calculations carried out in the absence of observational constraints which then came to define the prevailing paradigm (e.g., Kelvin's age of the

[3]Zircon ($ZrSiO_4$) is an accessory mineral amenable to precise U-Pb dating that is highly refractory in igneous, sedimentary and metamorphic environments.

Earth). A brief review in Chap. 2 of the history of such speculations is a good starting point to evaluate what can be said about earliest Earth from purely theoretical considerations and leads to a review of thermal evolution models of Earth underscoring the strengths and limitations of these calculations.

Complimentary to the isotopic signals contained in ancient zircons, both long- and short-lived radionuclides leave isotopic signatures in mantle rocks that bear on when and how the silicate Earth formed and differentiated (Chap. 3). The longstanding view that the Hadean mantle was compositionally undepleted was upset by the recognition that Earth may differ in important ways from chondrites[4] suggesting a very early enriched reservoir.[5] Although recent work indicates this difference reflects differing irradiation histories of Earth and meteorites, and thus have little bearing on silicate differentiation, both terrestrial and lunar Lu–Hf zircon data appear to require global silicate differentiation by 4.5 billion years. Tungsten isotopic data from mantle rocks provides evidence of either very early isotopic isolation of silicate reservoirs or disturbance by a late chondritic veneer.

The once intense bombardment of the inner solar system that is manifest in the lunar surface would have surely influenced early Earth and its habitability. The exact nature of this role depends on the accurate dating of such impact features and thus this topic is critically reviewed in some detail in Chap. 4. In light of recent results, I argue that the Late Heavy Bombardment (LHB) hypothesis should be viewed with skepticism (see Mann 2018 for a brief overview).

Armstrong (1981) emphasized that, like all other terrestrial bodies which rapidly developed primary crusts, Earth must have immediately differentiated into relatively constant-volume core, depleted mantle, enriched crust, and fluid reservoirs. That view, however, was long outside the mainstream in which others argued that exceptional circumstances had forestalled this process on Earth. Indeed, the longstanding assumption was that significant continental crust or plate interactions didn't emerge until about 3 billion years ago. This was argued on the basis of apparent changes at that time in diamond inclusion assemblages, shale composition, zircon age spectra, and arc rock associations. However, flaws in multiple interrelated assumptions (particularly that lithospheric thermal structure and zircon productivity are time independent and that the Archean rock record is unbiased) leave open the possibility that continental crust may have existed previously and even been relatively abundant during the Hadean. Chapter 5 attempts to separate what is truly known from model-based speculations to permit readers to judge for themselves independent of longstanding conventional wisdom.

The thermal models for early Earth, described in Chap. 2, led directly to efforts to assess when our planet's dominant geodynamic regime—plate tectonics—got underway. Estimates of when plate tectonics initiated (or re-initiated) range across 3 billion years and include the possibility that plate boundary interactions were

[4]Chondrites are primitive stony meteorites containing chondrules that have not experienced significant differentiation and thus broadly represent material condensed from the solar nebula.

[5]A reservoir is a chemically and isotopically homogeneous and isolated mass (e.g., atmosphere, hydrosphere, undepleted mantle, etc.) that can exchange with other geochemically distinct storages.

occurring during Hadean times. Chapter 6 reviews current thoughts regarding the conditions necessary for the emergence of plate tectonics and weighs the likelihood that this mechanism operated on early Earth.

Chapter 7 reviews results of geochemical investigations of >4 billion year old zircons from Jack Hills, Australia (Mojzsis et al. 2001; Wilde et al. 2001). These data underlie a now widespread consensus that liquid water was present at or near Earth's surface throughout much of the Hadean. Given general agreement that life could not have emerged until liquid water appeared at or near Earth's surface, a significant implication is that our planet may have been habitable as much as 500 Ma earlier than previously thought. But Jack Hills is but one of fifteen locations on Earth from which zircons older than the most ancient known rock (the 4.02 Ga Acasta gneiss) have been identified. Are zircons from the Jack Hills globally representative? Chapter 8 reviews Hadean zircon data acquired from the fourteen other terrestrial locations (as well as extraterrestrial sources) but concludes that too little work has been undertaken to address that question at the moment with any confidence. Chapter 9 discusses the full range of petrogenetic interpretations put forward to explain the origin of >4 billion year zircons. While there is disagreement regarding certain interpretations, there is a remarkable consensus that the data essentially requires abundant liquid water at or near Earth's surface during much of the Hadean. This marks a distinct break from the former paradigm of a hellish, fiery world.

Chapter 10 summarizes current thoughts on the requirements for life and the ten or so interdependent features of Earth dynamics that appear to have fostered its emergence and development. Recent carbon isotopic evidence obtained from inclusions in Hadean zircons is consistent with life having emerged by 4.1 Ga, or several hundred million years earlier that the hypothesized lunar cataclysm. In Chap. 11, I summarize what is known from the morpho- and chemo-fossil records regarding the timing of the emergence of life on Earth. Chapter 12 addresses the epistemic questions raised in the introductory remarks of this chapter and points to future directions in Hadean research.

A critical summary highlighting what the author considers ground truth takeaways is provided at the end of each of the subsequent chapters. If I have tended to err on the side of conservative interpretations it is because our legacy has been one of confident speculation about topics for which no observational evidence then existed.

1.3 Defining the Hadean Eon

The geologic timescale arose from early nineteenth century trans-European biostratigraphic correlations and was thus fundamentally rooted in the identification of macrofossils (Cuvier and Brongniart 1811; Smith 1815; Phillips 1841). The need for a geologic time convention requires a significant degree of scientific cooperation and thus a series of global organizations, beginning with the first International

Geological Congress in 1878 (Ellenberger 1999), emerged to provide that support. Since 1974, the International Commission on Stratigraphy (ICS), a sub-group within the International Union of Geological Sciences, has attempted to establish a standardized, global geologic time scale. But defining geologic time boundaries prior to the Cambrian biodiversity explosion has always borne a greater degree of ambiguity than establishing them for the past 542 Ma because macrofossils only occur over the last 15% of Earth history. Subdividing the oldest 85% requires other approaches and no period is this more true than for than the first 11%—the Hadean —for which there is no known macroscopic rock record (Fig. 1.1).

Preston Cloud (1972) first proposed the term "Hadean" as the earliest division of geologic time which "ended 3.6–3.5 (billion years) ago[6] by a world-wide thermal event". He assumed that all terrestrial "radiometric clocks have been reset by some global and perhaps cosmic thermal event" at that time. As such, he suggested that "Selenian" (from Selene, the Greek goddess of Moon) would be equally appropriate to "Hadean", imputing to that "cosmic thermal event" the same impact history as was thought to be recorded in the then recently returned lunar samples. My sense is that Cloud's (1972) principal motivation was the exploration of ways to expand the geological time scale to include all of Earth history. By relating the apparent absence of terrestrial rocks older than $\sim$3.6 Ga to the pre-Imbium lunar history, he felt he had identified an event that could be globally correlated, putting early Earth on a broadly similar footing to biostratigraphically controlled Phanerozoic time divisions. Four years later, Cloud (1976) reiterated his proposal of the Hadean as the earliest division of geologic time during which "high prevailing temperatures" had likely precluded formation of stable crust until after $\sim$4.1 Ga. Geochronologic discoveries over the preceding four years (e.g., Moorbath et al. 1973) had pushed back his Hadean-Archean boundary age to 3.8 Ga—the approximate age of the supracrustal sequence at Isua, Greenland, which then included the oldest known rocks. Gone was the inference of a lunar-like global thermal catastrophe in favor of a more benign view of the transition to Archean Earth, including the possibility of a hydrosphere supporting life.

Harland (1975) argued that geologic time should have two scales, a chronometric scale based on units of time (e.g., the ephemeris second; Sadler 1957) and a chronostratic scale of rock sequences with standardized reference points separating boundary stratotypes. Since most stratigraphic names are derived from Greek roots, he suggested using Latin for the geochronometric scale. Thus he introduced the term Priscoan (from *priscus*, the Latin word for ancient) to describe the interval of Earth history prior to the Archean and placed that boundary arbitrarily at 4.0 Ga. Harland et al. (1982) continued to use Priscoan to describe pre-Archean Earth but chronostratically adopted Cloud's (1976) use of the Isuan supracrustal sequence at 3.8 Ga to define the lower boundary of the Hadean eon (consistent with the practice that the terminal boundary be defined by the initial boundary of the succeeding division; Cowie et al. 1986). Harland et al. (1990) further subdivided the Hadean based on lunar chronostratigraphy, as had Cloud (1972), assuming that the age of

[6]then the oldest reliably known rock forming ages.

the large impact basins were well known. In Chap. 4, I argue that problematic interpretations of lunar chronologic (Boehnke et al. 2016) and surface imaging (Spudis et al. 2011) results have substantially eroded the confidence that was once held regarding knowledge of the timing of those events. Although Priscoan is appealing to me as it carries no preconception about the nature of earliest Earth, it was not widely adopted.

In a report issued under the auspices of the ICS, Gradstein et al. (2004) recommended that the lower bound of the Hadean be defined at 3.85 Ga, noting that the earlier period was characterized by "intense bombardment and its consequences, but no preserved supracrustals" (cf. Chap. 4). This was echoed by Bleeker (2004a, b), Moorbath (2005), and Van Kranendonk et al. (2012), who argued that the lower boundary of the Hadean Eon should be defined by the end of the Late Heavy Bombardment between 3.85 and 3.82 Ga. Judging from the 2010 to 2015 annual reports of the ICS's Subcommission on Precambrian Stratigraphy,[7] this group was aware of these recommendations but appears not to have acted to define the timing of a Hadean Eon. Nonetheless, the 2017 version of the ICS's International Chronostratigraphic Chart[8] shows the Hadean as extending from 4.0 to 4.6 Ga (Fig. 1.1).

The brief history above shows not only the ambiguity inherent in defining a chronostratic term for an eon without known strata, but the potential for codifying unconstrained assumptions as well. Take, for example, the widely shared argument (Cloud 1972; Harland et al. 1990; Gradstein et al. 2004; Bleeker 2004a, b; Moorbath 2005; Van Kranendonk et al. 2012) that the lower bound of the Hadean be defined effectively by the termination of the Late Heavy Bombardment given that the very existence of the LHB is currently being debated (see Mann 2018; 1.2.2; Chap. 4). Another curious feature that links these various proposals made over forty years (i.e., 1972–2012) is their confidence that the terrestrial crust had, at the moment at which the edict was made, revealed the full range of its preserved rock record and past history.[9] There appears no sense that the failure of earlier proposed time scales to anticipate discoveries of yet older rocks provided any cautionary feedback. Even today, vast regions of continental crust remain unexposed (Sect. 7.3) and seismic sections across it are clearly inconsistent with the assumption that surface rocks characterize the crustal column beneath (Sect. 5.2). Indeed, Harrison et al. (2017) calculated that less than 10^{-17} of the continental crust has as yet been geochronologically surveyed.

For the reasons discussed above and the simple utility of having a term that describes the period of Earth history for which we have no macroscopic rock record, I believe the timing and duration of the Hadean eon is best left elastic. Thus

[7]http://www.stratigraphy.org/images/Archive/ICS_SubcommReport2014.pdf.

[8]http://www.stratigraphy.org/ICSchart/ChronostratChart2017-02.pdf.

[9]This phenomenon has a long tradition. For example, in 1948 George Gamow wrote: "…modern geology arrives at a rather detailed picture of the solidification times of different parts of the Earth's crust. The general result of this survey reveals an important fact: no rock exhibits an age of more than two billion years from which we must conclude that *the solid crust of the Earth was formed from previously molten matter not more than about two billion years ago*" (Gamow 1948).

my preference is to define it as the interval prior to the formation of the oldest known rock outcrop—the 4.02 Ga Acasta gneiss (Bowring and Williams 1999; Stern and Bleeker 1998; Reimink et al. 2016; cf. O'Neil et al. 2008) and subsequent to the gross differentiation of Earth into metal and silicate layers and final solidification of the latter (Fig. 1.1). This maintains the Hadean as an informal term that can change once rocks older than the Acasta gneiss (and the ages of core formation and magma ocean crystallization) have been unambiguously documented. It also underscores the continuing need for skepticism about interpretations of Hadean environments as they must then be, by definition, based on other than a macroscopic rock record.

1.4 Is Hadean a Misnomer?

Use of the term Hadean to characterize the first half billion or so years of Earth history as a planetary inferno may prove ironic. In ancient Greek mythology, Hades was the god of a synonymous, mist-shrouded, riverine underworld. The realm of Hades, transliterated from Koine Greek, may have first appeared in printed English in the Tyndale-Coverdale Bible (1535) and later in the more widely disseminated King James Version (1611). Perhaps surprisingly, specific references to Hades in the King James New Testament as a fiery, tormenting hell are rather rare,[10] appearing in Mark (9:43), James (3:6), and Luke's (16:23–24) relating of the parable of Lazarus and the wealthy man in which the latter is "tormented in this flame". Despite their number, these few verses appear to have strongly influenced the Anglo-Saxon imagination. The eponym 'Hadean' had appeared in English literature by the early eighteenth century (e.g., Scriblerus 1731) gaining some popularity in poetry and scriptural interpretations during the Victorian era (e.g., Ogle 1839) (Fig. 1.2). The word then appears to have fallen out of favor until shortly after Cloud (1972) proposed his definition of the first eon of Earth history.

Ironically, designating the first half billion years or so of Earth history as the Hadean eon may well prove prescient, but in terms of the ancient Greek myth rather than the intended inference of a protracted, fiery hellscape. As already noted, the paradigm of a hellish early Earth began to be challenged in 2001 as results of geochemical investigations of >4 billion year old zircons from Jack Hills, Australia, began to emerge (Mojzsis et al. 2001; Wilde et al. 2001). These data were consistent with these zircons forming in a world more similar to today than long believed, including indications that sediment cycling had occurred in the presence of liquid water. This leaves open the possibility that plate tectonic-like behavior and even life had emerged shortly after Earth accretion (Hopkins et al 2008; Bell et al. 2015). But just because this new view of early Earth is based on tangible, empirical evidence doesn't mean that it's correct (e.g., evidence for Piltdown Man was

[10]Notwithstanding the dozen or so references to *gehenna*, a non-specific destination for the wicked, and the multiple references in Revelations to fiery torments (14:10–11, 20:10,14,15; 21:8) in unspecified locations.

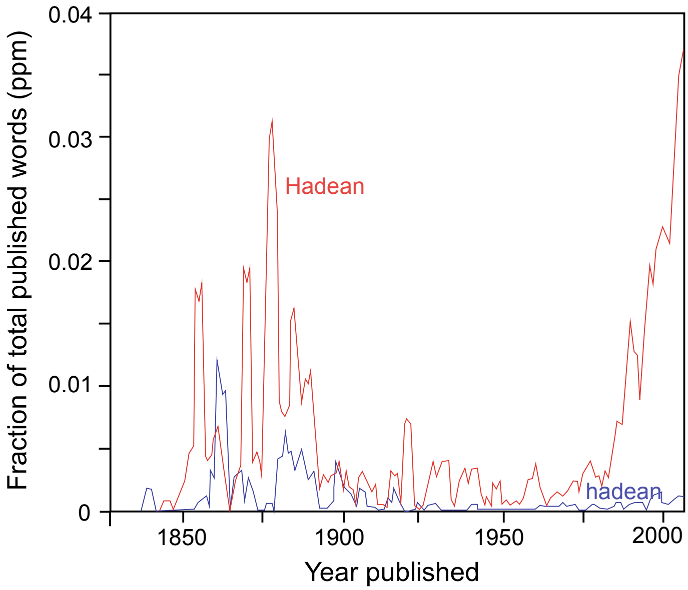

Fig. 1.2 Ngram Viewer (Michel et al. 2011) graph with a one year smoothing of the usage of *Hadean* and *hadean* (in ppm) between 1825 and 2007 relative to all words in the Google Books database published that year. Note that use of the capitalized version of the word increased significantly following Cloud's (1972) proposed definition of the earliest eon in Earth history

tangible). Even at its best, the effect of this new view should be to open up novel lines of investigation and to liberate the coming generation of geoscientists to think more freely and widely about possible origin scenarios than their mentors did. And this new view of early Earth might even prove to be correct.

1.5 When Did the Hadean Begin?

Because Earth formed by the protracted accretion of planetestimals and planetary embryos, formed themselves by condensation from a nebular cloud of gas and dust and variably differentiated thereafter, asking the age of our planet is akin to asking your friends theirs. They are unlikely to date themselves from the moment of conception but instead use the widely accepted convention of the date of their emergence from the womb. From a cosmochemical standpoint, we pinpoint the arrival of our solar system to the formation of the first solids that condensed from the circumstellar disk. Refractory Ca–Al-rich inclusions (CAIs) found in primitive chondrites were the first minerals to form as the hot nebula cooled. These first solids of the new solar system have been U-Pb[11] dated to as old as 4.568 ± 0.001 Ga (Amelin et al. 2010; Bouvier and Wadhwa 2010) and thus provide us with a convenient starting point in solar system evolution, if not the upper age bound on the Hadean.

The culmination of efforts to establish the age of Earth is generally credited to Patterson et al. (1955). They measured Pb isotopes in terrestrial rocks believed to be representative of the bulk Earth and found that they plotted on the same $^{207}Pb/^{206}Pb$ array (the "geochron") as primitive and iron meteorites, corresponding to an age of ~4.5 Ga. However, this was before it was appreciated that the rocks on Earth's surface are the products of extreme mantle differentiation and thus are not representative of its bulk composition. Patterson et al. (1955) had, not unreasonably for the times, assumed that oceanic sediments are a well-mixed, representative sample of the Earth and further assumed that crustal formation had largely partitioned U into the crust but excluded Pb. However, little was known about crust-mantle differentiation and nothing was known about plate tectonics. The apparent fit of oceanic sediments to the meteorite isochron (in fact, modern high precision analyses plot to the right of the "geochron") is in fact a geochemical coincidence from which no conclusions about the age of the Earth should be drawn. They are entirely crust-derived and thus compositionally very different from the much larger mantle reservoir. The above-mentioned coincidence is that uranium and lead, both highly enriched in the continental crust relative to the mantle, have average crust/mantle enrichment factors that happen to be nearly equal.

The early timing of volatile loss seen in the meteorite record strongly suggests Earth had accreted most of its present mass by 4.55 Ga (see Sect. 3.1) from planetesimals of broadly chondritic composition, albeit of a class not yet recognized in the meteorite record (e.g., Render et al. 2017). It was long assumed that the planetary embryos from which the terrestrial planets formed were initially enveloped by atmospheres similar to the nebular gas (e.g., Craig and Lupton 1976) leading to exceedingly high surface temperatures. That view subsided with the appreciation that such hydrogen-dominated atmospheres would be lost over million year timescales by hydrodynamic escape of molecules heated by photons in the extreme ultraviolet (e.g., Lunine et al. 2011). A second protoatmosphere arises when gases are released from the deep planetary interior during planetary differentiation, either catastrophically or gradually, creating a CO_2- and H_2O-rich atmosphere (e.g., Elkins-Tanton 2008).

Despite the lack of direct evidence for a collision shortly thereafter with a Mars-sized object, and some that appears inconsistent (e.g., Wiechert et al. 2001; cf. Pahlevan and Stevenson 2007), there is widespread agreement that Moon formed by such a process (Canup 2004). The importance of whether or not this collision scenario of lunar formation occurred rests with the thermal and compositional consequences of a $\sim 10^{32}$ J collision. Such an event would surely have vaporized a large portion of both impactor and target and melted the rest of the combined system, although little volatile loss would occur if temperatures were sufficiently

[11]From the ingrowth of daughter ^{206}Pb and ^{207}Pb from the radioactive decay of parent ^{238}U and ^{235}U, respectively.

high (i.e., >6000 K; Genda and Abe 2005; Abe 2007). Independent of this Moon-forming scenario, the energy associated with assembly of the Earth and core formation would likely create a thermal structure conducive to creation of a global magma ocean (Righter and Drake 1999; see 10.2.9). The timing of core formation —and thus an upper bound on the formation age of the metal-poor Moon—is not well known. An upper limit of ~100 Ma is estimated from the single-stage ^{207}Pb-^{206}Pb evolution of the most primitive known galena (Pidgeon 1978) and ^{182}Hf-^{182}W model ages generally suggest ~30 Ma (e.g., Lee and Halliday 1995; Jacobsen 2005; Touboul et al. 2007; Halliday 2008).

Timing constraints on the terrestrial magma ocean history (or histories) are even less well developed. Indeed, geochemical evidence requiring that such an event occurred is almost entirely lacking (e.g., Righter and Drake 1999). The consensus view of terrestrial magma ocean crystallization is that solidification proceeded from the bottom up, driving such initially vigorous convection such that the lower mantle (>28 GPa) crystallized within 10^3 years (Solomatov 2007). Calculations suggest that the remaining mantle would have been largely solid within 10^5–10^7 years, depending on volatile content (Elkins-Tanton 2008). Although a steam atmosphere would slow this process, the generally short timescales expected suggest that serial magma oceans, perhaps punctuated by clement conditions, were possible on earliest Earth (Elkins-Tanton 2008). Estimates of the depth of the last terrestrial magma ocean, based on apparent equilibration depths of moderately siderophile elements (e.g., Rubie et al. 2003; Elkins-Tanton et al. 2007) and geodynamic considerations (e.g., Solomatov 2000), range from relatively shallow to the core-mantle boundary. This range reflects, in part, the generally weak pressure dependence of siderophile element partitioning and uncertain extensive parameters (e.g., f_{O_2}).

Many possible permutations involving magma oceans and large impactors are consistent with what we actually know, but some proposed histories (e.g., Halliday 2008; Allègre et al. 2008) are contradicted by the Hadean zircon record (Chap. 7). While the oldest direct evidence of terrestrial crust formation are 4.38 Ga Jack Hills zircons (Holden et al. 2009), its existence can be inferred as early as 4.51 Ga from Lu–Hf data from terrestrial (Harrison et al. 2008) and lunar (Barboni et al. 2017) zircons, thus restricting the core formation-giant impactor-magma ocean phase to within ~70 Ma of the formation of CAIs at 4.568 ± 0.001 Ga (Krot et al. 2005; Amelin et al. 2010; Bouvier and Wadhwa 2010). Subject to future refinements, I take the upper bound of the Hadean to be the termination of globally disruptive formation and differentiation events, including a Moon-forming impact, core formation, and magma ocean(s), which had all occurred by 4.50 Ga (see Sects. 3.2–3.4).

1.6 The Challenge of Deep Time

Knowledge of time lies at the heart of geology and the concept of ‘deep time’ is what separates our field from all other disciplines, save astronomy. It is a rare geologist who has not surprised a layperson by describing a few million's-of-year-old feature as "youthful". When the concept of deep time emerged in the late eighteenth century, it held a semi-mystical quality in the geologic community. Hutton's (1788) statement that he could find "…no vestige of a beginning, no prospect of an end" for the planet was justifiable for its time but later adherents to uniformitarianism took this as a license to ignore physics. Lyell (1830) described Earth history as "indefinite" and "inconceivably vast" which his devotees effectively translated as 'infinite' at about the same time that the laws of thermodynamics—and particularly the concept of entropy—were being formulated (Clausius 1850). Indeed, it was the clash between uniformitarian lore and physical laws that led William Thomson (1863), later Lord Kelvin, to publically repudiate Huttonian fundamentalists leading to the ill-starred age of Earth debate during the Victorian era (see Chap. 2). Eventually, Lyell (1837) would go as far as to invoke perpetual motion to explain Earth's perennial peppiness.

The quantification of deep time (Boltwood 1907) gave the concept a prosaic touch at the same time catapulting the discussion of Earth's age from a few 10's of millions of years to billions. But vestiges of its once enchanted connotation linger. We are, as described in the opening paragraph of this chapter, a species of causal determinists driven by the need to feel that we understand the world around us (Dawkins 2007). Faced with what was once thought of as inconceivable durations and a famously incomplete rock record, comfort could be taken from orderly classification schemes. While geologists have been able to shed strict uniformitarianism when thinking about earliest Earth, they have tended to assume that it subsequently evolved in a monotonic fashion; from hot to cold (Christensen 1985; cf. Korenaga 2008), from simple to complex minerals (Hazen 2013; cf. Bell et al. 2018), from no continental crust to our complete complement via continuous growth today (Taylor and McLennan 1985; cf. Armstrong 1991). Think of this as our monotony bias. While having the superficial appearance of Occam's razor[12] in action, there is really no basis to assume that Earth, a collection of non-linear systems at all scales (Turcotte 1997), should be parsimonious with its evolutionary trajectory. It was long assumed that equilibrium was maintained between internal heat generation and its flux from the surface throughout Earth's history (Urey 1955; Tozer 1972; McKenzie and Weiss 1975; Bickle 1986). While possible, this speculation is hardly unique (cf. Korenaga 2006) but dominated thought for decades. The monotony bias, a recurring theme throughout this book, tends to lead to a group consensus temporizing for a true understanding, eventually ossifying into a community convention.

The discussion above is meant to invoke a sense of how our instinct to see deep time in a conservative fashion presents a continuing challenge to geologic interpretations. The further back in time we go, the spottier the rock record and the weaker is our understanding of boundary conditions (cf. Smith and Morowitz 2016). As already noted in Sect. 1.3, the geologic community tends to assume that the continental crust has already given up full knowledge of its preserved rock

[12]Occam's razor is the philosophical view that parsimonious explanations are preferable to complex ones because they are more easily falsifiable.

record and past history. Together with the monotony bias, these effects tend to incentivize narrowly focused explanations for the few remaining Archean exposures (which, as discussed in Chap. 5, are likely a biased record of that era) paving a path for unconstrained geodynamic models to be viewed as axiomatic (see Chap. 2). These two foci come at the expense of fresh ideas about the nature of the missing rock record which, of course, constitutes the vast majority of the history of petrogenesis.

While this book appears to be the first monograph specifically covering the first 500 million or so years of Hadean Earth, it is not a fact sheet thereof. No proposed model for earliest Earth is supported by what in the realm of the preserved rock record would constitute smoking gun evidence. It is hoped instead that it will inoculate the reader against adopting any specific speculation before they are aware of the now substantial literature across the various topics covered here, upon which they can arrive at their own best judgement of what the evidence currently permits, and then devise better experiments to probe more deeply.

References

Abe, Y. (1993). Physical state of the very early earth. *Lithos, 30,* 223–235.

Abe, Y. (2007). Behavior of water during terrestrial planet formation. *Geochimica et Cosmochimica Acta Suppl, 71,* A2.

Allègre, C. J., Manhès, G., & Göpel, C. (2008). The major differentiation of the earth at ~4.45 Ga. *Earth and Planetary Science Letters, 267,* 386–398.

Amelin, Y., Kaltenbach, A., Iizuka, T., Stirling, C. H., Ireland, T. R., Petaev, M., et al. (2010). U-Pb chronology of the solar system's oldest solids with variable $^{238}U/^{235}U$. *Earth and Planetary Science Letters, 300,* 343–350.

Armstrong, R. L. (1981). Radiogenic isotopes: The case for crustal recycling on a near-steady-state no-continental-growth earth. *Philosophical Transactions of the Royal Society London Ser. A, 301,* 443–471.

Armstrong, R. L. (1991). The persistent myth of crustal growth. *Australian Journal of Earth Science, 38,* 613–630.

Barboni, M., Boehnke, P., Keller, B., Kohl, I.E., Schoene, B., Young, E. D., & McKeegan, K.D. (2017). Early formation of the moon 4.51 billion years ago. *Science Advances*, *3*, e1602365.

Bell, E.A., Boehnke, P., Harrison, T.M., and Mao, W. (2015). Potentially biogenic carbon preserved in a 4.1 Ga zircon. *Proceedings of the National Academy of Sciences*, *112*, 14518–14521.

Bell, E. A., Boehnke, P., Harrison, T. M., & Wielicki, M. M. (2018). Mineral inclusion assemblage and detrital zircon provenance. *Chemical Geology, 477,* 151–160.

Berkman, M., & Plutzer, E. (2010). *Evolution, creationism, and the battle to control America's classrooms*.

Bickle, M. J. (1986). Implications of melting for stabilisation of the lithosphere and heat loss in the Archean. *Earth and Planetary Science Letters, 80,* 314–324.

Bleeker, W. (2004a). Taking the pulse of planet earth: A proposal for a new multi-disciplinary flagship project in Canadian solid earth sciences. *Geoscience Canada, 31,* 179–190.

Bleeker, W. (2004b). Towards a 'natural' time scale for the Precambrian—A proposal. *Lethaia, 37,* 219–222.

Boehnke, P., Harrison, T. M., Heizler, M. T., & Warren, P. H. (2016). A model for meteoritic and lunar $^{40}Ar/^{39}$ Ar age spectra: Addressing the conundrum of multi-activation energies. *Earth and Planetary Science Letters, 453,* 267–275.

Boltwood, B. (1907). On the ultimate disintegration products of the radioactive elements. Part II. The disintegration products of uranium. *American Journal of Science, 4,* 77–80.
Bouvier, A., & Wadhwa, M. (2010). The age of the Solar System redefined by the oldest Pb–Pb age of a meteoritic inclusion. *Nature Geoscience, 3,* 637.
Bowring, S. A., & Williams, I. S. (1999). Priscoan (4.00–4.02 Ga) orthogneisses from northwestern Canada. *Contributions to Mineralogy and Petrology, 134,* 3–16.
Canup, R. M. (2004). Simulations of a late lunar forming impact. *Icarus, 168,* 433–456.
Christensen, U. R. (1985). Thermal evolution models for the earth. *Journal of Geophysical Research: Solid Earth, 90,* 2995–3007.
Clausius, R. (1850). *On the motive power of heat, and on the laws which can be deduced from it for the theory of heat*. LXXIX (Dover Reprint): Poggendorff's Annalen der Physick.
Cloud, P. (1972). A working model of the primitive Earth. *American Journal of Science, 272,* 537–548.
Cloud, P. (1976). Major features of crustal evolution. *De Toit Lecture, Geological Society of South Africa, 79,* 1–33.
Cowie, J. W., Ziegler, W., Boucot, A. J., Basset, M.G. & Remane, J. (1986). Guidelines and Statues of the International Commission on-Stratigraphy (ICS). *Cour. Forsch.-lnst. Senckenberg*, *83*, 1–14.
Craig, H., & Lupton, J. E. (1976). Primoridial neon, helium, and hydrogen in oceanic basalts. *Earth and Planetary Science Letters, 32,* 369–385.
Cuvier, G., & Brongniart, A. (1811). *Essai sur la géographie minéralogique des environs de Paris: avec une carte géognostique, et des coupes de terrain*. Baudouin.
Davies, G. F. (1980). Thermal histories of convective earth models and constraints on radiogenic heat production in the earth. *Journal of Geophysical Research: Solid Earth, 85,* 2517–2530.
Dawkins, R. (2007). *The god delusion*. Random House.
Dundes, A. (1962). Earth-Diver: Creation of the mythopoeic male. *American Anthropologist, 64,* 1032–1051.
Elkins-Tanton, L. T. (2008). Linked magma ocean solidification and atmospheric growth for earth and mars. *Earth and Planetary Science Letters, 271,* 181–191.
Elkins-Tanton, L. T., Parmentier, E. M., & Hess, P. C. (2007). The effects of magma ocean depth and initial composition on planetary differentiation. In *Lunar and Planetary Science Conference* (pp. XXXVIII).
Ellenberger, F. (1999). The first international geological congress, Paris, 1878. *Episodes, 22,* 113–117.
Ernst, W. G. (1983). The early earth and the Archean rock record. In *Earth's earliest biosphere: Its origin and evolution* (pp. 41–52). Princeton, NJ: Princeton University Press.
Fyfe, W. S. (1978). The evolution of the earth's crust: Modern plate tectonics to ancient hot spot tectonics? *Chemical Geology, 23,* 89–114.
Gamow, G. A. (1948). *Biography of the earth: Its past, present and future* (p. 194). Mentor Books.
Genda, H., & Abe, Y. (2005). Enhanced atmospheric loss on protoplanets at the giant impact phase in the presence of oceans. *Nature, 433,* 842–844.
Gradstein, F. M., Ogg, J. G., Smith, A. G., Bleeker, W., & Lourens, L. J. (2004). A new geologic time scale, with special reference to Precambrian and Neogene. *Episodes, 27,* 83–100.
Halliday, A. N. (2008). Earth viewed from a late moon. *Geochimica et Cosmochimica Acta Suppl, 72,* A344.
Hamilton, W. B. (1998). Archean magmatism and deformation were not products of plate tectonics. *Precambrian Research, 91,* 143–179.
Harland, W. B. (1975). The two geological time scales. *Nature, 253,* 505.
Harland, W. B., Cox, A. V., Llewellyn, P. G., Pickton, C. A. G., Smith, A. G., & Walters, R. (1982). *A geologic time scale* (p. 131). Cambridge University Press.
Harland, W. B., Armstrong, R. L., Cox, A. V., Craig, L. E., Smith, A. G., & Smith, D. G. (1990). *A geologic time scale 1989*. Cambridge: Cambridge University Press.

Harrison, T. M., Schmitt, A. K., McCulloch, M. T., & Lovera, O. M. (2008). Early ($\geq$4.5 Ga) formation of terrestrial crust: Lu-Hf, δ^{18}O, and Ti thermometry results for Hadean zircons. *Earth and Planetary Science Letters, 268,* 476–486.

Harrison, T. M., Bell, E. A., & Boehnke, P. (2017). Hadean zircon petrochronology. *Reviews in Mineralogy and Geochemistry, 83,* 329–363.

Hazen, R. M. (2013). Paleomineralogy of the Hadean Eon: A preliminary species list. *American Journal of Science, 313,* 807–843.

Holden, P., Lanc, P., Ireland, T. R., Harrison, T. M., Foster, J. J., & Bruce, Z. P. (2009). Mass-spectrometric mining of Hadean zircons by automated SHRIMP multi-collector and single-collector U/Pb zircon age dating: The first 100 000 grains. *International Journal of Mass Spectrometry, 286,* 53–63.

Hopkins, M., Harrison, T. M., & Manning, C. E. (2008). Low heat flow inferred from >4 Ga zircons suggests Hadean plate boundary interactions. *Nature, 456,* 493–496.

Hume, D. (1738). *A treatise of human nature* (p. 368). London: John Noon.

Hutton, J. (1788). Theory of the earth; or an investigation of the land observable in the composition, dissolution and restoration of land upon the globe. *Earth and Environmental Science Transactions of The Royal Society of Edinburgh*, *1*, 209–304.

Jacobsen, S. (2005). The Hf-W isotopic system and the origin of the earth and moon. *Annual Review of Earth and Planetary Sciences, 33,* 531–570.

Korenaga, J. (2006). Archean geodynamics and the thermal evolution of Earth. In K. Benn, J.-C. Mareschal, K. Condie (Eds.), *AGU Geophysical Monograph Series: Vol.* 164. *Archean geodynamics and environments* (pp. 7–32).

Korenaga, J. (2008). Urey ratio and the structure and evolution of earth's mantle. *Reviews of Geophysics*, *46*, RG2007. https://doi.org/10.1029/2007RG000241.

Krot, A. N., Amelin, Y., Cassen, P., & Meibom, A. (2005). Young chondrules in CB chondrites from a giant impact in the early solar system. *Nature, 436,* 989–992.

Lee, D., & Halliday, A. (1995). Hafnium-tungsten chronometry and the timing of terrestrial core formation. *Nature, 378,* 771–774.

Leeming, D. A. (2010). *Creation myths of the world: An encyclopedia* (in two volumes). ABC-CLIO Inc., p. 553.

Lunine, J. I. (1999). *Earth: Evolution of a habitable world*. Cambridge University Press.

Lunine, J. I., O'Brien, D. P., Raymond, S. N., Morbidelli, A., Qinn, T., & Graps, A. L. (2011). Dynamical models of terrestrial planet formation. *Advanced Science Letters, 4,* 325–338.

Lyell, C. (1830). *Principles of geology* (Vol. 1). Murray.

Lyell, C. (1837) *Principles of geology: being an inquiry how far the former changes of the earth's surface are referable to causes now in operation* (Vol. 1). J. Kay, jun. and brother.

Maher, K. A., & Stevenson, D. J. (1988). Impact frustration of the origin of life. *Nature, 331,* 612–614.

Mann, A. (2018). Bashing holes in the tale of earth's troubled youth. *Nature, 553,* 393–395.

McKenzie, D. P., & Weiss, N. (1975). Speculation on the thermal and tectonic history of the earth. *Geophysical Journal International, 42,* 131–174.

Michel, J. B., Shen, Y. K., Aiden, A. P., Veres, A., Gray, M. K., Pickett, J. P., et al. (2011). Quantitative analysis of culture using millions of digitized books. *Science, 331,* 176–182.

Mojzsis, S. J., Harrison, T. M., & Pidgeon, R. T. (2001). Oxygen-isotope evidence from ancient zircons for liquid water at the earth's surface 4300 Myr ago. *Nature, 409,* 178–181.

Moorbath, S. (2005). Oldest rocks, earliest life, heaviest impacts, and the Hadean-Archaean transition. *Applied Geochemistry, 20,* 819–824.

Moorbath, S., O'Nions, R. K., & Pankhurst, R. J. (1973). Early Archaean age for the Isua iron formation, West Greenland. *Nature, 245,* 138–146.

Nevins, A., Pesetsky, D., & Rodrigues, C. (2009). Pirahã exceptionality: A reassessment. *Language, 85,* 355–404.

O'Neil, J., Carlson, R. W., Francis, D., & Stevenson, R. K. (2008). Neodymium-142 evidence for Hadean mafic crust. *Science, 321,* 1828–1831.

Ogle, N. (1839). *Mariamne, the last of the Asmonean Princesses: A historical novel of Palestine*. James Fraser.

Pahlevan, K., & Stevenson, D. J. (2007). Equilibration in the aftermath of the lunar-forming giant impact. *Earth and Planetary Science Letters, 262,* 438–449.

Patterson, C., Tilton, G., & Inghram, M. (1955). Age of the earth. *Science, 121,* 69–75.

Phillips, J. (1841). *Figures and descriptions of the Palaeozoic Fossils of Cornwall, Devon and West Somerset.* Longman Brown.

Pidgeon, R. T. (1978). Big Stubby and the early history of the earth. *U.S. Geological Survey Open File Report*, *78–701*, 334–335.

Reimink, J. R., Davies, J. H. F. L., Chacko, T., Stern, R. A., Heaman, L. M., Sarkar, C., et al. (2016). No evidence for Hadean continental crust within earth's oldest evolved rock unit. *Nature Geoscience, 9,* 777–780. https://doi.org/10.1038/ngeo2786.

Render, J., Fischer-Gödde, M., Burkhardt, C., & Kleine, T. (2017). The cosmic molybdenum-neodymium isotope correlation and the building material of the earth. *Geochemical Perspective Letters, 3,* 170–178.

Righter, K., & Drake, M. J. (1999). Effect of water on metal-silicate partitioning of siderophile elements a high pressure and temperature terrestrial magma ocean and core formation. *Earth and Planetary Science Letters, 171,* 383–399.

Rooth, A. B. (1957). The creation myths of the North American Indians. *Anthropos, 52,* 497–508.

Rubie, D. C., Melosh, H. J., Reid, J. E., Liebske, C., & Righter, K. (2003). Mechanisms of metal-silicate equilibration in the terrestrial magma ocean. *Earth and Planetary Science Letters, 205,* 239–255.

Sadler, D. H. (1957). 4. Commission des Ephemerides. *Transactions of the International Astronomical Union, 9,* 80–84.

Scriblerus, S. (1731). *Whistoneutes: Or, Remarks on Mr. Whiston's Historical Memoirs of the Life of Dr. Samuel Clarke, &c*. By a person of retirement and obscurity; But of the Antique Ffamily of the Scriblerians. Printed for T. Warner, at the Black-Boy in Pater-Noster-Row, London.

Smith, W. (1815). *A memoir to the map and delineation of the Strata of England and wales with part of Scotland*. John Cary.

Smith, J. V. (1981). The first 800 million years of earths history. *Philosophical Transactions of the Royal Society London Ser. A, 301,* 401–422.

Smith, E. and Morowitz, H.J. (2016) *The origin and nature of life on earth: the emergence of the fourth geosphere*. Cambridge University Press.

Solomatov, V. S. (2000). Fluid dynamics of a terrestrial magma ocean. In R. Canup & K. Righter (Eds.), *Origin of the earth and moon* (pp. 323–338). Tucson, TUS: Univ. Ariz. Press.

Solomatov, V. S. (2007). Magma oceans and primordial mantle differentiation. In G. Schubert (Ed.), *Treatise on geophysics 9* (pp. 91–120). Oxford: Elsevier.

Solomon, S. C. (1980). Differentiation of crusts and cores of the terrestrial planets: Lessons for the early earth? *Precambrian Research, 10,* 177–194.

Spudis, P. D., Wilhelms, D. E., & Robinson, M. S. (2011). The sculptured hills of the Taurus Highlands: Implications for the relative age of Serenitatis, basin chronologies and the cratering history of the moon. *Journal of Geophysical Research: Planets, 116,* E12.

Stern, R. A., & Bleeker, W. (1998). Age of the world's oldest rocks refined using Canada's SHRIMP the Acasta gneiss complex Northwest territories Canada. *Geoscience Canada, 25,* 27–31.

Taylor, S. R., & McLennan, S. M. (1985). *The continental crust: Its composition and evolution*. Oxford: Blackwell.

Thomson, W. (1863). On the secular cooling of the earth. *Philosophical Magazine Ser, 4*(25), 1–14.

Touboul, M., Kleine, T., Bourdon, B., Palme, H., & Wieler, R. (2007). Late formation and prolonged differentiation of the Moon inferred from W isotopes in lunar metals. *Nature, 450,* 1206–1209.

Tozer, D.C. (1972). The present thermal state of the terrestrial planets. *Physics of the Earth and Planetary Interiors*, *6*(1–3),182–197.

Turcotte, D. L. (1997). *Fractals and chaos in geology and geophysics* (p. 412). Cambridge University Press.

Urey, H. C. (1955). The cosmic abundances of potassium, uranium, and thorium and the heat balances of the earth, the moon, and mars. *Proceedings of the National Academy of Sciences of the United States of America, 41,* 127–144.

Van Kranendonk, M. J., Altermann, W., Beard, B. L., Hoffman, P. F., Johnson, C. M., Kasting, J. F., Melezhik, V. A., Nutman, A. P., & Papineau, D., Pirajno, F. (2012). A chronostratigraphic division of the Precambrian: possibilities and challenges. In F. M. Gradstein et al. (Eds.), *The geologic time scale* (pp. 299–392). Elsevier.

Waltham, J. (2014). *Lucky planet* (p. 198). New York, NY: Basic Books (Perseus).

Ward, P. D., & Brownlee, D. (2000). *Rare earth: Why complex life is uncommon in the universe*. New York: Copernicus Books.

Wetherill, G. W. (1972). The beginning of continental evolution. *Tectonophysics, 13,* 13–45.

Wiechert, U., Halliday, A. N., Lee, D. C., Snyder, G. A., Taylor, L. A., & Rumble, D. (2001). Oxygen isotopes and the moon-forming giant impact. *Science, 294,* 345–348.

Wilde, S. A., Valley, J. W., Peck, W. H., & Graham, C. M. (2001). Evidence form detrital zircons for the existence of continental crust and oceans 4.4 Ga ago. *Nature, 409,* 175–178.

2 Thermal Evolution Models

Abstract

The study of Earth as an object whose history can be understood by application of physical laws dates back 200 years. This tradition is, however, rife with missteps related to as yet undiscovered physics or fundamentally incorrect assumptions. While the former is unavoidable, the latter amounts to self-inflicted wounds that may have forestalled scientific progress. Even in the absence of knowledge of initial conditions, linear mathematical relationships such as first order loss (e.g., radioactive decay) have proved useful in predicting Hadean conditions. However, more complex physical systems cannot be uniquely extrapolated back in time. For example, mantle convection, a highly non-linear, dispersive, chaotic system is, by its very nature, uninvertible. This fact has not inhibited generations of modeler's from making ab initio predictions regarding early Earth evolution. Their results were initially limited by technological impediments and adoption of assumptions regarding the relationship between interior temperature and planetary heat loss that narrowed possible solutions. Radically new proposals regarding both the latter issue and discontinuous transitions between modes of heat loss have tempered earlier conclusions that plate-tectonic-like behavior could not arise on early Earth. Physical calculations have an important role to play in assessing the plausibility of Hadean geodynamic models, but should best be seen as "convenient fictions".

2.1 Background

We begin by picking up on a theme from the previous chapter. One element of how the scientific community came to adopt the paradigm of a hellish, pre-4 billion-year-old Earth comes from the first of our four avenues of Hadean investigation; the assumption that physical laws are time invariant and thus mathematical models can

T. M. Harrison, *Hadean Earth*, https://doi.org/10.1007/978-3-030-46687-9_2

be used to place limits on the nature of early Earth. The example given in the previous chapter of extrapolating the decay behavior of radioactivity back 4.5 billion years to estimate the planet's heat generation marks one endmember of the spectrum of possible calculations (see Sect. 2.2). At the other end of this spectrum, global thermal evolution models operate over highly non-linear landscapes and require input parameter values and boundary conditions that are poorly or unconstrainable. The influence that some of these models have had on geologic thought has been profound and suggests an intellectual vulnerability in our culture that may linger today. Let's start at the very beginning.

The mathematical analysis of Earth's thermal history began with Fourier (1820) who, upon deriving and solving the differential equation describing conductive heat flow near a semi-infinite boundary (i.e., an approximation of Earth's near surface), estimated the parameters needed to solve for the time that Earth would have taken to decay to its present, near-surface geotherm from the melting temperature of iron. Had Fourier actually evaluated this expression, his parameter choices would have led to a minimum age of many hundreds of thousands of years, although the melting temperature of iron was not then well known (Cloud 1818) and he overestimated the thermal diffusivity of iron by a factor of forty. He chose not to explicitly calculate an age, perhaps cognizant of the strong countervailing religious sentiments of the time and the icy reception that de Buffon's proposal of a 75,000 year age had received from religious authorities four decades earlier (de Buffon 1778). This approach was re-energized in the latter half of the nineteenth century by William Thomson (later Lord Kelvin), a prominent British physicist. Thomson (1863) adopted Fourier's (1820) model and concluded that Earth could not be in excess of 100 million years (Ma) old, later reducing his estimate to between 20 and 40 Ma (Kelvin 1899). Although many prominent geologists acceded to this outlook, several argued that the complexity of the geologic record demanded a much longer duration than Kelvin was advocating (see Burchfield 1975). However, other contemporary physicists (Perry 1895a, b, c; Heaviside 1899), using models incorporating the possibility of fluid circulation in the mantle, were able to accommodate time scales as great as 5 Ga (1 Ga = 10^9 years).

The discovery of radioactivity by Becquerel (1896) and the subsequent recognition that radioactive decay involves the release of substantial energy provided an apparent reconciliation of these divergent views, in part due to overestimated values of radioactive heat production (e.g., Strutt 1906). From a contemporary perspective (Richter 1986; Harrison 1987), the true resolution of this controversy occurred only recently when the importance of mantle convection and its role in global tectonics was recognized. The discovery of radioactivity did lay the foundation for directly measuring the physical age of rocks based upon the natural occurrence of long-lived radioactive isotopes. The nineteenth century debate regarding Earth's age remains worthy of mention today as traditions begun during that era brought greater clarity to our understanding of Earth history but also a heritage that tends to inhibit important discussions. In terms of the former, Kelvin was arguably the world's first geophysicist as he viewed our planet in much the same fashion as we would any object in our laboratory—as a physical system containing mass and energy that must be conserved (Richter 1986). Thus what we have come to learn about the present physical structure of Earth arguably derives from a culture born in the Victorian era. However, Kelvin was ultimately wrong because his simple physical model could not capture Earth's complexity. The tradition he began of unilaterally applying physics to geologic problems without a clear understanding of the physical system continues to the present (see Sect. 12.1). As we're about to see, the appeal of this approach reflects a challenge our field faces that few others do—the need to understand natural processes over multibillion year timescales. In response, geologists, armed only with a sporadically retained rock record, developed within their culture the capacity of endowing models borrowed from physicists—often unconstrained or in which parameter space had not been adequately explored—with the stature of theory, and, in some cases, eventually treated as fact (e.g., Mars-sized impact origin of Moon; Sect. 3.3). Astronomers of course also share the burden of, well, astronomical timescales but are greatly aided by their ability to directly observe photons whose age can approach that of the known Universe (Bennett et al. 2013) and the fact that stars have simpler physics than colder geologic systems where chemistry, phase changes, and biologic activity become important.

Kelvin has been kept in good company over the subsequent 150 years. The annals of physicists trying to be helpful to geology are replete with distinguished scientists drawing fundamentally incorrect conclusions about Earth's behavior based on poorly constrained calculations alone. Of course science is not about being right all the time but instead about iterating towards truth through open dialogue. In the latter regard, their perspectives have often been problematic. Consider the following firm conclusions:

Earth can be no older than 100 Ma. Thomson (1863): "No hypothesis as to internal fluidity … possessing the smallest vestige of probability, can justify this supposition"; Kelvin (1899): "very sure assumption…certain truth…no other possible alternatives" (also Chamberlin 1899).

Continents are static: Jeffreys (1924). "… best known argument for continental drift is the alleged fit of South America into Africa…coasts could not be brought within 100 s of km of each other without distortion".

The mantle is entirely molten. Gamow (1947): "The temperature of the Earth must reach the melting point…at a depth of only 50 km…all the material farther below must be in a completely molten state".

Seafloor magnetic stripes are not due to geomagnetic field reversal. Heirtzler and Le Pichon (1965): "The patterns of (seafloor magnetic) anomalies is such that we had no basis for including reversed magnetism in our models".

All petroleum is mantle derived: Gold (1987): "The deposits of hydrocarbons in the crust of the Earth (are directly) derived from materials incorporated in the mantle at the time of the Earth's formation".

The common theme amongst these cautionary examples is the certainty with which unexamined assumptions were held and the influence these views enjoyed until overwhelmed by observational evidence. While the repudiation of each of those concepts has the cosmetic appearance of the scientific method at work, it differs in an important way. Our willingness to endow an unconstrained calculation with the status of theory casts alternate, and potentially better, ideas as challengers that need to dislodge the prior model in order to be seen as successful. This inhibits thought and unnecessarily polarizes discussion. While the rock record ultimately permitted these various assertions to be falsified, the Hadean presents a fresh opportunity for mischief principally because *there is no macroscopic rock record*. Surely the role of modeling is to place observations in a physical framework but, as seen in the earlier discussion, our history is rife with calculations carried out in the absence of empirical constraints that, at least temporarily, became scientific dogma. As Box and Draper (1987) famously wrote, "all models are wrong; the practical question is how wrong do they have to be to not be useful". A partial answer to their question is that a model that is fundamentally wrong and provides no immediate basis for its falsification not only lacks utility, but also can be pernicious to the advancement of science.

Physical calculations do, of course, have a role to play in assessing the plausibility of interpretations, but Stevenson (1983) may have said it best. When quantitatively speculating on the nature of the Hadean, he wrote, it is best to view such calculations as "convenient fictions".

2.2 Arithmetic Models

The premise of this chapter is that the time invariance of physical laws permits us to place some limits on the nature of early Earth. Among the least controversial examples of this is the use of Rutherford's (1905) radioactive decay law, given by

$$\frac{D}{P} = e^{\lambda t} - 1 \tag{2.1}$$

where t is time, λ is the decay constant (the fraction of parent decaying to daughter per unit time), D is daughter product and P is parent concentration.[1] Our current estimates of bulk Earth K, Th, and U concentrations of about 200 ppm, 65 ppb, and 16 ppb (Lyubetskaya and Korenaga 2007; Arevalo et al. 2009, 2013), respectively, are probably known to better than a factor of two. When coupled with our knowledge of the heat generation of these three elements, we estimate the current terrestrial heat production due to radioactive decay to be $\sim$20 TW. We can use Eq. 2.1 to extrapolate each radioactive isotope (i.e., $^{238,235}U$, ^{232}Th, ^{40}K) back in time to 4 Ga to estimate their total combined heat production then to be about four times higher than today, and about five times higher at 4.5 Ga (Fig. 2.1). Other, shorter-lived isotopes were either extinct by the time the core formed (e.g., ^{26}Al) or participated only marginally to increasing Hadean heat production (e.g., ^{244}Pu). Coupled with assumptions about initial temperature, calculations using Eq. 2.1 led

[1]It is this equation, rewritten in terms of t, that permits us to calculate an age from knowledge of D/P.

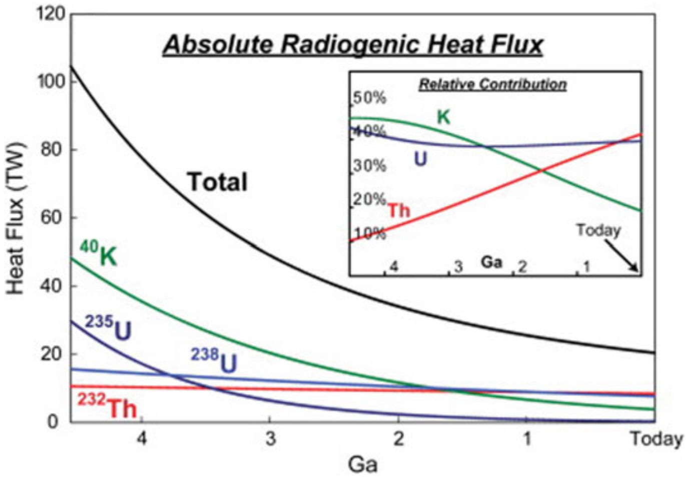

Fig. 2.1 Calculated heat flux from decay of long-lived radioisotopes of U, Th and K through time. Note in the inset that prior to 2.5 Ga, K was the dominant radiogenic heat source. Reproduced with permission from Arevalo et al. (2009)

to estimates of average Hadean heat flow between 200 and 400 mW/m^2 (Smith 1981; Sleep 2000) to ca. 70 mW/m^2 (Korenaga 2006) For comparison, the present global average heat flow is ~80 mW/m^2 (Sclater et al. 1980).

Similar calculations for short-lived nuclides with high decay energies, such as ^{26}Al ($t_{½}$ = 0.7 Ma), suggest that the interiors of even relatively small protoplanets were molten in the early phase of planetary assembly (see Sect. 10.2.8), implying that Earth's building blocks brought great heat along with mass. A simple calculation of the global temperature increase from full separation of rocky and metallic portions of the planet into core and mantle, requiring only knowledge of Earth's radius, gravitational acceleration (uniformly ~10 m/sec^2 from the surface to core-mantle boundary), and the heat capacity of rock, suggests as much as 2000 °C could be added to the planet's average temperature due to the release of gravitational potential energy (Solomon 1979; see Sect. 10.2.9). Alternatively, much of the silicate/metal segregation may have occurred on precursor planetesimals and thus have contributed relatively little to heating proto-Earth (see Sect. 3.2).

The above examples demonstrate how simple calculations came to influence thinking of the early Earth as an exceedingly hot and hostile world. But the real transition from 'cold' (e.g., Urey 1952) to 'hot' (Cameron 1962) accretion models came with a shift in the view from terrestrial planets forming by agglomeration of slow-moving objects (Safronov 1958) to high velocity collisions between planetesimals and planetary embryos (Cameron 1962) (see Sect. 12.1.2).

While the range of early Earth scenarios permitted by these simple calculations is significant, it is finite. Think of these as goal posts for our conversations about early Earth. Taking this approach much beyond this sort of back-of-the-envelope estimate to place limits on Earth's early evolution is tempting but fraught with potential for oversimplification. Had the planet cooled largely by thermal conduction according to Fourier's Law,[2] the linear nature of that heat transport mechanism would permit a high degree of confidence in predicting its entire thermal history (despite Kelvin's cautionary example). But hot Hadean mantle likely behaved as a fluid, engendering sustained thermal (and thus buoyancy) contrasts to drive a highly non-linear convection regime that was chaotic to the point of profound unpredictability (Turcotte 1997).

2.3 Mantle Convection Modelling

The thermal state of a planetary body reflects how much heat was initially present, the efficiency by which its heat is lost to space, the magnitude of internal heat sources, and its age. The rate at which Earth heats or cools reflects the balance between heat sources (H) and sinks (Q),

$$\mathrm{d}T/\mathrm{d}t \propto H - Q \tag{2.2}$$

where T is temperature and t is time. The ratio of H/Q, known at the Urey ratio (γ), gives a snapshot of the thermal state of a planet. While long supposed to today be ~ 0.7 (Turcotte and Schubert 2002), the bulk Earth γ is almost certainly closer to 0.4 (Korenaga 2006). Because the continental crust contains a disproportionate fraction of large ion lithophile elements, including K, Th, and U, the radiogenic heat driving mantle circulation probably corresponds to a convective γ closer to ~ 0.2 (Lyubetskaya and Korenaga 2007; Arevalo et al 2013). Heat added following accretion and core formation (which sets the initial thermal state) can include tidal dissipation (which increases with temperature until the onset of melting, and then decreases rapidly), latent heat from crystallization of the outer core (which began well after core formation and continues today), and heat from intermediate- and long-lived radioisotopes (which decline with time). Planets lose internal heat and cool over time through heat transport processes including; radiation to space from the surface ($\propto T^4$, but modulated by atmosphere opacity), conduction in solids (linear in T), melt extraction to the surface (a strong function of T at and above that of melting), and convection (boundary limited in a fluid; broadly increasing with T). The vigor of mantle convection is characterized by the Rayleigh number, the ratio of thermal and chemical buoyancy to dissipative forces, given by

$$Ra = (g\rho\Delta T\,\alpha\, d^3)/\kappa\mu \tag{2.3}$$

where g is gravity, ρ is density, T is temperature, α is thermal expansion coefficient, d is lengthscale, κ is thermal diffusivity, and μ is viscosity.

[2]heat flux = $-K\ \partial T/\partial x$, where K is thermal conductivity, T is temperature, and x is depth.

The possibility of feedbacks between Eqs. 2.2 and 2.3 long suggested to many (Urey 1955; Schubert et al. 1980; Davies 1980) that Earth's thermal evolution could have proceeded with the two terms on the right hand side of Eq. 2.2, heat sources (H) and heat loss (Q), broadly balanced through time (i.e., in a near equilibrium dynamical state). If planetary heat loss is insufficient to keep up with heat production (i.e., $Q < H$), the increased mantle temperature results in increased buoyancy contrasts (according to Eq. 2.3) that drive more vigorous convection and greater heat loss from the surface. Contrariwise, during periods in which surface heat loss is greater than internal heat production (i.e., $Q > H$), the planet cools, dampening convective vigor and, ultimately, surface heat flux.

As the thermal structure of Earth is only known with confidence today, one approach in mantle convection calculations is to forward model from an assumed initial condition and value of γ using Eq. 2.2 and a relationship for global heat loss given by the Nusselt number (Nu = total heat loss/heat loss due to conduction alone). Thus 'dead' bodies like Moon that lose heat only by conduction have $Nu = 1$. Thermal evolution calculations can be undertaken using a parameterized scheme in which the salient effects of heat transfer are coupled to an energy balance (e.g., Sharpe and Peltier 1978; Davies 1980) or in a spatially specified framework using numerical solutions of equations describing energy and momentum transfer (e.g., Richter and McKenzie 1978). In the latter case, models vary in dimensional coverage (2D versus 3D) and can involve many dozens of free parameters. To make computationally challenging models feasible, many are run without consideration of effects such as phase changes (Nakagawa and Tackley 2004), depth dependent thermal expansivity (Hansen et al. 1993), compressible convection (Dubuffet et al. 1999), or a realistic representation of the mixture of basal and internal heating (see Korenaga 2017). The challenge to the modeler is to understand which of these multiple parameters exerts first order control over the physical system under study, permitting computational simplification, without unduly influencing the outcome of the simulation.

Given the then relatively primitive computational capability, early numerical models of mantle convection were necessarily oversimplified, assuming, for example, isoviscosity in a 2D box. Results of such calculations were not easily reconciled with fluid dynamics experiments (e.g., Richter and McKenzie 1978). Due to what appears to be a protracted misunderstanding between the geochemical and geodynamical communities, modelers appear to have accepted that isotopic data from mantle-derived samples were strong evidence of two-layer mantle convection (DePaolo 1981) and thus emphasized convection confined to discrete layers. For example, Richter and McKenzie (1981) showed that a double thermal boundary layer, capable of supporting the large thermal contrast needed to maintain discrete layers, could occur at the interface between isoviscous layers at ca. 700 km depth. Geochemists in turn viewed the modelling results as support for their speculation that the 660 km mantle discontinuity separated previously melt depleted upper mantle from the region below, assumed to contain both juvenile and enriched materials.

However, the scaling between global heat loss (i.e., the *Nu* number) and the vigor of mantle convection (i.e., characterized by *Ra*) predicted from isoviscous calculations is quite different from those permitting non-linear responses, such as temperature dependent rheologies (Lenardic and Kaula 1993; Solomatov 1995). As computational power increased, the limitations of earlier models became clear to geodynamicists but information transfer to the geochemical community lagged. Three distinct convective regimes could now be discerned from numerical experiments: (1) one involving small viscosity contrasts, resembling results from isoviscous calculations, (2) a transitional regime controlled by the cold boundary layer, and (3) an asymptotic regime in which the cold boundary becomes stagnant and convection involves only the hottest part of the lid determined by a rheological temperature scale (Solomatov 1995). This latter regime is similar to the strongly temperature-dependent viscosity convection with rigid boundaries available to laboratory experiments. In particular, *Nu* scaling in a non-linear system is far different than that assuming convection in an isoviscous medium. For example, dissimilar viscosity contrasts between approaches can lead to very different physical inferences. This is especially true when considering early Earth due to the expected higher mantle temperatures, and thus higher *Ra* and viscosity contrasts. Consider as an example how limitations of the earlier generations of models came to long influence geologic thought.

2.4 Early Computational Limitations

Prior to the widespread use of numerical calculations capable of simulating large viscosity contrasts, models were run assuming constant mantle temperature (e.g., Christensen 1985; Davies 2002). Achieving *Ra* greater than $\sim 10^6$ was technically challenging then because the large attendant viscosity contrasts led to numerical instabilities. Limited to $Ra << 10^6$, Davies (2002) attempted to indirectly account for the higher temperature of the mantle in the past by running extended models with simulated times greater than the age of Earth. For conditions appropriate to the present mantle potential temperature, he arrived at a duration of 18 Ga by assuming that the rate of mantle convection scales according to the square of the global radioactive heat production (four to five times higher during the Hadean than present day). That is, he assumed that 18 Ga of model time would achieve the total number of mantle overturns that occurred since planet formation at 4.5 Ga. After 18 Ga of simulated convection, Davies (2002) models resulted in a highly heterogeneous mantle as subducted material, although highly attenuated, remained largely intact in the upper mantle.

A consequence of a having a relatively primitive (i.e., melt undepleted) upper mantle early in Earth history when the mantle was hotter, is that oceanic crust forming at mid-ocean ridges would have been very thick ($\sim$30 km) due to the deeper initiation and higher degrees of melting (McKenzie and Bickle 1988). This thicker lithosphere would require significantly greater time to cool to become neutrally buoyant, and thus subductable. As already noted, it was widely assumed that a hotter mantle would have convected faster and thus the average age of oceanic plates at subduction would have been less than the presently observed ca. 100 Ma. In a paper entitled "On the emergence of plate tectonics", Davies (1992) estimated that the crossover between these two regimes would have occurred between 0.9 and 1.4 Ga ago when the mantle was about 50 °C hotter than at present. He concluded that plate tectonics could not have accomplished the necessary rate of heat removal and was unlikely to have operated on early Earth. Another mechanism, such as sagduction or subcrustal delamination, was thought to be a more likely geodynamic regime (Davies 1992). This well-cited study was influential in convincing many Precambrian geologists that mobile lid tectonics was not viable on early Earth.

The inference that differences in $^{142}Nd/^{144}Nd$ between Earth and chondrites (Boyet and Carlson 2006) reflect an early mantle depletion event (subsequently superseded by recognition that Earth did not assemble from any of the know chondrite groups; see Sect. 3.1) motivated Davies (2006) to revisit this issue. When the above calculations were repeated using a numerical scheme capable of directly simulating high temperatures (1550 °C) and corresponding Ra ($>10^6$), a quite different result was found. The much lower upper mantle viscosities resulted in the rapid gravitational settling of subducted mafic crust creating a strongly melt depleted upper mantle and a dense, enriched layer forming at the base of the lower mantle. Melting of this strongly depleted upper mantle in turn yields ca. 5 km thick ocean crust. Crust that thin can become neutrally buoyant within only ten to twenty million years. Despite the high mantle temperature, Davies (2006) concluded that early mobile lid behavior (i.e., plate tectonics) was more attractive than previously thought. Indeed, the possibility of Archean (Hynes 2013) or Hadean subduction subsequently became part of mainstream thought (e.g., Korenega 2011; Sleep et al. 2014).

2.5 Transitions in Modes of Convection

Earth appears to be cooling ~100°C/Ga (e.g., Bedini et al. 2004; Herzberg et al. 2010) and is currently losing about 42 TW of heat (Sclater et al. 1980). Secular cooling is important and maybe essential for habitability for it drives the geodynamo which generates the geomagnetic shield. Among other qualities, the geomagnetic field prevents surface water from being lost to space (see Sect. 10.2.9). A Urey ratio of 0.35 (see Sect. 2.3; Korenaga 2006) implies that Earth is today losing heat about three times faster than it is being supplied. Such an imbalance cannot be sustained indefinitely and might, at first glance, appear to support the late initiation of plate tectonics. But the numerator in the Urey ratio is largely defined by radioactive heat generation which was about five times higher in the early Hadean than at present (see Sect. 2.2).

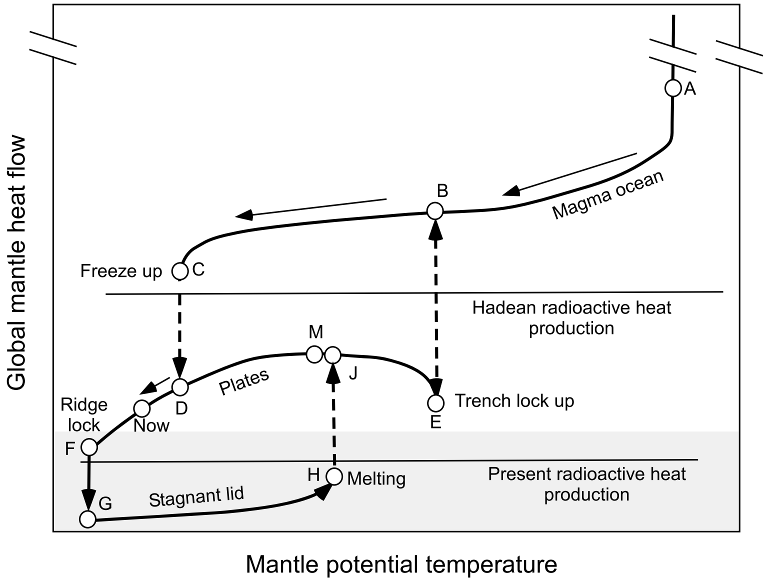

Fig. 2.2 Schematic diagram of global heat flow vs. mantle potential temperature showing three possible branches: magma ocean, plates and stagnant-lid convection. Magma ocean and plate regimes occur early in Earth history but only plates occur after the system evolves to between points D and M when radioactive heat production was less than M. A jump to stagnant-lid convection will occur in the future (shown as shaded region). Modified with permission from Sleep (2000)

Earth may have cooled continuously from formation but it is also possible that it has lurched through discontinuous transitions from very efficient cooling via melt extraction (i.e., a "heat pipe" that brings deep interior magmas directly to the surface as volcanism; Solomatov 2007; Moore and Webb 2013) to slow (conductive) cooling through a stagnant lid[3] (e.g., Venus; Gerya 2014) to the present-day mobile lid regime (i.e., plate tectonics; Forsyth and Uyeda 1975). Assuming a long-term balance between heat generation and surface heat loss, Sleep (2000) introduced a phenomenological model of plate tectonics in which globally averaged heat flow scales as the inverse of the square root of the mean age of oceanic crust at subduction (Fig. 2.2). Sleep (2000) then examined the circumstances in which global potential temperature would favor mobile lid tectonics relative to either stagnant lid convection or a magma ocean. He identified two transitions: (1) "ridge lock", when the mantle adiabat no longer intersects melting at shallow depths beneath ridges leading the cessation of plate generation and a stagnant lid regime (point F in Fig. 2.2), and (2) "trench lock", that occurs when mobile lid tectonics can no longer release all the heat produced by radioactivity resulting in planetary

[3]Stagnant lid tectonics arises on a convecting planet with an unbroken lithosphere. Since planetary heat can only be lost by conduction through the 'lid', the interior warms.

warming and, eventually, a magma ocean regime (point E in Fig. 2.2). Sleep (2000) showed qualitatively how these transitions would be expected to occur as a function of global heat flow and mantle potential temperature for both continuous and discontinuous transitions. An implication is that a very thermally energetic early Earth could have cycled between plate tectonic and magma ocean regimes multiple times (e.g., internal heating due to trench lock at point E could be sufficient to reform a magma ocean).

Korenaga's (2006) principal argument is that the mantle is not a simple fluid and may therefore require a very different scaling than that traditionally used. An earlier, hotter mantle would begin melting at greater depths than today with higher melt fractions resulting in thicker oceanic crust at spreading centers (McKenzie and Bickle 1988). Those hygroscopic melts would significantly dry out the upper mantle greatly altering its viscosity structure and creating stiffer lithospheric plates. This would produce slower plate velocities than today (Fig. 2.5), despite the hotter mantle, retarding global heat loss (Q) and thus causing mantle heating, potentially, creating a magma ocean.

2.6 Non-traditional Scaling

To this point, our discussion of geodynamic modelling has considered only a single relationship between global heat loss and convective vigor. Classically, it has been assumed that

$$Nu = Ra^{\beta} \tag{2.4}$$

where β is typically between 0.15 and 0.3 (e.g., Christensen and Hofmann 1994). This relationship implies that as the mantle gets hotter, convective vigor increases which has the effect of lowering Earth's interior temperature and thus slowing fluid motion (Fig. 2.3). This model, however, presupposes that the convective vigor of the mantle is a simple function of its temperature and that heat loss is broadly equivalent to its generation.

Assuming that β is a positive number provides a stabilizing feedback between mantle temperature, convective vigor, and global heat loss. If planetary refrigeration becomes less than internally generated heat, Eq. 2.2 becomes positive and the interior warms.[4] This, from Eq. 2.3, results in a higher Ra, greater convective vigor, and increased heat loss thus causing the planet to cool. Korenaga (2003, 2006) pointed out that this negative feedback in forward models reverses in a backward integration leading to a 'thermal catastrophe' at ~1.5 Ga (Fig. 2.4) in which temperature asymptotically tends toward infinity (i.e., a hotter earlier mantle must have lost heat faster requiring increasingly higher prior temperatures). Figure 2.4

[4]Although an unorthodox view now, the idea that Earth's interior has warmed was relatively popular in the first half of the twentieth century (e.g., Bowen 1928; Slichter 1941).

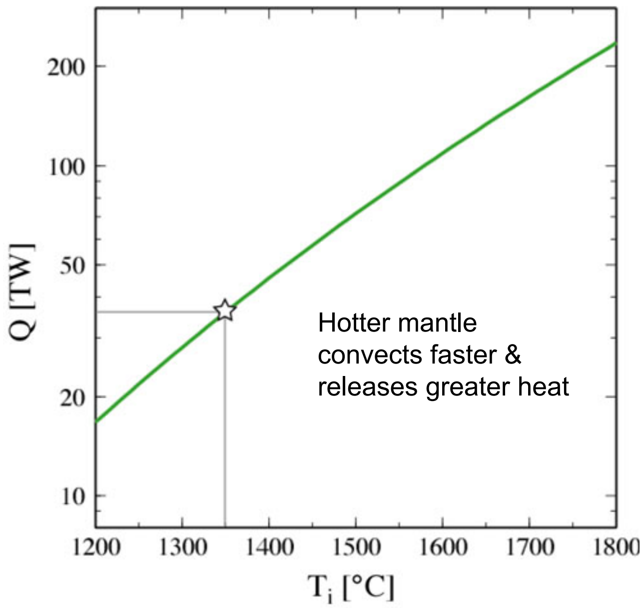

Fig. 2.3 Conventional parameterization of heat flux based on *Nu-Ra* scaling (Eq. 2.4) with $\beta = 0.15$ (assuming mantle rheology with activation energy = E = 300 kJ/mol). The star notes present mantle conditions. Reproduced with permission from Korenaga (2006)

Fig. 2.4 Thermal evolution modeling with conventional *Nu-Ra* scaling. Two present day Urey ratios (γ = H(0)/Q(0)) are shown: 0.15 inferred from petrological constraints (red) and 0.72 from Turcotte and Schubert (2002). Note that the higher the value of γ the further back in time the thermal catastrophe is shifted. Modified with permission from Korenaga (2006)

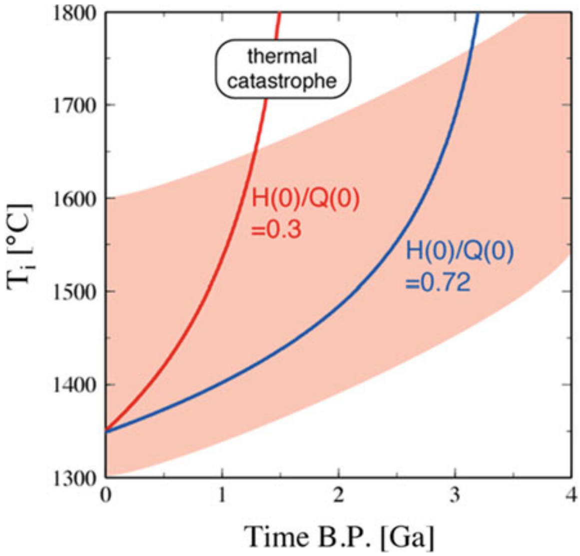

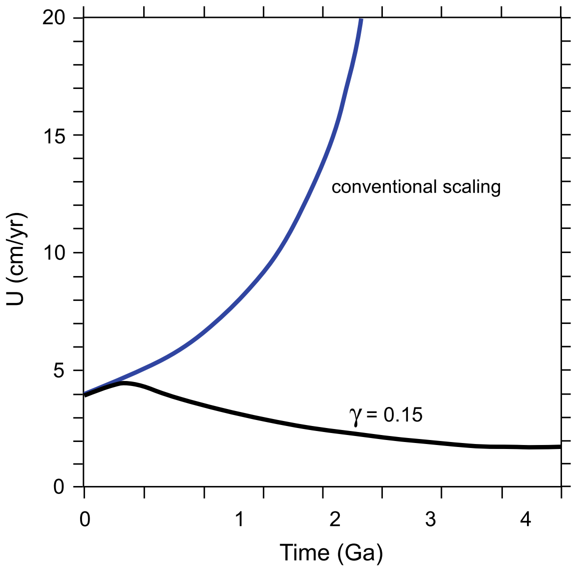

Fig. 2.5 Predicted plate velocity from a thermal evolution model using present day Urey ratio (γ) of 0.15 (black line). The blue line shows the result for a Urey ratio of 0.72 leading to a thermal catastrophe at ca. 2.5 Ga. Contrary to conventional parameterizations, Korenaga's (2006) model predicts lower plate velocities on early Earth relative to today. Modified with permission from Korenaga (2006)

shows the relationship between Urey ratio (γ) and onset of the thermal catastrophe. This in itself does not prove the conventional scaling wrong (but partially explains the interest of modelers in a high γ, which has the effect of pushing the thermal catastrophe back further in time). After all, time cannot run backwards. But it does illustrate how the conventional scaling limited thinking about possible solutions for global thermal evolution (Fig. 2.5).

Korenaga's (2003, 2006) model runs contrary to the traditional view that high mantle temperatures extant in early Earth would result in such thick (>30 km), fast-spreading oceanic lithosphere as to preclude it attaining the neutral buoyancy required for subduction (McKenzie and Bickle 1988; Davies 1992). Thus Hadean plate-tectonic-like behavior has historically been viewed as unlikely (e.g., Davies 1992). If, as Korenaga (2006) argues, Earth's surface heat flux was decoupled from internal heat production early in Earth history, mobile lid tectonics may have been heating and then cooling Earth independent of its overall, steadily decreasing heat production. Note that this last point stands in contrast to a longstanding assumption (e.g., Urey 1955) in many parameterized thermal models that Earth evolution proceeds with the two terms on the right hand side of Eq. 2.2, heat sources (H) and heat loss (Q), broadly balanced through time (i.e., in a quasi-equilibrium dynamical state). Indeed, Korenaga's (2006) plate tectonic model specifically precludes the possibility of a quasi-equilibrium dynamical evolution.

2.7 Can Plate Tectonics Exist Outside a State of Dynamic Thermal Equilibrium?

To further complicate an already complex picture, Weller and Lenardic (2012) showed that multiple tectonic regimes are possible for the same conditions of lithospheric strength and convective vigor. They found that as lithospheric yield stress increases in the mobile lid mode, an "episodic lid" regime occurs in which rapid pulses of lithospheric overturn are interspersed with periods of quiescence. Further increases in yield stress eventually overcome the internal driving stresses that break the lithosphere into plates leading to a stagnant lid. Moreover, when Weller and Lenardic (2012) performed simulations using an identical viscosity contrast between mantle and lithosphere, they found contrasting tectonic mode transitions depending on whether yield strength was increasing or decreasing. Although the transition from mobile to stagnant lid occurs over a relatively limited window of yield stress, regardless of the direction from which it is approached, much longer periods of episodic behavior occur when transitioning from high to low yield stress. They likened these divergent paths between increasing versus decreasing yield stress states, in which multiple tectono-convective regimes can exist at equivalent parameter values, as a hysteresis gap and termed it the Tectono-Convective Transition Window (TCTW). Restated, where multiple solutions exist, the global tectonic mode is pathway dependent and thus predicting its behavior requires knowledge of the dynamic pre-history of a planet.

Moore and Lenardic (2015) further explored this approach and found that if, as Korenaga (2006) suggested, planetary heat loss via mobile lid tectonics becomes less efficient at higher mantle temperatures, its failure to sustain quasi-equilibrium causes it to quickly evolve away from plate tectonic behavior. In this scenario, the planet would dwell longer in heat pipe mode resulting in a continuously lower Urey ratio (Fig. 2.6). The stability of these equilibria is determined by the relative slopes of the heat production and heat transport curves. When the slope of the heat transport is greater than the slope of the heat production, then slight perturbations from equilibrium cause the system to return to the stable mode (Tozer 1965). Conversely, when the slope of the heat transport is less than the slope of the heat production (either more negative or simply less positive), small perturbations grow, driving the system away from the unstable equilibrium (Fig. 2.6). These conclusions are based solely on the structure of the equilibria in a system with less efficient plate tectonics in the past and are independent of the mechanisms leading to this behavior.

One element missing from the Moore and Lenardic (2015) scenario is consideration of the lag time between a decrease in internal heating and its expression as reduced heat flow at the surface. This timescale has long been thought to be sufficiently short (i.e., ca. 200 Ma; Tozer 1972) to be approximated as quasi-equilibrium. Korenaga (2016, 2017) explicitly considered the time scale necessary for this feedback and found that when the effect of mantle melting on viscosity is accounted for, the adjustment timescale (he called the Tozer number) is too long to permit any style of mantle convection to self-regulate. This analysis supports the view that

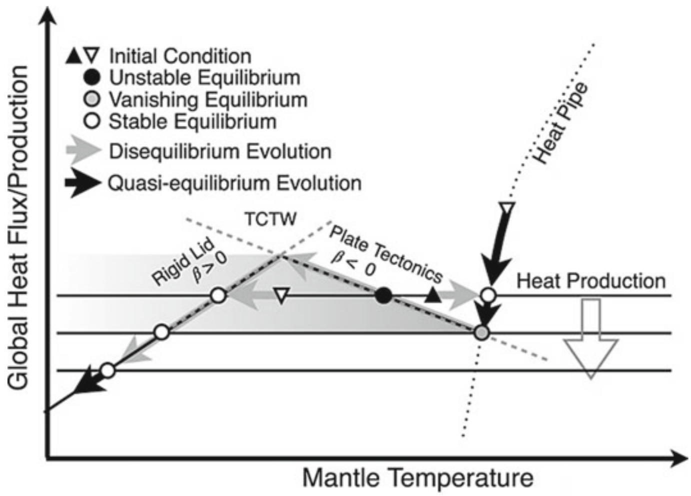

Fig. 2.6 Sketch of planetary heat flow and heat production in three heat flow regimes versus T (heat transport in rigid lid, β > 0, solid-dashed; plate tectonics, β > 0, solid-dashed; heat pipe, dotted). Radioactive heating is shown by horizontal lines with outlined arrows showing secular evolution. Metastable branches are shown in the TCTW (grey dashed). Stable equilibria are indicated by the circles, and initial conditions by triangles. Quasi-equilibrium evolution follows the black arrow. Reproduced with permission from Moore and Lenardic (2015)

Earth's mantle is likely to have evolved far from thermal equilibrium (e.g., Herzberg et al. 2010) with the result that its history would be sensitive to initial conditions and thus non-invertible (i.e., not yielding to a unique solution) via geodynamic models.

2.8 Critical Summary

The models discussed above are generally more attractive to physicists than to geo- or planetary scientists because none of them can ab initio predict the variations in convective and tectonics style in any of the four active silicate bodies that we know of (Earth, Venus Mars, Io). While the computational power available today to simulate mantle evolution is at least a million times greater[5] than what Richter and McKenzie (1978) then had available, we should resist the temptation to infer that our confidence in model predictions should be proportionately greater. That would be to mistake computational sophistication for enhanced accuracy of prediction. There are at least three reasons, drawn from the discussion above, why such models may never be capable of ab initio reconstruction of early Earth environments.

[5]https://en.wikipedia.org/wiki/Moore%27s_law.

Mantle convection, a highly non-linear, dispersive, chaotic system (Stewart and Turcotte 1989), is, by its very nature, uninvertible in the same way that the butterfly effect precludes using today's weather pattern to reconstruct last century's climate (Turcotte 1997). Weller and Lenardic's (2012) recognition that global tectonic mode is pathway dependent (i.e., multiple solutions exist simultaneously for the same equations) underscores the requirement of independent, pre-knowledge of the dynamic history of a planet as a prerequisite to accurate forward modelling. Lastly, even if the fundamental nature of the physics didn't preclude predicting early Earth evolution, the multitude of unknown parameter values and boundary conditions surely would (Korenaga 2017).

So, what is the utility of mantle convection modelling for understanding early Earth? Numerical models can be useful in exploring the effect that parameter variation has on a system (i.e., sensitivity analysis), but their primary value is heuristic. Models are only representations, useful for guiding further study but not susceptible to proof (Oreskes et al. 1994).

Then what's the path forward? Because mantle convection is chaotic (Turcotte 1997), one approach is to investigate the landscape of possible solutions (or attractors). How many stable states exist? How distinct are they? How noisy is a system? Do backward integrations of negative β values amplify or dampen noise greater or less than positive values? By understanding the fundamental nature of the system, limits to the range of possible thermal histories might be established. Another way forward is comparative planetology. Astronomers have come to understand complex stellar systems by imaging hundreds of thousands of stars and translating those observations into highly refined behavioral models (e.g., the Hertzsprung–Russell relationship). Although relatively few, other solar system bodies provide examples of stagnant lid (Venus), heat pipe (Io), and conduction-limited (Moon) tectonics for study that could help constrain the range of dynamic solutions.

Alternatively, with the provisos just discussed, forward modelling can investigate tectonic speculations under highly specified conditions (e.g., Sizova et al. 2015). As previously noted, it is best to build up complex models one step at a time, first understanding what each component does. The danger here, similar to that discussed in Sect. 2.4, is that while geodynamic modelers surely understand the limitations of their calculations, the geologist as consumer of models may not. The allure of forward modelling results to geologists was driven home to me during a 2016 field workshop on early Earth tectonics in the Barberton belt of southern Africa. Following a summary of the key conclusions from the Workshop on the Origin and Evolution of Plate Tectonics (Stern et al. 2017), held two months earlier in Ascona, Switzerland, which included quoting Slava Solomatov's statement that convection models are by their nature incapable of ab initio planetary thermal history reconstruction, an animation of a recent crust-mantle model was then shown. Audience members, including noted figures in Precambrian geology, asked (amid satisfied murmurs) that the animation be replayed in slow motion so that the elapsed time between onset of sagduction and generation of dacitic melt could be jotted down for future reference. While models like that of Sizova et al. (2015) are at the cutting edge of sophistication and could provide ground truth for the physical plausibility of their proposed mechanisms, they are at best "convenient fictions" (Stevenson 1983). In the absence of observational constraints, they have no inherent predictive value regarding the history of our planet.

References

Arevalo, R., McDonough, W. F., & Luong, M. (2009). The K/U ratio of the silicate Earth: Insights into mantle composition, structure and thermal evolution. *Earth and Planetary Science Letters, 278,* 361–369.

Arevalo, R., McDonough, W. F., Stracke, A., Willbold, M., Ireland, T. J., & Walker, R. J. (2013). Simplified mantle architecture and distribution of radiogenic power. *Geochemistry, Geophysics, Geosystems, 14,* 2265–2285.

Becquerel, H. (1896). On the rays emitted by phosphorescence. *Compt. Rend. Hebd. Seances Acad. Sci., 122,* 420–421.

Bedini, R. M., Blichert-Toft, J., Boyet, M., & Albarède, F. (2004). Isotopic constraints on the cooling of the continental lithosphere. *Earth and Planetary Science Letters, 223,* 99–111.

Bennett, C. L., Larson, D., Weiland, J. L., Jarosik, N., Hinshaw, G., Odegard, N., et al. (2013). Nine-year Wilkinson Microwave Anisotropy Probe (WMAP) observations: final maps and results. *The Astrophysical Journal Supplement Series, 208*(20), 1–54.

Bowen, N. L. (1928). *Evolution of igneous rocks.* Princeton University Press.

Box, G. E., & Draper, N. R. (1987). *Empirical model-building and response surfaces*. Wiley.

Boyet, M., & Carlson, R. W. (2006). A new geochemical model for the Earth's mantle inferred from ^{146}Sm-^{142}Nd systematics. *Earth and Planetary Science Letters, 250,* 254–268.

Burchfield, J. D. (1975). *Lord Kelvin and the age of the Earth*. London: Macmillan.

Cameron, A. G. W. (1962). The formation of the sun and planets. *Icarus, 1,* 13–69.

Chamberlin, T. C. (1899). Lord Kelvin's address on the age of the earth as an abode fitted for life. *Science, 9,* 889–901.

Christensen, U. R. (1985). Thermal evolution models for the Earth. *Journal of Geophysical Research, 90,* 2995–3007.

Christensen, U. R., & Hofmann, A. W. (1994). Segregation of subducted oceanic crust in the convecting mantle. *Journal of Geophysical Research, 99,* 19867–19884.

Cloud, J. (1818). An attempt to ascertain the fusing temperature of metals. *Transactions of the American Philosophical Society, 1,* 167–169.

Davies, G. F. (1980). Thermal histories of convective Earth models and constraints on radiogenic heat production in the Earth. *Journal of Geophysical Research: Solid Earth, 85,* 2517–2530.

Davies, G. F. (1992). On the emergence of plate tectonics. *Geology, 20,* 963–966.

Davies, G. F. (2002). Stirring geochemistry in mantle convection models with stiff plates and slabs. *Geochimica et Cosmochimica Acta, 66,* 3125–3142.

Davies, G. F. (2006). Gravitational depletion of the early Earth's upper mantle and the viability of early plate tectonics. *Earth and Planetary Science Letters, 243,* 376–382.

DePaolo, D. J. (1981). Nd isotopic studies: Some new perspectives on Earth structure and evolution. *Eos, Transactions American Geophysical Union, 62*, 137–137.

de Buffon, G. L. L. "Count". (1778). *Histoire Naturelle, Générale et Particulière. Supplément, Tome Cinquième*. L'Imprimerie Royale, Paris, pp. 615 + 8 + 23.

Dubuffet, F., Yuen, D. A., & Rabinowicz, M. (1999). Effects of a realistic mantle thermal conductivity on patterns of 3-D convection. *Earth and Planetary Science Letters, 171,* 401–409.

Forsyth, D., & Uyeda, W. S. (1975). On the relative importance of the driving forces of plate motion. *Geophysical Journal of the Royal Astronomical Society, 4,* 163–200.

Fourier, J. B. J. (1820). Extrait d'un mémoire sur le refroidissement séculaire du globe terrestre. *Bulletin des Sciences par la Société Philomathique de Paris, Ser., 3,* 58–70.

Gamow, G. (1947). *One Two Three Infinity: Facts and Speculations of Science*. Courier Corporation.

Gerya, T. V. (2014). Plume-induced crustal convection: 3D thermomechanical model and implications for the origin of novae and coronae on Venus. *Earth and Planetary Science Letters, 391,* 183–192.

Gold, T. (1987) *Power From the Earth: Deep Earth Gas—Energy for the Future*, London, Dent and Sons.

Hansen, U., Yuen, D. A., Kroening, S. E., & Larsen, T. B. (1993). Dynamical consequences of depth-dependent thermal expansivity and viscosity on mantle circulations and thermal structure. *Physics of the Earth and Planetary Interiors, 77,* 205–223.

Harrison, T. M. (1987). Comment on "Kelvin and the age of the earth". *Journal of Geology, 95,* 725–727.

Heaviside, O. (1899). *Electromagnetic theory* (Vol. II). New York: Van Nostrand.

Heirtzler, J. R., & Le Pichon, X. (1965). Crustal structure of the mid-ocean ridges: 3. Magnetic anomalies over the mid-Atlantic ridge. *Journal of Geophysical Research, 70,* 4013–4033.

Herzberg, C., Condie, K., & Korenaga, J. (2010). Thermal history of the Earth and its petrological expression. *Earth and Planetary Science Letters, 292,* 79–88.

Hynes, A. (2013). How feasible was subduction in the Archean? *Canadian Journal of Earth Sciences, 51,* 286–296.

Jeffreys, H. (1924). *The Earth. Its origin, history and physical constitution*. Cambridge University Press.

Kelvin. (1899). The age of the earth as an abode fitted for life. *Science, 9*, 665–674 and 704–711.

Korenaga, J. (2003). Energetics of mantle convection and the fate of fossil heat. *Geophysical Reseach Letters, 30,* 1437.

Korenaga, J. (2006). Archean geodynamics and the thermal evolution of Earth. In K. Benn, J. -C. Mareschal, & K. Condie (Eds.) *Archean Geodynamics and Environments* (vol. 164, pp. 7–32). AGU Geophysical Monograph Series.

Korenaga, J. (2011). Thermal evolution with a hydrating mantle and the initiation of plate tectonics in the early Earth. *Journal of Geophysical Research, 116,* B12403.

Korenaga, J. (2016). Can mantle convection be self-regulated? *Science Advances*, *2*(8), e1601168.

Korenaga, J. (2017). Pitfalls in modeling mantle convection with internal heat production. *Journal of Geophysical Research: Solid Earth,* 4064–4080. https://doi.org/10.1002/2016jb013850.

Lenardic, A., & Kaula, W. M. (1993). A numerical treatment of geodynamic viscous flow problems involving the advection of material interfaces. *Journal of Geophysical Research: Solid Earth*, *98,* 8243–8260.

Lyubetskaya, T., & Korenaga, J. (2007). Chemical composition of Earth's primitive mantle and its variance: 1 Method and results. *Journal of Geophysical Research, 112,* B03211. https://doi.org/10.1029/2005JB004223.

McKenzie, D., & Bickle, M. J. (1988). The volume and composition of melt generated by extension of the lithosphere. *Journal of Petrology, 29,* 625–679.

Moore, W. B., & Lenardic, A. (2015). The efficiency of plate tectonics and nonequilibrium dynamical evolution of planetary mantles. *Geophysical Research Letters, 42,* 9255–9260.

Moore, W. B., & Webb, A. A. G. (2013). Heat-pipe Earth. *Nature, 501,* 501–505.

Nakagawa, T., & Tackley, P. J. (2004). Effects of a perovskite–postperovskite phase change near core-mantle boundary in compressible mantle convection. *Geophysical Research Letters, 31,* L16611. https://doi.org/10.1029/2004GL020648.

Oreskes, N., Shrader-Frechette, K., & Belitz, K. (1994). Verification, validation, and confirmation of numerical models in the Earth sciences. *Science, 263,* 641–646.

Perry, J. (1895a). On the age of the earth. *Nature, 51,* 224–227.

Perry, J. (1895b). On the age of the earth. *Nature, 51,* 341–342.

Perry, J. (1895c). The age of the earth. *Nature, 51,* 582–585.
Richter, F. M. (1986). Kelvin and the age of the earth. *Journal of Geology, 94,* 395–401.
Richter, F. M., & McKenzie, D. P. (1978). Simple plate models of mantle convection. *Journal of Geophysics, 44,* 441–471.
Richter, F. M., & McKenzie, D. P. (1981) On some consequences and possible causes of layered mantle convection. *Journal of Geophysical Research: Solid Earth, 86*, 6133–6142.
Rutherford, E. (1905). *Radio-activity* (p. 580). Cambridge University Press.
Safronov, V. S. (1958). On the growth of terrestrial planets. Vopr. Kosmog., Akad. Nauk S.S.S.R. *6*, 63–77.
Schubert, G., Stevenson, D., & Cassen, P. (1980). Whole planet cooling and the radiogenic heat source contents of the Earth and Moon. *Journal of Geophysical Research, 85,* 2531–2538.
Sclater, J., Jaupart, C., & Galson, D. (1980). The heat flow through oceanic and continental crust and the heat loss of the Earth. *Reviews of Geophysics, 18,* 269–311.
Sharpe, H. N., & Peltier, W. R. (1978). Parameterized mantle convection and the Earth's thermal history. *Geophysical Research Letters, 5,* 737–740.
Sizova, E., Gerya, T., Stüwe, K., & Brown, M. (2015). Generation of felsic crust in the Archean: a geodynamic modeling perspective. *Precambrian Research, 271,* 198–224.
Sleep, N. H. (2000). Evolution of the mode of convection within terrestrial planets. *Journal of Geophysical Research, 105,* 17563–17578.
Sleep, N. H., Zahnle, K. J., & Lupu, R. E. (2014). Terrestrial aftermath of the Moon-forming impact. *Philosophical Transactions of the Royal Society A, 372,* 20130172.
Slichter, L. B. (1941). Cooling of the Earth. *Bulletin of the Geological Society of America, 52,* 561–600.
Smith, J. V. (1981). The first 800 million years of earths history. *Philosophical Transactions of the Royal Society London Ser. A* 301, 401–422.
Solomatov, V. S. (1995). Scaling of temperature-and stress-dependent viscosity convection. *Physics of Fluids, 7,* 266–274.
Solomatov, V. S. (2007). Magma oceans and primordial mantle differentiation. In G. Schubert (Ed.), *Treatise on Geophysics 9* (pp. 91–120). Oxford: Elsevier.
Solomon, S. C. (1979). Formation, history and energetics of cores in the terrestrial planets. *Physics of the Earth and Planetary Interiors, 19,* 168–182.
Stern, R. J., Gerya, T., & Tackley, P. J. (2017). Tackling unanswered questions on what shapes Earth. Eos 98. https://doi.org/10.1029/2017EO065791.
Stevenson, D. J. (1983). The nature of the earth prior to the oldest known rock record-The Hadean earth. *Earth's earliest biosphere: Its origin and evolution* (pp. 32–40). Princeton, NJ: Princeton University Press.
Stewart, C. A., & Turcotte, D. L. (1989). The route to chaos in thermal convection at infinite Prandtl number: 1. Some trajectories and bifurcations. *Journal of Geophysical Research: Solid Earth, 94,* 13707–13717.
Strutt, R. J. (1906). On the distribution of radium in the earth's crust and on the earth's internal heat. *Proceedings of the Royal Society of London. Series A, Containing Papers of a Mathematical and Physical Character, 77A,* 472–485.
Thomson, W. (1863). On the secular cooling of the earth. *Philosophical Magazine Series, 4*(25), 1–14.
Tozer, D. C. (1965). Heat transfer and convection currents. *Philosophical Transactions of the Royal Society A, 258,* 252–271.
Tozer, D. C. (1972). The present thermal state of the terrestrial planets. *Physics of the Earth and Planetary Interiors, 6,* 182–197.

Turcotte, D. L. (1997). *Fractals and Chaos in Geology and Geophysics* (p. 412). Cambridge University Press.

Turcotte, D. L., & Schubert, G. (2002). *Geodynamics: applications of continuum physics to geological problems* (2nd Edn.). New York, NY: Wiley.

Urey, H. C. (1952). *The planets: their origin and development* (p. 245). New Haven: Yale University Press.

Urey, H. C. (1955). The cosmic abundances of potassium, uranium, and thorium and the heat balances of the Earth, the Moon, and Mars. *Proceedings of the National Academy of Sciences of the United States of America, 41,* 127–144.

Weller, M. B., & Lenardic, A. (2012). Hysteresis in mantle convection: plate tectonics systems. *Geophysical Research Letters, 39*(L10202), 1–5.

3 Radionuclide Produced Isotopic Variations in Mantle Rocks

Abstract

Evidence from short- and long-lived radioisotope systems indicates that Earth was largely built from volatile-depleted planetesimals and planetary embryos during runaway accretion that occurred within 1–10 Ma of formation of the first solar system solids at 4.567 ± 0.001 Ga. Both long- and short-lived radionuclides leave isotopic signatures in mantle rocks that bear on when and how the silicate Earth formed and differentiated. The longstanding view that the Hadean mantle was compositionally undepleted appeared to be contradicted by differences between mantle and chondrite Nd isotopes which suggested a very early enriched terrestrial reservoir. Although recent work indicates this difference reflects differing irradiation histories of Earth-forming-materials and meteorites, and thus has little bearing on the timing of silicate differentiation, both terrestrial and lunar Lu–Hf zircon data appear to require global silicate differentiation by 4.50 ± 0.02 Ga billion years. Tungsten isotopic data from mantle rocks provides evidence of core formation by about 4.53 Ga and either very early isotopic isolation of silicate reservoirs or disturbance by a late chondritic veneer. Despite evidence that Moon formed substantially from proto-Earth material between about 4.53 and 4.50 Ga, the exact mechanism by which this occurred remains controversial. The once widely accepted model of collision of a Mars-sized body has lost support in light of contradictory evidence in the form of indistinguishable isotopic compositions of volatile and refractory elements between Earth and Moon. Models that appear to transcend this problem (hit-and-run collision, synestia, successive smaller collisions, magma ocean heating, etc.) are currently being evaluated. Although geochemical evidence requiring an early terrestrial magma ocean is almost entirely lacking, the sources of thermal energy available during accretion make such an appearance appear inevitable. If solidification proceeded from the bottom up, vigorous convection would have caused the lower mantle to rapidly crystallize with the upper mantle becoming largely solidified within several million years. The high abundance of highly siderophile elements in the upper mantle is strong evidence that Earth

T. M. Harrison, *Hadean Earth*, https://doi.org/10.1007/978-3-030-46687-9_3

added at least half a percent of its present mass following core formation but prior to the Mesoarchean. Preservation of mantle isotopic anomalies throughout the Hadean-Archean seem unlikely to reflect sluggish mantle convention in a stagnant lid tectonic regime during that period as the plate tectonic era is associated with a large range of isolated mantle isotopic domains.

3.1 Isotopes in the Early Solar System

As the nebular cloud began to gravitationally contract onto the midplane, dust condensates from the gas randomly collided with one another, either fragmenting or attaching. In the latter case, these two-body collisions created progressively larger objects. Some of the kinetic energy involved during these interactions was manifested as heat that could be trapped within growing planetesimals. Once these bodies reached about a kilometer in size they could begin to gravitationally attract each other leading to Moon-sized objects and, eventually, runaway planet formation (Chambers 2004). Observations of young stellar systems show that most protoplanetary disks dissipate within 2–6 million years after star formation implying rapid planetary formation (e.g., Williams and Cieza 2011; cf. Pfalzner et al. 2014).

The inner solar system appears to have been initially poorly mixed during planetesimal and planetary assembly as evidenced by the isotopic contrasts between the Earth-Moon system and meteorites (and Mars and Sun) (Clayton 1993; Dauphas et al. 2002; Carlson et al. 2007; Burkhardt et al. 2011; Warren 2011; McKeegan et al. 2011). The rapid growth of Jupiter may have first acted as a barrier against inward transport through the nebular disk, whereas its subsequent migration may be responsible for the later (within 5 Ma?) introduction of volatile rich outer solar system material into the terrestrial planets (Kruijer et al. 2017).

Relative to the bulk composition of the solar system, Earth is substantially deficient in volatile elements (those having condensation temperatures <900 °C under highly reducing conditions; Grossman 1972; Lodders 2003). The extent of this depletion correlates with the temperature at which a specific element condenses from a low pressure gas of solar composition (Fig. 3.1). Whether the depletion was inherited from the planetesimals that accreted to form Earth (Wetherill 1980; Drake 2005; Marty 2012) or occurred later by global outgassing can be addressed by comparing the radiogenic ingrowth from two decay systems with widely different half-lives—the decay of ^{53}Mn to ^{53}Cr ($t_{½}$ = 3.7 Ma) and ^{87}Rb to ^{87}Sr ($t_{½}$ = 49 Ga). Relative to primitive chondrites, mantle rocks have both low Mn/Cr and Rb/Sr (i.e., ratios of volatile to non-volatile elements; Lugmair and Shukolyukov 1998; Trinquier et al. 2008; Halliday and Kleine 2005) indicating that Earth bound materials were volatile-depleted within ca. 5 Ma of formation of the first solids from the nebular disc at 4.567 ± 0.001 Ga (Amelin et al. 2010). The relatively short

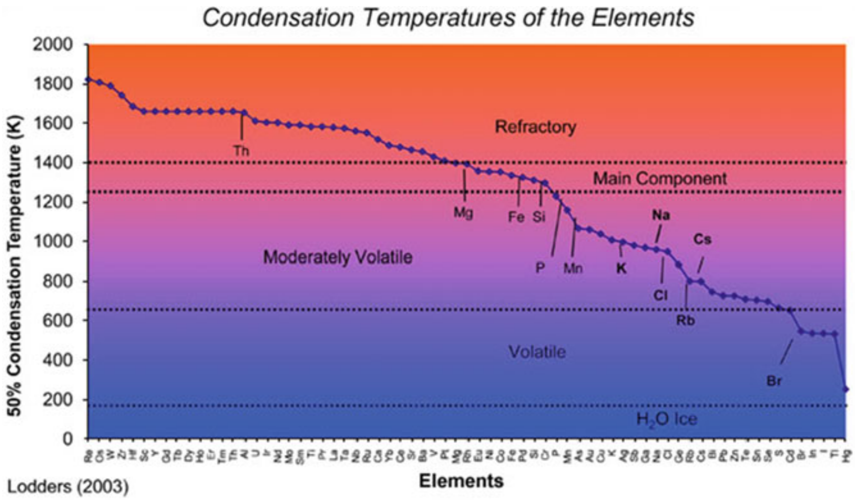

Fig. 3.1 Temperature for 50% condensation of an element, from high to low condensation temperatures, calculated for a hydrogen pressure of 10^{-4} bars. Condensation temperatures above 1400 K are regarded as refractory and those below ~1200 K as volatile. Data from Lodders (2003) reproduced with permission from Jeffrey Taylor

duration of this interval suggests that Earth grew from volatile-depleted planetesimals that would have then occupied the region between perhaps ~0.8 and 2 AU where temperatures were then high enough (Chambers 2004) to prevent highly volatile species (e.g., H_2O) from condensing (Carlson et al. 2014). Melting and volcanism on small planetesimals driven by nuclides with short-lived radioactivities such as ^{26}Al ($t_{½}$ = 0.7 Ma) would have transported volatile elements from planetary interiors to their surfaces where they could be lost, further depleting volatile element abundances in Earth's precursor building blocks.

In stark contrast to its substantial deficit in volatile elements, Earth's mantle has much higher concentrations of highly siderophile ("iron-loving") elements (HSE) than would be expected following core formation (see Sect. 3.5). Mo isotopes show that carbonaceous and non-carbonaceous meteorites plot on parallel, but separate, s-process[1] mixing lines (Budde et al. 2016). The terrestrial isotope composition is intermediate between these two arrays suggesting to Budde et al. (2018) that Earth's mantle incorporated about 40% of carbonaceous chondrites over the last ca. 10% of accretion (i.e., following core formation; see next section) which may have provided a significant portion of our planet's complement of water and other volatile species.

[1]The s-process is neutron-capture by atomic nuclei in stars that occurs at rates that are slow relative to the half-lives of their radioactive products.

3.2 Core Formation

Over the next few tens of millions of years as Earth accreted close to its present mass, heat generated by potential energy release, as dense metal sank to Earth's center, likely increased. How much is not known as evidence from iron meteorites suggests that many planetesimals differentiated within the first few hundreds of thousands of years following the formation of the first solids (Kruijer et al. 2014). Core formation may have been a continuing process such that there was no single moment or temperature at which a dominant silicate-metal differentiation event occurred (cf. Solomon 1979). The timing of the effective completion of core formation—and thus an upper bound on the formation age of the metal-poor Moon—is not directly datable, but two isotopic systems provide age constraints. Under chemical equilibrium, core formation would extract siderophile elements, such as Pb and W, from the mantle which in turn preferentially retains lithophile ("rock-loving") elements, such as U and Hf. Since $^{235,238}U$ decays to $^{207,206}Pb$ ($t_{½}$ = 0.70 and 4.4 Ga, respectively) and ^{182}Hf to ^{182}W ($t_{½}$ = 9 Ma), the separation of the metal and silicate portions of the planet would have profoundly fractionated parents from daughters imposing high U/Pb and Hf/W on mantle rocks (a record of which is preserved in daughter element isotope compositions). We can calculate the amount of radiogenic ingrowth that has occurred because we can obtain the initial $^{207}Pb/^{206}Pb$ and $^{182}W/^{184}W$ ratios of the solar system from, respectively, U and Hf poor components of primitive meteorites.

As already noted, core formation was unlikely to have occurred as a single, virtually instantaneous event, in part because the process must have been dynamic and we know that silicate-metal segregation was occurring on planetesimal precursors (Nimmo and Kleine 2015). However, that scenario does provide the simplest case for calculation which, given the many unknowns, provides an upper bound. With that premise, a lower age limit on core formation of ~4.45 Ga is estimated from a single-stage, back extrapolation of the $^{207}Pb/^{206}Pb$ composition of the most primitive known galena from the ca. 3.42 Ga Big Stubby deposit (Pidgeon 1978). Shorter timescales estimated from Pb isotopes (e.g., average accretion span of 28 Ma; Wood and Halliday 2005) are problematic. Since Pb is volatile, it is not clear if U-Pb model ages are dating core formation, volatile loss, or both. Since a large fraction of Earth's U and Pb, possibly a majority, is held within the continental crust, the global terrestrial U-Pb system is powerfully influenced by the history of continent formation and recycling. As documented in Chap. 5, this evolution is very poorly understood.

That the mantle today has a superchondritic $^{182}W/^{184}W$ (Fig. 3.2) requires that silicate-metal segregation began while ^{182}Hf (produced in supernovae or neutron star mergers; Vockenhuber et al. 2007) was still active (within ca. 50 Ma of first solids; Jacobsen 2005; Kleine et al. 2009), whether it occurred on Earth or on the planetesimals from which it formed. The average chondrite Hf/W ratio of ~1.3 would have been strongly fractionated upon core formation, with the rocky mantle inheriting a Hf/W of >10 and the core a Hf/W ≈ 0. Assuming a $^{180}Hf/^{183}W$

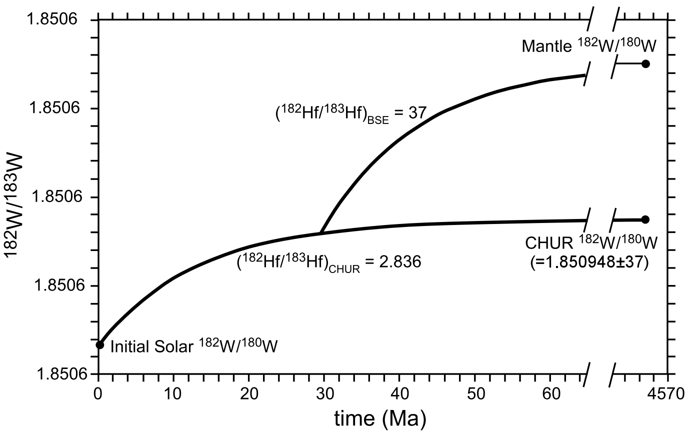

Fig. 3.2 Model ^{182}Hf-^{182}W evolution diagram showing Hf-W isotopic evolution of average chondrites (CHUR) and Earth's mantle for a core-mantle separation age of 4.54 Ga. Modified from Jacobsen (2005)

of ~40, ^{182}Hf-^{182}W model ages for terrestrial core formation range from ca. 20 to 50 Ma, depending on the assumed value of Hf/W in the silicate Earth, the extent of differentiation on precursor planetesimals, and the extent of W isotope equilibration during the hypothesized giant impact (Klein et al. 2002; Yin et al. 2002; Jacobsen 2005, Touboul et al. 2007, Halliday 2008; cf. Lee and Halliday 1995). Despite these complexities, the range of ^{182}W/^{184}W in Earth's mantle is broadly consistent with a single-stage model core separation about 30 Ma after formation of first solar system solids (e.g., Yin et al. 2002; Kleine et al. 2009; Puchtel et al. 2016; Fig. 3.2). So, for the purposes of constructing a timescale of Earth formation, let's adopt ~4.54 Ga as the effective age of core formation.

While the outer core is dominantly comprised of molten iron-nickel, its formation must have involved light elements as well. The density distribution through the outer core inferred from seismic wave travel times has long been known to be about 10% lower than expected for a $Fe_{90}Ni_{10}$ mixture (Birch 1964). A number of light elements, including oxygen, sulphur, silicon, carbon and hydrogen, have been proposed, but the mixture of these components depends on the redox conditions during Earth accretion and core formation. Badro et al. (2014) concluded that oxygen is almost certainly present with silicon and sulfur concentrations limited to no greater than 4.5% and 2.4%, respectively. However, Grewal et al. (2019) found that high core sulphur contents reduced carbon solubility while leaving nitrogen solubility unaffected. This could explain why the bulk silicate Earth has a C/N ratio of about 40, or twice the value seen in carbonaceous chondrites (albeit likely a minor Earth building block).

3.3 Moon-Forming Event

Although there is no direct evidence of a glancing collision with a Mars-sized object to form Moon shortly after Earth had accreted close to its present mass (e.g., Benz et al. 1986; Canup 2004), the Giant Impact Theory became the most widely accepted explanation for lunar formation (Halliday 2012). This is in spite of the fact that the simplest interpretation of cosmochemical evidence is that this scenario is unlikely to have occurred in exactly this fashion. Most such impact calculations indicate that Moon would consist of more than 70% impactor (e.g., Canup 2004). However, the indistinguishable isotopic compositions of O, Ti and Si between Earth and Moon (e.g., Wiechert et al. 2001; Dauphas et al. 2014; Magna et al. 2017) would require that the impactor have, to the ppm level, been of identical isotopic composition to proto-Earth (Wiechert et al. 2001). But apart from enstatite chondrites, no extraterrestrial materials we have sampled come close to that specification. This then requires the remarkable coincidence, advocated by some, that the Mars-sized impactor and proto-Earth shared the identical isotopic composition (Wiechert et al. 2001; Stevenson and Halliday 2014; Dauphas 2017) or completely mixed virtuously instantaneously (Young et al. 2016). However, the initial identical W composition of Earth and Moon argues against such an interpretation as radiogenic ^{182}W ingrowth into both proto-Earth and the giant impactor reflects both their respective core formation ages and the Hf/W ratios of their mantles (Walker 2016). That two isotopically identical bodies would have evolved to the same $^{182}W/^{184}W$ at the time of collision stretches credulity. Other ad hoc explanations have been proffered, such as chemical exchange within the vapor that resulted from impact (Pahlevan and Stevenson 2007), but lack specificity and would tend to remove angular momentum, leading to collapse of the post-impact disk (Melosh 2009).

The problems relating predictions of the Giant Impact Theory with cosmochemistry inspired, beginning in 2012, a spate of alternate models. Ćuk and Stewart (2012) examined the case of small impactors (as small $\sim$2% of present Earth mass) into a very fast-spinning (i.e., two to three times higher pre-impact angular momentum than today) early Earth. This would permit formation of Earth and Moon containing as little as 2% impactor materials in each body. They proposed that the Earth-Moon system then lost excess angular momentum through an orbital resonance between Sun and Moon that transferred it to Earth's orbit around the Sun. Whether by this orbital transfer mechanism or another (Wisdom and Tian 2015; Ćuk et al. 2016), this scenario is consistent with the isotopic homogeneity and angular momentum content of the Earth-Moon system. Canup (2012) investigated impactors that were somewhat larger than Mars-sized and proto-Earths much smaller than present Earth. This resulted in more equal mixtures of pre-collisional Earth and impactor in the final planet and satellite (indeed, in these scenarios, which of the two objects is proto-Earth and which is impactor is a matter of definition).

Reufer et al. (2012) investigated a "hit-and-run" collision scenario (Asphaug 2010) by a Mars-sized object at higher impact velocity and angle than the canonical scenario (Canup 2004), resulting in considerably higher temperatures (>10,000 K) in the resulting debris disk. Excess angular momentum is lost from the system by material ejection and the resultant Moon is composed of mostly proto-Earth (again, consistent with the isotopic similarity of the Earth-Moon system). More recently, Rufu et al. (2017) found that a succession of smaller collisions could potentially harvest terrestrial mantle into lunar orbit while satisfying the angular momentum constraint.

At the time of lunar formation, uranium-235 would have made up about one quarter of uranium. Although not considered weapons grade, that level of enrichment would nonetheless be capable of fueling crude nuclear fission weapons today (Albright et al. 1997). De Meijer et al. (2013) proposed that early concentration of U+Pu-bearing calcium perovskite at the core-mantle boundary could have (by an unspecified mechanism) triggered a nuclear explosion. They argue that the expanding plasma from the explosion could have sent a shock wave through the mantle expelling near surface material into orbit. De Meijer et al. (2013) argue that lunar Xe isotopic data are consistent with this version of the fission hypothesis but their proposal remains controversial. Lock et al. (2018) investigated a model that combines aspects of the fission and co-accretion hypotheses in which, for example, a very fast-spinning proto-Earth is heated so strongly that it expands beyond the Roche limit (Lock and Stewart 2017). The vapor cloud beyond that tidal boundary eventually condenses to form Moon. The equilibration of Moon-forming materials with terrestrial silicate vapor explains the identical Earth-Moon isotopic composition, the Moon-like pattern of moderately volatile element depletions (Lock et al. 2018), and the small lunar core.

Hosono et al. (2019) proposed a variant on the now traditional Mars-sized-impactor model in which the proto-Earth target contained a global-scale magma ocean. Because the magma ocean is heated more than impactor materials by the shock wave (due to the strong contrast in shock heating between silicate melts and solids), the expanding disk of Moon-forming ejecta contains about half of the original magma ocean. Their model can yield the appropriate amount of angular momentum and better explains the compositional similarities between Earth and Moon than the solid-solid impact scenario.

The importance of whether or not such a collision occurred rests with the thermal and compositional consequences of a $\sim 10^{32}$ J collision. As already noted, an event of this magnitude would have vaporized a large portion of both impactor and target and melted the rest of the combined system, although little volatile loss would occur if temperatures were sufficiently high (i.e., ≥ 6000 K; Genda and Abe 2005, Abe 2007; Nakajima and Stevenson 2018) as the vaporized silicate acts to shield hydrogen against escape from the system. Independent of this Moon-forming scenario, the energy associated with assembly of Earth and core formation would likely create a thermal structure conducive to magma ocean formation (Righter and Drake 1999).

Barboni et al. (2017) found that the very unradiogenic initial ^{176}Hf/^{177}Hf ratios in 4.10–4.35 Ga lunar zircons were so close to the solar system initial value (Iizuka et al. 2015a, b) that lunar formation and magma ocean solidification must have occurred prior to 4.51 ± 0.01 Ga. If Moon emerged from a collisional interaction with, or fission from, proto-Earth, then terrestrial core formation must have been largely complete by that time to explain the low lunar Fe content.

3.4 Magma Ocean(s)

While evidence of an early magma ocean is preserved on Moon (and perhaps Mars), the extent and timing of a terrestrial magma ocean phase are poorly understood. Although geochemical evidence requiring that such an event occurred on Earth is almost entirely lacking (e.g., Righter and Drake 1999), the multiple sources of thermal energy available in the first ca. 5 Ma of solar system history appear to make such an appearance inevitable. The current paradigm of terrestrial magma ocean crystallization is that solidification proceeded from the bottom up, driving such initially vigorous convection that the lower mantle (i.e., >28 GPa) crystallized within 10^3 years (Solomatov 2007). Calculations suggest that the remaining mantle would have been largely solid within 10^5–10^7 years, depending on volatile content (Elkins-Tanton 2008). Although a steam atmosphere would slow cooling, the generally short timescales expected suggest that serial magma oceans, perhaps punctuated by clement conditions, were possible on earliest Earth (Elkins-Tanton 2008). Estimates of the depth of the last terrestrial magma ocean, based on apparent equilibration depths of moderately siderophile elements (e.g., Rubie et al. 2003, Elkins-Tanton et al. 2007) and geodynamic considerations (e.g., Solomatov 2000), range from relatively shallow to the core-mantle boundary. This range reflects, in part, the generally weak pressure dependence of siderophile element partitioning and uncertain extensive parameters (e.g., f_{O_2}).

Many possible permutations involving magma oceans and large impactors are consistent with what we actually know (e.g., Puchtel et al. 2016), but some proposed histories (e.g., Halliday 2008; Allegre et al. 2008) are contradicted by the Hadean zircon record (see Chap. 7). While the oldest direct evidence of terrestrial crust formation is the presence of 4.38 Ga zircons, its existence can be inferred as early as 4.50 ± 0.02 Ga from Lu–Hf data (Harrison et al. 2008), thus restricting the collective core formation/giant Moon-forming impactor/global magma ocean phase to within ~ 70 Ma of the formation of CAIs at 4.567 Ga (Krot et al. 2005).

3.5 Late Accretion

As previously noted, Earth's mantle has much higher concentrations of highly siderophile elements (HSE) than would be expected from metal-silicate equilibration. Between about 0.5 and 1.5% of an Earth mass—termed the late veneer—must have been accreted following core formation (Chou 1978; Jones and Drake 1986; Dauphas and Marty 2002; Walker 2009; Willbold et al. 2011; cf. Righter 2003, 2015; Righter et al. 2008). The timing of the late veneer is not well understood but appears not to have involved significant carbonaceous chondrite input (ca. 4%; Budde et al. 2018) and thus import of their high corresponding volatile element contents. This veneer must have been largely acquired prior to the Mesoarchean as rocks of that era show high HSE contents (Bermingham et al. 2018; Rizo et al. 2013, 2016).

The high $^{182}W/^{184}W$ ratio seen in some Archean rocks could be interpreted as sampling a mantle source that had been depleted in W by core formation, but had not had chondritic W added by the late veneer. Measurement of $^{182}W/^{184}W$ in the ca. 3.8 Ga rocks at Isua, West Greenland, led Willbold et al. (2011) to infer that a mantle domain free of a major proportion of late accreted material had remained intact until that time. They argued that even the addition of only 0.5% of an Earth mass would significantly alter the mantle composition as chondrites are about 10 times higher in HSE and have strongly contrasting $\mu^{182}W$ (μ = ppm; White, 2015), although the advent of coupled ^{182}W-^{142}Nd studies appear to mitigate such an interpretation. As a note to the reader, Willbold et al. (2011) appear to have conflated the late veneer with the Late Heavy Bombardment, the latter conventionally thought to have brought an order of magnitude less material to Earth than that responsible for the high HSE abundances (see Chap. 4).

3.6 $^{182}W/^{184}W$ and $^{142}Nd/^{144}Nd$ in Archean Rocks

While few post-Archean rocks have been observed to contain non-bulk silicate Earth (BSE) signatures in ^{182}W or ^{142}Nd, some modern ocean island basalts (OIB) do (e.g., Rizo et al. 2016; de Leeuw et al. 2017; Mundl et al. 2017). Mundl et al. (2017) documented a clear negative correlation between $^{182}W/^{184}W$ and $^{3}He/^{4}He$ (i.e., depleted $\mu^{182}W$ corresponding to high $^{3}He/^{4}He$) in rocks from Hawaii, Samoa and Iceland (Fig. 3.3) indicating either that OIB sources contain domains that formed within the first ~50 Ma of solar system history or that a component of mantle ^{182}W was lowered over time by some exchange (i.e., limited W isotope equilibration) with the core. As the aforementioned OIB locations presently sit atop large ultralow-velocity zones, the latter have been suggested as the hosts of these primordial isotopic signals.

Ultramafic rocks older than 2.6 Ga generally contain up to −10 or +15 $\mu^{182}W$ deviations from bulk Earth (Rizo et al. 2013, 2016; Puchtel et al. 2016). The preservation of such anomalous domains throughout the Archean is often interpreted as indicating a relatively quiescent Hadean Earth (e.g., Puchtel et al. 2016). Most rock suites do not show coupled depletions in ^{182}W or ^{142}Nd. However, Puchtel et al. (2016) found negative values of both $\mu^{182}W$ and $\mu^{142}Nd$ in the Schapenburg komatiites, South Africa, suggesting that their incompatible trace-element-enriched source, or at least the HSEs, had separated from the global silicate reservoir within ~30 Ma of solar system formation. That the rock has both lower than average mantle HSE's and negative $\mu^{182}W$ appears consistent with its source having largely escaped contamination by the late veneer. Although a positive correlation between ^{182}W and ^{142}Nd is likely in a differentiated reservoir, the general lack of correlation between ^{182}W and ^{142}Nd is expected for several reasons (Rizo et al. 2016). While concentrations of Nd are similar between chondrites and

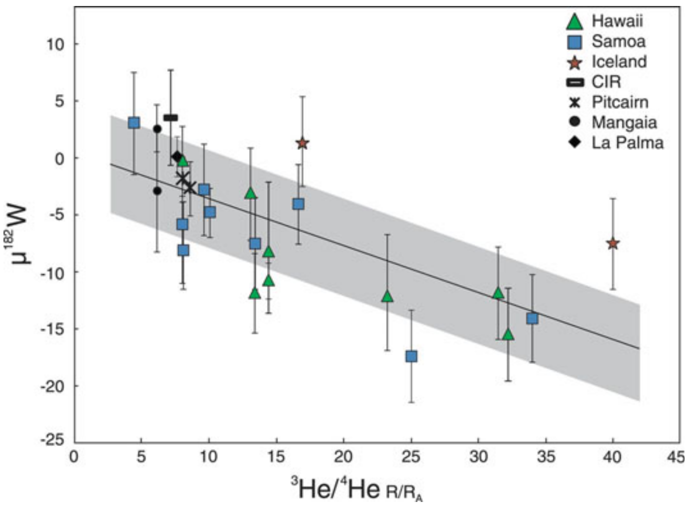

Fig. 3.3 Plot of $\mu^{182}W$ versus $^{3}He/^{4}He$ (relative to modern atmosphere) for ocean island basalts and a MORB from the Central Indian Ridge which show a remarkably high degree of correlation. Reproduced with permission from Mundl et al. (2017)

mantle (and thus the late veneer would have negligible effect on ^{142}Nd), as noted above, W differs substantially. Original correlations could subsequently have been decoupled by, for example, metasomatic processes (Rizo et al. 2016). Alternatively, since core formation strongly fractionates Hf/W but does not affect Sm/Nd, the W isotopic data might primarily reflect core formation while Sm/Nd could reflect a later (ca. 4.5 Ga) magma ocean, perhaps corresponding to lunar formation.

3.7 Isotopic Signatures Attributed to Hadean Evolution

In seeming contradiction to the widespread agreement that an early terrestrial magma ocean was inevitable, it was, until relatively recently, widely assumed that the silicate Earth remained largely undifferentiated until after 4 Ga (Taylor and McLennan 1985). This view began to change when investigations of early Archean rocks from West Greenland (Boyet et al. 2003; Caro et al. 2003) revealed distinctive ^{142}Nd variations, from the decay of ^{146}Sm ($t_{1/2}$ = 68–103 Ma, Kinoshita et al. 2012), from which an early Hadean mantle fractionation event was inferred. With some assumptions as to the Sm/Nd ratios of key terrestrial reservoirs, coupled $^{142,143}Nd/^{144}Nd$ systematics suggest a major differentiation of the silicate Earth within ~150 Ma of planetary accretion (Caro et al. 2003). To explain the apparent lack of covariance of Nd and Hf isotopes in ~3.7 Ga West Greenland gneisses, Caro et al. (2005) proposed an elaborate multi-stage model involving melt segregation from a crystallizing magma ocean, with Ca-perovskite playing a key role in fractionating the two isotopic systems. Subsequently, Lu–Hf data from terrestrial zircons as old as 4.37 Ga revealed unradiogenic compositions that require their source to have been sequestered in a low Lu/Hf environment as early as 4.50 Ga (Harrison et al. 2008). Since the protolith of those zircons could not have survived global melting, the last magma ocean must have ended by that time. As noted earlier, Barboni et al. (2017) found that the initial $^{176}Hf/^{177}Hf$ ratios in 4.10–4.35 Ga lunar zircons lie so close to the solar system initial value as to require lunar formation and its magma ocean to have solidified by 4.51 ± 0.01 Ga.

Correlated $^{142,143}Nd/^{144}Nd$ variations in rocks from Nuvvuagittuq, northern Quebec, are interpreted as recording a mantle fractionation event that produced an incompatible-element-enriched reservoir at $\sim$4.3 Ga (O'Neil et al. 2008). This age likely reflects an early mantle fractionation event as the youngest U-Pb ages of detrital zircons from meta-sediments within the same Nuvvuagittuq supracrustal successions that preserve low $^{142}Nd/^{144}Nd$ are 3.78 Ga, thus defining an upper age bound on the sequence (Cates et al. 2013).

The observation of Boyet and Carlson (2005, 2006) that chondrites have an apparent $\sim$20 ppm deficiency in ^{142}Nd relative to the observable silicate Earth appeared to push global silicate differentiation to even earlier times. The restricted range of Sm/Nd in terrestrial reservoirs and the short half-life of ^{146}Sm implied either that Earth's inferred superchondritic Sm/Nd formed from a global differentiation event within 30 Ma of Solar System formation, or that Earth inherited an Sm/Nd ratio that was fractionated at the ca. 5% level by solar nebula processes (Caro et al. 2008). This view began to change when it emerged (Becker and Walker 2003; Trinquier et al. 2008; Qin et al. 2010; Warren 2011; Dauphas et al. 2014) that carbonaceous chondrites and most other meteorite classes are isotopically distinct from Earth and Mars. Burkhardt et al. (2016) subsequently showed that, relative to chondrites, the materials contributing to Earth were enriched in s-process Nd isotopes that result in higher $^{142}Nd/^{144}Nd$ ratios relative to known chondrites. Once so corrected, terrestrial $^{142}Nd/^{144}Nd$ is indistinguishable from chondrites obviating the need for a hidden reservoir or a super-chondritic Earth (i.e., bulk Earth effectively has a chondritic Sm/Nd ratio).

Examining the isotopic composition of elements ranging from siderophile to lithophile provides insights into the nature of the materials that accreted to form Earth. Dauphas (2017) interpreted the mantle isotopic signatures of O, Ca, Ti and Nd (lithophile elements), Cr, Ni and Mo (moderately siderophile), and Ru (highly siderophile) as recording different phases of Earth's accretion. Their isotopic similarity to enstatite meteorites suggested to Dauphas (2017) that this group may have been a significant—perhaps as much as 90%—contributor to Earth's mass. However, Render et al. (2017) noted that nucleosynthetic Mo isotope anomalies in enstatite chondrites are not seen in terrestrial samples, precluding them from being Earth's dominant building materials (Fig. 3.4). Enstatite and ordinary chondrites and Earth's mantle plot on a Mo–Nd isotope correlation line that reflects varying proportions of s-process contributions. This correlation implied to Render et al. (2017) that the materials contributing to constructing Earth were of relatively

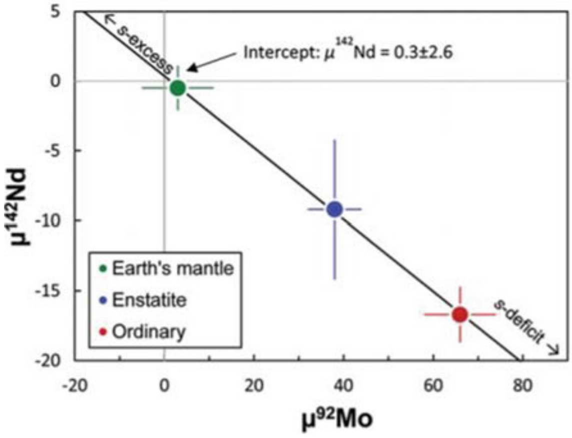

Fig. 3.4 Plot of μ^{142}Nd versus μ^{92}Mo showing lack of relationship of enstatite and ordinary chondrites to Earth's mantle. Such correlations indicate that all known chondrite groups are deficit in s-process nuclides relative to those bodies that formed Earth. Reproduced with permission from Render et al. (2017)

constant composition and formed closer to Sun than Earth (Fig. 3.4). Nothing we have yet sampled in the meteorite record or from extraterrestrial sample-return missions match Earth's composition at the ppm level. But given that virtually all meteorites in our collections accreted to Earth in the last few millennia, and are derived mostly from asteroids near Kirkwood gaps (see 10.2.7), they may not be spatially representative of either the asteroid belt or the solar nebula.

As noted in the previous section, erasure from post-2.6 Ga rocks of ^{182}W and ^{142}Nd (Fig. 3.5), as well as other (e.g., Byerly et al. 2017) isotopic anomalies that were perhaps pervasive throughout the Archean, reflects either subsequent homogenization of the mantle or the tapping of different reservoirs. Assuming the latter to be unlikely, do these data imply a lack of vigorous mantle circulation during the Hadean? Since anomalous ^{182}W can potentially be introduced by a late veneer or reflect its absence (Willbold et al. 2011), its presence in Archean rocks could represent snapshots of an accumulation-loss process in which the introduction of extraterrestrial contamination is slowly offset by convective mixing in the mantle. In this view, the gradual disappearance of the W isotopic signatures has less to do with the vigor of mantle circulation than the waning flux of extraterrestrial impactors.

Caro et al. (2017a, b) concluded that anomalous ^{142}Nd in rocks of the Eoarchean Nuvvuagittuq and Ukaliq terranes are inherited signatures from a crust-forming event at ca. 4.3–4.4 Ga. They interpreted these data as evidence of the stabilization of Hadean plates whose long-term stability implies inefficient lithospheric recycling and thus stagnant lid tectonics throughout that eon. Others have made similar arguments on the basis of ^{142}Nd signals preserved in ca. 2.7 Ga (Debaille et al. 2013), 3.4 Ga (Roth et al. 2014), and ca. 3.7 Ga rocks (Saji et al. 2018). While none

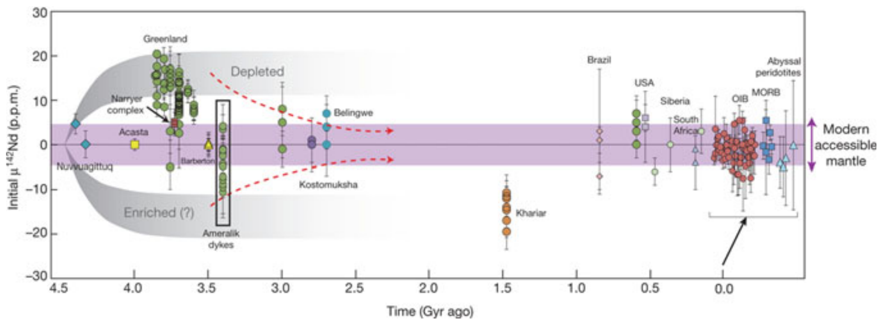

Fig. 3.5 Plot of μ^{142}Nd over geologic time (as of 2012). The purple region represents an isotopic ratio measurement error of ±5 ppm. The Eoarchean is characterized by ±20 ppm positive and negative anomalies which appear (with the exception of Khariar) to have disappeared from the record by 2.5 Ga. Samples derived from the present day accessible mantle are indicated by the purple shaded region. Reproduced with permission from Rizo et al. (2012)

of these studies offer an explanation for how Hadean zircons could have acquired the full range of their geochemical characteristics in such an environment, their presumption that the preservation of mantle isotopic signatures of short-lived radioactive nuclides requires long-term sluggish mantle circulation and thus the lack of mobile lid tectonics is problematic for at least three reasons.

First, the existence of plate tectonics does not imply a singular degree of mantle convective vigor. A variety of evidence (see summary in Rosas and Korenaga 2018) supports the view that plate tectonic rates may have been slower in the past than today and thus mantle mixing due to the related convection may have been less efficient (Korenaga 2006). Second, the slow (billion-year-scale) apparent disappearance of isotopic signals in mantle rocks can equally well be due to crustal recycling, which explains the full panoply of geologic evidence (Armstrong 1991; Rosas and Korenaga 2018; Chaps. 7 and 9). Third, the assertion that long term preservation of mantle isotopic domains is exclusive of plate tectonics is contradicted by what we know today with certainty. The modern mantle, is characterized by many different MORB and OIB sources (e.g., HIMU, FOZO, EM1, EM2, N-MORB, DMM, etc.) that are replete with isotopic variability indicating the lack of global homogenization over at least the past ca. 2 Ga (Brooks and Hart 1978; Zindler and Hart 1986; Stracke et al. 2005) and perhaps the past 4.54 Ga (Mundl et al. 2017; Fig. 3.3). Clearly these observations cannot imply that plate tectonics hasn't occurred on Earth over at least the past billion years (see Chap. 6). Erasure of mantle isotopic heterogeneity requires mixing at a variety of scales (Hofmann and Hart 1978; Schmalzl et al. 1996) that appear to have little or nothing to do with the vigor of mantle convection.

3.8 Critical Summary

Evidence from short- and long-lived radioisotopic systems indicates that Earth was largely built from volatile-depleted planetesimals and planetary embryos during runaway accretion that occurred within 1–10 Ma of formation of the first solids at 4.567 ± 0.001 Ga (Carlson et al. 2014). Although model ^{182}Hf-^{182}W ages of terrestrial silicate-metal fraction are complicated to interpret due to unknown planetesimal differentiation histories, semi-continuous core formation likely occurred over the first 30 Ma of Earth evolution. There is no direct evidence of a glancing collision with a Mars-sized object shortly after Earth accretion to form Moon and substantial evidence contradicting that particular scenario. However, impact models reveal a wide range of two body interactions, some involving little mass exchange between impactor and impactee, that appear physically plausible and consistent with accumulating evidence that Earth and Moon are isotopically identical at the ppm level. There is no clear geochemical evidence that Earth hosted a magma ocean following lunar formation (Righter and Drake 1999), but the abundant sources of thermal energy available in the first few tens of millions of years of Earth evolution (radiogenic heating, impact heating, gravitational potential energy) make such an event (or events) likely. Lu–Hf isotope constraints from Hadean zircons require any such global silicate homogenization event to have ended by 4.50 ± 0.02 Ga. The high abundance of highly siderophile elements in the upper mantle is strong evidence that Earth added at least half a percent of its present mass following core formation but prior to the Mesoarchean. Isotopic evidence from multiple sources (OIB's, zircons) appear to show that Earth's mantle and crust sequestered isotope signatures that formed within the first 50–70 Ma of planetary evolution, although core-mantle exchange could be responsible. Preservation of mantle isotopic anomalies throughout the Hadean-Archean seem unlikely to reflect sluggish mantle convention in a stagnant lid tectonic regime during that period as the plate tectonic era is associated with a veritable zoo of isolated mantle isotopic domains.

References

Abe, Y. (2007). Behavior of water during terrestrial planet formation. *Geochimica et Cosmochimica Acta Supplement, 71,* A2.

Albright, D., Berkhout, F. and Walker, W. (1997) Plutonium and highly enriched uranium 1996. *World inventories, capabilities and policies* (pp. 502). Oxford.

Allègre, C. J., Manhès, G., & Göpel, C. (2008). The major differentiation of the Earth at ~4.45 Ga. *Earth and Planetary Science Letters, 267,* 386–398.

Amelin, Y., Kaltenbach, A., Iizuka, T., Stirling, C. H., Ireland, T. R., Petaev, M., Jacobsen, S. B. (2010). U–Pb chronology of the solar system's oldest solids with variable ^{238}U/^{235}U. *Earth and Planetary Science Letters*, *300*, 343–350.

Armstrong, R. L. (1991). The persistent myth of crustal growth. *Australian Journal of Earth Science, 38,* 613–630.

Asphaug, E. (2010). Similar-sized collisions and the diversity of planets. *Chemie der Erde-Geochemistry, 70,* 199–219.

Badro, J., Côté, A. S., & Brodholt, J. P. (2014). A seismologically consistent compositional model of Earth's core. *Proceedings of the National Academy of Sciences, 111,* 7542–7545.

Barboni, M., Boehnke, P., Keller, B., Kohl, I. E., Schoene, B., Young, E. D., & McKeegan, K. D. (2017). Early formation of the Moon 4.51 billion years ago. *Science advances*, *3*, p.e1602365.

Becker, H., & Walker, R. J. (2003). In search of extant Tc in the early solar system: ^{98}Ru and ^{99}Ru abundances in iron meteorites and chondrites. *Chemical Geology, 196,* 43–56.

Benz, W., Slattery, W. L., & Cameron, A. G. W. (1986). The origin of the Moon and the single-impact hypothesis I. *Icarus, 66,* 515–535.

Bermingham, K. R., Worsham, E. A., & Walker, R. J. (2018). New insights into Mo and Ru isotope variation in the nebula and terrestrial planet accretionary genetics. *Earth and Planetary Science Letters, 487,* 221–229.

Birch, F. (1964). Density and composition of mantle and core. *Journal of Geophysical Research, 69,* 4377–4388.

Boyet, M., Blichert-Toft, J., Rosing, M., Storey, M., Telouk, P., & Albarède, F. (2003). ^{142}Nd evidence for early Earth differentiation. *Earth and Planetary Science Letters, 214,* 427–442.

Boyet, M., & Carlson, R. W. (2005). ^{142}Nd evidence for early (>4.53 billion years ago) global differentiation of the silicate Earth. *Science, 309,* 576–581.

Boyet, M., & Carlson, R. W. (2006). A new geochemical model for the Earth's mantle inferred from ^{146}Sm-^{142}Nd systematics. *Earth and Planetary Science Letters, 250,* 254–268.

Brooks, C., & Hart, S. R. (1978). Rb–Sr mantle isochrons and variations in the chemistry of Gondwanaland's lithosphere. *Nature, 271,* 220–223.

Budde, G., Burkhardt, C., Brennecka, G. A., Fischer-Gödde, M., Kruijer, T. S., Kleine, T. (2016). Molybdenum isotopic evidence for the origin of chondrules and a distinct genetic heritage of carbonaceous and non-carbonaceous meteorites. *Earth and Planetary Science Letters, 454*, 293–303.

Budde, G., Burkhardt, C., & Kleine, T. (2018). Earth's accretion history inferred from the molybdenum isotope dichotomy of meteorites. In *18th Goldschmidt Conference Abstracts, 123*.

Burkhardt, C., Kleine, T., Oberli, F., Pack, A., Bourdon, B., & Wieler, R. (2011). Molybdenum isotope anomalies in meteorites: Constraints on solar nebula evolution and origin of the Earth. *Earth and Planetary Science Letters, 312,* 390–400.

Burkhardt, C., Borg, L. E., Brennecka, G. A., Shollenberger, Q. R., Dauphas, N., & Kleine, T. (2016). A nucleosynthetic origin for the earth's anomalous ^{142}Nd composition. *Nature*, *537*, 394–398.

Byerly, B. L., Kareem, K., Bao, H., & Byerly, G. R. (2017). Early Earth mantle heterogeneity revealed by light oxygen isotopes of Archaean komatiites. *Nature Geoscience, 10,* 871–875.

Canup, R. M. (2004). Simulations of a late lunar forming Impact. *Icarus, 168,* 433–456.

Canup, R. M. (2012). Forming a Moon with an Earth-like composition via a giant impact. *Science, 338,* 1052–1055.

Carlson, R. W., Boyet, M., & Horan, M. (2007). Chondrite barium, neodymium, and samarium isotopic heterogeneity and early Earth differentiation. *Science, 316,* 1175–1178.

Carlson, R. W., Garnero, E., Harrison, T. M., Li, J., Manga, M., McDonough, W. F., et al. (2014). How did early Earth become our modern world? *Annual Review of Earth and Planetary Sciences, 42,* 151–178.

Caro, G., Bourdon, B., Birck, J. L., & Moorbath, S. (2003). ^{146}Sm-^{142}Nd evidence from Isua metamorphosed sediments for early differentiation of the Earth's mantle. *Nature, 423,* 428–432.

Caro, G., Bourdon, B., Wood, B. J., & Corgne, A. (2005). Trace element fractionation in Hadean mantle generated by melt segregation from a magma ocean. *Nature, 436,* 246–249.

Caro, G., Bourdon, B., Halliday, A.N., & Quitte, G. (2008). Non-chondritic Sm/Nd ratios in the terrestrial planets. *Geochimica et Cosmochimica Acta Supplement, 72*, A138.

Caro, G., Morino, P., Mojzsis, S. J., Cates, N. L., & Bleeker, W. (2017a). Sluggish Hadean geodynamics: Evidence from coupled ^{146,147}Sm–^{142,143}Nd systematics in Eoarchean supracrustal rocks of the Inukjuak domain (Québec). *Earth and Planetary Science Letters, 457,* 23–37.

Caro, G., Morino, P., Reisberg, L., Mojzsis, S. J., Cates, N.L. and Bleeker, W. (2017b). ^{146}Sm-^{142}Nd constraints on the nature and evolution of the Hadean crust. *Before life: The chemical, geological and dynamical setting for the emergence of an RNA World*. Workshop, Boulder, CO, 9–12 October, 27–28.

Cates, N. L., Ziegler, K., Schmitt, A. K., & Mojzsis, S. J. (2013). Reduced, reused and recycled: detrital zircons define a maximum age for the Eoarchean (ca. 3750–3780 Ma) Nuvvuagittuq Supracrustal Belt, Québec (Canada). *Earth and Planetary Science Letters, 362,* 283–293.

Chambers, J. (2004). Planetary accretion in the inner Solar System. *Earth Planet Sci. Lett., 223,* 241–252.

Chou, C. L. (1978). Fractionation of siderophile elements in the earth's upper mantle. In *Proceedings of the 9th Lunar and Planetary Science Conference* (pp. 219–230).

Clayton, R. N. (1993). Oxygen isotopes in meteorites. *Annual Review of Earth and Planetary Sciences, 21,* 115–149.

Ćuk, M., Hamilton, D. P., Lock, S. J., & Stewart, S. T. (2016). Tidal evolution of the Moon from a high-obliquity, high-angular-momentum Earth. *Nature, 539,* 402.

Ćuk, M., & Stewart, S. T. (2012). Making the Moon from a fast-spinning Earth: A giant impact followed by resonant despinning. *Science, 338,* 1047–1052.

Dauphas, N. (2017). The isotopic nature of the Earth's accreting material through time. *Nature, 541,* 521–524.

Dauphas, N., Burkhardt, C., Warren, P. H., & Fang-Zhen, T. (2014). Geochemical arguments for an Earth-like Moon-forming impactor. *Philosophical Transactions of the Royal Society A, 372,* 20130244.

Dauphas, N., & Marty, B. (2002). Inference on the nature and the mass of Earth's late veneer from noble metals and gases. *Journal of Geophysical Research, 107,* 1–7.

Dauphas, N., Marty, B., & Reisberg, L. (2002). Molybdenum evidence for inherited planetary scale isotope heterogeneity of the protosolar nebula. *Astrophysical Journal, 565,* 640–644.

de Leeuw, G. A. M., Ellam, R. M., Stuart, F. M., & Carlson, R. W. (2017). ^{142}Nd/^{144}Nd inferences on the nature and origin of the source of high ^{3}He/^{4}He magmas. *Earth and Planetary Science Letters, 472,* 62–68.

De Meijer, R. J., Anisichkin, V. F., Van Westrenen, W. (2013). Forming the moon from terrestrial silicate-rich material. *Chemical Geology*, *345*, 40–49.

Debaille, V., O'Neill, C., Brandon, A. D., Haenecour, P., Yin, Q., Mattielli, N., et al. (2013). Stagnant-lid tectonics in early Earth revealed by ^{142}Nd variations in late Archean rocks. *Earth and Planetary Science Letters, 373,* 83–92.

Drake, M. J. (2005). Origin of water in the terrestrial planets. *Meteoritics & Planetary Science, 40,* 519–527.

Elkins-Tanton, L. T. (2008). Linked magma ocean solidification and atmospheric growth for Earth and Mars. *Earth and Planetary Science Letters, 271,* 181–191.

Elkins-Tanton, L. T., Parmentier, E. M., & Hess, P. C. (2007). *The effects of magma ocean depth and initial composition on planetary differentiation*. XXXVIII: Lunar Planetary Science Conference.

Genda, H., & Abe, Y. (2005). Enhanced atmospheric loss on protoplanets at the giant impact phase in the presence of oceans. *Nature, 433,* 842–844.

Grewal, D. S., Dasgupta, R., Sun, C., Tsuno, K., & Costin, G. (2019). Delivery of carbon, nitrogen, and sulfur to the silicate Earth by a giant impact. *Science Advances 5*, eaau3669.

Grossman, L. (1972). Condensation in the primitive solar nebula. *Geochimica et Cosmochimica Acta, 36,* 597–619.

Halliday, A. N. (2008). Earth viewed from a late Moon. *Geochimica et Cosmochimica Acta Supplement, 72,* A344.

Halliday, A. N. (2012). The origin of the Moon. *Science, 338,* 1040–1041.

Halliday, A. N., & Kleine, T. (2005). Meteorites and the timing, mechanisms, and conditions of terrestrial planet accretion and early differentiation. In D. S. Lauretta & H. Y. McSween Jr. (Eds.), *Meteorites and the early solar system II* (pp. 775–801). Tucson: Univ. Ariz. Press.

Harrison, T. M., Schmitt, A. K., McCulloch, M. T., & Lovera, O. M. (2008). Early ($\geq$4.5 Ga) formation of terrestrial crust: Lu-Hf, $\delta^{18}O$, and Ti thermometry results for Hadean zircons. *Earth and Planetary Science Letters, 268,* 476–486.

Hofmann, A. W., & Hart, S. R. (1978). An assessment of local and regional isotopic equilibrium in the mantle. *Earth and Planetary Science Letters, 38,* 44–62.

Hosono, N., Karato, S. I., Makino, J., & Saitoh, T. R. (2019). Terrestrial magma ocean origin of the Moon. *Nature Geoscience, 12,* 418–423.

Iizuka, T., Yamaguchi, A., Haba, M. K., Amelin, Y., Holden, P., Zink, S., et al. (2015a). Timing of global crustal metamorphism on Vesta as revealed by high-precision U-Pb dating and trace element chemistry of eucrite zircon. *Earth and Planetary Science Letters, 409,* 182–192.

Iizuka, T., Yamaguchi, T., Hibiya, Y., & Amelin, Y. (2015b). Meteorite zircon constraints on the bulk Lu–Hf isotope composition and early differentiation of the Earth. *Proceedings of the National Academy of Sciences, 112,* 5331–5336.

Jacobsen, S. (2005). The Hf-W isotopic system and the origin of the Earth and Moon. *Annual Review of Earth and Planetary Sciences, 33,* 531–570.

Jones, J. H., & Drake, M. J. (1986). Geochemical constraints on core formation in the Earth. *Nature, 322,* 221–228.

Kinoshita, N., Paul, M., Kashiv, Y., Collon, P., Deibel, C. M., DiGiovine, B., et al. (2012). A shorter ^{146}Sm half-life measured and implications for ^{146}Sm-^{142}Nd chronology in the solar system. *Science, 335,* 1614–1617.

Kleine, T., Münker, C., Mezger, K., & Palme, H. (2002). Rapid accretion and early core formation on asteroids and the terrestrial planets from Hf–W chronometry. *Nature, 418,* 952–954.

Kleine, T., Touboul, M., Bourdon, B., Nimmo, F., Mezger, K., & Palme, H. (2009). Hf-W chronology of the accretion and early evolution of asteroids and terrestrial planets. *Geochimica et Cosmochimica Acta, 73,* 5150–5188.

Korenaga, J. (2006). Archean geodynamics and the thermal evolution of Earth. In K. Benn, J.-C. Mareschal, & K. Condie (Eds.), *Archean geodynamics and environments* (Vol. 164, pp. 7–32). AGU Geophysical Monograph Series.

Krot, A. N., Amelin, Y., Cassen, P., & Meibom, A. (2005). Young chondrules in CB chondrites from a giant impact in the early solar system. *Nature, 436,* 989–992.

Kruijer, T. S., Burkhardt, C., Budde, G., & Kleine, T. (2017). Age of Jupiter inferred from the distinct genetics and formation times of meteorites. *Proceedings of the National Academy of Sciences, 114,* 6712–6716.

Kruijer, T. S., Touboul, M., Fischer-Gödde, M., Bermingham, K. R., Walker, R. J., & Kleine, T. (2014). Protracted core formation and rapid accretion of protoplanets. *Science, 344,* 1150–1154.

Lee, D., & Halliday, A. (1995). Hafnium-tungsten chronometry and the timing of terrestrial core formation. *Nature, 378,* 771–774.

Lock, S. J., & Stewart, S. T. (2017). The structure of terrestrial bodies: Impact heating, corotation limits, and synestias. *Journal of Geophysical Research: Planets, 122,* 950–982.

Lock, S. J., Stewart, S. T., Petaev, M. I., Leinhardt, Z. M., Mace, M. T., Jacobsen, S. B., & Ćuk, M. (2018). The origin of the Moon within a terrestrial synestia. *Journal of Geophysical Research: Planets*. https://doi.org/10.1002/2017je005333.

Lodders, K. (2003). Solar system abundances and condensation temperatures of the elements. *Astrophysical Journal, 591,* 1220–1247.

Lugmair, G. W., & Shukolyukov, A. (1998). Early solar system timescales according to ^{53}Mn-^{53}Cr systematics. *Geochimica et Cosmochimica Acta, 62,* 2863–2886.

Magna, T., Dauphas, N., Righter, K., & Camp, R. (2017). Stable isotope constraints on the formation of Moon. *LPI Contrib. 1988.*

Marty, B. (2012). The origins and concentrations of water, carbon, nitrogen and noble gases on Earth. *Earth and Planetary Science Letters, 313,* 56–66.
McKeegan, K. D., Kallio, A. P. A., Heber, V. S., Jarzebinski, G., Mao, P. H., Coath, C. D., et al. (2011). The oxygen isotopic composition of the Sun inferred from captured solar wind. *Science, 332,* 1528–1532.
Melosh, H. J. (2009). An isotopic crisis for the giant impact origin of the Moon?. *Meteoritics and Planetary Science Supplement*, *72*, 5104–5015.
Mundl, A., Touboul, M., Jackson, M. G., Day, J. M., Kurz, M. D., Lekic, V., et al. (2017). Tungsten-182 heterogeneity in modern ocean island basalts. *Science, 356,* 66–69.
Nakajima, M., & Stevenson, D. J. (2018). Inefficient volatile loss from the Moon-forming disk: Reconciling the giant impact hypothesis and a wet Moon. *Earth and Planetary Science Letters, 487,* 117–126.
Nimmo, F., & Kleine, T. (2015). Early differentiation and core formation: Processes and timescales. *The Early Earth: Accretion and Differentiation*, 83–102.
O'Neil, J., Carlson, R. W., Francis, D., & Stevenson, R. K. (2008). Neodymium-142 evidence for Hadean mafic crust. *Science, 321,* 1828–1831.
Pahlevan, K., & Stevenson, D. J. (2007). Equilibration in the aftermath of the lunar-forming giant impact. *Earth and Planetary Science Letters, 262,* 438–449.
Pfalzner, S., Steinhausen, M., & Menten, K. (2014). Short dissipation times of proto-planetary disks: An artifact of selection effects? *The Astrophysical Journal Letters, 793,* L34.
Pidgeon, R. T. (1978). Big stubby and the early history of the Earth. *U.S. Geological Survey Open File Report, 78-701*, 334–335.
Puchtel, I. S., Blichert-Toft, J., Touboul, M., Horan, M. F., & Walker, R. J. (2016). The coupled ^{182}W-^{142}Nd record of early terrestrial mantle differentiation. *Geochemistry, Geophysics, Geosystems, 17,* 2168–2193.
Qin, L., Alexander, C. M. D., Carlson, R. W., Horan, M. F., & Yokoyama, T. (2010). Contributors to chromium isotope variation of meteorites. *Geochimica et Cosmochimica Acta, 74,* 1122–1145.
Render, J., Fischer-Gödde, M., Burkhardt, C., & Kleine, T. (2017). The cosmic molybdenum-neodymium isotope correlation and the building material of the Earth. *Geochemical Perspectives Letters, 3,* 170–178.
Reufer, A., Meier, M. M., Benz, W., & Wieler, R. (2012). A hit-and-run giant impact scenario. *Icarus, 221,* 296–299.
Righter, K. (2003). Metal-silicate partitioning of siderophile elements and core formation in the early Earth. *Annual Review of Earth and Planetary Sciences, 31,* 135–174.
Righter, K. (2015). Modeling siderophile elements during core formation and accretion, and the role of the deep mantle and volatiles. *American Mineralogist, 100,* 1098–1109.
Righter, K., & Drake, M. J. (1999). Effect of water on metal-silicate partitioning of siderophile elements a high pressure and temperature terrestrial magma ocean and core formation. *Earth and Planetary Science Letters, 171,* 383–399.
Righter, K., Humayun, M., & Danielson, L. (2008). Partitioning of palladium at high pressures and temperatures during core formation. *Nature Geosci., 1,* 321–323.
Rizo, H., Boyet, M., Blichert-Toft, J., O'Neil, J., Rosing, M. T., & Paquette, J. L. (2012). The elusive Hadean enriched reservoir revealed by ^{142}Nd deficits in Isua Archaean rocks. *Nature, 491,* 96–99.
Rizo, H., Touboul, M., Carlson, R. W., Boyet, M., & Walker, R. J. (2013). Early mantle composition and evolution inferred from ^{142}Nd and ^{182}W variation in Isua samples. *Goldschmidt 2013, abstract*.
Rizo, H., Walker, R. J., Carlson, R. W., Horan, M. F., Mukhopadhyay, S., Manthos, V., et al. (2016). Preservation of Earth-forming events in the tungsten isotopic composition of modern flood basalts. *Science, 352,* 809–812.

Rosas, J. C., & Korenaga, J. (2018). Rapid crustal growth and efficient crustal recycling in the early Earth: Implications for Hadean and Archean geodynamics. *Earth and Planetary Science Letters, 494,* 42–49.

Roth, A. S., Bourdon, B., Mojzsis, S. J., Rudge, J. F., Guitreau, M., & Blichert-Toft, J. (2014). Combined 147,146Sm-143,142Nd constraints on the longevity and residence time of early terrestrial crust. *Geochemistry, Geophysics, Geosystems, 15,* 2329–2345.

Rubie, D. C., Melosh, H. J., Reid, J. E., Liebske, C., & Righter, K. (2003). Mechanisms of metal-silicate equilibration in the terrestrial magma ocean. *Earth and Planetary Science Letters, 205,* 239–255.

Rufu, R., Aharonson, O., & Perets, H. B. (2017). A multiple-impact origin for the Moon. *Nature Geoscience, 10,* 89–94.

Saji, N. S., Larsen, K., Wielandt, D., Schiller, M., Costa, M. M., Whitehouse, M. J., et al. (2018). Hadean geodynamics inferred from time-varying ^{142}Nd/^{144}Nd in the early Earth rock record. *Geochemical Perspectives Letters 7*, https://doi.org/10.7185/geochemlet.1818.

Schmalzl, J., Houseman, G. A., & Hansen, U. (1996). Mixing in vigorous, time-dependent three-dimensional convection and application to earth's mantle. *Journal of Geophysical Research: Solid Earth*, *101*, 21847–21858.

Solomatov, V. S. (2000). Fluid dynamics of a terrestrial magma ocean. In R. Canup & K. Righter (Eds.), *Origin of the Earth and Moon* (pp. 323–338). Tucson, TUS: University of Arizona Press.

Solomatov, V. S. (2007). Magma oceans and primordial mantle differentiation. In G. Schubert (Ed.), *Treatise on Geophysics 9* (pp. 91–120). Oxford: Elsevier.

Solomon, S. C. (1979). Formation, history and energetics of cores in the terrestrial planets. *Physics of the Earth and Planetary Interiors, 19,* 168–182.

Stevenson, D. J., & Halliday, A. N. (2014). The origin of the Moon. *Philosophical Transactions of the Royal Society A*, *372*, https://doi.org/10.1098/rsta.2014.0289.

Stracke, A., Hofmann, A. W., & Hart, S. R. (2005). FOZO, HIMU, and the rest of the mantle zoo. *Geochemistry, Geophysics, Geosystems 6*, https://doi.org/10.1029/2004gc000824.

Taylor, S. R., & McLennan, S. M. (1985). *The continental crust: Its composition and evolution*. Oxford: Blackwell.

Touboul, M., Kleine, T., Bourdon, B., Palme, H., & Wieler, R. (2007). Late formation and prolonged differentiation of the Moon inferred from W isotopes in lunar metals. *Nature, 450,* 1206–1209.

Trinquier, A., Birck, J. L., Allègre, C. J., Göpel, C., & Ulfbeck, D. (2008). ^{53}Mn-^{53}Cr systematics of the early Solar System revisited. *Geochimica et Cosmochimica Acta, 72,* 5146–5163.

Vockenhuber, C., Dillmann, I., Heil, M., Käppeler, F., Winckler, N., Kutschera, W., et al. (2007). Stellar (n, γ) cross sections of ^{174}Hf and radioactive ^{182}Hf. *Physical Review C, 75,* 015804.

Walker, R. J. (2009). Highly siderophile elements in the Earth, Moon and Mars: Update and implications for planetary accretion and differentiation. *Chemie der Erde—Geochemistry, 69*, 101–125.

Walker, R. J. (2016). Siderophile elements in tracing planetary formation and evolution. *Geochemical Perspectives, 5,* 1–2.

Warren, P. H. (2011). Stable-isotopic anomalies and the accretionary assemblage of the Earth and Mars: A subordinate role for carbonaceous chondrites. *Earth and Planetary Science Letters, 311,* 93–100.

Wetherill, G. W. (1980). Formation of the terrestrial planets. *Annual Review of Astronomy and Astrophysics, 18,* 77–113.

White, W. M. (2015). *Isotope geochemistry*. John Wiley & Sons.

Wiechert, U., Halliday, A. N., Lee, D. C., Snyder, G. A., Taylor, L. A., & Rumble, D. (2001). Oxygen isotopes and the moon-forming giant impact. *Science, 294,* 345–348.

Willbold, M., Elliott, T., & Moorbath, S. (2011). The tungsten isotopic composition of the Earth's mantle before the terminal bombardment. *Nature, 477,* 195–198.

Williams, J. P., & Cieza, L. A. (2011). Protoplanetary disks and their evolution. *Annual Review of Astronomy and Astrophysics, 49,* 67–117.

Wisdom, J., & Tian, Z. (2015). Early evolution of the Earth-Moon system with a fast-spinning Earth. *Icarus, 256,* 138–146.

Wood, B. J., & Halliday, A. N. (2005). Cooling of the Earth and core formation after the giant impact. *Nature, 437,* 1345–1348.

Yin, Q., Jacobsen, S. B., Yamashita, K., Blichert-Toft, J., Télouk, P., & Albarede, F. (2002). A short timescale for terrestrial planet formation from Hf–W chronometry of meteorites. *Nature, 418,* 949–951.

Young, E. D., Kohl, I. E., Warren, P. H., Rubie, D. C., Jacobson, S. A., & Morbidelli, A. (2016). Oxygen isotopic evidence for vigorous mixing during the Moon-forming giant impact. *Science, 351,* 493–496.

Zindler, A., & Hart, S. (1986). Chemical geodynamics. *Annual Review of Earth and Planetary Sciences, 14,* 493–571.

4 The Lunar Surface and Late Heavy Bombardment Concept

Abstract

As much as half of lunar surface rocks may have originated between 4.4 and 3.9 billion years and thus observations of, and samples from, Moon could attest to conditions then extant in the inner solar system. The concept of a lunar cataclysm at ~3.9 Ga grew from seemingly contradictory observations of elemental fractionation in lunar highland rocks. U–Pb—and some Rb–Sr—data suggested recrystallization occurred between about 4.0 and 3.8 Ga. The Late Heavy Bombardment (LHB) concept that emerged appeared supported by ~3.9 Ga $^{40}Ar/^{39}Ar$ "plateau ages" of lunar impact melt rocks, although no similar spike in ages was seen in the likely more globally distributed lunar meteorites. While the $^{40}Ar/^{39}Ar$ step-heating method can reveal intragrain isotope variations, this capability has several method-specific requirements that, if not met, preclude thermochronologic interpretations. Three such issues effectively rule out the use of virtually all lunar $^{40}Ar/^{39}Ar$ data as support for the LHB hypothesis: (1) the "plateau age" approach used is an aphysical concept for the thermally disturbed samples typical of most lunar impact melt rocks, (2) laboratory artifacts destroy preserved diffusion information, or create false apparent age gradients; and (3) obtaining meaningful thermal history information from extraterrestrial samples that have differing activation energies for Ar diffusion in their K-bearing phases requires a different laboratory protocol than was used on lunar rocks. Possibly due to these issues, no case in which multiple chronometric techniques have yielded intrasample concordancy of a lunar melt rock has yet been documented. Advancements in mass spectrometry now permit $^{40}Ar/^{39}Ar$ and U–Pb dating to be undertaken on small (10 s-of-µm diameter) in situ spots on glasses and accessory minerals in lunar rocks. This approach has the potential to transcend the analytical challenge posed by the continuous impact reworking of the lunar regolith that produces fine-scale polygenetic breccias of multiple age and origins. The longstanding assumption that lunar melt rocks originated from discrete, basin-forming events is obviated by lunar

T. M. Harrison, *Hadean Earth*, https://doi.org/10.1007/978-3-030-46687-9_4

imaging that show impact melts formed in small highland craters and clusters of 'light plains' deposits radiating outward >2000 km from large impact basins. The latter underscores how poorly the spatial relationships between large basins and their surrounding deposits were understood when impact chronologies were developed in the 1970s. The assumption that a specific lunar melt rock from a given landing site is representative of one of the basin-forming impacts is deeply flawed. Establishing a reliable, quantitative planetary impact chronology requires that all analyzed rocks be equally suitable for the application of specific chronometers. This may not be possible given the large contrasts in incompatible trace element distributions across the lunar surface (e.g., Procellarum KREEP terrane, South Pole Aiken basin). A conservative view of the lunar chronological record is that the large nearside basins are older than 3.82 Ga but these data are consistent with most of them being older than 3.92 Ga and possibly older than 4.35 Ga.

4.1 Introduction

Tectonic activity coupled with surface erosion continuously destroys or reworks terrestrial rocks such that their average age (both continental and oceanic crust) at Earth's surface today is only about 900 million years. Although we know of no terrestrial rocks older than 4.02 Ga, samples returned from the six Apollo lander missions suggest that perhaps half the lunar surface is older than that (Anand et al. 2015). Together with surface imaging, chronologic analysis of these samples and lunar meteorites (Korotev 2005) can potentially establish a record of the physical conditions within the Earth-Moon system throughout the Hadean eon. In particular, geochronologic data from lunar highlands rocks has been long interpreted to reflect a pulse of impact activity termed the Late Heavy Bombardment (LHB) that, as we've seen from Chap. 1 (Sect. 1.3), was widely proposed to define the lower bound of the Hadean (Cloud 1972; Harland et al. 1990; Gradstein et al. 2004; Bleeker 2004a, b; Moorbath 2005a, b; Van Kranendonk et al. 2012). Unfortunately, most published isotopic chronometry data for lunar samples are complex and multiply interpretable. Simplistic interpretations of such data can mask geologic complexity and impede progress toward a better understanding of the inner Solar System during the Hadean eon. In this Chapter, I deconstruct the longstanding community consensus regarding the lunar bombardment chronology and identify possible constraints on lunar history obtainable from geochronology and paleomagnetism.

4.2 Lunar Origin

Investigations resulting from Apollo-era explorations revealed that Moon comprises a ca. 40 km thick crust, an ultramafic mantle, and a small core, likely a metallic iron alloy (Shearer et al. 2006). The strong scatter of seismic energy in the lunar regolith and limited sensitivity of the Apollo-era instruments precludes a more accurate size estimate (Weber et al. 2011). The lunar surface exposes two different kinds of crust: an old anorthositic portion in the highlands nearly saturated with impact craters; and younger mare flood basalts occupying huge impact basins. The longstanding paradigm for this dichotomy is that crystallization of a lunar magma ocean culminated in a plagioclase-dominated floatation crust (Wood et al. 1970). The magma ocean phase appears to have ended by 4.51 Ga (Barboni et al. 2017; see Sect. 3.3). Later, impacts fractured that anorthositic crust producing large basins, most of which were subsequently flooded with mantle-derived lava to create the maria.

Over the past five decades, hypothesis tests of theories of lunar origin have largely rested on the following constraints:

1. Angular momentum: Moon carries most of the angular momentum in the Earth-Moon system. The total angular momentum, conserved in the absence of an external torque, is four times greater than in rotational form and highly anomalous compared to other planet/satellite ratios in the Solar System (e.g., most are ca. 0.01). Moon is also unique in being larger relative to the size of its host than any other satellite in the Solar System (Stevenson and Halliday 2014).
2. Isotopic data. The stable isotopic compositions (e.g., Ti) of lunar samples are, at ultrahigh analytical precision (± 3 ppm), identical to Earth's mantle (Zhang et al. 2012; Magna et al. 2017).
3. Low density. Moon has only 60% of Earth density which, together with seismic data, limits the size of its core to ca. 300 km radius.
4. Crustal dichotomy. As noted above, the lunar surface exposes both 4.0–4.4 Ga anorthositic highland rocks and younger ($\sim$3.8–3.1 billion years) mare basins (Wieczorek and Zuber 2001).
5. Tidal dissipation. On formation, Moon was perhaps 13 times closer to Earth than at present and continues to move away at $\sim$4 cm/year causing Earth's rotation to slow (Stevenson and Halliday 2014).

Four hypotheses have been proposed to explain Moon's origin:

The *capture hypothesis* postulates that Moon was gravitationally apprehended and bound to Earth. For this mechanism to be effective requires an extended atmosphere around primitive Earth (for which there is no direct evidence) that would have slowed the movement of passing planetary debris. While this hypothesis does not explain the highly volatile-depleted nature of Moon, it could be consistent with the isotopic homogeneity of the Earth-Moon system if, as Dauphas et al. (2014) argue, the inner Solar System inner was derived from the same portion of the nebular reservoir and thus share a similar starting chemistry (see Chap. 3).

The *co-accretion hypothesis*, which arose from a proposal by Schmidt (1944), supposes that Earth and Moon formed together as a double system from a primordial accretion disk. This view was consistent with Urey's (1952a, b) conclusion that lunar formation occurred at sufficiently low temperature as to retain a primary chondritic composition. In light of the Apollo-era discovery that Moon is strongly volatile depleted, the inconsistency of this hypothesis with the high angular momentum in the Earth-Moon system, together with the small size of the lunar core, essentially removed it from debate. Recent modelling, however, suggests plausible ways in which this might have occurred (Lock and Stewart 2017; see Sect. 3.3).

The *fission hypothesis*, as originally conceived by Darwin (1879), proposed that the equatorial centrifugal force on a rapidly spinning Earth initially matched that of gravitational attraction such that minor solar gravity perturbations separated the terrestrial tidal bulge into lunar orbit. This view fell into disfavor as dynamical complexities were subsequently revealed, but was recently resurrected in a somewhat different form: a late glancing impact hit a fast-spinning proto-Earth producing a disk derived primarily from Earth's mantle that coalesced to form Moon. A very fast-spinning early Earth-Moon system could lose angular momentum and reach its present state through an orbital resonance between the Sun and Moon that transfers angular momentum to Earth's orbit around the Sun (Cuk and Stewart 2012). This orbital transfer mechanism, or another with similar effect (e.g., Wisdom and Tian 2015), is consistent with the isotopic homogeneity and angular momentum of the Earth-Moon system.

The most widely accepted model for Moon's origin is the *impact hypothesis* (e.g., Hartmann and Davis 1975; Cameron and Ward 1976; Benz et al. 1986; Canup 2014). Its current incarnation (Cameron and Ward 1976; Canup and Asphaug 2001) proposes that a Mars-sized object impacted Earth very early casting debris beyond the Roche limit (the distance beyond which a large satellite would not disintegrate by tidal forces). This process would create enough heat to produce a global magma ocean leading to an anorthositic floatation crust. Under most impact scenarios, such an event would increase angular momentum in the Earth-Moon system. However, most calculations (cf. Canup 2004) showed that Moon would consist of more than 70% of the impactor and thus not easily explain the isotopic similarity between Earth and Moon (cf. Dauphas 2017). Alternatively, a "hit and run" scenario, steeper impact angle, collision into a rapidly spinning Earth, or succession of smaller collisions could potentially harvest terrestrial material into lunar orbit while satisfying the angular momentum constraint (see Sect. 3.3).

4.3 Impacts in the Early Solar System

Models of Solar System formation generally suggest that the terrestrial and Jovian planets had largely accreted from the solar nebula parent molecular cloud within 10 million years of initiation of its gravitational collapse, but that remaining debris continued to be swept up for many tens of millions of years (e.g., Chambers 2004). At least for the past ~3.6 Ga, the impactor flux to the inner Solar System appears to have been relatively stable with size-frequency distributions similar to that of the asteroid belt (Neukum et al. 2001). While early simulations (e.g., Safronov 1954; Wetherill 1975) could roughly produce the observed number of planets in our system, they were less successful at creating bodies the mass of Jupiter (Wetherill 1995; Lineweaver et al. 2002) and could not account for subsequent events, such as the Terminal Lunar Cataclysm (Tera et al. 1974), later called the Late Heavy Bombardment (LHB; Wetherill 1975). The LHB hypothesis posits that at about 3.9 Ga, a discrete, intense bolide flux to the inner Solar System impacted Moon and Earth. Given Earth's twenty times greater gravitational cross-section, such an episode would have had a profound effect on terrestrial habitability, with consequences thought to range from 'impact frustration' or complete planetary sterilization (Maher and Stevenson 1988; Sleep et al. 1989) to enhanced habitats for extremophiles (Abramov and Mojzsis 2009).

Despite the many chemical and isotopic similarities between Earth and Moon, they differ significantly in at least one respect that is likely related to an impact episode they don't share. As early Earth differentiated, it is assumed that most highly siderophile elements (HSE; e.g., Au, Pt, Pd) were drawn into segregating metallic phases that subsequently coalesced to form the core (see Sect. 3.2). However, the levels of highly siderophile elements in the modern mantle are orders of magnitude higher than that expected from silicate/metal partition experiments (e.g., Holzheid et al. 2000; Righter et al. 2008). This addition corresponds to about 0.5–1.5 of an Earth mass and is presumed to have arrived via impacts that post-dated core formation (Sect. 3.5). As noted above, Earth is expected to have acquired about twenty times more of this 'late veneer' than Moon (Kimura et al. 1974). However, the lunar late veneer amounts to less than one thousandth that of Earth (e.g., Day and Walker 2015), leading Sleep et al. (1989) to suggest that the terrestrial late veneer could have been acquired during a single impact. The size frequency distribution of asteroids is most consistent with Earth's late veneer having accreted from a single ca. 4000 km-sized impactor (Brasser et al. 2016; Genda et al. 2017). Given the expectation that such large planetesimals were rare in the early Solar System, Moon was statistically unlikely to have an equivalent encounter, thus explaining its lower HSE concentrations.

Alternatively, Kraus et al. (2015) argued that the relatively low shock pressure needed to vaporize planetesimal cores could be responsible for dispersal of iron and HSE's over the surface of proto-Earth. In contrast, the much lower abundances of lunar HSE's simply reflect a significantly lower retention of vaporized core material on Moon due to its lower escape velocity.

Tera et al.'s (1974) concept of an episodic cataclysm grew from observations of elemental fractionation in samples of the heavily cratered lunar highlands (Fig. 4.1). Specifically, U–Pb, and Rb–Sr data corresponded to apparent recrystallization ages between about 4.0 to 3.8 Ga. Although the parent/daughter behavior in these two geochronologic systems are quite different (i.e., both U and Sr are highly refractory while Pb and Rb have similar volatility, both revealed evidence of an isotopic

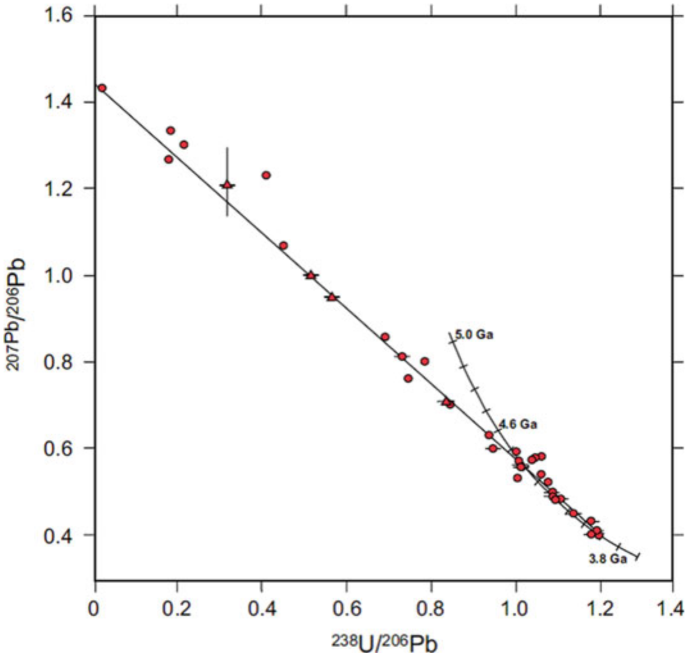

Fig. 4.1 U–Pb analyses of Apollo and Luna highland rocks (plus leachates and mineral separates) plotted on a concordia diagram yield a scattered array with apparent upper and lower intercept ages of approximately 4.4 and 3.9 Ga. Modified from Tera et al. (1974)

disturbance at ca. 3.9 Ga, albeit in different ways. While whole rock Rb–Sr systems appeared largely intact, the potassium-rich, interstitial groundmass, termed *quintessence,*[1] gave younger ages. For example, Apollo 17 sample 76,055, a recrystallized breccia, yielded an internal isochron age of 4.49 ± 0.05 Ga except for the coexisting quintessence which plotted on a line through the whole rock corresponding to an age of 3.86 ± 0.04 Ga. U–Pb analyses of samples of fifteen Apollo 14, 15, 16 and 17 rocks and soils (plus leachates, mineral separates and Luna 20 soils) array about a concordia slope with an apparent lower intercept age of ca. 3.9 Ga. There is notable scatter about the array but U-Pb analytical errors were not tabulated in Tera et al. (1974) precluding formal evaluation of uncertainty and MSWD. The contrasting results of the two isotopic systems represented something of a conundrum as Tera et al. (1974) interpreted Pb–U fractionation as due to Pb volatilization (perhaps as a halide) during metamorphism, but the undisturbed Rb–Sr whole rocks imply that Rb was not similarly affected (i.e., by yielding unrealistically old ages). They acknowledged that the lack of a mechanism to explain this differential behavior "remains a basic problem".

[1]A play on the Latin translation of Aristotle's hypothesized fifth element (*quinta essentia*) that forms the celestial realms.

Subsequently, the LHB concept came to be regarded as having been confirmed by $^{40}Ar/^{39}Ar$ geochronology of impact melt products found in lunar meteorites and samples returned by the Apollo and Luna missions (Fig. 4.2). Many studied samples were interpreted as yielding completely reset $^{40}Ar/^{39}Ar$ dates between 4.0 and 3.8 Ga (e.g., Turner 1977; Maurer et al. 1978; Dalrymple and Ryder 1993; Bogard 1995; Ryder et al. 2000; Cohen et al. 2000, 2005; Kring and Cohen 2002; Strom et al. 2005; Norman et al. 2006; Bottke and Norman 2017) caused by a significant increase in impactor flux during that interval. While some researchers continued to maintain that the large impact basins formed during a gradually decreasing impact flux (e.g., Hartmann et al. 2000; Chapman et al. 2007; Fassett and Minton 2013), the notion of a distinctive late impact event (Tera et al. 1974) became regarded as one of the most successful concepts to have emerged from the Apollo-era explorations. The concept had detractors (e.g., Baldwin 1974; Hartmann 1975) who argued that the lack of evidence of prior impact could have been erased by surface impact saturation and thus the accumulating age data instead reflect a slow decay of an initially intense bombardment era (Fig. 4.3).

In conjunction with geological inferences regarding the source regions for ejecta blankets found at the Apollo exploration sites, many of the $^{40}Ar/^{39}Ar$ dates for lunar impact melt breccias were then used to argue for specific ages of large impact basins. For example, Stöffler and Ryder (2001) recommended best estimates for the ages of the multi-ring basins and their related ejecta blankets (Nectaris, 3.92 ± 0.03 Ga; Crisium, 3.89 ± 0.02; Serenitatis, 3.89 ± 0.01 Ga; Imbrium, 3.85 ± 0.02 Ga) implying age accuracy of up to 0.25%. Such inferred ages in turn form the foundation for age calibrations of relative 'crater count' chronologies, used to establish surface histories of Moon and other Solar System bodies (e.g., Head 1976; Hartmann and Neukum 2001).

The collective suite of radiogenic chronologies, dominated by $^{40}Ar/^{39}Ar$ step-heating ages, inspired dynamical modelers to propose a series of explanations for a discrete episode of bombardment occurring relatively late in the evolution of the inner Solar System (Zappala et al. 1998; Ryder et al. 2000; Levison et al. 2001;

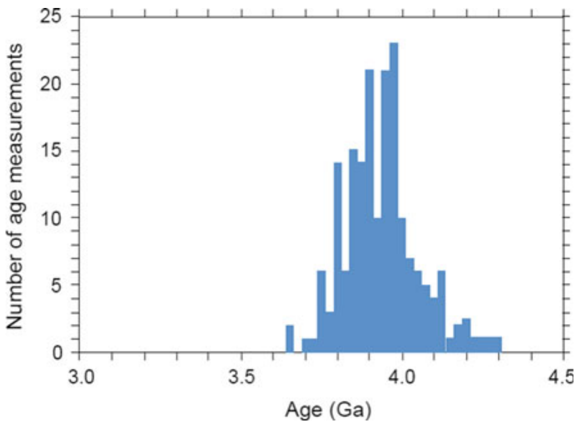

Fig. 4.2 Interpreted impact-reset $^{40}Ar/^{39}Ar$ and Rb-Sr ages of lunar highland rocks showing an apparent peak at ages between 3.8 and 3.9 Ga. Modified from Bogard (1995)

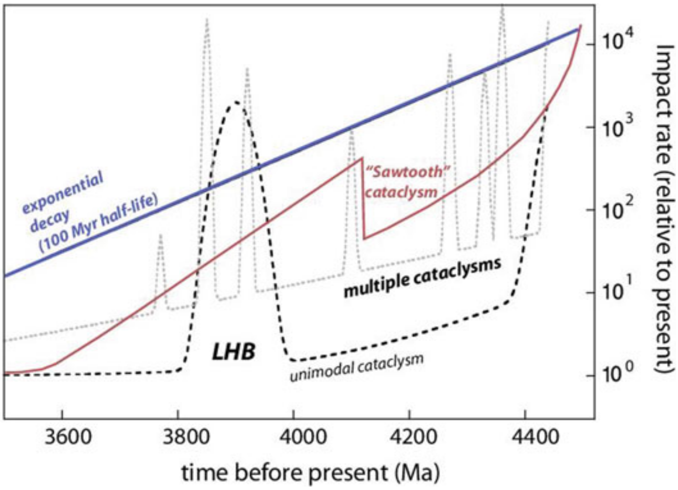

Fig. 4.3 Schematic diagram showing various possible impact histories that might be consistent with an apparent age spike in lunar rocks at ca. 3.9 Ga, including a slow decay from ca. 4.5 Ga with varying half-lives, and multiple, periodic cataclysms. Reproduced with permission from Zahnle et al. (2007)

Gomes et al. 2005). The "Nice model" (Gomes et al. 2005; Tsiganis et al. 2005) is based on dynamic simulations that track planetary evolution following the dissipation of the initial protoplanetary gas disk. Following ca. 600 Ma of planetary evolution, a fundamental shift in orbital resonance of the Giant planets caused a substantial disruption to the asteroid belt. In this scenario, the original, near-circular orbits of Jupiter, Saturn, Uranus, and Neptune were spaced more closely than present day. Gravitational encounters of planetesimals with Jupiter led to successive outward movements in the orbits of Uranus, Neptune, and Saturn. The cumulative effects of this migration led to Jupiter and Saturn to cross their 1:2 mean motion resonance, increasing their orbital eccentricities and destabilizing the configuration of the Jovian planets. This ultimately led to planetary debris scattering into the inner Solar System causing a sudden influx of massive impactors to the terrestrial planets. Later models assumed an LHB age of ∼4.1 Ga (Marchi et al. 2014).

The strong influence that the accumulated lunar $^{40}Ar/^{39}Ar$ dataset has had on the last 40 years of thinking about Solar System evolution warrants periodic critical examination of the assumptions underlying age interpretations. Surprisingly, such a response has been very limited, and arguably retrograde. In the latter regard, the pioneering studies that established $^{40}Ar/^{39}Ar$ as a viable dating method explicitly addressed the importance of diffusive $^{40}Ar^*$ loss in extra-terrestrial materials (Merrihue and Turner 1966) and devised corrections for partial resetting effects (Turner 1970; Turner et al. 1966). With rare exception (e.g., Shuster et al. 2010), this approach was abandoned over the intervening five decades. Instead, age significance was assigned to seemingly flat portions of lunar age spectra, termed "plateau ages", despite the highly disturbed nature of many of the release patterns (Sect. 4.7). Add to this both laboratory artifacts (McDougall and Harrison 1999; Sect. 4.8) and complexities arising from only recently understood diffusion phenomena (Boehnke et al. 2016; Sect. 4.8), and the need for a revaluation of the basis of the LHB hypothesis is evident. Thus I proceed by first introducing the reader to the $^{40}Ar/^{39}Ar$ age spectrum method and then deconstruct interpretations based on models that lack a sound physical basis.

4.4 The $^{40}Ar/^{39}Ar$ Dating Method

^{40}K (an alkaline metal) decays to both ^{40}Ca (an alkaline earth) or ^{40}Ar (an inert gas). The latter does not chemically bond in silicates so at mildly elevated temperatures (e.g., McDougall and Harrison 1999; Gardés and Montel 2009), Ar will tend to be lost from K-bearing minerals resulting in K–Ar ages younger than that of mineral formation. In the $^{40}Ar/^{39}Ar$ method, the sample is irradiated with fast neutrons to transform a portion of the ^{39}K atoms to $^{39}Ar_K$ via the $^{39}K(n,p)^{39}Ar$ reaction (see McDougall and Harrison 1999). Following irradiation, the sample is put in an ultrahigh vacuum system and heated to fusion to release Ar, which is then isotopically analyzed in a mass spectrometer. After correction of the measured isotope ratios for Ar produced by interfering neutron reactions and non-radiogenic ^{40}Ar, a radiogenic $^{40}Ar/^{39}Ar$ ratio is calculated. Because this ratio is proportional to the sample $^{40}Ar/^{39}K$, it can be calibrated to age by inclusion of a standard sample of accurately known K–Ar age along with the unknown during irradiation (McDougall and Harrison 1999).

Since the ratio of radiogenic daughter ^{40}Ar ($^{40}Ar^*$) to parent ^{40}K (via the $^{39}Ar_K$ proxy) is measured in a single isotopic analysis, an $^{40}Ar/^{39}Ar$ age can be measured more precisely and on smaller samples than a conventional K–Ar age. Furthermore, an irradiated sample can be heated in steps, eventually reaching fusion, that permits a series of apparent ages related to the amount of gas released at that step to be determined on a single sample (Fig. 4.4). This approach, known as the step-heating method, provides a wealth of additional information that can provide insights into the distribution of ^{40}Ar in the sample relative to the distribution of ^{39}K (and thus ^{40}K). In the ideal case, release of Ar in the laboratory vacuum extraction system occurs by diffusion as the sample is progressively heated. Thus, for a sample that has retained its ^{40}Ar since crystallization, both ^{40}Ar and ^{39}Ar likely occupy similar lattice sites as they have both been derived from potassium. In the likely case that the two isotopes have similar transport behavior, they will be degassed in similar proportions thus yielding an essentially constant $^{40}Ar/^{39}Ar$ ratio and age in each gas fraction extracted. A plot of the apparent $^{40}Ar/^{39}Ar$ age for each step against cumulative proportion of ^{39}Ar released (termed an "age spectrum") will yield a flat release pattern called a "plateau" (Dalrymple and Lanphere 1974) (Fig. 4.4a). Provided the underlying assumptions of the age spectrum method have been realized (i.e., phase stability throughout vacuum heating and Ar loss solely by diffusion), such a pattern can be interpreted to indicate that the sample always behaved as a closed system. In contrast, a sample that lost ^{40}Ar, say, during a thermal excursion associated with an impact, will have lower ratios of daughter ^{40}Ar to parent ^{40}K close to boundaries in which Ar can escape from the mineral host relative to those regions progressively further from diffusion boundaries (Fig. 4.4b). These differences may be revealed by variations in the $^{40}Ar/^{39}Ar$ ratio measured for gas fractions successively released from the sample, yielding a staircase-type pattern of increasing ages. The initially released $^{40}Ar/^{39}Ar$ ratio thus provides an estimate of the age of the thermal event (Last Heating Age; LHA) while the highest ratio in the gas released in the highest temperature steps yields a minimum age for the crystallization age, or complete resetting age, of the sample.

In contrast with the flat release patterns from which the plateau concept was first introduced (Dalrymple and Lanphere 1974; Fleck et al. 1977), lunar samples are rarely observed to have undisturbed age spectra. As can be gleaned from simple diffusion theory, once a K–Ar system has lost daughter ^{40}Ar, the oldest age in a staircase-type pattern will underestimate the rock-forming age (Fig. 4.4b). Even those cases in which an age spectrum reveals a truly uniform pattern of ages, potentially significant biases can be introduced that compromise interpretations. The simplest is the possibility that the effective length scale of Ar diffusion in a K-bearing phase (defined by grainsize or a sub-grainsize) has been reduced during sample preparation. Specifically, if a diffusion domain is broken during sample crushing, thereby exposing both grain surfaces and interiors, non-uniform distributions of $^{40}Ar^*$ created in Nature by diffusive loss will be homogenized during laboratory heating. In this way, a sample containing a profound internal gradient of $^{40}Ar^*$ will tend toward an apparently uniform 'plateau' age (McDougall and Harrison 1999). Thus internal age consistency across an age spectrum may either be evidence of closed system behavior or a signal that the experiment violated the underlying assumptions of the step-heating approach. Keep these points in mind later when you examine Fig. 4.11.

In those cases where an analysis can be shown to have met the requirements of the step-heating method, a variety of rules have been proposed regarding the minimum number of concordant age steps and the minimum proportion of the ^{39}Ar release required to define a plateau, and whether or not the chosen steps should be contiguous or define an isochron (see review in McDougall and Harrison 1999). But by framing the definition of a plateau in terms of a community convention rather than in purely physical terms, an element of subjectivity was introduced that opened the possibility that the true chronological information in a $^{40}Ar/^{39}Ar$ system could be obscured. As Norman et al. (2006) noted in context of dating Apollo 16 impact breccias, "Interpreting plateaus as crystallization ages can be somewhat arbitrary". This raises a fundamental question arising from a rules-based approach is: What is the basis on which an age step could be excluded from consideration of a plateau in an undisturbed sample? That this question has never been explicitly addressed in the literature is a measure of the extent to which this community compact has prevailed, although the approach has not been without its critics.

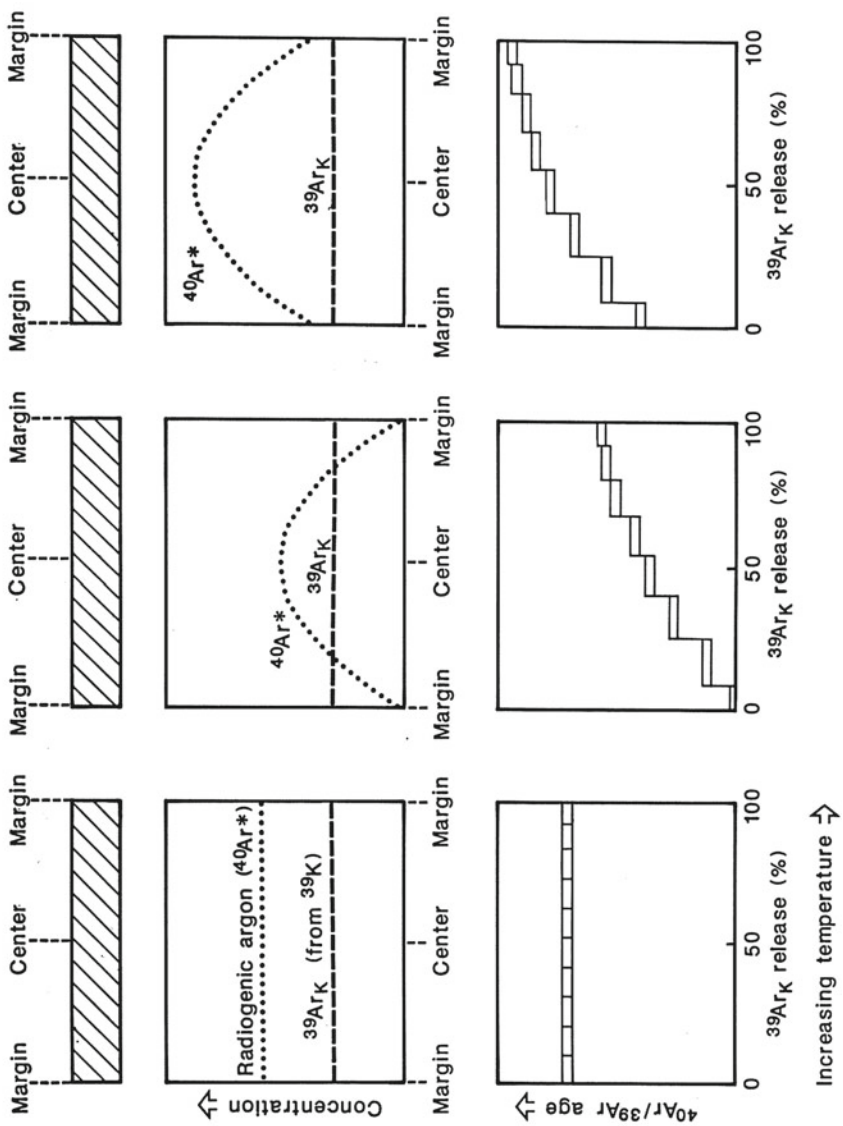

Fig. 4.4 The top diagram in each panel portrays an idealized crystal in cross section, the middle diagram the concentration of radiogenic ^{40}Ar ($^{40}Ar^*$) and neutron induced $^{39}Ar_K$ across the crystal, and the lower diagram the expected $^{40}Ar/^{39}Ar$ age spectrum for Ar extracted in successive steps. **a** The case of a system undisturbed since formation and rapid cooling. **b** The case in which partial loss of $^{40}Ar^*$ has occurred from the crystal in geologically recent times such that there is a marked gradient of $^{40}Ar^*$across the crustal from essentially zero at the boundary. **c** The same case as in *b* except that significant accumulation of $^{40}Ar^*$ has occurred since the reheating event owing to the passage of time. A maximum for the time of the reheating is given by the $^{40}Ar/^{39}Ar$ age for the gas release in the first step of the experiment and a minimum age of the formation of the crystal is given by the apparent age of the last gas released. Reproduced with permission from McDougall and Harrison (1999)

McDougall and Harrison (1999) noted that the lack of a physical basis for the plateau gives “the method somewhat elastic properties. Having defined a plateau, it is then incumbent on us not to apply the approach too literally”.

4.5 Thermal Effects of Impacts

Numerical simulations (Collins 2002) and analogue experiments (e.g., Schultz and Gault 1985) show that impact cratering occurs in three stages: contact, excavation, and collapse (Grieve et al. 2006; Collins et al. 2012). In the absence of an atmosphere, a projectile will strike the surface of a target at velocities equal to or greater than escape velocity of the target body (i.e. lunar escape velocity = 2.4 km/s). At the point of contact, two shock waves are generated that propagate into both the impactor and the target creating, at relevant velocities, pressures greater than >10 s of GPa. Release waves subsequently propagate inward releasing pressure along a near-adiabatic path (the Hugoniot) that can translate to temperatures sufficient for melting, or even vaporization. The initial kinetic energy is partitioned between thermal energy added to the target and the ejected material (Melosh 1989). Residual momentum behind the shock wave results in the excavation of material in a hemispherical path, creating a deep bowl at the surface many times larger than the impactor. In relatively low energy collisions, where target temperatures do not exceed the solidus, rebound of this bowl-shaped feature can lead to decompression melting. In general, however, the major source of melt production in a lunar impact scenario is from the shockwave itself. Melt sheets produced in this fashion can either remain within the crater or be ejected from it (Marchi et al. 2014). Heat from the melt sheets conducts into adjacent rock raising temperature and potentially disturbing isotopic systems, by, for example, causing radiogenic ^{40}Ar to diffuse out of potassium-bearing minerals (Young et al. 2013; Mercer and Hodges 2017).

4.6 The Lunar Highlands Impact Record

The heavily cratered lunar highlands, covered by a many kilometer thick megaregolith of brecciated material, is the exposed remnant of early lunar differentiation (Taylor et al. 2006). That is, the highlands comprise rocks thought to represent primordial lunar crust and may be an analog for a similar process that led to formation of the first felsic crust on Hadean Earth (see Sect. 5.1). The majority of the samples recovered from the highlands are complex breccias, commonly exhibiting breccia-in-breccia textures. There is also ample evidence of impact-induced melting and multiple impact events, although a number of ‘pristine’ rock fragments have been recognized (Warren 1985). Some $^{40}Ar/^{39}Ar$ ages provide evidence that at least a few portions of the lunar surface have not been thermally disturbed since 4.35 ± 0.05 Ga (Dominik and Jessberger 1978; see summary in

McDougall and Harrison 1999). This raises the question, what proportion of the lunar highlands was isotopically reset during a relatively brief LHB? The principal problem in addressing that question is that evidence for a ca. 3.9 Ga cataclysm comes largely from sites representing less than 4% of the lunar surface (Warren 2004), clustered in the central nearside which was significantly influenced by just three or four basin-forming impacts (Imbrium, Serenitatis, Nectaris and possibly Orientale) (Fig. 4.5). Lunar meteorites, which likely also sample different parts of Moon than were accessed by past human and robotic explorations (Gladman et al. 1995), show a relatively broad and uniform distribution of $^{40}Ar/^{39}Ar$ ages from 2.5 to 4 Ga (e.g., Cohen et al. 2000, 2005) strongly suggesting that the returned Apollo samples are unrepresentative of the global lunar age distribution.

If Apollo-era samples are insufficient to define a global cataclysm, do they at least have the capacity to date the major nearside impact basins? Of the six Apollo sample return missions, the first two were situated in maria whereas the last four investigated regions of lunar highland basement. The criteria that led to the targeting of those sites implicitly assumed that dateable stratigraphic relationships could be found in what appeared to be coherent rock formations. Specifically, it was assumed that the

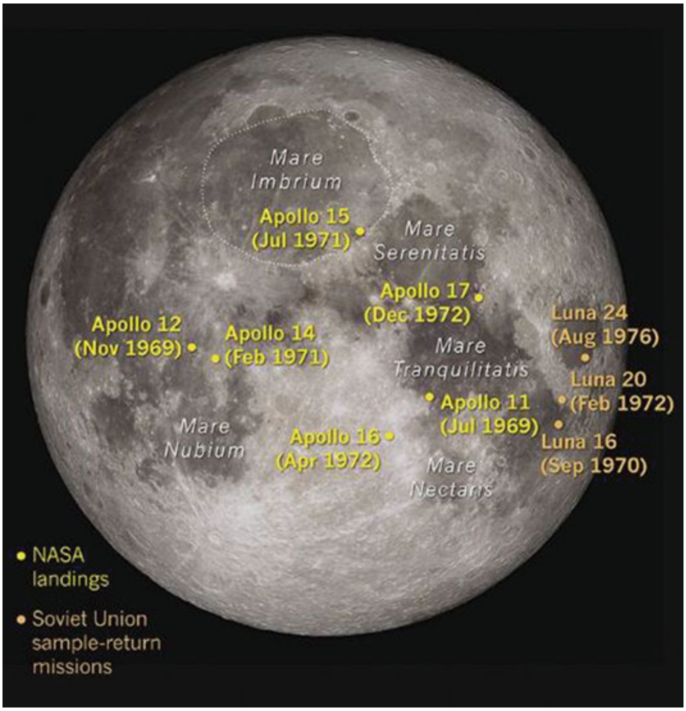

Fig. 4.5 Image of the lunar nearside showing locations of the Apollo and Luna lander missions with five major impact basins identified. Historically, Apollo 16 was thought to sample Imbrium, Apollo 15 Serenitatis, and Apollo 16 Nectaris. Reproduced with permission from Mann (2018)

process of ejecting molten debris from nearby basin-forming impacts fully reset radiogenic chronometers thus forming dateable chronostratigraphic units which correspond to the age of basin formation. In 1971, the first of the highland missions, Apollo 14, landed ~500 km from the edge of the Imbrium crater in the Fra Mauro Formation (Fig. 4.5). This formation had been mapped remotely from Earth-based telescopes and appeared to be widely distributed across the nearside of Moon (Wilhelms 1965, 1970). As such it would provide a stratigraphic marker separating pre-Imbrium rocks from younger deposits as well as the age of the melt rocks thus establishing an absolute chronostratigraphic framework for lunar evolution. In a report defining targeting criteria for the Apollo highland landers, Binder and Roberts (1970) wrote: "The Fra Mauro is a stratigraphic unit which consists of the material ejected from the Imbrium basin. This site is excellent in terms of the level 2 criteria" which requires that "individual mission sites must be chosen to represent homogeneous provinces". The specific location of the Apollo 14 landing site was chosen to be adjacent Cone Crater, a small, youthful impact feature, that was expected to have excavated fresh rock from beneath the lunar regolith.

Apollo 15 landed on the mare near the frontal scarp of the Apennine Mountains, which was interpreted as the boundary of the Imbrium Basin (Fig. 4.5). Apollo 16 and Apollo 17 both landed on lunar highlands, the latter at the eastern rim of the Serenitatis basin about 750 km from the Apollo 15 landing site (although two melt rocks from Apollo 15 were assumed to be from the Imbrium impact; Bottke and Norman 2017). In general, material sampled by Apollo 14 and 17 were interpreted as Imbrium and Serenitatis melt ejecta, respectively, while units from the Apollo 16 site were seen as deposits from Imbrium and Nectaris (see below).

While the above inferences appeared sensible starting points in the early 1970s, by 1974 serious concerns with the chronostratigraphic model had arisen as deeper knowledge of the lunar near-surface developed in the wake of investigations of lunar highland deposits. In particular, the underlying assumption implicit in the targeting of Apollo highland lander sites was that dateable stratigraphic relationships in seemingly coherent rock formations, such as Fra Mauro, could lead to clear insights into the absolute timing of basin forming events. Rather, it became clear that the upper few kilometers of highland crust is typically characterized by a ejecta from multiple basin-forming events mixed with surface materials and continuously reworked by later, smaller impacts producing dominantly breccia-in-breccia textures (Fig. 4.6). Atop this km-scale 'megaregolith' (Fig. 4.7), numerous local impacts modified the upper ca. 10 m to produce a fine-grained regolith. Megaregolith breccias are, in essence, sedimentary rocks containing clasts for which no stratigraphic information is preserved. This recognition led to the counterintuitive view that geochronology should be the preferred tool to guide and test stratigraphic interpretations. However, interpretting isotopic age data from bulk dating methods was complicated by Oberbeck et al.'s (1974, 1975) conclusion that ejecta from major basin forming events was in most cases subsequently intermixed with material derived from local, medium-sized impacts. This effect increases in proportion with distance from the basin forming event and thus was seen as significant for the distal Apollo 14 and 16 sites.

Fig. 4.6 Apollo 14 sample 14,306,21, illustrates the polymict nature of lunar brecccias. The rock is about 6 cm across. The crystalline matrix breccias are thought to be from the Fra Mauro Formation. Note the black glass vein which likely formed from a late impact. NASA photo no. 77-22103

Crater ejecta models can yield surprisingly varied results. While early models applied to the Apollo 16 site supported the view that nearby Nectaris was the principal source of ejecta, with Imbrium contributing relatively little (McGetchin et al. 1973; Head 1974), Oberbeck et al. (1974) concluded that the Imbrium was the dominant basin that modified the Apollo 16 region. Using a refined model accounting for both basin ejecta and megaregolith mixing, Petro and Pieters (2006) found coequal abundances (ca. 10%) of primary ejecta from the Imbrium, Serenitatis, and Nectaris basins in the Apollo 16 regolith with equal fraction from other impact basins with close to two-thirds of the rock being derived from ancient highlands crust.

Although it was long assumed that lunar melt rocks had to have originated in large, basin-forming events, images from the Lunar Reconnaissance Orbiter Camera (LROC) documented impact melt deposits in lunar highland craters as small as 170 m (Plescia and Cintala 2012) (Fig. 4.9). LROC images have also radically altered other longstanding assumptions about the distal distribution of impact debris from basin-forming events. For example, a global map showing clusters of 'light plains' deposits (Meyer et al. 2016, 2018) radiating outward more than 2000 km from the rim of the $\sim$930 km diameter Orientale Basin (Fig. 4.10) underscores how poorly the spatial relationships between large basins and their surrounding deposits were understood when impact chronologies were being developed in the 1970s. Thus the assumption that a specific lunar melt rock from a given landing site is representative of one of the basin-forming impacts is deeply flawed; a lunar grab sample could be from a basin-forming impact, a tiny, inconsequential impact of arbitrary age, or a mixture of those materials. And, of course, impacts are not the only source of heat early in lunar history capable of resetting K–Ar systematics. For example, juvenile basaltic magmatism began early on Moon and continued episodically for more than three billion years (Ziethe et al. 2009) (Fig. 4.8).

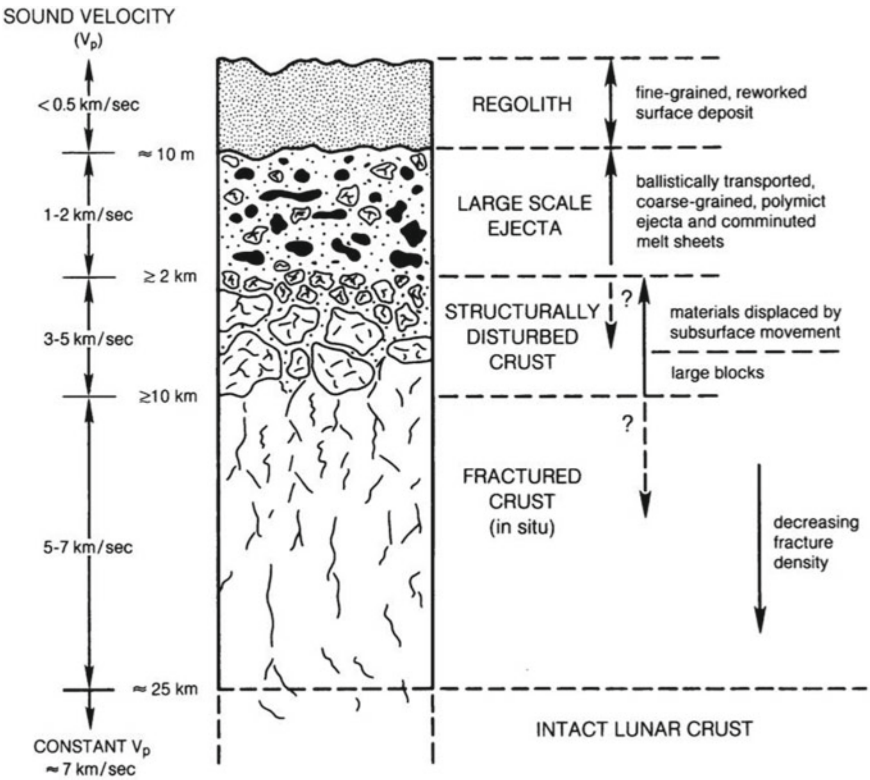

Fig. 4.7 Conceptual cross section showing effects of large-scale cratering on the shallow lunar crust as inferred from surface observations and seismic velocity measurements. Note that the depth scale remains uncertain. Reproduced with permission from Hörz et al. (1991)

So it's clear that the early assumption that coherent lunar rock formations contain simple chronostratigraphic relationships was incorrect, but what about the associated premise of ejecta deposits containing fully reset radiogenic chronometers? Schaeffer and Schaeffer (1977) recognized that the breccia matrix typically did not fully degas during impact shock and heating and thus that $^{40}Ar/^{39}Ar$ ages of molten felsic clasts could be masked by an older component. A case study that illustrates these complications well is provided by the thoughtful analysis of $^{40}Ar/^{39}Ar$ analyses of Apollo 16 and 17 highland rocks, and an Apollo 17 mare basalt, by Turner and Cadogan (1975). The basalt yielded an age of 3.78 ± 0.04 Ga which they took as "a well-defined lower limit to the bombardment". They criticized the general lack of petrological integration in lunar dating studies stating "…a large number of rather precise ages of highland rocks have been obtained over the past few years. Unfortunately, the precision of ages is not matched by any precise understanding of the events to which they refer". Specifically

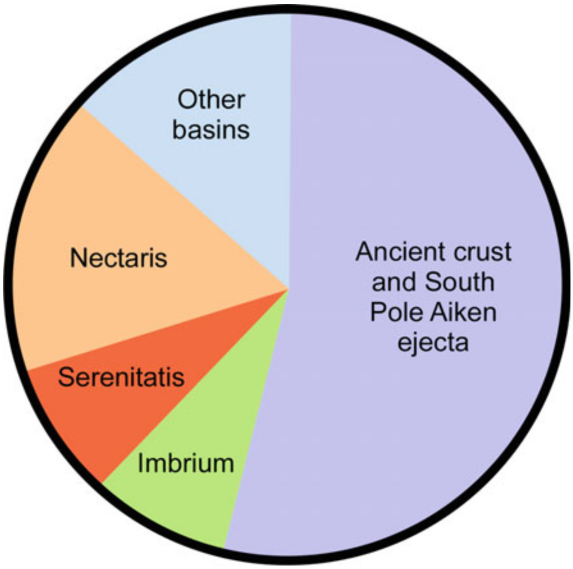

Fig. 4.8 Results of crater ejecta model for Apollo 16 lander site showing that, contrary to an initial assumption that this site would be dominated by ejecta from Nectaris, it likely contains coequal abundances of primary ejecta from Imbrium, Serenitatis, and Nectaris, with nearly two-thirds derived from ancient highlands crust and other basins. SPA = South Pole Aiken crater. Reproduced with permission from Pietro and Peters (2006)

they noted that "it is tacitly assumed that, at the sites so far sampled, the age distribution is dominated by these events and that the effects of local smaller cratering events are of secondary importance. The possibility of alternative interpretations, in which the ages reflect the outgassing resulting from the much larger number of medium-sized cratering events…individual ages cannot be realistically assigned to specific event and the age distribution must be interpreted statistically". Turner and Cadogan (1975) noted the "basic assumption made by most authors in connection with Imbrium is that the Apollo 14 site is dominated by Imbrium ejecta, which generally leads to the conclusion that the age of 3.95 Ga…represents an upper limit to the time of the Imbrium event". Indeed, Chao (1973) found that "The geochronologic clocks of fragments in the Fra Mauro Formation, with textures ranging from unannealed to strongly annealed, were not reset or strongly modified by the Imbrian event. Strongly annealed breccia clasts and basalt clasts are pre-Imbrian, and probably existed as ejecta mixed with basalt flows in the Imbrium Basin prior to the Imbrian event". It must be clear at this point in the discussion that the view that the Fra Mauro Formation is solely an annealed Imbrium ejecta blanket is almost certainly incorrect (Spudis 1993, Merle et al. 2014; Snape et al. 2016) (Fig. 4.9).

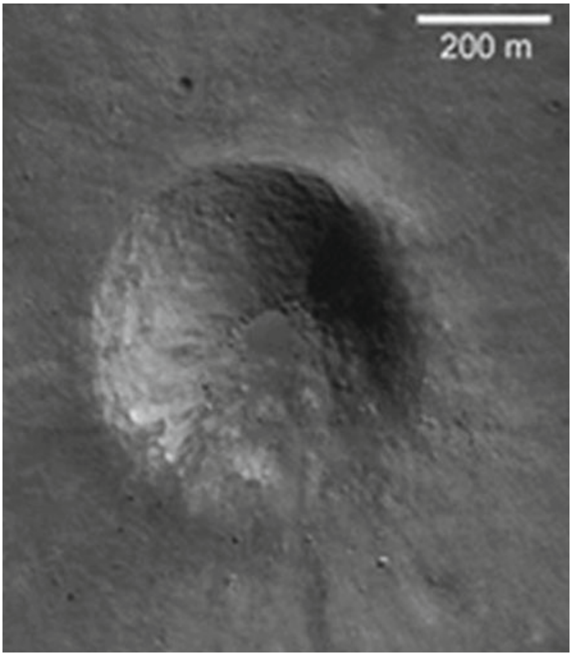

Fig. 4.9 Lunar reconnaissance orbiter camera images showing impact melt deposit (flat, uncratered region) in floor of a lunar highland crater less than 200 m across. Clearly, lunar melt rocks are not solely a consequence of major basin forming impacts. Reproduced with permission from Plescia and Cintala (2012)

However, the $^{40}Ar/^{39}Ar$ data presented in Turner and Cadogan (1975) range from one simple age spectrum (e.g., isochronous at 4.22 ± 0.04 Ga over >90% of gas release; 78,115) to a range of variably disturbed patterns. Implicit in their interpretation of these release patterns in terms of impact history is that an impact event completely resets the $^{40}Ar/^{39}Ar$ dating system. While this will surely be true within an impact melt sheet, pure melt rock is rare among investigated lunar samples. Furthermore, the diffusive thermal halo produced outside the crater produces a uniform probability distribution of ^{40}Ar loss (Boehnke 2016). That is, the fraction of material that experienced between 1 and 99% loss is essentially equal and thus disequilibrium should be at least as common as complete re-setting following an impact. But for the moment, let's accept the assumption that rock forming ages can be inferred from such data, although we'll later describe significant problems with this view that were then unknown to those authors in the 1970s.

Although Turner and Cadogan (1975) suggested that a special case might be made that the large proportion of chemically similar melt rocks from the Apollo 17 site was consistent with a single nearby event (i.e., the Serenitatis cratering event), they argued on statistical grounds "*that the 3.9–4.0 Ga cluster represents at least two events* (conceivably it may represent many more)" (see Sect. 4.11.2). Thus the picture that emerges from the early days of Apollo sample $^{40}Ar/^{39}Ar$ dating is of sensible hypotheses being framed in context of mission targets. That, for example, ages of impact ejecta from the Apollo 17 site would date the formation age of the Serenitatis basin. However, recent imaging shows that the Apollo 17 impact melts

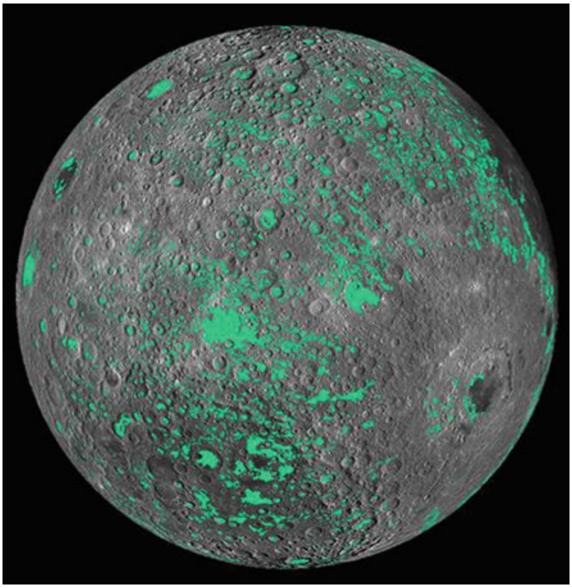

Fig. 4.10 Lunar Reconnaissance Orbiter Camera image (Meyer et al. 2018) showing 'light plains' deposits radiating out more than 2000 km from the rim of Orientale Basin (lower right). From lroc.sese.asu.edu/posts/1016

may not sample the Serenitatis basin-forming impact but instead could contain significant debris from Imbrium (Spudis et al. 2011) (Fig. 4.10).

Despite the above-mentioned complications and limitations of using lunar highland samples to directly date basin-forming events, a consensus supportive of those underlying assumptions emerged through the 1980s that had the effect of removing them from critical scrutiny (see Bottke and Norman 2017, for an historical review).

4.7 Assignment of Lunar $^{40}Ar/^{39}Ar$ Plateau Ages

Quite independent of the problematic nature of using polymict breccias returned from the Apollo missions to constrain lunar stratigraphic relationships, the lack of a basis in physical theory for the prevailing interpretive model of $^{40}Ar/^{39}Ar$ step-heating data, as well as numerous significant analysis artifacts fundamental to lunar samples, opens the possibility that the chronologic information content of lunar K–Ar systems has been seriously misinterpreted over many decades. Interpreting $^{40}Ar/^{39}Ar$ dating of meteorite and lunar samples as impact ages in the vast majority of cases has involved assigning plateau ages (Sect. 4.4) rather than using either total fusion ages or inferring corrected ages from diffusion modeling. The literature is vast but virtually all relevant criticisms are exemplified in two studies well-regarded by Bottke and Norman (2017) that used 1) $^{40}Ar/^{39}Ar$ analyses of Apollo 17 glass-bearing samples in an attempt to establish the age of the Serenitatis basin (Dalrymple and Ryder 1996), and 2) $^{40}Ar/^{39}Ar$ data from Apollo 16 impact melt breccias to infer the influence of four discrete impact events (Norman et al. 2006).

Norman et al. (2006) $^{40}Ar/^{39}Ar$ dated twenty-nine Apollo 16 samples comprising 846 individual heating steps, but used only 37% of these data in their construction of plateau ages (Fig. 4.11). In some cases, replicate splits could not be reproduced but drew no further comment. For example, sample 63,525 yielded two plateaus regarded as "good" or "excellent" but differed considerably from one another (3.895 ± 0.036 vs. 4.190 ± 0.024 Ga). While Norman et al. (2006) identified correlations between sample petrology and chemistry and age, the arbitrary nature by which ages were assigned diminishes confidence in their conclusions (Fig. 4.11). For example, in assigning an age for the mafic poikilitic class of samples, only half of the steps in the seven age spectra were used in the calculation.

Dalrymple and Ryder (1996) undertook $^{40}Ar/^{39}Ar$ step-heating analyses of Apollo 17 phenocryst-bearing melt rocks, aphanitic melt rocks, melt clasts, and granulite and gabbro clasts. Their twenty-three samples comprise 1047 individual step heating analyses. Significantly, in light of the earlier discussion of the definition of a plateau (Sect. 4.4), less than a third of these data were used to calculate plateau ages. None of their release patterns approximates that expected from closed system behavior (McDougall and Harrison 1999) and over three-quarters of their age spectra have patterns indicative of ^{40}Ar loss subsequent to 3.4 Ga (thus potentially reducing the age of the oldest components present). Dalrymple and Ryder (1996) stated that they were "conservative in selecting plateaus, choosing to exclude steps rather than to include them if there is doubt" but did not explain why isochroneity in middle portions of anomalous release patterns would necessarily define an impact age. Arguably, the conservative option was instead to assume that the bulk $^{40}Ar/^{39}Ar$ age of a reworked regolith sample represents a lower bound on the age of formation.

Contrast these studies with the rare case in which diffusion theory was used to interpret lunar $^{40}Ar/^{39}Ar$ data. Shuster et al. (2010) undertook high-resolution measurements on seven splits of Apollo 16 regolith and found age spectra whose high temperature gas release corresponded to ages between 3.9 and 4.2 Ga. All samples shared an age spectrum form that indicated they had experienced ^{40}Ar loss due to subsequent heating. Diffusion modelling to those spectra showed that all observations were consistent with ^{40}Ar degassing due to a brief thermal event at 3.3 Ga that likely corresponds to a local impact that mixed preexisting ejecta units. This observation underscores a point made earlier—that the least ambiguous signal of impact heating in lunar samples comes from the $^{40}Ar/^{39}Ar$ ratio of the initially released gas, or Last Heating Age. Such subsequent events have the effect of reducing the apparent age of the gas released at the higher laboratory extraction temperatures from which plateau ages would be estimated. A review of the literature suggested to Shuster et al. (2010) that such episodic pulses in the impactor flux are common in the inner solar system. When coupled with the underappreciated effects of smaller, local impacts on $^{40}Ar/^{39}Ar$ systematics in major ejecta blankets (e.g., Turner and Cadogan 1974), this effect has the potential to lead to significant misestimates of the age of those deposits.

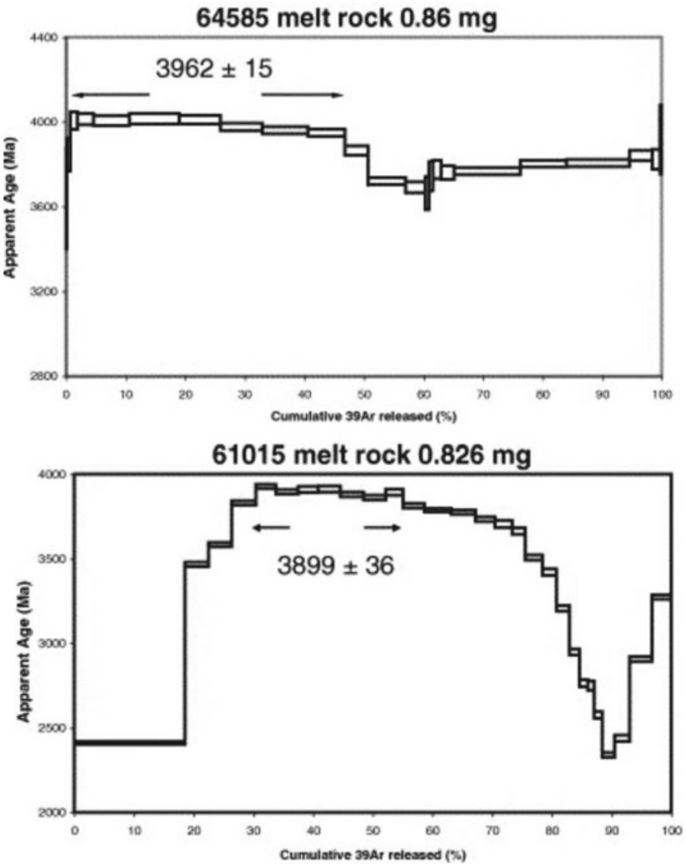

Fig. 4.11 The lower $^{40}Ar/^{39}Ar$ age spectrum was regarded by as a "Fair" plateau, although only 7 of the 29 steps constituting ¼ of gas release was used. The plateau in upper figure was judged as "Good" with 8 of 23 steps being utilized. In either case, there is no physical basis to select between any of the steps to determine a rock forming age. The misbehavior of the age spectra relative to that expected from simple theory is sufficient reason to abandon attempts to estimate impact ages from disturbed lunar $^{40}Ar/^{39}Ar$ age spectra. Reproduced with permission from Norman et al. (2006)

4.8 Laboratory Artifacts and Diffusion Effects

As noted earlier, lunar $^{40}Ar/^{39}Ar$ step-heating results, a pivotal source of evidence for the LHB, may be biased not only by sampling limitations and aphysical plateau theory, but analysis artifacts as well. Specifically, the complexity of analyzed lunar samples (multiphase materials containing a non-uniform distribution of grain sizes) has not been rigorously interpreted in terms of diffusion, recoil and/or multi-activation energy effects that have the potential to produce misleading artifacts. Ironically, most of these artifacts were clearly identified in the lunar context shortly after the end of the lunar sample return missions (Hunecke 1976). Instead, many ca. 3.9 Ga 'plateau ages' ages are arbitrarily assigned (more on this shortly) belying the fact that the vast majority of samples have bulk ages much younger or older than the interpreted age (e.g., Culler et al. 2000; McDougall and Harrison 1999; Boehnke and Harrison 2016). Below, a brief primer on the interpretation of $^{40}Ar/^{39}Ar$ dating is followed by a description of the three interconnected issues that collectively preclude interpreting results of this method in terms of impact histories.

Lunar samples are appealing targets for $^{40}Ar/^{39}Ar$ dating in that they are anhydrous and generally very ancient. The former is significant because K-bearing lunar phases are stable up to very high temperatures during vacuum heating, the latter because the method is based upon the accumulation of radiogenic ^{40}Ar so the antiquity of lunar samples generally ensures the accumulation of sufficient radiogenic ^{40}Ar for reasonably precise $^{40}Ar/^{39}Ar$ dating (McDougall and Harrison 1999). On the downside, lunar rocks are typically very low in potassium (and thus accumulate radiogenic ^{40}Ar slowly with time), of typically mixed provenance (brecciated samples are typically admixtures of rocks of differing origins), contain non-uniform grain sizes and fine-grained phases (and thus are susceptible to other laboratory artifacts, such as nuclear recoil), and contain K-bearing phases with contrasting activation energies for Ar diffusion (and thus not amenable for simple age spectrum interpretation; McDougall and Harrison 1999; Harrison et al. 1991; Boehnke et al. 2016). Although models to quantitatively assess multi-domain, diffusive ^{40}Ar loss have been applied to terrestrial samples since Lovera et al. (1989), their use on extra-terrestrial materials has been surprisingly limited.

The recoil energy of ^{39}Ar produced by the $^{39}K(n,p)^{39}Ar$ reaction during neutron irradiation typically results in a mean displacement of ~ 0.1 μm. Early studies of lunar samples recognized that ^{39}Ar recoil transfer could be expected to affect age spectra of samples in which potassium is principally located in fine-grained phases adjacent to potassium-poor minerals (Turner and Cadogan 1974). This can result in creation of more than one apparent plateau in the same age spectrum in the likely case where the two phases have differing Ar diffusion behavior. In extreme cases, apparent ages older than the Solar System can result (Jessberger and Dominik 1979; cf. Villa et al. 1983), in which case identification of the pathologic behavior is straightforward. However, this effect can also produce smoothly varying $^{40}Ar/^{39}Ar$ age gradients that could be misinterpreted as containing meaningful chronological information (McDougall and Harrison 1999).

Boehnke et al. (2016) recognized that radiogenic ^{40}Ar is held in two dominant phases in many extraterrestrial samples—plagioclase and clinopyroxene. Because activation energies for Ar in these phases differ substantially (Cassata et al. 2009, 2011), they developed a multi-activation energy, multi-diffusion domain model and applied it to $^{40}Ar/^{39}Ar$ temperature-cycling, step-heating data for meteorite and lunar samples. They showed that non-ideal, complex age spectra for extra-terrestrial materials—commonly interpreted as indicative of either laboratory artifacts or localized shock heating of pyroxene—are, in fact, meaningful and can be understood in context of the presence of multi-diffusion domains with multiple activation energies. However, they demonstrated that the form of an age spectrum of a sample containing more than one activation energy for Ar diffusion was an artifact of monotonic laboratory heating; the presence of multiple Ar activation energies dictates that an $^{40}Ar/^{39}Ar$ age spectrum is a function of both the natural and laboratory heating histories rather than an intrinsic property of the sample. Only by using temperature cycling during laboratory analysis is it possible to derive appropriate kinetic parameters and thermal histories. Unfortunately, to date, all other $^{40}Ar/^{39}Ar$ age spectrum analyses of lunar rocks have involved monotonic heating while only a rare few are known to contain a single activation energy (e.g., Albarede 1978).

If, at this point, the reader is wondering if it would make more sense to abandon step-heating in favor of the $^{40}Ar/^{39}Ar$ laser microprobe approach (e.g., Mercer et al. 2015; Sect. 4.11.1), the answer is surely yes. The spatial specificity of that method permitting ages to be related to melt textures can provide unambiguous age information, even in samples of mixed provenance. While it is not possible to recover Ar diffusion kinetics from the laser microprobe method, such information is superfluous if the chronological system remained closed. That said, recent results using in situ methods (see Sect. 4.11) appear to yield confusing or contradictory results.

4.9 Can Peaks in Histograms of Lunar $^{40}Ar/^{39}Ar$ Step-Heating Ages Date a Cataclysm?

Putting aside for the moment the serious concerns that have been raised regarding the use of $^{40}Ar/^{39}Ar$ plateau ages of lunar samples to date impact events, the question arises: If $^{40}Ar/^{39}Ar$ plateau ages actually yielded valid chronological information, could they then uniquely define an episode of heavy bombardment on Moon? Assuming that apparent ages are produced and destroyed by random impacts which occur at an exponentially decreasing rate (i.e., the probability of survival of an age is related to the total number of craters formed from that moment to the present), Hartung (1974) found that a crater-production-rate half-life of 0.07 Ga yielded an $^{40}Ar/^{39}Ar$ age distribution that broadly matched the observed histogram. To examine how well histograms of plateau ages represent the actual impact record and its support of an LHB-type event, Boehnke and Harrison (2016) took this approach a step further by reinterpreting the lunar $^{40}Ar/^{39}Ar$ data using a model that describes $^{40}Ar^*$ diffusive loss during post-formation heating events. Their model, which accounts for partial resetting, permits an assessment whether or not $^{40}Ar/^{39}Ar$ data can, even in principle, act as evidence for an impact spike or if the apparent spikes are simply artifacts due to episodic crust formation. Boehnke and Harrison (2016) assumed that the lunar crust formed in a relatively brief interval between about 4.3 and 4.5 Ga and that subsequent impacts onto that surface systematically reduced $^{40}Ar/^{39}Ar$ ages by diffusion processes. They compiled a large number (267) of Last Heating Ages (i.e., the last time a sample had been thermally disturbed) and, under a range of assumptions about the form of ^{40}Ar loss and using only monotonically decreasing impact fluxes, found apparent age peaks that were a robust feature of their simulations. That is, the nature of the evidence used to define the Late Heavy Bombardment has an intrinsic tendency to create apparent, but illusory, age spikes that can mistakenly be interpreted in terms of bombardment history. Apparent age spikes between 3.5 and 4 Ga seen in compilations of dated H-chondrites and HED meteorites (Bogard and Garrison 2003; Bogard 2011; Marchi et al. 2013; Swindle et al. 2014), also previously interpreted in terms of impact activity, appear to have a similar cause.

Michael et al. (2018) similarly revisited lunar K–Ar ages with a view to determining if they support the LHB concept. While they took a very different approach to Boehnke and Harrison (2016), they also concluded that the data are not consistent with a lunar-wide impact event at ca. 3.9 Ga. Specifically, they utilized several longstanding lunar ^{40}Ar/^{39}Ar databases in which interpreted "plateau" ages are the form of the chronological information. As noted previously, these compilations are compromised by aphysical selection criteria that lead to arbitrary age assessment. Michael et al. (2018) added a further criterion of dubious value by using, in cases where multiple ages were obtained from the same sample, "the age value with the smallest error bars". As noted previously, isochroneity is only a useful concept in ^{40}Ar/^{39}Ar age spectrum interpretation for samples that have remained closed K–Ar systems. Unsurprisingly, they found an overall strong age peak centered on 3.87 Ga which their modelling suggested could be a record of a late bombardment event. However, that same model predicts that such a signature should be a universal feature of all near lunar surface samples. Instead, prominent 3.87 Ga peaks are only found in Apollo 14 and 15 samples. Apollo 16 and 17 sites yield more complex age distributions and, as noted earlier, the distribution of lunar meteorite ages (likely a more random spatial sample) shows no such peak. Both observations appear to Michael et al. (2018) inconsistent with the LHB hypothesis. They argued instead that this discrepancy is due to a bias from oversampling Imbrium basin ejecta (Apollo 14 and 15) and that those with more complicated signatures contain ejecta from Nectaris (Apollo 16) and Serenitatis (Apollo 17). Michael et al. (2018) concluded that evidence supports formation of "local terminal cataclysms" between 3.87 and 4.25 Ga with other basins (most importantly South Pole-Aitken) as yet undated.

Bottke and Norman (2017) stated that because "pronounced clustering of lunar melt rock ages in the interval typically associated with the Terminal Cataclysm is apparent in diverse isotopic systems, including Rb–Sr, Sm–Nd, U–Pb, and ^{40}Ar/^{39}Ar", the "excellent agreement obtained by multiple techniques provides confidence that the ages are meaningful". They did not, however, specifically point to an example of such concordancy. Indeed, the next section well documents age discordance between coexisting U–Pb and ^{40}Ar/^{39}Ar systems in lunar rocks. Lunar basalt sample 14,310, found half buried in lunar soil and thus not linkable to the Fra Mauro Formation, has been cited informally as an exemplar of such concordancy (e.g., Barbara Cohen to Adam Mann, December 2017, pers. comm.). Although

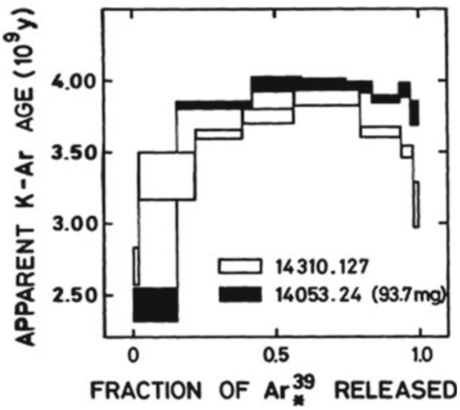

Fig. 4.12 Although $^{40}Ar/^{39}Ar$ ages for 14,310 (white blocks) range over a billion years, a 'plateau' age of 3.88 ± 0.06 Ga was inferred from the single step in the mid portion of ^{39}Ar release. There is no physical basis from which to conclude that this age represents that of rock formation (see text). Reproduced with permission from Stettler et al. (1973)

different ^{87}Rb decay constants were in use at the time, five separate international groups dated 14,310 by the Rb–Sr method within uncertainty to 3.90 Ga (see Meyer 2009). In particular, Mark et al. (1974) obtained a relatively precise Rb–Sr age of 3.94 ± 0.03 Ga. 14,310 proved not to be amenable to U–Th–Pb dating (Tatsumoto et al. 1972). However, $^{40}Ar/^{39}Ar$ ages for 14,310 (Fig. 4.12) range over a billion years (e.g., Stettler et al. 1973) and the total fusion K–Ar age of 3.63 Ga is clearly discordant to the Rb–Sr results. Recently, Haber et al. (2017) undertook $^{176}Lu–^{176}Hf$ mineral isochron dating of 14,310 and obtained a neutron-corrected crystallization age of 4.01 ± 0.06 Ga, clearly statistically distinct from, and older than, the weighted mean age of the five Rb–Sr dates. Not to belabor the point, but I remain unaware of any lunar highland rock that yields 'excellent agreement obtained by multiple techniques'.

4.10 The Nice Model Revisited and the LHB in Decline

An underappreciated consequence of a late LHB Nice model are the instabilities that at imposes on the terrestrial planets, possibly leading to their annihilation (Brasser et al. 2009; Clement et al. 2019). The recent understanding (Nesvorný et al. 2018) that the Jupiter Trojan binaries would not have survived if the giant planets' instability occurred later than 100 Ma into the history of the solar system, as well as structural details of Kuiper Belt objects and aspects of Neptune's evolution, led to reinvestigations (Deienno et al. 2017; de Sousa Ribeiro et al. 2020) of aspects of the Nice model. These studies found that an instability of the giant planets within a few tens of millions years of nebular collapse was far more likely to have occurred than the conditions required to maintain planets in stable orbits for hundreds of millions of years (as needed for the late Nice model). Clement et al. (2018) found that models most consistent with the structure of the inner solar system (e.g., that yield the correct mass of Mars) arise when the giant planet instability occurs during primary accretion of the terrestrial planets, or within 10 Ma of dissipation of the primordial gas disk. Subsequent modeling led Clement et al. (2019) to further reduce their preferred timing for the instability to within one million years following dispersal of the gas disk.

Many longstanding supporters of the LHB, including progenitors of the 'Nice' suite of models have abandoned the concept (e.g., Michael et al. 2018; Zellner 2017; Deienno et al. 2017; cf. Nesvorný et al. 2018; de Sousa Ribeiro et al. 2020; see Mann 2018), at least in part reflecting the accumulating concerns of the classical interpretation of lunar geochronologic data. Alexandro Morbidelli, the father of the Nice model, admits that the early models took fine-tuning to get the instability to occur so late. He no longer believes in a late LHB ("My prediction is people will abandon the cataclysm"; Mann 2018), particularly having reconciled the low lunar HSE concentrations with a monotonically declining bombardment flux (Morbidelli et al. 2018; Zhu et al. 2019). Even Bottke and Norman (2017) recently concluded that "The strongest version of the Terminal Cataclysm hypothesis in which all of the lunar basins formed within a brief interval ($\leq$200 Ma)…can be excluded as a viable hypothesis".

In a paper entitled "History of the Terminal Cataclysm Paradigm: Epistemology of a planetary bombardment that never (?) happened", Hartmann (2019) reviews the evolution of this debate and the degree to which the tentacles of the hypothesis still influence allied disciplines:

> Given that the four-decade acceptance of the "classic terminal cataclysm" paradigm is declining, if not collapsing, it is disturbing to find that papers from biological, climatic, and terrestrial geological communities, not to mention textbooks, popular-level articles, and press releases continue to invoke the putative cataclysm as a constraint on their interpretations and models of life's origin and geologic/climatic evolution. Thus, analysis focusing on the epistemology and history of the terminal cataclysm paradigm seems timely, if not overdue. How did the cataclysm ideas arise? Why were they so widely accepted? When did contrary ideas arise? Why did they have little effect?

This exhaustive treatment hints at similar sociological effects to those that fed the enduring appeal of a hellish Hadean and the reader is directed to the relevant sections in Chaps. 1 and 12 (Sects. 1.1, 12.1, 12.2, 12.5) for my speculative answer to Hartmann's (2019) last question above.

4.11 In Situ Geochronologic Studies

4.11.1 ^{40}Ar/^{39}Ar Laserprobe Dating

Advancements in mass spectrometer sensitivity and extraction system backgrounds now permit ^{40}Ar/^{39}Ar dating to be undertaken on small (10 s of micron diameter) spots on thin sections using a laser to degas irradiated samples (see review in McDougall and Harrison 1999). Mercer et al. (2015) undertook laser microprobe dating of two Apollo 17 impact melt breccias. While one sample yielded evidence of a single melt-forming event at 3.83 ± 0.02 Ga, data from the second yielded texturally correlated age peaks at 3.81 ± 0.01, 3.66 ± 0.02 and ca. 3.3 Ga (Fig. 4.13). Note that these ages are significantly younger than that ascribed to Serenitatis by Turner and Cadogan (1975) and Stöffler and Ryder (2001). Incidentally, in an earlier study of the same sample, Grange et al. (2009) presented U–Pb dates for various accessory minerals which they interpreted as indicative of two older generations of impact melt produced at 4.335 ± 0.005 and 3.934 ± 0.012 Ga.

Mercer et al. (2015) emphasized the unlikelihood that this fine-scale chronology could have been obtained using the step-heating method and underscores the profound limitations in interpreting $^{40}Ar/^{39}Ar$ step-heating ages of bulk breccia samples.

4.11.2 U–Pb Accessory Mineral Dating

An alternative approach to $^{40}Ar/^{39}Ar$ step-heating to assess lunar impact ages is in situ U–Pb dating of U-bearing phosphate minerals using a Secondary Ion Mass Spectrometer (SIMS), often referred to as an ion microprobe. Thiessen et al. (2017) dated phosphates from Apollo 17 breccias and found a restricted range of ages of 3.920 ± 0.003 Ga, 3.922 ± 0.005 Ga, and 3.930 ± 0.005 Ga; all significantly older than the 'best estimate' of 3.89 ± 0.01 Ga for Serenitatis (Stöffler and Ryder 2001). While in principal the ion microprobe has the potential to resolve spatial variations in the daughter to parent ratio (i.e., Pb/U), and thus evaluate the assumption of closed system behavior, only $^{207}Pb/^{206}Pb$ ages were reported in this study. That in itself does not preclude observing lateral age variations but the high uncertainties on individual measurements led the authors to average numerous dates to obtain overall weighted means, in much the same way Mercer et al. (2015) did in their laser microprobe study of Apollo 17 breccias. Thiessen et al. (2017) recognized that their analyzed phosphates likely originated from different source rocks, but assumed that their $^{207}Pb/^{206}Pb$ ages were reset at the time of the breccia forming event. They based this assumption on what they characterized as the low closure temperatures of the U–Pb system in phosphates of 450–550 °C, which "should result in significant Pb mobility during an impact event and complete Pb loss". However, closure temperature is exponentially dependent on the timescale of heating. The 450–550 °C estimate assumes cooling rates of 1–10°C/Ma for the grainsizes used (Cherniak et al. 1991) whereas likely rates during breccia formation are of the order 10^9°C/Ma. Since virtually all lunar breccias include subsolidus material, the complete isotopic equilibration of Pb in phosphate minerals appears an unlikely consequence of impact mixing (Young et al. 2013).

Thiessen et al. (2017) concluded that the observed ~10 Ma spread in ages between their chemically and texturally different samples is evidence of three distinct impact events. It is unclear how they reconciled their result with the

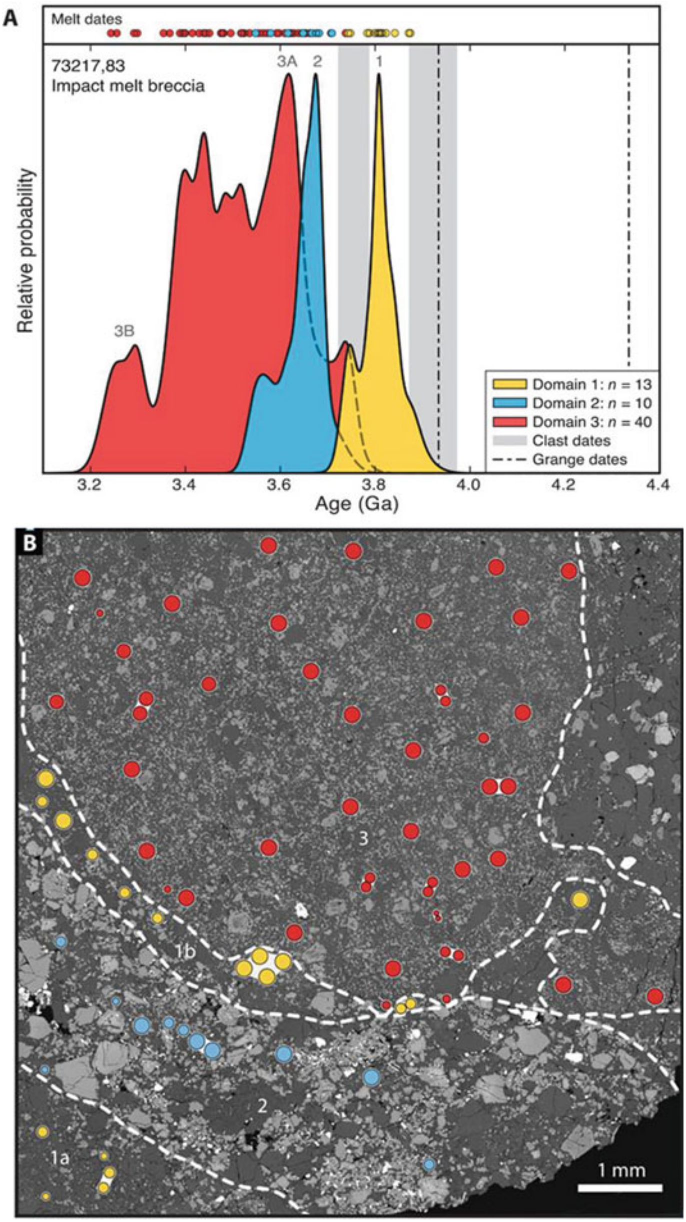

Fig. 4.13 (top) $^{40}Ar/^{39}Ar$ laserprobe ages, color coded by textural position, of an Apollo 17 impact melt breccia. Locations of age clusters are shown on the micrograph (bottom). This sample yields three distinctively different age domains which vary over 500 Ma. A remarkable aspect of this result is the apparent lack of resetting that the latter introduced melts appear to have had on earlier ages. Reproduced with permission from Mercer et al. (2015)

abovementioned study of Mercer et al. (2015) who found significantly younger ages from Apollo 17 melt rocks as Thiessen et al. (2017) made no mention of that study in their paper. Such contradictory conclusions from two, recent, in situ chronologic studies whose ages span more than a billion years, underscores the provenance complexity of Apollo 17 impact breccias (Oberbeck et al. 1974; Plescia and Cintala 2012). This discordant behavior also raises the possibility that any mineral-specific chronologic approach presents an implicit mineralogical bias. That is, that a method based solely on phosphate minerals can only provide impact chronologies on melt rocks that were saturated in that phase during the heating event (see Sect. 4.11.3).

The results of Thiessen et al. (2017) appear to create a substantial problem for the traditional view that Serenitatis is the sole source of the Apollo 17 breccias. Furthermore, these ages are similar to those inferred from dating Apollo 14 phosphates (Snape et al. 2016), possibly from the Imbrium impact, and Apollo 12 impact melt breccias (Liu et al. 2012). Thus, unless all major impact basins between Serenitatis and Imbrium formed within a ~10 Ma time span, in contradiction of the conventional view of lunar stratigraphy as well as the previous interpretations of ^{40}Ar/^{39}Ar plateau ages, one might conclude that no Apollo 17 breccia is derived from Serenitatis impact ejecta. Indeed, the same concern goes for all of the data from all of the landing sites.

Zhang et al. (2018) dated zircons from Apollo 17 sample 73,155 using SIMS and obtained a weighted mean ^{207}Pb–^{206}Pb age of 3.928 ± 0.010 Ga. The concordancy of this age with the interpreted ^{40}Ar–^{39}Ar plateau age of one sample of 73,155 of 3.937 ± 0.016 Ga (Dalrymple and Ryder 1996) was cited as evidence that the Apollo 17 site was substantially influenced by Imbrium ejecta rather than Serenitatis. However, as alluded to earlier (Sect. 4.7), the total gas ^{40}Ar/^{39}Ar ages of the four samples of 73,155 that Dalrymple and Ryder (1996) dated range over 240 Ma and are as young as 3.67 Ga. The average %^{39}Ar used for the calculation of the plateaus is only 30%, thus over two-thirds of the gas release was ignored in their age determinations.

There is no more reason to believe that Snape et al. (2016) or Zhang et al. (2018) actually dated the Imbrium impact than that Mercer et al. (2015) or Thiessen et al. (2017) or Snape et al. (2016) dated the Serenetatis impact. These collective studies and others all appear to have dated distinctive melt components that include, and go beyond (both above and below), the nominal age range for the LHB. The notion that we can uniquely ascribe any date, no matter how precise, to a particular basin-forming impact with a confidence in accuracy of 0.25% (Stöffler and Ryder 2001) is unsupported by the evidence. Can an educated guess be made based on U–Pb age consistency—did Imbrium form at 3.93 ± 0.01 Ga (e.g., Grange et al. 2009; Thiessen et al. 2017)? I suppose, but it remains just that—a conjecture—which is a weak basis on which to build the solar system cratering chronology.

4.11.3 Petrothermal Considerations in Interpreting U–Pb Accessory Mineral Ages

Accessory minerals such as apatite or zircon tend to concentrate parent U over daughter Pb during their formation thus making them attractive U–Pb selenochronometers. However, establishing a reliable, quantitative impact chronology requires that all candidate target rocks be equally amenable to producing the dateable phase. In the case of K–Ar dating, the broad presence of at least trace amounts of potassium in lunar rocks provides a somewhat level playing field, although rocks with a significant KREEP component (see below) will tend to have higher signal-to-noise ratios. However, there is an underappreciated aspect of the use of accessory minerals in dating lunar events, or for that matter any other planetary body, that limits their value in establishing global phenomena.

The presence of accessory phases in a melt depends dominantly on its thermal state and chemistry. In regard to the latter, zircon solubility in metaluminous melts is governed by the molar parameter M = [(Na + K+2Ca)/(Al·Si)] and Zr concentration, whereas apatite solubility is proportional to SiO_2 and P_2O_5 abundances (Watson and Harrison 1983; Harrison and Watson 1984). Stability of these two phases appears unaffected by pressure or water content (Boehnke et al. 2013; Harrison and Watson 1984). Zircon and apatite can form in magmas generated by both volcanic and impact processes so are not diagnostic of a particular mechanism. Because not every pair of target rock composition and impact condition can lead to formation of either of these two phases, there is an inherent bias implicit in using them to establish impact chronologies. That is, only melts of appropriate chemistry and thermal history will produce crystals large enough (i.e., >10 μm) for in situ chronologic investigation. For example, melts of mafic composition (M > 2.5) close to the anhydrous liquidus require unavailably large Zr contents to stabilize zircon (e.g., 4.5% Zr at 1225°C for M = 2.6; Boehnke et al. 2013). Melts that cool very rapidly will grow only microcrystalline apatite unless that phase was stable on the liquidus, requiring very high P concentration (e.g., 3.6% P_2O_5 at 1080°C for 40% SiO_2; Green and Watson 1982). Thus whole suites of melt rocks will simply not have the appropriate chemistry or thermal history to produce these phases in a manner suitable for dating and thus cannot preserve a record of a given impact event. Indeed, as discussed in Sect. 8.7.2, impacts are unlikely to be the primary source of lunar zircons (Taylor et al. 2009; Wielicki and Harrison 2015).

As discussed in more detail in Sect. 8.7.2, the incompatible trace element enriched KREEP component (i.e., potassium-, rare-earth-element-, phosphorous-rich), produced in the late stage of fractional crystallization of the lunar magma ocean, is the likely source of the high levels of P and Zr needed to crystallize magmatic apatite and zircon. Using Lunar Prospector gamma-ray spectrometry data, Gillis et al. (2004) found globally heterogeneous K and Th (two incompatible elements) distributions across the lunar surface, ranging from 0 ppm Th and 190 ppm K on the northeastern far side, to 11 ppm Th and 4300 ppm K in the Fra Mauro Formation (see Sect. 4.6). In general, the anorthositic highland terranes are low in incompatible elements whereas the Procellarum KREEP-rich terrane

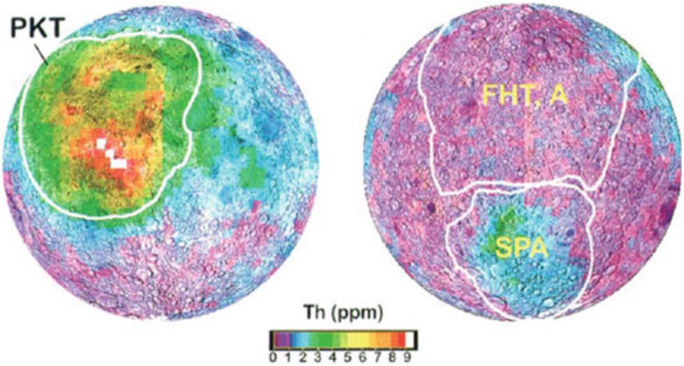

Fig. 4.14 Th concentration map draped over a global relief image of Moon. Outlined regions include Procellarum Kreep Terrane (PKT), anorthositic central region of Feldspathic Highlands Terrane (FHT,A) and South Pole-Aitken Terrane (SPAT). The PKT boundary is drawn at the 3.5 ppm Th boundary. Reproduced with permission from Jolliff et al. (2000)

(Jolliff et al. 2000), which contains both highlands and volcanic rocks, is characterized by high values (Fig. 4.14). Thus impacts into these KREEP-rich rocks would tend to form zircon, apatite and other dateable accessory minerals relative to most other lithologies.

4.12 Moon as a Repository of Early Earth Materials

Based on distinctive isotopic, mineralogic or chemical characteristics, both martian (Bogard et al. 1984) and lunar (Marvin 1983) meteorites have been recovered on Earth. Their existence is testament that interplanetary transfer of rock can occur following large impacts. Likewise, large terrestrial impacts can have launch velocities close to or greater than the escape velocity, potentially transferring Earth materials to Moon. Moon is currently about 60 Earth radii from Earth but was probably about one-third of that distance at the close of the Hadean eon (Zharkov 2000). Assuming a broadly exponentially declining impactor flux, Armstrong et al. (2002) calculated that orbital transfer of terrestrial materials to Moon would have averaged 7 ppm since $\sim$3 Ga and been markedly higher prior to that time.

While 7 ppm may seem a small amount, consider that our primary "mine" for Hadean zircons is the quartzite at Jack Hills. This rock contains about 100 ppm Zr and thus zircon constitutes only about 10^{-4} by weight of the rock. Given that >4 Ga grains are only a couple of percent of the zircon population, an average lunar highlands rock could potentially hold more terrestrial material than the Jack Hills quartzite does Hadean zircons. The place to start looking for this evidence is in the $\sim$400 kg of lunar samples returned from the lunar surface as Armstrong et al. (2002) estimate that about 3 g of terrestrial material could be present. How might terrestrial material be identified within lunar surface samples? Discovery of bedded siliceous or carbonate sediments, microfossils, or banded iron formation would, for example, be immediately distinctive of an Earth origin. However, the similarity in isotopic compositions between Earth and Moon across an array of elements (see Sect. 4.2) removes a powerful genetic signature, and some rocks types could be common to planet and satellite alike. Based on its relatively low formation temperature under oxidized conditions, Bellucci et al. (2019) argued that a "granite" clast from an Apollo 14 breccia could be a fragment of a terrestrial meteorite, potentially making it the first known 4.32 Ga (Meyer et al. 1996) terrestrial rock.

4.13 What Else Can We Learn About the Hadean from the Lunar Rock Record?

4.13.1 Lunar Magnetism

One of the clearest results that emerged from Apollo-era exploration was evidence indicating a high degree of lunar differentiation (i.e., the anorthositic highlands and magma ocean produced KREEP), which stood in contrast to the longstanding view that Moon coalesced cold from chondritic materials (e.g., Urey 1952a, b). This latter view reflected the view that the low lunar mass could not provide sufficient gravitational potential energy release to melt rock in the deep interior, and the giant impact hypothesis had not yet been formulated (i.e., Benz et al. 1986). But is Moon fully differentiated? Its moment of inertia (0.392) is so close to that of a sphere of uniform density (0.400) as to call into question the existence of a lunar core (Gapcynski et al. 1975). While the low resolution data provided by Apollo-era seismometers left open the possibility of a small core, modern data processing methods have permitted detection of a solid inner and fluid outer core, the latter of which may still be $\sim$60% liquid (Weber et al. 2011).

Moon today does not generate a measurable magnetic field at its surface, but magnetic studies of lunar rocks are interpreted to indicate that it possessed a core-driven dynamo from 4.25 to at least 2.5 Ga, although the mechanisms responsible remain unclear (Shea et al. 2012; Tikoo et al. 2017). Given the small size of the lunar core (ca. 4% by mass), it seems unlikely that such a long-lived lunar dynamo could be powered by thermochemical convection driven by secular cooling. Even more surprising is that the intensity of the natural remanent magnetism of lunar samples implies a magnetic strength at the then lunar core-mantle boundary (CMB) forty times higher than that at Earth's CMB today. Several alternate mechanisms have been proposed to explain this, including core stirring from mantle precession when Moon was close to the Roche limit (see Sect. 3.3) and transient plasmas generated by meteoroid impacts on the lunar surface (Hood and Artemieva 2008). The latter model, which if correct would mean that paleomagnetic measurements may have no geophysical significance with respect to processes operating in planetary interiors, appears to have been shown to be implausible

(Weiss & Tikoo, 2014), in part as such an effect has not been observed in terrestrial impact craters.

The relevance of a lunar magnetic field to this book's theme is the possibility that Earth-Moon could have exchanged ionized gases early in solar system history. Specifically, could a more proximal Moon with high surface magnetism have attracted Earth atmosphere via ionized gases along field lines, or could ion flows from the atmosphere of a non-magnetic Earth be implanted into the lunar surface (Ozima et al. 2005)? If early interactions between Earth's atmosphere and the near-side lunar surface implanted terrestrial atmospheric gases in lunar soils, they could preserve a record of, for example, when biotic oxygen began to accumulate in Earth's atmosphere (Seki et al. 2001; Ozima et al. 2008). This proposal was given some support from recent observations (Terada et al. 2017) of low energy O^+ ions transported moonward during the five days of each lunar orbit when it is shielded from solar wind bombardment by Earth's magnetosphere. They conclude that biogenic terrestrial oxygen is currently been implanted into the lunar surface and may have done so for billions of years. These studies hold the promise of the lunar surface storing information of ancient terrestrial atmospheric gas composition that might be able to address the onset timing of Earth's geodynamo, the rise of oxygen in the atmosphere, and the dynamical evolution of the Earth-Moon system.

4.14 Critical Summary

Lunar differentiation leading to formation of its crust occurred by 4.51 Ga (Barboni et al. 2017), requiring formation of Moon within the first ~60 million years of solar system history. The paradigm of a lunar magma ocean that culminated in creation of an anorthositic floatation crust (Wood et al. 1970) has stood largely unchallenged for nearly 50 years and appears to well-describe most observations. Moon subsequently experienced intense bombardment by impactors perhaps as big as ~1000 km but the timing of that history has come under intense scrutiny. Confidence that Moon experienced a ca. 100 Ma pulse of bombardment at ca. 3.9 Ga has significantly eroded in light of four lines of inquiry. The first is clear evidence that lunar highland melt rocks used to establish a radiogenic chronology typically contain multiple generations of impact melts, have little or no stratigraphic context, and can be formed by small impacts. Thus age variations in samples from Apollo lander sites may reflect either local events or basin-forming impacts. The second is recognition that interpretation of $^{40}Ar/^{39}Ar$ dates for lunar melt rocks is much more complex than originally thought. Specifically, assigning plateau ages based on aphysical criteria together with underappreciated laboratory artifacts and diffusion effects virtually preclude histograms of selected $^{40}Ar/^{39}Ar$ dates of having chronological meaning regarding impact history. The third is that, even if the first two of these concerns were not at issue, the nature of most evidence used to define the Late Heavy Bombardment has an intrinsic tendency to create apparent, but illusory, age spikes. The fourth is that the most recent and sophisticated dynamic simulations of the early Solar System are consistent with giant planet gravitational instabilities occurring within the first 10s of millions of years following dissipation of the primordial gas disk. In principle, use of in situ dating methods (U–Pb microprobe and $^{40}Ar/^{39}Ar$ laserprobe) could transcend the second and third issues, but results to date using both the U–Pb and $^{40}Ar/^{39}Ar$ methods yield complex or seemingly contradictory results. One possible cause is a preservation bias inherent in using accessory minerals which form preferentially from KREEP-rich sources. A conservative view of the lunar chronological record is that all of the nearside basins are older than 3.82 Ga but the data is consistent with most of them being older than 3.92 Ga and possibly older than 4.35 Ga (Deienno et al. 2017).

Am I confident that Moon did not experience a global impact cataclysm at ca. 3.9 Ga? Not only can I not prove a negative, I caution against reading more into this critique than is meant. In this chapter I document pseudoscientific practices used to support what should be a testable hypothesis using lunar meteorites and samples returned from Moon—that a high flux of planetary debris impacted the inner solar system at about 3.9 Ga causing a near planetary-wide resurfacing of Moon. In Sect. 9.11, I describe both analyses of the outermost rims of Hadean Jack Hills zircons and recrystallization of Jack Hills zircons that occurred between about 3.9 and 3.8 Ga. These data provide intriguing hints that Earth may have experienced an anomalous thermal episode at that time leaving open the possibility of an impact spike at that time.

References

Abramov, O., & Mojzsis, S. J. (2009). Microbial habitability of the Hadean Earth during the late heavy bombardment. *Nature, 459,* 419–422.

Albarède, F. (1978). The recovery of spatial isotope distributions from stepwise degassing data. *Earth and Planetary Science Letters, 39,* 387–397.

Anand, M., Barnes, J. J., & Hallis, L. J. (2015). Lunar geology. In M. R. Lee & H Leroux (Eds.), *Planetary mineralogy* (Vol. 15, pp. 129–164). European Mineralogical Union Notes in Mineralogy.

Armstrong, J. C., Wells, L. E., & Gonzalez, G. (2002). Rummaging through Earth's attic for remains of ancient life. *Icarus, 160,* 183–196.

Baldwin, R. B. (1974). Was there a "terminal lunar cataclysm" 3.9–4.0 x 10^9 years ago? *Icarus, 23,* 157–166.

Barboni, M., Boehnke, P., Keller, B., Kohl, I.E., Schoene, B., Young, E.D., & McKeegan, K.D. (2017). Early formation of the Moon 4.51 billion years ago. *Science Advances*, *3*, e1602365.

Bellucci, J. J., Nemchin, A. A., Grange, M. L., Robinson, K. L., Collins, G., Whitehouse, M. J., et al. (2019). *Earth and Planetary Science Letters, 510*, 173–185.

Benz, W., Slattery, W. L., & Cameron, A. G. W. (1986). The origin of the Moon and the single-impact hypothesis I. *Icarus, 66,* 515–535.

Binder, A. B., & Roberts, D. L. (1970). *Criteria for lunar site selection*. IIT Research Institute, Report P-30, 38 pp.

Bleeker, W. (2004a). Taking the pulse of planet Earth: A proposal for a new multi-disciplinary flagship project in Canadian solid Earth sciences. *Geoscience Canada, 31,* 179–190.

Bleeker, W. (2004b). Towards a 'natural' time scale for the Precambrian—A proposal. *Lethaia, 37,* 219–222.

Boehnke, P. (2016). *A Tale of Two Earths: Reconciling the Lunar and Terrestrial Hadean Records* (Ph.D. thesis). University of California, Los Angeles.

Boehnke, P., & Harrison, T. M. (2016). Illusory late heavy bombardments. *Proceedings of the National Academy of Sciences, 113,* 10802–10806.

Boehnke, P., Harrison, T. M., Heizler, M. T., & Warren, P. H. (2016). A model for meteoritic and lunar ^{40}Ar/^{39} Ar age spectra: Addressing the conundrum of multi-activation energies. *Earth and Planetary Science Letters, 453,* 267–275.

Boehnke, P., Watson, E. B., Trail, D., Harrison, T. M., & Schmitt, A. K. (2013). Zircon saturation re-revisited. *Chemical Geology, 351,* 324–334.

Bogard, D. D. (1995). Impact ages of meteorites: A synthesis. *Meteoritics, 30,* 244–268.

Bogard, D. D. (2011). K-Ar ages of meteorites: clues to parent-body thermal histories. *Chemie der Erde-Geochemistry, 71,* 207–226.

Bogard, D. D., & Garrison, D. H. (2003). ^{39}Ar-^{40}Ar ages of eucrites and thermal history of asteroid 4 Vesta. *Meteoritics & Planetary Science, 38,* 669–710.

Bogard, D. D., Nyquist, L. E., & Johnson, P. (1984). Noble gas contents of shergottites and implications for the Martian origin of SNC meteorites. *Geochimica et Cosmochimica Acta, 48,* 1723–1739.

Bottke, W. F., & Norman, M. D. (2017). The late heavy bombardment. *Annual Review of Earth and Planetary Sciences, 45,* 619–647.

Brasser, R., Mojzsis, S. J., Werner, S. C., Matsumura, S., & Ida, S. (2016). Late veneer and late accretion to the terrestrial planets. *Earth and Planetary Science Letters, 455,* 85–93.

Brasser, R., Morbidelli, A., Gomes, R., Tsiganis, K., & Levison, H. F. (2009). Constructing the secular architecture of the solar system II: The terrestrial planets. *Astronomy & Astrophysics, 507,* 1053–1065.

Cameron, A. G., & Ward, W. R. (1976). The origin of the Moon. *Lunar and Planetary Science Conference, 7,* 120.

Canup, R. M. (2004). Simulations of a late lunar forming Impact. *Icarus, 168,* 433–456.

Canup, R. M. (2014). Lunar-forming impacts: processes and alternatives. *Philosophical Transactions of the Royal Society A, 372,* 20130175.

Canup, R. M., & Asphaug, E. (2001). Origin of the Moon in a giant impact near the end of the Earth's formation. *Nature, 412,* 708.

Cassata, W. S., Renne, P. R., & Shuster, D. L. (2009). Argon diffusion in plagioclase and implications for thermochronometry: A case study from the Bushveld Complex, South Africa. *Geochimica et Cosmochimica Acta, 73,* 6600–6612.

Cassata, W. S., Renne, P. R., & Shuster, D. L. (2011). Argon diffusion in pyroxenes: Implications for thermochronometry and mantle degassing. *Earth and Planetary Science Letters, 304,* 407–416.

Chambers, J. (2004). Planetary accretion in the inner Solar System. *Earth Planet Science Letters, 223,* 241–252.

Chao, E. C. T. (1973). Geologic implications of the Apollo 14 Fra Mauro breccias and comparison with ejecta from the Ries crater, Germany. *U.S. Geological Survey Journal Research*, 1–18.

Chapman, C. R., Cohen, B. A., & Grinspoon, D. H. (2007). What are the real constraints on the existence and magnitude of the late heavy bombardment? *Icarus, 189,* 233–245.

Cherniak, D. J., Lanford, W. A., & Ryerson, F. J. (1991). Lead diffusion in apatite and zircon using ion implantation and Rutherford backscattering techniques. *Geochimica et Cosmochimica Acta, 5,* 1663–1673.

Clement, M. S., Kaib, N. A., Raymond, S. N., & Walsh, K. J. (2018). Mars' growth stunted by an early giant planet instability. *Icarus, 311,* 340–356.

Clement, M. S., Kaib, N. A., Raymond, S. N., Chambers, J. E., & Walsh, K. J. (2019). The early instability scenario: terrestrial planet formation during the giant planet instability, and the effect of collisional fragmentation. *Icarus*, *321*, 778–790.

Cloud, P. (1972). A working model of the primitive Earth. *American Journal of Science, 272,* 537–548.

Cohen, B. A., Swindle, T. D., & Kring, D. A. (2000). Support for the lunar cataclysm hypothesis from lunar meteorite impact melt ages. *Science, 290,* 1754–1756.

Cohen, B. A., Swindle, T. D., & Kring, D. A. (2005). Geochemistry and ^{40}Ar-^{39}Ar geochronology of impact-melt clasts in feldspathic lunar meteorites: Implications for lunar bombardment history. *Meteoritics & Planetary Science, 40,* 755–777.

Collin, G. S., Melosh, H. J., & Osinski, G. R. (2012). The impact cratering process. *Elements, 8,* 25–30.

Collins, G. (2002). Hydrocode simulations of Chicxulub Crater collapse and peak-ring formation. *Icarus, 157,* 24–33.

Ćuk, M., & Stewart, S. T. (2012). Making the Moon from a fast-spinning Earth: A giant impact followed by resonant despinning. *Science, 338,* 1047–1052.

Culler, T. S., Becker, T. A., Muller, R. A., & Renne, P. R. (2000). Lunar impact history from 40Ar/39Ar dating of glass spherules. *Science, 287,* 1785–1788.

Dalrymple, G. B., & Lanphere, M. A. (1974). ^{40}Ar/^{39}Ar age spectra of some undisturbed terrestrial samples. *Geochimica et Cosmochimica Acta, 38,* 715–738.

Dalrymple, G. B., & Ryder, G. (1993). ^{40}Ar/^{39}Ar age spectra of Apollo 15 impact melt rocks by laser step-heating and their bearing on the history of lunar basin formation. *Journal of Geophysical Research: Planets, 98,* 13085–13095.

Dalrymple, G. B., & Ryder, G. (1996). Argon-40/argon-39 age spectra of Apollo 17 highlands breccia samples by laser step heating and the age of the Serenitatis basin. *Journal Geophysics Research: Planets 101*, 26069–26084.

Darwin, G. H. (1879). On the bodily tides of viscous and semi-elastic spheroids, and on the ocean tides upon a yielding nucleus. *Philosophical Transactions of the Royal Society London, Pt., 1,* 1–35.

Dauphas, N. (2017). The isotopic nature of the Earth's accreting material through time. *Nature, 541,* 521–524.

Dauphas, N., Burkhardt, C., Warren, P. H., & Fang-Zhen, T. (2014). Geochemical arguments for an Earth-like Moon-forming impactor. *Philosophical Transactions of the Royal Society, 372,* 20130244.

Day, J. M. D., & Walker, R. J. (2015). Highly siderophile element depletion in the Moon. *Earth and Planetary Science Letters, 423,* 114–124.

de Sousa Ribeiro, R., Morbidelli, A., Raymond, S. N., Izidoro, A., Gomes, R., & Neto, E. V. (2020). Dynamical evidence for an early giant planet instability. *Icarus, 339,* 113605.

Deienno, R., Morbidelli, A., Gomes, R. S., & Nesvorný, D. (2017). Constraining the giant planets' initial configuration from their evolution: Implications for the timing of the planetary instability. *The Astronomical Journal, 153,* 153.

Dominik, B., & Jessberger, E. K. (1978). Early lunar differentiation: 4.42–AE–old plagioclase clasts in Apollo 16 breccia 67435. *Earth and Planetary Science Letters, 38,* 407–415.

Fassett, C. I., & Minton, D. A. (2013). Impact bombardment of the terrestrial planets and the early history of the Solar System. *Nature Geoscience, 6,* 520–524.

Fleck, R. J., Sutter, J. F., & Elliot, D. H. (1977). Interpretation of discordant ^{40}Ar/^{39}Ar age-spectra of Mesozoic tholeiites from Antarctica. *Geochimica et Cosmochimica Acta, 41,* 15–32.

Gapcynski, J. P., Blackshear, W. T., Tolson, R. H., & Compton, H. R. (1975). A determination of the lunar moment of inertia. *Geophysical Reseach Letters, 2,* 353–356.

Gardés, E., & Montel, J. M. (2009). Opening and resetting temperatures in heating geochronological systems. *Contributions to Mineralogy and Petrology, 158,* 185–195.

Genda, H., Brasser, R., & Mojzsis, S. J. (2017). The terrestrial late veneer from core disruption of a lunar-sized impactor. *Earth and Planetary Science Letters, 480,* 25–32.

Gillis, J. J., Jolliff, B. L., & Korotev, R. L. (2004). Lunar surface geochemistry: Global concentrations of Th, K, and FeO as derived from lunar prospector and Clementine data. *Geochimica et Cosmochimica Acta, 68*(3791–380), 5.

Gladman, B. J., Burns, J. A., Duncan, M. J., & Levison, H. F. (1995). The dynamical evolution of lunar impact ejecta. *Icarus, 118,* 302–321.

Gomes, R., Levison, H. F., Tsiganis, K., & Morbidelli, A. (2005). Origin of the cataclysmic Late Heavy Bombardment period of the terrestrial planets. *Nature, 435,* 466–470.

Gradstein, F. M., Ogg, J. G., Smith, A. G., Bleeker, W., & Lourens, L. J. (2004). A new geologic time scale, with special reference to Precambrian and Neogene. *Episodes, 27,* 83–100.

Grange, M. L., Nemchin, A. A., Pidgeon, R. T., Timms, N., Muhling, J. R., & Kennedy, A. K. (2009). Thermal history recorded by the Apollo 17 impact melt breccia 73217. *Geochimica et Cosmochimica Acta, 73,* 3093–3107.

Green, T. H., & Watson, E. B. (1982). Crystallization of apatite in natural magmas under high pressure, hydrous conditions, with particular reference to 'orogenic'rock series. *Contributions to Mineralogy and Petrology, 79,* 96–105.

Grieve, R. A. F., Cintala, M. J., & Therriault, A. M. (2006). Large-scale impacts and the evolution of the Earth's crust: The early years. *Geological Society of America Special Paper, 405,* 22–31.

Haber, T., Scherer, E. E., Bast, R., & Sprung, P. (2017). ^{176}Lu-^{176}Hf isochron dating of strongly cosmic ray exposed samples—A case study on Apollo 14 impact melt rock 14310. *Lunar and Planetary Science Conference, 48,* 2911.

Harland, W. B., Armstrong, R. L., Cox, A. V., Craig, L. E., Smith, A. G., & Smith, D. G. (1990). *A geologic time scale 1989*. Cambridge: Cambridge University Press.

Harrison, T. M., Lovera, O. M., & Heizler, M. T. (1991). ^{40}Ar/^{39}Ar results for alkali feldspars containing diffusion domains with differing activation energy. *Geochimica et Cosmochimica Acta, 55,* 1435–1448.

Harrison, T. M., & Watson, E. B. (1984). The behavior of apatite during crustal anatexis: Equilibrium and kinetic considerations. *Geochimica et Cosmochimica Acta, 48,* 1467–1477.

Hartmann, W. K. (1975). Lunar "cataclysm": A misconception? *Icarus, 24,* 181–187.

Hartmann, W. K. (2019). History of the Terminal Cataclysm Paradigm: Epistemology of a planetary bombardment that never (?) happened. *Geosciences, 9,* 285.

Hartmann, W. K., & Davis, D. R. (1975). Satellite-sized planetesimals and lunar origin. *Icarus, 24,* 504–515.

Hartmann, W. K., & Neukum, G. (2001). Cratering chronology and the evolution of Mars. *Space Science Reviews, 96,* 165–194.

Hartmann, W. K., Ryder, G., Dones, L., & Grinspoon, D. (2000). The time-dependent intense bombardment of the primordial Earth/Moon system. In R. Canup & K. Righter (Eds.), *Origin of the Earth and Moon* (493–512), University of Arizona Press.

Hartung, J. B. (1974). Can random impacts cause the observed ^{39}Ar/^{40}Ar age distribution for Lunar Highland rocks? *Meteoritics, 9,* 349.

Head, J. W. (1974). Stratigraphy of the Descartes region (Apollo 16)—Implications for the origin of samples. *Moon, 11,* 77–99.

Holzheid, A., Sylvester, P., O'neill, H.S.C., Rubie, D. C., & Palme, H. (2000). Evidence for a late chondritic veneer in the Earth's mantle from high-pressure partitioning of palladium and platinum. *Nature 406*, 396–399.

Hood, L. L., & Artemieva, N. A. (2008). Antipodal effects of lunar basin-forming impacts: Initial 3D simulations and comparisons with observations. *Icarus, 193,* 485–502.

Hörz, F., Grieve, R., Heiken, G., Spudis, P., & Binder, A. (1991). Lunar surface processes. In G. H. Heiken et al. (Eds.), *Lunar sourcebook* (61–120). Cambridge Press.

Huneke, J. C. (1976). Diffusion artifacts in dating by stepwise thermal release of rare gases. *Earth and Planetary Science Letters, 28,* 407–417.

James W. Head, (1976). Lunar volcanism in space and time. *Reviews of Geophysics*, *14*(2), 265.

Jessberger, E. K., & Dominik, B. (1979). Gerontology of the Allende meteorite. *Nature, 277,* 554.

Jolliff, B. L., Gillis, J. J., Haskin, L. A., Korotev, R. L., & Wieczorek, M. A. (2000). Major lunar crustal terranes: Surface expressions and crust-mantle origins. *Journal of Geophysical Research: Planets, 105,* 4197–4216.

Kimura, K., Lewis, R. S., & Anders, E. (1974). Distribution of gold and rhenium between nickel-iron and silicate melts: Implications for the abundances of siderophile elements on the Earth and Moon. *Geochimica et Cosmochimica Acta, 38,* 683–701.

Korotev, R. L. (2005). Lunar geochemistry as told by lunar meteorites. *Chemie der Erde-Geochemistry, 65,* 297–346.

Kraus, R. G., Root, S., Lemke, R. W., Stewart, S. T., Jacobsen, S. B., & Mattsson, T. R. (2015). Impact vaporization of planetesimal cores in the late stages of planet formation. *Nature Geoscience, 8,* 269–272.

Kring, D. A., & Cohen, B. A. (2002). Cataclysmic bombardment throughout the inner solar system 3.9–4.0 Ga. *Journal of Geophysical Research: Planets 107*(E2).

Levison, H. F., Dones, L., Chapman, C. R., Stern, S. A., Duncan, M. J., & Zahnle, K. (2001). Could the lunar "Late Heavy Bombardment" have been triggered by the formation of Uranus and Neptune? *Icarus, 151,* 286–306.

Lineweaver, C. H., Grether, D., & Hidas, M. (2002). How common are Earths? How common are Jupiters? *Bioastronomy 2002: Life Among the Stars*, *ASP Conference Series* (Vol. 28, pp. 1–4), arXiv preprint astro-ph/0209383.

Liu, D., Jolliff, B. L., Zeigler, R. A., Korotev, R. L., Wan, Y., Xie, H., et al. (2012). Comparative zircon U-Pb geochronology of impact melt breccias from Apollo 12 and lunar meteorite SaU 169, and implications for the age of the Imbrium impact. *Earth and Planetary Science Letters, 319,* 277–286.

Lock, S. J., & Stewart, S. T. (2017). The structure of terrestrial bodies: Impact heating, corotation limits, and synestias. *Journal of Geophysical Research: Planets, 122,* 950–982.

Lovera, O. M., Richter, F. M., & Harrison, T. M. (1989). The ^{40}Ar/^{39}Ar thermochronometry for slowly cooled samples having a distribution of diffusion domain sizes. *Journal of Geophysical Research: Solid Earth, 94,* 17917–17935.

Magna, T., Dauphas, N., Righter, K., & Camp, R. (2017). Stable isotope constraints on the formation of Moon. *LPI Contrib. 1988*.

Maher, K. A., & Stevenson, D. J. (1988). Impact frustration of the origin of life. *Nature, 331,* 612–614.

Mann, A. (2018). Bashing holes in the tale of Earth's troubled youth. *Nature, 553,* 393–395.

Marchi, S., Bottke, W. F., Elkins-Tanton, L. T., Bierhaus, M., Wuennemann, K., Morbidelli, A., et al. (2014). Widespread mixing and burial of Earth's Hadean crust by asteroid. *Nature, 511,* 578–582.

Marchi, S., Bottke, W. F., Cohen, B. A., Wünnemann, K., Kring, D. A., McSween, H. Y., De Sanctis, M. C., O'Brien, D. P., Schenk, P., Raymond, C. A., Russell, C. T. (2013). High-velocity collisions from the lunar cataclysm recorded in asteroidal meteorites. *Nature Geoscience*, *6*(4), 303–307.

Mark, R. K., Lee-Hu, C. N., & Wetherill, G. W. (1974). Rb-Sr age of lunar igneous rocks 62295 and 14310. *Geochimica et Cosmochimica Acta, 38,* 1643–1648.

Marvin, U. B. (1983). The discovery and initial characterization of Allan Hills 81005: The first lunar meteorite. *Geophysical Reseach Letters, 10,* 775–778.

Maurer, P., Eberhardt, P., Geiss, I., Gršgler, N., Stettler, A., Brown, G. M., et al. (1978). Pre-Imbrian craters and basins: Ages, compositions and excavation depths of Apollo 16 breccias. *Geochimica et Cosmochimica Acta, 42,* 1687–1720.

McDougall, I., & Harrison, T. M. (1999). *Geochronology and Thermochronology by the ^{40}Ar/^{39}Ar Method*. Oxford University Press.

McGetchin, T. R., Settle, M., & Head, J. W. (1973). Radial thickness variation in impact crater ejecta: Implications for lunar basin deposits. *Earth and Planetary Science Letters, 20,* 226–236.

Melosh, H. J. (1989). Impact cratering: A geologic process. *Oxford University Press (Oxford Monographs on Geology and Geophysics, No. 11)* (253 pp).

Mercer, C. M., & Hodges, K. V. (2017). Diffusive loss of argon in response to melt vein formation in polygenetic impact melt breccias. *Journal of Geophysical Research: Planets, 122,* 1650–1671.

Mercer, C. M., Young, K. E., Weirich, J. R., Hodges, K. V., Jolliff, B. L., Wartho, J. A., et al. (2015). Refining lunar impact chronology through high spatial resolution ^{40} Ar/^{39} Ar dating of impact melts. *Science Advances, 1,* e1400050.

Merle, R. E., Nemchin, A. A., Grange, M. L., Whitehouse, M. J., & Pidgeon, R. T. (2014). High resolution U-Pb ages of Ca-phosphates in Apollo 14 breccias: Implications for the age of the Imbrium impact. *Meteoritics & Planetary Science, 49,* 2241–2251.

Merrihue, C., & Turner, G. (1966). Potassium-argon dating by activation with fast neutrons. *Journal of Geophysical Research, 71,* 2852–2857.

Meyer, C. (2009). 14310. Lunar Sample Compendium, 1–12 (https://www.lpi.usra.edu/lunar/samples/atlas/compendium/14310.pdf).

Meyer, H. M., Denevi, B. W., Boyd, A. K., & Robinson, M. S. (2016). The distribution and origin of lunar light plains around orientale basin. *Icarus, 273*, 135–145. https://doi.org/10.1016/j.icarus.2016.02.014.

Meyer, H. M., Denevi, B. W., Boyd, A. K., & Robinson, M. S. (2018). A new global map of light plains from the lunar reconnaissance orbiter camera. In *49th Lunar and Planetary Science Conference, Abstract #1474*.

Meyer, C., Williams, I. S., & Compston, W. (1996). Uranium-lead ages for lunar zircons: Evidence for a prolonged period of granophyre formation from 4.32 to 3.88 Ga. *Meteoritics & Planetary Science, 31,* 370–387.

Michael, G., Basilevsky, A., Neukum, G. (2018). On the history of the early meteoritic bombardment of the moon: was there a terminal lunar cataclysm? *Icarus*, *302*, 80–103.

Moorbath, S. (2005a). Palaeobiology: Dating earliest life. *Nature, 434,* 155–156.

Moorbath, S. (2005b). Oldest rocks, earliest life, heaviest impacts, and the Hadean-Archaean transition. *Applied Geochemistry, 20,* 819–824.

Morbidelli, A., Nesvorny, D., Laurenz, V., Marchi, S., Rubie, D. C., Elkins-Tanton, L., Wieczorek, M., Jacobson, S. (2018). The timeline of the lunar bombardment: revisited. *Icarus*, *305*, 262–276.

Nesvorný, D., Vokrouhlický, D., Bottke, W. F., & Levison, H. F. (2018). Evidence for very early migration of the Solar System planets from the Patroclus–Menoetius binary Jupiter Trojan. *Nature Astronomy, 2*. https://doi.org/10.1038/s41550-018-0564-3.

Neukum, G., Ivanov, B. A., & Hartmann, W. K. (2001). Cratering records in the inner solar system in relation to the lunar reference system. *Chronology and evolution of Mars* (pp. 55–86). Dordrcht: Springer.

Norman, M. D., Duncan, R. A., & Huard, J. J. (2006). Identifying impact events within the lunar cataclysm from 40Ar–39Ar ages and compositions of Apollo 16 impact melt rocks. *Geochimica et Cosmochimica Acta, 70,* 6032–6049.

Oberbeck, V. R., Quaide, W. L., Gault, D. E., Hoerz, F., & Morrison, R. H. (1975). On the origin of the lunar smooth-plains. *Moon, 12,* 19–54.

Oberbeck, V. R., Quaide, W. L., Gault, D. E., Morrison, R. H., & Hörz, F. (1974). Smooth plains and continuous deposits of craters and basins. In *5th Proceedings of Lunar Science Conference* (pp. 111–136).

Ozima, M., Seki, K., Terada, N., Miura, Y. N., Podosek, F. A., & Shinagawa, H. (2005). Terrestrial nitrogen and noble gases in lunar soils. *Nature, 436,* 655–659.

Ozima, M., Yin, Q. Z., Podosek, F. A., & Miura, Y. N. (2008). Toward understanding early Earth evolution: Prescription for approach from terrestrial noble gas and light element records in lunar soils. *Proceedings of the National Academy of Sciences, 105,* 17654–17658.

Pietro, N. E., & Pieters, C. M. (2006). Modeling the provenance of the Apollo 16 regolith. *Journal of Geophysical Research: Planets, 111*(E09005), 1–13.

Plescia, J. B., & Cintala, M. J. (2012). Impact melt in small lunar highland craters. *Journal of Geophysical Research: Planets, 117,* E12.

Righter, K., Humayun, M., & Danielson, L. (2008). Partitioning of palladium at high pressures and temperatures during core formation. *Nature Geoscience, 1,* 321–323.

Ryder, G., Koeberl, C., & Mojzsis, S. J. (2000). Heavy bombardment of the Earth at ~3.85 Ga: The search for petrographic and geochemical evidence. In R. Canup & K. Righter (Eds.), *Origin of the Earth and Moon* (pp. 475–492), University of Arizona Press.

Safronov, V. S. (1954). On the growth of planets in the protoplanetary cloud. *Astrron. Zh., 31,* 499–510.

Schaeffer, G. A., & Schaeffer, O. A. (1977). ^{39}Ar/^{40}Ar ages of lunar rocks. In *Proceedings, Lunar and Planetary Science Conference VIII* (pp. 2253–2300).

Schmidt, O. Y. (1944). Meteorite theory of origin of Earth and planets. *Doklady Akademii Nauk SSSR, 45,* 245–249.

Schultz, P. H., & Gault, D. E. (1985). Clustered impacts: Experiments and implications. *Journal Geophysics Research, 90,* 3701–3732.

Seki, K., Elphic, R. C., Hirahara, M., Terasawa, T., & Mukai, T. (2001). On atmospheric loss of oxygen ions from Earth through magnetospheric processes. *Science, 291,* 1939–1941.

Shea, E. K., Weiss, B. P., Cassata, W. S., Shuster, D. L., Tikoo, S. M., & Gattacceca, J. (2012). A long-lived lunar core dynamo. *Science, 335,* 453–456.

Shearer, C. K., Hess, P. C., Wieczorek, M. A., Pritchard, M. E., Parmentier, E. M., Borg, L. E., et al. (2006). Thermal and magmatic evolution of the Moon. *Reviews in Mineralogy and Geochemistry, 60,* 365–518.

Shuster, D. L., Balco, G., Cassata, W. S., Fernandes, V. A., Garrick-Bethell, I., & Weiss, B. P. (2010). A record of impacts preserved in the lunar regolith. *Earth and Planetary Science Letters, 290,* 155–165.

Sleep, N. H., Zahnle, K. J., Kasting, J. F., & Morowitz, H. J. (1989). Annihilation of ecosystems by large asteroid impacts on the early earth. *Nature, 342,* 139–142.

Snape, J. F., Nemchin, A. A., Grange, M. L., Bellucci, J. J., Thiessen, F., & Whitehouse, M. J. (2016). Phosphate ages in Apollo 14 breccias: Resolving multiple impact events with high precision U-Pb SIMS analyses. *Geochimica et Cosmochimica Acta, 174,* 13–29.

Spudis, P. D. (1993). *The geology of multi-ring impact basins: The Moon and other planets*. Cambridge, UK: Cambridge University Press.

Spudis, P. D., Wilhelms, D. E., & Robinson, M. S. (2011). The Sculptured Hills of the Taurus Highlands: Implications for the relative age of Serenitatis, basin chronologies and the cratering history of the Moon. *Journal of Geophysical Research: Planets, 116,* E12.

Stettler, A., Eberhardt, P., Geiss, J., Grögler, N., & Maurer, P. (1973). Ar^{39}-Ar^{40} ages and Ar^{37}-Ar^{38} exposure ages of lunar rocks. *Lunar and Planetary Science Conference Proceedings, 4,* 1865–1888.

Stevenson, D. J., & Halliday, A. N. (2014). The origin of the Moon. *Philosophical Transactions of the Royal Society A*, A 372. https://doi.org/10.1098/rsta.2014.0289.

Stöffler, D., & Ryder, G. (2001). Stratigraphy and isotope ages of lunar geologic units: Chronological standard for the inner solar system. *Chronology and evolution of Mars* (pp. 9–54). Dordrecht: Springer.

Strom, R. G., Malhotra, R., Ito, T., Yoshida, F., & Kring, D. A. (2005). The origin of planetary impactors in the inner solar system. *Science, 309,* 1847–1850.

Swindle, T. D., Kring, D. A., & Weirich, J. R. (2014). ^{40}Ar/^{39}Ar ages of impacts involving ordinary chondrite meteorites. *Geological Society, London, Special Publications*, *378*, 333–347.

Tatsumoto, M., Hedge, C. E., Doe, B. R., & Unruh, D. M. (1972). U-Th-Pb and Rb-Sr measurements on some Apollo 14 lunar samples. *Lunar and Planetary Science Conference Proceedings, 3,* 1531–1555.

Taylor, D. J., McKeegan, K. D., & Harrison, T. M. (2009). ^{176}Lu-^{176}Hf zircon evidence for rapid lunar differentiation. *Earth and Planetary Science Letters, 279,* 157–164. https://doi.org/10.1016/j.epsl.2008.12.030.

Taylor, S. R., Taylor, G. J., & Taylor, L. A. (2006). The moon: A Taylor perspective. *Geochimica et Cosmochimica Acta, 70,* 5904–5918.

Tera, F., Papanastassiou, D. A., & Wasserburg, G. J. (1974). Isotopic evidence for a terminal lunar cataclysm. *Earth and Planetary Science Letters, 22,* 1–21.

Terada, K., Yokota, S., Saito, Y., Kitamura, N., Asamura, K., & Nishino, M. N. (2017). Biogenic oxygen from earth transported to the moon by a wind of magnetospheric ions. *Nature Astronomy*, *1*, 1–5.

Thiessen, F., Nemchin, A. A., Snape, J. F., Whitehouse, M. J., & Bellucci, J. J. (2017). Impact history of the Apollo 17 landing site revealed by U-Pb SIMS ages. *Meteoritics & Planetary Science, 52,* 584–611.

Tikoo, S. M., Weiss, B. P., Shuster, D. L., Suavet, C., Wang, H., & Grove, T. L. (2017). A two-billion-year history for the lunar dynamo. *Science Advances, 3,* e1700207.

Tsiganis, K., Gomes, R., Morbidelli, A., & Levison, H. F. (2005). Origin of the orbital architecture of the giant planets of the Solar System. *Nature, 435,* 459–461.

Turner, G. (1970). Argon–40/argon–39 dating of lunar rock samples. *Science, 167,* 466–468.

Turner, G. (1977). Potassium–argon chronology of the moon. *Physics and Chemistry of the Earth, 10,* 145–195.

Turner, G., & Cadogan, P. H. (1974). Possible effects of ^{39}Ar recoil in ^{40}Ar–^{39}Ar dating. *Geochimica et Cosmochimica Acta Suppl. 5* (Proceedings of the Fifth Lunar Science Conference, pp. 1601–1615).

Turner, G., & Cadogan, P. H. (1975). The history of lunar bombardment inferred from Ar-40-Ar-39 dating of highland rocks. In *Lunar and Planetary Science Conference Proceedings* (Vol. 6, pp. 1509–1538). New York, NY: Pergamon.

Turner, G., Miller, J. A., & Grasty, R. L. (1966). The thermal history of the Bruderheim meteorite. *Earth and Planetary Science Letters, 1,* 155–157.

Urey, H. C. (1952a). *The planets: Their origin and development* (p. 245). New Haven: Yale University Press.

Urey, H. C. (1952b). The origin of the Earth. *Scientific American, 187*(October), 53–61.

Van Kranendonk, M. J., Altermann, W., Beard, B. L., Hoffman, P. F., Johnson, C. M., Kasting, J. F., et al. (2012) A chronostratigraphic division of the Precambrian: possibilities and challenges. In F. M. Gradstein, et al. (Eds.), *The geologic time scale* (pp. 299–392). Elsevier.

Villa, I. M., Huneke, J. C., & Wasserburg, G. J. (1983). ^{39}Ar recoil losses and presolar ages in Allende inclusions. *Earth and Planetary Science Letters, 63,* 1–12.

Warren, P. H. (1985). The magma ocean concept and lunar evolution. *Annual Review of Earth and Planetary Sciences, 13,* 201–240.

Warren, P. H. (2004). The Moon. In H. D. Holland, & K. K. Turekian (Eds.), *Treatise on geochemistry* (pp. 559–599), Elsevier, Amsterdam.

Watson, E. B., & Harrison, T. M. (1983). Zircon saturation revisited: Temperature and composition effects in a variety of crustal magma types. *Earth and Planetary Science Letters, 64,* 295–304.

Weber, R. C., Lin, P. Y., Garnero, E. J., Williams, Q., & Lognonne, P. (2011). Seismic detection of the lunar core. *Science, 331,* 309–312.

Weiss, B. P., & Tikoo, S. M. (2014). The lunar dynamo. *Science*, *346*(6214), 1246753.

Wetherill, G. W. (1975). Late heavy bombardment of the moon and terrestrial planets. In *Proceedings 6th Lunar Science Conference* (pp. 1539–1561), March 17–21, Houston, TX, Pergamon, New York.

Wetherill, G. W. (1995). How special is Jupiter? *Nature, 373,* 470.

Wieczorek, M. A., & Zuber, M. T. (2001). The composition and origin of the lunar crust: Constraints from central peaks and crustal thickness modeling. *Geophysical Reseach Letters, 28,* 4023–4026.

Wielicki, M. M., & Harrison, T. M. (2015). Zircon formation in impact melts: Complications for deciphering planetary impact histories. *Large Meteorite Impacts and Planetary Evolution V: Geological Society of America Special Paper, 518,* 127–134.

Wilhelms, D. E. (1965). Fra Mauro and Cayley Formations in the Mare Vaporum and Julius Caesar quadrangles. *U. S. Geological Survey open-file report 13*, 28 pp.

Wilhelms, D. E. (1970). Summary of lunar stratigraphy-telescopic observations. *U.S. Geological Survey Professional Paper No. 599-F*, 47 pp.

Wisdom, J., & Tian, Z. (2015). Early evolution of the Earth-Moon system with a fast-spinning Earth. *Icarus, 256,* 138–146.

Wood, J. A., Dickey, J. S., Marvin, U. B., & Powell, B. N. (1970). Lunar anorthosites. *Science, 167,* 602–604.

Young, K. E., van Soest, M. C., Hodges, K. V., Watson, E. B., Adams, B. A., & Lee, P. (2013). Impact thermochronology and the age of Haughton impact structure, Canada. *Geophysical Research Letters, 40,* 3836–3840.

Zahnle, K., Arndt, N., Cockell, C., Halliday, A., Nisbet, E., Selsis, F., et al. (2007). Emergence of a habitable planet. *Space Science Reviews, 129,* 35–78.

Zappala, V., Cellino, A., Gladman, B. J., Manley, S., & Migliorini, F. (1998). Asteroid showers on Earth after family breakup events. *Icarus, 134,* 176–179.

Zellner, N. E. (2017). Cataclysm no more: New views on the timing and delivery of lunar impactors. *Origins of Life and Evolution of Biospheres, 47,* 261–280.

Zhang, J., Dauphas, N., Davis, A. M., Leya, I., & Fedkin, A. (2012). The proto-Earth as a significant source of lunar material. *Nature Geoscience, 5,* 251.

Zhang, B., Lin, Y., Moser D. E., Shieh, S. R., & Bouvier, A. (2018). Imbrium zircon age for Apollo 73155 Serenitatis impact melt breccia: Implications for the lunar bombardment. Bombardment: Shaping planetary surfaces and their environments 2018, *LPI Contrib. No. 2107*, Abstract 2021.

Zharkov. (2000). On the history of the lunar orbit. *Solar System Research 34*, 1–11.

Zhu, M. H., Artemieva, N., Morbidelli, A., Yin, Q. Z., Becker, H., & Wünnemann, K. (2019). Reconstructing the late-accretion history of the Moon. *Nature*, *571*(7764), 226–229.

Ziethe, R., Seiferlin, K., & Hiesinger, H. (2009). Duration and extent of lunar volcanism: Comparison of 3D convection models to mare basalt ages. *Planetary and Space Science, 57,* 784–796.

5 Models of Continental Growth and Destruction

Abstract

We don't know with confidence the mechanisms by which primitive arc basalts are modified to produce the broadly granodioritic continental crust but there is widespread agreement that plate tectonics has been doing just that for at least the past billion years. We also don't fully understand the structure of the continental crust; popular layered models lack mechanisms to produce such structures or to recover them following tectonic homogenization. The geochemical community long favored the view that early crust was mafic, in part owing to misconceptions regarding feldspar buoyancy on a hydrous magmatic substrate and the deep stabilization of garnet (which retards crystallization of more buoyant aluminous phases from the magma). But early felsic crusts with the potential for long term stability could have emerged via crystallization of tonalitic liquids fractionated from ultramafic magmas in equilibrium with olivine or differentiating magma sheets following large impacts into early basaltic crusts. The remarkable range of estimates of the growth history of continental crust reflects a number of influences but, generally speaking, earlier growth has been increasingly favored as new age survey methodologies became available and as the effects that crustal reworking and recycling have on apparent surface age provinces became better appreciated. Isotopic data once thought to support rapid growth at ~2.7 Ga are now recognized as equally consistent with constant volume continental crust. The longstanding misapprehension that the present-day distribution of crust formation ages is equivalent to the growth history of continents strongly influenced some estimates. Instead, today's crust represents a running balance between new growth, internal overprinting, and crustal recycling. The difficulty in deconvolving these processes is one of the two principal challenges in establishing the growth history of continental crust. The other is that crust recycled back into the mantle and thoroughly mixed leaves no trace of its past incarnations. Although the rock record has yet to yield clear, direct evidence from which to constrain the magnitude of Hadean continental crust, optimal solutions to modelling mantle isotopic data are at least as consistent with

T. M. Harrison, *Hadean Earth*, https://doi.org/10.1007/978-3-030-46687-9_5

constant volume continental crust since ca. 4.4 Ga as with slow monotonic growth. Radiogenic isotopic data used to argue for an early mafic crust are contradicted by stable isotopic results that appear to support a continuously felsic continental crust of unknown volume.

5.1 How Is Continental Crust Made?

The origin of continental crust[1] remains enigmatic. While there is little question today that it ultimately derives from mantle-derived basaltic crust formed at mid-ocean ridges which then interacts with the mantle wedge at convergent plate boundaries to form andesitic (60–65% SiO_2) crust, the details of the latter transition are poorly understood. Andesite magmas were once thought to be the dominant composition in arcs and thus their addition at convergent margins explained how continents grew (Taylor and White 1965; Taylor 1967). Subsequently it was recognized that, since arc magmas are derived from mantle wedge melting, they are instead broadly basaltic ($\sim$50% SiO_2) in composition (Brown et al. 1977). The challenge then is to conceive of ways in which primitive arc basalts could transmute into felsic crust. Most mechanisms proposed to accomplish this chemical fractionation assume some form of differentiation followed by loss of a mafic cumulate to the mantle. For example, Lee and Anderson (2015) suggested that the parental basalt differentiates into a mafic garnet pyroxenitic residue along with a complementary silicic magma. The dense cumulate then founders at the Moho eventually causing delamination of the lithosphere. Compelling evidence for such a mechanism was compiled by Ducea and Saleeby (1998) for the eastern Sierra Nevada batholith of California. From geophysical, geochronologic and petrologic data, they argued that a dense residuum had delaminated beginning in the Late Miocene leading to basaltic underplating. Subsequent seismic studies appear to support the view that the hypothesized mafic residuum at the base of the eastern Sierran batholith had been removed (Jones et al. 2014). Lee and Anderson (2015) calculated the recycled flux of garnet pyroxenitic residue to be 5–20% that of oceanic crust recycling by subduction and that loss of this residue would create complimentary trace-element compositions consistent with that observed in continental crust. While seemingly successful in explaining how continental crust acquired its felsic nature, the mechanism is problematic in other ways.

Xenolith dating indicates that most cratonic roots formed relatively rapidly and are a similar age to the overlying crust (Pearson 1999), possibly forming beneath mid-ocean ridges (Servali and Korenaga 2018). This implies that the crust and mantle portions of continental lithosphere have generally remained coupled since formation, perhaps billions of years ago, despite semi-continuous Wilson cycle activity (see Fig. 6.1). If the subcontinental mantle is continuously lost at

[1]Herein, any reference to crust without a modifier is of the continental variety.

convergent margins, how do ancient cratons maintain deep roots retaining ancient isotopic signals? While the case for Sierran delamination appears strong, the generality of the process remains unclear in light of this observation.

The above discussion presupposes the existence of plate tectonics to mediate the production of continental crust. How might the first terrestrial continental crust have formed before the advent of mobile lid tectonics? It was long thought that Earth could not have grown an early anorthositic crust similar to that which developed on Moon (Sect. 4.2) because plagioclase is negatively buoyant in hydrous silicate melts (Condie 1982; Taylor 1982; Taylor and McLennan 1985; cf. Shaw 1976). But Warren (1989) pointed out that even calcic plagioclase floats atop magmas containing water contents well in excess of that present in terrestrial upper mantle magmas.

Models of crustal growth on early Earth tended to favor mafic over felsic compositions, in part owing to the aforementioned erroneous view regarding plagioclase buoyancy in hydrous magmas. Whether or not an early basaltic crust formed on a magma ocean can have long term stability or instead founder on the underlying peridotitic liquid may depend on the nature of the terminal phase of global melting. Given the relatively short durations estimated for magma ocean crystallization (10^3–10^7 years; Sect. 3.4), Earth may have experienced multiple such episodes (Sect. 3.4). Forming an early felsic crust during solidification upwards of a completely molten primitive mantle would have been inhibited by the stabilization of garnet at depths greater than $\sim$250 km, which removes the 'feldspar' component from the magma, leading to a mafic solute. However, as the magma ocean shallowed to depths less than that, olivine crystallized at the magma base would yield a light, evolved liquid that, upon ascent to shallow depths, would be expected to rapidly nucleate feldspar in a highly polymerized melt (Morse 1986). This potentially results in rapid crystallization of tonalitic, network-rich, high viscosity liquids that could coalesce into 'rockbergs' of stable, felsic crust.

Melting experiments using a primitive mantle composition in the CaO–MgO–Al_2O_3–SiO_2 system at 6.5 GPa and 1850 °C (Asahara and Ohtani 2001) yield liquids with up to 52% SiO_2. Zou and Harrison (2007) used the MELTS algorithm (Ghiorso and Sack 1995) to model the compositional change that this magma would experience during ascent to the near surface. Their model magmas rapidly evolve during crystallization to produce hydrous (1–2% H_2O), tonalitic (57% SiO_2) melts at 950–1000 °C. At the surface, such a proto-crust might migrate to down-welling loci where they could be stabilized by locally cooler conditions (Morse 1986). As the base of this crust heats up in response to shutdown of the descending cell, felsic liquids produced would tend to ascend diapirically, creating a self-stabilizing feedback.

Alternatively, large impactors into an early basaltic or intermediate crust would create thick, magma sheets. Their subsequent differentiation could produce felsic crust with the potential for long term stability. Consider the Sudbury Igneous Complex as an analogue. Internal differentiation of this 1.85 Ga igneous complex, formed largely from melting of Archean granite-greenstone target rocks (Grieve 1991; Latypov et al. 2019), produced sequential layers from norite to granophyre that have sufficient buoyancy to resist mantle reincorporation. Preservation of such protocontinental crust during the Hadean eon would, however, require the underlying mantle lithosphere to have cooled below the dry fusion temperature of granite (ca. 930 °C) lest the lower crust flow laterally away.

The intent of the above discussion is not to advocate a particular process of early crust production—there is little or no evidence to support either view—but to instead suggest that formation of a stable crust of intermediate or felsic composition almost immediately following Earth formation cannot be ruled out for lack of plausible mechanisms. As to the answer to the question posed in the title of this section, first order questions regarding how continental crust is formed remain without adequate explanation today to the point where essentially any of the models reviewed in this chapter could be valid.

5.2 Internal Structure of Continental Crust

If we're not exactly sure how continental crust formed, how do we know its internal structure? A longstanding assumption is that the continental crust is vertically stratified upward from low to high SiO_2 (McLennan and Taylor 1982, 1991; Taylor and McLennan 1985). This concept assumes that the high seismic velocities observed in the deep crust are evidence of mafic lithologies. However, garnet-bearing metapelites have velocities that overlap the complete velocity range displayed by meta-igneous rocks (Rudnick and Fountain 1995). If we don't confidently know the internal structure of continental crust, then how do we know its composition?

It was also long assumed that U, Th, K are redistributed upward to create a thin radioactive layer in the upper continental crust (e.g., Roy et al. 1968). However, in the fullness of time the mechanisms proposed to explain upward transport in the crust have been shown to be unviable. For example, Taylor and McLennan (1985) assumed that large ion lithophile elements like U and Th would be preferentially partitioned into buoyant, granitoid magmas during anatexis in the deep crust that would then ascend to shallower levels. But because of the low solubilities of accessory minerals such as zircon and monazite in crustal melts (the phases in which U and Th are concentrated), anatexis would typically enrich the lower crust in U and Th as more restitic zircon or monazite remains in the source than is dissolved in the magma (Watson and Harrison 1983, 1984; Rapp and Watson 1986; Harrison et al. 1986; Bea and Montero 1999; Alessio et al. 2018). Although this doesn't hold true for K, exhumed continental granulites, as a population, are not characterized by depletions in U, Th, or K (Rudnick et al. 1985).

The relationship between surface heat flux and heat generation was long interpreted as indicating that radioactivity is concentrated in the upper continental crust (Lachenbruch 1970). This now seems unlikely for at least two reasons. First, seismic cross sections of continental crust are inconsistent with assumption that surface rocks characterize the crustal column (e.g., Lewry et al. 1994). Second, the apparent heat flow/production relationship is likely an artifact of the 1D nature of the calculation and instead reflects heterogeneously distributed crustal heat generation (Morgan et al. 1987). Estimates of lower crustal heat sources that satisfy continental heat flow and seismic wavespeed constraints (Rudnick and Gao 2003; Hacker et al. 2011) differ in lower crustal heat generation by factor of three (Fig. 5.1) underscoring the poorly known geochemical and petrologic character of the deep continental crust.

Lastly, orogenesis is seen by some geochemists as bit player in establishing crustal architecture rather than a first-order mechanism that juxtaposes and thoroughly mixes rocks at all crustal levels. For example, Rudnick and Fountain (1995) state that orogenic P-T paths "are probably not representative of the deep crust but are merely upper crustal rocks that have been through an orogenic cycle". This supposes a mechanism that retrieves to the surface all rocks that experienced, say,

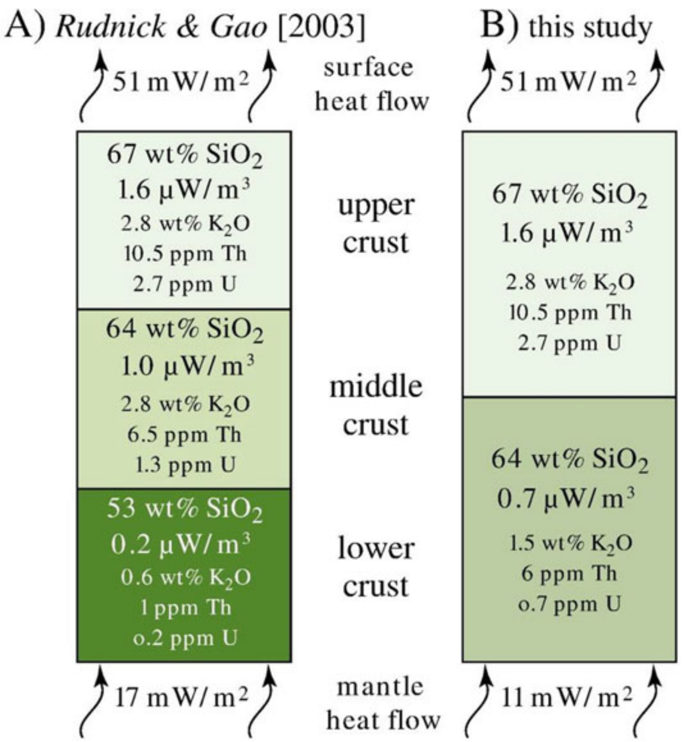

Fig. 5.1 Two models of continental composition and heat generation consistent with seismic wavespeeds yield similar surface heat flows but contrasting internal structures. **a** The model of Rudnick and Gao (2003) employs a three layers with a mafic lower crust. **b** The Hacker et al. (2011) model assume only two layers and features a felsic lower crust with three times great radiogenic heat production than Rudnick and Gao (2003). Reproduced with permission from Hacker et al. (2011)

underthrusting to great depths during continental collision. Since > 90% of continental crust has been processed through at least one orogenic cycle, the mafic-to-felsic stratified model appears problematic in the absence of a physical mechanism that could rapidly return a tectonic 'plum pudding' crust to a highly stratified state.

From the inner core to the atmosphere, the continental crust is almost certainly the terrestrial shell furthest from thermodynamic equilibrium. As an illustration of how poor our understanding of the composition of continental crust is, note that there is far less variance in estimates of the amount of light elements in the outer core (ca. 30%; see Badro et al. 2014, and references therein) than there is regarding the K, U, and Th concentrations of the lower crust (ca. 100%; Rudnick and Gao 2003; Hacker et al. 2011). In the absence of plausible mechanisms that could explain how the spatial heterogeneity imposed on continental crust during, say, continental collision, could vertically segregate into increasingly SiO_2-rich layers toward the surface, this longstanding model should be viewed with considerable skepticism.

5.3 Continental Crust Growth History Estimates

5.3.1 Introduction

Of the roughly 40% of Earth's surface that is continent, about half is inferred to be exposed or buried Precambrian crust, with only 14% of that thought to be Archean or older (Cogley 1984; Goodwin 1991). This age distribution reflects the continuous resurfacing of the planet through the coupled effects of erosion and plate tectonics. These two processes drive the growth of new continental crust, the internal reworking of existing crust, and the recycling of that crust back into the mantle, either via subduction of continental-derived sediment (subduction erosion) or delamination. In the process of crustal reworking during orogeny, primary rock-forming ages are unlikely to survive and thus a bias to younger ages is expected.

In the 50 years that geologists have felt sufficiently confident to quantitatively reconstruct the growth history of the continental crust, estimates for the age at which half of the present mass was attained range from 1.2 Ga to 4.4 Ga (Fig. 5.2). This remarkable range reflects a number of influences but, generally speaking, earlier growth has been increasingly favored as new age survey methodologies became available and as the effects that crustal reworking and recycling have on apparent surface age provinces became better appreciated. The longstanding misapprehension that the present-day distribution of crust formation ages is equivalent to the growth history of continents strongly influenced some estimates (see recent review in Korenaga 2018b). Instead, today's crust represents a running balance between new growth, internal overprinting, and crustal recycling. The difficulty in deconvolving these processes is one of the two principal challenges in establishing

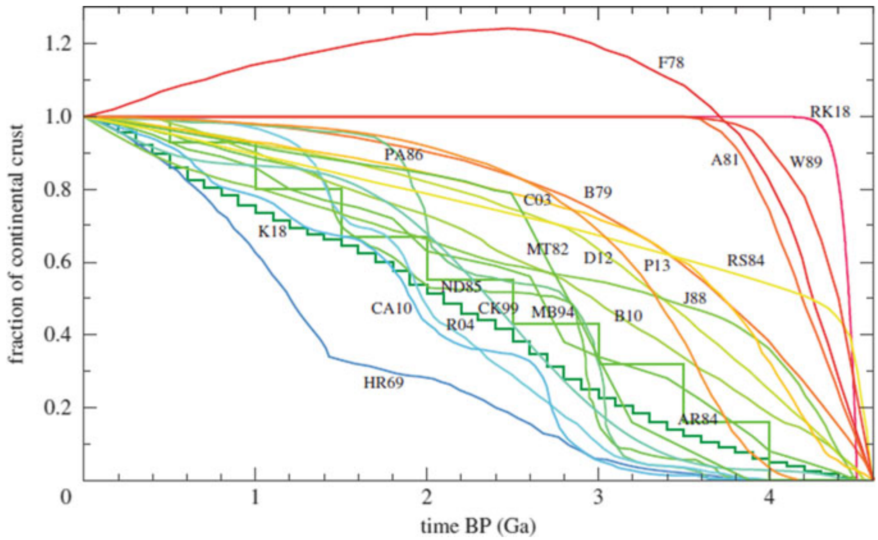

Fig. 5.2 Schematic curves showing the diversity of continental crust growth histories (cool to hot color gradation represents progressively earlier growth estimates). Early models based on surface age provinces skewed to relatively recent growth, expanding to earlier histories as new age survey methodologies and an appreciation of crustal reworking and recycling arose. Reference key: HR67: Hurley and Rand 1969; F78: Fyfe 1978; B79: Brown 1979; A81: Armstrong 1981; MT82: McLennan and Taylor 1982; RS84: Reymer and Schubert 1984; AR84: Allègre and Rousseau 1984; ND85: Nelson and DePaolo 1985; PA86: Patchett and Arndt 1986; J88: Jacobsen 1988; W89: Warren 1989; CK99: Collerson and Kamber 1999; C03: Campbell 2003; R04: Rino et al. 2004; CA10: Condie and Aster 2010; B10: Belousova et al. 2010; D12: Dhuime et al. 2012; K18: Korenaga, 2018b; RK18: Rosas and Korenaga 2018). Reproduced with permission from Korenaga (2018b)

the growth history of continental crust. The other is that crust recycled back into the mantle and thoroughly mixed leaves no trace of its past incarnations.

The earliest approach, an outgrowth of the rise of K-Ar and Rb-Sr geochronology as a geologist's tool in the 1960s, was to establish the global distribution of age provinces and assume that continental crust formed at that time (Hurley and Rand 1969). This provided only a lower limit due to the relative ease with which the geochronometers, particularly K–Ar, could be reset during orogeny. Subsequently, geochronometers thought to be more resistant to resetting, such as U–Pb, Sm–Nd and Lu–Hf, were employed (DePaolo 1981; Allègre and Rousseau 1984; Condie 1998; Rino et al. 2004; Belousova et al. 2010; Dhuime et al. 2012; Roberts and Spencer 2015). However, these methods provide no information regarding the amount of continental crust lost to the mantle through recycling and thus constrain only lower bounds on net crustal growth (Korenaga 2018a). A third approach is the use of tracers of juvenile involvement which can track the history of mantle-derived elements preferentially taken up in, or excluded from, the continental crust (e.g., DePaolo 1980; Jacobsen 1988; Armstrong 1991; Campbell 2003). The extraction of incompatible elements into continental crust depletes the mantle of those species which can only be replenished through subduction of recycled crust. Thus knowledge of the secular history of mantle depletion is potentially a proxy for knowing the time-varying mass of coexisting continental crust. The extent to which this estimate differs from the surface age distribution of crustal rocks is then a measure of crustal reworking and recycling.

The longstanding paradigm or, as characterized by Moorbath (1983), the "majority view" of continental crust growth history, is that its formation did not begin until after ~4 Ga with monotonic growth to its present mass (e.g., Moorbath 1975; Veizer and Jansen 1979; McLennan and Taylor 1982, 1991; Taylor and McLennan 1985). This view largely reflects the apparent absence of a >4 Ga rock record and the distribution of surface age provinces, but the post-3 Ga evolution of $^{143}Nd/^{144}Nd$ and $^{176}Hf/^{177}Hf$ in samples thought to represent the depleted mantle attracted new proponents of that longstanding view (e.g., McCulloch and Bennett 1993; Bowring and Williams 1999; Vervoort and Blichert-Toft 1999). However, the observation of early Nd (Galer and Goldstein 1991) and Hf (Blichert-Toft and Arndt 1999; Blichert-Toft et al. 2004) isotopic heterogeneities left open the possibility of earlier global fractionations. This sustained a minority view that continental crust may have been present during the Hadean Eon (e.g., Armstrong 1981, 1991; Reymer and Schubert 1984, Bowring and Housh 1995; Harrison 2009), but the view that continental mass increased slowly and monotonically through the first half of Earth history (Veizer and Jansen 1979, McLennan and Taylor 1991, McCulloch and Bennett 1993) remained broadly popular.

Although the existence of Hadean zircons had been known since the early 1980s (Froude et al. 1983; Compston and Pidgeon 1986), they were largely seen more as curiosities unrelated to the existence of continental crust rather than helpful in understanding its origins (e.g., McCulloch and Bennett 1993). For example, their origin was widely speculated to have been in Icelandic-type magmas (e.g., Taylor and McLennan 1985; Galer and Goldstein 1991; Valley et al. 2002; Martin and Sigmarsson 2005), although geochemical evidence essentially precludes such an environment for their formation (Carley et al. 2014). In addition to the distribution of age provinces and the absence of > 4 Ga crust, supporters of the slow growth paradigm also pointed to Archean-Proterozoic sediment REE patterns, the lack of fractionation of the Nd–Hf isotopic systems, the uniformity of Ce/Pb in basalts throughout time, Nb–U–Th systematics in mantle-derived rocks, and the general implausibility of making early felsic crust. But, as discussed in more detail below, none of these lines of evidence can be particularly compelling given the unknown history of recycling continental crust back into the mantle.

At the other extreme of this debate, advocates for massive early continental growth pointed to early silicate differentiation in other planets, continental freeboard, and the relationship between rates of arc magma production relative to sediment subduction to support their viewpoint. Armstrong (1981) emphasized that, like all other terrestrial bodies, Earth must have immediately differentiated into relatively constant-volume core, depleted mantle, enriched crust, and fluid reservoirs. Others argued that, unlike Mercury, Mars, and Moon which all rapidly developed primary crusts, exceptional circumstances (see earlier arguments; Smith 1981; Taylor and McLennan 1985) forestalled this occurrence on Earth.

While it is possible that the mass of continental crust could have been greater in the past than at present day, or experienced periodic increases and decreases (e.g., Fyfe 1978; Stern and Scholl 2010; Fig. 5.2), two lines of reasoning suggest that the present continental-oceanic crustal division of 40:60 may reflect a balance between optimization of planetary heat loss and maintenance of a global stress balance. Lenardic et al. (2005) argued that the insulating effect of the present surface extent of continental crust does not result in an overall reduction in mantle heat loss, but instead helps to cool Earth by increasing the velocity and thus subduction rate of oceanic lithosphere. However, increasing surface area of continental crust beyond the present area will eventually exceed a critical value whereupon the global plate system will lock up. Sandiford (2010) proposed that the near equivalence between the total gravitational potential energy of continental lithosphere with that of the mid-ocean ridge system reflects a planetary-scale modulation of the density configuration of the continents. This implies a feedback mechanism between the internal architecture and extent of continental and oceanic lithosphere that results in continents being everywhere critically stressed. Taken together, these two mechanisms appear to support attainment of something approaching the present 40:60 division of continental-oceanic crust relatively early in Earth history.

5.3.2 ^{146,147}Sm–^{142,143}Nd Model Ages

^{147}Sm and ^{146}Sm decay to ^{143}Nd and ^{142}Nd, with half-lives of 106 Ga and 70-100 Ma, respectively. Historically, the secular evolution in the ^{143}Nd/^{144}Nd depleted mantle has been attributed to the continuous extraction of the continental crust component (e.g., DePaolo 1981) whereas ^{142}Nd/^{144}Nd variations were generally thought to reflect sluggish mantle convection on early Earth (Debaille et al. 2013; Caro et al. 2017). The latter view is based on the aforementioned observation of significant ^{142}Nd/^{144}Nd anomalies in Neoarchean rocks that appear to gradually disappear from the geologic record by ca. 2.5 Ga. That seemingly long residence time is assumed by many to reflect inefficient mixing due to a stagnant lid tectonic regime inhibiting vigorous mantle convection (see Sect. 3.6).

Compilations of Sm–Nd model mantle extraction ages from exposed continental crust (e.g., McCulloch and Bennett 1993) tend to yield peaks at about 2.7, 1.9, 1.2, and ~0.4 Ga, arguably reflecting supercontinent assembly (Condie 2000). However, this approach is limited by sampling artifacts (e.g., glacially-scoured bedrock exposures in developed nations actively engaged in mineral resource exploration are overrepresented), irregular or poor exposure, ice cover, and sampling limitations (i.e., 99%+ of the volume of continental crust has not been radiometrically age characterized; Harrison et al. 2017).

Although such data provide a lower bound on continental growth, they are often interpreted in terms of the rate of continental addition with time (e.g., Taylor and

McLennan 1985) rather than the record of crustal preservation in light of reworking and crustal recycling. Morgan (1985, 1989) noted that the anomalously low K, Th, and U contents seen in Archean rocks is evidence that complementarily high heat production >2.5 Ga crust has been preferentially recycled into the mantle during subsequent orogenesis. In this interpretation, the extent of exposed Archean crust is only a fraction of what existed prior to 2.5 Ga. What remains is highly biased to compositions most likely to resist deformation and thus exposure to erosion at newly rifted continental margins, specifically those portions containing both low heat production and water content. This bias influences all subsequent approaches which assume the present distribution of continental crust is a true growth, rather than preservation, record.

As previously noted in Sect. 3.7, plate tectonics can potentially exist under a range of convective intensities and the slow apparent disappearance of ^{142}Nd signals in mantle rocks could equally well be explained by crustal recycling. Rosas and Korenaga (2018) modeled the evolution of ^{146,147}Sm–^{142,143}Nd and found these data were best explained by rapid continental growth at ca. 4.5 Ga followed by declining crustal recycling (Fig. 5.3a). The apparent paucity of Hadean zircons preserved today reflects this early, efficient crustal recycling. Perhaps fortuitously, their preferred inverse model predicts within uncertainties the present-day formation age distribution estimated from a global database of detrital zircon U-Pb ages (Fig. 5.3b) (Korenaga 2018a).

5.3.3 Coupled Rb-Sr/Sm–Nd Model Ages

Dhuime et al. (2015) introduced an intriguing approach in which they corrected ^{87}Sr/^{86}Sr at the time of crystallization for decay of ^{87}Rb using the measured Rb/Sr

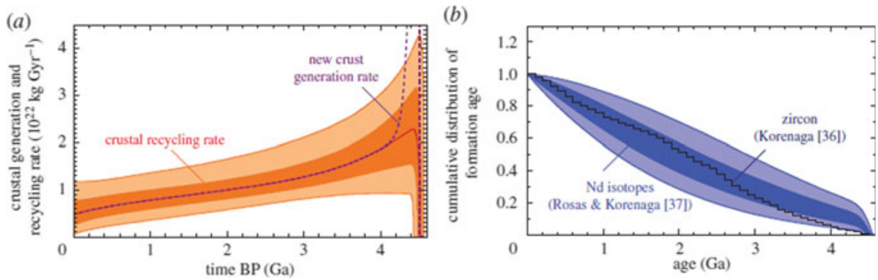

Fig. 5.3 **a** Crustal recycling rate corresponding to the net crustal growth from Rosas and Korenaga's (2018) joint inversion of ^{146,147}Sm–^{142,143}Nd data. For comparison note that the present-day recycling rate is $\sim 0.8 \times 10^{22}$ kg/Ga. The rate of new crust generation is shown in purple dashed line and recycling rate in red. **b** The present-day formation age distribution predicted from modelling Nd isotope evolution compared with that estimated from the global database of detrital zircon. In both figures, dark and light shades denote the 50 and 90% confidence limits. Reproduced with permission from Korenaga (2018a)

and known crystallization age. Using a large database of igneous rocks, they then calculated a “juvenile” Rb/Sr ratio by assuming that these rocks had separated from the depleted mantle at the time corresponding to their Sm/Nd model age. Under the assumption that Rb/Sr monotonically increased in the same fashion with SiO_2 over time as modern rock suites, they concluded that the continental crust was mafic early in Earth history becoming increasingly felsic over time (Fig. 5.4). However, Dhuime et al. (2015) did not address whether rocks of a given SiO_2 content could have had time varying Rb/Sr ratios. As noted in Chap. 2, the early Earth mantle was almost certainly hotter than today resulting in higher degrees of mantle partial melting and, as a result, incompatible element abundances were almost certainly lower than today.

Keller and Harrison (2020) tested the Dhuime et al. (2015) model by comparing it with a reference model in which a mix of mafic, intermediate and felsic rocks maintains a constant SiO_2 content over geologic time. Because of significant changes in compatible and incompatible element concentrations occur due to secular cooling, they found that ancient rocks would as a result have had lower Rb/Sr than today, regardless of SiO_2 content. That is, temporal changes in concentrations of compatible and incompatible elements occur as a function of SiO_2, not because the crust changed from mafic to felsic. They further found that Rb/Sr variations in their constant SiO_2 crust model well-tracked the apparent time variation seen in the Dhuime et al. (2015) model compilation. Thus the assumption of a time-invariant relationship between Rb/Sr and SiO_2 appears to be overly simplistic. In a similar fashion, Keller and Harrison (2020) noted that other approaches that assumed

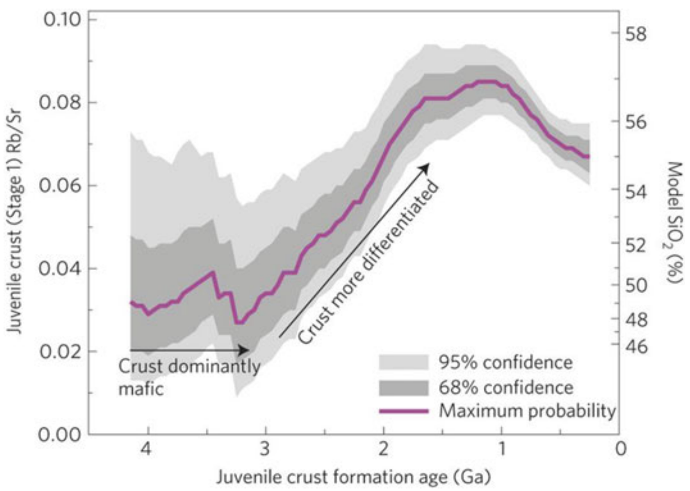

Fig. 5.4 Model evolution of silica content of continental crust using a large database of analyzed rocks for an assumed monotonic relationship between Rb/Sr and SiO_2. Reproduced with permission from Dhuime et al. (2015)

constant inter-elemental ratios over time (e.g., relationships between Ni/Co, Cr/Zn, and MgO content to SiO_2, Tang et al. 2016 (see Fig. 6.5); Cr/U to SiO_2, Smit and Mezger 2017) can equally well be explained by constant SiO_2 crust or make problematic assumptions regarding the constancy of redox conditions through geologic time. In a related study, Ptáček et al. (2020) reprocessed the sediment geochemistry data previously used to argue for a mafic Archaean crust with a view to correcting for effects of chemical and physical weathering. Their results indicate that these data are consistent with an upper continental crust containing >50% felsic material since 3.5 Ga; i.e., the ratio of mafic to felsic rocks in the crust has remained broadly constant through time (see Sect. 6.3.3).

5.3.4 U-Pb (and Lu–Hf) Zircon Dating

Patchett et al. (1984) argued that because zircon-rich turbiditic sands have much lower Lu/Hf than superchondritic pelagic sediments, the broad coherence between the Nd and Hf isotopic systems in mantle-derived rocks is evidence that continental sediment had not been substantially subducted over geologic time. Armstrong (1991) counter argued that subduction of the mix of sediments characteristic of the ocean floor today would retain the mantle Nd–Hf array and thus no inference of global tectonic behavior could be taken.

With the advent of methods for rapid, in situ U–Pb dating of zircon, large age databases began to become available for evaluation in the late 1990s (e.g., Condie 1998). Many authors found age peaks in these compilations similar to that seen from model mantle extraction ages and inferred rapid continental crust growth at those times (e.g., Condie and Kroner 2008; Condie and Pease 2008; Condie et al. 2009, Condie and Aster 2010; Roberts and Spencer 2015). Such interpretations are problematic for two reasons. The first is, as noted above, the overrepresentation of data from developed nations. The second, as described above, is subtler. Keller et al. (2017) observed that igneous rocks show increasing depletions in incompatible elements, including Zr, with increasing age. They interpreted this to reflect the hotter early Earth experiencing significantly higher degrees of mantle partial melting (thus diluting the concentration of incompatible trace elements like Zr). In effect, a cubic kilometer of rock added to the crust early in Earth history is represented by significantly fewer zircons than at present. Interpreting zircon U–Pb age spectra without taking this effect into account results in underestimates of early continental crust mass. Depending on assumptions regarding pressure and water content during melting, this could result in a bias of up to a factor of four (Keller et al. 2017). This issue is further discussed in Sect. 6.3.2.

In an effort to transcend the abovementioned limitation, it became popular to couple U-Pb age and Hf isotope analyses of detrital zircons (e.g., Hawkesworth and Kemp 2006; Kemp and Hawkesworth 2012). The ability of zircon to retain the U-Pb crystallization age and Hf isotopic signature of its host rock through multiple orogenic cycles seemingly simultaneously provides crust formation ages and the extent of depletion of the mantle reservoir from which the zircon host arose (Rino et al. 2004; Iizuka et al. 2010; Belousova et al. 2010; Dhuime et al. 2012). Again, note that this cannot permit reconstruction of continental growth histories without independent knowledge of the magnitude of subduction recycling of continental crust throughout Earth history.

Korenaga (2018a) approached interpretation of a global U-Pb/Lu–Hf zircon database (Roberts and Spencer 2015) from a perspective incorporating corrections for both crustal reworking and recycling. He argued that previous interpretive models (e.g., Belousova et al. 2010) were flawed because (1) they only corrected for crustal reworking but not crustal recycling, and (2) their correction for crustal reworking had been incorrectly formulated. He utilized a "reworking index" (Iizuka et al. 2010) that modifies the relationship between the apparent U–Pb and associated depleted mantle Lu–Hf model ages, and the age of the reworked crustal component. The distribution of crust formation ages estimated by this approach from the database of Roberts and Spencer (2015) provide a lower bound to the true crustal growth history (Fig. 5.3b). As such, deviations of the zircon record from growth models based on mantle depletion reflect the important role of crustal recycling rather than confirm a record of slow continental growth. However, the reworking index shows some variations in real data (Iizuka et al. 2010), reflecting temporally varying effects, including the rate of continental crust generation, changes in granitoid formation processes, and increasing crustal thickness with time (i.e., thin crust permits less crustal assimilation than thick crust under the same heat flow regime).

5.3.5 Ti Isotopes

Greber et al. (2017) found that the titanium isotopic composition of shales of all ages have a uniform composition. Because Ti isotopes correlate with SiO_2 content, the uniform composition suggests that the source of shales had ~72% silica since at least 3.5 Ga. Titanium is a particularly good tracer in this regard as it is highly insoluble in surface environments, present on Earth in a single oxidation state, biologically inert, and not preferentially sorted into a particular sediment grain size (Greber et al. 2017). Recent work showing that tholeiitic rocks are more isotopically fractionated in Ti than calc-alkaline rocks (e.g., Deng et al. 2019) is unlikely to influence this conclusion as continental basalts record a constant proportion of subduction magmatism since the Neoarchean (Keller and Schoene, 2018). Greber et al. (2017) inference supports the underlying perspectives of Keller and Harrison (2020) and Ptáček et al. (2020) who found geochemical data to be consistent with a mix of crustal lithologies that maintain a constant SiO_2 content since ca. 4 Ga (Sect. 5.3.3).

5.3.6 Sediment Geochemistry

Distinct differences in chemistry between fine-grained Archean and Proterozoic sediments have been interpreted as indicating that >2.5 Ga upper crust was substantially more mafic and less abundant than <2.5 Ga upper crust (Taylor and McLennan 1985). One reason for this is that fine-grained Archean sediments are nearly all hosted in greenstone belts and thus represent material eroded from island arc volcanics built on oceanic floor. Thus Taylor and McLennan (1985) are more likely to have identified an environmental, rather than a temporal, difference. Higher ratios of incompatible to compatible elements (e.g., Th/Sc) in post-Archean sediments may reflect lesser vertical mixing in compositionally stratified crust rather than a fundamentally different crustal composition. In any case, inferences regarding crustal volume drawn from trace element data are without basis; *there is simply no definable relationship between sediment chemistry and continental growth history* (Armstrong 1991).

5.3.7 Nb–U–Th

Modern mid-ocean ridge basalts (MORB) and oceanic island basalts (OIB) show uniformity in incompatible trace element ratios (e.g., Ce/Pb; Hofmann et al. 1986) while mafic volcanics appear to increase in Nb/U (and Nb/Th) through time (Sylvester et al. 1997; Collerson and Kamber 1999; Campbell 2003). Thus secular variations in ratios of Nb–U–Th have been used to estimate the fraction of continental crust extracted from the mantle over time. The basis of this approach is that, while Nb, U, and Th are equally incompatible during mantle melting, they are fractioned in the processes of continental crust formation such that Nb/U of the continental crust, primitive, and depleted mantle are today approximately 10, 30, and 50, respectively. Thus, documenting an Archean basalt with Nb/U $\approx$ 50 could be evidence that a similar magnitude of continental crust existed then as today. This approach, however, supports diverse conclusions. While Collerson and Kamber (1999) concluded that growth of the continental crust mostly occurred since Archean time, with less than 20% of the present mass of continental crust present at 3.1 Ga, Campbell (2003) used the same approach to estimate that 70% of the continental crust had been extracted by $\sim$3.1 Ga. This disparity appears to reflect the vagaries in the way in which trace element ratios of ancient rocks are averaged (see Condie 2003). In any case, trace element ratios retain no clear or convincing record of the state of continental extraction prior to the beginning of the rock record at $\sim$4 Ga.

Korenega (2018b) notes that the similarity of the mantle-derived model of Campbell (2003) to the crust-derived model of Dhiume et al. (2015) would imply that there has been no continental crust recycled into the mantle over at least the past billion years (Fig. 5.2). This would appear to be difficult to reconcile with the general recognition that plate tectonics operated over that same period (Stern 2007) and that subduction erosion is an inevitable consequence of that mechanism (Scholl and von Huene 2007).

5.3.8 Geophysical Estimates

Assuming that the oceans maintained a constant volume over the past 3 Ga, the semicontinuous geologic record of shallow water sedimentation on stable cratons could be seen as evidence that sea level has not significantly deviated from the present base level of erosion. This is referred to as “constant continental freeboard”. In detail, however, such an inference is complicated by the isostatic response to changing thermal conditions in the mantle, the unknown thickness of oceanic crust in the distant past, whether or not plate tectonics operated continuously in the past, and the role of mantle plumes on ancient Earth (Eriksson 1999).

Despite the many assumptions and uncertainties, there is general agreement that the thickness and areal extent of continents has been relatively constant since the Late Archean (Armstrong 1981; Taylor and McLennan 1985). Schubert and Reymer (1985) argued that, because the mantle cools over time, mid-ocean ridges would have diminished in volume and thus constant freeboard implies some continental growth since ~3 Ga. Armstrong (1991) countered that the diminishing volume of mid-ocean ridge would be compensated for by the subsidence of continental lithosphere as a result of its thickening (~40 km) over the past 2.5 Ga. In the author’s view, the present constraints are essentially equally supportive of the full range of continental growth models since ~3 Ga and freeboard arguments provide no useful quantitative constraints on earlier histories.

5.4 Recycling Model

The crux of Armstrong’s (1968, 1981, 1991) recycling model is that additions to the continental crust over time have been compensated by the recycling of similar amounts of continental material back into the mantle, mostly via sediment subduction. That is, there may have been a coequal mass of continental crust during the Hadean as today, but continuous subduction erosion has left virtually no vestige of that material in the geologic record. An appealing aspect of this model is that today, Earth appears to be in such a balance. A generation ago, estimates of sediment subduction rates were typically a fraction of a km^3/year (Dewey and Windley 1981; Reymer and Schubert 1984; Taylor and McLennan 1985), while others ruled out the possibility of this process operating altogether (e.g., Moorbath 1976). It now seems irrefutable from geochemical data (Pb–Nd–Hf isotopes and the presence of ^{10}Be in arc volcanics; Armstrong 1968; DePaolo 1983; Tera et al. 1986) and seismic imaging of accretionary arcs (e.g., Vannucchi et al. 2003, 2016) that significant amounts of continental sediment are being subducted into the mantle. Scholl and von Huene (2007) estimate that a minimum of ~3 km^3/yr of continental crust has been introduced into the mantle via subduction processes through the Cenozoic. Other mechanisms, such as crustal delamination or continental subduction, would only add to this figure. Scholl and von Huene’s (2007) estimate implies that a volume of continental crust equal to the present mass (~6×10^9 km^3) has been removed from the surface of Earth since 2.5 Ga. Estimates of magmatic additions at arcs, which long hovered around 1 km^3/year (see Condie 2005), lately have increased to values up to ~5 km^3/year (Scholl and von Huene 2007) suggesting an approximate balance between production and destruction.

In contrast to the assumption that peaks in Sm–Nd model ages correspond directly to crustal growth episodes (see Sect. 5.3.2), Rosas and Korenaga (2018) used a geochemical box modeling approach incorporating crustal growth, reworking and recycling to extract a best fit evolution of ε^{143}Nd and μ^{142}Nd in the continental crust and depleted mantle. Their preferred model is that net growth of continental crust was complete by the end of the Hadean and gradually decreased since then (Figs. 5.2 and 5.3). This continental crustal evolution model is consistent with the present-day distribution of crustal formation ages, a global compilation of zircon U-Pb ages (Korenaga 2018a, b), and the observed modern rate of subduction erosion (Scholl and von Huene 2007).

The discussion above is intended to emphasize only that our present knowledge of continental additions and losses is consistent with planet's continental crust budget being in steady-state. Armstrong (1981) recognized that, even if this were the case, the present magnitude of recycling would be insufficient to remove surface vestiges of once widespread Hadean continental crust. He instead proposed that the rate of crustal recycling scales according to the square of the internal heat generation (i.e., ~10 times faster at 4 Ga than today)—a relationship then thought to be supported by geodynamic modeling (e.g., Davies 2002)—and his model achieved a good fit with what was then taken to be the age distribution of continents. Armstrong's (1981) model was limited by his implementation of mantle-crust recycling that had no spatial dependence (i.e., mantle-crust box reservoirs were randomly accessed and mixed). The approach of Rosas and Korenaga (2018) greatly improved on Armstrong's pioneering work and their conclusions bolster the view that the seeming absence of pre-Archean crust today may more reflect early reworking and recycling than its non-existence.

5.5 Critical Summary

The rock record contains no direct evidence with which to constrain the magnitude of Hadean continental crust. Isotopic data (e.g., Sr–Nd isotopes of basalts) once thought to support rapid growth at ~2.7 Ga (e.g., Taylor and McLennan 1985) are recognized as equally consistent with constant volume continental crust (DePaolo 1983). The possibility of unrecognized crust-mantle recycling removes the ability to use such a relationship to predict the absence of a significant continental crustal mass prior to 4 Ga. Indeed, optimal solutions of modelling ^{146,147}Sm–^{142,143}Nd data are at least as consistent with constant volume continental crust since ca. 4.4 Ga as with slow monotonic growth. Radiogenic isotopic data used to argue for an early mafic crust are contradicted by stable isotopic results that appear to support a continuously felsic continental crust.

References

Alessio, K. L., Hand, M., Kelsey, D. E., Williams, M. A., Morrissey, L. J., & Barovich, K. (2018). Conservation of deep crustal heat production. *Geology, 46,* 335–338.

Allègre, C. J., & Rousseau, D. (1984). The growth of the continent through geological time studied by Nd isotope analysis of shales. *Earth and Planetary Science Letters, 67,* 19–34.

Armstrong, R. L. (1968). A model for the evolution of strontium and lead isotopes in a dynamic Earth. *Reviews of Geophysics, 6,* 175–199.

Armstrong, R. L. (1981). Radiogenic isotopes: The case for crustal recycling on a near-steady-state no-continental-growth Earth. *Philosophical Transactions of the Royal Society London Series, A, 301,* 443–471.

Armstrong, R. L. (1991). The persistent myth of crustal growth. *Australian Journal of Earth Science, 38,* 613–630.

Asahara, Y., & Ohtani, E. (2001). Melting relations of the hydrous primitive mantle in the CMAS-H_2O system at high pressures and temperatures, and implications for generation of komatiites. *Physics of the Earth and Planetary Interiors, 125,* 31–44.

Badro, J., Côté, A. S., & Brodholt, J. P. (2014). A seismologically consistent compositional model of Earth's core. *Proceedings of the National Academy of Sciences, 111,* 7542–7545.

Bea, F., & Montero, P. (1999). Behavior of accessory phases and redistribution of Zr, REE, Y, Th, and U during metamorphism and partial melting of metapelites in the lower crust: an example from the Kinzigite formation of Ivrea-Verbano, NW Italy. *Geochimica et Cosmochimica Acta, 63,* 1133–1153.

Belousova, E. A., Kostitsyn, Y. A., Griffin, W. L., Begg, G. C., O'Reilly, S. Y., & Pearson, N. J. (2010). The growth of the continental crust: Constraints from zircon Hf-isotope data. *Lithos, 119,* 457–466.

Blichert-Toft, J., & Arndt, N. T. (1999). Hf isotope compositions of komatiites. *Earth and Planetary Science Letters, 171,* 439–451.

Blichert-Toft, J., Arndt, N. T., & Gruau, G. (2004). Hf isotopic measurements on Barberton komatiites: effects of incomplete sample dissolution and importance for primary and secondary magmatic signatures. *Chemical Geology, 207,* 261–275.

Bowring, S. A., & Housh, T. (1995). The Earth's early evolution. *Science, 269,* 1535–1540.

Bowring, S. A., & Williams, I. S. (1999). Priscoan (4.00–4.02 Ga) Orthogneisses from northwestern Canada. *Contributions to Mineralogy and Petrology, 134,* 3–16.

Brown, G. C. (1979). The changing pattern of batholith emplacement during Earth history. In M. P. Atherton & J. Tarney (Eds.), *Origin of Granite Batholiths, geochemical evidence*. Nantwich: Shiva.

Brown, G. M., Holland, J. G., Sigurdsson, H., Tomblin, J. F., & Arculus, R. J. (1977). Geochemistry of the Lesser Antilles volcanic island arc. *Geochimica et Cosmochimica Acta, 41,* 785–801.

Campbell, I. J. (2003). Constraints on continental growth models from Nb/U ratios in the 3.5 Ga Barberton and other Archaean basalt-komatiite suites. *American Journal of Science, 303,* 319–351.

Carley, T. L., Miller, C. F., Wooden, J. L., Padilla, A. J., Schmitt, A. K., Economos, R. C., et al. (2014). Iceland is not a magmatic analog for the Hadean: Evidence from the zircon record. *Earth and Planetary Science Letters, 405,* 85–97.

Caro, G., Morino, P., Mojzsis, S. J., Cates, N. L., & Bleeker, W. (2017). Sluggish Hadean geodynamics: Evidence from coupled ^{146,147}Sm–^{142,143}Nd systematics in Eoarchean supracrustal rocks of the Inukjuak domain (Québec). *Earth and Planetary Science Letters, 457,* 23–37.

Cogley, J. G. (1984). Continental margins and the extent and number of the continents. *Reviews of Geophysics, 22,* 101–122.

Collerson, K. D., & Kamber, B. (1999). Evolution of the continents and the atmosphere inferred from Th-U-Nb systematics of the depleted mantle. *Science, 283,* 1519–1522.

Compston, W., & Pidgeon, R. T. (1986). Jack Hills, evidence of more very old detrital zircons in Western Australia. *Nature, 321,* 766–769.

Condie, K. C. (1982). *Plate tectonics and crustal evolution*. New York, NY: Pergamon.

Condie, K. C. (1998). Episodic continental growth and supercontinents: a mantle avalanche connection? *Earth and Planetary Science Letters, 163,* 97–108.

Condie, K. C. (2000). Episodic continental growth models: Afterthoughts and extensions. *Tectonophysics, 322,* 153–162.

Condie, K. C. (2003). *Incompatible element ratios in oceanic basalts and komatiites: Tracking deep mantle sources and continental growth rates with time., G3*(4), 1005. https://doi.org/10.1029/2002GC000333.

Condie, K. C. (2005). *Earth as an evolving planetary system*. Amsterdam: Elsevier Academic Press.

Condie, K. C., & Aster, R. C. (2010). Episodic zircon age spectra of orogenic granitoids: The supercontinent connection and continental growth. *Precambrian Research, 180,* 227–236.

Condie, K. C., Belousova, E., Griffin, W. L., & Sircombe, K. N. (2009). Granitoid events in space and time: constraints from igneous and detrital zircon age spectra. *Gondwana Research, 15,* 228–242.

Condie, K. C., & Kröner, A. (2008). When did plate tectonics begin? Evidence from the geologic record. *Geological Society of America Special Paper, 440,* 281–294.

Condie, K. C., & Pease, V. (2008). When did plate tectonics begin on planet Earth? *Geological Society of America Special Paper, 440,* 294.

Davies, G. F. (2002). Stirring geochemistry in mantle convection models with stiff plates and slabs. *Geochimica et Cosmochimica Acta, 66,* 3125–3142.

Debaille, V., O'Neill, C., Brandon, A. D., Haenecour, P., Yin, Q., Mattielli, N., et al. (2013). Stagnant-lid tectonics in early Earth revealed by ^{142}Nd variations in late Archean rocks. *Earth and Planetary Science Letters, 373,* 83–92.

Deng, Z., Chaussidon, M., Savage, P., Robert, F., Pik, R., & Moynier, F. (2019). Titanium isotopes as a tracer for the plume or island arc affinity of felsic rocks. *Proceedings of the National Academy of Sciences*, *116*, 1132–1135.

DePaolo, D. J. (1980). Crustal growth and mantle evolution: Inferences from models of element transport and Nd and Sr isotopes. *Geochimica et Cosmochimica Acta, 44,* 1185–1196.

DePaolo, D. J. (1981). Nd isotopic studies: Some new perspectives on Earth structure and evolution. *EOS, Transactions American Geophysical Union, 62,* 137.

DePaolo, D. J. (1983). The mean life of continents: estimates of continent recycling rates from Nd and Hf isotopic data and implications for mantle structure. *Geophysical Reseach Letters, 10,* 705–708.

Dewey, J. F., & Windley, B. F. (1981). Growth and differentiation of the continental crust. *Philosophical Transactions of the Royal Society London Series A 301*, 189–206.

Dhuime, B., Hawkesworth, C. J., Cawood, P. A., & Storey, C. D. (2012). A change in the geodynamics of continental growth 3 billion years ago. *Science, 335,* 1334–1336.

Dhuime, B., Wuestefeld, A., & Hawkesworth, C. J. (2015). Emergence of modern continental crust about 3 billion years ago. *Nature Geoscience, 8,* 552–555.

Ducea, M., & Saleeby, J. (1998). A case for delamination of the deep batholithic crust beneath the Sierra Nevada, California. *International Geology Review, 40,* 78–93.

Eriksson, P. G. (1999). Sea level changes and the continental freeboard concept: general principles and application to the Precambrian. *Precambrian Research, 97,* 143–154.

Froude, D. O., Ireland, T. R., Kinny, P. D., Williams, I. S., & Compston, W. (1983). Ion microprobe identification of 4100–4200 Myr-old terrestrial zircons. *Nature, 304,* 616–618.

Fyfe, W. S. (1978). The evolution of the Earth's crust: Modern plate tectonics to ancient hot spot tectonics? *Chemical Geology, 23,* 89–114.

Galer, S. J. G., & Goldstein, S. L. (1991). Early mantle differentiation and its thermal consequences. *Geochimica et Cosmochimica Acta, 55,* 227–239.

Ghiorso, M. S., & Sack, R. O. (1995). Chemical mass-transfer in magmatic processes 4. A revised and internally consistent thermodynamic model for the interpolation and extrapolation of liquid-solid equilibria in magmatic systems at elevated-temperatures and pressures. *Contributions to Mineralogy and Petrology, 119,* 197–212.

Goodwin, A. M. (1991). *Precambrian geology: The dynamic evolution of the continental crust*. Academic Press.

Greber, N. D., Dauphas, N., Bekker, A., Ptáček, M. P., Bindeman, I. N., & Hofmann, A. (2017). Titanium isotopic evidence for felsic crust and plate tectonics 3.5 billion years ago. *Science, 357,* 1271–1274.

Grieve, R. A. F. (1991). The Sudbury structure: Controversial or misunderstood? *Journal of Geophysical Research, 96,* 22753–22764.

Hacker, B. R., Kelemen, P. B., & Behn, M. D. (2011). Differentiation of the continental crust by relamination. *Earth and Planetary Science Letters, 307,* 501–516.

Harrison, T. M. (2009). The Hadean crust: Evidence from >4 Ga zircons. *Annual Reviews of Earth and Planetary Sciences, 37,* 479–505.

Harrison, T. M., Bell, E. A., & Boehnke, P. (2017). Hadean zircon petrochronology. *Reviews in Mineralogy and Geochemistry, 83,* 329–363.

Harrison, T. M., Watson, E. B., & Rapp, R. P. (1986). Does anatexis deplete the lower crust in heat-producing elements? Implications from experimental studies. *EOS, 67,* 386.

Hawkesworth, C. J., & Kemp, A. I. S. (2006). Using hafnium and oxygen isotopes in zircons to unravel the record of crustal evolution. *Chemical Geology, 226,* 144–162.

Hofmann, A. W., Jochum, K. P., Seufert, M., & White, W. M. (1986). Nd and Pb in oceanic basalts: New constraints on mantle evolution. *Earth and Planetary Science Letters, 79,* 33–45.

Hurley, P. M., & Rand, J. R. (1969). Pre-drift continental nuclei. *Science, 164,* 1229–1242.

Iizuka, T., Komiya, T., Rino, S., Maruyama, S., & Hirata, T. (2010). Detrital zircon evidence for Hf isotopic evolution of granitoid crust and continental growth. *Geochimica et Cosmochimica Acta, 74,* 2450–2472.

Jacobsen, S. B. (1988). Isotopic and chemical constraints on mantle-crust evolution. *Geochimica et Cosmochimica Acta, 52,* 1341–1350.

Jones, C. H., Reeg, H., Zandt, G., Gilbert, H., Owens, T. J., & Stachnik, J. (2014). P-wave tomography of potential convective downwellings and their source regions, Sierra Nevada, California. *Geosphere, 10,* 505–533.

Keller, B., & Schoene, B. (2018). Plate tectonics and continental basaltic geochemistry throughout Earth history. *Earth and Planetary Science Letters*, *481*, 290–304.

Keller, B., & Harrison, T. M. (2020). Constraining crustal silica on ancient earth. EarthArXiv. https://doi.org/10.31223/osf.io/75evw.

Keller, C. B., Boehnke, P., & Schoene, B. (2017). Temporal variation in relative zircon abundance throughout Earth history. *Geochemical Perspectives Letters, 3,* 179–189.

Kemp, A. I. S., & Hawkesworth, C. J. (2012). *Growth and differentiation of the continental crust from isotope studies of accessory minerals*. Treatise on Geochemistry.

Korenaga, J. (2018a). Estimating the formation age distribution of continental crust by unmixing zircon ages. *Earth and Planetary Science Letters, 482,* 388–395.

Korenaga, J. (2018b). Crustal evolution and mantle dynamics through Earth history. *Philosophical Transactions of the Royal Society A: Mathematical, Physical and Engineering Sciences, 376,* 20170408.

Lachenbruch, A. H. (1970). Crustal temperature and heat production: Implications of the linear heat-flow relation. *Journal of Geophysical Research, 75,* 3291–3300.

Latypov, R., Chistyakova, S., Grieve, R., & Huhma, H. (2019). Evidence for igneous differentiation in Sudbury Igneous Complex and impact-driven evolution of terrestrial planet proto-crusts. *Nature Communications*, *10*. https://doi.org/10.1038/s41467-019-08467-9.

Lee, C. T. A., & Anderson, D. L. (2015). Continental crust formation at arcs, the arclogite "delamination" cycle, and one origin for fertile melting anomalies in the mantle. *Science Bulletin, 60,* 1141–1156.

Lenardic, A., Moresi, L. N., Jellinek, A. M., & Manga, M. (2005). Continental insulation, mantle cooling, and the surface area of oceans and continents. *Earth and Planetary Science Letters, 234,* 317–333.

Lewry, J. F., Hajnal, Z., Green, A., Lucas, S. B., White, D., Stauffer, M. R., et al. (1994). Structure of a Paleoproterozoic continent-continent collision zone: A LITHOPROBE seismic reflection profile across the Trans-Hudson Orogen, Canada. *Tectonophysics, 232,* 143–160.

Martin, E., & Sigmarsson, O. (2005). Trondhjemitic and granitic melts formed by fractional crystallization of an olivine tholeiite from Reykjanes Peninsula, Iceland. *Geological Magazine, 142,* 651–658.

McCulloch, M. T., & Bennett, V. C. (1993). Progressive growth of the Earth's continental crust and depleted mantle: constraints from ^{143}Nd-^{142}Nd isotopic systematics. *Lithos, 30,* 237–255.

McLennan, S. M., & Taylor, S. R. (1982). Geochemical constraints on the growth of continental crust. *Jour. Geol., 9,* 342–354.

McLennan, S. M., & Taylor, S. R. (1991). Sedimentary rocks and crustal evolution: Tectonic setting and secular trends. *Jour. Geol., 99,* 1–21.

Moorbath, S. (1975). Evolution of Precambrian crust from strontium isotopic evidence. *Nature, 254,* 395–398.

Moorbath, S. (1976). Age and isotope constraints for the evolution of Archean crust the Earth. In B. F. Windley (Ed.), *The early history of the earth* (pp. 351–364). Wiley: London.

Moorbath, S. (1983). Precambrian geology: The most ancient rocks? *Nature, 304,* 585–586.

Morgan, P. (1985). Crustal radiogenic heat production and the selective survival of ancient continental crust. *Proc. Lunar Planet. Scientific Conference on Journal Geophysics and Research Suppl. 90*, C561–570.

Morgan, P. (1989) Thermal factors controlling crustal stabilization. *28th International geological congress Washington, DC. Abstract, 3*, 333.

Morgan, P., Sawka, W. N., & Furlong, K. P. (1987). Introduction: Background and implications of the linear heat flow-heat production relationship. *Geophysical Research Letters, 14,* 248–251.

Morse, S. A. (1986). Origin of earliest planetary crust: Role of compositional convection. *Earth and Planetary Science Letters, 81,* 118–126.

Nelson, B. K., & DePaolo, D. J. (1985). Rapid production of continental crust 1.7 to 1.9 b.y. ago: Nd isotopic evidence from the basament of the North American mid-continent. *Geological Society of America Bulletin, 96,* 746–754.

Patchett, P. J., & Arndt, N. T. (1986). Nd isotopes and tectonics of 1.9–1.7 Ga crustal genesis. *Earth and Planetary Science Letters, 78,* 329–338.

Patchett, P. J., White, W. M., Feldmann, H., Kielinczuk, S., & Hofmann, A. (1984). Hafnium/rare earth element fractionation in the sedimentary system and crustal recycling into the Earth's mantle. *Earth and Planetary Science Letters, 69,* 365–378.

Pearson, D. G. (1999). The age of continental roots. *Lithos, 48,* 171–194.

Ptáček, M.P., Dauphas, N., & Greber, N.D. (2020). Chemical evolution of the continental crust from a data-driven inversion of terrigenous sediment compositions. *Earth and Planetary Science Letters*, *539*, 116090.

Rapp, R. P., & Watson, E. B. (1986). Monazite solubility and dissolution kinetics: Implications for the thorium and light rare earth chemistry of felsic magmas. *Contributions to Mineralogy and Petrology, 94,* 304–316.

Reymer, A., & Schubert, G. (1984). Phanerozoic addition rates to the continental crust and crustal growth. *Tectonics, 3,* 63–77.

Rino, S., Komiya, T., Windley, B. F., Katayama, I., Motoki, A., & Hirata, T. (2004). Major episodic increases of continental crustal growth determined from zircon ages of river sands; implications for mantle overturns in the Early Precambrian. *Physics of the Earth and Planetary Interiors, 146,* 369–394.

Roberts, N. M. W., & Spencer, C. J. (2015). The zircon archive of continent formation through time. In N. M. W. Roberts et al. (Eds.), *Continent formation through time* (Vol. 389, pp. 197–225). Geological Society of London Special Publications.

Rosas, J. C., & Korenaga, J. (2018). Rapid crustal growth and efficient crustal recycling in the early Earth: Implications for Hadean and Archean geodynamics. *Earth and Planetary Science Letters, 494,* 42–49.

Roy, R. F., Blackwell, D. D., & Birch, F. (1968). Heat generation of plutonic rocks and continental heat flow provinces. *Earth and Planetary Science Letters, 5,* 1–12.

Rudnick, R. L., & Fountain, D. M. (1995). Nature and composition of the continental crust: a lower crustal perspective. *Reviews of Geophysics, 33,* 267–309.

Rudnick, R. L., & Gao, S. (2003). Composition of the continental crust. *Treatise on Geochemistry, 3,* 1–64.

Rudnick, R. L., McLennan, S. M., & Taylor, S. R. (1985). Large ion lithophile elements in rocks from high-pressure granulite facies terrains. *Geochimica et Cosmochimica Acta, 49,* 1645–1655.

Sandiford, M. (2010). Why are the continents just so…? *Journal of Metamorphic Geology, 28,* 569–577.

Scholl, D. W., & von Huene, R. (2007). Crustal recycling at modern subduction zones applied to the past - issues of growth and preservation of continental basement, mantle geochemistry and supercontinent reconstruction. *Geological Society of America Special Paper, 200,* 9–32.

Schubert, G., & Reymer, A. P. S. (1985). Continental freeboard throughout geologic time. *Nature, 316,* 336–339.

Servali, A., & Korenaga, J. (2018). Oceanic origin of continental mantle lithosphere. *Geology, 46,* 1047–1050.

Shaw, D. M. (1976). Development of the early continental crust. In B. F. Windley (Ed.), *The early history of the Earth* (pp. 33–46). London: Wiley.

Smit, M. A., & Mezger, K. (2017). Earth's early O_2 cycle suppressed by primitive continents. *Nature Geoscience*, *10*, 788–781.

Smith, J. V. (1981). The first 800 million years of earths history. *Philosophical Transactions of the Royal Society London Series A, 301*, 401–422.

Stern, R. J. (2007). When and how did plate tectonics begin? Theoretical and empirical considerations. *Chinese Science Bulletin, 52,* 578–591.

Stern, R. J., & Scholl, D. W. (2010). Yin and yang of continental crust creation and destruction by plate tectonic processes. *International Geology Review, 52,* 1–31.

Sylvester, P. J., Campbell, I. H., & Bowyer, D. A. (1997). Niobium/uranium evidence for early formation of the continental crust. *Science, 275,* 521–523.

Tang, M., Chen, K., & Rudnick, R. L. (2016). Archean upper crust transition from mafic to felsic marks the onset of plate tectonics. *Science, 351,* 372–375.

Taylor, S. R. (1967). The origin and growth of continents. *Tectonophysics, 4,* 17–34.

Taylor, S. R. (1982). *Planetary science: A lunar perspective*. Houston, TX: Lunar Planet. Inst.

Taylor, S. R., & McLennan, S. M. (1985). *The Continental crust: Its composition and evolution*. Oxford: Blackwell.

Taylor, S. R., & White, A. J. R. (1965). Geochemistry of andesites and the growth of continents. *Nature, 208,* 271–273.

Tera, F., Brown, L., Morris, J., Sacks, I. S., Klein, J., & Middleton, R. (1986). Sediment incorporation in island-arc magmas: inferences from ^{10}Be. *Geochimica et Cosmochimica Acta, 50,* 535–550.

Valley, J. W., Peck, W. H., King, E. M., & Wilde, S. A. (2002). A cool early Earth. *Geology, 30,* 351–354.

Vannucchi, P., Morgan, J. P., & Balestrieri, M. L. (2016). Subduction erosion, and the de-construction of continental crust: The Central America case and its global implications. *Gondwana Research, 40,* 184–198.

Vannucchi, P., Ranero, C. R., Galeotti, S., Straub, S. M., Scholl, D. W., & McDougall-Ried, K. (2003). Fast rates of subduction erosion along the Costa Rica Pacific margin: Implications for nonsteady rates of crustal recycling at subduction zones. *Journal Geophysical Research, 108,* 2511.

Veizer, J., & Jansen, S. L. (1979). Basement and sedimentary recycling and continental evolution. *Journal of Geology, 87,* 341–370.

Vervoort, J. D., & Blichert-Toft, J. (1999). Evolution of the depleted mantle: Hf isotope evidence from juvenile rocks through time. *Geochimica et Cosmochimica Acta, 63,* 533–556.

Warren, P. H. (1989). Growth of the continental crust: A planetary-mantle perspective. *Tectonophysics, 161,* 165–199.

Watson, E. B., & Harrison, T. M. (1983). Zircon saturation revisited: temperature and composition effects in a variety of crustal magma types. *Earth and Planetary Science Letters, 64,* 295–304.

Watson, E. B., & Harrison, T. M. (1984). Accessory minerals and the geochemical evolution of crustal magmatic systems: a summary and prospectus of experimental approaches. *Physics of the Earth and Planetary Interiors, 35,* 19–30.

Zou, H., & Harrison, T. M. (2007). Formation of 4.5 Ga continental crust. *Geochimica et Cosmochimica Acta Suppl. 71*, A1176.

Plate Boundary Interactions Through Geologic History

6

Abstract

Estimates of when plate tectonics began range from the last 20% of Earth history to within the first 5%. While there is no observation that precludes plate tectonics from operating at 4.3 Ga, evidence that it was is indirect. Although subduction initiation is a robust feature of the modern plate tectonic system and we can calculate with some accuracy when oceanic lithosphere attains negative buoyancy, we don't yet understand how strong the lithosphere weakens sufficiently for subduction to initiate. Most approaches used to estimate when Earth first entered the mobile lid regime—preservation of modern plate tectonic features, detrital zircon age spectra, trace element and radiogenic isotope geochemistry, atmosphere-crust-mantle exchange, and model-based estimates—can be interpreted in multiple ways and are all underlain by assumptions that cannot be independently tested. All share the flaw that absence of evidence is not evidence of absence. Of special concern is that the Precambrian geologic record is likely biased to rock compositions most likely to resist deformation and thus exposure to erosion at newly rifted continental margins where loss to subduction erosion could occur. Thus any look-back comparison is flawed to some degree by a preservation bias. A more recently recognized limitation is the failure to consider how a hotter, early Earth would differ petrologically from, say, Phanerozoic behavior (e.g., lower incompatible trace element concentrations in mantle magmas, higher geothermal gradients). Historically, computational limitations in early geophysical modelling methods led to skepticism regarding the possibility of plate tectonics on early Earth. Influenced by this view, the geologic community was reluctant to take a dynamic view of the preserved crustal record, instead inferring the apparent absence of a Hadean rock record as evidence that there never was one. The unknown extent to which ancient continental crust was recycled into the mantle and thoroughly mixed, the

T. M. Harrison, *Hadean Earth*, https://doi.org/10.1007/978-3-030-46687-9_6

abovementioned selection biases in the rock record, and the assumption of uniformitarian conditions throughout Earth history limit virtually all continental growth estimates to providing only lower age bounds and thus minimum estimate on the initiation age of subduction.

6.1 Characteristics of Modern Plate Tectonics

Earth's present structure is a complex function of its composition, thermal state, and differentiation history (Chap. 2). Its present surface consists of about a dozen or so major lithospheric plates which interact at divergent, convergent and transform boundaries. The near surface lithosphere/asthenosphere dichotomy reflects the substantially different mechanical properties of these domains which result in contrasting modes of heat transfer—conduction within the relatively cool lithosphere and fluid convection in the hotter asthenosphere. Lateral weaknesses in the relatively cool and stiff lithosphere permit cracks to periodically separate it into discrete plates by an unknown or speculative mechanisms (Bercovici and Ricard 2014, 2016).

Positive and negative buoyancies—created by thermal contrasts at the global scale as Earth cools and more locally by compositional contrasts and phase changes—are the primary driving forces of the mobile-lid convection that powers plate tectonics. But density contrasts between the surface and deep Earth alone are insufficient to maintain plate tectonics; by itself, that leads to a stagnant-lid regime rather than plate tectonics. Mobile lid convection also requires negative buoyancy of the surface boundary layer and mechanically weak convergent plate boundaries (Sobolev 2016). Forces acting on subducting plates are the dominant contribution to the global energy balance but, because each plate must be in dynamic equilibrium, the velocity at which a slab is dragged downward must be nearly balanced by the sum of the resistive forces on that plate. Tractions at the base of lithosphere transferred by the underling convecting asthenosphere are thought to represent only a minor force contribution to the global tectonic system (Forsyth and Uyeda 1975).

The mantle gains thermal energy from radioactive decay and heat transfer from the core which increase mantle temperature and lowers its density by thermal expansion (it is estimated that about one quarter of that gravitational potential energy increase is spent on *PV* work; Arevalo et al. 2013). The hot buoyant mantle rises, but in doing so both cools and loses gravitational energy. Upon reaching the surface, much of the transported heat is lost to space by radiation causing the lithosphere to cool and densify, increasing gravitational potential energy which eventually causes it to sink into the mantle. Some of that potential energy gained through cooling is converted back to thermal energy by friction as plates subduct raising temperature locally and thus reducing negative buoyancy. While plate tectonics is fundamentally characterized by the recycling of mass, it also recycles a portion of its internal energy as well.

In the subsequent discussion, we adopt Stern and Gerya's (2018) definition of plate tectonics:

> A theory of global tectonics powered by subduction in which the lithosphere is divided into a mosaic of strong lithospheric plates, which move on, and sink into, weaker ductile asthenosphere…The negative buoyancy of old dense oceanic lithosphere, which sinks in subduction zones, mostly powers plate movements. The role of the subduction process and subduction zones is thus integral in this redefinition, and a strong case could be made that "subduction tectonics" is a more accurate and thus better name for modern-style global plate tectonics. Insofar as this is true, our understanding of plate tectonics is no better than our understanding of the subduction process from its initiation to its fate. It is also obvious that subduction initiation is needed to start plate tectonics.

6.2 How Did Plate Tectonics Initiate?

Immediately following accretion, silicate-metal differentiation, and lunar formation (Sects. 3.1–3.3), Earth was likely sufficiently thermally energized to create a silicate magma ocean (Sect. 3.4). Its subsequent crystallization could have led to a global scale mantle overturn that produced a stable density stratification in the mantle that forestalled, or even prevented, the initiation of plate tectonics (Schaefer and Elkins-Tanton 2018). Eventually, internal thermal contrasts would have overcome this resisting force.

While the energy balance within the modern plate tectonic system is broadly understood, the origin of subduction is not. Despite Earth being the only known planet with plate tectonics, it is hardly its perfect exemplar. Pure plate tectonics would feature only oceanic lithosphere subduction whereas the presence of compositionally buoyant continental crust inhibits that full process. In effect, Earth today is a hybrid of plate and stagnant lid tectonics complicating our understanding of Earth dynamics (e.g., O'Neill et al. 2007).

Although the lithosphere's resistance to bending works against the initiation and maintenance of subduction (McKenzie 1977), modelers broadly agree that attaining the needed negative buoyancy (subductability) of oceanic lithosphere is a negligible hurdle for a planet to produce a mobile lid tectonic regime (e.g., Sobolev 2016). The far greater challenge is overcoming the strength of the lithosphere, a challenge that only increases as Earth cools and oceanic lithosphere thickens. The long term stability of a stiff thermal boundary layer is provided by continuous surface heat loss to space, but this raises a chicken-or-egg paradox: what caused this strong layer to generate weakened planar features on which subduction could initiate? Specifically, what was the yield stress of the lithosphere that permitted plate tectonics to get underway and how did values approaching that develop? Answering these questions requires an understanding of, and the interrelationships between the full range of relevant lithospheric rheologies (i.e., elasto-visco-plastic-brittle behaviors). While there are presently few firm conclusions with regard to these issues, several interesting perspectives have recently emerged. One transcendent possibility is that plate tectonics began before the magma ocean phase was finished and Earth's surface was not entirely solid (Solomatov 2016). Numerical simulations suggest that while calculated yield stresses appear higher than that expected in the modern lithosphere, our planet may be the optimum size to approach the needed values (Wong and Solomatov 2016).

Alternatively, it may be that it is the application of conventional rheologies that confounds reconciliation. Bercovici and Ricard (2014, 2016) argue that an as yet incompletely understood memory of grain-damage in the lithosphere may allow future plate boundaries to accumulate damage until that weakening reaches similar values to the mantle. Or perhaps subduction initiation has an extraterrestrial origin (e.g., Hansen 2007; Yin 2012). Baes et al. (2016) argued that the very low values of friction ($\mu \approx 0.03$) required to match plate velocities in convection models could be attained by "aquaplaning" on subducting sediments following large impacts. A related model suggests that the breaking of the lithosphere by a mantle plume head could initiate self-sustaining subduction (Ueda et al. 2008; Gerya et al. 2015). A review of the full range of subduction initiation mechanisms is provided by Stern and Gerya (2018). Incongruously, although the manner in which subduction initiates continues to confound modelers, it appears to occur on Earth with surprising ease and frequency. For example, Gurnis et al. (2004) found that nearly one third of active subduction zones formed over the past 65 Ma.

6.3 When Did Plate Tectonics Initiate

Speculations on the timing of when subduction first initiated have been made since the dawn of the plate tectonic revolution (Dewey and Spall 1975). But identifying when plate tectonics began brings us back to defining what exactly it is. Stern and Gerya's (2018) definition focuses almost exclusively on subduction while others (e.g., Shirey and Richardson 2011) emphasize the importance of documenting the entire Wilson Cycle (Fig. 6.1)—the periodic opening and closing of ocean basins resulting in the aggregation and dispersal of continental crust (Wilson 1968; Fig. 6.1).

Estimates of the initiation age of plate tectonics rest on a range of assumptions, but can be broadly grouped as five distinct types: (1) preservation of modern plate tectonic features, (2) detrital zircon age spectra, (3) trace element and isotope geochemistry, (4) atmosphere-crust-mantle exchange, and (5) model-based estimates. While assumptions embodied in these different approaches have individual limitations, described below, all share at least one flaw; even if demonstrable evidence is obtained for the timing of the emergence of plate tectonics at a specified time, the fragmentary geologic record potentially masks earlier episodes that had previously terminated. My own view was influenced by the late, great geologist Kevin Burke who argued that the null hypothesis coupled with the community's broad acceptance of modern terrestrial plate tectonics puts the scientific onus on demonstrating when plate tectonics was *not* extant on Earth rather than the guilty-until-proven-innocent approach of requiring definitive proof that it was operating at a specified time in the past. From that perspective (as summarized in Chap. 9), in my opinion, the evidence at hand supports the null hypothesis back to

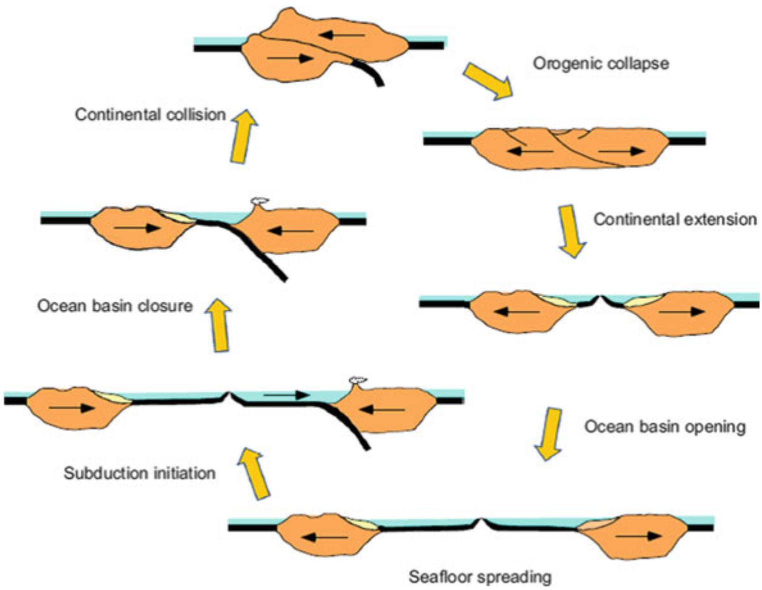

Fig. 6.1 The Wilson cycle, named after its originator J. Tuzo Wilson, is the concept that plate tectonics continuously cycles through phases of continental extension, ocean basin opening, seafloor spreading, subduction initiation, ocean basin closure, continental collision followed by orogenic collapse which leads again to continental extension

nearly 4.5 Ga. It remains, however, controversial (as discussed in the summary of Jun Korenaga's work; Sect. 2.4). Indeed, an alternate hypothesis arising from comparative planetology might be that a stagnant lid is the normal mode of convection on an active, roughly Earth mass planetary body with a silicate mantle, and that any such object—including Earth—should be assumed to be in stagnant lid mode unless strong evidence for mobile lid convection exists (see Stern et al. 2017).

6.3.1 Preservation of Modern Plate Tectonic Features

Modern-style plate tectonics imparts distinctive features to the geologic record and thus has formed the basis of numerous past efforts to assess its past activity (e.g., Davies 1992, 2006; Hamilton 1998; de Wit 1998; Griffin et al. 2003; Brown 2006, 2007; Stern 2007, 2018; O'Neill et al. 2007; van Hunen and van den Berg 2008; Condie 2008; Halla et al. 2009; Sizova et al. 2010; Gerya 2011; van Hunen and Moyen 2012; Holder et al. 2019). But because plate tectonics tends to consume evidence of its past existence (for example, we know of no oceanic lithosphere older than 220 Ma), we need to exercise caution in drawing hard-and-fast constraints from such forms of evidence. Indeed, such an approach, if valid, can only provide a lower bound.

Stern (2007, 2018) examined the geologic record for earliest preserved evidence of plate tectonics. He emphasized that any indications of plate tectonics initiation must be regarded as a minimum age and cautioned that geologic evidence is continuously removed by orogeny and erosion on an active planet. Since modern subduction produces ophiolites (preserved oceanic crust), blueschists (glaucophane-bearing schists formed from oceanic crust under high pressure-low temperatures metamorphism), ultra-high pressure (UHP) metamorphic belts, eclogites, and passive margins, he favored using the appearance of these features over inferences obtained from paleomagnetism and igneous geochemistry which, to varying degrees, require secondary interpretations to establish a link to plate tectonics. While Stern (2007, 2018) acknowledges the unstable nature of (1) ophiolites, (2) blueschist facies accretionary rocks, and (3) UHP terranes, their limited occurrence in the geologic record prior to about 900 Ma led him to suggest that modern style plate tectonics with deep subduction began at that time following about $\sim$1 Ga of a primitive form of plate tectonics (also see Hamilton 2011). However, those three features are so susceptible to erosion or overprinting that their disappearance from the geologic record may more likely be due to their lack of preservation than as marking a clear lower age bound to the onset of subduction. I note that the collision boundary between India and Asia—an orogeny that began only ca. 60 million years ago—has retained exposed ophiolites along less than 30% of its suture zone and eliminated half of the associated accretionary complex rocks and virtually all UHP rocks. And this continent-continent collision is still underway (Yin and Harrison 2000)!

Moyen et al. (2006) reported mineral assemblages in ca. 3 Ga metamorphic rocks that record high pressure-low temperature metamorphism corresponding to apparent geotherms of $\sim$15 °C/km. As such low values are typical of the footwall in modern convergent margins, they concluded that these data represent evidence of cold and strong lithosphere in an ancient subduction zone. Brown (2008) compiled a large database of metamorphic rocks of all ages and observed that granulite facies ultrahigh temperature metamorphism was found dominantly in Neoarchean to Cambrian rocks, and that medium-temperature eclogite-high pressure granulite metamorphism is characteristic from the Neoarchean intermittently through to the Paleozoic. He inferred that the initiation of the latter was consistent with a shift to lower heat flows, possibly due to subduction, while coeval belts of the former were analogous to modern arcs. Brown (2008) noted, as did Stern (2007, 2018), that blueschists and related assemblages first appear during the Neoproterozoic which he took to mark the onset of the low to intermediate apparent thermal gradients characteristic of modern subduction. Holder et al. (2019) interpreted the gradual appearance of bimodal thermobarometric patterns in metamorphic rocks as indicating a gradual transition to plate tectonics since $\sim$2.5 Ga. They did not address the effect that preservation biases in the rock record might have on their conclusion but acknowledged that metamorphism at convergent margins in the past might have been characterized by different thermal structures than today. A further feature of modern subduction is the generation of a second, adjacent metamorphic belt characterized by high-temperature-low pressure metamorphism. Van Hunen and Moyen (2012) coupled geological and geochemical observations with inferences from modelling to argue that arc-like signatures in igneous rocks (see below), in the presence of paired metamorphic belts, are evidence that subduction operated at least intermittently during the Archean.

While contemporary magmatism in subduction zones arises largely from melting in the mantle wedge in response to the introduction of fluids fluxed from the adjacent dehydrating, down going plate, higher thermal gradients on early Earth may have permitted direct melting of ocean crust. Tonalite-trondhjemite-granodiorite (TTG) rocks, thought to be formed by partial melting of hydrated basalt (Rapp and Watson 1995), are widespread in Eoarchean crust (Martin et al. 2005). One school of thought is that TTGs reflect melting in a convergent plate boundary setting under significantly higher thermal gradients than accessible today (e.g., Martin 1986; Moyen 2011). Keller and Schoene (2018) investigated a large database of analyzed continental igneous rocks dating back to nearly 4 Ga. They found their average composition evolved in a broadly continuous fashion, with decreasing compatible element concentrations and increasing incompatible element concentrations they interpreted as due to a declining mantle potential temperature (and thus extent of mantle melting) throughout Earth history (see Sect. 6.3.2). They concluded that continental basalts record an essentially constant proportion of subduction magmatism since the early Archean.

Alternatively, Johnson et al. (2017) argued that the arc-like signature in TTGs rocks from the Pilbara region of Western Australia was inherited through a multistage process involving TTG formation at the base of thick basaltic crust and thus "the production and stabilization of the first continents…is incompatible with modern-style plate tectonics". But their characterization of this particular ca. 3.5 Ga granite-greenstone association as part of Earth's first stable continent in essence seeks to prove a negative. The paucity of rocks older than 4 Ga could reflect their non-existence but alternatively may be due to a preservation bias (see Sect. 6.3.2) or crustal recycling at similar rates to that seen today (see Sect. 5.4). Turner et al. (2014) used recent investigations of the Izu-Bonin-Mariana forearc (Ishizuka et al. 2011), which documented both the stratigraphy and geochemistry of a newly formed island arc, to argue that their close match to that found in the 3.8 Ga (cf., 4.3 Ga; O'Neil et al. 2011) Nuvvuagittuq supracrustal belt, northern Quebec, suggests an Eoarchean (or Hadean) initiation of subduction.

Condie and Kröner (2008) followed a similar approach as Stern (2007) but interpreted petrotectonic assemblages characteristic of modern plate tectonics to indicate that subduction had initiated by, or prior to, 3 Ga but did not become pervasive until 2.7 Ga. They explained the paucity of >1 Ga ophiolites as reflecting the difficulty of obducting the thicker oceanic crust expected on an earlier, hotter Earth while the apparent absence of blueschists and UHP rocks prior to that time was thought due to the resulting steeper subduction geotherms. What sets the latter two inferences apart from the most of the abovementioned studies searching for ancient signs of modern convergent margins is that Condie and Kröner (2008) considered possible non-uniformitarian conditions that may have applied on early Earth. As a case illustrating the potential ambiguities of uniformitarian interpretations, consider the study of Shirey and Richardson (2011). Their literature search showed that prior to 3 Ga, only diamonds with peridotitic inclusion assemblages have been found (Fig. 6.2) whereas eclogitic inclusions are dominant in post-3 Ga assemblages (although in many cases, the apparent Sm–Nd ages of silicate inclusions are discordant with Re–Os ages in sulfide inclusions in diamonds from the same sources). They interpreted this transition as due to the capture of eclogite material formed in subducting lithosphere by the subcontinental mantle during continental collision, and thus, evidence of Wilson cycle activity. They concluded with certainty that plate tectonics initiated over the past 3.5 Ga. However, as noted in Chap. 5, Armstrong (1991) pointed out that the continental mantle lithosphere thickens slowly over time due to secular cooling. Thus young continental masses on early Earth may have had mantle roots extending only a few 10 s of km beneath relatively thin continental crust. In such a case, the eclogite transition in an adjacent downgoing slab would occur at depths *greater* than the base of the continental lithosphere precluding capture of lower plate material. In this view, Shirey and Richardson's (2011) observation has nothing to do with the Wilson cycle but is instead a potentially powerful thermal constraint on Earth evolution.

In a similar fashion, Palin and White (2016) suggested that the absence of blueschists in the ancient geological record is attributable to the changing composition of oceanic crust throughout Earth history that resulted from mantle cooling. Oceanic crust formed on a hotter, early Earth was enriched in MgO relative to today and that composition does not react under high pressure-low temperature conditions to form glaucophane-bearing assemblages. Instead, MgO-rich oceanic crust would have created the greenschist-like metamorphic rocks like those commonly throughout the Phanerozoic.

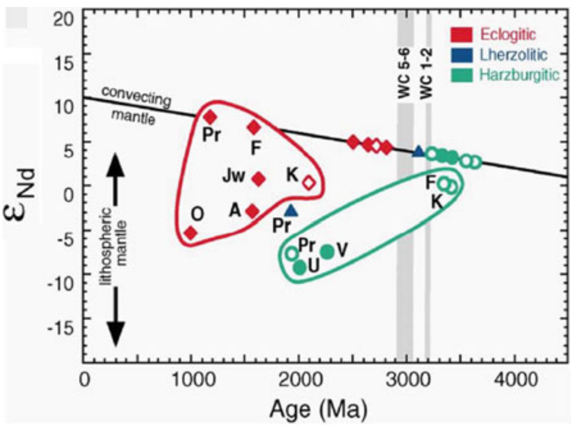

Fig. 6.2 Silicate inclusion initial Nd isotopic composition versus Sm–Nd age for diamonds of peridotitic (circles), lherzolitic (triangles), and eclogitic (diamonds) parageneses. Solid symbols are composite garnet and clinopyroxene isochrons; open symbols are model age studies for composites of garnet only. Unlabeled points on convecting mantle curve are mantle extraction ages extrapolated from labeled points. Reproduced with permission from Shirey and Richardson (2011)

6.3.2 Detrital Zircon Age Spectra

A number of studies, notably by Kent Condie and coworkers, have used literature compilations of detrital zircon U–Pb ages as a proxy for Wilson cycle activity (Condie and Kroner 2008; Condie and Pease 2008; Condie et al. 2009a; Condie and Aster 2010; Voice et al. 2011). Their view is that observed age peaks of orogenic plutonism reflect the activity of local or global subduction systems. Condie and Pease (2008) interpret this database in light of other geologic controls and inferred onset of modern plate tectonics by 3 Ga. In certain variants, age gaps in such spectra are thought related to a shutdown of planetary-scale plate tectonics between (e.g., at 2450–2200 Ma, Condie et al. 2009b). Condie and Aster (2010) concluded that eight peaks ranging from 750 to 2930 Ma reflect subduction system episodicity on local or regional scales but that five of them (at 2700, 1870, 1000, 600, and 300 Ma) are due to supercontinent formation. The corresponding minima of the age spectra occurred during supercontinent stasis or breakup. Condie (2018) concludes that these features in zircon age spectra are consistent with the appearance of plate tectonics on Earth at about 3 Ga and its widespread propagation by 2 Ga.

Beyond the fundamental flaw that all such approaches share (i.e., that absence of evidence is not evidence of absence), there are several aspects of this approach which remain of concern. The first is that the Precambrian geologic record appears biased to rock compositions most likely to resist deformation (e.g., low heat production and water content) and thus exposure to erosion at newly rifted continental margins where loss to subduction erosion could occur (Morgan 1985, 1989; Harrison 2009; see Chap. 5). Thus any look-back comparison is flawed to some degree by a preservation bias. The second concern is that most such studies examined unfiltered zircon age spectra without regard to geographic coverage. This was in part addressed by Puetz et al. (2017) who weighted detrital zircon ages in proportion to continental surface areas, resulting in generally similar age spectra. That notwithstanding, there remain large portions of continents buried beneath ice or debris that remain unrepresented in global zircon age compilations (e.g., Africa, Antarctica). For example, recent data acquisition no longer supports a previously suggested crustal age gap at 2.4–2.2 Ga (Kent Condie, pers. comm., 2018).

A third complication (discussed in Sect. 5.3.3) arises from the observed trend of increasing Zr depletions in igneous rocks with increasing age (Keller et al. 2017). That is, an early zircon represents a greater amount of new continental crust that one formed later in Earth history when the mantle is cooler and thus zircon age spectrum intercomparisons will underestimate ancient continental crust mass. Thus, as shown in Fig. 6.3a, observed detrital zircon age spectra require a relative abundance correction specific to crystallization conditions. This point is driven home in Fig. 6.3b which shows the average mass of magma required to produce an equivalent mass of zircon as a function of crust age. A fourth problem is that zircon age peaks may reflect periods of enhanced crustal preservation trapped during continent-continent collisions (Condie and Aster 2009, 2010; Hawkesworth et al. 2010; Voice et al. 2011) rather than peaks in production of new arc crust (Stein and Hofmann 1994; Condie 1998; Albarède 1998). Condie et al. (2017) estimated the relative magnitudes of these two effects by modelling the proportion of juvenile Nd input into the continental crust and found that zircons formed and preserved from juvenile crust in accretionary orogens are at least three times more abundant than that preserved during the collisional phase of orogens. This conclusion is countervailed to some degree by the very low solubility of zircon during anatexis (Watson and Harrison 1983) which makes continental collisions poor recorders of Wilson cycle activity.

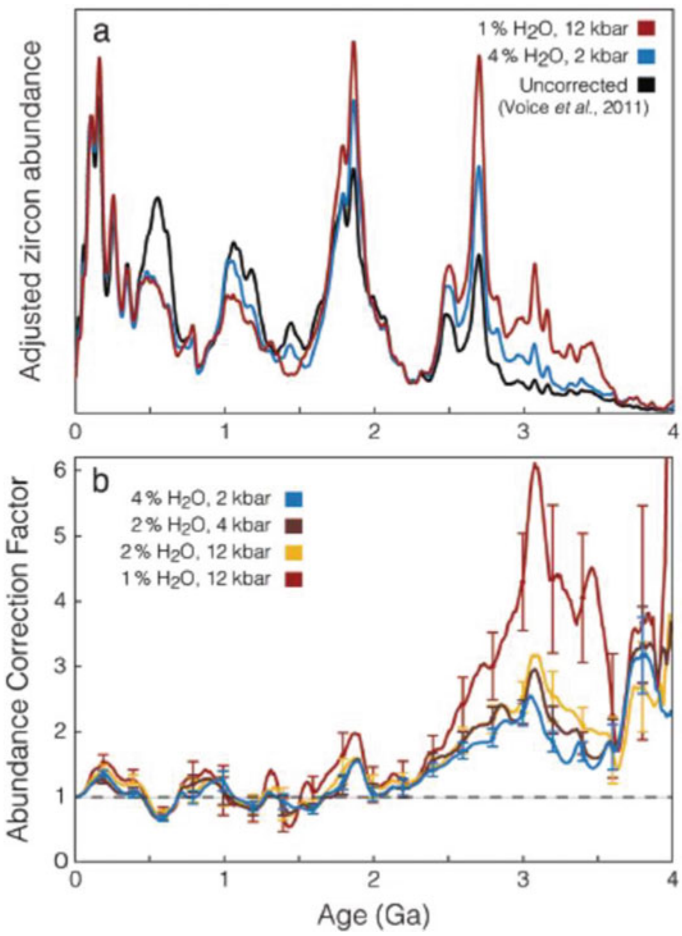

Fig. 6.3 **a** The effect of applying a relative zircon abundance correction (see text for explanation) to the detrital zircon age spectrum of Voice et al. (2011) for several crystallization conditions. **b** The average mass of magma throughout Earth history required to produce the same mass of zircon as a unit mass of average present-day magma. Reproduced with permission from Keller et al. (2017)

6.3.3 Estimates from Trace Elements

Geochemists have long ascribed differences in chemistry between fine-grained sediments (thought to be good aggregators of average crustal composition) across the Archean-Proterozoic boundary to indicate that >2.5 Ga upper crust was substantially more mafic and less abundant than <2.5 Ga upper crust (e.g., Taylor and McLennan 1985). Tang et al. (2016) adopted this approach using both ancient shales and glacial diamictites (poorly sorted terrigenous sediments) to estimate secular variations in crustal MgO, a proxy for degree of silicate differentiation (Fig. 6.4). However, soluble elements like Mg are not retained during weathering (seawater is 0.2% MgO) and thus require a suitable proxy. They chose Ni/Co and Cr/Zn in this role and concluded that the upper continental crust changed from a highly mafic (i.e., high MgO) composition prior to 3 Ga to a felsic composition by 2.5 Ga. That this transition is not reflected in the mineralogy of Archean clastic sediments (which are dominantly felsic) was ascribed to the preferential weathering of mafic minerals. In order to overcome the buffering effect of an assumed mafic Archean upper crust, they further argued that this compositional change had to have been accompanied by a fivefold increase in the mass of the upper continental crust via massive granitoid additions. Because felsic magmatism of this magnitude requires an external supply of water, the authors concluded that global arc magmatism initiated at ~3 Ga.

A significant limitation of this approach is that virtually all known occurrences of fine-grained Archean sediments are in greenstone belts (Taylor and McLennan 1985; Tang et al. 2016) where they represent material eroded from island arcs built on oceanic floor. Thus these authors are almost certainly documenting purely environmental, and not temporal, changes in local crust composition. Furthermore, higher ratios of incompatible to compatible elements (e.g., Ni/Co, Cr/Zn, Th/Sc) in

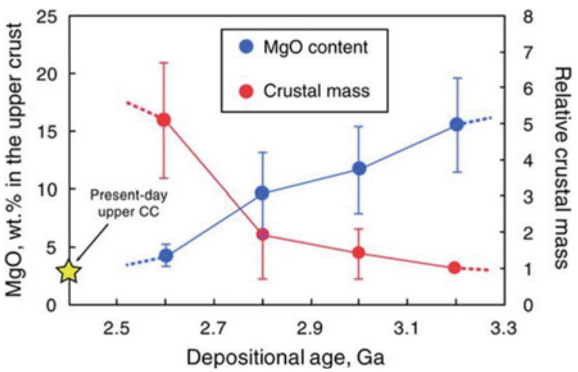

Fig. 6.4 Plot showing MgO content of fine-grained Archean sediments estimated from average Ni/Co and Cr/Zn ratios. Crustal mass is calculated from a mass balance assuming knowledge of the composition of Mesoarchean upper continental crust. These apparent shifts imply to the authors the timing of the onset of plate tectonics at ca. 3 Ga. Reproduced with permission from Tang et al. (2016)

post-Archean sediments may reflect lesser vertical mixing in a compositionally stratified crust rather than a fundamentally different crustal composition. As for estimating crustal volume from trace element data, there is simply no definable relationship between sediment chemistry and continental growth (Armstrong 1991). But let's say for argument sake that the source of the fine-grained Archean sediments is the same as post-Archean. To test exactly that scenario, Keller and Harrison (2020) developed a reference model in which crustal SiO_2 content remains constant but significant changes occur in compatible and incompatible element concentrations over time simply due to secular cooling (e.g., Keller et al. 2017; see Sect. 5.3.3). They found that models that propose such a change through time can equally well be explained by constant crustal SiO_2 content (Fig. 6.5). Ptáček et al. (2020) reprocessed the sediment geochemistry data used to argue for a mafic Archaean crust with a view to correcting for effects of chemical and physical weathering. Their results indicate that these data are consistent with an upper continental crust containing >50% felsic material at 3.5 Ga; i.e., the ratio of mafic to felsic rocks in the crust has remained essentially constant through time. They conclude that their finding "is consistent with an early onset of plate tectonics".

6.3.4 Atmosphere-Ocean-Crust-Mantle Exchange

As well as ubiquitous features, such as ophiolites and blueschists, modern plate tectonics also leads to rare mineral occurrences, such as diamond, jade, and ruby. Stern et al. (2016) inferred that kimberlites result from subduction of hydrated

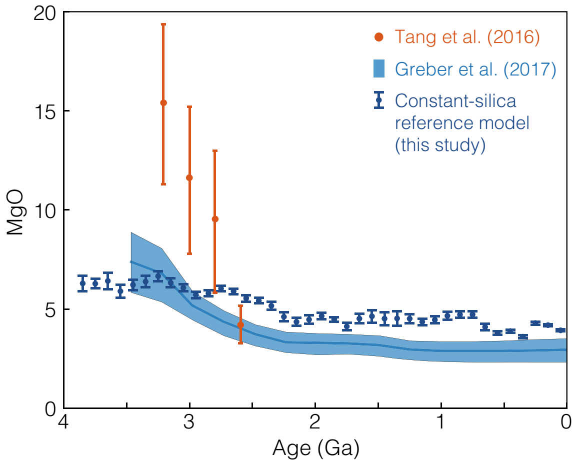

Fig. 6.5 MgO content predicted over past 3.5 Ga from the reference model of Keller and Harrison (2020) (i.e., This study) together with that calculated from the constancy of Ti isotopes (Greber et al. 2017) and that from Ni/Co and Cr/Zn ratios in fine-grained sediments by Tang et al. (2016). Only the Tang et al. (2016) model shows the very high (>10%) MgO values prior to ca. 3 Ga. Reproduced with permission from Keller and Harrison (2020)

oceanic crust and sediments deep into the mantle. Such recycling of fluids substantially enriched the mantle in CO_2 and H_2O leading to the explosive ascent of diamond-bearing kimberlite magmas. Jadeitite forms when supercritical fluids released from subducting oceanic crust condense in the overlying mantle wedge whereas ruby forms from Al-rich metasediments during continental collision (Stern et al. 2013). Such 'plate tectonic gemstones' are argued to be diagnostic of mobile lid behavior, but their very rarity would seem to preclude their presence as required signatures of plate tectonics.

Farquhar et al. (2002) found atmosphere-produced, mass-independent sulfur isotopes preserved in sulfides within ~2.9 Ga diamonds. They interpreted these data as evidence that following photochemical fractionation of volcanic, sulfur-bearing gases in the upper Archean atmosphere, that material had settled out onto surface sediments which were subsequently introduced into the mantle. In the absence of another plausible transport mechanism (sagduction of stagnant lid crust?), the authors interpreted this observation as evidence for Archean atmosphere-mantle exchange via subduction.

6.3.5 Stable Ti Isotopes

Titanium stable isotope ratios of terrestrial magmas correlate well with SiO_2 content, likely the result of fractional crystallization of Ti-bearing oxides, and appear unaffected by partial melting (Greber et al. 2017). The uniformity in the isotopic composition of Ti in shales dating back to ~3.5 Ga has been taken as evidence that their sources were dominantly felsic throughout back to that time (see also Sect. 5.3.5). Greber et al. (2017) concluded that the most plausible mechanism to explain this observation is subduction of oceanic crust and thus is plate tectonics was already been operating by at least at 3.5 Ga and possibly earlier. Recent work showing that tholeiitic rocks are more isotopically fractionated in Ti than calc-alkaline rocks (e.g., Deng et al., 2018) is unlikely to influence this conclusion as continental basalts record a constant proportion of subduction magmatism since the Neoarchean (Keller and Schoene, 2018). Greber et al. (2017) inference is consistent with the conclusions of Keller and Harrison (2020) and Ptáček et al. (2020) who found geochemical data to be consistent with a mix of crustal lithologies that maintain a constant SiO_2 content since ca. 4 Ga.

6.3.6 Model-Based Estimates

Numerical modeling permits simulation of possible conditions on early Earth that allow possible geodynamic behaviors to be explored (see Chap. 2). However, efforts to simulate early Earth mantle circulation prior to the ability to simulate realistic viscosity contrasts (e.g., Davies 1992, 2002; Sect. 2.4) promulgated the view that plate boundary interactions were unlikely during the Hadean. In some ways, the community is only now recovering from this rush to judgement.

As noted earlier, Earth is a hybrid of plate and stagnant lid tectonics. This complicates modeling but has led to proposals that suggest early plate tectonic regimes may necessarily have been intermittent (e.g., Silver and Behn 2008). Several authors suggest that the combination of early high mantle temperatures and supercontinent assembly led plate tectonics to have multiple false starts, returning each time to a stagnant lid regime ("episodic overturn") until the modern style emerged (Moresi and Solomatov 1998; O'Neill et al. 2007, 2013; O'Neill and Debaille 2014). Others see no barrier to subduction occurring throughout the Archean (e.g. Hynes 2013).

O'Neill et al. (2009) focused on an apparent magmatic gap between 2.4 and 2.2 Ga and inferred that aspects of their modelling were relevant to Earth history. These included a shift from high to negligible plate velocities (thus explaining an apparent early Proterozoic magmatic age gap) and a subsequent rise of upper mantle temperatures leading to the emplacement of ca. 2.2 Ga anorogenic granitoid belts, for which several examples could be cited (e.g., Fetter et al. 1997). This case is in some ways a cautionary tale as recent acquisition of detrital U–Pb zircon data has closed the apparent 2.4–2.2 Ga crustal age gap (Condie 2018; see Sect. 6.3.2). It is certainly the role of physical modelling to attempt to place geologic observations in a physical framework, but, at a time when less than 10^{-17} of the continental crust has been geochronologically characterized (Harrison et al. 2017), it may be premature to draw overly detailed scenarios from such data compilations.

Sizova et al. (2010) used the results of 2D thermomechanical numerical models of oceanic subduction to infer three transitionary geodynamic regimes: (1) no-subduction, (2) pre-subduction and (3) modern subduction. The transition between mode 1 and 2 occurs when the mantle potential temperature is $\sim$250 °C higher than present day with the transition between mode 2 and 3 occurring abruptly at $\sim$170 °C higher. They suggested that this latter transition to the modern plate tectonic regime might have occurred between 3.2 and 2.5 Ga. In their models, the key parameter is the degree of lithospheric weakening produced when sub-lithospheric melts are emplaced into the lithosphere. At high mantle potential temperatures (>170 °C above the present), continuously produced melts weaken the overlaying lithosphere which lose coherency and do not produce self-sustaining one-sided subduction.

Models of early Earth like that of Sizova et al. (2010) require numerous, unconstrained parameters and are, by the very nature of the problem, free of unambiguous observational constraints (see Chap. 2). Convection is a nonlinear, chaotic phenomenon (Turcotte 1997) and thus slab initiation times determined in such models are highly non-unique. While such calculations are useful in gaining insight into possible early Earth behaviors, they are perhaps best thought of as "convenient fictions" (Stevenson 1983).

As emphasized in Sect. 2.8, the role of mantle convection modelling in understanding early Earth cannot be ab initio reconstruction, but, at its best, to seek insights into possible dynamic behaviors under different assumptions. For example, Nakagawa and Tackley (2015) undertook calculations to assess the relationships between coupled core-mantle cooling and the mode of lithospheric behavior (mobile-, episodic-, and stagnant-lid) by varying the friction coefficient in a model lithosphere featuring brittle failure. They found that deep mantle structure exerts a strong influence on surface tectonic mode. Whereas episodic lid behavior results in an unrealistically thick layer of subducted basalt adjacent the core-mantle boundary (CMB), and stagnant lid mode produces no such layer at all, a mobile lid regime results in the sort of isolated, large low shear velocity provinces that are seismically imaged at the CMB today (e.g., Garnero and McNamara 2008). Interestingly, Nakagawa and Tackley (2015) found that tectonic style is established quickly in their models; in the mobile lid case, subduction initiates prior to a model time corresponding to an age of ca. 4.5 Ga. Because of the contrasting thickness of subducted piles at the CMB in the various scenarios, the tectonic mode strongly effects core cooling, and thus implicitly, the intensity of the geodynamo. Nakagawa and Tackley (2015) concluded that a continuous mobile-lid mode existing from shortly after Earth formation best matches Earth's present mantle structure and core evolution.

6.4 Critical Summary

Estimates of when plate tectonics began range from the last 20% of Earth history to within the first 5%. In fact, we don't know with any confidence when plate tectonics initiated. There is no observation that precludes it from operating at 4.5 Ga and some that convinces some that it didn't start in its present form until a billion years ago.

The force balance within the modern plate tectonic system is broadly understood and subduction initiation appears to be one of its most robust features. However, when and how subduction first began remains poorly understood. Most approaches used to estimate when Earth first entered the mobile lid regime—preservation of modern plate tectonic features, detrital zircon age spectra, trace element and radiogenic isotope geochemistry, atmosphere-crust-mantle exchange, and model-based estimates—can be interpreted in multiple ways and are all underlain by assumptions that cannot be independently tested. The incomplete geologic record precludes a definitive answer. Historically, limitations in early geophysical modelling methods (see Sect. 2.4) led to skepticism regarding the possibility of plate tectonics on early Earth. Influenced by this view, the geologic community was largely reluctant to take a dynamic view of the preserved crustal record, instead inferring the apparent absence of a Hadean rock record as evidence that there never was one.

The community appears to be in the act of creating a meme reminiscent of the billion-year-magma-ocean myth (see Sect. 1.1) that served as the consensus paradigm—that plate tectonics initiated 3 billion years ago (e.g., Van Kranendonk et al. 2007; Condie and Kröner 2008; Shirey and Richardson 2011; Dhuime et al. 2015; Bercovici and Ricard 2016; Condie 2018). The above described limitations of all the approaches making such estimates warn against coalescing around a convention at the present time lest we further stunt the intellectual quality of this debate. Too many interpretations of the nature of the early continental crust and the tectonic regime(s) responsible for its rise are characterized by simplistic thinking and the aforementioned historical legacies. It is an exceedingly rare paper on the topic that takes a balanced look at the entire range of evidence available. Instead decades-old arguments are recycled in the guise of a novel methodology that ultimately fails to transcend the three very real limitations of this debate—the extent to which ancient continental crust was recycled into the mantle and thoroughly mixed, the selection biases in the present rock record, and the assumption of uniformitarian conditions throughout Earth history (see Sect. 12.4).

References

Albarède, F. (1998). The growth of continental crust. *Tectonophysics, 296,* 1–14.

Arevalo, R., McDonough, W. F., Stracke, A., Willbold, M., Ireland, T. J., & Walker, R. J. (2013). Simplified mantle architecture and distribution of radiogenic power. *Geochemistry, Geophysics, Geosystems, 14,* 2265–2285.

Armstrong, R. L. (1991). The persistent myth of crustal growth. *Australian Journal of Earth Science, 38,* 613–630.

Baes, M., Gerya, T., & Sobolev, S. V. (2016). 3-D thermo-mechanical modeling of plume-induced subduction initiation. *Earth and Planetary Science Letters, 453,* 193–203.

Bercovici, D., Ricard, Y. (2014). Plate tectonics, damage and inheritance. *Nature*, *508*(7497), 513–516.

Bercovici, D., & Ricard, Y. (2016). Grain-damage hysteresis and plate tectonic states. *Physics of the Earth and Planetary Interiors, 253,* 31–47.

Brown, M. (2006). Duality of thermal regimes is the distinctive characteristic of plate tectonics since the Neoarchean. *Geology*, *34*(11), 961.

Brown, M. (2007). Metamorphism, plate tectonics, and the supercontinent cycle. *Earth Science Frontiers*, *14*(1), 1–18.

Brown, M. (2008). Characteristic thermal regimes of plate tectonics and their metamorphic imprint throughout Earth history: When did Earth first adopt a plate tectonics mode of behavior. *Geological Society of America Special Paper, 440,* 97–128.

Condie, K. C. (1998). Episodic continental growth and supercontinents: A mantle avalanche connection? *Earth and Planetary Science Letters, 163,* 97–108.

Condie, K. C. (2008). Did the character of subduction change at the end of the Archean? Constraints from convergent-margin granitoids. *Geology*,*36*(8), 611–614.

Condie, K. C. (2018). A planet in transition: the onset of plate tectonics on earth between 3 and 2 Ga? *Geoscience Frontiers*, *9*(1), 51–60.

Condie, K. C., & Kröner, A. (2008). When did plate tectonics begin? Evidence from the geologic record. *Geological Society of America Special Paper, 440,* 281–294.

Condie, K. C., & Pease, V. (2008). When did plate tectonics begin on planet Earth? *Geological Society of America Special Paper, 440,* 294.

Condie, K. C., O'Neill, C., & Aster, R. C. (2009). Evidence and implications for a widespread magmatic shutdown for 250 my on earth. *Earth and Planetary Science Letters*, *282*(1–4), 294–298.

Condie, K. C., & Aster, R. C. (2010). Episodic zircon age spectra of orogenic granitoids: the supercontinent connection and continental growth. *Precambrian Research*, *180*(3–4), 227–236.

Condie, K. C., Belousova, E., Griffin, W. L., & Sircombe, K. N. (2009a). Granitoid events in space and time: Constraints from igneous and detrital zircon age spectra. *Gondwana Research, 15,* 228–242.

Condie, K. C., O'Neill, C., & Aster, R. C. (2009b). Evidence and implications for a widespread magmatic shutdown for 250 My on Earth. *Earth and Planetary Science Letters, 282,* 294–298.

Condie, K. C., Arndt, N., Davaille, A., & Puetz, S. J. (2017). Zircon age peaks: Production or preservation of continental crust? *Geosphere, 13,* 227–234.

Davies, G. F. (1992). On the emergence of plate tectonics. *Geology, 20,* 963–966.

Davies, G. F. (2002). Stirring geochemistry in mantle convection models with stiff plates and slabs. *Geochimica et Cosmochimica Acta, 66,* 3125–3142.

Davies, G. F. (2006). Gravitational depletion of the early Earth's upper mantle and the viability of early plate tectonics. *Earth and Planetary Science Letters, 243,* 376–382.

Deng, Z., Moynier, F., Sossi, P. A., & Chaussidon, M. (2018). *Bridging the depleted MORB mantle and the continental crust using titanium isotopes*.

Dewey, J. F., & Spall, H. (1975). Pre-Mesozoic plate tectonics: How far back in Earth history can the Wilson Cycle be extended? *Geology, 3,* 422–424.

de Wit Maarten, J. (1998). On Archean granites, greenstones, cratons and tectonics: does the evidence demand a verdict?. *Precambrian Research*, 91(1–2), 181–226.

Dhuime, B., Wuestefeld, A., & Hawkesworth, C. J. (2015). Emergence of modern continental crust about 3 billion years ago. *Nature Geoscience, 8,* 552–555.

Farquhar, J., Wing, B. A., McKeegan, K. D., Harris, J. W., Cartigny, P., & Thiemens, M. H. (2002). Mass-independent sulfur of inclusions in diamond and sulfur recycling on early Earth. *Science, 298,* 2369–2372.

Fetter, A. H., Van Schmus, W. R., Santos, T. S., Arthaud, M., & Nogueira Neto, J. (1997). Geologic history and framework of Ceará State: Northwest Borborema Province, NE Brazil (Extended Abstract). In *South American Symposium on Isotope Geology* (pp. 112–114), Brazil.

Forsyth, D., & Uyeda, W. S. (1975). On the relative importance of the driving forces of plate motion. *Geophysical Journal of the Royal Astronomical Society, 4,* 163–200.

Garnero, E. J., & McNamara, A. K. (2008). Structure and dynamics of Earth's lower mantle. *Science, 320*(5876), 626–628.

Gerya, T. (2011). Future directions in subduction modeling. *Journal of Geodynamics*, *52*(5), 344–378.

Gerya, T. V., Stern, R. J., Baes, M., Sobolev, S. V., & Whattam, S. A. (2015). Plate tectonics on the earth triggered by plume-induced subduction initiation. *Nature*, *527*(7577), 221–225.

Greber, N. D., Dauphas, N., Bekker, A., Ptáček, M. P., Bindeman, I. N., & Hofmann, A. (2017). Titanium isotopic evidence for felsic crust and plate tectonics 3.5 billion years ago. *Science, 357,* 1271–1274.

Griffin, W. L., O'Reilly, S. Y., Abe, N., Aulbach, S., Davies, R. M., Pearson, N. J. et al. (2003). The origin and evolution of Archean lithospheric mantle. *Precambrian Research*, *127*(1–3), 19–41.

Gurnis, M., Hall, C., & Lavier, L. (2004). Evolving force balance during incipient subduction. *Geochemistry, Geophysics, Geosystems*, *5*(7).

Halla, J., van Hunen, J., Heilimo, E., & Hölttä, P. (2009). Geochemical and numerical constraints on Neoarchean plate tectonics. *Precambrian Research*, *174*(1–2), 155–162.

Hamilton, W. B. (1998). Archean magmatism and deformation were not products of plate tectonics. *Precambrian Research, 91,* 143–179.

Hamilton, W. B. (2011). Plate tectonics began in Neoproterozoic time, and plumes from deep mantle have never operated. *Lithos, 123,* 1–20.

Hansen, V. L. (2007). Subduction origin on early Earth: A hypothesis. *Geology, 35,* 1059–1062.

Harrison, T. M. (2009). The Hadean crust: Evidence from >4 Ga zircons. *Annual Reviews of Earth and Planetary Sciences, 37,* 479–505.

Harrison, T. M., Bell, E. A., & Boehnke, P. (2017). Hadean zircon petrochronology. *Reviews in Mineralogy and Geochemistry, 83,* 329–363.

Hawkesworth, C., Dhuime, B., Pietranik, A., Cawood, P., Kemp, A. I. S., & Storey, C. (2010). The generation and evolution of the continental crust. *Journal of Geological Society of London, 167,* 229–248. https://doi.org/10.1144/0016-76492009-072.

Holder, R. M., Viete, D. R., Brown, M., & Johnson, T. E. (2019). Metamorphism and the evolution of plate tectonics. *Nature*, *572*(7769), 378–381.
Hynes, A. (2013). How feasible was subduction in the Archean? *Canadian Journal of Earth Sciences, 51,* 286–296.
Ishizuka, O., Tani, K., Reagan, M. K., Kanayama, K., Umino, S., Harigane, Y., et al. (2011). The timescales of subduction initiation and subsequent evolution of an oceanic island arc. *Earth and Planetary Science Letters, 306,* 229–240.
Johnson, T. E., Brown, M., Gardiner, N. J., Kirkland, C. L., & Smithies, R. H. (2017). Earth's first stable continents did not form by subduction. *Nature, 543,* 239–242.
Keller, B., & Harrison, T. M. (2020). Constraining crustal silica on ancient earth. *Earth and Space Science Open Archive*, https://doi.org/10.31223/osf.io/75evw.
Keller, B., & Schoene, B. (2018). Plate tectonics and continental basaltic geochemistry throughout Earth history. *Earth and Planetary Science Letters, 481,* 290–304.
Keller, C. B., Boehnke, P., & Schoene, B. (2017). Temporal variation in relative zircon abundance throughout Earth history. *Geochemical Perspectives Letters, 3,* 179–189.
Martin, H. (1986). Effect of steeper Archean geothermal gradient on geochemistry of subduction-zone magmas. *Geology, 14,* 753–756.
Martin, H., Smithies, R. H., Rapp, R., Moyen, J. F., & Champion, D. (2005). An overview of adakite, tonalite–trondhjemite–granodiorite (TTG), and sanukitoid: Relationships and some implications for crustal evolution. *Lithos, 79,* 1–24.
McKenzie, D. P. (1977). The initiation of trenches: A finite amplitude instability. In M. Talwani & W. C. Pittman (Eds.), *Island arcs, deep sea trenches, and back-arc basins* (pp. 57–61). Washington, DC: Maurice Ewing Ser. I., AGU.
Moresi, L., & Solomatov, V. S. (1998). Mantle convection with a brittle lithosphere: Thoughts on the global tectonic styles of the Earth and Venus. *Geophysical Journal International, 133,* 669–682.
Morgan, P. (1985). Crustal radiogenic heat production and the selective survival of ancient continental crust. *Journal of Geophysical Research, 90,* C561–C570.
Morgan, P. (1989). Thermal factors controlling crustal stabilization. In *28th International Geological Congress*, Washington, DC, Abstracts 3, 333.
Moyen, J. F. (2011). The composite Archaean grey gneisses: Petrological significance, and evidence for a non-unique tectonic setting for Archaean crustal growth. *Lithos, 123,* 21–36.
Moyen, J. F., Stevens, G., & Kisters, A. (2006). Record of mid-Archaean subduction from metamorphism in the Barberton terrain, South Africa. *Nature, 442,* 559–562.
Nakagawa, T., & Tackley, P. J. (2015). Influence of plate tectonic mode on the coupled thermochemical evolution of Earth's mantle and core. *Geochemistry, Geophysics, Geosystems, 16,* 3400–3413.
O'Neil, J., Francis, D., & Carlson, R. W. (2011). Implications of the Nuvvuagittuq greenstone belt for the formation of Earth's early crust. *Journal of Petrology, 52,* 985–1009.
O'Neill, C., Debaille, V., & Griffin, W. (2013). Deep earth recycling in the Hadean and constraints on surface tectonics. *American Journal of Science*, *313*(9), 912–932.
O'Neill, C., & Debaille, V. (2014). The evolution of Hadean-Eoarchaean geodynamics. *Earth and Planetary Science Letters, 406,* 49–58.
O'Neill, C., Lenardic, A., Moresi, L., Torsvik, T. H., & Lee, C.-T. A. (2007). Episodic Precambrian subduction. *Earth and Planetary Science Letters, 262,* 552–562.
Palin, R. M., & White, R. W. (2016). Emergence of blueschists on Earth linked to secular changes in oceanic crust composition. *Nature Geoscience, 9,* 60–64.
Ptáček, M.P., Dauphas, N., & Greber, N.D. (2020). Chemical evolution of the continental crust from a data-driven inversion of terrigenous sediment compositions. *Earth and Planetary Science Letters*, *539*, 116090.
Puetz, S. J., Condie, K. C., Pisarevsky, S., Davaille, A., Schwarz, C. J., & Ganade, C. E. (2017). Quantifying the evolution of the continental and oceanic crust. *Earth-Science Reviews, 164,* 63–83.

Rapp, R. P., & Watson, E. B. (1995). Dehydration melting of metabasalt at 8–32 kbar: Implications for continental growth and crust-mantle recycling. *Journal of Petrology, 36,* 891–931.

Schaefer, L., & Elkins-Tanton, L. T. (2018). Magma oceans as a critical stage in the tectonic development of rocky planets. *Philosophical Transactions of the Royal Society A: Mathematical, Physical and Engineering Sciences, 376,* 20180109.

Shirey, S. B., & Richardson, S. H. (2011). Start of the Wilson cycle at 3 Ga shown by diamonds from subcontinental mantle. *Science, 333,* 434–436.

Silver, P. G., & Behn, M. D. (2008). Intermittent plate tectonics? *Science, 319,* 85–88.

Sizova, E., Gerya, T., Brown, M., & Perchuk, L. L. (2010). Subduction styles in the Precambrian: Insight from numerical experiments. *Lithos, 116,* 209–229.

Sobolev, S. V. (2016). Plate tectonics initiation as running hurdles. In *Workshop on the Origin and Evolution of Plate Tectonics*, Monte Verità.

Solomatov, V. (2016). Why plate tectonics is rare and how it started on earth. *Bulletin of the American Physical Society*, *61*, 15.

Stein, M., & Hofmann, A. W. (1994). Mantle plumes and episodic crustal growth. *Nature, 372,* 63–68.

Stern, R. J. (2007). When and how did plate tectonics begin? Theoretical and empirical considerations. *Chinese Science Bulletin, 52,* 578–591.

Stern, R. J. (2018). The evolution of plate tectonics. *Philosophical Transactions of the Royal Society A, 376,* 20170406.

Stern, R. J., Tsujimori, T., Harlow, G., & Groat, L. A. (2013). Plate tectonic gemstones. *Geology, 41,* 723–726.

Stern, R. J., Leybourne, M. I., & Tsujimori, T. (2016). Kimberlites and the start of plate tectonics. *Geology, 44,* 799–802.

Stern, R. J., Gerya, T., & Tackley, P. J. (2017). Tackling unanswered questions on what shapes Earth. *Eos, 98*. https://doi.org/10.1029/2017EO065791.

Stern, R. J., & Gerya, T. (2018). Subduction initiation in nature and models: a review. *Tectonophysics*, *746*, 173–198.

Stevenson, D. J. (1983). The nature of the earth prior to the oldest known rock record—The Hadean earth. In *Earth's earliest biosphere: Its origin and evolution* (pp. 32–40). Princeton, NJ: Princeton University Press.

Tang, M., Chen, K., & Rudnick, R. L. (2016). Archean upper crust transition from mafic to felsic marks the onset of plate tectonics. *Science, 351,* 372–375.

Taylor, S. R., & McLennan, S. M. (1985). *The continental crust: Its composition and evolution*. Oxford: Blackwell.

Turcotte, D. L. (1997). *Fractals and chaos in geology and geophysics* (p. 412). Cambridge University Press.

Turner, S., Rushmer, T., Reagan, M., & Moyen, J. F. (2014). Heading down early on? Start of subduction on Earth. *Geology, 42,* 139–142.

Ueda, K., Gerya, T., & Sobolev, S. V. (2008). Subduction initiation by thermal-chemical plumes: Numerical studies. *Physics of the Earth and Planetary Interiors, 171,* 296–312.

van Hunen, J., & van den Berg, A. P. (2008). Plate tectonics on the early earth: limitations imposed by strength and buoyancy of subducted lithosphere. *Lithos*, 103(1–2), 217–235.

Van Hunen, J., & Moyen, J. F. (2012). Archean subduction: Fact or fiction? *Annual Reviews of Earth and Planetary Sciences, 40,* 195–219.

Van Kranendonk, M. J., Hugh Smithies, R., Hickman, A. H., & Champion, D. C. (2007). Secular tectonic evolution of Archean continental crust: Interplay between horizontal and vertical processes in the formation of the Pilbara Craton, Australia. *Terra Nova, 19,* 1–38.

Voice, P. J., Kowalewski, M., & Eriksson, K. A. (2011). Quantifying the timing and rate of crustal evolution: Global compilation of radiometrically dated detrital zircon grains. *Journal of Geology, 119,* 109–126.

Watson, E. B., & Harrison, T. M. (1983). Zircon saturation revisited: Temperature and composition effects in a variety of crustal magma types. *Earth and Planetary Science Letters, 64,* 295–304.

Wilson, T.W. (1968). Static or mobile earth: the current scientific revolution. *American Philosophical Society Proceedings*, *112*, 309–320.

Wong, T., & Solomatov, V. S. (2016). Constraints on plate tectonics initiation from scaling laws for single-cell convection. *Physics of the Earth and Planetary Interiors, 257,* 128–136.

Yin, A., & Harrison, T. M. (2000). Geologic evolution of the Himalayan-Tibetan orogen. *Annual Review of Earth and Planetary Sciences, 28*, 211–280.

Yin, A. (2012). An episodic slab-rollback model for the origin of the Tharsis rise on Mars: Implications for initiation of local plate subduction and final unification of a kinematically linked global plate-tectonic network on Earth. *Lithosphere, 4,* 553–593.

Hadean Jack Hills Zircon Geochemistry

7

Abstract

Geochemical analysis of zircons older than 4 billion years, found in Early Archean metasediments at Jack Hills, Western Australia, provide insights into the nature of Hadean Earth. Oxygen isotopes have been interpreted as indicating that protoliths of magmas from which Hadean zircons crystallized were formed in the presence of water at or near Earth's surface. Apparent crystallization temperatures of Hadean zircons cluster at 680 °C. Given the low porosity expected in rocks under anatectic conditions, dehydration melting of micas as the principal source of the melts from which these zircons crystallized can be ruled out. Instead, a regulated mechanism producing near minimum-melting conditions during the Hadean is inferred. Combined, these results have been interpreted to reflect chemical weathering and sediment cycling in the presence of liquid water shortly after Earth accretion. ^{176}Hf/^{177}Hf ratios of Hadean Jack Hills zircons show large heterogeneities indicating a major differentiation of the silicate Earth by 4.50 Ga. A possible consequence of this differentiation is the formation of continental crust of similar order to the present. Studies of mineral inclusions within Hadean zircons indicate their crystallization from hydrous, granitoid magmas at pressures greater than 6 kbars, implying low near-surface geothermal gradients which in turn suggests their origin in underthrust environments. Given general agreement that life could not have emerged until liquid water appeared at or near Earth's surface, a significant implication is that our planet may have been habitable as much as 500 Ma earlier than previously thought. Indeed, carbon isotopic evidence obtained from inclusions in a Hadean zircon is consistent with life having emerged by 4.1 Ga, or several 100 million years earlier that the hypothesized lunar cataclysm. Trace element analyses of aluminum, halogens, sulfur, phosphorus, rare earth elements in Hadean zircons are consistent with their origin in a range of granitoid magma types and redox conditions. Although some of the above interpretations remain subject to debate, there is now a widespread consensus that molecular water was present at or near Earth's surface since at least 4.3 Ga. Perhaps the most remarkable feature of inferences drawn from investigations of these ancient zircons is that none were

T. M. Harrison, *Hadean Earth*, https://doi.org/10.1007/978-3-030-46687-9_7

predicted from theory, underscoring the importance of observations in testing models of early Earth.

7.1 Hadean Zircon Characteristics

Zircon ($ZrSiO_4$), a tetragonal neosilicate, is the principal host of Zr in the continental crust. Because that crust on average contains only ca. 200 ppm Zr (Rudnick and Gao 2003), zircon exists as a near ubiquitous but rare mineral in igneous, metamorphic and sedimentary rocks. Its inherent resistance to alteration by weathering, dissolution, shock, and diffusive exchange, coupled with its enrichment in U and Th relative to daughter product Pb (Hanchar and Hoskin 2003), has long made the U-Pb zircon dating the premier crustal geochronometer. While highly valued in that role, the trace element and isotopic compositions of zircon have become recognized as valuable probes of environmental conditions experienced during crystallization. Even in cases where zircon has been removed from its original rock context, such as detrital grains in clastic rocks, inclusions, trace element and isotopic signatures can yield important information regarding source conditions if the record is undisturbed. Despite zircon's remarkable refractory nature and resistance to diffusive exchange (Cherniak and Watson 2003), it is sensitive to radiation damage and can degrade into heterogeneous microcrystalline zones encompassed by amorphous material (Ewing et al. 2003). Nature has, to some degree, already selected out those grains most susceptible to metamictization from detrital zircon populations as high U and Th grains are unlikely to survive sediment transport (e.g., Hadean Jack Hills zircons with original U concentrations of >600 ppm are exceedingly rare). Thus care must be taken to ensure that effects of post-crystallization alteration are not mistaken as primary features.

The importance of Hadean zircons is then their great antiquity, amenability to U-Pb dating, and capacity to retain geochemical information. Although first documented at nearby Mt. Narryer (Froude et al. 1983; see Sect. 12.2), the vast majority of investigations of >4 Ga zircons sampled heavy-mineral-rich quartz-pebble conglomerates from a locality in the Erawondoo region of the Jack Hills (Fig. 7.1) (Compston and Pidgeon 1986; Maas et al. 1992; Spaggiari et al. 2007). Zircons are typically extracted from these rocks using separatory methods based on their high density and low magnetic susceptibility, handpicked and secured in an epoxy mount which is then polished and analyzed using the $^{207}Pb/^{206}Pb$ ion microprobe dating approach (see Holden et al. 2009).

Although zircon is dominantly a mineral of the continental crust, its formation is not restricted to that environment nor, for that matter, to Earth. However, zircons of continental affinity can be readily distinguished from those derived from the mantle or oceanic crust by trace element characteristics (e.g., U/Y vs. Y) and significantly lower crystallization temperatures (Grimes et al. 2007; Hellebrand et al. 2007). Lunar and meteoritic zircons can be distinguished from terrestrial counterparts by

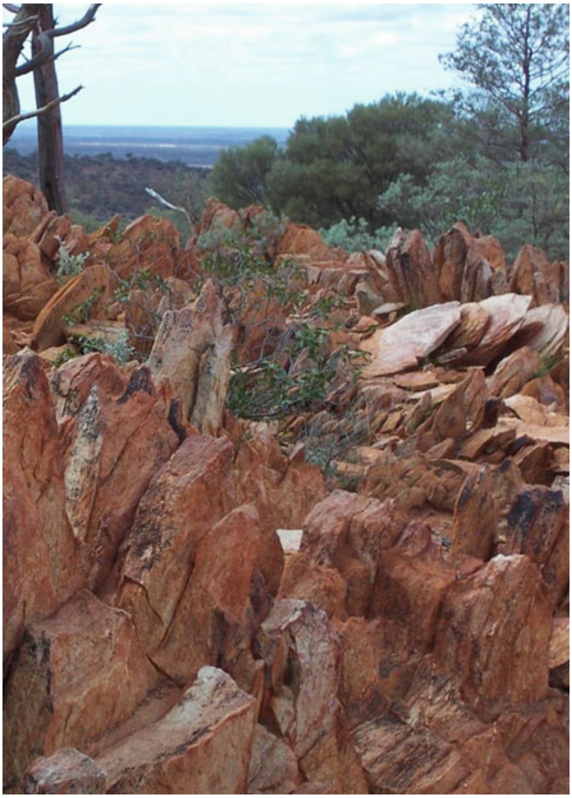

Fig. 7.1 Quartz-pebble conglomerates on Erawondoo Hill, Jack Hills region of Western Australia. Samples collected within ~100 m of this site have produced >95% of all Hadean zircons yet documented. *Photo credit* Bruce Watson

their REE signature (e.g., lack of a Ce anomaly; Hoskin and Schaltegger 2003). Furthermore, apparent crystallization temperatures for lunar zircons range from 900 to 1100 °C (Taylor et al. 2009) in contrast to terrestrial Hadean zircons which are restricted to 600–780 °C (Harrison et al. 2007; Fu et al. 2008). Thus it is amply clear that the vast majority of Hadean zircons are derived from terrestrial continental lithologies. Furthermore, textural characteristics of Hadean zircons from Jack Hills (e.g., growth zoning, inclusion mineralogy) indicate that most are derived from igneous sources (e.g., Cavosie et al. 2004, 2006; Hopkins et al. 2008).

Geochemical studies using upwards of half of the total Hadean grains thus far documented have inspired a variety of interpretations. However, there is a broad consensus that evidence derived from these ancient zircons implies abundant water at or near Earth's surface during that era (e.g., Wilde et al. 2001; Mojzsis et al. 2001; Rollinson 2008; Shirey et al. 2008; Harrison 2009). This represents a dramatic reversal from the conception of an uninhabitable, hellish world from which this time period gets its name (e.g., Wetherill 1972; Solomon 1980; Smith 1981; Maher and Stevenson 1988; Abe 1993; Ward and Brownlee 2000).

There are, of course, intrinsic limitations (including preservation bias) of the Hadean zircon record that could prevent 'smoking gun' conclusions about earliest Earth from ever being drawn. For example, the 70% of Earth's surface that is today nderlain by oceanic basalts contributes essentially nothing to the archive of detrital or xenocrystic zircons so the record is likely to be dominated by continental sources. Concerns that the Jack Hills locality may not be representative of early Earth may be resolved as >4 Ga zircons are documented from a growing number of globally diverse locations (see Appendix).

7.2 Modes of Investigation

Most investigations of Hadean zircons to date have emphasized ion microprobe analysis in order to minimize the volume of mineral excavated during the age survey process thus maximizing the signals in subsequent analyses (i.e., $\delta^{18}O$, $^{176}Hf/^{177}Hf$, Ti, etc.). This made sense for early studies of Jack Hills zircons (e.g., Compston and Pidgeon 1986; Mojzsis et al. 2001) as there were then no serious alternatives to the ion microprobe. Typical practice was to handpick individual zircons and mount them on double-sided adhesive tape in systematic grids together with zircon standards. This enabled the most ancient grains identified by the $^{207}Pb/^{206}Pb$ age survey to be easily located for subsequent analysis. When I began the program to date over 100,000 Jack Hills zircons in 2001, this laborious mounting process was not the rate limiting step in creating a large archive of Hadean zircons as then no ion microprobe yet had automated analysis capability. Indeed, that project led to the development of the automated stage on the Sensitive, High Resolution, Ion MicroProbe (SHRIMP) instruments (see Sect. 12.2) followed shortly thereafter by CAMECA's 'chain analysis' tool. Arguably the most remarkable analytical development over the subsequent 20 years has been the development and refinement of laser ablation, inductively-coupled mass spectrometry (LA-ICPMS). Effective yields have increased by over an order of magnitude dropping both analytical time and the mass of material needed to attain a specified precision (see Appendix).

7.3 Age Distributions

Over 200,000 Jack Hills zircons have been $^{207}Pb/^{206}Pb$ dated in this fashion with over 6000 yielding ages older than 4 Ga. Most of the ~3% of the analyzed grains that are >4 Ga were then U-Pb dated using an ion microprobe, with several found to be as old as 4.38 Ga (Compston and Pidgeon 1986; Holden et al. 2009; Valley et al. 2014; Wang and Wilde 2018). Numerous age studies of Jack Hills detrital zircons all show a characteristic bimodal distribution with peaks close to 3.4 and 4.1 Ga with some grains as old as nearly 4.4 Ga (Compston and Pidgeon 1986; Maas and McCulloch 1991; Maas et al. 1992; Amelin 1998; Amelin et al. 1999; Mojzsis et al.

2001; Cavosie et al. 2004; Trail et al. 2007; Holden et al. 2009; Bell et al. 2011, 2014; Bell and Harrison 2013; Wang and Wilde 2018). As noted above, to maximize selection of >4 Ga zircons a rapid survey of $^{207}Pb/^{206}Pb$ ages of typically 400 zircons in a polished epoxy mount is first undertaken. This is often accomplished during an automated overnight session as, unlike U-Pb dating, it requires no standardization. Grains with apparent ages older than ~3.9 Ga (typically a dozen or so per mount) are then analyzed using the more time consuming U-Pb dating protocol. A histogram and probability density function plot of a subsample of those ages are shown in Fig. 7.2a and the distribution of concordant >4.2 Ga zircons in Fig. 7.2b (Holden et al. 2009).

How abundant are Hadean zircons on Earth? Most of the fifteen localities for which at least one >4 Ga zircon has been documented (Chap. 8) were not targeted for that purpose but rather discovered serendipitously. Ancient metasediments and orthogneisses for which 10–100 s of zircons have been U-Pb dated without identifying at least one Hadean zircon fall into two categories: (1) those in which >4 Ga zircons are present at a level of less than ~1% but haven't yet been detected, and (2) those in which they are simply absent. How many zircons should be dated to ascertain to which category a sample belongs? The probability of detecting at least a single >4 Ga zircon as a function of their abundance in a population is discussed in the Appendix. To the authors knowledge, only the Erawondoo locality in the Jack Hills has had more than ca 5000 zircons dated making intercomparisons difficult (Chap. 8).

The significance of Hadean zircons is sometimes dismissed by their seeming rarity—without even a heaping handful of these grains (the total mass acquired is less than 6 g), how can one begin to tell a story about the nature of early Earth? Harrison et al. (2017) note that this is akin to asking how the Big Bang could possibly be characterized by capture of a vanishingly small fraction ($<10^{-70}$) of the photons in the observable universe. There are two principal factors that inform this view. The first is, we don't expect to preserve a significant proportion of early formed crust on a dynamic planet (Korenaga 2018). Assuming that Earth has recycled crust since formation at least as efficiently as we recognize it has throughout the Phanerozoic, only a few percent at most would likely remain (Armstrong 1981; Rosas and Korenaga 2018). The second is that we simply haven't tried particularly hard to find these remnants; we've geochronologically characterized less than 10^{-17} of the continental crust (Harrison et al. 2017), and support for reconnaissance dating surveys (i.e., "fishing trips") is notoriously difficult to obtain.

7.4 Isotope Geochemistry

Several elements abundant in zircon comprise isotopic systems relevant to petrogenesis and have a significant role in defining conditions not only during the Hadean but throughout Earth history. The $^{18}O/^{16}O$ of magmas contains information

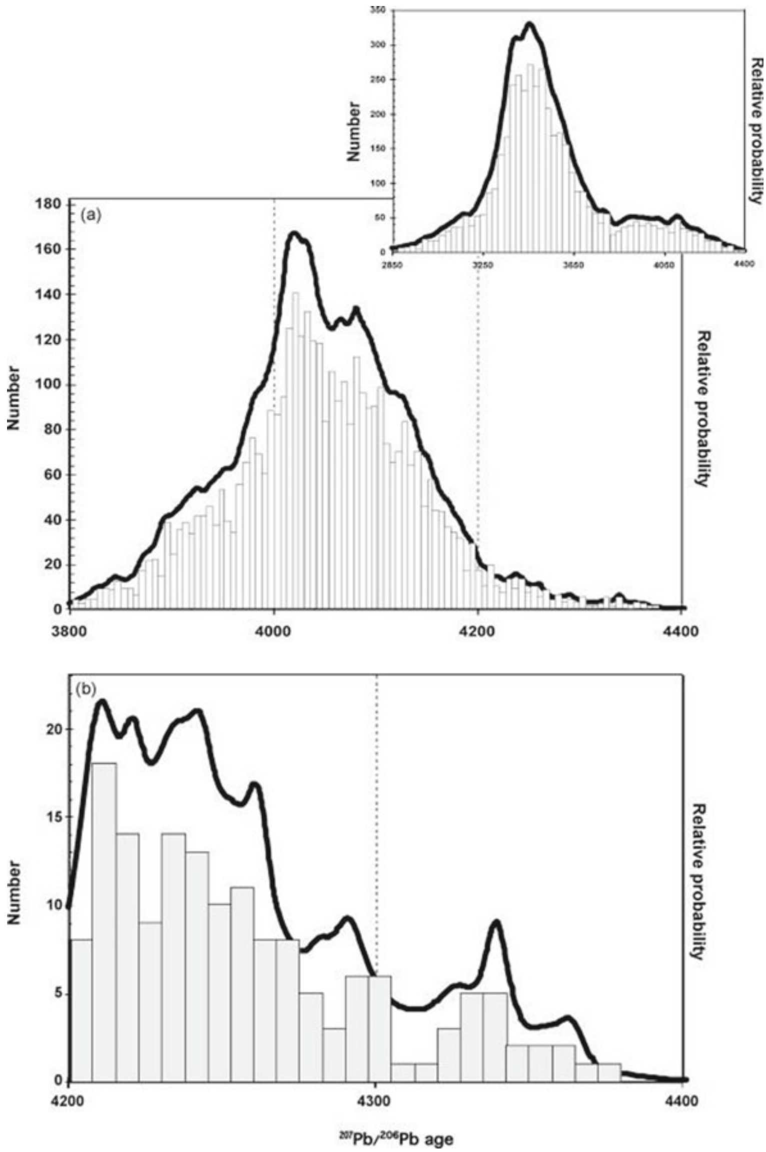

Fig. 7.2 Histograms and probability-density curves for concordant Jack Hills zircons. **a** Histogram of ages obtained from rapid initial survey of individual $^{207}Pb/^{206}Pb$ ages from which the >3.9 Ga population is identified. Inset shows the whole population of 4500 rapidly scanned $^{207}Pb/^{206}Pb$ ages. **b** Histogram and probability density for the concordant >4.2 Ga zircons. The small peak at 4.35 Ga may be the oldest surviving crustal remnant. Reproduced with permission from Holden et al. (2009)

regarding their sources with primary variations often reflecting incorporation of aqueously altered materials. Mantle-derived magmas display a narrow range of $^{18}O/^{16}O$, corresponding to zircons with an average $\delta^{18}O_{SMOW}$ of 5.3 ± 0.3‰ (Valley et al. 1998). Aqueous alteration at low temperatures results in clay-rich sediments with higher $\delta^{18}O$, whereas hydrothermal alteration generally imparts lower $\delta^{18}O$ values. Incorporation of these altered materials into later magmas results in significant deviation from the mantle average value (e.g., O'Neil and Chappell 1977) which are reflected in all silicate and oxide phases present, including zircon. That some Hadean Jack Hills zircons are significantly above the mantle value suggests abundant liquid water in the surface or near-surface environment as early as ca. 4.3 Ga (e.g., Mojzsis et al. 2001; Peck et al. 2001).

The Lu–Hf system is based on the decay of ^{176}Lu to ^{176}Hf ($t_{½}$ = 37 Ga; Söderlund et al. 2004). Lu and Hf are fractionated during partial melting, leading over Earth history to higher Lu/Hf ratios (and therefore ^{176}Hf relative to the stable, primordial isotope ^{177}Hf; represented in parts per 10,000 relative to average chondrite by ε_{Hf}) in the depleted mantle and lower Lu/Hf in the continental crust. The spread in ε_{Hf} between the continental crust and depleted mantle allows for the calculation of a model age of mantle extraction for igneous rocks. This isotopic system is useful on the level of individual zircons due to the incorporation of abundant (up to several weight percent) Hf in zircon and the lesser, ca. 100 ppm-level incorporation of Lu (e.g., Hoskin and Schaltegger 2003), which allows zircon to preserve the original magma ε_{Hf} with very little age-correction needed to account for ^{176}Lu ingrowth. Hadean Jack Hills zircons show dominantly negative (i.e., old crustal) ε_{Hf} with some grains requiring separation of very low-Lu/Hf (i.e., felsic) reservoirs by ca. 4.5 Ga (Harrison et al. 2008; Bell et al. 2014).

7.5 Mineral Inclusions

As zircon crystallizes in the solid state or from magmas, it almost invariably traps exotic phases such as crystals and melt or other fluids (e.g., Maas et al. 1992; Chopin and Sobolev 1995; Tabata et al. 1998; Liu et al. 2001; Fig. 7.3). Inclusions in zircon vary from submicron to 10 s of microns in size but most range from 1 to 10 μm. Coupled with the capacity for accurate U-Pb dating of the zircon host, these inclusions are a potentially rich source of information about petrogenetic conditions of formation and/or provenance.

Although mineral inclusions in magmatic zircon can record diagnostic information about the environment in which they formed, the extent to which the mineralogy and chemistry of zircons and their inclusion can be used to reconstruct petrogenesis and provenance is only now becoming clear. Darling et al. (2009) concluded that mineral inclusions in zircons grown in intermediate to felsic melts within the Sudbury impact melt sheet imply somewhat more felsic melt conditions than the associated whole rock in terms of the modal proportions of quartz, alkali feldspar, and plagioclase. However, Jennings et al. (2011) showed that the

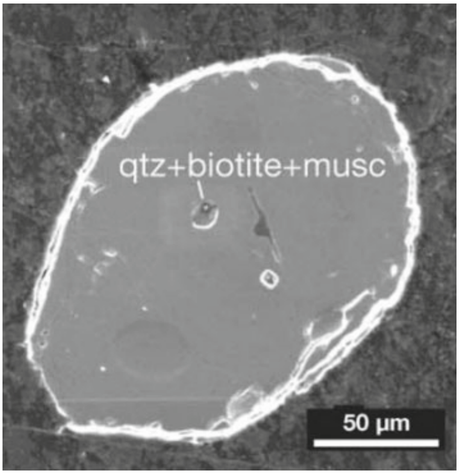

Fig. 7.3 Electron microscope image of Hadean Jack Hills zircon RSES67-3.2 with an inclusion containing coexisting quartz, biotite and muscovite. The white mica has a high celadonite component indicative of an origin at high pressure. From Hopkins et al. (2008)

chemistry of igneous apatite and mafic phases is typically similar between crystals included in zircon and those in the whole rock. Establishing the primary nature of inclusions and contamination introduced during sample preparation are potentially serious concerns that need to be explicitly addressed.

Mineral inclusions coupled with the chemistry of their host zircon are an underexploited resource for establishing internally consistent evidence for host rock character. The advent of the Ti-in-zircon thermometer, for instance, underscored the potential for thermodynamic relationships between included phases and elements partitioned into the zircon structure. Similarly, the incorporation of aluminous and carbonaceous inclusions into zircon (Hopkins et al. 2008; Rasmussen et al. 2011; Harrison and Wielicki 2016; Bell et al. 2015a) raises the possibility of calibrating trace elements in zircon as an indicator of host melt chemistry or volatile content.

7.6 Zircon Geochemistry

Zircon incorporates many elements at the trace or minor level during crystallization, some of which are useful petrologic indicators. For example, the content of Ti in zircon serves as a crystallization thermometer given knowledge of the melt a_{SiO_2} and a_{TiO_2} (Watson and Harrison 2005; Ferry and Watson 2007). Ce/Ce*, or the excess in Ce over the other light rare earth elements (LREE) La and Pr, is a proxy for magma f_{O_2}(Trail et al. 2011b). Th/U can generally be used to distinguish magmatic from metamorphically grown zircons, with metamorphic zircons typically <0.07 and igneous zircon at higher values (Rubatto 2002). Other trace element concentrations have less quantitative ties to petrogenesis but may have the potential to yield important information.

Rare earth elements (REE) occur in terrestrial zircon with a characteristic chondrite-normalized abundance pattern featuring relatively low LREE and increasingly abundant REE with increasing atomic number (e.g., Hoskin and Schaltegger 2003). Two exceptions to this rule include the aforementioned excess in Ce (Ce/Ce*) which is seen among virtually all unaltered terrestrial zircons and a deficit in Eu (Eu/Eu*). The steady increase in compatibility with increasing atomic mass for most REE in the zircon lattice results from the steady decrease in ionic radius coupled with the trivalent oxidation state in which most REE are found in the crustal and surficial environments. Significant amounts of tetravalent Ce (which is more compatible in zircon) and divalent Eu (largely taken up by plagioclase) lead to their respective anomalous contents. However, interpreting REE patterns in terms of zircon petrogenesis requires distinguishing pristine from altered zircon chemistry, and hydrothermal alteration of zircon is usually accompanied by an increase in LREE relative to the other REE and a flattening of the LREE pattern, obscuring the Ce/Ce* and potentially the Eu/Eu*.

7.7 Isotopic Results

7.7.1 U-Pb Age

Various age surveys of detrital zircons from the Erawondoo Hill discovery site conglomerate (e.g., Crowley et al. 2005; Holden et al. 2009) generally show the zircons to have a bimodal age distribution with major peaks at ca. 3.4 and 4.1 Ga. Concordant zircons older than ca. 3.8 Ga make up approximately 5% of the population, and zircons become much less abundant with age older than ca. 4.2 Ga (Holden et al. 2009; Fig. 7.2). The remaining 95% of the population is mostly concentrated between 3.3 and 3.6 Ga, with a relative lack of zircon between 3.6 and 3.8 Ga (Bell and Harrison 2013).

The confidence with which one can interpret the meaning of a U-Pb date of a >4 Ga zircon is challenged by the potential for later fluid alteration and thermal disturbances. While the concordance of U-Pb analyses (or lack thereof) can be used to assess the robustness of an interpreted age, this is generally insensitive to early Pb loss. Therefore assessing the general reliability of ion microprobe U-Pb ages is an open challenge, especially given that most Hadean Jack Hills zircons contain multiple age domains. Valley et al. (2014) examined the possibility of Pb redistribution in a 4.38 Ga zircon core, imaged using atom probe tomography, encompassed by a ca. 3.4 Ga, 10–20 µm rim. In this analytical technique, a zircon sliver extracted using a focused ion beam is evaporated and the emergent ions mass analyzed with a spatial resolution of <1 nm. Results from their analysis show Pb redistribution into "nanoclusters" with ~10 nm diameter and spacing of ~10–50 nm. The ^{207}Pb/^{206}Pb age of the zircon outside of the "nanoclusters" is ~3.4 and ~4.4 Ga for the entire analyzed volume. These data are consistent with an event at 3.4 Ga that mobilized radiogenic Pb accumulating since the zircon's crystallization at 4.38 Ga into "nano clusters" on a length scale of <50 nm, which is below the lateral spatial resolution of an ion microprobe. This finding supports the view that due to the generally slow diffusion of Pb in zircon and zircon's resistance to alteration, concordant U-Pb analyses likely record actual zircon crystallization ages.

7.7.2 Oxygen and Silicon

Elevated values of $\delta^{18}O_{SMOW}$ observed in Hadean Jack Hills zircons led two independent groups to simultaneously propose (Mojzsis et al. 2001; Wilde et al. 2001) that the protolith of these grains contained ^{18}O-enriched clay minerals, in turn implying that liquid water was present at or near Earth's surface by $\sim$4.3 Ga. Numerous follow-up measurements (e.g., Cavosie et al. 2005; Trail et al. 2007; Harrison et al. 2008; Bell et al. 2016) confirmed that a significant fraction of Hadean Jack Hills zircons contain ^{18}O-enrichments of 2–3‰ above the mantle zircon value of 5.3‰ (Valley et al. 1998). As the oxygen isotope fractionation between zircon and granitoid melt is approximately −2‰ (Valley et al. 1994; Trail et al. 2009), $\delta^{18}O$ values of the melt from which the zircons crystallized are inferred to be up to +9‰.

Phanerozoic granitoids derived largely from orthogneiss protoliths (I-types) tend to have $\delta^{18}O$ between 8 and 9‰, whereas those derived by melting of clay-rich (i.e., ^{18}O enriched) metasedimentary rocks (S-types) have higher $\delta^{18}O$ (O'Neil and Chappell 1977). Granitoids with $\delta^{18}O$ values significantly less than 5‰ likely reflect hydrothermal interaction with meteoric water (Taylor and Sheppard 1986) rather than weathering. In general, S-type granitoids form by anatexis of metasediments enriched in ^{18}O, compared with I-type granitoids that form directly or indirectly from arc processes (Chappell and White 1974). Jack Hills zircons enriched in $\delta^{18}O$ thus provide evidence suggesting the presence in the protolith of recycled crustal material that had interacted with liquid water under surface, or near surface, conditions (i.e., low temperature).

A limitation to this interpretation is the possibility of oxygen isotope exchange under hydrous conditions, even at post-depositional temperatures experienced by Jack Hills zircons (i.e., $\sim$450 °C). For example, the characteristic diffusion distance for oxygen in zircon at 500 °C for 1 Ma is $\sim$1 μm (Watson and Cherniak 1997). Thus it is conceivable that oxygen isotope exchange during protracted thermal events could have introduced the heavy oxygen signature. This concern is somewhat mitigated by the relative unlikelihood of hydrothermal fluids being highly $\delta^{18}O$ enriched given the observed oxygen isotopic heterogeneity in Jack Hills zircons. However, it does not preclude isotopic equilibration from having occurred prior to their deposition at ca. 3 Ga.

In addition to concentrating the heavy isotope of oxygen, low temperature clay formation tends to select for lighter Si isotopes, particularly low silica clays, and is thus is a potentially good indicator of pelitic source materials. Recently, Trail et al. (2018) developed a method for simultaneous measurement of $\delta^{18}O$ and $\delta^{30}Si$ and applied this approach to Hadean zircons. They found the range of Si and O isotope compositions to be consistent with melt generation from isotopically heterogeneous sources in the fashion proposed by Chappell and White (1974) for the origin of the I- and S-type granitoids of southeastern Australia. Note that the hypothesis of Kemp et al. (2010) that Hadean zircon source melts were entirely derived from mafic rocks (Sect. 9.8) fails the test presented by this result. The preferred model of Trail et al. (2018) for their combined $\delta^{18}O$ and $\delta^{30}Si$ analyses is of a mixture of sources involved anatexis of siliceous sediments, felsic schists and metabasalts.

7.7.3 Lutetium-Hafnium

Studies of initial $^{176}Hf/^{177}Hf$ in >4 Ga Jack Hills zircons show large deviations in $\varepsilon_{Hf(T)}$ from bulk silicate Earth (Kinny et al. 1991; Amelin et al. 1999; Harrison et al. 2005, 2008; Blichert-Toft and Albarède 2008; Bell et al. 2011, 2014; Kemp et al. 2010) that have been generally interpreted to reflect an early major differentiation of the silicate Earth (Fig. 7.4). Modeling these data by associating $\varepsilon_{Hf(T)}$ with the range of $^{176}Lu/^{177}Hf$ observed in large datasets of analyzed crustal rocks are consistent with the formation of crust occurring essentially continuously since 4.5 Ga. Several data (Harrison et al. 2008; Bell et al. 2014) yield $\varepsilon_{Hf(T)}$ within uncertainty of the solar system initial ratio (Iizuka et al. 2015) requiring that the zircon protoliths had been removed from a chondritic uniform reservoir (CHUR) by 4.50 $\pm$ 0.02 Ga. Harrison et al. (2005) initially reported several Hadean Jack Hills zircons with positive $\varepsilon_{Hf(T)}$, but subsequent in situ studies have not confirmed significantly positive values.

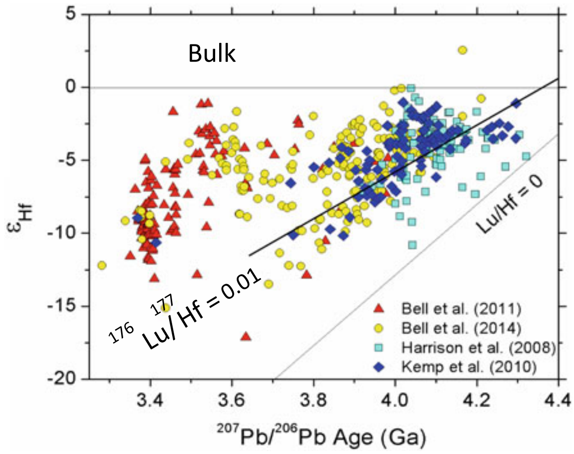

Fig. 7.4 $\varepsilon_{Hf(T)}$ versus $^{207}Pb/^{206}Pb$ age of Jack Hills zircons. Reference $^{176}Lu/^{177}Hf$ ratios for continental crust (0.01) is shown along with value for Bulk Earth (0.034) and primordial $^{176}Hf/^{177}Hf$ (i.e., Lu/Hf = 0). These data are consistent with the formation of continental crust occurring essentially continuously since 4.5 Ga. Modified from Bell et al. (2014)

This likely reflects complications arising from the lack of simultaneous age and Hf isotope analysis, as described by Harrison et al. (2005).

The most robust aspect of this now large dataset is the cluster of results along a line corresponding to a Lu/Hf ≈ 0.01, a value characteristic of continental crust. Such a low-Lu/Hf reservoir at ~4 Ga is consistent with either early extraction of this very felsic crust or its generation by remelting of a primordial more basaltic reservoir, but in either case extrapolation of this trend yields a present-day $\varepsilon_{Hf(T)}$ of approximately −100. This is substantially lower than the most negative value yet seen ($\varepsilon_{Hf(T)} = -35$; Guitreau et al. 2012). The lack of such a signal suggests substantial cycling of crust into the mantle during the early Archean (Bell et al. 2011, 2014). More specifically, zircons with $\varepsilon_{Hf(T)}$ consistent with continuing evolution of this reservoir appear absent from the Jack Hills record after 3.7 Ga (Bell et al. 2014). Combined with Hf isotopic evidence for juvenile mantle melts at ca. 3.9–3.7 Ga at both Jack Hills (Bell et al. 2014) and the nearby Mt. Narryer site with similarly aged zircon (Nebel-Jacobsen et al. 2010), this likely points to a recycling event ca. 3.9–3.7 Ga which resembles the Hf isotopic evolution of modern subduction-related orogens (e.g., Collins et al. 2011) and so may have additional tectonic significance.

7.7.4 Plutonium-Xenon

Xenon isotope measurements of meteorites reveals that ^{244}Pu was present in the early solar system with an initial Pu/U abundance of ~0.007 (Ozima and Podosek 2002). However, its use as a geochemical tracer is restricted by its relatively short half-life ($t_{½} = 82$ Ma). As the only certain relics of Earth's earliest crust, analysis of Xe in Hadean zircons offers a way to determine terrestrial Pu/U ratios and potentially investigate Pu geochemistry during early crust forming events. Since these ancient zircons are detrital and of unknown provenance, it is essential that individual grains be analyzed. Turner et al. (2004) discovered the first evidence of extinct terrestrial ^{244}Pu in individual 4.15–4.22 Ga Jack Hills zircons. These measurements yielded initial Pu/U ratios ranging from chondritic (~0.007) to essentially zero. The latter results were first interpreted to be due to Xe loss during later metamorphism. This assumption was tested by irradiating 3.98-4.16 Ga zircons with thermal neutrons to generate Xe from ^{235}U neutron fission in order to determine Pu/U simultaneously with U-Xe apparent ages. Comparison of U-Pb and U-Xe ages showed varying degrees of Xe loss, but about a third of the zircons yield ^{207}Pb/^{206}Pb and U-Xe ages that are concordant within uncertainty (Turner et al. 2007). Given that U becomes oxidized to the soluble uranyl ion (UO_2^{2+}) under even mildly oxidized aqueous conditions while the solubilities of essentially all Pu species are generally much lower, this mechanism has been suggested as a potential indicator of aqueous alteration in the Jack Hills zircon protoliths (Harrison 2009). Bell (2013) collected a multivariate dataset on eleven zircons including analysis of Xe isotopic ratios, U-Pb age, trace element contents, and δ^{18}O and found no obvious correlations with the exception of Nd/U. High-Nd/U zircons display only low Pu/U, while low Nd/U zircons show more heterogeneous Pu/U. The high-Nd/U group appears less magmatically evolved than other Hadean zircons, has REE patterns suggestive of some degree of alteration, either by hydrothermal fluid interaction or phosphate replacement, and consists of solely low-Pu/U zircons with a range of Hadean to Proterozoic U-Xe ages. The higher diversity of Pu/U among the rest of the population may reflect more heterogeneous processes, including possible primary Pu/U variations from a variety of processes that were not well-constrained. Thus the early promise that Pu/U variations might record aqueous fractionation events in the Hadean may not be realized.

7.7.5 Lithium

δ^7Li analyses of Hadean Jack Hills zircons range from −19 to +13‰ (Ushikubo et al. 2008). These authors interpreted highly negative values to reflect zircon crystallization from a source that experienced intense weathering thus placing the protolith at one time at Earth's surface. A limitation of this interpretation is that Li diffuses readily in zircons at relatively low temperatures (Cherniak and Watson 2010) and thus could have exchanged with hydrogen species during metamorphism (Trail et al. 2011a). Ushikubo et al. (2008) speculated that Li migration might be limited by coupling with the very slow REE diffusion in zircons thus limiting its geological transport rate. Trail et al. (2016) examined this relationship experimentally and found relatively fast diffusion and no detectable link between Li and rare earth diffusion. However, Tang, Rudnick et al. (2017) modeled natural zircon concentration profiles and inferred that Li may diffuse in two modes; a fast mechanism (presumably that experimentally interrogated by Trail et al. 2016) and a slow mode coupled with REE + Y transport. They also observed large, natural Li isotope fractionation and suggested that the δ^7Li variations observed in Hadean Jack Hills zircons by Ushikubo et al. (2008) are due to kinetic effects rather than a record of ancient weathering of granitic source materials.

7.7.6 Uranium

Tissot et al. (2019) made high precision, single grain, U isotope measurements on 31 Jack Hills zircons and found small, but resolvable, differences in δ^{238}U ranging from −0.60 to −0.12‰. This range spans that between chondritic and bulk continental crust values indicating that Oklo-type natural nuclear reactors were unlikely to be widespread during the Hadean. The absence of cases with significant ^{238}U excesses suggest they were not derived from mineralized ores. Tissot et al. (2019) interpreted the isotopic variability to be due to vibrational isotope fractionations rather than from a nuclear field shift during magmatic differentiation. The small observed range in δ^{238}U has implications for the reliability of U-Pb and ^{207}Pb/^{206}Pb ages. Although U-Pb dates are in principle independent of the sample ^{238}U/^{235}U, modern isotope dilution-thermal ionization mass spectrometry analyses are made using mixed ^{233}U-^{235}U spikes (e.g., Condon et al. 2015), requiring knowledge of the sample U isotope composition. However, the full range in observed $\delta^{238}U$ results in calculated $^{207}Pb/^{206}Pb$ age differences of less than one million years, even for Hadean zircons.

7.7.7 Zirconium

ID-TIMS investigations of mass dependent Zr isotope effects in igneous samples revealed resolvable inter-grain $\delta^{94}Zr/^{90}Zr$ variability among coexisting minerals (zircon and baddeleyite; Ibanez-Mejia and Tissot 2018; Zhang et al. 2019) and whole rock suites (N-MORB, felsic volcanics; Inglis et al. 2019). Inglis et al. (2019) inferred that this was due to the preferential incorporation of lighter Zr isotopes within the 8-fold coordinated sites of zircon resulting in heavier values in residual melts. Kirkpatrick et al. (2019) undertook SIMS measurements on 11 zircons standards and zircons from well characterized Phanerozoic I-type S-type granitoids and Hadean Jack Hills grains. Hadean zircons show a limited range with an average $^{94/90}Zr_{NIST}$ of -0.4 ± 0.5‰. In contrast, large ($\sim$7‰) inter- and intra-grain variations were seen in several younger zircons, underscoring the value of using a high spatial resolution method. Zr isotopes could be a useful tool in characterizing protolith composition of detrital, igneous zircons. For example, the isotopic uniformity seen in the Hadean Jack Hills zircons is consistent with their origin in late crystallizing or undifferentiated (e.g., leucogranite) granitoids relative to that expected in a fractionating igneous complex.

7.8 Inclusion Results

The plentiful mineral inclusions preserved in detrital zircons from the Jack Hills, Western Australia, have been the subject of several studies beginning with Maas et al. (1992) who recognized their dominantly granitic character.

7.8.1 Muscovite

Hopkins et al. (2008, 2010) followed up the Maas et al. (1992) study by examining >1700 inclusion bearing zircons from Jack Hills. Their examination revealed that quartz and muscovite are the principal inclusion phases, potentially pointing to some of the granitic sources being aluminous in nature (see example in Fig. 7.3). Hopkins et al. (2010) used a thermodynamic solution model for celadonite substitution in muscovite (White et al. 2001) to estimate pressures for muscovite inclusions in magmatic zircons. In all cases, pressures greater than 5 kbar (unsurprising given the presence of magmatic muscovite) were obtained, consistent with the lower bound on the pressure of the quartz + muscovite reaction at anatectic temperatures. In many instances where a case for a preserved primary inclusion assemblage might be made, analyses cannot currently be undertaken due to size limitations. Indeed, only 6 of the 31 muscovites documented in the Hopkins et al. (2008) study could be reliably analyzed using EMPA due to their small (<2 μm on shortest dimension) size and the effects of secondary fluorescence. Typically, the oldest zircons (>4.2 Ga) contain the smallest white mica inclusions. For example, my group has identified a zircon as old as 4.34 Ga containing white mica that, except for its size, is a candidate for thermobarometric analysis.

The primary nature of these inclusions was brought into question by Rasmussen et al. (2011), who surveyed 1000 Jack Hills zircons from 4.2 to 3.0 Ga and showed that some inclusions fall on cracks in their host zircons and that phosphate inclusions generally record post-depositional U-Pb ages. They then suggested that the entire mineral inclusion record was due to secondary mineralization, and, specifically, that the hexagonal cross section habit of muscovite inclusions was due to their secondary precipitation in voids created from dissolved apatite inclusions. A closer look at the Jack Hills mineral inclusion record reveals complexities not well explained by a largely secondary origin and argues for the preservation of many primary inclusions. Inclusions that intersect cracks in their host zircons display a different modal mineralogy than those isolated from cracks (Bell et al. 2015b). Muscovite inclusions record a wide range of silica substitution with Si-per-formula-unit ranging from 2.91 to 3.45, unlikely to all form from the same metamorphic fluid. The assemblage that intersects cracks is roughly intermediate between the isolated assemblage and the assemblage of secondary phases seen filling void space along cracks, probably showing partial replacement (Bell et al. 2015b). The isolated and likely primary assemblage is muscovite-dominated with abundant quartz, still suggestive of aluminous granitic protoliths, and minor phases such as biotite, apatite, and feldspars vary in abundance with zircon age (Bell et al. 2015b). Certain phases present in the isolated assemblage and absent in the crack-intersecting assemblage probably point to selective destruction of the minerals apatite and feldspar. Because of the relatively low numbers of identified rare phases (e.g., aluminosilicates), it is difficult at present to determine their significance for zircon provenance or for identifying the nature of the altering fluids which invaded the zircons along cracks over geologic time.

Rasmussen et al. (2011) did not address implications of the bimodal distribution of Si_{pfu} values in the white mica inclusions, including a distinct population at ~3.45 (i.e., implying pressure of >12 kbars). That the Si_{pfu} distributions differ appears to strengthen the interpretation of Hopkins et al. (2008, 2010) that most of the mica inclusions are primary as it is unclear how low temperature/pressure alteration could create such a heterogeneous distribution. Indeed, unless all Hadean Jack Hills muscovite inclusions coincidentally precipitated during subsolidus reactions that imparted crystal forms characteristics of igneous muscovite together with virtually the full range of of Si/Al ratios seen in crustal rocks, at least a portion of these inclusion assemblages must be primary (Hopkins et al. 2012).

For those muscovite-bearing inclusion assemblages for which a primary origin can be ascribed, Hopkins et al. (2008, 2010) then coupled the pressure estimates with the relatively low host zircons crystallization temperature (ca. 700 °C; Sect. 7.9.1) which yields near surface apparent geotherms. To do so requires several assumptions, such as overburden density (i.e., 3 g/cm^3) and knowledge of surface temperature. Given that the Hadean Sun was $\sim$30% less luminous than today, surface temperature was likely limited to the range 200–300 K (e.g., Budyko 1969; Pierrehumbert 2005; Zahnle 2006). Note that if the magmas from which the zircons formed had ascended buoyantly from the source of melting prior to crystallization/inclusion trapping, then the apparent geotherm would be overestimated. Hopkins et al. (2010) noted that the calculated geotherms were subparallel to the slope of the Si_{pfu} isopleths in the phengite barometer and thus underestimating crystallization temperature due to sub-unit a_{TiO_2} is compensated by lower calculated pressure (i.e., apparent gradients are insensitive to changes in calculated zircon crystallization temperature). Assuming that the host granitoids formed within a thermal boundary layer in which conduction was the dominant heat flow mechanism, an apparent geotherm can be translated into average heat flow between the surface and depth of crystallization using Fourier's Law (see Sect. 2.2). For a thermal conductivity of 2.5 W/m C (Turcotte and Schubert 2002), near-surface ($\leq$60 km) heat flows range from 40 to 85 mW/m^2, with an average of $\sim$60 mW/m^2. This range largely overlaps that of Earth today (Pollack et al. 1993) and is substantially less than that generally inferred for global heat flow during both the Archean (150–200 mW/m^2; Bickle 1978; Abbott and Hoffman 1984) and postulated for the Hadean (160–400 mW/m^2; Smith 1981; Sleep 2000).

7.8.2 Fe Oxides

The development of textural criteria for identifying primary inclusions (Bell et al. 2015b) opens up possibilities for recognizing zircons' changing provenance with time and investigating their post-depositional alteration history. One intriguing aspect of zircon provenance that could be further understood through the inclusion record is that of protolith magma f_{O_2} and its evolution. As described in more detail in the next section, Trail et al. (2011b) demonstrated that the Ce anomaly of a zircon (Ce/Ce*) is a quantitative estimate for host magma f_{O_2}, and furthermore that Hadean Jack Hills zircons show a range in f_{O_2} with an average near FMQ (or, similar to the modern upper mantle). Granitoids form at a range of f_{O_2}, controlled both by source region and assimilation of wall rock material during ascent. The observation of both ilmenite and magnetite inclusions in >4 Ga Jack Hills granitoid zircons implies a range of redox environments for their origin. Characteristic series of granites with contrasting f_{O_2} in accretionary environments are identified by their accessory Fe–Ti oxides, with more oxidized granites dominated by magnetite and more reduced granites dominated by ilmenite (Ishihara 1977).

Fe–Ti oxides occur commonly as inclusions in zircon (Rasmussen et al. 2011) and appear to be a robust if minor component of the Hadean primary assemblage (Bell et al. 2015b). Primary Fe-oxide inclusions may preserve geomagnetic information and multiple groups are currently investigating whether such signals are the oldest known records of a Hadean dynamo. Knowing when the geodynamo arose potentially constrains Earth's early thermal structure and potential for atmospheric loss and when compositionally-driven core convection began. At present, the oldest reliable determination of the terrestrial magnetic field is 3.45 Ga (Biggin et al. 2011). Tarduno et al. (2015) interpreted Jack Hills zircons as containing magnetite inclusions that retained primary remanent magnetization as old as 4.2 Ga (cf., Weiss et al. 2015) but failed to demonstrate whether they had been remagnetized by thermal processes subsequent to formation. Tarduno et al. (2015) argued that their zircons had not experienced high-temperature metamorphism, as Pb would be redistributed in an inhomogeneous fashion at the nm-scale (Valley et al. 2014) resulting in non-systematic Pb/U variations during SIMS depth profiling that they did not observe. That view misrepresents their ion microprobe capability in three ways: (1) the sputtering process mixes near surface atoms at the ~10 nm-scale, (2) the SHRIMP instrument they used cannot truly depth profile as sputtered atoms from both crater bottom and surface are simultaneously accelerated into the mass spectrometer, and (3) the 10–20 μm diameter spot they used is three orders of magnitude larger than would be needed to reveal such heterogeneities, even if they existed. As described in Sect. 7.9.3, Trail et al. (2016) suggested that zircons exhibiting Li concentration heterogeneities, including oscillatory zoning, could be calibrated in this role as a peak temperature geothermometer for paleomagnetic studies, although multiple diffusion mechanisms may preclude this application (Tang, Rudnick et al. 2017; Sect. 10.2.9).

7.8.3 Biotite

Biotite inclusions in magmatic zircon are relatively common (Rasmussen et al. 2011) and appear to reflect the composition of biotite in the host (Jennings et al. 2011), which varies considerably among granitoids (e.g., Buda et al. 2004; Abdel-Rahman 1994). Biotite shows characteristic variations in FeO, MgO, and Al_2O_3 contents that can discriminate among calc-alkaline, peraluminous, and alkaline anorogenic granitoids (Abdel-Rahman 1994). Thus, identifying and analyzing primary Hadean biotite inclusions could better constrain the nature of Hadean melt compositions that may have tectonic implications. Three biotite inclusions identified in Hadean zircons appear to derive from metaluminous as well as reduced peraluminous magmas (Bell et al. 2018). In addition, rare sulfide (Mojzsis et al. 2007) and carbonaceous (see Sect. 7.8.5) phases have also been identified in Hadean zircons. A systematic survey for these and other rare phases will further illuminate the volatile contents of Hadean magmas and their source materials.

7.8.4 Quartz

Although quartz makes up about 35% of the total inclusion population (Hopkins et al. 2008), its monomolecular structure limits its geochemical utility. Nonetheless, the Ti content of such inclusions have been used as a thermobarometer (Hopkins et al. 2010). Cameron et al. (2016) found that most quartz inclusions in zircons from the Jack Hills were in isotopic equilibrium and had not exchanged with the host quartzite. They concluded that primary inclusions can be used to infer properties of Hadean parent magmas at the time zircon crystallized.

7.8.5 Graphite

A key challenge in pondering the existence of life elsewhere is that we know of only one occurrence. While Earth is the only planet on which life is known to have emerged, we remain largely ignorant of the conditions, timing and mechanisms by which this occurred (see Chap. 10). A broad array of morphological and isotopic evidence supports the view that by 3.8–3.5 Ga, our planet hosted microbiota, including some with relatively sophisticated metabolisms (e.g., Mojzsis et al. 1996; Rosing 1999; McKeegan et al. 2007; Schopf 2014; Brasier et al. 2015).

As noted earlier, geochemical studies of Hadean Jack Hills zircons have led several authors to suggest relatively clement conditions on earliest Earth (e.g., Wilde et al. 2001; Mojzsis et al. 2001; Harrison 2009). This leaves open the possibility that our planet became habitable, and life emerged, during the first 500 million years of Earth history. Knowing when and under what conditions life emerged could tell us a great deal about the likelihood of life elsewhere. Were conditions clement or hellacious? Did life emerge virtually immediately or only after a half billion years of planetary preparation?

Thus reports of abundant diamond and graphite inclusions in the Jack Hills zircons (4% of each in the zircons investigated) and the spectrum of light carbon isotopic compositions they contained (Menneken et al. 2007; Nemchin et al. 2008) was met with both excitement and skepticism; the latter reflecting the seeming inconsistency of the presence of diamonds with the many inferences drawn from other zircon inclusions (e.g., their derivation from arc or crustal melts; Hopkins et al. 2010; Mojzsis et al. 2001; Peck et al. 2001; Watson and Harrison 2005; Bell et al. 2015a). Subsequently, the diamonds were shown definitively to be contamination from the polishing compound that was used during sample preparation (Dobrzhinetskaya et al. 2014). The origin of the graphite was less certain but deemed also likely due to contamination. This left the true occurrence rate and nature of carbonaceous materials in the Jack Hills zircons uncertain.

Bell et al. (2015a) optically examined a large number of >3.8 Ga Jack Hills zircons and found $\sim 25\%$ contain opaque inclusions. Imaging these selected grains by Raman spectroscopy revealed two isolated carbonaceous inclusions in a concordant, 4.10 Ga zircon (RSES 61-18.8; Fig. 7.5). To ensure that these inclusions were never in contact with the laboratory environment prior to structural and isotopic analyses, Bell et al. (2015a) extracted a ~ 160 ng sliver of the zircon containing the two carbonaceous phases via focused ion beam milling and examined it using X-ray nanotomography (Fig. 7.5). The 40 nm spatial resolution of this imaging method revealed no cracks associated with the graphite inclusions. Their isolation within the zircon crystal and from cracks indicated a primary origin.

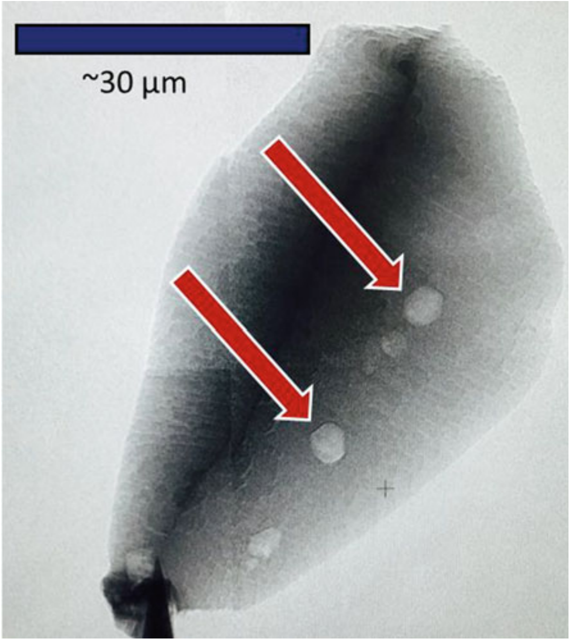

Fig. 7.5 High resolution transmission X-ray image of RSES 61-18.8 with arrows pointing to the two graphite inclusions analyzed for carbon isotopes. Reproduced with permission from Bell et al. (2015a)

Carbon isotopic measurements using SIMS yielded an average $\delta^{13}C_{PDB}$ of -24 ± 5‰. As carbon isotopic fractionation between gaseous and condensed species in magmas is expected to be relatively small (e.g., ≤ 4‰; Javoy et al. 1978), this result is consistent with a biogenic origin. While there are possible inorganic mechanisms that could also produce such a signal (see Sect. 11.5.1), they require an unlikely chain of geologic events (Bell et al. 2015a). Alternatively, House (2015) proposed the "wild" suggestion that a high carbon content in Earth's core could have resulted in an initially isotopically light mantle. If the Bell et al. (2015a) result does indeed represent an isotopic signal of biologic activity, it would extend our knowledge of the timing of terrestrial life back to at least 4.1 Ga, or ≥ 300 Ma earlier than the previously suggested and coincident with estimates derived from molecular divergence among prokaryotes (Battistuzzi et al. 2004).

Reports of graphite in S-type granites are relatively rare but cases have been documented in which it was inherited from the source (Seifert et al. 2010; Zeng et al. 2001), incorporated via wallrock assimilation (Duke and Rumble 1986), or precipitated during subsolidus interactions with CO_2 (Frezzotti et al. 1994; also see Carroll and Wyllie 1989). Graphite inclusions have been reported in metamorphic zircon (Song et al. 2005) but, to my knowledge, Bell et al. (2015a) is the first documented case of primary graphite in magmatic zircon. Given the relative paucity of investigations of zircon inclusion populations, it is difficult to know whether this reflects their low abundance or simply the lack of a concerted search.

The oxygen fugacity over which graphite can be stable in a granitic magma depends on H_2O and H_2 activities (Ohmoto and Kerrick 1977), but relatively reducing conditions (i.e., below the fayalite-magnetite-oxygen buffer assemblage; FMQ) are implied. The highly reduced redox state of the magma from which the Hadean zircon crystallized is consistent with a metasedimentary protolith containing some form of reduced carbon (Bell et al. 2015a). This would be the case for any, say, Phanerozoic S-type granitoid formed by melting of shales bearing carbnaceous residues of life. At anatexis, the only remaining evidence of biologic activity would be graphite formed from sequential decomposition of kerogen. Clearly zircon RSES 61-18.8 provides proof that the relevant surface energetics permit graphite to be incorporated into magmatic zircon during crystallization.

7.9 Trace Element Geochemistry Results

7.9.1 Titanium

Because the abundance of a trace element partitioned between mineral and melt is temperature dependent, crystallization temperatures can in principle be estimated from knowledge of the concentration of that element in the solid phase if the magma is appropriately buffered. The advent of the Ti-in-zircon thermometer permits zircon crystallization temperatures to be assessed provided the activities of quartz and rutile in the melt can be accurately estimated (Watson and Harrison 2005; Watson et al. 2006; Ferry and Watson 2007). The diffusion of Ti in zircon is vanishingly slow under crustal conditions (Cherniak and Watson 2007) and thus the potential for re-equilibration of the thermometer is very low. In the case in which zircon co-exists with both quartz and rutile (i.e., $a_{SiO_2} \approx a_{TiO_2} \approx 1$), an accurate and precise temperature (i.e., ±15 °C) can routinely be determined.

The first application of the Ti-in-zircon thermometer was to Hadean zircons from Jack Hills. Watson and Harrison (2005) measured Ti in zircons ranging from 3.91 to 4.35 Ga, the vast majority of these plotting in a normal distribution. Excluding high temperature outliers yielded an average temperature of 680 ±25 °C (data shown in Fig. 7.6). However, a limitation in applying this thermometer to detrital zircons is the unknown a_{TiO_2} of the parent magma. In the case of zircons containing both primary quartz and rutile, an accurate crystallization temperature is expected. However, unless co-crystallization with rutile is known, the calculated temperature it is a minimum estimate. In the absence of rutile inclusions, Watson and Harrison (2005) argued that a_{TiO_2} is largely restricted to between ~0.5 and 1 in continental igneous rocks as the general nature of evolving magmas leads to high a_{TiO_2} prior to zircon saturation (Watson and Harrison 1983; Boehnke et al. 2013). Thus for Hadean zircons of magmatic origin, it would be a rare case in which zircon formed in the absence of a Ti-rich phase (e.g., rutile, ilmenite, titanite), thus generally restricting a_{TiO_2} to ≥ 0.5. In case of $a_{TiO_2} \approx 0.5$, calculated temperatures in the range 650–700 °C would be underestimated by 40–50 °C, although similar

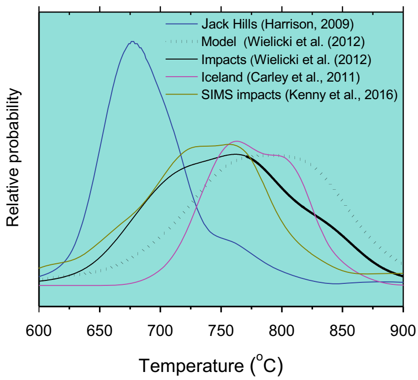

Fig. 7.6 Probability plot of apparent zircon crystallization temperature comparing Hadean data (blue) with data for Icelandic (magenta) and impact formed (black and green) zircons. The dashed curve shows the distribution predicted by a model incorporating impact thermal effects, continental rock chemistry, and zircon saturation behavior. Modified from Wielicki et al. (2012)

sub-unity activities SiO_2 and TiO_2 are compensatory (Ferry and Watson 2007). Hofmann et al. (2009) inferred that enhanced Ti contents could be incorporated during non-equilibrium crystallization resulting in higher than actual calculated temperatures. If this effect were significant in the generation of granitic Jack Hills zircons this would further support their low-temperature origin.

7.9.2 Rare Earths

As previously noted, the abundance ratio of Ce in zircon relative to that interpolated from the light rare earth pattern (Ce/Ce*) has been developed as a quantitative estimate for host magma f_{O_2} (Trail et al. 2011b). Most Hadean Jack Hills zircons are within error of FMQ (similar present-day upper mantle) but range as low as iron-wüstite (IW) suggesting a diversity of source materials (Trail et al. 2011b). Another, qualitative estimate for magma oxygen fugacity can be inferred from the mineralogy of Fe–Ti oxide phases (see Sect. 7.8.2). Ishihara (1977) observed that both oxidized and reduced series of granitoids occur in accretionary settings, with the oxide mineralogy of highly oxidized granites dominated by magnetite and that of the reduced granites dominated by ilmenite. Since oxide inclusions are often a minor constituent of igneous zircon inclusion suites (e.g., Rasmussen et al. 2011), the coupled investigation of oxide inclusion mineralogy with Ce/Ce* in the host zircon provides the ability to check for internal consistency between these two estimates of Hadean magma redox conditions.

It will be helpful to establish both the characteristic ranges of zircon Ce/Ce* for magnetite versus ilmenite series granitoids and whether the oxide mineralogy of the whole rock is accurately reflected by the mineralogy included in zircons.

Reconnaissance electron microscope observations (Hopkins et al. 2010; reported by Bell et al. 2015b) suggest that Hadean opaque inclusions are dominated by Fe oxides, potentially magnetite. Further investigation of the mineralogy of Hadean oxide inclusions, coupled with their host zircon Ce/Ce*, may help to better classify the granitoids they derive from or potentially to diagnose alteration affecting the inclusions or host zircon. This coupled approach will better illuminate the redox conditions in the Hadean crust and any potential complexities that igneous zircon may record.

Petrologically important trace element signatures such as Ce/Ce* (and Ti content) can be obscured by alteration or contamination (e.g., cracks, inclusions, etc.). Hydrothermal alteration of zircon is often diagnosed by a high, flat light rare earth element (LREE) pattern. Among Jack Hills zircons, such alteration is dominantly characterized by anomalously high Ti, Fe, P, U, and LREE contents (Bell et al. 2016). To remediate this issue, Bell et al. (2016) developed a trace element indicator (i.e., the LREE-Index) which permits altered and hydrothermal zircons to be clearly identified.

Melts from oceanic settings (MORB, oceanic arc, Iceland) typically have higher HREE contents and shallower MREE-HREE slopes than those from continental settings (arcs, TTGs). Model melts calculated from elemental partition coefficients and Hadean zircon REE patterns (Bell et al. 2016, 2017) are similar to that expected for continental arcs, including TTGs (i.e., strong HREE depletion with a slope reversal at the heaviest REE) indicating the influence of garnet and amphibole in low temperature, high (≥ 7 kbar) pressure environments (Carley et al. 2018, 2020). The oldest (>4.25 Ga) Jack Hills zircons yield model melts that show elevated REE, LREE/HREE and Zr/Hf relative to that for younger zircons.

7.9.3 Lithium

As noted earlier, Trail et al. (2016) proposed the use of Li zoning in zircon as a peak temperature indicator, particularly for use in ascertaining the retention of primary remenant magnetic signals. The general preservation of micron-scale lamella requires that peak heating temperature(s) did not exceed $\sim$500 °C (and thus the Curie temperature for magnetite of 585 °C) for million-year-scale timescales. Each detrital zircon in a population may have a different pre-depositional thermal history, but documenting such evidence even once indicates that, post deposition, the metaconglomerates at Erawondoo Hill did not experience temperatures greater than 500 °C. This is consistent with other thermometric determinations at that location (Rasmussen et al. 2010). However, Tang, Rudnick et al. (2017) modeled natural zircon concentration profiles and inferred that Li may diffuse in two modes—a fast mechanism and a slow mode coupled with REE + Y transport—thus complicating thermometric interpretations.

7.9.4 Aluminum

Trail et al. (2016) found that zircons from peraluminous granitoids contain average Al concentrations of ~10 ppm (with a range from 0 to 23 ppm), in contrast to I- and A-type zircons which average ~1.3 ppm. Although alumina activity appears not to be a simple function of the degree of the peraluminosity, they inferred that zircon Al concentration could be calibrated as a proxy for melt $Al_2O_3/(CaO + Na_2O + K_2O)$ with inferred molar values of >1 reflecting an origin from recycled pelitic material. They applied this approach to Hadean Jack Hills zircons and found both metaluminous and peraluminous sources, with the former apparently dominating the population. Although the low occurrence of high Al contents from Hadean zircons suggests that metaluminous crustal rocks may have been more common than peraluminous rocks in the Hadean, the ~20% overlap of low Al (i.e., <5 ppm) in S-type zircons somewhat obscures this inference.

7.9.5 Carbon

As carbon is long known to dissolve in silicates at trace levels (e.g., Freund et al. 1980; Oberheuser et al. 1983; Mathez et al. 1984; Tingle et al. 1988; Keppler et al. 2003; Rosenthal et al. 2015), the coexistence of zircon and graphite raises the possibility that C could be present at measurable levels in zircon. As SIMS has the potential for detection levels of C as low as ~1 ppb, it is ideally suited for such a search.

The lack of dependency of carbon solubility in silicates on oxygen fugacity suggested to Shcheka et al. (2006) that C^{4+} substitutes for Si^{4+}, with increased levels as the volume of the SiO_4 tetrahedron decreases. In this regard, they emphasized that the relatively small volume of the SiO_4 tetrahedron in zircon should enhance carbon solubility. Alternatively, Sen et al. (2013) found evidence of C substituting for nonbridging oxygen in synthesized silicate nanodomains. As such they hypothesized that trace carbon could be incorporated into silicates across a broader range of oxygen fugacity than previously thought and speculated that this incorporation mechanism might have been preferentially important during the Hadean eon.

In the same way that a zircon co-crystallizing with rutile contains a predictable temperature-dependent Ti concentration, zircons growing in the presence of a carbonaceous species appear to partition C in a fashion that could be calibrated as a magma volatile probe. Having an approach with which to detect Hadean crustal C could potentially reconcile the disparate views regarding the magnitude of carbon in the crust during that eon. Some authors argue for a net increase in crustal carbon from essentially zero at 4 Ga (e.g., Hayes and Waldbauer 2006; Kelemen and Manning 2015) to its present day inventory in a broadly linear fashion. Marty et al. (2013) envisioned an essentially continuous transfer of carbon from undegassed mantle reservoirs implying a net increase to the crust over time. In contrast, Dasgupta (2013) advocates for higher than present day concentration on early Earth.

The development of a proxy to detect the presence of carbon in Hadean (and younger) melts may eventually permit selection among these models.

7.9.6 Halogens

Tang et al. (2019) investigated halogen abundances in Jack Hills zircons along with Proterozoic-Phanerozoic zircons of known provenance. All zircons show halogen contents above measurement background and appear not be due to secondary alteration or inclusions. In general, the younger zircons (0.1–1.1 Ga) show low and uniform F and Cl contents of 1.80 ± 0.11 ppm and 0.31 ± 0.04 ppm, respectively. Fluorine contents in all 58 Jack Hills zircons are higher (2.28 ± 0.19 ppm) than post Archean zircons whereas chlorine contents in analyzed Jack Hills zircons show a secular trend. Specifically, much higher Cl concentrations (1.19 ± 0.32 ppm) are observed in a subset of zircons between 3.8 and 3.9 Ga whereas younger and older grains have Cl contents consistent with the young zircons (0.34 ± 0.04 ppm). Significantly, that age range corresponds to a dicrete part of the classification scheme of Bell and Harrison (2013) who found zircons between 3.91 and 3.84 Ga are distinctly different than both older and younger grains in the Jack Hills population (see Sect. 9.11). These grains, termed "Group II" are characterized by high U and Hf, low-Ti, and Ce, P, Th/U relative to "Group I" which resemble the majority of Hadean zircons in terms of trace element concentrations. Bell and Harrison (2013) interpreted Group II to have formed from thermally-driven, transgressive recrystallization (Hoskin and Schaltegger 2003) between 3.91 and 3.84 Ga. An implication of the high Cl contents of this cohort is that recrystallization occurred in the presence of a hydrothermal brine.

Tang et al. (2019) experimentally determined a partition coefficient between zircon and a highly saline aqueous fluid of ($D_{\text{zircon-fluid}}$) $\approx 2.5 \times 10^{-4}$, demonstrating that Cl can substitute into zircon when crystallizing in fluid-rock systems. This translates to a fluid concentration of between 10^3 and 10^4 ppm Cl during the recrystallization of Group II zircons. This range is similar to Cl concentrations in modern Cl-rich, hydrothermal systems (e.g., Stefánsson and Barnes 2016) and is testament to the local presence of high halogen levels during the Hadean to Archean transition.

7.9.7 Sulfur

The geochemistry of sulfur makes it a potentially powerful probe of volatile evolution and redox conditions and with which to distinguish lithophile/chalcophile environments. Tang, Bell et al. (2017) found that sulfur contents of zircons varied systematically with changes in protolith and redox. I-type zircons contain very low (~0.4 ppm S) concentrations relative to those from S-type granitoids (~1.3 ppm S). When correlated with f_{O_2} via the Ce/Ce* method (see Sect. 7.9.2) they found a systematic relationship with S-type zircons plotting distinctively in high S, low f_{O_2}

space. Three of ten Jack Hills zircons analyzed showed sulfur contents consistent with that of S-type zircons with the others yielding the lower abundances consistent with an I-type source.

7.9.8 Phosphorus/Rare-Earths

Burnham and Berry (2017) showed that most zircons crystallizing from I-type magmas show a different geochemical signature to those derived from S-type magmas. Unlike I-type zircons, the phosphorus/rare-earth ratio (i.e., the xenotime solid solution) is close to unity in many S-type zircons which also typically have higher P contents. Applying this discriminant to Hadean Jack Hills zircons, they concluded that most formed from I-type granitoids, consistent with a source from melted pre-existing mafic lower crust and suggesting a minor role for S-type magmas. However, Bell (2017) pointed out that many zircons with lower phosphorus contents could derive from sediment-rich sources which could account for other geochemical evidence from the Hadean Jack Hills that are strongly suggestive of an S-type origin, albeit for a minority of the population. Specifically, only one in seventy-five Hadean zircon grains contain primary muscovite, one in thirty-nine yield high aluminium contents, one in five show elevated $\delta^{18}O$, and one in nine show high S (Bell 2017; Tang, Bell et al. 2017). A sedimentary origin for the protoliths of these zircons is thus likely indicated.

7.10 Petrologic Constraints

7.10.1 Water Activity During Melting

While it is widely acknowledged that water saturation in intracrustal magmas is rare and that the vast majority of intermediate to siliceous anatectic magmas form by dehydration melting under vapor absent conditions (Clemens 1984), Watson and Harrison (2005) concluded that the tight cluster of Hadean zircon crystallization temperatures at 680 ± 25 °C (Fig. 7.6) reflects prograde melting under conditions at or near water saturation. They arrived at this interpretation because prograde, vapor-absent melting of metapelites and orthogneisses containing typical crustal Zr concentrations (i.e., 150–200 ppm; Harrison et al. 2007) at 5–10 kbar would be expected to record zircon crystallization temperature peaks corresponding to the relevant dehydration melting equilibria (e.g., muscovite at ca. 740 °C, biotite at ca. 770–800 °C, amphibole at $\geq$ 800 °C; Spear 1993). Thus, for example, Hamilton's (2007) assertion that Hadean zircons were derived solely through melting resulting from hornblende breakdown is fundamentally inconsistent with all thermometric results to date.

Rock porosities in the middle and deep crust are typically <0.1% (Ingebritsen and Manning 2002) and thus less than 0.03 wt% free H_2O would be available to

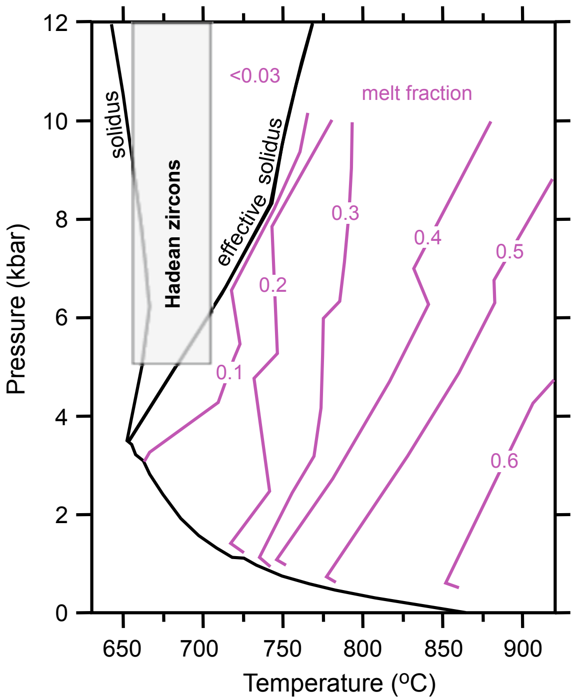

Fig. 7.7 *P-T* pseudosection for a model pelite in the NCKFMASH system containing 20 mol% added H_2O. Note that even in the presence of this free water, the *P-T* region populated by Hadean zircons would result in essentially melt-free conditions indicating that very high water contents (>9 wt%; Burnham 1975) would be required to create significant, mobile magmas. Modified from White et al. (2001)

flux melting. During metamorphism, water is progressively lost from rocks via discontinuous, subsolidus dehydration reactions through the greenschist and amphibolite facies (Spear 1993). Structural water is stored in hydrous minerals (e.g., ~4% in muscovite, ~3% in biotite, ~2% in hornblende, ~2–4% in altered basalt at greenschist facies; Clemens and Vielzeuf 1987; Franzson et al. 2010). The correspondingly low water contents of pelitic (~1.2%) and quartzofeldspathic rocks (~0.6%) are expected to produce only small amounts of melt at temperatures close to 700 °C (Clemens and Vielzeuf 1987). The calculations of White et al. (2001) (Fig. 7.7) underscore the limited melting potential of metapelite (represented by the Na_2O–CaO–K_2O–FeO–MgO–Al_2O_3–SiO_2–H_2O system) for the temperatures (up to 730 °C) and pressures (>6 kbars) inferred for Hadean Jack Hills zircons, which fall below their "effective solidus" melt fraction of 0.03 (even in the presence of 20 mol% H_2O). That is, under vapor absent conditions at the pressure-temperature range documented for Hadean zircons (Hopkins et al. 2010), both pelitic and quartzofeldspathic source rocks would be effectively melt free.

Concluding that Hadean Jack Hills zircons largely formed under near water-saturated conditions sharply limits the possible tectonic settings in which they formed. The key issue is that silicate magmas at pressures above 6 kbar dissolve much more H_2O than is available in rocks (up to 70 mol% at 10 kbar; Burnham 1975; Clemens 1984) and thus appear to require an external source of water for saturation to be achieved.

7.10.2 A Himalayan Analogue?

In general, Phanerozoic zircons showing magmatic zoning appear to form at somewhat higher apparent temperatures than the average value of Hadean Jack Hills zircons of ca. 680 °C. Harrison and Wielicki (2016) found that zircons from the rutile-bearing, ~20 Ma Arunachal leucogranites, a suite of dykes and sills in the eastern Himalaya, to be a rare exception. The spectrum of their magmatic crystallization temperatures of about 660 °C is remarkably similar to the Hadean distribution, but distinctly different to the pluton-scale Himalayan leucogranites, including the nearby Tsona granites (Fig. 7.8). Furthermore, the Arunachal leucogranites show large-ion lithophile covariance trends indicative of wet basement melting.

Incongruent, fluid-absent melting of both muscovite and biotite is expected to lead to strong Rb enrichment in the melt. Figure 7.9 shows a Rb/Sr versus Ba covariance diagram for the suite of Arunachal leucogranites along with a variety of High Himalayan leucogranites and averages of the Greater Himalayan Crystallines for comparison (Colchen et al. 1986; Harris and Inger 1992 Aikman et al. 2012). The variance within the Greater Himalayan Crystallines is shown in Fig. 7.9 by the grey field defined by the results of Vidal et al. (1982) for hangingwall gneisses in the central Himalaya. Covariance vectors for muscovite dehydration melting, biotite dehydration melting, and water-saturated minimum melting are also shown (Inger and Harris 1992). The clear trend of the High Himalayan leucogranites, including

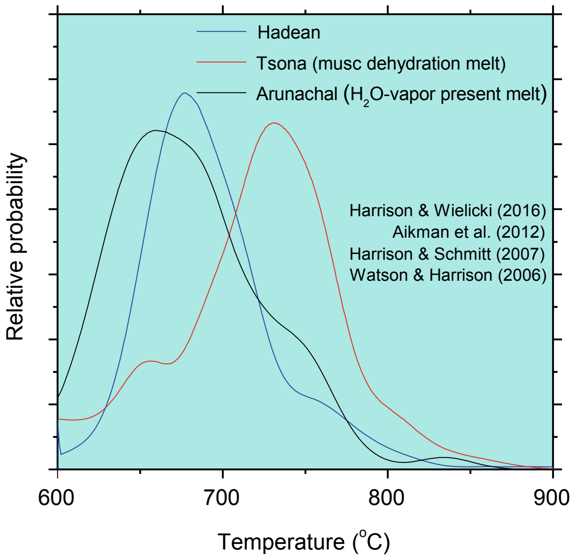

Fig. 7.8 Relative probability plot of zircon crystallization temperatures for the Tsona and Arunachal leucogranites (eastern Himalaya). Zircons from the Arunachal leucogranites resemble the distribution for the Jack Hills zircon population. Reproduced with permission from Harrison and Wielicki (2016)

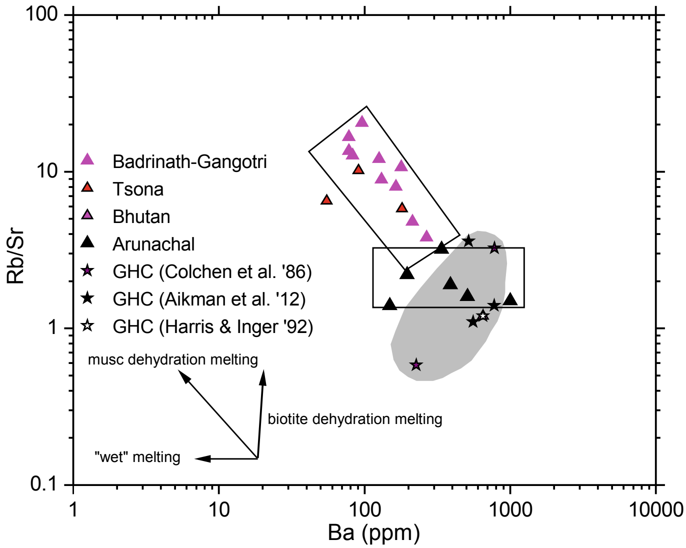

Fig. 7.9 Rb/Sr versus Ba plot for Himalayan leucogranites (in warm colors), the Arunachal leucogranites (black triangles), averages for the Greater Himalayan Crystallines (stars) and the field of GHC gneisses from the study of Vidal et al. (1982) in grey. Note that the covariance vector expected for muscovite vapor absent melting is parallel to the trend exhibited by the large Himalayan plutons but not the Arunachal leucogranites, which plot in the field of the basement rocks but within the variance shown in grey. Reproduced with permission from Harrison and Wielicki (2016)

the Tsona leucogranites, parallel to the muscovite fluid-absent melting vector is evidence that these large plutons formed by dehydration melting.

In contrast, the average Rb/Sr of the Arunachal leucogranites of ~2 is similar to the host Greater Himalayan Crystallines average. The lack of enrichment in Rb/Sr is evidence that the Arunachal leucogranites formed via water-saturated minimum melting, a process that more equally consumes feldspar, quartz and mica than does muscovite dehydration melting. Thus their low crystallization temperature (ca. 660 °C) is unsurprising. Harrison and Wielicki (2016) took this as support of the view that the formation of the Hadean Jack Hills zircons under conditions of near water-saturation.

7.11 Critical Summary

A significant portion of the Jack Hills detrital zircon population is too metamict and otherwise altered/overprinted to retain reliable information regarding their petrogenetic origins. But other grains appear to have remained closed chemical and isotopic systems for as long as 4.38 Ga. Evidence from oxygen isotopes, primary hydrous inclusion assemblages, and Ti thermometry have driven a consensus that molecular water was present at or near Earth's surface since at least 4.3 Ga.

References

Abbott, D. H., & Hoffman, S. E. (1984). Archaean plate tectonics revisited. Part 1. Heat flow, spreading rate, and the age of subducting oceanic lithosphere and their effects on the origin and evolution of continents. *Tectonics, 3,* 429–448.

Abdel-Rahman, A. F. M. (1994). Nature of biotites from alkaline calc-alkaline and peraluminous magmas. *Journal of Petrology, 35,* 525–541.

Abe, Y. (1993). Physical state of the very early Earth. *Lithos, 30,* 223–235.

Aikman, A. B., Harrison, T. M., & Herman, J. (2012). The origin of Eo- and Neohimalayan granitoids, Eastern Tibet. *Journal of Asian Earth Sciences, 58,* 143–157.

Amelin, Y. V. (1998). Geochronology of the Jack Hills detrital zircons by precise U-Pb isotope dilution analysis of crystal fragments. *Chemical Geology, 146,* 25–38.

Amelin, Y. V., Lee, D. C., Halliday, A. N., & Pidgeon, R. T. (1999). Nature of the Earth's earliest crust from hafnium isotopes in single detrital zircons. *Nature, 399,* 252–255.

Armstrong, R. L. (1981). Radiogenic isotopes: The case for crustal recycling on a near-steady-state no-continental-growth Earth. *Philosophical Transactions of the Royal Society London Series A, 301*, 443–471.

Battistuzzi, F. U., Feijão, A., & Hedges, S. B. (2004). A genomic timescale of prokaryote evolution: Insights into the origin of methanogenesis, phototrophy, and the colonization of land. *B.M.C. Evolutionary Biology, 4,* 44–51. https://doi.org/10.1186/1471-2148-4-44.

Bell, E. A. (2013). *Hadean-Archean transitions: Constraints from the Jack Hills detrital zircon record* (Ph.D. thesis). University of California, Los Angeles, U.S.A.

Bell, E. (2017). Petrology: Ancient magma sources revealed. *Nature Geoscience, 10,* 397.

Bell, E. A., Boehnke, P., & Harrison, T. M. (2016). Recovering the primary geochemistry of Jack Hills zircons through quantitative estimates of chemical alteration. *Geochimica et Cosmochimica Acta, 191,* 187–202.

Bell, E. A., Boehnke, P., Harrison, T. M., & Mao, W. (2015a). Potentially biogenic carbon preserved in a 4.1 Ga zircon. *Proceedings of the National Academy of Sciences, 112,* 14518–14521.

Bell, E. A., Boehnke, P., Harrison, T. M., & Wielicki, M. M. (2018). Mineral inclusion assemblage and detrital zircon provenance. *Chemical Geology, 477,* 151–160.

Bell, E. A., Boehnke, P., Hopkins-Wielicki, M. D., & Harrison, T. M. (2015b). Distinguishing primary and secondary inclusion assemblages in Jack Hills zircons. *Lithos, 234,* 15–26.

Bell, E. A., & Harrison, T. M. (2013). Post-Hadean transitions in Jack Hills zircon provenance: A signal of the Late Heavy Bombardment? *Earth and Planetary Science Letters, 364,* 1–11.

Bell, E. A., Harrison, T. M., Kohl, I. E., & Young, E. D. (2014). Eoarchean evolution of the Jack Hills zircon source and loss of Hadean crust. *Geochimica et Cosmochimica Acta, 146,* 27–42.

Bell, E. A., Harrison, T. M., McCulloch, M. T., & Young, E. D. (2011). Early Archean crustal evolution of the Jack Hills Zircon source terrane inferred from Lu-Hf, $^{207}Pb/^{206}Pb$, and $\delta^{18}O$ systematics of Jack Hills zircons. *Geochimica et Cosmochimica Acta, 75,* 4816–4829.

Bickle, M. J. (1978). Heat loss from the Earth: Constraints on Archaean tectonics from the relation between geothermal gradients and the rate of plate production. *Earth and Planetary Science Letters, 40,* 301–315.

Biggin, A. J., de Wit, M. J., Langereis, C. G., Zegers, T. E., Voûte, S., Dekkers, M. J., & Drost, K. (2011) Palaeomagnetism of Archaean rocks of the Onverwacht Group Barberton Greenstone Belt (southern Africa): Evidence for a stable and potentially reversing geomagnetic field at ca. 3.5 Ga. *Earth and Planetary Science Letters, 302*, 314–328.

Blichert-Toft, J., & Albarède, F. (2008). Hafnium isotopes in Jack Hills zircons and the formation of the Hadean crust. *Earth and Planetary Science Letters, 265,* 686–702.

Boehnke, P., Watson, E. B., Trail, D., Harrison, T. M., & Schmitt, A. K. (2013). Zircon saturation re-revisited. *Chemical Geology, 351,* 324–334.

Brasier, M. D., Antcliffe, J., Saunders, M., & Wacey, D. (2015). Changing the picture of Earth's earliest fossils (3.5-1.9 Ga) with new approaches and new discoveries. *Proceedings of the National Academy of Sciences, 112,* 4859–4864.

Buda, G., Koller, F., Kovács, J., & Ulrych, J. (2004). Compositional variation of biotite from Variscan granitoids in Central Europe: a statistical evaluation. *Acta Mineralogica-Petrographica, Szeged, 45,* 21–37.

Budyko, M. I. (1969). The effect of solar radiation variations on the climate of Earth. *Tellus, 21,* 611–619.

Burnham, C. W. (1975). Water and magmas; A mixing model. *Geochimica et Cosmochimica Acta, 39,* 1077–1084.

Burnham, A. D., & Berry, A. J. (2017). Formation of Hadean granites by melting of igneous crust. *Nature Geoscience, 10,* 457–460.

Cameron, E., Valley, J., Ortiz-Cordero, D., Kitajima, K., & Cavosie, A. (2016). Detrital Jack Hills zircon-quartz $\delta^{18}O$ analysis tests alteration of zircon and zircon inclusions. In *16th Goldschmidt Conference Abstracts, 349*.

Carley, T. L., Bell, E. A., Miller, C. F., Claiborne, L. L., & Harrison, T. M. (2018). *Striking similarities and subtle differences across the Hadean-Archean boundary: Model melt insight into the early Earth using new zircon/melt Kds*. Geological Society of America. Abstracts.

Carley, T. L., Bell, E. A., Miller, E. A., Claiborne, L. L., & Harrison, T. M. (2020). Hadean, Archean, and modern Earth: Zircon-modeled melts clarify the formation of Earth's earliest crust. Earth and Space Science Open Archive. https://doi.org/10.1002/essoar.10502994.1.

Carroll, M. R., & Wyllie, P. J. (1989). Experimental phase relations in the system tonalite-peridotite-H_2O at 15 kb; Implications for assimilation and differentiation processes near the crust-mantle boundary. *Journal of Petrology, 30,* 1351–1382.

Cavosie, A. J., Valley, J. W., Wilde, S. A, & E.I.M.F. (2005). Magmatic $\delta^{18}O$ in 4400-3900 Ma detrital zircons: A record of the alteration and recycling of crust in the Early Archean. *Earth and Planetary Science Letters, 235*, 663–681.

Cavosie, A. J., Valley, J. W., Wilde, S. A., & EIMF. (2006). Correlated microanalysis of zircon: Trace element, $\delta^{18}O$, and U-Th-Pb isotopic constraints on the igneous origin of complex >3900 Ma detrital grains. *Geochimica et Cosmochimica Acta, 70*, 5601–5616.

Cavosie, A. J., Wilde, S. A., Liu, D., Weiblen, P. W., & Valley, J. W. (2004). Internal zoning and U-Th-Pb chemistry of Jack Hills detrital zircons: A mineral record of early Archean to Mesoproterozoic (4348–1576 Ma) magmatism. *Precambrian Research, 135,* 251–279.

Chappell, B. W., & White, A. J. R. (1974). Two contrasting granite types. *Pacific Geology, 8,* 173–174.

Cherniak, D. J., & Watson, E. B. (2003) Diffusion in zircon. In J. M. Hanchar & P.W.O Hoskin (Eds.), *Zircon* (pp. 89–112) Chantilly. VA: Reviews in Mineralogy and Geochemistry.

Cherniak, D. J., & Watson, E. B. (2007). Ti diffusion in zircon. *Chemical Geology, 242,* 470–483.

Cherniak, D. J., & Watson, E. B. (2010). Li diffusion in zircon. *Contributions to Mineralogy and Petrology, 160,* 383–390.

Chopin, C., & Sobolev, N. V. (1995). Principal mineralogic indicators of UHP in crustal rocks. In R. G. Coleman & X. M. Wang (Eds.) *Ultrahigh-pressure metamorphism* (pp. 96–133). Cambridge University Press.

Clemens, J. D. (1984). Water contents of silicic to intermediate magmas. *Lithos, 17,* 273–287.

Clemens, J. D., & Vielzeuf, D. (1987). Constraints on melting and magma production in the crust. *Earth and Planetary Science Letters, 86,* 287–306.

Colchen, M., LeFort, P., & Pêcher, A. (1986). *Recherches géologiques dans l'Himalaya du Népal Annapurna, Manaslu, Ganesh: Paris* (p. 136). Paris: Editions du Centre National de la Recherche Scientifique.

Collins, W. J., Belousova, E. A., Kemp, A. I. S., & Murphy, J. B. (2011). Two contrasting Phanerozoic orogenic systems revealed by Hf isotopic data. *Nature Geoscience, 4,* 333–337.

Compston, W., & Pidgeon, R. T. (1986). Jack Hills, evidence of more very old detrital zircons in Western Australia. *Nature, 321,* 766–769.

Condon, D. J., Schoene, B., McLean, N. M., Bowring, S. A., & Parrish, R. R. (2015). Metrology and traceability of U-Pb isotope dilution geochronology (EARTHTIME Tracer 624 Calibration Part I). *Geochimica et Cosmochimica Acta, 164,* 464–480.

Crowley, J. L., Myers, J. S., Sylvester, P. J., & Cox, R. A. (2005). Detrital zircon from the Jack Hills and Mount Narryer, Western Australia: Evidence for diverse >4.0 Ga source rocks. *The Journal of Geology, 113,* 239–263.

Darling, J., Storey, C., & Hawkesworth, C. (2009). Impact melt sheet zircons and their implications for the Hadean crust. *Geology, 37,* 927–930.

Dasgupta, R. (2013). Ingassing storage and outgassing of terrestrial carbon through geologic time. *Reviews in Mineralogy and Geochemistry, 75,* 183–229.

Dobrzhinetskaya, L., Wirth, R., & Green, H. (2014). Diamonds in Earth's oldest zircons from Jack Hills conglomerate Australia are contamination. *Earth and Planetary Science Letters, 387,* 212–218.

Duke, E. F., & Rumble, D. (1986). Textural and isotopic variations in graphite from plutonic rocks South-Central New Hampshire. *Contributions to Mineralogy and Petrology, 93,* 409–419.

Ewing, R. C., Meldrum, A., Wang, L., Weber, W. J., & Corrales, L. R. (2003). Radiation effects in zircon. *Revs. Mineral. Geochem., 53,* 387–425.

Ferry, J. M., & Watson, E. B. (2007). New thermodynamic models and revised calibrations for the Ti-in-zircon and Zr-in-rutile thermometers. *Contributions to Mineralogy and Petrology, 154,* 429–437.

Franzson, H., Guðfinnsson, G. H., Helgadóttir, H. M., & Frolova, J. (2010). Porosity, density and chemical composition relationships in altered Icelandic hyaloclastites. In P. Birkle & S. Torres-Alvarado (Eds.) *Water-rock interactions* (pp. 199–202). Taylor and Francis Group, London.

Freund, F., Kathrein, H., Wengeler, H., Knobel, R., & Heinen, H. J. (1980). Carbon in solid solution in forsterite—A key to the intractable nature of reduced carbon in terrestrial and cosmogenic rocks. *Geochimica et Cosmochimica Acta, 44,* 1319–1333.

Frezzotti, M.L., Di Vincenzo, G., Ghezzo, C., and Burke, E.A. (1994) Evidence of magmatic CO_2-rich fluids in peraluminous graphite-bearing leucogranites from Deep Freeze Range (northern Victoria Land Antarctica) *Contributions to Mineralogy and Petrology, 117*, 111–123.

Froude, D. O., Ireland, T. R., Kinny, P. D., Williams, I. S., & Compston, W. (1983). Ion microprobe identification of 4100–4200 Myr-old terrestrial zircons. *Nature, 304,* 616–618.

Fu, B., Page, F. Z., Cavosie, A. J., Fournelle, N. T. Kita, N. T., Lackey, J. S., Wilde, S. A., & Valley, J. W. (2008). Ti-in-zircon thermometry: applications and limitations. *Contributions to Mineralogy and Petrology, 156*, 197–215.

Grimes, C. B., John, B. E., Kelemen, P. B., Mazdab, F. K., Wooden, J. L., Cheadle, M. J., et al. (2007). Trace element chemistry of zircons from oceanic crust: A method for distinguishing detrital zircon provenance. *Geology, 35,* 643–646.

Guitreau, M., Blichert-Toft, J., Martin, H., Mojzsis, S. J., & Albarède, F. (2012). Hafnium isotope evidence from Archean granitic rocks for deep-mantle origin of continental crust. *Earth and Planetary Science Letters, 337,* 211–223.

Hamilton, W. B. (2007). Earth's first two billion years—The era of internally mobile crust. *Geological Society of America-Memoirs, 200,* 233–296.

Hanchar, J. M., & Hoskin, P. W. O. (2003). *Zircon* (Vol. 53). Washington, DC: Revs. Mineral. Geochem.

Harris, N., & Inger, S. (1992). Trace element modelling of pelite-derived granites. *Contributions to Mineralogy and Petrology, 110,* 46–56.

Harrison, T. M. (2009). The Hadean crust: Evidence from >4 Ga zircons. *Annual Reviews of Earth and Planetary Sciences, 37,* 479–505.

Harrison, T. M., Bell, E. A., & Boehnke, P. (2017). Hadean zircon petrochronology. *Reviews in Mineralogy and Geochemistry, 83,* 329–363.

Harrison, T. M., Blichert-Toft, J., Müller, W., Albarede, F., Holden, P., & Mojzsis, S. J. (2005). Heterogeneous Hadean hafnium: Evidence of continental crust by 4.4–4.5 Ga. *Science, 310,* 1947–1950.

Harrison, T. M., Schmitt, A. K., McCulloch, M. T., & Lovera, O. M. (2008). Early ($\geq$ 4.5 Ga) formation of terrestrial crust: Lu-Hf, δ18O, and Ti thermometry results for Hadean zircons. *Earth and Planetary Science Letters, 268,* 476–486.

Harrison, T. M., Watson, E. B., & Aikman, A. K. (2007). Temperature spectra of zircon crystallization in plutonic rocks. *Geology, 35,* 635–638.

Harrison, T. M., & Wielicki, M. M. (2016). From the Himalaya to the Hadean. *American Mineralogist, 101,* 1348–1359.

Hayes, J. M., Waldbauer, J. R. (2006). The carbon cycle and associated redox processes through time. *Philosophical Transactions of the Royal Society B: Biological Sciences, 361*, 931–950.

Hellebrand, E., Möller, A., Whitehouse, M., & Cannat, M. (2007). Formation of oceanic zircons. *Geochimica et Cosmochimica Acta Suppl., 71,* A391.

Hofmann, A. E., Valley, J. W., Watson, E. B., Cavosie, A. J., & Eiler, J. M. (2009). Sub-micron scale distributions of trace elements in zircon. *Contributions to Mineralogy and Petrology, 158,* 317–335.

Holden, P., Lanc, P., Ireland, T. R., Harrison, T. M., Foster, J. J., & Bruce, Z. P. (2009). Mass-spectrometric mining of Hadean zircons by automated SHRIMP multi-collector and single-collector U/Pb zircon age dating: The first 100,000 grains. *International Journal of Mass Spectrometry, 286,* 53–63.

Hopkins, M., Harrison, T. M., & Manning, C. E. (2008). Low heat flow inferred from >4 Ga zircons suggests Hadean plate boundary interactions. *Nature, 456,* 493–496.

Hopkins, M., Harrison, T. M., & Manning, C. E. (2010). Constraints on Hadean geodynamics from mineral inclusions in >4 Ga zircons. *Earth and Planetary Science Letters, 298,* 367–376.

Hopkins, M., Harrison, T. M., & Manning, C. E. (2012). Comment: Metamorphic replacement of mineral inclusions in detrital zircon from Jack Hills, Australia: Implications for the Hadean Earth. *Geology, 40*, e281–e281.

Hoskin, P. W. O., & Schaltegger, U. (2003). The composition of zircon and igneous and metamorphic petrogenesis. *Reviews in Mineralogy and Geochemistry, 53,* 27–62.

House, C. H. (2015). Penciling in details of the Hadean. *Proceedings of the National Academy of Sciences, 112,* 14410–14411.

Ibanez-Mejia, M., & Tissot, F. (2018). Zr stable isotope fractionation during magmatic processes. *Goldschmidt Abstracts*, 1115.

Iizuka, T., Yamaguchi, T., Hibiya, Y., & Amelin, Y. (2015). Meteorite zircon constraints on the bulk Lu − Hf isotope composition and early differentiation of the Earth. *Proceedings of the National Academy of Sciences, 112,* 5331–5336.

Ingebritsen, S. E., & Manning, C. E. (2002). Diffuse fluid flux through orogenic belts: Implications for the world ocean. *Proceedings of the National Academy of Sciences, 99,* 9113–9116.

Inger, S., & Harris, N. B. W. (1992). Tectonothermal evolution of the High Himalayan crystalline sequence, Langtang Valley, northern Nepal. *Journal of Metamorphic Geology, 10,* 439–452.

Inglis, E. C., Moynier, F., Creech, J., Deng, Z., Day, J. M., Teng, F. Z., et al. (2019). Isotopic fractionation of zirconium during magmatic differentiation and the stable isotope composition of the silicate Earth. *Geochimica et Cosmochimica Acta, 250,* 311–323.

Ishihara, S. (1977). The magnetite-series and ilmenite-series granitic rocks. *Mining Geology, 27,* 293–305.

Javoy, M., Pineau, F., & Iiyama, I. (1978). Experimental determination of the isotopic fractionation between gaseous CO_2 and carbon dissolved in tholeiitic magma. *Contributions to Mineralogy and Petrology, 67,* 35–39.

Jennings, E. S., Marschall, H. R., Hawkesworth, C. J., & Storey, C. D. (2011). Characterization of magma from inclusions in zircon: Apatite and biotite work well feldspar less so. *Geology, 39,* 863–866.

Kelemen, P. B., & Manning, C. E. (2015). Reevaluating carbon fluxes in subduction zones, what goes down, mostly comes up. *Proceedings of the National Academy of Sciences, 112,* E3997–E4006.

Kemp, A. I. S., Wilde, S. A., Hawkesworth, C. J., Coath, C. D., Nemchin, A., Pidgeon, R. T., et al. (2010). Hadean crustal evolution revisited: New constraints from Pb-Hf isotope systematics of the Jack Hills zircons. *Earth and Planetary Science Letters, 296,* 45–56.

Keppler, H., Wiedenbeck, M., & Shcheka, S. S. (2003). Carbon solubility in olivine and the mode of carbon storage in the Earth's mantle. *Nature, 424,* 414–416.

Kinny, P. D., Compston, W., & Williams, I. S. (1991). A reconnaissance ion-probe study of hafnium isotopes in zircons. *Geochimica et Cosmochimica Acta, 55,* 849–859.

Kirkpatrick, H., Harrison, T. M., Liu, M. C., Tissot, F., & Ibanez-Mejia, M. (2019). In situ $\delta^{94/90}$Zr variations in zircon. *Goldschmidt Abstracts*.

Korenaga, J. (2018). Crustal evolution and mantle dynamics through Earth history. *Philosophical Transactions of the Royal Society A: Mathematical, Physical and Engineering Sciences, 376,* 20170408.

Liu, J., Ye, K., Maruyama, S., Cong, B., & Fan, H. (2001). Mineral inclusions in zircon from gneisses in the ultrahigh-pressure zone of the Dabie Mountains China. *The Journal of Geology, 109,* 523–535.

Maas, R., Kinny, P. D., Williams, I. S., Froude, D. O., & Compston, W. (1992). The Earth's oldest known crust: A geochronological and geochemical study of 3900–4200 Ma old detrital zircons from Mt. Narryer and Jack Hills Western Australia. *Geochimica et Cosmochimica Acta, 56,* 1281–1300.

Maas, R., & McCulloch, M. T. (1991). The provenance of Archean clastic metasediments in the Narryer Gneiss Complex, Western Australia: Trace element geochemistry, Nd isotopes, and U-Pb ages for detrital zircons. *Geochimica et Cosmochimica Acta, 55*(7), 1915–1932.

Maher, K. A., & Stevenson, D. J. (1988). Impact frustration of the origin of life. *Nature, 331,* 612–614.

Marty, B., Alexander, C. M. D., & Raymond, S. N. (2013). Primordial origins of Earth's carbon. *Reviews in Mineralogy and Geochemistry, 75,* 149–181.

Mathez, E. A., Blacic, J. D., Beery, J., Maggiore, C., & Hollander, M. (1984). Carbon abundances in mantle minerals determined by nuclear reaction analysis. *Geophysical Research Letters, 11,* 947–950.

McKeegan, K. D., Kudryavtsev, A. B., & Schopf, J. W. (2007). Raman and ion microscopic imagery of graphitic inclusions in apatite from older than 3830 Ma Akilia supracrustal rocks, west Greenland. *Geology, 35,* 591–594.

Menneken, M., Nemchin, A. A., Geisler, T., Pidgeon, R. T., & Wilde, S. A. (2007). Hadean diamonds in zircon from Jack Hills Western Australia. *Nature, 448,* 917–920.

Mojzsis, S. J. (2007). Sulphur on the early earth. *Developments in Precambrian Geology, 15,* 23–970.

Mojzsis, S. J., Arrhenius, G., McKeegan, K. D., Harrison, T. M., Nutman, A. P., & Friend, C. R. L. (1996). Evidence for life on Earth by 3800 Myr. *Nature, 384,* 55–59.

Mojzsis, S. J., Harrison, T. M., & Pidgeon, R. T. (2001). Oxygen-isotope evidence from ancient zircons for liquid water at the Earth's surface 4,300 Myr ago. *Nature, 409,* 178–181.

Nebel-Jacobsen, Y., Munker, C., Nebel, O., Gerdes, A., Mezger, K., & Nelson, D. R. (2010). Reworking of Earth's first crust: constraints from Hf isotopes in Archean zircons from Mt. Narryer Australia. *Precambrian Research, 182,* 175–186.

Nemchin, A. A., Whitehouse, M. J., Menneken, M., Geisler, T., Pidgeon, R. T., & Wilde, S. A. (2008). A light carbon reservoir recorded in zircon-hosted diamond from the Jack Hills. *Nature, 454*(7200), 92–95.

O'Neil, J. R., & Chappell, B. W. (1977). Oxygen and hydrogen isotope relations in the Berridale Batholith, Southeastern Australia. *Journal of the Geological Society, London, 133,* 559–571.

Oberheuser, G., Kathrein, H., Demortier, G., Gonska, H., & Freund, F. (1983). Carbon in olivine single crystals analyzed by the ^{12}C(d p)^{13}C method and by photoelectron spectroscopy. *Geochimica et Cosmochimica Acta, 47,* 1117–1129.

Ohmoto, H., & Kerrick, D. M. (1977). Devolatilization equilibria in graphitic systems. *American Journal of Science, 277,* 1013–1044.

Ozima, M., & Podosek, F. A. (2002). *Noble Gas Geochemistry*. Cambridge, UK: Cambridge Univ. Press.

Peck, W. H., Valley, J. W., Wilde, S. A., & Graham, C. M. (2001). Oxygen isotope ratios and rare earth elements in 3.3 to 4.4 Ga zircons: Ion microprobe evidence for high $\delta^{18}O$ continental crust and oceans in the Early Archean. *Geochimica et Cosmochimica Acta, 65,* 4215–4229.

Pierrehumbert, R. T. (2005). Climate dynamics of a hard snowball Earth. *Journal of Geophysical Research, 110*. https://doi.org/10.1029/2004jd005162.

Pollack, H. N., Hurter, S. J., & Johnson, J. R. (1993). Heat flow from the earth's interior: Analysis of the global data set. *Reviews of Geophysics, 31,* 267–280.

Rasmussen, B., Fletcher, I. R., Muhling, J. R., Gregory, C. J., & Wilde, S. A. (2011). Metamorphic replacement of mineral inclusions in detrital zircon from Jack Hills Australia: Implications for the Hadean Earth. *Geology, 39,* 1143–1146.

Rasmussen, B., Fletcher, I. R., Muhling, J. R., & Wilde, S. A. (2010). In situ U-Th-Pb geochronology of monazite and xenotime from the Jack Hills belt: Implications for the age of deposition and metamorphism of Hadean zircons. *Precambrian Research, 180,* 26–46.

Rollinson, H. (2008). Ophiolitic trondhjemites: A possible analogue for Hadean felsic 'crust'. *Terra Nova, 20,* 364–369.

Rosas, J. C., & Korenaga, J. (2018). Rapid crustal growth and efficient crustal recycling in the early Earth: Implications for Hadean and Archean geodynamics. *Earth and Planetary Science Letters, 494,* 42–49.

Rosenthal, A., Hauri, E. H., & Hirschmann, M. M. (2015). Experimental determination of C F and H partitioning between mantle minerals and carbonated basalt CO_2/Ba and CO_2/Nb systematics of partial melting and the CO_2 contents of basaltic source regions. *Earth and Planetary Science Letters, 412,* 77–87.

Rosing, M. T. (1999). ^{13}C-depleted carbon microparticles in >3700-Ma sea-floor sedimentary rocks from West Greenland. *Science, 283,* 674–676.

Rubatto, D. (2002). Zircon trace element geochemistry: partitioning with garnet and the link between U-Pb ages and metamorphism. *Chemical Geology, 184,* 123–138.

Rudnick, R. L., & Gao, S. (2003). Composition of the continental crust. *Treatise on Geochemistry, 3,* 1–64.

Schopf, J. W. (2014). Geological evidence of oxygenic photosynthesis and the biotic response to the 2400–2200 Ma "Great Oxidation Event". *Biochemistry (Moscow), 79,* 165–177.

Seifert, W., Thomas, R., Rhede, D., & Förster, H. J. (2010). Origin of coexisting wüstite Mg-Fe and REE phosphate minerals in graphite-bearing fluorapatite from the Rumburk granite. *European Journal of Mineralogy, 22,* 495–507.

Sen, S., Widgeon, S. J., Navrotsky, A., Mera, G., Tavakoli, A., Ionescu, E., et al. (2013). Carbon substitution for oxygen in silicates in planetary interiors. *Proceedings of the National Academy of Sciences, 110,* 15904–15907.

Shcheka, S. S., Wiedenbeck, M., Frost, D. J., & Keppler, H. (2006). Carbon solubility in mantle minerals. *Earth and Planetary Science Letters, 245,* 730–742.

Shirey, S. B., Kamber, B. S., Whitehouse, M. J., Mueller, P. A., & Basu, A. R. (2008). A review of the isotopic and trace element evidence for mantle and crustal processes in the Hadean and Archean: Implications for the onset of plate tectonic subduction. *Geological Society of America Special Paper, 440,* 1–29.

Sleep, N. H. (2000). Evolution of the mode of convection within terrestrial planets. *Journal of Geophysical Research: Planets, 105,* 17563–17578.

Smith, J. V. (1981). The first 800 million years of earths history. *Philosophical Transactions of the Royal Society London Ser. A 301*, 401–422.

Söderlund, U., Patchett, P. J., Vervoort, J. D., & Isachsen, C. E. (2004). The ^{176}Lu decay constant determined by Lu–Hf and U–Pb isotope systematics of Precambrian mafic intrusions. *Earth and Planetary Science Letters, 219*, 311–324.

Solomon, S. C. (1980). Differentiation of crusts and cores of the terrestrial planets: Lessons for the early Earth? *Precambrian Research, 10,* 177–194.

Song, S., Zhang, L., Niu, Y., Su, L., Jian, P., & Liu, D. (2005). Geochronology of diamond-bearing zircons from garnet peridotite in the North Qaidam UHPM belt Northern Tibetan Plateau: A record of complex histories from oceanic lithosphere subduction to continental collision. *Earth and Planetary Science Letters, 234,* 99–118.

Spaggiari, C. V., Pidgeon, R. T., & Wilde, S. A. (2007). The Jack Hills greenstone belt, Western Australia Part 2: lithological relationships and implications for the deposition of $\geq$4.0 Ga detrital zircons. *Precambrian Research, 155,* 261–286.

Spear, F. S. (1993). *Metamorphic phase equilibria and pressure-temperature-time-paths*. Chantilly, VA: Mineral Society of America.

Stefánsson, A., & Barnes, J. D. (2016). Chlorine isotope geochemistry of Icelandic thermal fluids: Implications for geothermal system behavior at divergent plate boundaries. *Earth and Planetary Science Letters, 449,* 69–78.

Tabata, H., Yamauchi, K., Maruyama, S., & Liou, J. G. (1998) Tracing the extent of a UHP metamorphic terrane: Mineral-inclusion study of zircons in gneisses from the Dabie Shan. In *When Continents Collide: Geodynamics and geochemistry of ultrahigh-pressure rocks* (pp. 261–273). Netherlands, NL: Springer.

Tang, H., Bell, E. A., Boehnke, P., Barboni, M., & Harrison, T. M. (2017, December). Sulfur in zircons: A new window into melt chemistry. In *AGU Fall Meeting Abstracts*.

Tang, M., Rudnick, R. L., McDonough, W. F., Bose, M., & Goreva, Y. (2017). Multi-mode Li diffusion in natural zircons: Evidence for diffusion in the presence of step-function concentration boundaries. *Earth and Planetary Science Letters, 474,* 110–119.

Tang, H., Trail, D., Bell, E. A., & Harrison, T. M. (2019). Zircon halogen geochemistry: Insights into Hadean-Archean fluids. *Geochemical Perspectives Letters*, 49–53.

Tarduno, J. A., Cottrell, R. D., Davis, W. J., Nimmo, F., & Bono, R. K. (2015). A Hadean to Paleoarchean geodynamo recorded by single zircon crystals. *Science, 349,* 521–524.

Taylor, H.P., & Sheppard, S. M. F. (1986). Igneous rocks. I. Processes of isotopic fractionation and isotope systematics. In J. W. Valley, H. P. Taylor, Jr, & J. R. O'Neil (Eds.), *Stable isotopes in high temperature processes*. *Reviews in Mineralogy* (Vol. 16, pp. 227–271).

Taylor, D. J., McKeegan, K. D., & Harrison, T. M. (2009). ^{176}Lu-^{176}Hf zircon evidence for rapid lunar differentiation. *Earth and Planetary Science Letters*, *279*, 157–164.

Tingle, T. N., Green, H. W., & Finnerty, A. A. (1988). Experiments and observations bearing on the solubility and diffusivity of carbon in olivine. *Journal of Geophysical Research: Solid Earth, 93,* 15289–15304.

Tissot, F. L. H., IIbanez-Mejia, M., Boehnke, P., Dauphas, N., McGee, D., Grove, T. L. and Harrison, T. M. (2019). Variable ^{238}U/^{235}U between single zircon grains. *Journal of Analytical Atomic Spectrometry*. https://doi.org/10.1039/c9ja00205g.

Trail, D., Bindeman, I. N., Watson, E. B., & Schmitt, A. K. (2009). Experimental calibration of oxygen isotope fractionation between quartz and zircon. *Geochimica et Cosmochimica Acta, 73,* 7110–7126.

Trail, D., Boehnke, P., Savage, P. S., Liu, M. C., Miller, M. L., & Bindeman, I. (2018). Origin and significance of Si and O isotope heterogeneities in Phanerozoic, Archean, and Hadean zircon. *Proceedings of the National Academy of Sciences, 115,* 10287–10292.

Trail, D., Cherniak, D. J., Watson, E. B., Harrison, T. M., Weiss, B. P., & Szumila, I. (2016). Li zoning in zircon as a potential geospeedometer and peak temperature indicator. *Contributions to Mineralogy and Petrology, 171,* 1–15.

Trail, D., Mojzsis, S. J., Harrison, T. M., Schmitt, A. K., Watson, E. B., & Young, E. D. (2007). Constraints on Hadean zircon protoliths from oxygen isotopes, REEs and Ti-thermometry. *G3, 8,* Q06014.

Trail, D., Thomas, J. B., & Watson, E. B. (2011a). The incorporation of hydroxyl into zircon. *American Mineralogist, 96,* 60–67.

Trail, D., Watson, E. B., & Tailby, N. D. (2011b). The oxidation state of Hadean magmas and implications for early Earth's atmosphere. *Nature, 480,* 79–82.

Turcotte, D. L., & Schubert, G. (2002). *Geodynamics: Applications of continuum physics to geological problems*, 2nd edn. Wiley, New York, NY.

Turner, G., Busfield, A., Crowther, S. A., Harrison, T. M., Mojzsis, S. J., & Gilmour, J. (2007). Pu-Xe, U-Xe, U-Pb chronology and isotope systematics of ancient zircons from Western Australia. *Earth and Planetary Science Letters, 261,* 491–499.

Turner, G., Harrison, T. M., Holland, G., Mojzsis, S. J., & Gilmour, J. (2004). Xenon from extinct ^{244}Pu in ancient terrestrial zircons. *Science, 306,* 89–91.

Ushikubo, T., Kita, N. T., Cavosie, A. J., Wilde, S. A., Rudnick, R. L., & Valley, J. W. (2008). Lithium in Jack Hills zircons: Evidence for extensive weathering of Earth's earliest crust. *Earth and Planetary Science Letters, 272,* 666–676.

Valley, J. W., Cavosie, A. J., Ushikubo, T., Reinhard, D. A., Lawrence, D. F., Larson, D. J., et al. (2014). Hadean age for a post-magma-ocean zircon confirmed by atom-probe tomography. *Nature Geoscience, 7,* 219–223.

Valley, J. W., Chiarenzelli, J. R., & McLelland, J. M. (1994). Oxygen isotope geochemistry of zircon. *Earth and Planetary Science Letters, 126,* 187–206.

Valley, J. W., Kinny, P. D., Schulze, D. J., & Spicuzza, M. J. (1998). Zircon megacrysts from kimberlite: Oxygen isotope variability among mantle melts. *Contributions to Mineralogy and Petrology, 133,* 1–11.

Vidal, P., Cocherie, A., & Le Fort, P. (1982). Geochemical investigations of the origin of the Manaslu leucogranite (Himalaya, Nepal). *Geochimica et Cosmochimica Acta, 46,* 2279–2292.

Wang, Q., & Wilde, S. A. (2018). New constraints on the Hadean to Proterozoic history of the Jack Hills belt, Western Australia. *Gondwana Research, 55,* 74–91.

Ward, P. D., & Brownlee, D. (2000). *Rare earth: Why Complex Life is Uncommon in the Universe*. New York: Copernicus Books.

Watson, E. B., & Cherniak, D. J. (1997). Oxygen diffusion in zircon. *Earth and Planetary Science Letters, 148,* 527–544.

Watson, E. B., & Harrison, T. M. (1983). Zircon saturation revisited: temperature and composition effects in a variety of crustal magma types. *Earth and Planetary Science Letters, 64,* 295–304.

Watson, E. B., & Harrison, T. M. (2005). Zircon thermometer reveals minimum melting conditions on earliest Earth. *Science, 308,* 841–844.

Watson, E. B., Wark, D. A., & Thomas, J. B. (2006). Crystallization thermometers for zircon and rutile. *Contributions to Mineralogy and Petrology, 151,* 413–433.

Weiss, B. P., Maloof, A. C., Tailby, N., Ramezani, J., Fu, R. R., Hanus, V., et al. (2015). Pervasive remagnetization of detrital zircon host rocks in the Jack Hills Western Australia and implications for records of the early geodynamo. *Earth Planet Sci. Lett., 430,* 115–128.

Wetherill, G. W. (1972). The beginning of continental evolution. *Tectonophysics*, *13*, 13–45.

White, R. W., Powell, R. W., & Holland, T. J. B. (2001). Calculation of partial melting equilibria in the system Na_2O-CaO-K_2O-FeO-MgO-Al_2O_3-SiO_2-H_2O (NCKFMASH). *Journal of metamorphic Geology, 19,* 139–153.

Wielicki, M. M., Harrison, T. M., & Schmitt, A. K. (2012). Geochemical signatures and magmatic stability of terrestrial impact produced zircon. *Earth and Planetary Science Letters, 321,* 20–31.

Wilde, S. A., Valley, J. W., Peck, W. H., & Graham, C. M. (2001). Evidence form detrital zircons for the existence of continental crust and oceans 4.4 Ga ago. *Nature, 409,* 175–178.

Zahnle, K. J. (2006). Earth's earliest atmosphere. *Elements, 2,* 217–222.

Zeng, Y., Zhu, Y., & Liu, J. (2001). Carbonaceous material in S-type Xihuashan granite. *Geochemical Journal, 35,* 145–153.

Zhang, W., Zaicong, W. A. N. G., Moynier, F., Inglis, E. C., Tian, S., Liu, Y., et al. (2019). Determination of Zr isotopic ratio in zircons using laser-ablation multiple-collector inductively-coupled-plasma mass-spectrometry. *Journal of Analytical Atomic Spectrometry*. https://doi.org/10.1039/c9ja00192a.

8 Hadean Zircons Elsewhere in the Solar System

Abstract

Hadean zircons have been documented from fifteen terrestrial localities in Australia, Asia, Africa, and North and South America, in stony and martian meteorites, and in lunar rocks. Extraterrestrial zircons are characterized by the absence of the positive Ce anomaly, seen in virtually all terrestrial zircons, much higher formation temperatures, and a unique suite of mineral inclusions. Remarkably little effort has been directed toward characterizing the geochemical nature of Hadean zircons from terrestrial localities beyond the Jack Hills region and thus it remains unclear how representative it is of the Hadean world. A massive analysis campaign is indicated to better understand Earth's last true 'dark age'.

8.1 Introduction

The previous chapter illustrated how investigations of Jack Hills zircons can reveal information about Hadean environments (e.g. H_2O activity, redox conditions, *P-T* of formation, near surface heat flow, melt chemistry, etc.) as well as to document >4 Ga carbon isotope variations. Although the vast majority of documented Hadean zircons come from that one locality, at least one Hadean zircon has been documented from fourteen other localities across five continents (Fig. 8.1). For the most part, these occurrences have not been the result of age surveys organized to identify >4 Ga zircons but rather have been serendipitous discoveries. To my knowledge, no locality outside the Jack Hills has catalogued more than a few hundred Hadean zircons compared to the >6000 documented from a single outcrop at the Erawondoo Hills location. Zircons older than 4 Ga have also been documented in differentiated stony and martian meteorites and in lunar rocks.

T. M. Harrison, *Hadean Earth*, https://doi.org/10.1007/978-3-030-46687-9_8

Fig. 8.1 Location map showing the approximate location of the 15 sites from which >4 Ga zircons have been documented

8.2 Other Western Australian Localities

8.2.1 Mt. Narryer

The original discovery of Hadean zircons was at Mt. Narryer (Froude et al. 1983), a massif outcropping within the Narryer Gneiss Complex that also hosts the Jack Hills. Ion microprobe U-Pb dating of detrital zircons from several quartzites show that Hadean zircons range from ~2% (Froude et al. 1983) to 12% of the detrital population (Pidgeon and Nemchin 2006), with zircons as young as ca. 3 Ga. An LA-ICPMS study of Mt. Narryer zircons across the range of ages suggested that they generally display higher U contents and lower Ce/Ce* than those at Jack Hills (Crowley et al. 2005). Our ion microprobe data for 80 zircons between ca. 3 and 3.75 Ga from two Mt. Narryer quartzites suggests that zircons with unaltered magmatic chemistry (i.e. via the LREE-Index) do indeed show slightly higher U contents and lower Ce/Ce* than Jack Hills zircons of similar age, although there is significant overlap between the populations. However, crystallization temperatures for these zircons is higher than at Jack Hills, averaging 750 ± 50 °C. All but one of our studied zircons has Th/U >0.2, indicative of magmatic origins. Calculated oxygen fugacities for these zircons suggests values on average several log units below the FMQ buffer, although overlapping the range of many less-oxidized Hadean Jack Hills zircons. Although we have not yet identified >4 Ga zircons from Mt. Narryer in our preliminary survey, these differences in chemistry likely point to a diversity of Eoarchean-Hadean source rocks represented in Western Australia, as also suggested by Crowley et al. (2005), and by Hf isotopic compositions (Nebel-Jacobsen et al. 2010).

8.2.2 Churla Wells

Ion microprobe dating of a zircon from an orthogneiss from near Churla Wells, ~25 km west of the Mt. Narryer site (Fig. 10), yielded a subpopulation with $^{207}Pb/^{206}Pb$ ages of 4.14 to 4.18 Ga (Nelson et al. 2000). Electron microprobe traverses show that the core containing the oldest ages has much lower Hf, REE, U and Th than the outer regions. Nonetheless, U contents in the core ranging up to 666 ppm, Th/U as high as 0.6, and trace element concentrations and ratios strongly suggest its origin in a granitic magma.

8.2.3 Maynard Hills

Thick (up to 900 m), quartz-rich, metasedimentary rocks in the Illaara and Maynard Hills greenstone belts, parts of the Southern Cross Granite-Greenstone Terrane), central Yilgarn, have been found to host Hadean zircons (Wyche et al. 2004). Ion microprobe dating of a single zircon from a quartzite within the Maynard Hills greenstone belt (Wyche et al. 2004; Wyche 2007) yielded a subpopulation with a mean $^{207}Pb/^{206}Pb$ age of 4.35 ± 0.01 Ga. Our unpublished U-Pb dating of Maynard Hills zircons yielded one >4 Ga grain out of an analyzed population of over 2000 zircons (E. Bell, & H. Kirkpatrick, pers. comm.).

8.2.4 Mt. Alfred

At the Mt. Alfred locality of the Illaara Greenstone Belt further south along strike from the Maynard Hills, Nelson (2005) documented a concordant zircon with an age of 4.17 ± 0.01 Ga. Thern and Nelson (2012) reported three additional Hadean zircon ages from this sample ranging from 4.23 to 4.34 Ga. To our knowledge, no geochemistry for Hadean zircons from this sample have been published.

Kielman et al. (2018) subsequently undertook a larger survey of U-Pb ages from Mt. Alfred and found a small number of Hadean grains up to an age of 4.11 ± 0.01 Ga. They found the detrital zircon distribution from this location to be more similar to that of Mt. Narryer than at the Jack Hills. My laboratory has U-Pb dated over 4000 detrital zircons from multiple samples from this area and found a generally low yield of Hadean ages (<1%).

8.3 North American Hadean Zircon Occurrences

8.3.1 Northwest Territory, Canada

The Acasta tonalite orthogneiss from the Western Slave craton (Fig. 10) yields a range of U-Pb zircon ages interpreted to date protolith crystallization at

3.96–4.02 Ga (Bowring and Williams 1999; Stern and Bleeker 1998; Mojzsis et al. 2014). However, Iizuka et al. (2006) documented a 4.20 ± 0.06 Ga zircon grain using the laser ablation, inductively-coupled, plasma mass spectrometer multi-collector (LA-ICPMS) method. This apparent xenocryst has a light rare earth pattern (Bell et al. 2016) within the field associated with unaltered zircon. Its Th/U suggests a magmatic origin which, along with other trace element concentrations and ratios, argue for derivation from a felsic melt by a process other than differentiation of a mafic magma. Pronounced Ce and Eu anomalies correspond, respectively, to an oxygen fugacity close to the fayalite-magnetite-quartz (FMQ) buffer (assuming a crystallization temperature of 750 °C) and a crustal, as opposed to mantle, origin.

8.3.2 Akilia Island, Greenland

A suite of granulite grade supracrustal rocks, termed the Akilia association (McGregor and Mason 1977; Griffin et al. 1980; see 11.3.1) after its type locality at the southern tip of Akilia Island, southwestern Greenland, are intruded by orthogneisses. Within this package is a pyroxene-magnetite rock, interpreted to be the oldest known marine sediment (Manning et al. 2006). A crosscutting metatonalite yields U-Pb zircon ages of 3.83 ± 0.01 Ga (Mojzsis and Harrison 2002) providing a lower age bound for the metachert unit. In the course of this geochronologic survey, a single inherited zircon, concordant within uncertainty, was identified with a $^{207}Pb/^{206}Pb$ age of 4.08 ± 0.02 Ga (Mojzsis and Harrison 2002).

8.4 Asian Hadean Zircon Occurrences

8.4.1 Buring County, Southwestern Tibet

Duo et al. (2007) report a 4.1 Ga U-Pb ion microprobe age for a zircon from a quartz schist within the Indus-Tsangpo suture zone in southwestern Tibet (Fig. 10). Th/U ratios greater than 0.7 suggest an ultimately magmatic origin for this detrital grain but no other geochemical data was reported.

8.4.2 North Qinling

Wang et al. (2007) reported an LA-ICPMS age of 4.08 ± 0.01 Ga for a xenocrystic zircon from Ordovician volcanics of the Caotangou Group, North Qinling Orogenic Belt (Fig. 10). Subsequent ion microprobe and LA-ICPMS analyses identified additional Hadean grains with ages ranging from 4.02 to 4.08 Ga (Diwu et al. 2010, 2013). Hafnium isotope analyses of these grains are consistent with origin in crust extracted between 4–4.4 Ga (Diwu et al. 2013).

8.4.3 North China Craton

Cui et al. (2013) reported an LA-ICPMS U-Pb date of 4.17 ± 0.05 Ga, concordant within uncertainly, for a xenocrystic zircon from the Anshan-Benxi Archaean supracrustal greenstone belt (Fig. 10). Correction of common Pb was made using ^{208}Pb and assumed concordancy between the U-Pb and Th–Pb systems. The zircon was separated from fine-grained amphibolites intruded into banded iron formation and bedded coarse-grained amphibolites. Its Th/U of 0.46 suggests a magmatic origin.

8.4.4 Southern China

Xing et al. (2014) separated zircons from a quartzite within Neoproterozoic metasediments from the Cathaysia Block in southwestern Zhejiang (Fig. 10). Two Hadean detrital zircons were documented using ion microprobe U-Pb dating. One zircon core yielded a ^{207}Pb/^{206}Pb age of 4.13 ± 0.01 Ga with a δ^{18}O = 5.9 ± 0.1‰. The other zircon grain has a 4.12 ± 0.01 Ga magmatic core, a δ^{18}O of 7.2 ± 0.2‰, a positive Ce anomaly indicative of highly oxidizing conditions, and a high apparent Ti-in-zircon crystallization temperature 910 °C. While the authors interpreted these results to suggest the zircons originated via dry melting of oxidized and hydrothermally altered supracrustals, closer examination of the high apparent Ti content may be warranted due to Ti contamination effects (Harrison and Schmitt 2007). Rare earth patterns and trace element discrimination diagrams place the zircon core within the continentally-derived field.

8.4.5 Junggar Basin

Huang et al. (2013) reported a single detrital zircon ICP-MS age of 4.04 Ga from a population of 141 grains in a Paleozoic sedimentary sequence of the Aermantai ophiolitic mélange, East Junggar basin. They also obtained an $\varepsilon_{Hf(t)}$ value of −5.2 for the zircon suggesting to them a model source age of 4.47 Ga. No other geochemical characteristics were reported.

8.4.6 Singhbhum Craton, India

Two zircons from the Singhbhum Craton, northeastern India were recently documented to have Hadean ages. The Older Metamorphic Group is comprised of interlayered amphibolites and metapelitic rocks (Chaudhuri et al. 2018). One oscillatory zoned grain yielded concordant, SIMS $^{207}Pb/^{206}U$ ages of 4.031 ± 0.005, 4.036 ± 0.015, and 4.057 ± 0.008 Ga and a second, smaller subhedral grain with a homogenous core in its CL image and yielded concordant ages of 4.241 ± 0.014 and 4.239 ± 0.004 Ga. Initial $^{176}Hf/^{177}Hf$ compositions range from $\varepsilon_{Hf[t]}$ −2.5 to −5.2. From these data, the authors inferred separation of the enriched reservoir from chondritic Earth at ~4.5 Ga (Harrison et al. 2008). Th/U ratios of the Hadean grains ranged from 0.44 to 0.65 suggestive of a igneous origin, but no other trace element data was provided. Miller et al. (2018) measured U-Pb ages by LA-ICPMS on detrital zircons from a river whose drainage is limited within the Singhbhum craton. One essentially concordant grain yielded a $^{207}Pb/^{206}Pb$ age of 4.02 ± 0.01 Ga together with a $\varepsilon_{Hf[t]}$ of −5.3, which the authors interpreted to reflect an episode of Hadean felsic crust formation similar to that proposed for the Jack Hills.

8.5 South American Hadean Zircon Occurrences

8.5.1 Southern Guyana

In the course of a joint Guyanese-Brazilian geological mapping program along their common border, 18 rocks from Southern Guyana were dated by LA-ICPMS yielding about 450 U-Pb zircon ages. A single xenocrystic zircon from a felsic volcanic unit of the Iwokrama Formation, Guyana Shield (Fig. 10), yielded a single concordant LA-ICPMS U-Pb age of 4.22 ± 0.02 (Nadeau et al. 2013). No other geochemical analyses of this zircon have been reported.

8.5.2 Eastern Brazil

The Archean core of the São Francisco Craton, northeastern Brazil (Fig. 10), contains meta-volcano-sedimentary supracrustal rocks including the Ibitira–Ubirac greenstone belt. Paquette et al. (2015) analyzed a zircon from an amphibolite facies pelite from this belt by LA-ICPMS yielding a distribution of U-Pb ages that intersected concordia at 4.22 ± 0.02 Ga (four $^{207}Pb/^{206}Pb$ ages >4.01 Ga). The core Th/U ratios of 0.8 and high U contents (up to 1400 ppm) suggest a felsic magmatic origin of this probably detrital grain.

8.6 African Hadean Zircon Occurrence

8.6.1 Barberton Greenstone Belt

A greenish sandstone within a chert unit of the Mendon Formation (part of the 3.55–3.22 Ga Onverwacht Group) contains a rich assemblage of heavy detrital minerals, including spinel, zircon, and rutile. Of the 2033 zircons dated by ICP-MS that are highly radiogenic and within uncertainty of concordance, 11 yield $^{207}Pb/^{206}Pb$ ages between 4.1 and 4.0 Ga (i.e. 0.5% of the total), with the oldest at 4.10 ± 0.1 Ga (Byerly et al. 2018). The Hadean zircons are interpreted to be igneous in origin and yield Ti-in-zircon crystallization temperatures ranging from 650 to 820 °C (assuming $a_{TiO_2} = 1$).

This discovery is particularly notable for the low degree of metamorphism of the host rocks, in general thought not to have exceeded 300 °C in many parts of the Barberton greenstone belt (Tice et al. 2004), and apparent bimodal distribution of zircon crystallization temperatures at ~680 and ~750 °C. The former temperature corresponds closely to the peak seen in Hadean zircons from Jack Hills and the latter is more characteristic of zircons produced in mafic igneous complexes and impact melts (Fu et al. 2008; Carley et al. 2014; Harrison et al. 2007; Wielicki et al. 2012a; see Sects. 9.2 to 9.5).

8.7 Extraterrestrial Zircons (Moon, Mars, Meteorites)

8.7.1 Meteorites

Ireland and Wlotzka (1992) U-Pb dated and undertook geochemical characterization of zircons from two meteorites, the Simmern H5 chondrite and Vaca Muerta mesosiderite, a stony-iron type of meteorite. Meteoritic zircons show similar HREE enrichments to terrestrial zircons but Ireland and Wlotzka (1992) found what was subsequently recognized as a hallmark of extraterrestrial zircons—the absence of the positive Ce anomaly, seen in virtually all terrestrial zircons, reflecting their more reducing source conditions. One of the Vaca Muerta zircon occurrences was in a eucrite clast. Eucrites are basaltic meteorites—part of the howardite-eucrite-diogenite (HED) grouping—thought from their spectral reflectivity (McCord et al. 1970) to have originated from the surface of the asteroid 4 Vesta (Drake 1979). Ireland and Wlotzka (1992) obtained a $^{207}Pb/^{206}Pb$ age of 4.56 ± 0.02 Ga on a eucritic zircon consistent with the magmatic phase of achondrite evolution lasting only as long as short-lived radioactivities, such as ^{26}Al, were extant (i.e. <10 Ma). Srinivasan et al. (2007) used short-lived ^{182}Hf as a relative chronometer to confirm that eucrite zircons crystallized within ~7 Ma of metal-silicate segregation (see Sect. 3.2).

Haba et al. (2017) undertook U-Pb dating and REE analyses of zircons from the Estherville mesosiderite. These data constrained the metal-silicate mixing event to have occurred 42 Ma after primary magmatic zircon formation at 4.52 ± 0.03 Ga. The shared isotope composition and petrology of the HEDs and mesosiderites indicate a genetic link in their origin (Greenwood et al. 2006).

Zhou et al. (2013) undertook U-Pb ion microprobe dating of non-cumulate basaltic eucrite zircons from five different eucrites and obtained a collective $^{207}Pb/^{206}Pb$ age of 4.54 ± 0.01 Ga suggesting protracted magmatism on 4 Vesta. An age contrast between zircons from cumulate versus non-cumulate zircons might be expected if protracted high temperatures in deep cumulates forestalled zircon crystallization. Iizuka et al. (2015) undertook high-precision U-Pb age and trace element analyses of zircons from the non-cumulate eucrite Agoult which yielded a collective $^{207}Pb/^{206}Pb$ age of 4.555 ± 0.002 Ga. Ti-in-zircon temperatures of ~900 °C suggested a metamorphic origin when Zr was released during ilmenite exsolution followed by reaction with SiO_2. Since that age is coincident with the oldest ^{53}Mn-^{53}Cr date for cumulate eucrites (Lugmair and Shukolyukov 1998), they concluded that thermal metamorphism was due to rising temperature from burial by basaltic crust rather than an exogenous source. Hopkins et al. (2015) used the depth profiling capability of the ion microprobe to examine intragrain age relationships in eucrite zircons. Their results confirmed earlier determinations that Vesta's crust solidified within ca. 10 Ma of solar system formation but also documented younger ages interpreted to reflect an impact origin.

8.7.2 Lunar Zircons

Upon examination of the early returned Apollo samples, lunar scientists almost immediately adopted the concept of an early magma ocean to explain two phenomena: the plagioclase-dominated floatation crust preserved in the lunar highlands and the pervasive presence of an incompatible trace element enriched component termed KREEP (i.e. a potassium-, rare-earth-element-, phosphorous-rich reservoir). It was believed that progressive crystallization of a planetary-scale magma ocean left atop a thin, incompatible-trace-element residue (Wood et al. 1970; see Sect. 3.4). As that residue was rich in the essential structural constituents of accessory phases (e.g. Zr for zircon, P for apatite), otherwise of globally low abundance, those phases could eventually saturate late in the crystallization sequence. This model explained the occurrence of Zr-rich phases, such as tranquillityite ($Fe^{2+}_8Ti_3Zr_2Si_3O_{24}$; Ramdohr and El Goresy 1970; Lovering et al. 1971), baddeleyite, and zircon (Hubbard et al. 1971). Lunar zircons proved too small and scarce to separate and analyze by methods then available, but the advent of the ion microprobe permitted in situ U-Pb dating of zircons from an Apollo 17 breccia as old as 4.36 ± 0.02 Ga (Compston et al. 1984).

A large number of U-Pb and geochemical analyses of lunar zircons separated from soils and breccias have now been published and several trends are apparent (Meyer et al. 1996; Nemchin et al. 2008, 2009a, b, 2012; Taylor et al. 2009; Hopkins and Mojzsis 2015). First, they show the same absence of a Ce anomaly as seen in meteorite zircons. Second, age peaks at ca. 3.95, 4.25 and 4.35 Ga are evident with the oldest age yet reported at 4.417 ± 0.006 Ga. Since the KREEP residuum is the likely source of lunar igneous zircons, the latter age provides a lower bound on magma ocean solidification. Barboni et al. (2017) used the very unradiogenic initial $^{176}Hf/^{177}Hf$ ratios in 4.1 to 4.35 Ga lunar zircons to extend the age of magma ocean solidification back to 4.51 ± 0.01 Ga. The U-Pb zircon age distribution suggests either a continuum of magmatism from 4.5 to 3.9 Ga or several pulses of crust formation. Lunar zircons yield oxygen isotope values similar to Earth's mantle (Whitehouse and Nemchin 2009).

Zircon crystallization temperatures from Ti concentrations (Watson and Harrison 2005) range from 920 °C to ~1500 °C, with a minor peak at 925 °C and major peak at 1025 °C (Taylor et al. 2009; Crow et al. 2017). This result is broadly consistent with that expected for zircon crystallization from dry basaltic magmas and strongly contrasts with the ~680 °C peak observed for terrestrial Hadean zircons. In contrast to Hadean terrestrial zircons which support a range of included minerals (see Sect. 7.5), inclusions in lunar zircons are mostly trapped melt.

As discussed in Sect. 9.5, Wielicki et al. (2012a) showed that crystallization temperature of neoformed zircons from five large terrestrial impact basins are on average more than 100 °C higher than that for >4 Ga Jack Hills zircons and thus impacts cannot represent a dominant source for that Hadean population. They supported their conclusion using a model that incorporated the expected lithospheric thermal structure during a major bombardment, the stability of zircon in silicate melts as a function of temperature and composition, and a large database of Archean rock compositions. Simulations using this model predicted temperatures similar to their observations strongly suggesting that results from this handful of impact melt sheets is indeed globally representative. Wielicki et al. (2012b) adapted this impact model for the specific physical attributes of Moon, using the selenotherm of Dyal et al. (1973) and lunar zircon saturation model of Dickinson and Hess (1982). The most salient feature of their modelling is that zircon crystallized in only ~2% of their simulations, reflecting the high Zr concentrations needed to nucleate zircon in the predominantly mafic lunar compositions. While their model predicts lunar zircon crystallization temperatures between ca. 900 °C and 980 °C, or ~200 °C higher than that expected from terrestrial impacts (Wielicki et al. 2012a), this is substantially lower than most of the results of Taylor et al. (2009) suggesting impacts are unlikely to be the primary source of lunar zircons.

Hopkins and Mojzsis (2015) measured U-Pb ages and Ti contents of zircons separated from an Apollo 14 lunar impact breccia. These data revealed three age populations at 4.33 ± 0.01, 4.25 ± 0.01 and 3.95 ± 0.01 Ga with the youngest peak corresponding to the highest average zircon crystallization temperature. They observed the same two temperature peaks seen by Taylor et al. (2009), at ca. 925 °C and 1025 °C, but a higher proportion of the former suggesting to them that while most were sourced from primary KREEP magmas, some of the lower temperature zircons could have grown in impact melt sheets.

8.7.3 Martian Zircons

While no samples have yet been brought to Earth by a lander mission to Mars, we've had documented samples in our possession for over 30 years. Examining gases trapped in impact glass in an Antarctic shergottite, Becker and Pepin (1984) found elemental and isotopic compositions of N and Ar virtually identical with the martian atmosphere (as measured by the Viking landers). They surmised that this rock had been ejected from the martian crust by an impact, absorbing atmospheric gases in the processes, and was eventually captured from an Earth-crossing orbit. This and other samples with a direct tie to Mars were found to lie on an essentially unique oxygen isotope fractionation line (Clayton 1993), thus permitting samples not containing impact generated glass to be ascribed to a martian origin. It became clear that the entire SNC group of meteorites (shergottites, nakhlites, chassignites) shared a martian origin which explained their broad range of formation ages (4.45–0.18 Ga) and aqueous alteration (Treiman et al. 2000).

Humayun et al. (2013) documented the presence of zircons in felsic clasts of a martian polymict breccia (NWA 7533), thought to be compositionally representative of the martian highlands. U-Pb analyses yielded a crystallization age of 4.43 ± 0.03 Ga. Nemchin et al. (2014) interpreted oxygen isotopic variations seen in these zircons as due to continued low-temperature rock-water-atmosphere interactions. McCubbin et al. (2016) found evidence for hydrothermal alteration in another martian meteorite, NWA 7034.

Bizzarro et al. (2018) obtained $^{207}Pb/^{206}Pb$ ages from martian meteorite NWA 7034 ranging from 4.430 ± 0.001 to 4.476 ± 0.001 Ga. The latter age is the oldest yet found from martian samples and about 100 Ma older that the most ancient zircon documented from Jack Hills (see Sect. 7.3). Bouvier et al. (2018) undertook Lu–Hf analysis of these grains and found unradiogenic initial Hf isotope compositions they interpreted had been inherited from an enriched, andesitic-like crust extracted from a primitive mantle by 4.547 Ga. This implies that a stable, primordial crust had formed on Mars, and global planetary differentiation was completed, by this time.

Although not of Hadean age, of interest is the combined nanostructural analyses and U-Pb measurements of fine-grained baddeleyite from a highly shock-metamorphosed basaltic shergottite establishing that it formed during basalt crystallization at 187 ± 33 Ma (Moser et al. 2013). However, during impact ejection from Mars at ca. 22 Ma, portions reacted with felsic glass pockets to form 'launch-generated' zircon crystals.

8.8 Critical Summary

Hadean zircons have been documented from fifteen terrestrial localities on five continents, in stony and martian meteorites, and in lunar rocks. Extraterrestrial zircons are characterized by the absence of the positive Ce anomaly, seen in virtually all terrestrial zircons, and generally much higher formation temperatures (ca. 1000° vs. 700 °C). Inclusions in extraterrestrial zircons are starkly different to those in zircons from Earth. Although systematic studies have not been undertaken, it is virtually certain that extraterrestrial meteoritic and martian zircons do not plot on the terrestrial oxygen isotope fractionation line.

It is astonishing to me that virtually no effort has been directed toward characterizing the geochemical nature of Hadean zircons from terrestrial localities beyond the Jack Hills region. The import of that latter site rests on how representative it is of the Hadean world. In the Appendix, I describe how a global program of U-Pb age surveying and geochemical characterization could lead to fundamental new information on earliest Earth.

References

Barboni, M., Boehnke, P., Keller, B., Kohl, I. E., Schoene, B., Young, E. D., & McKeegan, K. D. (2017). Early formation of the Moon 4.51 billion years ago. *Science advances*, *3*, e1602365.

Becker, R. H., & Pepin, R. O. (1984). The case for a Martian origin of the shergottites: Nitrogen and noble gases in EETA 79001. *Earth and Planetary Science Letters, 69,* 225–242.

Bell, E. A., Boehnke, P., & Harrison, T. M. (2016). Recovering the primary geochemistry of Jack Hills zircons through quantitative estimates of chemical alteration. *Geochimica et Cosmochimica Acta, 191,* 187–202.

Bizzarro, M., Costa, M. M., & Connelly, J. N. (2018). High-resolution U-Pb chronology of ancient martian zircons. 28th Goldschmidt Conference Abstracts.

Bouvier, L. C., Costa, M. M., Connelly, J. N., Jensen, N. K., Wielandt, D., Storey, M., et al. (2018). Evidence for extremely rapid magma ocean crystallization and crust formation on Mars. *Nature, 558,* 586.

Bowring, S. A., & Williams, I. S. (1999). Priscoan (4.00–4.02 Ga) orthogneisses from northwestern Canada. *Contributions to Mineralogy and Petrology, 134,* 3–16.

Byerly, B. L., Lowe, D. R., Drabon, N., Coble, M. A., Burns, D. H., & Byerly, G. R. (2018). Hadean zircon from a ∼3.3 Ga sandstone, Barberton greenstone belt. *Geology*. https://doi.org/10.1130/g45276.1.

Carley, T. L., Miller, C. F., Wooden, J. L., Padilla, A. J., Schmitt, A. K., Economos, R. C., et al. (2014). Iceland is not a magmatic analog for the Hadean: Evidence from the zircon record. *Earth and Planetary Science Letters, 405,* 85–97.

Chaudhuri, T., Wan, Y., Mazumder, R., Ma, M., & Liu, D. (2018). Evidence of enriched, hadean mantle reservoir from 4.2–4.0 Ga zircon xenocrysts from paleoarchean TTGs of the Singhbhum craton, Eastern India. *Scientific Reports, 8*(7069), 12.

Clayton, R. N. (1993). Oxygen isotopes in meteorites. *Annual Review of Earth and Planetary Sciences, 21,* 115–149.

Compston, W., Williams, I. S., & Meyer, C. (1984). U-Pb geochronology of zircons from lunar breccia 73217 using a sensitive high mass-resolution ion microprobe. *Journal of Geophysical Research: Solid Earth, 89,* B525–B534.

Crow, C. A., McKeegan, K. D., & Moser, D. E. (2017). Coordinated U-Pb geochronology, trace element, Ti-in-zircon thermometry and microstructural analysis of Apollo zircons. *Geochimica et Cosmochimica Acta, 202,* 264–284.

Crowley, J. L., Myers, J. S., Sylvester, P. J., & Cox, R. A. (2005). Detrital zircon from the Jack Hills and Mount Narryer, Western Australia: Evidence for diverse >4.0 Ga source rocks. *Journal Geologica, 113,* 239–263.

Cui, P. L., Sun, J. G., Sha, D. M., Wang, X. J., Zhang, P., Gu, A. L., et al. (2013). Oldest zircon xenocryst (4.17 Ga) from the North China Craton. *International Geology Reviews, 55,* 1902–1908.

Dickinson, J. E., Jr., & Hess, P. C. (1982). Zircon saturation in lunar basalts and granites. *Earth and Planetary Science Letters, 57,* 336–344.

Diwu, C. R., Sun, Y., Dong, Z. C., Wang, H. L., Chen, D. L., Chen, L., et al. (2010). In situ U-Pb geochronology of Hadean zircon xenocryst (4.1-3.9 Ga) from the western of the Northern Qinling Orogenic Belt. *Acta Petrol. Sin. 26,* 1171–1174.

Diwu, C., Sun, Y., Wilde, S. A., Wang, H., Dong, Z., Zhang, H., et al. (2013). New evidence for ~4.45 Ga terrestrial crust from zircon xenocrysts in Ordovician ignimbrite in the North Qinling Orogenic Belt China. *Gondwana Research, 23,* 1484–1490.

Drake, M. J. (1979). Geochemical evolution of the eucrite parent body-Possible nature and evolution of asteroid 4 vesta. In *Asteroids. (A80-24551 08-91) Tucson, Ariz* (pp. 765–782). University of Arizona Press.

Duo, J., Wen, C. Q., Guo, J. C., Fan, X. P., & Li, X. W. (2007). 4.1 Ga old detrital zircon in western Tibet of China. *Chinese Science Bulletin, 52,* 23–26.

Dyal, P., Parkin, C. W., & Daily, W. D. (1973). Surface magnetometer experiments: Internal lunar properties. *Lunar and Planetary Science Conference Proceedings, 4,* 2925–2945.

Froude, D. O., Ireland, T. R., Kinny, P. D., Williams, I. S., & Compston, W. (1983). Ion microprobe identification of 4100–4200 Myr-old terrestrial zircons. *Nature, 304,* 616–618.

Fu, B., Page, F. Z., Cavosie, A. J., Fournelle, J., Kita, N. T., Lackey, J. S., Wilde, S. A., & Valley, J. W. (2008). Ti-in-zircon thermometry: applications and limitations. *Contributions to Mineralogy and Petrology*, *156*, 197–215.

Greenwood, R. C., Franchi, I. A., Jambon, A., Barrat, J. A., & Burbine, T. H. (2006). Oxygen isotope variation in stony-iron meteorites. *Science, 313,* 1763–1765.

Griffin, W. L., McGregor, V. R., Nutman, A., Taylor, P. N., & Bridgwater, D. (1980). Early archaean granulite-facies metamorphism south of ameralik, West Greenland. *Earth and Planetary Science Letters, 50,* 59–74.

Haba, M. K., Yamaguchi, A., Kagi, H., Nagao, K., & Hidaka, H. (2017). Trace element composition and U-Pb age of zircons from Estherville: Constraints on the timing of the metal-silicate mixing event on the mesosiderite parent body. *Geochimica et Cosmochimica Acta, 215,* 76–91.

Harrison, T. M., & Schmitt, A. K. (2007). High sensitivity mapping of Ti distributions in Hadean zircons. *Earth and Planetary Science Letters, 261,* 9–19.

Harrison, T. M., Schmitt, A. K., McCulloch, M. T., & Lovera, O. M. (2008). Early ($\geq$4.5 Ga) formation of terrestrial crust: Lu-Hf, $\delta^{18}O$, and Ti thermometry results for hadean zircons. *Earth and Planetary Science Letters, 268,* 476–486.

Harrison, T. M., Watson, E. B., & Aikman, A. K. (2007). Temperature spectra of zircon crystallization in plutonic rocks. *Geology, 35,* 635–638.

Hopkins, M. D., & Mojzsis, S. J. (2015). A protracted timeline for lunar bombardment from mineral chemistry, Ti thermometry and U-Pb geochronology of Apollo 14 melt breccia zircons. *Contributions to Mineralogy and Petrology, 169,* 30.

Hopkins, M. D., Mojzsis, S. J., Bottke, W. F., & Abramov, O. (2015). Micrometer-scale U-Pb age domains in eucrite zircons, impact re-setting, and the thermal history of the HED parent body. *Icarus, 245,* 367–378.

Huang, G., Niu, G., Zhang, Z., Wang, X., Xu, X., Guo, J., et al. (2013). Discovery of ~4.0 Ga detrital zircons in the aermantai ophiolitic mélange, East Junggar, northwest China. *Chinese Science Bulletin, 58,* 3645–3663.

Hubbard, N. J., Gast, P. W., Meyer, C., Nyquist, L. E., Shih, C., & Wiesmann, H. (1971). Chemical composition of lunar anorthosites and their parent liquids. *Earth and Planetary Science Letters, 13,* 71–75.

Humayun, M., Nemchin, A., Zanda, B., Hewins, R. H., Grange, M., Kennedy, A., et al. (2013). Origin and age of the earliest Martian crust from meteorite NWA 7533. *Nature, 503,* 513–516.

Kielman, R. B., Nemchin, A. A., Whitehouse, M. J., Pidgeon, R. T., & Bellucci, J. J. (2018). U-Pb age distribution recorded in zircons from Archean quartzites in the Mt. Alfred area, Yilgarn Craton, Western Australia. *Precambrian Research, 310*, 278–290.

Iizuka, T., Horie, K., Komiya, T., Maruyama, S., Hirata, T., Hidaka, H., et al. (2006). 4.2 Ga zircon xenocryst in an acasta gneiss from northwestern Canada: Evidence for early continental crust. *Geology, 34,* 245–248.

Iizuka, T., Yamaguchi, T., Hibiya, Y., & Amelin, Y. (2015). Meteorite zircon constraints on the bulk Lu—Hf isotope composition and early differentiation of the Earth. *Proceedings of the National Academy of Sciences, 112,* 5331–5336.

Ireland, T. R., & Wlotzka, F. (1992). The oldest zircons in the solar-system. *Earth and Planetary Science Letters, 109,* 1–10.

Lovering, J. F., et al. (1971). Tranquillityite: A new silicate mineral from Apollo 11 and Apollo 12 basaltic rocks. *Proceedings of the Lunar Science Conference, 2,* 39–45.

Lugmair, G. W., & Shukolyukov, A. (1998). Early solar system timescales according to ^{53}Mn-^{53}Cr systematics. *Geochimica et Cosmochimica Acta, 62,* 2863–2886.

Manning, C. E., Mojzsis, S. J., & Harrison, T. M. (2006). Geology, age and origin of supracrustal rocks at Akilia, West Greenland. *American Journal of Science, 306,* 303–366.

McCord, T. B., Adams, J. B., & Johnson, T. V. (1970). Asteroid vesta: Spectral reflectivity and compositional implications. *Science, 168,* 1445–1447.

McCubbin, F. M., Boyce, J. W., Novák-Szabó, T., Santos, A. R., Tartèse, R., Muttik, N., et al. (2016). Geologic history of Martian regolith breccia Northwest Africa 7034: Evidence for hydrothermal activity and lithologic diversity in the Martian crust. *Journal of Geophysical Research: Planets, 121,* 2120–2149.

McGregor, V. R., & Mason, B. (1977). Petrogenesis and geochemistry of metabasaltic and metasedimentary enclaves in the Amıtsoq gneisses, West Greenland. *American Mineralogist, 62,* 887–904.

Meyer, C., Williams, I. S., & Compston, W. (1996). Uranium-lead ages for lunar zircons: Evidence for a prolonged period of granophyre formation from 4.32 to 3.88 Ga. *Meteoritics and Planetary Science, 31,* 370–387.

Miller, S. R., Mueller, P. A., Meert, J. G., Kamenov, G. D., Pivarunas, A. F., Sinha, A. K., et al. (2018). Detrital zircons reveal evidence of Hadean crust in the Singhbhum craton, India. *Journal of Geology, 126,* 541–552.

Mojzsis, S. J., Cates, N. L., Caro, G., Trail, D., Abramov, O., Guitreau, M., et al. (2014). Component geochronology in the polyphase ca. 3920 Ma acasta gneiss. *Geochimica et Cosmochimica Acta, 133,* 68–96.

Mojzsis, S. J., & Harrison, T. M. (2002). Establishment of a 3.83-Ga magmatic age for the Akilia tonalite (southern West Greenland). *Earth and Planetary Science Letters, 202*, 563–576.

Moser, D. E., Chamberlain, K. R., Tait, K. T., Schmitt, A. K., Darling, J. R., Barker, I. R., et al. (2013). Solving the Martian meteorite age conundrum using micro-baddeleyite and launch-generated zircon. *Nature, 499,* 454–457.

Nadeau, S., Chen, W., Reece, J., Lachhman, D., Ault, R., Faraco, M. T. L., et al. (2013). Guyana: The lost hadean crust of South America? *Brazilian Journal Geological, 43,* 601–606.

Nebel-Jacobsen, Y., Munker, C., Nebel, O., Gerdes, A., Mezger, K., & Nelson, D. R. (2010). Reworking of Earth's first crust: Constraints from Hf isotopes in archean zircons from Mt. Narryer Australia. *Precambrian Research, 182,* 175–186.

Nelson, D. R. (2005). *Compilation of geochronology data 2003*. No. 2005/2 Western Australia Geological Survey.

Nelson, D. R., Robinson, B. W., & Myers, J. S. (2000). Complex geological histories extending for $\geq$4.0 Ga deciphered from xenocryst zircon microstructures. *Earth and Planetary Science Letters, 181,* 89–102.

Nemchin, A. A., Grange, M. L., Pidgeon, R. T., & Meyer, C. (2012). Lunar zirconology. *Australian Journal of Earth Sciences, 59,* 277–290.

Nemchin, A. A., Humayun, M., Whitehouse, M. J., Hewins, R. H., Lorand, J. P., Kennedy, A., et al. (2014). Record of the ancient martian hydrosphere and atmosphere preserved in zircon from a martian meteorite. *Nature Geoscience, 7,* 638–642.

Nemchin, A. A., Pidgeon, R. T., Whitehouse, M. J., Vaughan, J. P., & Meyer, C. (2008). SIMS U-Pb study of zircon from Apollo 14 and 17 breccias: Implications for the evolution of lunar KREEP. *Geochimica et Cosmochimica Acta, 72*, 668–689.

Nemchin, A. A., Pidgeon, R. T., Healy, D., Grange, M. L., Whitehouse, M. J., & Vaughan, J. (2009a). The comparative behavior of apatite–zircon U-Pb systems in Apollo 14 breccias: Implications for the thermal history of the Fra Mauro Formation. *Meteoritics and Planetary Science, 44,* 1717–1734.

Nemchin, A., Timms, N., Pidgeon, R., Geisler, T., Reddy, S., & Meyer, C. (2009b). Timing of crystallization of the lunar magma ocean constrained by the oldest zircon. *Nature Geoscience, 2,* 133.

Paquette, J. L., Barbosa, J. S. F., Rohais, S., Cruz, S. C., Goncalves, P., Peucat, J. J., et al. (2015). The geological roots of South America: 4.1 Ga and 3.7 Ga zircon crystals discovered in NE Brazil and NW Argentina. *Precambrian Research, 271,* 49–55.

Pidgeon, R. T., & Nemchin, A. A. (2006). High abundance of early Archaean grains and the age distribution of detrital zircons in a sillimanite-bearing quartzite from Mt Narryer, Western Australia. *Precambrian Research, 150,* 201–220.

Ramdohr, P., & El Goresy, A. (1970). Opaque minerals of the lunar rocks and dust from are Tranquillitatis. *Science, 167,* 615–618.

Srinivasan, G., Whitehouse, M. J., Weber, I., & Yamaguchi, A. (2007). The crystallization age of eucrite zircon. *Science, 317,* 345–347.

Stern, R. A., & Bleeker, W. (1998). Age of the world's oldest rocks refined using Canada's SHRIMP the acasta gneiss complex northwest territories Canada. *Geosciences Canada, 25,* 27–31.

Taylor, D. J., McKeegan, K. D., & Harrison, T. M. (2009). ^{176}Lu-^{176}Hf zircon evidence for rapid lunar differentiation. *Earth and Planetary Science Letters, 279,* 157–164. https://doi.org/10.1016/j.epsl.2008.12.030.

Thern, E. R., & Nelson, D. R. (2012). Detrital zircon age structure within ca. 3 Ga metasedimentary rocks Yilgarn craton: Elucidation of hadean source terranes by principal component analysis. *Precambrian Research, 214,* 28–43.

Tice, M. M., Bostick, B. C., & Lowe, D. R. (2004). Thermal history of the 3.5–3.2 Ga Onverwacht and fig tree groups, Barberton greenstone belt, South Africa, inferred by Raman microspectroscopy of carbonaceous material. *Geology, 32,* 37–40.

Treiman, A. H., Gleason, J. D., & Bogard, D. D. (2000). The SNC meteorites are from Mars. *Planetary and Space Science, 48,* 1213–1230.

Wang, H., Chen, L., Sun, Y., Liu, X., Xu, X., Chen, J., et al. (2007). ~4.1 Ga xenocrystal zircon from Ordovician volcanic rocks in western part of North Qinling Orogenic Belt. *Chinese Science Bulletin, 52,* 3002–3010.

Watson, E. B., & Harrison, T. M. (2005). Zircon thermometer reveals minimum melting conditions on earliest Earth. *Science, 308,* 841–844.

Whitehouse, M. J., & Nemchin, A. A. (2009). High precision, high accuracy measurement of oxygen isotopes in a large lunar zircon by SIMS. *Chemical Geology, 261,* 32–42.

Wielicki, M. M., Harrison, T. M., Boehnke, P., & Schmitt, A. K. (2012b). Modeling zircon saturation within simulated impact events: Implications on impact histories of planetary bodies. *Lunar and Planetary Science Conference Proceeding*s, 43.

Wielicki, M. M., Harrison, T. M., & Schmitt, A. K. (2012a). Geochemical signatures and magmatic stability of terrestrial impact produced zircon. *Earth and Planetary Science Letters, 321,* 20–31.

Wood, J. A., Dickey, J. S., Marvin, U. B., & Powell, B. N. (1970). Lunar anorthosites. *Science, 167,* 602–604.

Wyche, S., Nelson, D.R., & Riganti, A. (2004). 4350-3130 Ma detrital zircons in the Southern Cross Granite Greenstone Terrane Western Australia: Implications for the early evolution of the Yilgarn Craton. *Australia Journal of Earth Sciences*, *51*, 31-45.

Wyche, S. (2007). Evidence of pre-3100 Ma crust in the Youanmi and South West Terranes, and Eastern Goldfields superterrane, of the Yilgarn craton. *Developments in Precambrian Geology, 15,* 113–123.

Xing, G., Wang, X., Wan, Y., Chen, Z., Yang, J., Jitajima, K., Ushikubo, T., & Gopon, P. (2014) Diversity in early crustal evolution: 4100 Ma zircons in the cathaysia block of southern China. *China Science Reports*, *4*, 51–43.

Zhou, Q., Yin, Q. Z., Young, E. D., Li, X. H., Wu, F. Y., Li, Q. L., et al. (2013). SIMS Pb-Pb and U-Pb age determination of eucrite zircons at <5 μm scale and the first 50 Ma of the thermal history of Vesta. *Geochimica et Cosmochimica Acta, 110,* 152–175.

Proposed Sources of Hadean Zircons

9

Abstract

Any successful geodynamic or environmental model for early Earth must be consistent with ten robust lines of evidence derived from geochemical and petrologic observations of Hadean Jack Hills zircons. These are: (1) a zircon sub-population enriched in ^{18}O and depleted in ^{30}Si relative to mantle values; (2) low crystallization temperatures; (3) the presence of primary hydrous mineral inclusions; (4) the predominance of magmatic muscovite, quartz, and biotite inclusions; (5) zircon formation in relatively low heat flow environments; (6) sub-chondritic initial $^{176}Hf/^{177}Hf$ ratios consistent with source isolation as early as 4.50 Ga; (7) fission Xe isotope compositions indicating variable fractionation of Pu from U; (8) the absence of ultra-high pressure mineral inclusions; (9) zircon formation under a wide range of redox conditions; and (10) geochemical signatures diagnostic of felsic continental crust. Numerous models have been proposed to explain these characteristics, including an origin similar to Icelandic rhyolites or lunar KREEP terranes, crystallization from mafic igneous rocks, formation in impact melts or sagduction, plate boundary and heat pipe tectonic environments, and multi-stage scenarios involving several of these mechanisms. While an origin of Jack Hills Hadean zircons in felsic and intermediate granitoids in a plate-boundary-type setting is consistent with all ten geochemically-derived constraints, competitor models are either only partially consistent or inconsistent with the evidence.

9.1 Introduction

Interpreting the environmental conditions of Hadean zircon formation from their geochemical analysis and the inclusions they host is challenging due to the possibility that these signals may reflect later alteration (Sect. 7.8). Furthermore,

T. M. Harrison, *Hadean Earth*, https://doi.org/10.1007/978-3-030-46687-9_9

as described in the previous two chapters, the vast majority of such data comes from a single location and thus conclusions drawn may be limited to local environments rather than evidence of global phenomena. Thus in this section we limit the discussion to those signatures that can confidently be interpreted to be primary. Leaving aside all but the Jack Hills zircon population, there are ten lines of evidence described in Chap. 7 that any successful interpretive model needs to explain. The Hadean Jack Hills zircon population:

(1) includes a minority population enriched in ^{18}O and depleted in ^{30}Si relative to mantle values suggesting their igneous origin includes clay-rich protoliths (Sect. 7.7.2);
(2) crystallized at low temperatures ($\sim$680 °C) indicating conditions close to or at water saturation (Sect. 7.10.1);
(3) contain hydrous (e.g., muscovite, biotite, hornblende) mineral inclusions (Sect. 7.8)
(4) contain predominantly magmatic muscovite + quartz + biotite inclusion assemblages (Sect. 7.8);
(5) yield thermobarometric results suggestive of their formation in relatively low ($\sim$40–80 mW/m^2) heat flow environments (Sect. 7.8.1);
(6) yield generally low radiogenic initial $^{176}Hf/^{177}Hf$ ratios, some of which require that global silicate homogenization ended by 4.50 Ga (Sect. 7.7.3);
(7) yield fission Xe isotopes indicating variable fractionation of Pu from U (Sect. 7.7.4);
(8) do not contain ultra-high pressure mineral inclusions (Sect. 7.8);
(9) formed under redox conditions ranging from reduced to as oxidized as the present upper mantle (Sect. 7.9.2); and
(10) contain geochemical signatures diagnostic of felsic continental rocks (Sect. 7.9).

The following nine sections summarize interpretations of the above data in terms of formation environment. Note that the shifting nature of these interpretations reflects to some degree the emergence of new geochemical proxies (e.g., $\delta^{18}O$, Ti thermometry) with which to test such models.

9.2 Icelandic Rhyolites

Iceland's unusual geochemical character and thick basaltic crust couple to produce an unusually high proportion ($\sim$10%) of silicic magmatism. As these rocks contain relatively abundant zircon, Icelandic rhyolites become an attractive model to those wishing to explain the production of Hadean zircons in the absence of continental-type crust (Moorbath 1983; Taylor and McLennan 1985; Galer and Goldstein 1991; Valley et al. 2002). However, in a paper strikingly entitled "Iceland is not a magmatic analog for the Hadean: Evidence from the zircon record", Carley et al. (2014) undertook a comprehensive investigation of the trace element and oxygen isotope composition of Icelandic zircons that showed the two populations to be distinctively different (also see Carley et al. 2011; cf. Reimink et al. 2014). In contrast to the heavy ^{18}O signature in some Hadean zircons, Icelandic zircons are characterized by ^{18}O-depleted values. Zircon crystallization temperatures are similarly different, with Icelandic zircons yielding an average of 780 °C compared to the 680 °C average of Jack Hills Hadean zircons (Harrison 2009). Contrasting trace elements compositions further suggest the origin of Icelandic and Hadean Jack Hills zircons in magmas of very different nature (Fig. 9.1).

As noted in the previous chapter, higher crystallization temperatures seen in the Mt. Narryer and southwestern Zhejiang zircons may indicate their formation in different environments relative to the Jack Hills population.

9.3 Intermediate Igneous Rocks

Calc-alkaline rocks in the basaltic andesite and dacite fields (Streckeisen 1979) and their phaneritic equivalents (e.g., quartz diorite, tonalite, granodiorite) are widely understood to be limited to convergent plate tectonic margins. Thus inferring that a portion of the Hadean Jack Hills zircons crystallized from intermediate composition igneous rocks suggests the presence of plate boundary interactions prior to 4 Ga. However, several authors have argued that the low temperature Hadean peak dominantly reflects zircon saturation at low temperatures in rocks specifically of the tonalite-trondhjemite-granodiorite (TTG) suite (Nutman 2006; Glikson 2006). Glikson (2006) proposed that Hadean zircons could have originated in TTG's that formed at high-temperatures but did not crystallize zircon until near eutectic temperatures were reached. Similarly, Nutman (2006) argued on the basis of calculated saturation temperatures (Watson and Harrison 1983) for TTG's that high-temperature melts do not crystallize zircon until they cool to temperatures of ca. 750 °C (i.e., that zircons from both wet tonalite and minimum melts would yield similarly low crystallization temperatures). However, Harrison et al. (2007) showed bulk rock saturation thermometry to be inapplicable to zircons crystallizing from TTGs. Rather, a cooling magma system first crystallizes modal phases which increases the Zr concentration in the residual melt while moving the melt towards compositions with much lower capacities to dissolve zircon. Thus temperatures calculated from bulk rock chemistry would typically significantly underestimate the onset temperature of zircon crystallization of many TTGs by ca. 100 °C (Harrison et al. 2007).

Although zircons crystallized from most tonalite melts (as documented by, for example, electron imaging studies) are generally expected to yield higher temperatures than that seen in the Hadean Jack Hills population (e.g., Harrison et al. 2007). Kielman et al. (2018) documented the case of an Archean tonalite sample from southern West Greenland that yielded variable zircon temperatures similar to the Jack Hills population. From the low apparent temperatures they inferred the zircons formed late in the crystallization sequence. While a single sample out of context of its complete magmatic series is unlikely to predict the character of the detrital population that

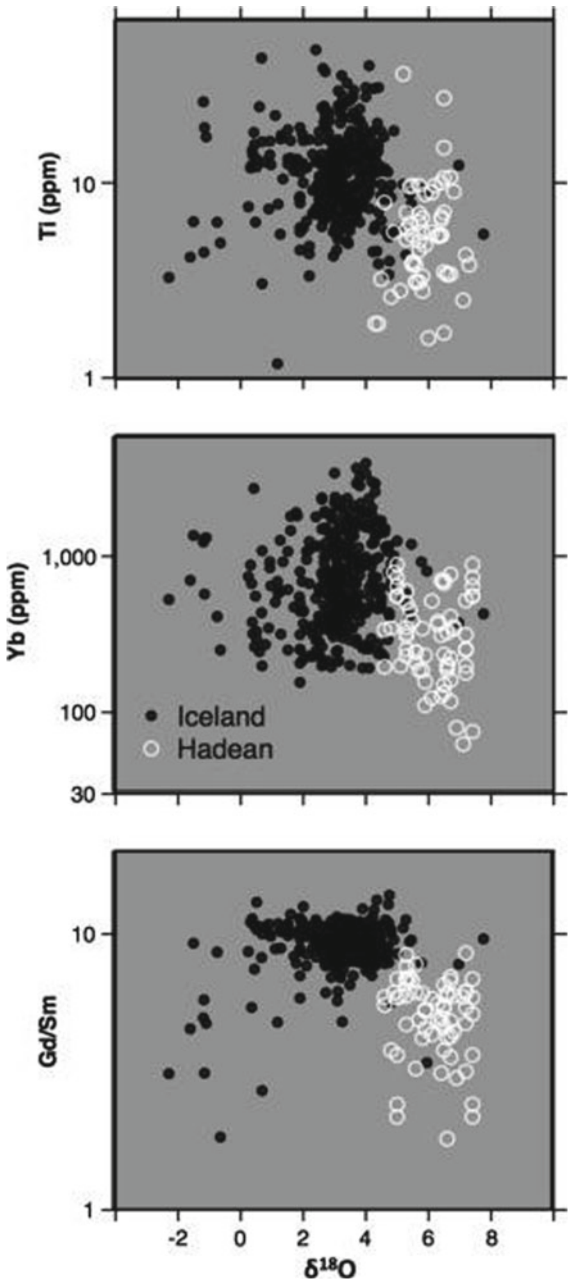

Fig. 9.1 Discrimination diagrams showing differences between Icelandic and Hadean Jack Hills zircons in Ti (top), Yb (middle), and Gd/Sm (lower) as a function of $\delta^{18}O$. These elemental and isotopic contrasts rule out Icelandic rhyolites as a likely source of Hadean Jack Hills zircons. Reproduced with permission from Carley et al. (2014)

would be regionally derived, the geochemistry of the oldest (>4.25 Ga) Jack Hills zircons yield model melts more similar to TTGs than other likely sources, suggesting to Carley et al. (2018, 2020) a subduction origin at relatively high pressure, consistent with thermobarometric results (Sects. 7.8.1 and 7.9.2; see also Reimink et al. 2020). Geochemical evidence is consistent with most Hadean Jack Hills zircons having formed in an subduction-like setting, with a relatively small subset exhibiting characteristics of anatectic S-type granitoids (see Sect. 7.9.8). Thus this suite likely included a significant portion of, for example, granodiorite sources.

9.4 Mafic Igneous Rocks

A variety of authors have suggested that the >4 Ga Jack Hills zircon temperature distribution could be derived from zircons originating in mafic magmas (Valley et al. 2006; Coogan and Hinton 2006; Rollinson 2008). However, zircon formation temperatures in these environments (Fig. 7.6) are significantly higher (>750 °C) than the Hadean peak (e.g., Harrison et al. 2007; Hellebrand et al. 2007). As a case in point, Rollinson (2008) argued that the $\delta^{18}O$ and trace element signatures in Hadean Jack Hills zircons were consistent with their origin in ophiolitic trondhjemites rather than continental crust. The author pointed to water-saturated, low pressure melting experiments on oceanic gabbros at >900 °C that yielded trondhjemitic melts. While the origin of the excess water is potentially explicable in this scenario, the origin of muscovite, a mineral uncharacteristic of trondhjemite but a common inclusion in Jack Hills Hadean zircons (Hopkins et al. 2008), was not addressed. Although we noted earlier the clear separation between Hadean and MORB zircons on a plot of U/Yb vs. Y plot (Grimes et al. 2007), Rollinson (2008) argued that data on such discrimination diagrams showed a ~20% overlap and were thus permissive of such an origin. While this is true when plotting present U concentrations, the separation becomes essentially complete once an appropriate correction for U decay has been made (e.g., a 4.3 Ga zircon presently containing 100 ppm U crystallized with 244 ppm).

As noted earlier, zircons derived from a wide range of mafic rocks yield much higher average temperatures (~770 °C; Valley et al. 2006; Fu et al. 2008) than the Hadean population (Harrison et al. 2007) (Fig. 7.6). In the absence of a natural selection mechanism that preferentially excludes zircons formed at high temperature (the opposite of what is expected from preservation effects on high radioactivity zircons), mafic sources are unlikely to have contributed significantly to the Hadean Jack Hills population. However, the limited higher temperature data from the Mt. Narryer and southwestern Zhejiang locations (Chap. 8) are consistent with such an origin, which could be tested by studies of their inclusion populations.

9.5 Impact Melts

Given the likelihood of high bolide fluxes to early Earth, the potential for impact melts to be a source of Hadean zircons requires investigation. Studies of neo-formed zircon in preserved terrestrial basins large enough to have created melt sheets (e.g., Sudbury, Morokweng, Manicouagan, Vredefort) show that their crystallization temperatures (Fig. 7.6) average more than 100 °C greater than that for >4 Ga Jack Hills zircons and thus impacts do not represent a dominant source for that Hadean population (Darling et al. 2009; Wielicki et al. 2012a). This observation is supported by modeling that relates expected impact thermal anomalies with early crustal rock chemistry (Wielicki et al. 2012a, b; see Fig. 7.6) and suggests that results from this handful of impact melt sheets is indeed globally representative.

Kenny et al. (2016) argued that zircon crystallization temperatures for the granophyre layer at the Sudbury impact crater had been underemphasized and proposed this rock type as a source of at least a portion of Hadean Jack Hills zircons. They raised the prospect of an unspecified selection process that had preferentially destroyed high temperature Hadean zircons and thus biased the detrital record to low temperatures. Nature does tend to bias the detrital zircon record but that mechanism operates in exactly the opposite sense. Late crystallizing, thus low temperature, granitoid zircons are known to contain elevated U and Th concentrations which lead to metamictization (Claiborne et al. 2010) and thus their likely removal from the detrital record. This results in preferential preservation of higher temperature zircons in clastic deposits (Harrison and Schmidt 2007). Wielicki et al. (2016) tested the Kenny et al. (2016) hypothesis statistically and showed that the probability of extracting the Hadean Jack Hills Ti-in-zircon temperature distribution from their data, or any permutation of the published dataset of impact-produced zircons, is vanishingly small. Kenny et al. (2016) were also skeptical that LA-ICPMS could accurately determine Ti concentrations and limited their analysis to SIMS data. Fig. 7.6 shows the probability density function for all Ti temperatures measured by SIMS (i.e., Wielicki et al. 2012a; Kenny et al. 2016) which differs little from that formed from all impact zircon analyses but is distinctly different from Hadean Jack Hills zircons.

Despite the seeming clarity of the conclusion that terrestrial impacts contributed little or nothing to the Hadean zircon population, Marchi et al. (2014) proposed that an intense bombardment event at 4.1–4.2 Ga reprocessed Earth's surface and covered it with ca. 20 km of flood basalt beneath which zircons were formed (Fig. 9.2). Despite their calculation that up to 600% of the surface was processed between 4.50 and 4.15 Ga, they concluded that large unaffected areas of surface water could exist in order to explain the elevated $\delta^{18}O$ seen in some Hadean zircons (Mojzsis et al. 2001). They argued that burial by impact-generated melt could produce a sufficient increase in crustal temperatures adjacent the impact site to generate eutectic melting of buried, wet, crustal material and thus satisfy constraint 2 (i.e., ca. 700 °C melting indicative of conditions close to or at water saturation). However, as described in Sect. 7.10.1, the amount of pore water or structural water

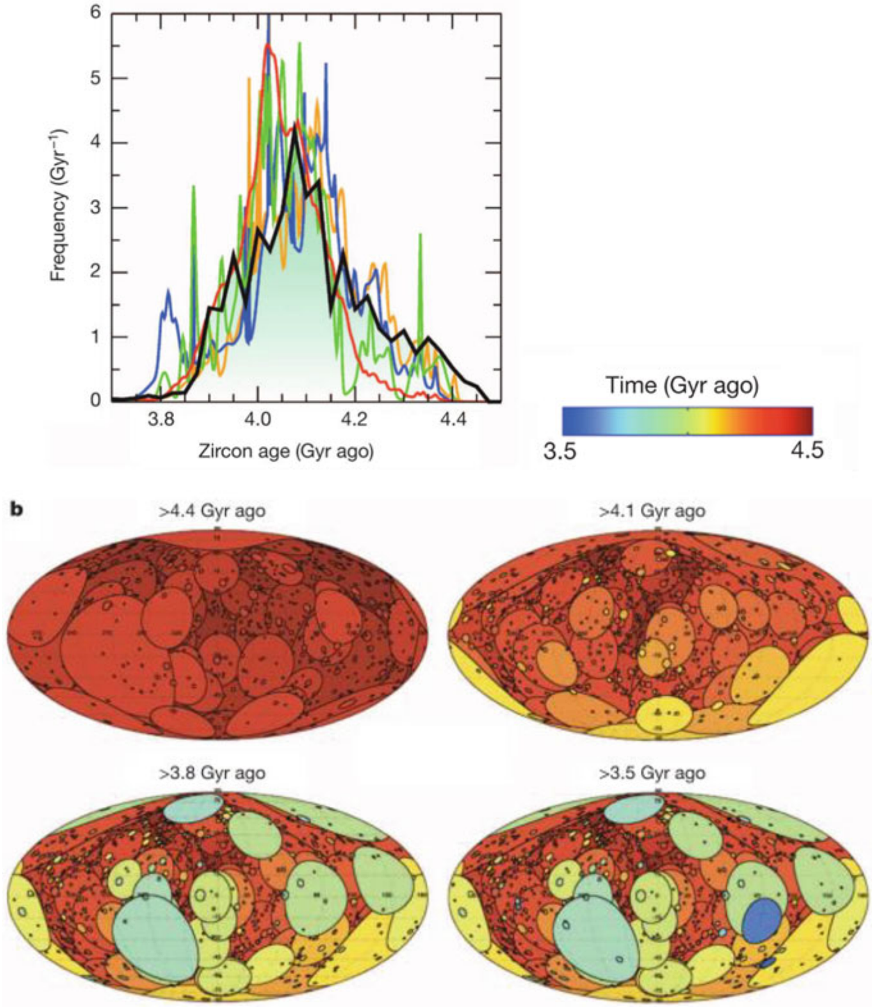

Fig. 9.2 Marchi et al. (2014) compiled Jack Hills zircon ages and inferred that the apparent peak (top) at 4.1–4.2 Ga represented a period of intense bombardment on Earth that led to formation of the Hadean zircons. The bottom four maps show the cumulative record of craters between 4.4 and 3.5 Ga (color coding indicates the time of impact). The outlined regions show the final calculated crater size and not the associated ejecta blankets and melt extrusion on the surface. Reproduced with permission from Marchi et al. (2014)

in hydrous phases under the conditions they posit (ca. 0.1–2%) is unlikely to create water-saturated, granitoid magmas capable of crustal transport (see Fig. 7.7). In the absence of a mechanism to introduce water-rich fluids to the site of anatexis, it is difficult to see how a dominant population of zircons forming at ca. 700 °C could result from this mechanism unless large quantities of surface water were introduced to deep Earth by the impact itself. As noted in Chap. 4, the concept of a late episode of intense bombardment to the inner solar system has lost traction recently in light of the improbable circumstances that scenario requires (see Sect. 4.10).

The above statements are specifically relevant to the Hadean Jack Hills zircons and conclusions drawn should be tempered by the reconnaissance-scale data obtained for samples from Mt. Narryer and southwestern Zhejiang, both of which yield apparent zircon crystallization temperatures of 750° and 910 °C, respectively. While these results are subject to potential Ti contamination effects, developing a comprehensive geochemical database from the fourteen other locations for which >4 Ga zircons have been documented should be a research priority.

9.6 Sagduction

A feature of modern plate tectonics is that oceanic lithosphere older than about 20 Ma is negatively buoyant and thus gravitationally unstable and vulnerable to subduction. At 80–120 km depths, the basaltic crust undergoes a transformation to much denser eclogite and the additional pull (ca. 30%) on the cold, dense down-going slab adds to the global plate tectonic driving force. In the hotter mantle of early Earth, it has been assumed that oceanic lithosphere would have been thicker and thus may not have been able to achieve the neutral buoyancy required for

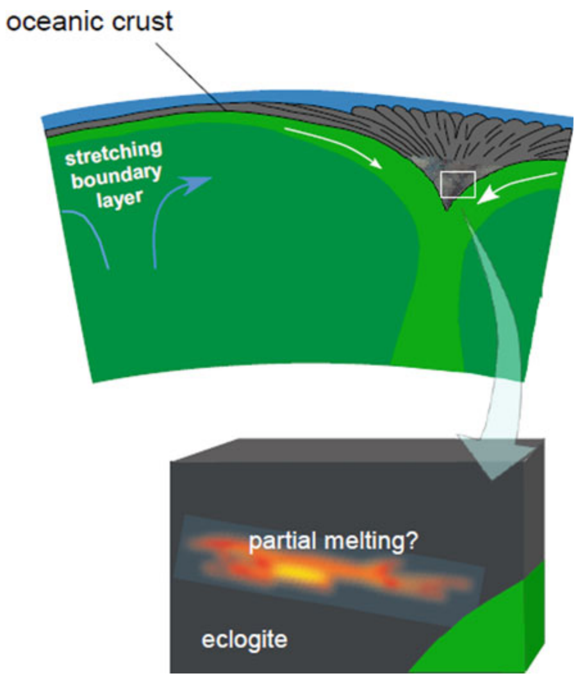

Fig. 9.3 (Top) Davies (1992) conjectured a pre-plate tectonic regime in which a thin, soft, thermal boundary layer forms under thick basaltic crust that then 'drips' back into the mantle. In this view, basaltic crust could accumulate over downwellings and produce deep eclogite (bottom). Partial melting in this region could occur with sufficiently high temperatures but is unlikely to lead to formation of zircons under minimum-melting conditions. Modified from Davies (1992)

subduction making plate tectonic-type behavior uncertain (Davies 1992; cf., Korenaga 2013). Under such conditions, a low apparent geotherm could be achieved locally where thermally and/or compositionally dense crust sinks into the mantle as downwardly moving drips (sagduction; Macgregor 1951). While this can insulate the descending mass from reaching melting temperature until high pressures are attained (e.g., Davies 1992; Fig. 9.3), more nuanced scenarios are also possible (e.g., François et al. 2014). Such a mechanism was invoked by several authors (Williams 2007; Nemchin et al. 2008) to explain the anomalously low (<10 °C/km) geotherms required by the apparent occurrence of diamond in Hadean Jack Hills zircons, although recognition that the diamonds they observed were contamination introduced during sample preparation (Dobrzhinetskaya et al. 2014) obviated the need for such models.

The sagduction model shares similar limitations to those discussed above, the source of the needed water and, in the case of blocks delaminated into the mantle, the lack of a mechanism to return zircons formed by this mechanism to the surface. Consider the case of a sagducting block of mafic eclogite. As noted earlier, below the brittle-ductile transition rock porosities are typically <0.1% (Ingebritsen and Manning 2002). Structural water stored in hydrous minerals is limited to $\leq 2\%$ of virtually all rock types and is lost progressively via discontinuous, subsolidus dehydration reactions through the greenschist and amphibolite facies (Spear 1993).

Any water liberated by dehydration is likely to ascend from the sagducting drip into colder, overlying rocks. Thus fusion is likely to be forestalled until temperatures greatly exceeding that of minimum melting are reached. In the case of complete devolatilization, temperatures of >900 °C would be required for melting. As noted earlier, the absence of peaks in the Hadean zircon crystallization spectrum corresponding to dehydration melting does not support such a mechanism and such melts are unlikely to be characterized by quartz and muscovite inclusions. Even the most appealing such scenario involving eclogitized pelite containing a 50:50 mixture of muscovite and quartz contains only ~ 2 wt% water and vapour absent melting of such a protolith produces highly water-undersaturated melts (e.g., Patiño Douce and Harris 1998).

Sagduction models lack a mechanism to introduce water-rich fluids into fertile source rocks capable of yielding both peraluminous and metaluminous magmas at temperatures close to minimum melting (as required by Ti thermometry) and then sustain the supply of water until the rock's melt fertility is essentially exhausted (thus resulting in the single Hadean zircon peak at ca. 680 °C). The twofold appeal of a plate boundary environment (Sect. 9.10) is the continuous source of water available in the hangingwall of a submarine underthrust and the potential for long-term (i.e., >4 Ga) preservation of any zircons created by water-fluxed melting. In contrast, how zircons formed during dehydration melting in a block sagducting into the mantle will reappear and be preserved at Earth's surface is unclear.

9.7 Heat Pipe Tectonics

Moore and Webb (2013) investigated the thermal effects of “heat-pipe” magmatism in which volcanism dominates the near surface thermal structure early in planetary evolution. Their simulations showed that low geotherms could develop in response to frequent volcanic eruptions that advect surface material downwards. They argued that Hadean zircons arose in ascending TTG plutons within the diamond stability field produced at the intersection of the wet basalt solidus and their exceedingly low calculated geotherms (Fig. 9.4). Unfortunately, this constraint was predicated on a report that diamonds had been included in these grains during formation (Menneken et al. 2007). This was subsequently shown to be due to contamination during sample preparation (Dobrzhinetskaya et al. 2014). Even putting this issue aside, left unaddressed was the source of sufficient water to saturate an intermediate melt (>25 wt%; Mysen and Wheeler 2000) at depths of >100 km. As noted earlier, the geochemistry of Hadean Jack Hills zircons is inconsistent with low water activity melting and the inclusion assemblage unlikely to arise from a basaltic source.

Rozel et al. (2017) simulated the production of tonalite-trondhjemite-granodiorite (TTG) type magmas from both heat-pipe and stagnant “squishy” lid scenarios (see Chap. 2)—both non-plate tectonic mechanisms—and found the latter more capable of reproducing the observed proportions of Archean TTG rocks. However, the thermal conditions under which these magmas are produced would result in zircon formation temperatures in excess of that observed from the Hadean population (Harrison et al. 2007).

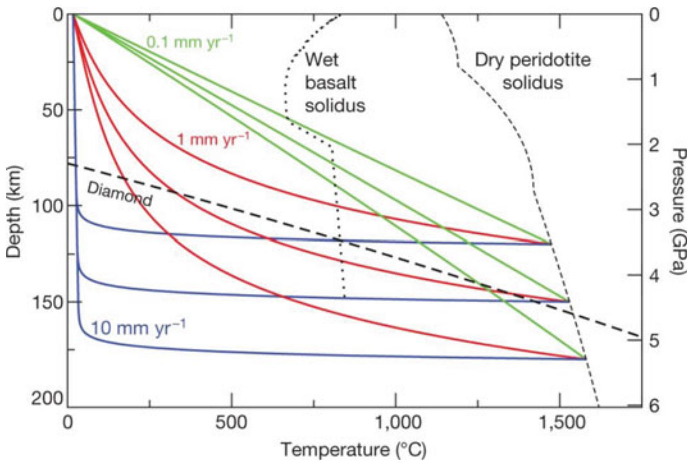

Fig. 9.4 Pressure-depth vs. temperature plot showing thermal model results with varying volcanic burial rates (0.1–10 mm/yr) for lithosphere thicknesses from 120 to 180 km. Wet basalt (dotted) and dry peridotite (thin dashed) solidi delineate partial melting regions. The diamond stability limit (thick dashed) is shown as it was then erroneously thought that Hadean Jack Hills zircons were diamondiferous. Reproduced with permission from Moore and Webb (2013)

9.8 Terrestrial KREEP

As noted earlier, initial $^{176}Hf/^{177}Hf$ of Jack Hills zircons show large deviations in $\varepsilon_{Hf(T)}$ from bulk silicate Earth (see summary in Bell et al. 2014). The initial report of Harrison et al. (2005) of positive ε_{Hf} results utilizing ion microprobe U-Pb age spots with LA-ICPMS Lu–Hf results on differing portions of the analyzed zircon were not reproduced in a follow-up study (Harrison et al. 2008) in which age and Hf isotopes were measured on the same volume. This was ascribed to non-linear mixing effects between zircon rims and cores (see Harrison et al. 2007) that almost certainly also affected the bulk results of Blichert-Toft and Albarède (2008).

Kemp et al. (2010) chose a small subset of the Jack Hills ε_{Hf} data that aligned along a subchondritic array which extrapolated back to 4.4–4.5 Ga. Indeed, they identified only a single grain of the roughly fifty they examined as having an unaltered igneous microstructure and thus likely to be isotopically undisturbed. They interpreted the coherence of their limited dataset to reflect its formation of an enriched reservoir during solidification of a magma ocean—in effect, a terrestrial KREEP layer (see Sects. 4.11.3 and 8.7.2). In their model, $\sim$400 Ma of subsequent intra-crustal melting of basalt hydrated by interaction with an early atmosphere/hydrosphere builds a thick volcanic pile which eventually produces the Hadean Jack Hills zircons (Fig. 9.5), including those with high ^{18}O. They interpreted the results of an experimental study of the simple system CaO + MgO + Al_2O_3 + SiO_2 + H_2O (Ellis and Thompson 1986), which produced peraluminous melts at $\geq$800 °C under water-saturation, as explaining the presence of muscovite inclusions in Jack Hills zircons and thus obviating the requirement for a metasedimentary source. While true that corundum-normative melts are produced under these conditions, muscovite was, of course, not present in the K-free system and is an unlikely modal phase to form from a basaltic protolith, particularly one altered in the presence of a steam atmosphere. Lastly, as noted in Sect. 7.7.2, the variations in Si and O isotope compositions in Hadean Jack Hills zircons were found to require a mixture of sources involved anatexis of siliceous sediments, felsic schists and metabasalts (Trail et al. 2018). This appears to preclude the Kemp et al. (2010) hypothesis that Hadean zircon source melts were entirely derived from mafic rocks.

As with most of the above hypotheses, the principal limitation of the Kemp et al. (2010) model—a variant of the Moore and Webb (2013) heat pipe mechanism—is the lack of a source for the copious amounts of water required to saturate melts at high pressure (Sect. 7.10.1) and the implied high zircon formation temperatures. As described in the Sagduction and Heat pipe sections, carrying water from the surface through a continuous series of dehydration reactions during burial would only result in production of inextractable amounts of melt below 750 °C (Fig. 7.7).

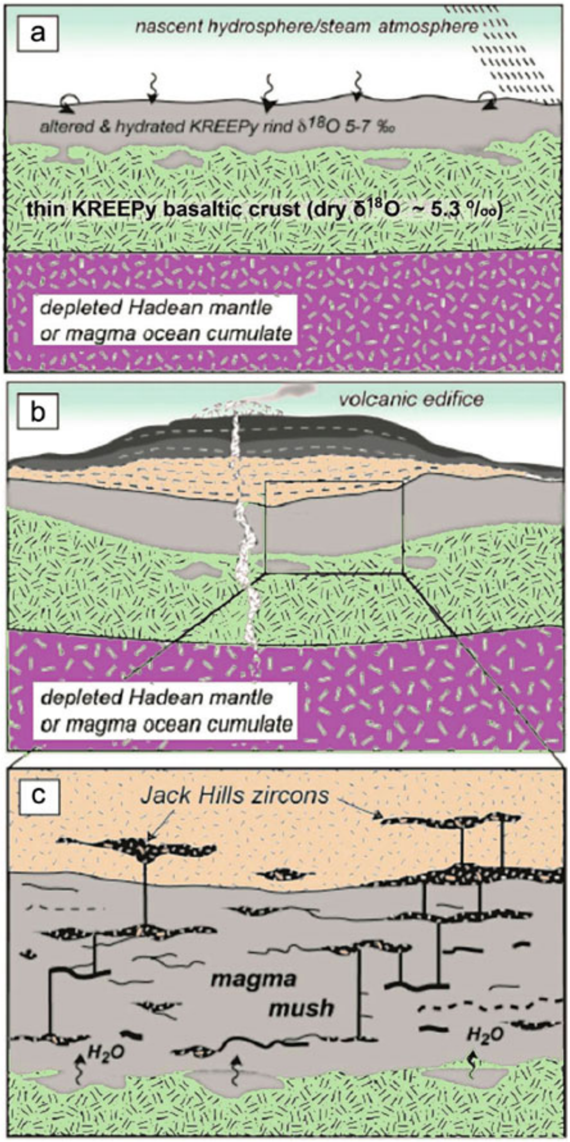

Fig. 9.5 Kemp et al. (2010) model for the evolution of Hadean crust and formation of Jack Hills zircons. **a** Accumulation of a thin, trace-element rich KREEPy crustal layer at ~4.5 Ga following magma ocean crystallization, and the interaction between this crust and the hydrosphere; **b** burial of the altered KREEPy rind beneath thick, mafic-ultramafic flows; and **c** remelting of the hydrated, chemically-fertile portion of the KREEPy source layer due to radioactive heating and the insulating effect of the overlying volcanic pile, generating small volume silicic melts from which the Jack Hills zircons are hypothesized to have crystallized. The age range of the Jack Hills zircons implies that partial melting was sustained over ~400 Ma. Modified by Nick Arndt and reproduced with permission from Kemp et al. (2010)

9.9 Multi-stage Scenarios

While some of the earlier described models are arguably more elaborate than justified given the nature of the observational constraints (e.g., Kemp et al. 2010), Shirey et al. (2008) interpreted the origin of Hadean zircons through a multi-part model that included: (1) global separation of an early (>4.4 Ga) enriched reservoir,

(2) deep mantle fractionation of Ca-silicate and Mg-silicate perovskite from a terrestrial magma ocean following lunar formation, (3) formation of a mafic to ultramafic crust, and (4) repeated cycles of remelting of that crust under "wet" conditions to produce progressively more silica-oversaturated TTGs. Their arguments against Hadean Jack Hills zircons forming in a dominantly granitic crust were that they were better explained by formation in a MORB or Icelandic setting (see *Icelandic rhyolites* and *Mafic igneous rocks* sections as well as the requirement of water-saturated melting for counter arguments). Shirey et al. (2008) note that latter environment would permit hydrothermally altered basalt to be buried to the depths of wet melting to produce zircons of similar character to the Jack Hills zircons. However, no such population has been documented in extensive studies of Icelandic zircons (Carley et al. 2011, 2014).

9.10 Plate Boundary Interactions on a Terrestrial Waterworld

With the exception of zircon formation in intermediate magmatic rocks at convergent margins, all the above models lack a mechanism to introduce water-rich fluids into fertile source rocks capable of yielding both peraluminous and metaluminous magmas at temperatures close to minimum melting (constraints 1–4) and then sustain the supply of water until the rock's melt fertility is essentially exhausted (thus resulting in the single Hadean zircon temperature peak). Perhaps the simplest model is that Earth's tectonic regime at ca. 4.3 Ga was more similar to today than long thought. Hopkins et al. (2010) argued that melting of mature continental sediment during continuous, submarine underthrusting (i.e., subduction) beneath a stable upper plate capable of long-term (i.e., ca. 4 Ga) preservation of a geologic record satisfies the ten constraints enumerated in the introduction to this chapter (Sect. 7.1). In this view, melting could occur in two scenarios: (1) water fluxed melting of underthrust material (including sediments), or (2) fluxed melting in the upper plate due to water delivery to the melting site from either the lower plate or degassing of a proximal crystallizing hydrous magma derived from the underthrust environment. In both scenarios, the presence of abundant water, derived from either open porosity at relatively shallow depths or lower plate dehydration, is consistent with constraints 1–4 and 8; the mix of source rocks is consistent with constraints 1, 4, 6, 7, 9, and 10; the stable upper plate is required by constraints 1, 2, 4, 5 and 7; melting is consistent with constraints 2–4, 7, and 8; and an underthrust regime meets constraint 5.

The choice between the two aforementioned scenarios depends on the weighting placed on our thermobarometric results. Pressure-temperature estimates derived solely from muscovite and zircon compositions constrain crystallization conditions of host magma(s), and yield conditions corresponding to modern, mid-crustal depths. However, the pressures derived from Ti-in-quartz barometry and the more Si-rich muscovite compositions correspond to deeper melting conditions, and are

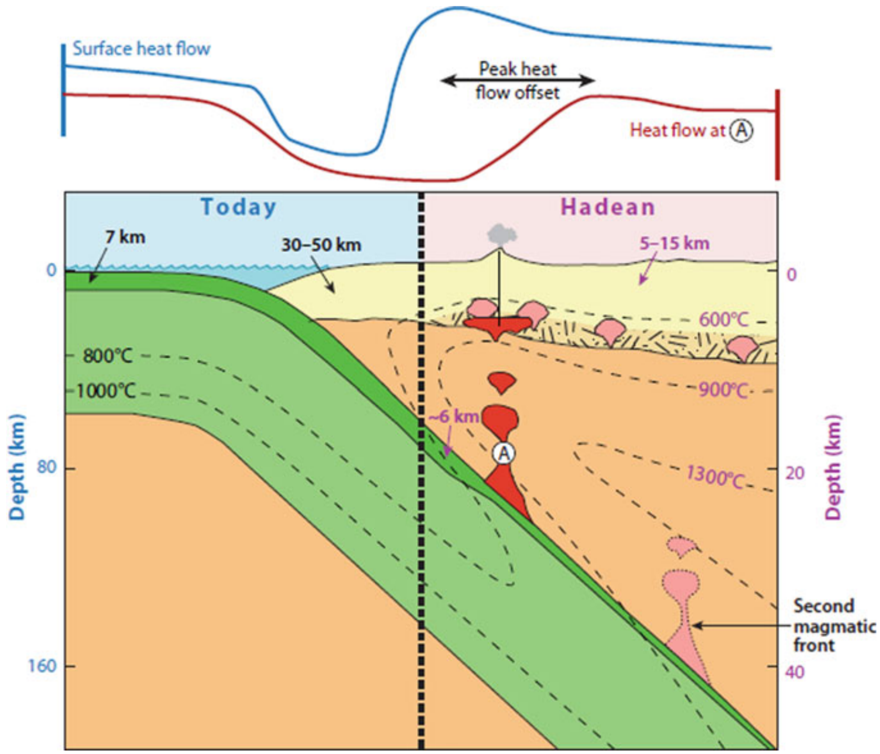

Fig. 9.6 Model of plate boundary interactions today (left) and during the Hadean (right) showing the refrigerating effects of underthrusting. Note that melting at location A today corresponds to ~900 °C at 80 km (~10 °C/Ma) and ~700 °C and 20 km for the Hadean (~35 °C/km). Both represent heat flow that is about ¼ of the expected global average. Relative surface heat flow is represented at the top of the figure and for location A at the bottom. Note that although surface heat flow in the magmatic arc is high (due to magmatic advection of heat), it is much lower at the source of melting. The dashed melting region shows location of the second magmatic front seen in modern arcs which appears absent in the Hadean zircon temperature spectrum (i.e., no temperature peaks are associated with dehydration of muscovite, biotite or amphibole). Reproduced with permission from Harrison (2009)

consistent with slab-top pressures of modern hot subduction zones at temperatures of wet sediment melting (e.g., Hermann and Spandler 2008). This would imply that zircon was on the liquidus from melt generation to crystallization, and that inclusions were trapped both at an early stage, during melting, and later, during crystallization.

This model (Fig. 9.6) is of course similar to melt production in a modern convergent margin setting—the only terrestrial magmatic environment characterized by heat flow of around one third to one quarter of the global average (i.e., the geotherm to the site of basaltic andesite production is today typically only ~12 °C/km). The model does run contrary to the traditional view that high mantle temperatures extant in early Earth would result in thick ($\sim$40 km), fast-spreading oceanic crust that resists subduction (McKenzie and Bickle 1988; Davies 1992), potentially leading to trench lock (Sleep 2000). But, as discussed in Sects. 2.4 and 6.3, this longstanding assumption about early Earth is largely axiomatic and alternate scenarios (e.g., Korenaga 2013) support the possibility of Hadean plate boundary interactions.

An oft made argument against Hadean plate boundary interactions is that high surface heat flow would prevent formation of a lithosphere of sufficient strength or density to permit mobile lid tectonics (e.g., Sizova et al. 2010, 2014, 2015; Fischer and Gerya 2016; Rozel et al. 2017). Such an argument is difficult to quantitatively establish with confidence as Hadean surface heat flow estimates range over a factor of six (see Sect. 2.2), but in any case the cooling effects of a surface ocean would act to mitigate both factors.

9.11 A Link to the Late Heavy Bombardment?

A curious feature of the Jack Hills detrital zircon age distribution, which contains two peaks at about 3.4 and 4.1 Ga (Holden et al. 2009; see Sect. 7.3), is the relative rarity of zircons between 3.9 and 3.6 Ga (Bell and Harrison 2013). This period includes a hypothesized spike in impacts to the Earth-Moon system, termed the Late Heavy Bombardment (LHB; see Chap. 4). Evidence of such an event was first seen in ca. 3.9 Ga isotopic disturbances of lunar samples (Tera et al. 1974), although others (e.g., Hartmann 1975) interpreted this as the tail of a decreasing bolide flux. The lack of an identifiable signature in the fragmentary terrestrial rock record from the LHB era (ca. 3.9 Ga) has limited the study of this period of solar system history almost entirely to extraterrestrial samples. Given its scaling to Moon in terms of gravitational cross section and surface area, Earth likely experienced $\sim$20 times the impact flux to Moon which would have caused widespread crustal thermal disturbances (Sleep et al. 1989). Thus it is somewhat surprising that the Jack Hills zircon population does not contain a significant proportion grown in impact melt sheets (Wielicki et al. 2012a, 2016; see Sect. 9.5).

Because of their crustal origin, Hadean Jack Hills zircons share one feature in common—they all must have resided within 10 s of km of Earth's surface during the LHB era. Thermal perturbations in the crust during this time, perhaps due to impacts, could mobilize Zr to form epitaxial growths on Hadean-age zircons. Trail et al. (2007) U-Pb depth profiled four Hadean zircons and found that they preserved 3.94–3.97 Ga rims. While they could not rule out endogenic processes as the precipitating event, they speculated that this common trait might be the terrestrial evidence of the LHB. Abbott et al. (2012) followed up this study by simultaneously depth profiling U-Pb age and crystallization temperature of overgrowths on Hadean zircons. Of the eight grains examined, four had 3.85–3.95 Ga rims that yield significantly higher formation temperatures (>840 °C) than either younger rims or older cores. While this was again seen as suggestive of an LHB link, can the

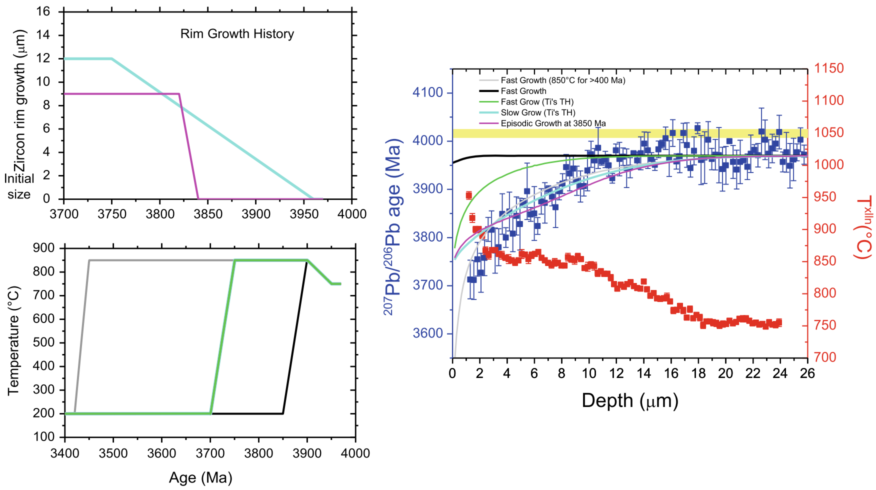

Fig. 9.7 (Right) U-Pb–Ti depth profiling results for 4.02 ± 0.01 Ga Jack Hills zircon RSES71-7.2. (Left top) Two model growth histories of 9- (magenta) and 12 μm-thick (cyan) rims. Their corresponding age gradients (right) are consistent with the measured age profile. (Left bottom) Three thermal histories without epitaxial growth (black, green, gray). The black and green histories clearly do not fit the empirical data, but the grey curve provides the best overall fit of the five example histories shown. This ambiguity limits the thermal history information retrievable from Hadean zircons regarding late bombardment episodes (Lovera et al. 2019)

continuous age-temperature profiles be inverted to uniquely identify the intensity and duration of the thermal episode?

Consider the case of zircon RSES71-7.2, which yielded a $^{207}Pb/^{206}Pb$ age of 4.02 ± 0.01 Ma from a polished, internal surface (Abbott et al. 2012). This grain was then plucked from its epoxy mount and reoriented so that a natural, unpolished crystal face was exposed at the surface of a second epoxy mount. Over three steps in which ca. 9 μm deep craters were sputtered, followed by removal of most of the adjacent material by polishing, a 26 μm-deep age-temperature depth profile was obtained before the zircon core was breached. As seen in Fig. 9.7, $^{207}Pb/^{206}Pb$ ages rise from 3.64 to ~4.0 Ga as Th/U drops from 3.9 to 0.6. This is accompanied by a general increase, with some oscillation, of U-Pb concordance and radiogenic fraction. After accounting for near surface Ti contamination, temperatures decrease from about 950° to 755 °C by the end of the profile (Fig. 9.7).

If the near surface age and temperature distributions reflect only epitaxial growth, then it is possible to find a limited range of possible temperature-time histories that satisfy the age gradient constraint. Two examples, growth of a 9-μm-thick rim between 3.840 and 3.825 Ga (magenta) and growth of a 12-μm-thick rim between 3.955 and 3.750 Ga (cyan), are shown in Fig. 9.7 (Lovera et al. 2019). Their corresponding age gradients (Fig. 9.7) are broadly consistent with the actual age profile which might suggest the viability of this approach to constrain zircon rim growth histories in the era associated with the LHB. This is true unless very high temperatures induce loss of radiogenic Pb. In such cases, interpretation requires separation of thermal and growth contributions and no unique solution is possible. As an illustration, consider the three cases shown in Fig. 9.7 (Left bottom): a temperature excursion from 750° to 850 °C between 3.95 and 3.90 Ga followed by cooling to 200°C (black), the same history except cooling is forestalled until 3.75 Ga (green), and the same history with cooling beginning at 3.45 Ga (grey). While the first two of those thermal evolutions do not visually conform to the empirical data, the last one (grey curve) provides the best overall fit of the five example temperature histories. Thus while it is possible to place some limits on possible rim growth and heating durations, this approach is unlikely to reveal unambiguous information of a terrestrial role in the hypothesized Late Heavy Bombardment.

As already noted, a curious feature of the Jack Hills zircon population is the relative absence of grains in the age range 3.9–3.6 Ga. Bell and Harrison (2013) undertook an intensive age survey to archive a large number (>100) of Jack Hills zircons formed during that period. Geochemical analyses on this population showed surprising differences. Specifically, zircons between ca. 3.91 and 3.84 Ga were found to be unique in the >3.6 Ga Jack Hills zircon record in having two distinct trace element groupings. The existence of a distinct high-U (and Hf), low-Ti (and Ce, P, Th/U) zircon provenance (termed “Group II”) and a low-U (and Hf), high-Ti population (termed “Group I”) is specific to this ca. 70 million year period between 3.91 and 3.84 Ga. The older and younger grains resemble the majority of Hadean

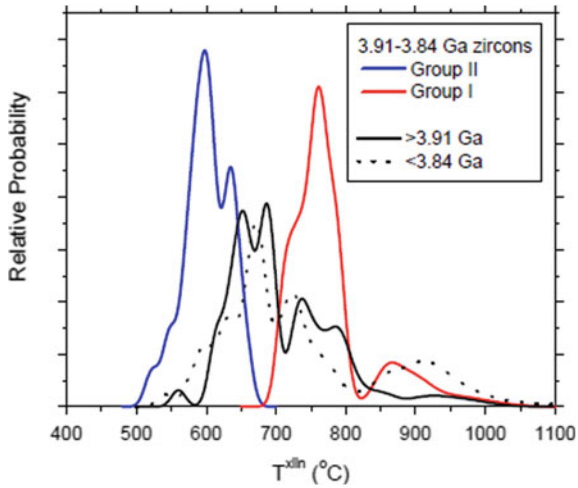

Fig. 9.8 Ti-in-zircon thermometry of Jack Hills zircons showing contrast between those formed prior to 3.91 Ga and after 3.84 Ga with those yielding crystallization ages in between. The latter groups yield distinct peaks at ~750 °C (Group I) and ~600 °C (Group II) interpreted to result from recrystallization during a thermal event between 3.91 and 3.84 Ga. Modified from Bell and Harrison (2013)

zircons both in apparent crystallization temperature and numerous other trace elements. These patterns in trace element depletion and enrichment, the seemingly paradoxical coincidence of the highest U contents with high degrees of concordance, and the homogeneous nature or very faint zoning found in many Group II grains, were interpreted to result from thermally-driven, transgressive recrystallization (Hoskin and Black 2000) at 3.91–3.84 Ga (Fig. 9.8).

Note that the discussion above is not inconsistent with criticisms of interpretations of lunar $^{40}Ar/^{39}Ar$ data marshalled in Chap. 4. Misinterpretations of such isotopic data don't prove that an LHB didn't occur. Rather, the case I laid out underscores how poorly the link between age spectra and impact history has been in a lunar context. The persistent coincidence of an apparent thermal event within the period postulated for the LHB suggests that the terrestrial archive of Hadean material may potentially be superior to lunar samples for establishing the timing, and even existence (Boehnke and Harrison 2016), of an exogenous thermal spike at ca. 3.9 Ga, possibly related to the event that produced the Imbrium crater.

9.12 Critical Summary

As noted in Sect. 7.11, evidence from oxygen isotopes, primary hydrous inclusion assemblages, and Ti thermometry suggests to all the authors of all the above mentioned models that water was present at or near Earth's surface when zircons as old as 4.3 Ga crystallized. From our present perspective, this conclusion seems inescapable but caution should be exercised in extrapolating results from a thimbleful of zircons to a planet wide phenomenon. Could Earth have been in a Snowball state, due to the faint early Sun (Gough 1981), during which water-rock interactions were limited to the ice-bedrock interface? What, for example, is the evidence for a globally-connected ocean? The only evidence I am aware of that makes that connection is Mojzsis et al.'s (2001) argument that the presence of hydrated mineral inclusions of broadly peraluminous character in the Hadean zircons (i.e., muscovite + quartz + biotite + K-feldspar) implies the then existence of shales. They reasoned that since the dominant Phanerozoic mechanism to create peraluminous granitoids is the melting of a pelitic protolith (White and Chappell 1977), the simplest explanation for the presence of this inclusion assemblage in Hadean zircons is that there was a salty ocean present prior to ~ 4 Ga. Why? When granitoid rocks (ultimately derived from mantle partial melting) are exposed at Earth's surface in the presence of water, feldspar (the most abundant mineral in the continental crust) decomposes to form aluminosilicate-rich clays and dissolved alkali and alkaline earth salts (e.g., chlorides of Na, K, Ca, Mg). These components are partitioned into different reservoirs when the clays are deposited as shales in a continental shelf environment while the latter remain in solution, ultimately contributing to ocean salinity. Subsequent anatexis of those pelitic sediments due to thrust burial during, say, continent-continent collision produces S-type magmas with molar $Al_2O_3 > CaO + Na_2O + K_2O$ (i.e., peraluminous). Although small amounts of peraluminous melts can be generated by fractional crystallization of mantle-derived magmas, muscovite inclusion chemistry supports the view that at least a small proportion of the Hadean Jack Hills zircon host magmas contained a metasedimentary component rather than being minor fractionates of mantle-derived melts (Hopkins et al. 2008). If this mechanism was indeed responsible for generating those peraluminous Hadean melts, it would rule out a Snowball Earth scenario which would not have the capacity to segregate Si–Al from K-Na–Ca-Mg. While an internally consistent argument, there is no obvious way to test this speculation so it doesn't really rise to the level of a hypothesis.

Even if plate boundary interactions are ultimately found to be source of the Hadean zircon geochemical signals, it still leaves numerous questions unanswered. Was the process continuous throughout the Hadean or did it repeatedly start and stop? Is the inferred convergent boundary an island arc, a continent-continent collision, a mixture of the two, or an entirely different kind of setting unique to early Earth?

Lastly, several lines of evidence drawn from Hadean terrestrial zircons suggest the interval 3.84–3.92 Ga was a period of unusually intense thermal activity at or near Earth's surface leaving open the possibility that the classically defined Late Heavy Bombardment may have actually occurred but that we've been justifying its existence using information obtained from the wrong planetary body.

References

Abbott, S. S., Harrison, T. M., Schmitt, A. K., & Mojzsis, S. J. (2012). A search for thermal excursions from ancient extraterrestrial impacts using Hadean zircon Ti-U-Th-Pb depth profiles. *Proceedings of the National Academy of Sciences, 109,* 13486–13492.

Bell, E. A., & Harrison, T. M. (2013). Post-Hadean transitions in Jack Hills zircon provenance: A signal of the late heavy bombardment? *Earth and Planetary Science Letters, 364,* 1–11.

Bell, E. A., Harrison, T. M., Kohl, I. E., & Young, E. D. (2014). Eoarchean evolution of the Jack Hills zircon source and loss of Hadean crust. *Geochimica et Cosmochimica Acta, 146,* 27–42.

Blichert-Toft, J., & Albarède, F. (2008). Hafnium isotopes in Jack Hills zircons and the formation of the Hadean crust. *Earth and Planetary Science Letters, 265,* 686–702.

Boehnke, P., & Harrison, T. M. (2016). Illusory late heavy bombardments. *Proceedings of the National Academy of Sciences, 113,* 10802–10806.

Carley, T. L., Bell, E. A., Miller, E. A., Claiborne, L. L., & Harrison, T. M. (2020). Hadean, Archean, and modern Earth: Zircon-modeled melts clarify the formation of Earth's earliest crust. *Earth and Space Science Open Archive*. https://doi.org/10.1002/essoar.10502994.1.

Carley, T. L., Miller, C. F., Wooden, J. L., Bindeman, I. N., & Barth, A. P. (2011). Zircon from historic eruptions in Iceland: Reconstructing storage and evolution of silicic magmas. *Mineralogy and Petrology, 102,* 135–161.

Carley, T. L., Miller, C. F., Wooden, J. L., Padilla, A. J., Schmitt, A. K., Economos, R. C., et al. (2014). Iceland is not a magmatic analog for the Hadean: Evidence from the zircon record. *Earth and Planetary Science Letters, 405,* 85–97.

Carley, T. L., Bell, E. A., Miller, C. F., Claiborne, L. L., Harrison, T. M. (2018). Striking similarities and subtle differences across the Hadean-Archean boundary: Model melt insight into the early earth using new zircon/melt Kds. In Geol. Soc. Am. Abstracts.

Claiborne, L. L., Miller, C. F., & Wooden, J. L. (2010). Trace element composition of igneous zircon: A thermal and compositional record of the accumulation and evolution of a large silicic batholith, Spirit Mountain, Nevada. *Contributions to Mineralogy and Petrology, 160,* 511–531.

Coogan, L. A., & Hinton, R. W. (2006). Do the trace element compositions of detrital zircons require Hadean continental crust? *Geology, 34,* 633–636.

Darling, J., Storey, C., & Hawkesworth, C. (2009). Impact melt sheet zircons and their implications for the Hadean crust. *Geology, 37,* 927–930.

Davies, G. F. (1992). On the emergence of plate tectonics. *Geology, 20,* 963–966.

Dobrzhinetskaya, L., Wirth, R., & Green, H. (2014). Diamonds in earth's oldest zircons from Jack Hills conglomerate Australia are contamination. *Earth and Planetary Science Letters, 387,* 212–218.

Ellis, D. J., & Thompson, A. B. (1986). Subsolidus and partial melting reactions in the quartz-excess $CaO + MgO + Al_2O_3 + SiO_2 + H_2O$ system under water-excess and water-deficient conditions to 10 kb: some implications for the origin of peraluminous melts from mafic rocks. *Journal of Petrology, 27,* 91–121.

Fischer, R., & Gerya, T. (2016). Regimes of subduction and lithospheric dynamics in the Precambrian: 3D thermomechanical modeling. *Gondwana Research, 37,* 53–70.

François, C., Philippot, P., Rey, P., & Rubatto, D. (2014). Burial and exhumation during Archean sagduction in the east Pilbara granite-greenstone terrane. *Earth and Planetary Science Letters, 396,* 235–251.

Fu, B., F. Z. Page, A. J. Cavosie, J. Fournelle, N. T. Kita, N. T., Lackey, J. S., Wilde, S. A., & Valley, J. W. (2008). Ti-in-zircon thermometry: Applications and limitations. *Contributions to Mineralogy and Petrology, 156*, 197–215.

Galer, S. J. G., & Goldstein, S. L. (1991). Early mantle differentiation and its thermal consequences. *Geochimica et Cosmochimica Acta, 55,* 227–239.

Glikson, A. (2006). Comment on "Zircon thermometer reveals minimum melting conditions on earliest Earth". *Science, 311,* A779.

Gough, D. O. (1981). Solar interior structure and luminosity variations. *Physics of Solar Variations* (pp. 21–34). Dordrecht: Springer.

Grimes, C. B., John, B. E., Kelemen, P. B., Mazdab, F. K., Wooden, J. L., Cheadle, M. J., et al. (2007). Trace element chemistry of zircons from oceanic crust: A method for distinguishing detrital zircon provenance. *Geology, 35,* 643–646.

Harrison, T. M. (2009). The Hadean crust: Evidence from >4 Ga zircons. *Annual Reviews of Earth and Planetary Sciences, 37,* 479–505.

Harrison, T. M., & Schmitt, A. K. (2007). High sensitivity mapping of Ti distributions in Hadean zircons. *Earth and Planetary Science Letters, 261,* 9–19.

Harrison, T. M., Blichert-Toft, J., Müller, W., Albarede, F., Holden, P., & Mojzsis, S. J. (2005). Heterogeneous Hadean hafnium: Evidence of continental crust by 4.4–4.5 Ga. *Science, 310,* 1947–1950.

Harrison, T. M., Watson, E. B., & Aikman, A. K. (2007). Temperature spectra of zircon crystallization in plutonic rocks. *Geology, 35,* 635–638.

Harrison, T. M., Schmitt, A. K., McCulloch, M. T., & Lovera, O. M. (2008). Early ($\geq$4.5 Ga) formation of terrestrial crust: Lu-Hf, $\delta^{18}O$, and Ti thermometry results for Hadean zircons. *Earth and Planetary Science Letters, 268,* 476–486.

Hartmann, W. K. (1975). Lunar "cataclysm": A misconception? *Icarus, 24,* 181–187.

Hellebrand, E., Möller, A., Whitehouse, M., & Cannat, M. (2007). Formation of oceanic zircons. *Geochimica et Cosmochimica Acta Suppl, 71,* A391.

Hermann, J., & Spandler, C. J. (2008). Sediment melts at sub-arc depths: An experimental study. *Journal of Petrology, 49,* 717–740.

Holden, P., Lanc, P., Ireland, T. R., Harrison, T. M., Foster, J. J., & Bruce, Z. P. (2009). Mass-spectrometric mining of Hadean zircons by automated SHRIMP multi-collector and single-collector U/Pb zircon age dating: The first 100,000 grains. *International Journal of Mass Spectrometry, 286,* 53–63.

Hopkins, M., Harrison, T. M., & Manning, C. E. (2008). Low heat flow inferred from >4 Ga zircons suggests Hadean plate boundary interactions. *Nature, 456,* 493–496.
Hopkins, M., Harrison, T. M., & Manning, C. E. (2010). Constraints on Hadean geodynamics from mineral inclusions in >4 Ga zircons. *Earth and Planetary Science Letters, 298,* 367–376.
Hoskin, P. W. O., & Black, L. P. (2000). Metamorphic zircon formation by solid-state recrystallization of protolith igneous zircon. *Journal of metamorphic Geology, 18*(4), 423–439.
Ingebritsen, S. E., & Manning, C. E. (2002). Diffuse fluid flux through orogenic belts: Implications for the world ocean. *Proceedings of the National Academy of Sciences, 99,* 9113–9116.
Kemp, A. I. S., Wilde, S. A., Hawkesworth, C. J., Coath, C. D., Nemchin, A., Pidgeon, R. T., et al. (2010). Hadean crustal evolution revisited: New constraints from Pb-Hf isotope systematics of the Jack Hills zircons. *Earth and Planetary Science Letters, 296,* 45–56.
Kenny, G. G., Whitehouse, M. J., & Kamber, B. S. (2016). Differentiated impact melt sheets may be a potential source of Hadean detrital zircon. *Geology, 44,* 435–438.
Kielman, R., Whitehouse, M., Nemchin, A., & Kemp, A. (2018). A tonalitic analogue to ancient detrital zircon. *Chemical Geology*. https://doi.org/10.1016/j.chemgeo.2018.08.028.
Korenaga, J. (2013). Initiation and evolution of plate tectonics on Earth: Theories and observations. *Annual Review of Earth and Planetary Sciences, 41,* 117–151.
Lovera, O. M., Harrison, T. M., Abbott. (2019). Can Hadean zircons constrain the Late Heavy Bombardment? American Geophysical Union Fall Abstracts V31G-0131 (Available at Earth and Space Science Open Archives).
Macgregor, A. M. (1951). Some milestones in the Precambrian of Southern Rhodesia. *Proceedings of the Geological Society of South Africa, 54,* 27–71.
Marchi, S., Bottke, W. F., Elkins-Tanton, L. T., Bierhaus, M., Wuennemann, K., Morbidelli, A., et al. (2014). Widespread mixing and burial of Earth's Hadean crust by asteroid. *Nature, 511,* 578–582.
McKenzie, D., & Bickle, M. J. (1988). The volume and composition of melt generated by extension of the lithosphere. *Journal of Petrology, 29,* 625–679.
Menneken, M., Nemchin, A. A., Geisler, T., Pidgeon, R. T., & Wilde, S. A. (2007). Hadean diamonds in zircon from Jack Hills Western Australia. *Nature, 448,* 917–920.
Mojzsis, S. J., Harrison, T. M., & Pidgeon, R. T. (2001). Oxygen-isotope evidence from ancient zircons for liquid water at the Earth's surface 4,300 Myr ago. *Nature, 409,* 178–181.
Moorbath, S. (1983). Precambrian geology: The most ancient rocks? *Nature, 304,* 585–586.
Moore, W. B., & Webb, A. A. G. (2013). Heat-pipe earth. *Nature, 501,* 501–505.
Mysen, B. O., & Wheeler, K. (2000). Solubility behavior of water in haploandesitic melts at high pressure and high temperature. *American Mineralogist, 85,* 1128–1142.
Nemchin, A. A, Whitehouse, M. J., Menneken, M., Geisler, T., Pidgeon, R. T., & Wilde, S. A. (2008). A light carbon reservoir recorded in zircon-hosted diamond from the Jack Hills. *Nature, 454*(7200), 92–95.
Nutman, A. P. (2006). Comments on "Zircon thermometer reveals minimum melting conditions on earliest Earth". *Science, 311,* 779b.
Patiño Douce, A., & Harris, N. (1998). Experimental constraints on Himalayan anatexis. *Journal of Petrology, 39,* 689–710.
Reimink, J. R., Chacko, T., Stern, R. A., & Heaman, L. M. (2014). Earth's earliest evolved crust generated in an Iceland-like setting. *Nature Geoscience, 7,* 529–533.
Reimink, J. R., Davies, J. H., Bauer, A. M., & Chacko, T. (2020). A comparison between zircons from the Acasta Gneiss Complex and the Jack Hills region. *Earth and Planetary Science Letters, 531*, 115975.
Rollinson, H. (2008). Ophiolitic trondhjemites: A possible analogue for Hadean felsic 'crust'. *Terra Nova, 20,* 364–369.
Rozel, A. B., Golabek, G. J., Jain, C., Tackley, P. J., & Gerya, T. (2017). Continental crust formation on early earth controlled by intrusive magmatism. *Nature, 545,* 332–335.
Shirey, S. B., Kamber, B. S., Whitehouse, M. J., Mueller, P. A., & Basu, A. R. (2008). A review of the isotopic and trace element evidence for mantle and crustal processes in the Hadean and

Archean: Implications for the onset of plate tectonic subduction. *Geological Society of America Special Paper, 440,* 1–29.
Sizova, E., Gerya, T., Brown, M., & Perchuk, L. L. (2010). Subduction styles in the Precambrian: Insight from numerical experiments. *Lithos, 116*(3–4), 209–229.
Sizova, E., Gerya, T., & Brown, M. (2014). Contrasting styles of Phanerozoic and Precambrian continental collision. *Gondwana Research, 25*(2), 522–545.
Sizova, E., Gerya, T., Stüwe, K., & Brown, M. (2015). Generation of felsic crust in the Archean: A geodynamic modeling perspective. *Precambrian Research, 271*, 198–224.
Sleep, N. H. (2000). Evolution of the mode of convection within terrestrial planets. *Journal of Geophysical Research, 105,* 17563–17578.
Sleep, N. H., Zahnle, K. J., Kasting, J. F., & Morowitz, H. J. (1989). Annihilation of ecosystems by large asteroid impacts on the early earth. *Nature, 342,* 139–142.
Spear, F. S. (1993). *Metamorphic phase equilibria and pressure-temperature-time-paths*. Chantilly, VA: Mineral Society of America.
Streckeisen, A. (1979). Classification and nomenclature of volcanic rocks, lamprophyres, carbonatites, and melilitic rocks: Recommendations and suggestions of the IUGS Subcommission on the Systematics of Igneous Rocks. *Geology, 7*(7), 331.
Taylor, S. R., & McLennan, S. M. (1985). *The continental crust: Its composition and evolution*. Oxford: Blackwell.
Tera, F., Papanastassiou, D. A., & Wasserburg, G. J. (1974). Isotopic evidence for a terminal lunar cataclysm. *Earth and Planetary Science Letters, 22,* 1–21.
Trail, D., Mojzsis, S. J., Harrison, T. M., Schmitt, A. K., Watson, E. B., & Young, E. D. (2007). Constraints on Hadean zircon protoliths from oxygen isotopes, REEs and Ti-thermometry. *Geochemistry, Geophysics, Geosystems, 6*(8), Q06014.
Trail, D., Boehnke, P., Savage, P. S., Liu, M. C., Miller, M. L., & Bindeman, I. (2018). Origin and significance of Si and O isotope heterogeneities in Phanerozoic, Archean, and Hadean zircon. *Proceedings of the National Academy of Sciences, 115,* 10287–10292.
Valley, J. W., Peck, W. H., King, E. M., & Wilde, S. A. (2002). A cool early earth. *Geology, 30,* 351–354.
Valley, J. W., Cavosie, A. J., Fu, B., Peck, W. H., Wilde, S. A. (2006). Comment on "Heterogeneous Hadean Hafnium: Evidence of continental crust at 4.4 to 4.5 Ga". *Science, 312*, 1139a.
Watson, E. B., & Harrison, T. M. (1983). Zircon saturation revisited: Temperature and composition effects in a variety of crustal magma types. *Earth and Planetary Science Letters, 64,* 295–304.
White, A. J. R., & Chappell, B. W. (1977). Ultrametamorphism and granitoid genesis. *Tectonophysics, 43,* 7–22.
Wielicki, M. M., Harrison, T. M., & Schmitt, A. K. (2012a). Geochemical signatures and magmatic stability of terrestrial impact produced zircon. *Earth and Planetary Science Letters 321*, 20–31.
Wielicki, M. M., Harrison, T. M., Boehnke, P., & Schmitt, A. K. (2012b). Modeling zircon saturation within simulated impact events: Implications on impact histories of planetary bodies. *Lunar and Planetary Science Conference Proceeding*s 43.
Wielicki, M. M., Harrison, T. M., & Schmitt, A. K. (2016). Comment on Kenny et al. "Differentiated impact melt sheets may be a potential source of Hadean detrital zircon". *Geology*, *44*, e398-e398.
Williams, I. S. (2007). Old diamonds and the upper crust. *Nature, 448,* 880–881.

Could the Hadean Eon Have Been Habitable?

10

Abstract

Given the absence of a macroscopic Hadean rock record, evaluating terrestrial habitability is largely a thought experiment, but data from Hadean zircons can provide some constraints. We are certain that life as we know it would not be possible without four requirements; soluble bioactive elements (carbon, hydrogen, oxygen, nitrogen, sulfur and phosphorous), free energy, liquid water, and time. Beyond these essential ingredients, there is broad agreement that there are ten secondary factors that separate us from the other, uninhabited terrestrial planets and maintain our planet's homeostasis. They are: (1) a galactic and planetary sanctuary for life; (2) liquid water at the planetary surface to mediate biochemistry and efficiently cool the planet; (3) dissolved water in the deep planetary interior to enhance mantle circulation and catalyze the eclogite transition; (4) a broadly solar chemical composition to provide sufficient metallicity for a stable surface platform; (5) sufficient planetary mass to retain an atmosphere and heat; (6) planetary satellite(s) to stabilize climate zones; (7) extra-planetary impactors to introduce organic building blocks and water and to create satellites; (8) long-term interior heat generation to maintain mantle circulation and the geodynamo; (9) a self-sustaining dynamo to protect the atmosphere is erosion; and (10) a mechanism to recycle surface carbon into the interior and back. Evaluating how these various factors interact is complicated but our speculations can be guided by inferences from Hadean zircon geochemistry which potentially bear on six of the ten ingredients for life—the presence of surface and interior water, the role of impacts on early Earth, internal heat generation, surface recycling, and the existence of a Hadean geodynamo. Knowledge of the geochemistry and inclusion population of Hadean zircons also permits constraints to be placed on whether mineral phases and trace elements key to biopoiesis were present during the Hadean eon.

T. M. Harrison, *Hadean Earth*, https://doi.org/10.1007/978-3-030-46687-9_10

10.1 What Makes a Planet Habitable?

10.1.1 The Four Requirements for Life

A key challenge for astrobiology—the science of extraterrestrial life—is conceiving of ways to find evidence of its existence elsewhere in the cosmos from a conceptual framework that knows of only one occurrence of abiogenesis (or biopoiesis, the development of a living organism[1] from abiotic matter). Understanding when and by what mechanisms life on Earth arose potentially constrains the nature of early terrestrial environments (and vice versa), but tells us little (cf. Lineweaver and Chopra 2012) about alternate biologic strategies that might exist under conditions well outside that experienced at or near Earth's surface. This limits our understanding of habitable conditions to those under which life as we know it could have emerged and been continuously sustained. In general, this either assumes that life originated elsewhere in the universe and was subsequently introduced to Earth, either by natural, non-sentient (Arrhenius 1908) or intentional (Crick and Orgel 1973) panspermia, or that terrestrial conditions permitted introduced alien life to flourish here. The latter is problematic as it requires that panspermia occurred only in the very earliest phase of Earth history and that all living organisms appear genetically to sit on the Tree of Life (Woese et al. 1990; Castelle and Banfield 2018). In any case, knowing when and under what conditions life arose or arrived would tell us a great deal about its likelihood elsewhere (Lineweaver and Davis 2002). Were conditions clement or hellacious? Did life emerge virtually immediately upon Earth's formation or only after a half billion years of planetary preparation?

Terrestrial life would not be possible without four essential requirements; soluble bioactive elements (carbon, hydrogen, oxygen, nitrogen, sulfur and phosphorous; herein CHONSP), free energy (in the form of chemical disequilibria), liquid water, and time. The ability of carbon to form polymeric chains is key to fabrication of organic molecules and the ability of H, O and N to bond in these polymers leads to an astronomical number of possible stable molecular configurations. Phosphorous is fundamental to the assembly of nucleic acid (RNA/DNA) and adenosine triphosphate (ATP), respectively the recipe for, and energy currency of, life. Sulfur is required by all living organisms. As life is fundamentally a disequilibrium process, an external energy source is required to drive the needed chemistry. It is widely thought that life could not have emerged until liquid water appeared at or near Earth's surface. The polar nature of the water molecule makes it an outstanding solvent for much of the periodic table while its volatility can make it a concentrating agent of bioactive elements. Lastly, some believe that tens to hundreds of millions of years would be needed for nature to survey nonfunctional biopolymer sequence space in order to form macromolecules on prebiotic Earth (e.g., Carter 1983; Neveu et al. 2013; Adamala et al. 2014).

[1]For our purposes, life is defined as a chemically-based cellular organism with the capacity for metabolism, reproduction, variation and heredity.

The first four elements of CHONSP were surely available at or near Earth's surface throughout the Hadean. While the P and S were then present (see Sect. 10.3.1), low concentrations of both may have acted as a governor on biopoiesis. Energy sources widely available on early Earth could have included photonic energy (from the Sun), electrical energy (from lightning, at least during abiotic synthesis), and chemical energy (from seafloor vents). The key remaining question then is—and seemingly the rate limiting step in making our planet habitable—when was liquid water first available? While this has already been addressed to some degree in Chap. 7, before discussing this issue further, let's take a more expansive view of terrestrial habitability.

10.2 The Ten Ingredients for Terrestrial Habitability

The above discussion of the four requirements for life is overly glib as it provides no geologic framework for the transition from a prebiotic world to one teeming with life. Many questions need to be addressed to provide that context. For example, once consumed, how were bioactive elements made available for subsequent use? What was the geologic platform on which the key chemical reactions occurred during this transition? Was the ancient atmosphere transparent to the portion of the solar spectrum that drives the needed prebiotic chemistry? Was there an ocean that hosted hydrothermal vents?

Since Earth provides our only example of life, it stands to reason that the geologic conditions that prevailed during its emergence are key factors in maintaining its habitability. In strong form, this view approaches the Gaia hypothesis, which proposes that living organisms acquired control of the planetary environment via a self-regulating mechanism that perpetuates life (Lovelock and Margulis 1974; cf. Chopra and Lineweaver 2016). In weaker forms (Kirchner 1991), this seeming interdependence is seen either as a manifestation of the anthropic principle (Waltham 2014) or simply an acknowledgment of specific cases of the coevolution of the planet's physical and biologic realms (e.g., Snowball Earth; Hoffman et al. 1998).

So what more is needed beyond the four requirements for life? A consensus has emerged over the past twenty years that a host of secondary factors is needed to maintain planetary homeostasis. They are:

1. A galactic and planetary sanctuary
2. Water at the planetary surface
3. Water in the deep planetary interior
4. A near solar chemical composition
5. Sufficient planetary mass
6. Planetary satellites
7. Extra-planetary impactors
8. Deep interior heat generation

9. A self-sustaining dynamo
10. Surface recycling.

Before we evaluate each of these factors, let's briefly consider what rests beneath these criteria. The ten factors are, in effect, the geologic and/or cosmologic context missing from the four requirements for life. The second and third factors are, of course, restatements of the third requirement for life but the others largely reflect how we think Earth evolved over the past 4.5 Ga and, in their totality, are what separate us from the other, apparently uninhabited, terrestrial planets. Without some form of surface recycling, mantle CO_2 degassing to the atmosphere leads to a runaway greenhouse of the sort that makes the surface of Venus today inhospitable to life. Without a mechanism to recycle bioactive elements, the planetary surface would soon become bionutrient depleted. On our planet today, this surface recycling is provided by plate tectonics which has the added benefits of both creating long-lived crustal platforms on which life can develop, and extracting sufficient heat from the core to drive a geodynamo that protects both life and our atmosphere by deflecting the solar wind (Gonzalez et al. 2001; Lammer et al. 2010).

10.2.1 Habitable Zones

Ever since Darwin (1871) speculated that life may have emerged in a "warm little pond", the notion of a surficial 'primordial soup' has dominated discussions of biopoiesis (Haldane 1929; Oparin 1957; Crick 1981; Schopf 2002). Thus a long-standing view has been that life arises in circumstellar habitable zones (CHZ)—orbital paths around stars which maintain surface temperatures between the boiling and freezing temperature of water permitting long-term photosynthetic biomass production (Hart 1979). The discoveries of deep marine biomes adjacent seafloor vents (e.g., Macdonald et al. 1980) and subsurface oceans formed by tidal heating on ice-covered Galilean satellites (e.g., Europa; Khurana et al. 1998) required revision of this view to include the possibility of life outside the CHZ, albeit restricted to internal thermal sources, but it remains a guiding premise underlying origin of life investigations (e.g., Neveu et al. 2013).

Assuming a mixed CO_2–H_2O–N_2 atmosphere, Kasting et al. (1993) modelled the width of the circumstellar habitable zone (CHZ) around main sequence stars. The inner boundary is defined by the loss of surface water via photolysis and subsequent H_2 escape while the outer edge is marked by the formation of refrigerating CO_2 clouds. In their model, climate stability is ensured by a greenhouse feedback between atmospheric CO_2 content and surface temperature which also define the width of the CHZ. They found the current range for the CHZ to be between 0.95 and 1.37 AU (Fig. 10.1) but, because the Sun increases in luminosity as it ages, they estimated the zone width at the time of Earth formation to have been limited to between 0.95 and 1.15 AU.

Recent refinements of such models suggest that the inner edge of the CHZ moves outward for smaller planets (with presumably less dense atmospheres) due to

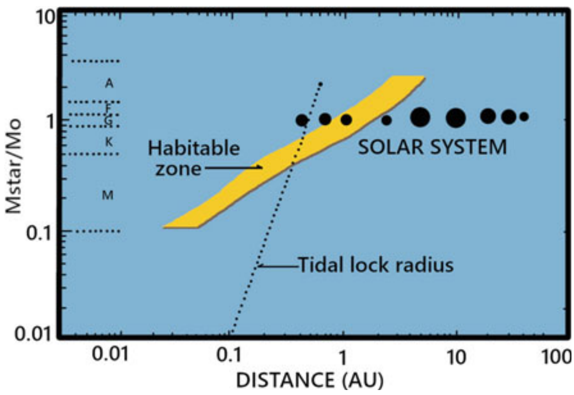

Fig. 10.1 Relationship between star mass and size of its habitable zone. M_{star}/M_O is ratio of star mass to the Sun; A, F, G, K, M refer to the spectral type of the star (see text); AU = astronomical unit; "tidal lock radius" is distance from star within which one planet hemisphere will always face the star. Modified from Kasting et al. (1993) with permission

a larger greenhouse effect owing to the increased 'water column depth' in the atmosphere (see Kopparapu et al. 2014). For larger planets, the water column depth is smaller and thus higher temperatures are needed before water vapor dominates the outgoing longwave radiation. As a result, the inner edge of the CHZ moves inward and supports a wider zone (i.e., 0.95–1.67 AU; Kopparapu et al. 2014).

Of course, not all stars are created equal. The above mentioned calculations were specifically for a G type star—like ours—in the Hertzsprung-Russell (abbreviated H-R) diagram of stellar luminosity against temperature. Habitable zones appear possible around other stars in the central Main Sequence (i.e., spectral types: F, G and K characterized by photospheric temperatures ranging from 8000 to 4000 K) but the shorter lifetimes of hotter stars (H-R types O, B and A) appear to make them unsuitable candidates. Stars dimmer than our Sun may possibly both host terrestrial-like planets and maintain CHZ's but these must necessarily be in orbits closer to the star (Mulders et al. 2015; see Fig. 10.1). As a result, the CHZ may occur within the tidal locking zone—the region within which tidal interactions have slowed down the spin of the planet (Fig. 10.1). If orbital eccentricity and obliquity are low, this can result in the same side of a planet consistently facing, in this case, the star about which it rotates. Having one side of a planet either in perpetual darkness or facing a stellar furnace—an "eyeball planet"—was recognized early in discussions of extrasolar life as a challenging environment for life as surface water would evaporate on the hot side and be frozen and permanently sequestered on the cold (Dole 1964). Although atmospheric circulation could help create a narrow habitable region at the boundary between the temperature extremes, a "weathering runaway" effect driven by greenhouse forcing of increased surface area above the freezing point of water might cause rapid and significant (thousand-fold) atmospheric pressure changes, further shrinking or eliminating whatever limited habitable zone might exist (Kite et al. 2011).

Proxima Centauri, a red dwarf type M star and our nearest stellar neighbor, hosts a tidally locked planet of roughly Earth mass (Anglada-Escudé et al. 2016). Its $\sim$0.05 AU orbital radius lies within what is regarded to be the CHZ for an M star (Kopparapu et al. 2014). While Anglada-Escudé et al. (2016) acknowledge that the strong stellar magnetic fields, flares and high ultraviolet and X-ray fluxes present on M stars could create a hostile environment for life, they argue that tidal locking does not preclude a stable atmosphere if global atmospheric circulation can redistribute sufficient heat. Moreover, planetary magnetic fields in tidally locked planets may be sufficiently strong to prevent atmospheric erosion by strong stellar magnetic fields (Vidotto et al. 2013) and flares (Zuluaga et al. 2013). Perhaps the greatest limitation on habitability around M stars is the very luminous (10–100 times more than CHZ luminosity) pre-main sequence life time of nearly one billion years that would likely devolatilize any rocky planet.

In an analogous fashion to circumstellar habitable zones, Gonzalez et al. (2001) pointed out the importance of galactic chemical evolution in creating a habitable world. In particular, they argued that a metallicity at least half that of the Sun is required to build a habitable, terrestrial-like planet and concluded that many galaxies are too metal-poor to contain Earth-mass planets. Lineweaver et al. (2004) extended this model to include four space-time prerequisites for complex life to emerge: a host star of intermediate mass, sufficient metallicity to form a rocky planet, sufficient time for biological evolution, and an environment free of life-extinguishing supernovae (Frank et al. 2014). These requirements circumscribed a galactic habitable zone as an annular region between 7 and 9 kiloparsecs from the galactic center that broadens with time. Too close to the center of the galaxy risks sterilizing radiation, too far out and there are insufficient heavy elements to form a terrestrial-like planet with long-term, internal, heat generation. Lineweaver et al. (2004) argued that galaxies formed during the first five billion years following the Big Bang (at $\sim$14 Ga) may have lacked the necessary metallicity while those younger than 4 Ga are unlikely as yet to have evolved complex life (Fig. 10.2).

Moore et al. (2017) offer a cautionary note regarding the term circumstellar habitable zone. A planet in a CHZ is not necessarily habitable, for instance, by having liquid water at its surface. As an example, Venus is nominally within the habitable zone of our Solar System (Fig. 10.1), but surely is currently sterile and may never have been otherwise (Hamano et al. 2013). Instead, occupancy in the zone only implies that such a state is not impossible. Furthermore, the term was coined before the concept of deep, chemosynthetic biospheres on icy satellites was conceived (see 10.2.6) and thus ignores alternate planetary refugia.

10.2.2 Surface Water

Water not only has manifold special properties that cause it to play a central role in autoregulation of both physical and biologic systems, but Nature has organized to make it widely available. Water is the most common triatomic molecule in the

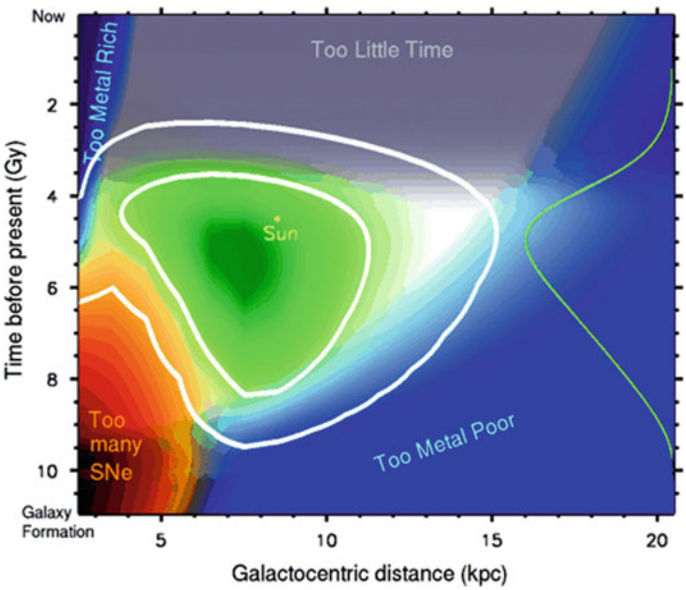

Fig. 10.2 The galactic habitable zone (green) calculated for the Milky Way constrained by star formation rate, metallicity (blue), the time thought required for biopoiesis (gray), and supernovae activity (red). The white contours show the one and two sigma bounds for stars with the highest potential to be harboring complex life today. Reproduced with permission from Lineweaver et al. (2004)

Universe and, in liquid form, is stable over a relatively wide pressure-temperature range. It is assumed to be essential for biopoiesis and has numerous roles in living organisms, including as a thermoregulator (due to its high enthalpy of vaporization) and metabolite. Its high surface energy enhances aggregation of organic compounds and its highly polar nature makes it an excellent solvent for bioactive elements.

Beyond its seemingly central role in the creation and sustenance of life, water also mediates the so-called Urey reaction (the carbonate-silicate cycle) which is widely thought to regulate atmospheric temperature over virtually all geologic timescales. Silicates make up about 90% of the crust and thus subaerial weathering of (mostly) feldspars yields free cations and silica that can react with the bicarbonate (HCO_3^-) washed out of a CO_2-bearing atmosphere to yield carbonate minerals. The model reaction typically assumes that the model mineral $CaSiO_3$, wollastonite,[2] is broadly representative of the silicate crust:

$$CaSiO_3 + CO_2 + H_2O \rightarrow SiO_2 + H_2O + CaCO_3 \tag{10.1}$$

[2]Wollastonite is a rare mineral but a useful analogue for plagioclase feldspar which constitutes a plurality of continental crust.

The products of this reaction are either returned to the atmosphere-hydrosphere system (i.e., H_2O) or washed into the ocean to be available to make silica (e.g., radiolarian) or calcium carbonate (e.g., coral) skeletons of marine organisms or chemical sediments. The carbon sequestered by this process accumulates on the seafloor eventually to be subducted, thus either recharging that reservoir for further volcanic degassing of CO_2 back into the atmosphere, or stored indefinitely in accreted sedimentary rocks. As previously noted, without this mechanism for recycling surface carbon, mantle-derived CO_2 would accumulate in the atmosphere, eventually leading to a runaway greenhouse and global sterilization. Indeed, it is generally thought that a majority of terrestrial carbon has at one time or another been oxidized to carbonate in this fashion (Zeebe 2012).

As plausible and widely held as this view of the central role of the Urey reaction in planetary homeostasis is, there is little in the way of empirical evidence that requires such a predominant role. In examining the main locus of sedimentary detritus from the uplifting Himalayan range, an orogenic event of a magnitude that may have occurred only a handful of times in Earth history (Harrison et al. 1992), France-Lanord and Derry (1997) showed that CO_2 draw down from the burial of organic carbon was two to three times greater than that resulting from the weathering of Himalayan silicates.

Isson and Planavsky (2018) proposed that during marine authigenic clay formation, the loss of alkalinity from the oceans and resulting decreased pH work to retain carbon within the ocean-atmosphere system. The strong negative feedback between marine pH and clay formation amounts to 'reverse' weathering that would lead to climate stability by buffering atmospheric CO_2 at a relatively constant levels.

From the perspective of planetary temperature regulation, it doesn't matter which of these mechanisms (i.e., silicate weathering creating sequestered carbonates, direct burial of reduced carbon, or reverse weathering) is most responsible—unless, in the case of the former two, life emerged relatively late in Earth history.

How Earth came to acquire and hold on to its complement of water is actively debated (e.g., Alexander et al. 2012, 2018). Its formation at 1 AU seemingly places it within a region too hot to permit primary water to have condensed (Grossman 1972; Chambers 2004; cf. Drake 2005) but water could have been introduced by late stage accretion of planetesimals originating further from Sun (i.e., beyond the planetary "snow line") (Wetherill 1980). The terrestrial D/H is very different from that of the solar nebula (Marty 2012 and references therein) and comets originating in the Oort Cloud, but within the range of meteorites (Altwegg et al. 2015; Woo et al. 2018), some Kuiper belt comets (Hartogh et al. 2011; Lis et al. 2013) and the Jupiter family comet 46P/Wirtanen (Lis et al. 2019).

As noted in Chap. 3, modelling suggests that even a giant impact of a possible Moon-forming variety, which melted the combined system, would result in little volatile loss from Earth if the impactor size, and thus resulting temperatures, were sufficiently high (i.e., >6000 K) to volatilize silicates (Abe 2007). However, Genda and Abe (2005) found that the presence of an ocean would significantly enhance atmospheric loss during a giant impact owing to ocean evaporation and the lower shock impedance of the ocean/atmosphere interface compared to that of the solid Earth/atmosphere.

As discussed in some detail in Chap. 6, it is the positive and negative buoyancies created by global scale cooling that are primarily responsible for the mobile-lid convection that drives terrestrial plate tectonics. That mechanism is a far more efficient planetary radiator than either thermal conduction or stagnant-lid convection. That over half of Earth's heat loss occurs by circulating ocean water during the creation of lithosphere at mid-ocean ridges (Sclater et al. 1980; Davies and Davies 2009) inspired the metaphor that our planet has a 'water cooled radiator'. Without surface water, plate tectonics as we recognize it would not be possible thus jeopardizing the surface recycling mechanism argued earlier to be a *sine qua non* of life on Earth.

10.2.3 Interior Water

The existence of mantle convection alone doesn't guarantee the mobile-lid behavior needed for continuous global cycling between surface and interior. A stagnant lid regime of the kind hypothesized for Venus (Turcotte 1993), in which global overturn occurs episodically, would ultimately cycle material between the surface and interior but the rarity of such events would in general not be conducive to the emergence of life (Stern 2016). More to the point, a dry basaltic surface cannot react with atmospheric CO_2 and thus such global overturns would not sequester carbon via the Urey reaction leading to, as in the present case of Venus, a runaway greenhouse effect resulting in surface temperatures of ca. 500 ºC which certainly precludes life as we know it.

A key step among the interlocking mechanisms that make plate tectonics possible on Earth is the decompression melting that occurs in ascending mantle currents beneath mid-ocean ridges (Fig. 10.3). Partial melting of fertile mantle (e.g., 'pyrolite'; Ringwood 1962) creates incompatible-element-enriched basaltic oceanic crust with its complementary peridotitic residuum whose later physical separation at convergent margins provides another key link in the plate tectonic chain when the basaltic crust portion transforms to denser eclogite (Ito and Kennedy 1967) providing slab pull. For this process to first occur, the adiabatically ascending solid mantle must reach the basalt solidus at sufficient depth beneath the ridge to generate a subductable basaltic crust. Too thick crust and 'trench lock' could occur (Sleep 2000; cf. Korenaga 2013; see Chap. 6); too thin and there might be insufficient 'slab pull' to drive the tectonic system (Forsyth and Uyeda 1975). But the present day average mantle potential temperature of ca. 1320 °C (McKenzie 1970) is close to the anhydrous, or "dry", solidus of 'pyrolite' and thus the required amount of partial melt cannot be generated in the absence of an impurity that depresses melting temperature. That impurity is water, or more correctly, a dissolved hydrogen species, such as OH^-. As an aside, I note that the mantle potential temperature appears to have dropped below the solidus in certain places. For

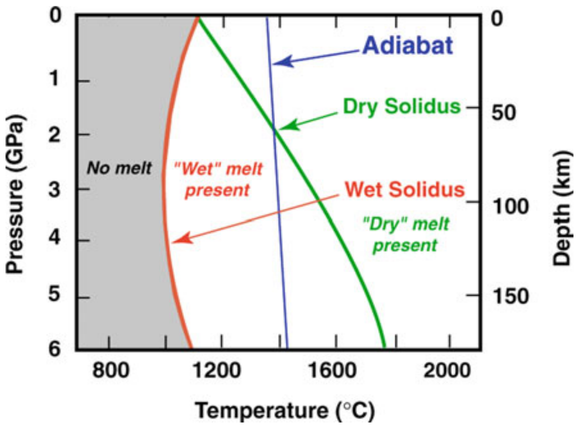

Fig. 10.3 Generalized diagram showing mantle melting fields and their relationship with the wet (water vapor-present) and dry (water absent) solidi and the mantle adiabat along which heat content is constant. Melting near Earth's surface can occur if mantle temperature exceeds any of the three curves. Modified from Hirth & Kohlstedt (1996)

example, the slow-spreading Southeast Indian Ridge has been amagmatic for many millions of years (Dick et al. 2003).

The dominant storehouse of water in the mantle is in nominally anhydrous phases, such as olivine, wadsleyite and ringwoodite, with global estimates equivalent to levels between one to three modern ocean's worth (Hirschmann 2006; Pearson et al. 2014; Fei et al. 2017). In addition to depressing melting temperature (Fig. 10.3), it has long been known that hydrogen species dramatically weaken silicate minerals (Griggs and Blacic 1965). Upper mantle viscosities can drop several orders of magnitude (Fig. 10.4) relative to the 'dry' equivalent upon the addition of several hundreds of ppm H (Hirth and Kohlstedt 1996). Thermochemical mantle convection simulations suggest enhanced plate motion through the lubricating effect of hydrous oceanic crust, but such water cycling between surface and deep interior has competing feedback effects (Nakagawa et al. 2015). While transport of water into the deep mantle reduces viscosity, resulting in a lower temperature, that cooling causes mantle viscosity to increase. Thus the presence of water in Earth's deep interior directly influences the 'running temperature' of mantle convection. Without the weakening effect of water on mineral strength, a stiffer terrestrial mantle would be more resistive to convective circulation, potentially limiting global heat loss below an amount needed to, for example, drive the geodynamo (see Sect. 10.2.9).

The earlier allusion to the transformation of basaltic oceanic crust to denser ecolgite (the gabbro-garnet granulite-eclogite transformation) is what provides much of the slab pull within the global plate tectonic force balance (Chap. 6). However, laboratory experiments show that, under anhydrous conditions and the inferred temperatures at which the natural reactions proceed, this phase transition

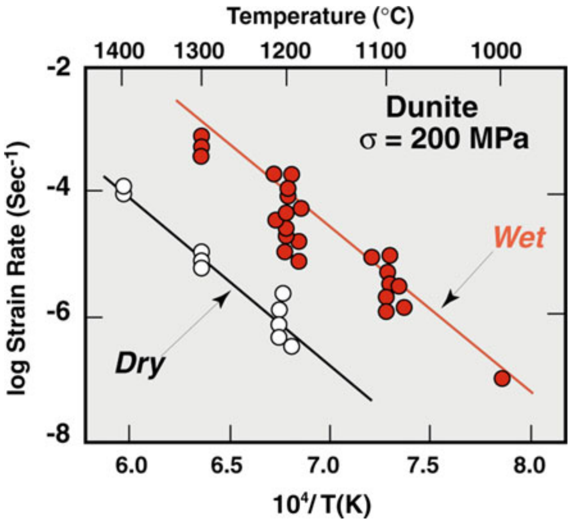

Fig. 10.4 Plot of strain rate in peridotite versus temperature for both water present ("wet") and absent ("dry") cases. Upper mantle viscosities can drop by a factor of 180 relative to the 'dry' equivalent upon the addition of several hundreds of ppm H. Modified with permission from Hirth and Kohlstedt (1996)

could not occur over the geologic durations relevant to subduction (i.e., 0–20 Ma) (Ito and Kennedy 1970). It is the presence of relatively small amounts of water ($\sim$0.5–1.0 kbar P_{H2O}) that overcomes that kinetic barrier, permitting the transformation, even at relatively low (<500 °C) temperatures (Ahrens and Schubert 1975).

10.2.4 Composition

Terrestrial planets cannot form unless "metals"—viewed by astronomers as elements heavier than helium—are available. Heavy elements have gradually built up over the $\sim$14 Ga history of the known Universe. Most with masses less than 56 amu form by semi-continuous fusion reactions within stars and virtually all those with greater masses are synthesized during brief, but intensely creative, supernova events.

Early observations of extrasolar planets suggested that the presence of giant planets at small distances ("hot Jupiters") from their host stars is strongly correlated with high metallicity of the host stars. Thus Lineweaver (2001) inferred that a close-orbiting giant is incompatible with the existence of Earth-like planets and proposed a 'Goldilocks' selection effect: too little metallicity (<0.1 solar Fe/H ratio) and terrestrial-type planets are unable to form for lack of appropriate elements, but significantly increase that metallicity and giant planets destroy them during inward migrations. Gonzalez et al. (2001) inferred a minimum metallicity of at least half that of the Sun is required to build a habitable terrestrial planet. The effect of "hot Jupiters" on terrestrial planets remains an open question (e.g., Raymond et al. 2011) but they now appear to represent a smaller fraction of exoplanets than originally thought (Bryan et al. 2016).

The relative global abundances of Si and Mg to Fe, which influences the core/mantle mass ratio of a terrestrial planet, vary spatially and temporally within the galaxy (Gonzalez et al. 2001). Thus planetary systems that have a similar metallicity to the Sun, but formed elsewhere and earlier in the Milky Way, may not be capable of forming habitable, Earth-like planets. That Earth's upper mantle is dominated by olivine reflects the global silicate Mg/Si of ~ 1.2, which fractionated from the solar Mg/Si ratio of ~ 1 during planetary formation (Ringwood 1989; Lodders et al. 2010). Had our solar nebula instead inherited an Mg/Si ratio, say, 20% lower (due, for example, to a different mix of stellar fusion and supernova products or a younger mix of galactic debris; Frank et al. 2014), pyroxene would likely dominate the upper mantle, potentially imposing significantly greater mechanical resistance to tectonic stresses (see previous section). Perhaps counter-intuitively, small changes to non-redox sensitive elements, like Mg or Si, can influence the oxidation state of the mantle, potentially influencing planetary habitability. Unlike pyroxene, olivine has no capacity to dissolve ferric Fe (Fe^{3+}). Thus any ferric Fe in our olivine-dominated upper mantle is hosted by spinel, (Mg,Fe) Al_2O_4. Although a minor modal phase (typically at the few percent level in lherzolites), its near ubiquity imposes a relatively high oxygen fugacity across the upper mantle (Hugh O'Neill, pers. comm.) in equilibrium with a CO–CO_2–N_2 mixture, potentially explaining why conditions close to the fayalite-magnetite-quartz buffer were present on Hadean Earth (Trail et al. 2011). Under such relatively oxidized conditions, the early mantle is unlikely to have degassed the mix of highly reducing gases proposed (NH_4–CH_4–H_2) to synthesize organic building blocks, like amino acids, in the fashion proposed by the classic Miller-Urey experiments (Miller and Urey 1959). Indeed, Cleaves et al. (2008) found that the relatively more oxidized atmospheres create nitrites which rapidly break down amino acids. The relevance of the Miller-Urey approach as a source of organic building blocks was significantly diminished by discovery of more than 60 amino acids in the Murchison chondrite (Koga and Naraoka 2017) (see Sect. 10.2.7).

The scenario above exemplifies how sensitive a planet could be to initial conditions in that small changes in one parameter, in this case Mg/Si, could lead to very different evolutionary trajectories.

Lastly, as discussed in Sect. 10.1.1, life as we know it needs soluble biophilic elements (CHONSP) and thus requires relatively high bulk planetary metallicity, including S and P contents sufficient for at least local concentration to levels permitting biopoiesis.

10.2.5 Planetary Mass/Size

The mass and size of a planet strongly influences the retention of both its atmosphere and interior heat.

The greater gravity that comes with higher mass impedes atmospheric loss. For a given molecule to be retained in Earth's atmosphere, its mass must exceed $3kTR/2\mu$, where k is Boltzmann's constant, T is absolute temperature, R is planetary radius, and μ is the standard gravitational parameter. Thus Earth, with a surface temperature of 288 K, can retain all gases heavier than He. Although H_2 (and H produced by photo-dissociation) well exceed Earth's escape velocity (11.2 km/s), the average molecular weight of our atmosphere of 29 g/mol ensures its retention. This is vital as the atmosphere shields surface lifeforms from potentially sterilizing ultraviolet radiation by photolysis of free O_2 to O_3 (i.e., ozone). Ratner and Walker (1972) calculated that an oxygen content as little as one thousandth of Earth's present atmosphere could still produce a biologically effective ozone screen. However, the observation that mass independent fractionation of sulfur isotopes ceased to be retained in the rock record subsequent to the Great Oxygenation Event at 2.4 Ga (Farquhar et al. 2000) suggests a higher threshold. At the other end of the size spectrum, too big a planet could lead to atmospheric densities so high that solar radiation cannot penetrate the cloudy atmosphere to the surface. Planets greater than about five to ten times Earth mass are at the threshold of transitioning to gas giants, depending on details of nebular evolution.

Although increasing planetary size decreases surface to volume ratio, thus inhibiting conductive heat loss (which scales inversely with the square of the radius), internal convection is enhanced because Rayleigh number scales as the cube of lengthscale (see Eq. 2.3, all other influences remaining equal). The role of planetary mass in the initiation and propagation of plate tectonics is debated in context of the behavior of so-called 'superearths'—terrestrial bodies with masses between two and five times that of Earth. Modelling that includes the enhanced role of gravity in locking near surface faults, suggests that greater size inhibits plate boundary interactions by decreasing the ratio of driving to resisting stresses (O'Neill and Lenardic 2007). In contrast, Valencia et al. (2007) found that with increasing planetary mass, the shear stress available to overcome resistance to plate motion increases while plate thickness decreases, both of which encourage lithospheric subduction. In their view, plate tectonics is inevitable on superearths, which are likely volatile-rich. Van Heck and Tackley (2011) may have reconciled these diverging views by noting that plate tectonics driven by internally-heated convection is equally probable for planets of any size, whereas plate tectonics becomes more likely with increasing planet size for basally-heated convection (also see Valencia and O'Connell 2009).

10.2.6 Satellites

Earth-Moon gravitational interactions stabilize the orbital characteristics of, and create tides on, both bodies. Tidal environments (Oparin 1957) have long been seen as an attractive environment for the creation of "Darwin ponds" (see Sect. 10.2.1), where repeated supply-and-evaporation cycles concentrate bioactive elements and support polymerization reactions. The presence of Moon stabilizes Earth's spin axis thereby moderating extreme climate oscillations that may be detrimental to the evolution of complex life forms. Specifically, Earth's current obliquity of 23.3° varies by only ±1.3°. But if Moon were not present, possible solutions range from 0° up to about 85° (Laskar and Robutel 1993; cf. Lissauer et al. 2012). Such large changes in obliquity would likely result in substantial climate instability and temperature extremes, arguably diminishing the likelihood of complex life arising (Ward and Brownlee 2000). However, the preceding argument assumes a planetary distribution much like our Solar System.

Piro (2018) investigated scenarios in which an exoplanet in the habitable zone of a low-mass star (0.1–0.6 $M_{\odot}$) experiences sub-equal tidal influences from its moon and star and found that the moon's orbital evolution depends on the parent planet's initial spin period rate. When low, transfer of the planet's angular momentum to the moon's orbit can result in its outward migration with the star eventually wresting it free. When the spin period is large, the star's tidal influence decelerates the planet's rate of rotation and the moon migrates inward until it is tidally disrupted by the planet. Piro (2018) noted that these effects did not necessarily preclude low-mass star planets having satellites as the timescales for their loss or destruction range up to the age of the Universe.

Waltham (2014) suggested that a planet's rate of rotation, the circularity of its orbit, and the locations of other planets could influence the rise of life. For example, Earth-Moon tidal dissipation has continuously expanded the lunar orbit and slowed Earth's rotation. A rapidly spinning proto-Earth may have had too short a day to permit effective meridional heat flow from poles to equator. But by quickly increasing the length of the terrestrial day, Moon insured that Earth was not perpetually bound in a "snowball" state (Waltham 2014).

The potential for satellites to host life beyond the planetary 'snow line' (Podolak and Zucker 2004) is enhanced for those orbiting giant planets as tidal heating could warm their interiors sufficiently to create sub-surface liquid oceans in contact with nutrient-bearing rock. For example, Europa has been suggested as a potentially "procreative satellite" following recognition that it hosts a subsurface ocean (Khurana et al. 1998).

10.2.7 Impacts

Impacts are a double-edged sword for life and its planetary habitats. They can destroy large portions of lithosphere hosting nascent life, or produce large melt sheets in the earliest stages of planetary evolution that differentiate to form stable, continental crust on which life can emerge and evolve. Vaporization of the global ocean due to a very large (>400 km diameter) impact was thought to cause planetary sterilization (e.g., Sleep et al. 1989), but smaller impacts could actually enhance ecological niches of extremophiles (Sleep and Zahnle 1998; Abramov and Mojzsis 2009). Impacts can cause near global extinctions, but survivors can get an evolutionary kick from new fitness landscapes that drive rapid evolution (e.g., the rise of mammals following the K-T impact; Alvarez and Asaro 1990). Also on the plus side, giant impacts can potentially make large satellites which, as described in the previous section, may aid development of complex life. Smaller impacts import both bioactive elements (CHONSP; Sect. 10.1.1) and organic molecular building blocks, such as amino acids (see Sect. 10.2.4). Impacts add thermal energy to the accreting planet and thus can aid in prolonging internal activity on small to medium sized bodies.

The relative advantages and disadvantages discussed above are based on a broad understanding of how our solar system has evolved. For example, Jupiter's gravitational scattering acts to shield the inner planets from impacts by long period comets. Wetherill (1994) argued that if Jupiter had failed to capture sufficient nebular gas during the early stages of solar system accretion and remained, say, the size of Uranus or Neptune, the cometary source region would be much more densely populated. In such a case he calculated that the cometary impact flux to the inner solar system could have been one thousand times greater than experienced over the past 4.5 Ga. Given their size (diameters up to 60 km; Fernández 2003) and relative velocities (e.g., the 1910 passage of Halley's comet was 70 km/s), cometary impacts might impede development of life if it had not yet appeared or potentially extinguish it if it had. Knowing in 1994 of no other solar system with which to compare, Wetherill (1994) lamented that ours "tells us nothing about the probability of similar gas giants occurring in other planetary systems" but that this "would be corrected by observation of an unbiased sample of planetary systems". Wetherill did not have to wait long as the modern era of exoplanetology began the following year (Mayor and Queloz 1995), and with it, the recognition that Jupiter-sized bodies appear to be relatively common feature of other planetary systems (although arguably not an unbiased sample).

Jupiter's presence may also have indirectly led to an audience for this book. Gravitational resonances, created through interactions between Jupiter and individual asteroids under specific orbital conditions, expel those bodies creating dynamical gaps within the asteroid belt. Repeated prodding by the giant planets of asteroids in such orbital resonances eventually creates dynamically barren regions—Kirkwood gaps—within the belt (Wetherill 1985). Some of the ejected objects are put into Earth crossing orbits and the larger of those (>10 km) would cause local or global species extinctions on impact. But, as noted earlier, alternation between brief impact events and long term (tens of millions of years) stability can provide surviving species with manifold opportunities for evolutionary innovation. For example, the rise of mammals in the wake of the K-T impact 66 million years ago which extinguished more than half of all life on Earth (Alvarez and Asaro 1990). In this view, the lack of a Jupiter-sized gas giant could doom inner solar system worlds by leaving excessive debris with which to pummel them to sterility. But, if by chance those worlds escaped that fate, the lack of a true gas giant might then deny them the "pump" provided by periodic impacts that would explore the fuller range of evolutionary landscapes perhaps necessary to promote complex lifeforms such as ourselves (Cramer 1986). Alternatively, Horner and Jones (2009) noted that the giant planets act on objects in Centaur-like orbits to significantly change the impact rate of short-period comets to Earth, greatly increasing the impact flux over what would be expected in the absence of a gas giant.

10.2.8 Internal Heating

Short-lived nuclides with high abundances and decay energies, such as ^{26}Al ($t_{½}$ = 0.72 Ma), can rapidly lead to melting of the interiors of even relatively small protoplanets (e.g., Hevey and Sanders 2006) provided the nucleosynthetic event that produced them occurred within a few of half-lives of those isotopes. Long-lived radioactivities from ^{40}K, $^{235,238}U$, and ^{232}Th can keep planetary interiors sufficiently hot to maintain internal circulation for billions of years (Fig. 2.1). However, a consequence of the temporal decline in star-forming activity in the Milky Way is a commensurate lowering of nucleosynthesis from supernova explosions. Thus the abundance of those geophysically important, lithophile, long-lived radioactive isotopes is in decline (relative to, say, Fe which is used as a metric of metallicity) (Frank et al. 2014). The specific mix and abundances of those radioactive isotopes in a given nebular cloud varies spatially and temporally within the galaxy (see Sect. 10.2.4) so there is little reason to expect that the exact complement that our solar system inherited immediately prior to nebular condensation at 4.567 Ga is typical of most others in the Milky Way galaxy (Frank et al. 2014). Had their abundances been perhaps a factor of two or so lower, our species may never have arisen due to the shutdown of the global tectonic engine billions of years ago when only microbiota roamed the planet.

Earth is estimated to today contain about 200 ppm K, 16 ppb U and 65 ppb Th (Lyubetskaya and Korenaga 2007), generating about 20 TW of heat (note that additional ~4 TW escapes to space in the form of neutrinos; Dye 2012). The distribution of the radiogenic heat produced by these isotopes on Earth is highly non-uniform, with about 50% estimated to be held within the continental crust (McDonough and Sun 1989; Rudnick and Gao 2003), leaving only about 10 TW to drive the convecting mantle. In this way, continental formation can cool the mantle by drawing out the heat-generating isotopic species and placing them adjacent the surface to radiate the heat into space. But continents, particularly supercontinents, can locally heat the underlying mantle by acting as thick, poorly conductive lids that trap heat beneath (Anderson 1982).

The other major source of Earth's internal heat generation comes from the latent heat of crystallization released as iron alloy plates onto the inner core. But the timing of initiation of inner core formation is poorly known (see Sect. 10.2.9), with estimates ranging from as young as 2.5–1 Ga (Labrosse et al. 2001; Buffett 2003) to potentially as early as the Hadean (Tarduno et al. 2015; cf. Weiss et al. 2018). Thus knowledge of the secular release of that heat is poorly constrained.

More speculatively, in investigating exoplanet-moon interactions in the habitable zone of a low-mass stars, Piro (2018) (Sect. 10.2.6) found that the combined tidal torques force the exoplanet to spin asynchronously with respect to both its moon and parent star. This causes the planet to tidally heat at rates comparable to Earth's current thermal flux for up to a billion years. Thus combined tides could potentially drive tectonic activity on worlds in closely spaced planetary systems.

10.2.9 Core Formation and the Geodynamo

The segregation of Earth into a distinct metallic core and encompassing silicate shell must have resulted in substantial heating from the conversion of potential energy into heat via viscous dissipation. Instantaneous full core-mantle separation would have yielded ca. 10^{31} J, potentially representing an average global temperature increase of as much as 2000 °C (Solomon 1979), depending on the initial distribution of metal-silicate and the segregation mechanism. The modern consensus is that the combined kinetic, gravitational and radiogenic sources of thermal energy available during Earth formation would have resulted in initial mantle potential temperatures in excess of 1600 °C and the formation of one or more successive global magma oceans (Elkins-Tanton 2008; cf. Urey 1952). Despite the seeming likelihood of a magma ocean phase early in Earth history, it's important to note that no unambiguous evidence of its existence has yet been documented (e.g., Righter and Drake 1999). As noted in Sect. 3.2, core formation was likely complete within about 30 Ma, and no later than 70 Ma, of the condensation of first solids from the solar nebula (see Sect. 3.1).

Earth's magnetic field arises in the outer core where electric currents moving in the convecting liquid iron-alloy interact with planetary rotation to create a self-generating geodynamo (Elsasser 1958). Knowing when Earth's magnetic field first arose has important implications for planetary thermal evolution, the physics of dynamo generation, and the oxidation state of the atmosphere (Gubbins et al. 2004; Lammer et al. 2010; Nimmo et al. 2004; Tarduno et al. 2014; Ziegler and Stegman 2013). The oldest known sedimentary rocks of sufficiently low metamorphic grade to preserve evidence of a dynamo indicate its presence at 3.45 Ga (Biggin et al. 2011), but its existence during the first billion years of Earth history remains unknown. A delayed onset of the geodynamo could be due to the persistence of a hot, molten lower mantle or the late initiation of plate tectonics (Labrosse et al. 2007; Nimmo and Stevenson 2000; O'Neill and Debaille 2014). Alternatively, an active early Hadean geodynamo could imply an important role for compositionally-driven convection in the core, a magma ocean overturn event, or even a magma ocean dynamo (Ziegler and Stegman 2013; O'Rourke and Stevenson 2016). More importantly, from the standpoint of habitability, the state of the early geomagnetic field may exert a control on the rate of atmospheric loss. Specifically, Earth's magnetic field essentially prevents solar wind erosion of upper atmospheric gases dissociated by extreme ultraviolet photon irradiation and also shields life forms from some cosmic radiation (e.g., Hunten and Donahue 1976; Lammer et al. 2008, 2011). That said, Venus lacks a planetary magnetic field but still maintains an atmosphere almost one hundred times denser than Earth's.

While no rocks older than 4.02 Ga are known, Jack Hills zircons date to as old as nearly 4.4 Ga. As noted in Sect. 7.5, virtually all magmatic zircons contain mineral inclusions incorporated during growth in the host melt. If ferromagnetic minerals were so included, it might be possible to measure primary remanent magnetization imposed at the time of crystallization. A significant proviso is that some form of thermometry is required to demonstrate that the zircon had not, in the case of a magnetite record, exceeded the Curie temperature of 585 °C and thus been reset. Tarduno et al. (2015) measured magnetic properties of Jack Hills zircons and argued that they retain natural remanent magnetization dating back to their U–Pb crystallization ages as old as 4.2 Ga. They did not, however, robustly demonstrate that the zircons had not been thermally or aqueously remagnetized since formation (see Weiss et al. 2015, 2016; Sect. 7.8.2). Weiss et al. (2018) showed ferromagnetic minerals in most Jack Hills zircons are located in cracks and on grain exteriors. Tang et al. (2019) showed by transmission electron microscopy that magnetite in Jack Hills zircons could be introduced along dislocations in radiation damaged grains. Hematite dominates the magnetization of many zircons with lesser quantities of magnetite and goethite. Thus the magnetization of most Jack Hills zircons appears to be dominantly carried by secondary minerals of unknown age. It remains possible that primary magnetite inclusions could be found in Hadean zircons and paleothermometric methods to ascertain post-crystallization thermal histories of zircons in the Curie temperature range are being investigated.

10.2.10 Surface Recycling

As laid out extensively in Chap. 6, Earth's surface recycling occurs by a self-regulating system in which internal circulation, driven largely by a sinking thermal boundary layer, results in surface horizontal forces that continuously expose rock to weathering. Some of the detritus produced by this process is carried back into the mantle. We call this mechanism plate tectonics. In this way, a tectonically and erosionally active planet (with an ocean and atmosphere) can cycle carbon between its surface and deep interior providing a feedback mechanism that helps stabilize long-term atmospheric temperature.

As just discussed in the previous section, Earth's magnetic field appears to play a role in shielding atmospheric gasses from solar wind erosion by solar ultraviolet radiation, particularly early in its history. That field is maintained by a geodynamo driven by fluid convection in the liquid outer core. As noted in Chap. 2, convective intensity is characterized by the Rayleigh number (Eq. 2.3), the ratio of thermal and chemical buoyancy to dissipative forces. Compositional buoyancy in this case comes from the segregation of light elements (e.g., O, C, Si) into the outer core with growth of the solid inner core. However, as also previously mentioned, inner core crystallization may have been forestalled for some time during which the thermal gradient across the core would be dictated by the magnitude of heat transfer from the core to the mantle. Assuming little core radioactivity, it was long thought that secular cooling of about ca. 4 TW could have alone powered an early dynamo. However, recent estimates of the thermal conductivity of the outer core (Pozzo et al. 2012) appear to require higher (15 TW) power than core cooling could provide in a long-lived geodynamo. Attaining this magnitude of core cooling would probably require a form of mobile lid convection—plate tectonics—to sustain Earth's magnetic field (de Montserrat Navarro et al. 2016).

While 98% of all ocean biomass is microbial, marine environments are not ideal environments for their abiotic synthesis. Hydrothermal circulation at mid-ocean ridges might have supported the energy requirements of early chemotrophs (Wächtershäuser 1990; Shock and Canovas 2010), and their submarine locations provided some shelter from extraterrestrial impactors (Sleep and Zahnle 1998), but the deep marine environment is unlikely to provide mechanisms to, say, concentrate the phosphorous and boron needed to create and stabilize self-replicating RNA molecules (see Sect. 10.3).

The 'primordial soup' is likely to have been something more akin to the "warm little pond" speculated by Darwin (Sect. 10.2.1), such as the tidal zone along continental margins where repeated cycles of evaporation and recharge occur (Commeyras et al. 2002; Lathe 2004), than in the deep ocean. Although small solar tides would still have occurred on early Earth in the absence of a satellite, lunar tides at the end of the Hadean, when Moon was less than one third of its present distance from Earth, were likely frequent (ca. 7 h) and sufficiently high (ca. 100 m) to flood inland hundreds of kilometers, potentially creating vast sabkhas (Zharkov 2000; Lathe 2006). There is widespread agreement that plate tectonics is responsible for the growth of continental crust, albeit in ways we have yet to fully understand (Chap. 5). Thus it is at least arguable that the appearance of felsic crust is prerequisite to the emergence of life. By first providing the nursery for biopoiesis (cf., Stern 2016) and then constantly changing fitness landscapes as continents drifted through climate zones, or through isolating species by rifting and mountain building, plate tectonics may have been a key driver of evolutionary change and biodiversity.

10.2.11 Interrelationships

It isn't possible here to explore all the possible permutations among the above ten factors for terrestrial habitability but several salient interrelationships are shown in Fig. 10.5. In this diagram, moving from left to right transitions from fundamental physical requirements common to most terrestrial planets (e.g., sufficient metallicity and size) to higher order specifications unique, to our knowledge, to Earth (i.e., surface-interior element cycling, surface liquid water). The red arrows show evolutions that are thought to be contraindicative for the emergence of life whereas the green arrows lead to states that are more conducive to biopoiesis. As an example, consider the inputs and outcomes of compositional state. Conservatively, the minimum requirement is for an Fe/H ratio approximately between 0.1 and 2 times the solar value. The position with respect to the star dictates first order details of the planets composition during accretion with more distant worlds richer in low temperature condensates and those close to the stellar center more likely to have early atmospheres stripped. The metal to silicate ratio influences planetary mass and thus surface gravity. Impacts, particularly large ones, modify planetary composition by, for example, introducing volatile species such as water. If long lived radioactivities and water contents are too low, internal circulation is unlikely to persist over billion year timescales and thus preclude long term surface-interior element cycling. As shown in Fig. 10.5, composition dictates whether the planet will have regulated element cycling, an atmosphere and CHONSP (see Sect. 10.2).

While cluttered, Fig. 10.5 is still too simplistic to permit representation of self-regulating mechanisms that might drive the co-evolution of life and geology (e.g., Lovelock and Margulis 1974). For example, the appearance of surface life likely modulates weathering, potentially increasing sedimentary input in subduction trenches. Höning et al. (2014) modeled mantle hydration and continental coverage for model biotic and abiotic Earths and found that a biosphere tends to promote a

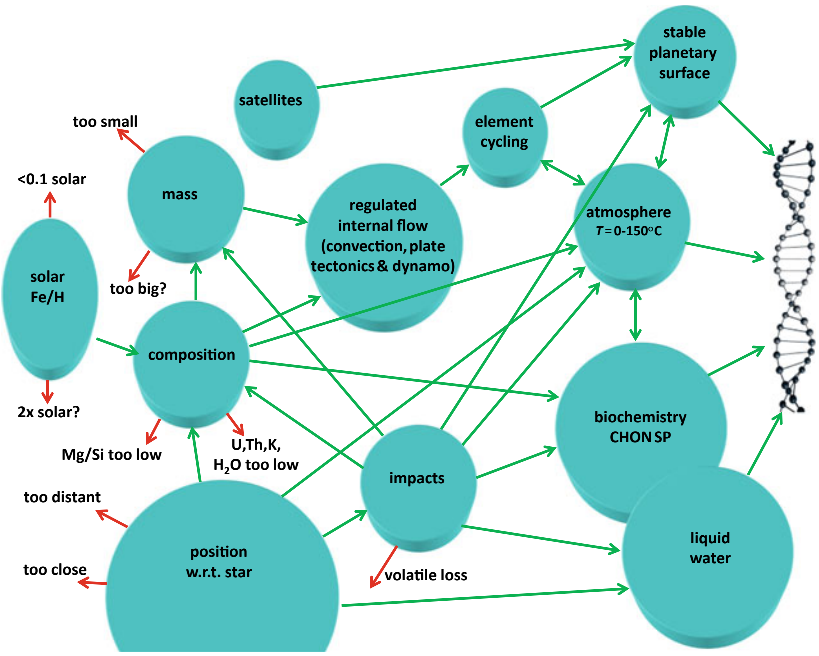

Fig. 10.5 Schematic representation of possible interactions between the ten factors proposed in this chapter that exert controls on planetary habitability. The flow from left to right transitions from zeroth order requirements for a terrestrial planet to those mechanisms thought to be responsible for maintaining a habitable Earth Red arrows show planetary histories contraindicative to biopoiesis whereas green arrows link to paths potentially leading to life

wet mantle and large continental surface area whereas an abiotic Earth tends to develop a dry mantle and low continental coverage. Thus the rise of biologic activity could help prolong plate tectonics (and thus element cycling) even as internal heat generation wanes.

The reasoning behind most of the interrelationships shown in Fig. 10.5 is drawn from the forgoing discussion of the ten ingredients for terrestrial life but is, in most cases, highly speculative. My hope is that it might help the reader to intuit other possible interrelationships while also stimulating a critical appraisal as this form of analysis remains in its infancy. The complexity implicit in this figure may give the reader the impression that the likelihood of biologic activity appearing on a planet is vanishingly small and thus there must be more robust mechanisms that short circuit this convolution of processes leading to intelligent life. But recall the anthropic principle from Sect. 10.2. Our ability to observe the universe only means that the large number of low-probability events leading to habitability happened once (Chopra and Lineweaver 2016). And the known universe is a big place.

10.2.12 Is Life Common in the Universe?

As just noted, a discussion of possible interrelationships between a planet's physical state and biologic destiny inevitably leads to the question: Is abiogenesis inevitable elsewhere in the universe or highly improbable? If habitation is likely, does complex or intelligent life necessarily follow? Does the fact that microbial life appears to have arisen relatively quickly on Earth—from virtual certainty by 3.5 Ga to possibly as early as 4.4 Ga (Betts et al. 2018; Sect. 11.6.3)—mean that it is abundant elsewhere? Beginning with the last question, from a purely statistical perspective, the lack of information about life elsewhere precludes drawing a clear conclusion (Lineweaver and Davis 2002; Spiegel and Turner 2012). However, finding a single additional example of life arising independent of ours would dramatically increase confidence that biopoiesis is a universal feature of the cosmos (Spiegel and Turner 2012).

Hubble's (1926) discovery of galaxies beyond the Milky Way began an exploration of the size of the observable universe which we now estimate holds at least two trillion galaxies (Conselice et al. 2016). By the early 1960s, radio astronomers had begun to estimate the number of civilizations within just our own galaxy that might be capable of communicating with Earth. Beginning in 1961, the well-known Drake equation (in essence, the rate of star formation times the cumulative fractions that define the time averaged number of civilizations sending detectable signs of their existence into space) was used to estimate the likelihood of extraterrestrial contact. Early estimates ranged up to many tens of millions of such worlds (Sagan and Drake 1975; Drake and Sobel 1992) leading many to infer that the probability of ours being the only advanced civilization among 'billions and billions' of potentially habitable planets was very low. The advent of exoplanetology increased all the astrophysical terms embodied in the Drake equation making contact seemingly more plausible. For example, Frank and Sullivan (2016) calculated that a probability of a habitable zone planet developing a technological species even as low as 1 in 10^{24} would mean that we are unlikely to be the only technological intelligence in the galaxy.

However, the very scale of the 'billions and billions' of Milky Way planets led to the 'Fermi Paradox'. Even at 10% of the speed of light, long-lived civilizations could by now have traveled anywhere in the galaxy and yet we have not seen any evidence of extraterrestrial contact (Hart 1975; Tipler 1981). This 'Great Silence' suggests that we could be the only technologically advanced civilization in the galaxy (Brin 1983). But does biopoiesis inevitably lead to complex life—or a technologically capable species? In *Rare Earth*, Ward and Brownlee (2000) argued that the conditions required to host complex life (in effect, the ten ingredients for life) are so exceptional in the universe that it is unlikely to be widespread. Publication of *Rare Earth* greatly stimulated this debate and in the ensuing period books advocating both viewpoints—a galaxy potentially teeming with complex life (e.g., Darling 2001; Kasting 2010) or one without (e.g., Waltham 2014)—have appeared.

This lack of convergence is a reflection of the single biggest limitation in the debate: that since Earth provides our only example of life, assumptions about the geologic conditions that pertained during its emergence directly influence views on the likelihood of widespread planetary habitability. For example, Ward and Brownlee (2000) view the Hadean in bleak terms: "For the first several 100 of millions of years of its existence…this constant rain of comets and asteroids would have driven temperatures high enough to melt surface rock. No water formed as a liquid on the surface. Clearly there would be no chance for life to form or survive on the planet's surface. It was hell on Earth". Thus their pessimism about life advancing elsewhere is in some ways unsurprising.

10.2.13 Constraints from Hadean Zircons

The arguments developed in this chapter are largely an academic exercise as we presently have no way of acquiring sufficiently detailed knowledge to test most of these speculations. That said, it is worth pointing out that the interpretations developed from Hadean zircon geochemical results reviewed in Chaps. 7–9 and this chapter potentially bear on six of the ten ingredients for life—the presence of surface and interior water, the role of impacts on early Earth, internal heat generation, surface recycling, and the existence of a Hadean geodynamo.

10.3 Mineralogic Considerations

10.3.1 Hadean Mineralogy

Because we define the Hadean eon (pre-4.02 Ga) by the absence of a known terrestrial rock record (Sect. 1.3), acquiring knowledge of what minerals then existed must necessarily be by implication. Neither of the two approaches thus far utilized, thought experiments (Hazen 2013) and documenting primary inclusions in Hadean detrital zircons (Bell et al. 2018), is likely to provide a complete inventory, but the former has the potential for misdirection that is worth pointing out here.

The presence or absence of key mineral phases during the Hadean eon has significant implications for the plausibility of certain pathways to life. The recognition of the catalytic properties of RNA (i.e., RNA can be both genetic material and a biologic catalyst; Kruger et al. 1982) led to the RNA world hypothesis. This posits an evolutionary stage in which self-replicating RNA molecules arose before the emergence of DNA and proteins (Neveu et al. 2013). Each nucleotide in RNA contains a ribose sugar with an attached base (A, C, G or U) and a phosphate group. Thus a postulated paucity of terrestrial phosphate minerals on early Earth as a source of reactive phosphorous (Griffith et al. 1977; cf. Planavsky et al. 2010) could imply that biopoiesis was forestalled until new geologic conditions prevailed. The observation of leachable apatite inclusions in Hadean Jack Hills zircons (Bell et al. 2018) suggests that dissolved phosphate was available by $\sim$4.3 Ga. Although ribose is unstable in many environments, aqueous solutions containing high borate concentrations stabilize that molecule. Several authors have argued that borate minerals didn't exist in sufficient quantities when the prebiotic synthesis processes that led to RNA occurred (Hazen 2013; Grew et al. 2011). However, laboratory partition experiments coupled with boron contents of >4 Ga zircons (Trail et al. 2017) suggest that Hadean crustal boron concentrations were similar to that of modern Earth.

Hazen (2013) concluded that Hadean Earth supported fewer than 10% of the $\sim$4800 known mineral species and that the "relative Hadean mineralogical parsimony is a consequence of the limited modes of mineral paragenesis prior to 4 Ga". Four criteria were enumerated that eliminated minerals from consideration as significant Hadean phases. These assumptions are: (1) rare minerals today were never widely distributed or volumetrically significant, (2) minerals arising primarily at convergent boundaries didn't exist because plate tectonics had not yet initiated, (3) biologically-mediated minerals were absent because all life is post-Hadean, and (4) redox-sensitive minerals requiring a high oxygen partial pressure f didn't predate the Great Oxidation Event. But note that (i) since only ¼ of known minerals are documented from more than 25 localities, criterion (1) is also true for all but $\sim$15% of the presently known mineral species; (ii) while there is no evidence that plate tectonics was not operating on Earth during Hadean times, there is some evidence that it was (Hopkins et al. 2008; Sect. 9.10); (iii) while there is no evidence that life did not arise during the Hadean, light carbon isotope signatures in carbonaceous inclusions in a 4.1 Ga zircon suggest that it may have (Bell et al. 2015; Sect. 11.4.2).

While redox-sensitive minerals requiring an oxygen fugacity higher than the hematite-magnetite buffer were probably rare on early Earth (Aulbach and Stagno 2016; Nicklas et al. 2019), local conditions might have supported them in microenvironments much as anaerobic microbiota thrive in near-surface conditions today (Bell et al. 2015; Morrison et al. 2018).

Bell et al. (2018) identified thirteen minerals as primary inclusions in Hadean Jack Hills zircons; quartz, plagioclase, alkali feldspar, muscovite, biotite, hornblende, sphene, apatite, monazite, ilmenite, rutile, Fe-oxides, Al_2SiO_5 and graphite. As two-thirds of all documented primary inclusions are quartz and muscovite, they inferred that I- and S-type felsic granitoids coexisted during the Hadean while quartz-deficient tonalites and trondhjemites (Sect. 9.3) were a less abundant source (cf. Hazen 2013). Bell et al. (2018) also surveyed a large number of zircons from Phanerozoic I-, S-, and A-type granitoids and found them to host thirty-one distinct mineral inclusions (i.e., a 0.65% occurrence rate relative to the known total), ranging from the expected granitic species (e.g., quartz, feldspars, micas) to the surprising (e.g., NaCl, Cu). However, as any one locality contains only three to nineteen included mineral species (10 ± 4), Bell et al. (2018) viewed the Jack Hills suite as potentially reflecting similar mineralogic complexity to today. But many of $\sim$5000 known minerals form by fluid interactions in the upper few km of crust, a zone almost exclusive of zircon formation. Thus not finding zeolites, sulfates, borates or other such inclusions in Hadean zircons is not evidence they didn't then exist, but rather that they either haven't yet been observed or, more likely, were not amenable to capture by zircon.

Bell et al. (2018) concluded that geochemistry provides no significant limitation on the type or abundance of minerals that may have been present on Hadean Earth and that speculations seeking to impose such restrictions risk inhibiting thought regarding possible scenarios for the emergence of life on Earth. Morrison et al. (2018) expanded Hazen's (2013) list of possible Hadean minerals by considering those that could have formed by direct precipitation from organic compounds, those produced by impacts, and those formed via abiological redox processes. Hazen et al. (2019) acknowledged that phases in which elements key to biologic processes (e.g., B and Mo) are essential structural components, are not required for biopoiesis as modal crustal minerals incorporate them as trace or minor constituents.

10.3.2 How Do Pink and White Granites Tell You a Planet Was Inhabited?

Anyone who has ever wondered why some granite countertops have a pinkish hue and others are white is asking a question that is ultimately related to the existence of life on Earth. As previously noted, Earth's upper mantle appears to have remained relatively oxidized since Hadean times, close to the fayalite-magnetite-quartz (FMQ) oxygen fugacity buffer, whereas Hadean zircons range from as oxidized as FMQ to several orders of magnitude more reduced (see Sects. 7.8.2 and 7.8.5).

Under relatively reducing conditions in which Fe^{2+} is the dominant species, iron is insoluble in alkali feldspar which, as a result, retains a milky white appearance. Pink granites are pink because under more oxidizing conditions, the constituent alkali feldspars can incorporate Fe^{+3} into their crystal lattice. The interaction between Fe and the adjacent ligand causes changes in *d*-orbital energies that alter optical absorption properties giving alkali feldspar a pinkish coloration.

Convergent margin magmatic belts are often characterized by an ilmenite-magnetite line parallel to the arc which separates more oxidized (magnetite-bearing) granites intruded into oceanic basement, from reduced (ilmenite-bearing) granites intruded into continental metasediments (Ishihara 1977). This boundary is often coincident with the I-S line which separates granites arising from purely igneous sources (I-type) from those dominated by melting of pelitic rocks (S-type), and a transition from white to pink alkali feldspar (e.g., Todd et al. 2003). The lower redox state in the hinterland reflects incorporation of reduced carbon, largely in the form of fossil plant and microbial remains, into the terrestrial metasediments. During burial, kerogens present in the sediments thermally decompose, eventually leaving only a graphitic residuum. Upon anatexis, the presence of that residue scrubs free oxygen by reacting it to CO or CO_2 resulting in a very low partial pressure of oxygen.

In effect, an alien probe landing on the Lachlan granite belt of southeastern Australia (the type location of the I-S designation; White and Chappell 1977) could infer from the appearance of both white and pink granites alone that there had been life on Earth when the protoliths of these rocks were created. The observation of both ilmenite and magnetite inclusions (and graphite and I- and S-type inclusion assemblages) in >4 Ga Jack Hills granitoid zircons (Sects. 7.8.2 and 7.8.5) implies their origin in a range of redox environments that is consistent with life having emerged during the Hadean.

10.4 Critical Summary

So, was the Hadean habitable? We don't know with confidence how or when life began on this planet and thus are uncertain of the circumstances under which it occurred other that it must surely have arisen prior to ca. 3.5 Ga (see Chap. 11). While there is little question that the emergence of life on Earth required soluble bioactive elements, an energy source, and liquid water, this chapter is otherwise a tour across the landscape of astrobiologic speculation. If there is value in this exercise, it is to draw attention to possible connections between specific aspects of the geologic evolution of our planet and the emergence of life as the two appear to be inexorably linked.

References

Abe, Y. (2007). Behavior of water during terrestrial planet formation. *Geochimica et Cosmochimica Acta, 71,* A2.

Abramov, O., & Mojzsis, S. J. (2009). Microbial habitability of the Hadean Earth during the late heavy bombardment. *Nature, 459,* 419–422.

Adamala, K., Anella, F., Wieczorek, R., Stano, P., Chiarabelli, C., & Luisi, P. L. (2014). Open questions in origin of life: Experimental studies on the origin of nucleic acids and proteins with specific and functional sequences by a chemical synthetic biology approach. *Computational and Structural Biotechnology Journal, 9,* e201402004.

Ahrens, T. J., & Schubert, G. (1975). Gabbro-eclogite reaction rate and its geophysical significance. *Reviews of Geophysics, 13,* 383–400.

Alexander, C. M. D., Bowden, R., Fogel, M. L., Howard, K. T., Herd, C. D. K., & Nittler, L. R. (2012). The provenances of asteroids, and their contributions to the volatile inventories of the terrestrial planets. *Science, 337,* 721–723.

Alexander, C. M. D., McKeegan, K. D., & Altwegg, K. (2018). Water reservoirs in small planetary bodies: Meteorites, asteroids, and comets. *Space Science Reviews, 214*(36), 1–47.

Altwegg, K., Balsiger, H., Bar-Nun, A., Berthelier, J. J., Bieler, A., Bochsler, P., et al. (2015). 67P/Churyumov-Gerasimenko, a Jupiter family comet with a high D/H ratio. *Science, 347*. https://doi.org/10.1126/science.1261952.

Alvarez, W., & Asaro, F. (1990). An extraterrestrial impact. *Scientific American, 263,* 78–84.

Anderson, D. L. (1982). Hotspots, polar wander, Mesozoic convection and the geoid. *Nature, 297,* 391–393.

Anglada-Escudé, G., Amado, P. J., Barnes, J., Berdinas, Z. M., Butler, R. P., Coleman, G. A., et al. (2016). A terrestrial planet candidate in a temperate orbit around Proxima Centauri. *Nature, 536,* 437–440.

Arrhenius, S. (1908). *Worlds in the making: The evolution of the universe*. Harper and Brothers.

Aulbach, S., & Stagno, V. (2016). Evidence for a reducing Archean ambient mantle and its effects on the carbon cycle. *Geology, 44,* 751–754.

Bell, E. A., Boehnke, P., Harrison, T. M., & Mao, W. L. (2015). Potentially biogenic carbon preserved in a 4.1 billion-year-old zircon. *Proceedings of the National Academy of Sciences, 112*(47), 14518–14521.

Bell, E. A., Boehnke, P., Harrison, T. M., & Wielicki, M. M. (2018). Mineral inclusion assemblage and detrital zircon provenance. *Chemical Geology, 477,* 151–160.

Betts, H. C., Puttick, M. N., Clark, J. W., Williams, T. A., Donoghue, P. C., & Pisani, D. (2018). Integrated genomic and fossil evidence illuminates life's early evolution and eukaryote origin. *Nature Ecology & Evolution, 2*, 1556–1562.

Biggin, A. J., de Wit, M. J., Langereis, C. G., Zegers, T. E., Voûte, S., Dekkers, M. J., & Drost, K. (2011). Palaeomagnetism of Archaean rocks of the Onverwacht Group, Barberton Greenstone Belt (southern Africa): Evidence for a stable and potentially reversing geomagnetic field at ca. 3.5 Ga. *Earth and Planetary Science Letters, 302*, 314–328.

Brin, G. D. (1983). The great silence—The controversy concerning extraterrestrial intelligent life. *Quarterly Journal of the Royal Astronomical Society, 24,* 283–309.

Bryan, M. L., Knutson, H. A., Howard, A. W., Ngo, H., Batygin, K., Crepp, J. R., et al. (2016). Statistics of long period gas giant planets in known planetary systems. *The Astrophysical Journal, 821,* 89.

Buffett, B. A. (2003). The thermal state of Earth's core. *Science, 299,* 1675–1677.

Carter, B. (1983). The anthropic principle and its implications for biological evolution. *Philosophical Transactions of the Royal Society of London. Series A, Mathematical and Physical Sciences, 310,* 347–363.

Castelle, C. J., & Banfield, J. F. (2018). Major new microbial groups expand diversity and alter our understanding of the tree of life. *Cell, 172,* 1181–1197.

Chambers, J. (2004). Planetary accretion in the inner solar system. *Earth and Planetary Science Letters, 223,* 241–252.

Chopra, A., & Lineweaver, C. H. (2016). The case for a Gaian bottleneck: The biology of habitability. *Astrobiology, 16,* 7–22.

Cleaves, H. J., Chalmers, J. H., Lazcano, A., Miller, S. L., & Bada, J. L. (2008). A reassessment of prebiotic organic synthesis in neutral planetary atmospheres. *Origins of Life and Evolution of Biospheres, 38,* 105–115.

Commeyras, A., Collet, H., Boiteau, L., Taillades, J., Vandenabeele-Trambouze, O., Cottet, H., et al. (2002). Prebiotic synthesis of sequential peptides on the Hadean beach by a molecular engine working with nitrogen oxides as energy sources. *Polymer International, 51,* 661–665.

Conselice, C. J., Wilkinson, A., Duncan, K., & Mortlock, A. (2016). The evolution of galaxy number density at $z < 8$ and its implications. *The Astrophysical Journal, 830,* 83–93.

Cramer, J. G. (1986). The pump of evolution. *Analog Science Fiction & Fact Magazine, 106,* 124–127.

Crick, F. H. (1981). *Life itself: Its origin and nature* (p. 192). New York: Simon and Schuster.

Crick, F. H., & Orgel, L. E. (1973). Directed panspermia. *Icarus, 19,* 341–346.

Darling, D. (2001). *Life everywhere: The maverick science of astrobiology* (p. 206). New York, NY: Basic Books.

Darwin, C. R. (1871). *The descent of man and selection in relation to sex* (p. 589). London: John Murray.

Davies, J. H., & Davies, D. R. (2009). Earth's surface heat flux. *Solid Earth Discussions, 1,* 1–45.

de Montserrat Navarro, A., Morgan, J. P., Vannucchi, P., Connolly, J. A. (2016). Has Earth's plate tectonics led to rapid core cooling? *AGU Fall Meeting Abstracts*.

Dick, H. J., Lin, J., & Schouten, H. (2003). An ultraslow-spreading class of ocean ridge. *Nature, 426,* 405–412.

Dole, S. H. (1964). *Habitable planets for man*. New York: Blaisdell Publ. Co.

Drake, M. J. (2005). Origin of water in the terrestrial planets. *Meteoritics & Planetary Science, 40,* 519–527.

Drake, F., & Sobel, D. (1992). *Is anyone out there?: The scientific search for extraterrestrial intelligence*. Delacorte Press.

Dye, S. T. (2012). Geoneutrinos and the radioactive power of the Earth. *Reviews of Geophysics, 50*, 2012RG000400, 19 pp.

Elkins-Tanton, L. T. (2008). Linked magma ocean solidification and atmospheric growth for Earth and Mars. *Earth and Planetary Science Letters, 271,* 181–191.

Elsasser, W. M. (1958). The earth as a dynamo. *Scientific American, 198,* 44–49.

Farquhar, J., Bao, H., & Thiemens, M. (2000). Atmospheric influence of Earth's earliest sulfur cycle. *Science, 289,* 756–758.

Fei, H., Yamazaki, D., Sakurai, M., Miyajima, N., Ohfuji, H., Katsura, T., et al. (2017). A nearly water-saturated mantle transition zone inferred from mineral viscosity. *Science Advances, 3,* e1603024.

Fernández, Y. R. (2003). The nucleus of comet Hale-Bopp (C/1995 O1): Size and activity. In *International Astronomical Union Colloquium* (Vol. 186, pp. 3–25). Cambridge University Press.

Forsyth, D., & Uyeda, W. S. (1975). On the relative importance of the driving forces of plate motion. *Geophysical Journal of the Royal Astronomical Society, 4,* 163–200.

France-Lanord, C., & Derry, L. A. (1997). Organic carbon burial forcing of the carbon cycle from Himalayan erosion. *Nature, 390,* 65–67.

Frank, A., & Sullivan, W. T. (2016). A new empirical constraint on the prevalence of technological species in the universe. *Astrobiology, 16,* 359–362.

Frank, E. A., Meyer, B. S., & Mojzsis, S. J. (2014). A radiogenic heating evolution model for cosmochemically Earth-like exoplanets. *Icarus, 243,* 274–286.

Genda, H., & Abe, Y. (2005). Enhanced atmospheric loss on protoplanets at the giant impact phase in the presence of oceans. *Nature, 433,* 842–844.

Gonzalez, G., Brownlee, D., & Ward, P. (2001). The galactic habitable zone: Galactic chemical evolution. *Icarus, 152,* 185–200.

Grew, E. S., Bada, J. L., & Hazen, R. M. (2011). Borate minerals and origin of the RNA world. *Origins of Life and Evolution of Biospheres, 41,* 307–316.

Griffith, E. J., Ponnamperuma, C., & Gabel, N. W. (1977). Phosphorus, a key to life on the primitive earth. *Origins of Life and Evolution of Biospheres, 8,* 1–85.

Griggs, D. T., & Blacic, J. D. (1965). Quartz: Anomalous weakness of synthetic crystals. *Science, 147,* 292–295.

Grossman, L. (1972). Condensation in the primitive solar nebula. *Geochimica et Cosmochimica Acta, 36,* 597–619.

Gubbins, D., Alfe, D., Masters, G., Price, G. D., & Gillan, M. (2004). Gross thermodynamics of two-component core convection. *Geophysical Journal International, 157,* 1407–1414.

Haldane, J. B. S. (1929). The orgin of life. *Rationalist Annual, 3,* 3–10.

Hamano, K., Abe, Y., & Genda, H. (2013). Emergence of two types of terrestrial planet on solidification of magma ocean. *Nature, 497,* 607–610.

Harrison, T. M., Copeland, P., Kidd, W. S. F., & Yin, A. N. (1992). Raising Tibet. *Science, 255,* 1663–1670.

Hart, M. H. (1975). Explanation for the absence of extraterrestrials on earth. *Quarterly Journal of the Royal Astronomical Society, 16,* 128–135.

Hart, M. H. (1979). Habitable zones about main sequence stars. *Icarus, 37,* 351–357.

Hartogh, P., Lis, D. C., Bockelée-Morvan, D., de Val-Borro, M., Biver, N., Küppers, M., et al. (2011). Ocean-like water in the Jupiter-family comet 103P/Hartley 2. *Nature, 478,* 218.

Hazen, R. M. (2013). Paleomineralogy of the Hadean Eon: A preliminary species list. *American Journal of Science, 313,* 807–843.

Hazen, R. M., Gagné, O. C., Liu, C., Morrison, S. M., & Runyon, S. E. (2019). Mineral environments of the Hadean Eon: Implications for Earth's geochemical evolution and the origins of life. In *Abstracts, 2019 Astrobiology Conference*.

Hevey, P. J., & Sanders, I. S. (2006). A model for planetesimal meltdown by ^{26}Al and its implications for meteorite parent bodies. *Meteoritics & Planetary Science, 41,* 95–106.

Hirschmann, M. M. (2006). Water, melting, and the deep Earth H_2O cycle. *Annual Review of Earth and Planetary Sciences, 34,* 629–653.

Hirth, G., & Kohlstedt, D. L. (1996). Water in the oceanic upper mantle: Implications for rheology, melt extraction and the evolution of the lithosphere. *Earth and Planetary Science Letters, 144,* 93–108.

Hoffman, P. F., Kaufman, A. J., Halverson, G. P., & Schrag, D. P. (1998). A neoproterozoic snowball Earth. *Science, 281,* 1342–1346.

Höning, D., Hansen-Goos, H., Airo, A., & Spohn, T. (2014). Biotic vs. abiotic Earth: A model for mantle hydration and continental coverage. *Planetary and Space Science, 98,* 5–13.

Hopkins, M., Harrison, T. M., & Manning, C. E. (2008). Low heat flow inferred from >4 Ga zircons suggests Hadean plate boundary interactions. *Nature, 456,* 493–496.

Horner, J., & Jones, B. W. (2009). Jupiter—Friend or foe? II: The Centaurs. *International Journal of Astrobiology, 8,* 75–80.

Hubble, E. (1926). Extragalactic nebulae. *Astrophysical Journal, 64,* 321–369.

Hunten, D. M., & Donahue, T. M. (1976). Hydrogen loss from the terrestrial planets. *Annual Review of Earth and Planetary Sciences, 4,* 265–292.

Ishihara, S. (1977). The magnetite-series and ilmenite-series granitic rocks. *Mining Geology, 27,* 293–305.

Isson, T. T., & Planavsky, N. J. (2018). Reverse weathering as a long-term stabilizer of marine pH and planetary climate. *Nature, 560,* 471.

Ito, K., & Kennedy, G. C. (1967). Melting and phase relations in a natural peridotite to 40 kilobars. *American Journal of Science, 265,* 519–538.

Ito, K., & Kennedy, G. C. (1970). The fine structure of the basalt-eclogite transition. *Mineralogical Society of America Special Papers, 3,* 77–83.

Kasting, J. (2010). *How to find a habitable planet*. Princeton University Press.

Kasting, J. F., Whitmire, D. P., & Reynolds, R. T. (1993). Habitable zones around main sequence stars. *Icarus, 101,* 108–128.

Khurana, K. K., Kivelson, M. G., Stevenson, D. J., Schubert, G., Russell, C. T., Walker, R. J., et al. (1998). Induced magnetic fields as evidence for subsurface oceans in Europa and Callisto. *Nature, 395,* 77–780.

Kirchner, J. W. (1991). The Gaia hypotheses: Are they testable? Are they useful? In S. Schneider (Ed.), *Scientists on Gaia*. Cambridge, MA: MIT Press.

Kite, E. S., Gaidos, E., & Manga, M. (2011). Climate instability on tidally locked exoplanets. *The Astrophysical Journal, 743*, 41 (12 pp.).

Koga, T., & Naraoka, H. (2017). A new family of extraterrestrial amino acids in the Murchison meteorite. *Scientific Reports, 7*.

Kopparapu, R. K., Ramirez, R. M., SchottelKotte, J., Kasting, J. F., Domagal-Goldman, S., & Eymet, V. (2014). Habitable zones around main-sequence stars: Dependence on planetary mass. *The Astrophysical Journal Letters, 787*(L29), 1–6.

Korenaga, J. (2013). Initiation and evolution of plate tectonics on Earth: Theories and observations. *Annual Review of Earth and Planetary Sciences, 41*, 117–151.

Kruger, K., Grabowski, P. J., Zaug, A. J., Sands, J., Gottschling, D. E., & Cech, T. R. (1982). Self-splicing RNA: Autoexcision and autocyclization of the ribosomal RNA intervening sequence of Tetrahymena. *Cell, 31,* 147–157.

Labrosse, S., Poirier, J. P., & Le Mouël, J. L. (2001). The age of the inner core. *Earth and Planetary Science Letters, 190,* 111–123.

Labrosse, S., Hernlund, J. W., & Coltice, N. (2007). A crystallizing dense magma ocean at the base of the Earth's mantle. *Nature, 450,* 866–869.

Lammer, H., Kasting, J. F., Chassefière, E., Johnson, R. E., Kulikov, Y. N., & Tian, F. (2008). Atmospheric escape and evolution of terrestrial planets and satellites. *Space Science Reviews, 139,* 399–436.

Lammer, H., Kislyakova, K. G., Odert, P., Leitzinger, M., Schwarz, R., Pilat-Lohinger, E., Kulikov, Y. N., Khodachenko, M. L., Güdel, M., & Hanslmeier, A. (2011). Pathways to earth-like atmospheres. *Origins of Life and Evolution of Biospheres, 41*(6), 503–522.

Lammer, H., Selsis, F., Chassefière, E., Breuer, D., Grießmeier, J. M., Kulikov, Y. N., et al. (2010). Geophysical and atmospheric evolution of habitable planets. *Astrobiology, 10,* 45–68.

Laskar, J., & Robutel, P. (1993). The chaotic obliquity of the planets. *Nature, 361,* 608–612.

Lathe, R. (2004). Fast tidal cycling and the origin of life. *Icarus, 168,* 18–22.

Lathe, R. (2006). Early tides: Response to Varga et al. *Icarus, 180*, 277–280.

Lineweaver, C. H. (2001). An estimate of the age distribution of terrestrial planets in the universe: Quantifying metallicity as a selection effect. *Icarus, 151,* 307–313.

Lineweaver, C. H., & Chopra, A. (2012). What can life on Earth tell us about life in the universe? In *Genesis—In the beginning* (pp. 799–815). Dordrecht: Springer.

Lineweaver, C. H., & Davis, T. M. (2002). Does the rapid appearance of life on Earth suggest that life is common in the universe? *Astrobiology, 2,* 293–304.

Lineweaver, C. H., Fenner, Y., & Gibson, B. K. (2004). The galactic habitable zone and the age distribution of complex life in the Milky Way. *Science, 303,* 59–62.

Lis, D. C., Biver, N., Bockelée-Morvan, D., Hartogh, P., Bergin, E. A., Blake, G. A., et al. (2013). A Herschel study of D/H in water in the Jupiter-family comet 45P/Honda-Mrkos-Pajdušáková and prospects for D/H measurements with CCAT. *The Astrophysical Journal Letters, 774,* L3.

Lis, D. C., Bockelée-Morvan, D., Güsten, R., Biver, N., Stutzki, J., Delorme, Y., et al. (2019). Terrestrial deuterium-to-hydrogen ratio in water in hyperactive comets. *Astronomy & Astrophysics, 625,* L5.

Lissauer, J. J., Barnes, J. W., & Chambers, J. E. (2012). Obliquity variations of a moonless Earth. *Icarus, 217,* 77–87.

Lodders, K., Palme, H., & Gail, H. P. (2010). Solar system abundances of the elements. In *Principles and perspectives in cosmochemistry* (pp. 379–417).

Lovelock, J. E., & Margulis, L. (1974). Atmospheric homeostasis by and for the biosphere: The Gaia hypothesis. *Tellus, 26,* 2–10.
Lyubetskaya, T., & Korenaga, J. (2007). Chemical composition of Earth's primitive mantle and its variance: 1. Method and results. *Journal of Geophysical Research, 112,* B03211. https://doi.org/10.1029/2005JB004223.
Macdonald, K. C., Becker, K., Spiess, F. N., & Ballard, R. D. (1980). Hydrothermal heat flux of the "black smoker" vents on the East Pacific Rise. *Earth and Planetary Science Letters, 48,* 1–7.
Marty, B. (2012). The origins and concentrations of water, carbon, nitrogen and noble gases on Earth. *Earth and Planetary Science Letters, 313*, 56–66.
Mayor, M., & Queloz, D. (1995). A Jupiter-mass companion to a solar-type star. *Nature, 378,* 355–359.
McDonough, W. F., & Sun, S. S. (1989). The composition of the Earth. *Chemical Geology, 120,* 223–253.
McKenzie, D. P. (1970). Temperature and potential temperature beneath island arcs. *Tectonophysics, 10,* 357–366.
Miller, S. L., & Urey, H. C. (1959). Origin of life. *Science, 130,* 1622–1624.
Moore, W. B., Lenardic, A., Jellinek, A. M., Johnson, C. L., Goldblatt, C., & Lorenz, R. D. (2017). How habitable zones and super-Earths lead us astray. *Nature Astronomy, 1*. https://doi.org/10.1038/s41550-017-0043.
Morrison, S., Runyon, S., & Hazen, R. (2018). The paleomineralogy of the Hadean Eon revisited. *Life, 8,* 64.
Mulders, G. D., Pascucci, I., & Apai, D. (2015). A stellar-mass-dependent drop in planet occurrence rates. *Astrophysical Journal, 798*, 112, 18 pp.
Nakagawa, T., Nakakuki, T., & Iwamori, H. (2015). Water circulation and global mantle dynamics: Insight from numerical modeling. *Geochemistry, Geophysics, Geosystems, 16,* 1449–1464.
Neveu, M., Kim, H. J., & Benner, S. A. (2013). The "strong" RNA world hypothesis: Fifty years old. *Astrobiology, 13,* 391–403.
Nicklas, R. W., Puchtel, I. S., Ash, R. D., Piccoli, P. M., Hanski, E., Nisbet, E. G., et al. (2019). Secular mantle oxidation across the Archean-Proterozoic boundary: Evidence from V partitioning in komatiites and picrites. *Geochimica et Cosmochimica Acta, 250,* 49–75.
Nimmo, F., & Stevenson, D. J. (2000). Influence of early plate tectonics on the thermal evolution and magnetic field of Mars. *Journal of Geophysical Research: Planets, 105,* 11969–11979.
Nimmo, F., Price, G. D., Brodholt, J., & Gubbins, D. (2004). The influence of potassium on core and geodynamo evolution. *Geophysical Journal International, 156,* 363–376.
O'Neill, C., & Debaille, V. (2014). The evolution of Hadean-Eoarchaean geodynamics. *Earth and Planetary Science Letters, 406,* 49–58.
O'Neill, C., & Lenardic, A. (2007). Geological consequences of super-sized Earths. *Geophysical Research Letters, 34*. https://doi.org/10.1029/2007gl030598.
O'Rourke, J. G., & Stevenson, D. J. (2016). Powering Earth's dynamo with magnesium precipitation from the core. *Nature, 529*, 387–389.
Oparin, A. I. (1957). *The origin of life on the Earth*. London: Oliver and Boyd.
Pearson, D. G., Brenker, F. E., Nestola, F., McNeill, J., Nasdala, L., Hutchison, M. T., et al. (2014). Hydrous mantle transition zone indicated by ringwoodite included within diamond. *Nature, 507,* 221–224.
Piro, A. L. (2018). Exoplanets torqued by the combined tides of a moon and parent star. *Astronomical Journal, 156*, 54, 10 pp.
Planavsky, N. J., Rouxel, O. J., Bekker, A., Lalonde, S. V., Konhauser, K. O., Reinhard, C. T., et al. (2010). The evolution of the marine phosphate reservoir. *Nature, 467,* 1088–1090.
Podolak, M., & Zucker, S. (2004). A note on the snow line in protostellar accretion disks. *Meteoritics & Planetary Science, 39,* 1859–1868.
Pozzo, M., Davies, C., Gubbins, D., & Alfe, D. (2012). Thermal and electrical conductivity of iron at Earth's core conditions. *Nature, 485,* 355–358.

Ratner, M. I., & Walker, J. C. (1972). Atmospheric ozone and the history of life. *Journal of the Atmospheric Sciences, 29,* 803–808.

Raymond, S. N., Armitage, P. J., Moro-Martín, A., Booth, M., Wyatt, M. C., Armstrong, J. C., et al. (2011). Debris disks as signposts of terrestrial planet formation. *Astronomy & Astrophysics, 530*(A62), 1–23.

Righter, K., & Drake, M. J. (1999). Effect of water on metal-silicate partitioning of siderophile elements a high pressure and temperature terrestrial magma ocean and core formation. *Earth and Planetary Science Letters, 171,* 383–399.

Ringwood, A. E. (1962). A model for the upper mantle. *Journal of Geophysical Research, 67,* 857–867.

Ringwood, A. E. (1989). Significance of the terrestrial Mg/Si ratio. *Earth and Planetary Science Letters, 95,* 1–7.

Rudnick, R. L., & Gao, S. (2003). Composition of the continental crust. *Treatise on Geochemistry, 3,* 1–64.

Sagan, C., & Drake, F. (1975). The search for extraterrestrial intelligence. *Scientific American, 232,* 80–89.

Schopf, J. W. (Ed.). (2002). *Life's origin: The beginnings of biological evolution*. University of California Press.

Sclater, J., Jaupart, C., & Galson, D. (1980). The heat flow through oceanic and continental crust and the heat loss of the Earth. *Reviews of Geophysics, 18,* 269–311.

Shock, E., & Canovas, P. (2010). The potential for abiotic organic synthesis and biosynthesis at seafloor hydrothermal systems. *Geofluids, 10,* 61–192.

Sleep, N. H. (2000). Evolution of the mode of convection within terrestrial planets. *Journal of Geophysical Research, 105,* 17563–17578.

Sleep, N. H., & Zahnle, K. (1998). Refugia from asteroid impacts on early Mars and the early Earth. *Journal of Geophysical Research, 103,* 28529–28544.

Sleep, N. H., Zahnle, K. J., Kasting, J. F., & Morowitz, H. J. (1989). Annihilation of ecosystems by large asteroid impacts on the early earth. *Nature, 342,* 139–142.

Solomon, S. C. (1979). Formation, history and energetics of cores in the terrestrial planets. *Physics of the Earth and Planetary Interiors, 19,* 168–182.

Spiegel, D. S., & Turner, E. L. (2012). Bayesian analysis of the astrobiological implications of life's early emergence on Earth. *Proceedings of the National Academy of Sciences, 109,* 395–400.

Stern, R. J. (2016). Is plate tectonics needed to evolve technological species on exoplanets? *Geoscience Frontiers, 7,* 573–580.

Tang, F., Taylor, R. J. M., Einsle, J. F., Borlina, C. S., Fu, R. R., Weiss, B. P., Williams, H. M., Williams, W., Nagy, L., Midgley, P., Lima, E. A., Bell, E. A., Harrison, T. M., & Harrison, R. (2019). Secondary magnetite in ancient zircon precludes analysis of a Hadean-Paleoarchean geodynamo. *Proceedings of the National Academy of Sciences, 116*, 407–412.

Tarduno, J. A., Blackman, E. G., & Mamajek, E. E. (2014). Detecting the oldest geodynamo and attendant shielding from the solar wind: Implications for habitability. *Physics of the Earth and Planetary Interiors, 233,* 68–87.

Tarduno, J. A., Cottrell, R. D., Davis, W. J., Nimmo, F., & Bono, R. K. (2015). A Hadean to Paleoarchean geodynamo recorded by single zircon crystals. *Science, 349,* 521–524.

Tipler, F. J. (1981). A brief history of the extraterrestrial intelligence concept. *Quarterly Journal of the Royal Astronomical Society, 22,* 133–145.

Todd, V. R., Shaw, S. E., & Hammarstrom, J. M. (2003). Cretaceous plutons of the Peninsular Ranges batholith, San Diego and westernmost Imperial Counties, California: Intrusion across a Late Jurassic continental margin. *Geological Society of America Special Paper, 374,* 185–235.

Trail, D., Buettner, J., Chowdhury, W., Bell, E. A., & Liu, M.-C. (2017). Decoding old zircons. In *Before life: The chemical, geological and dynamical setting for the emergence of an RNA world* (pp. 29–30). Workshop, Boulder, CO, October 9–12.

Trail, D., Watson, E. B., & Tailby, N. D. (2011). The oxidation state of Hadean magmas and implications for early Earth's atmosphere. *Nature, 480*(7375), 79–82.

Turcotte, D. L. (1993). An episodic hypothesis for Venusian tectonics. *Journal of Geophysical Research: Planets, 98,* 17061–17068.

Urey, H. C. (1952). *The planets: Their origin and development* (p. 245). New Haven: Yale University Press.

Valencia, D., & O'Connell, R. J. (2009). Convection scaling and subduction on Earth and super-Earths. *Earth and Planetary Science Letters, 286,* 492–502.

Valencia, D., O'Connell, R. J., & Sasselov, D. D. (2007). Inevitability of plate tectonics on super-Earths. *The Astrophysical Journal Letters, 670,* L45.

Van Heck, H. J., & Tackley, P. J. (2011). Plate tectonics on super-Earths: Equally or more likely than on Earth. *Earth and Planetary Science Letters, 310,* 252–261.

Vidotto, A. A., Jardine, M., Morin, J., Donati, J. F., Lang, P., & Russell, A. J. B. (2013). Effects of M dwarf magnetic fields on potentially habitable planets. *Astronomy & Astrophysics, 557*, A67 (11 pp.).

Wächtershäuser, G. (1990). Evolution of the first metabolic cycles. *Proceedings of the National Academy of Sciences, 87,* 200–204.

Waltham, J. (2014). *Lucky planet* (p. 198). New York, NY: Basic Books (Perseus).

Ward, P. D., & Brownlee, D. (2000). *Rare earth: Why complex life is uncommon in the universe*. New York: Copernicus Books.

Weiss, B. P., Maloof, A. C., Tailby, N., Ramezani, J., Fu, R. R., Hanus, V., et al. (2015). Pervasive remagnetization of detrital zircon host rocks in the Jack Hills Western Australia and implications for records of the early geodynamo. *Earth and Planetary Science Letters, 430,* 115–128.

Weiss, B. P., Maloof, A. C., Harrison, T. M., Swanson-Hysell, N. L., Fu, R. R., Kirschvink, J. L., et al. (2016). Reply to comment on "Pervasive remagnetization of detrital zircon host rocks in the Jack Hills, Western Australia and implications for records of the early dynamo". *Earth and Planetary Science Letters, 450,* 409–412.

Weiss, B. P., Fu, R. R., Einsle, J. F., Glenn, D. R., Kehayias, P., Bell, E. A., et al. (2018). Secondary magnetic inclusions in detrital zircons from the Jack Hills, Western Australia, and implications for the origin of the geodynamo. *Geology, 46,* 427–430.

Wetherill, G. W. (1980). Formation of the terrestrial planets. *Annual Review of Astronomy and Astrophysics, 18,* 77–113.

Wetherill, G. W. (1985). Asteroidal source of ordinary chondrites. *Meteoritics, 20,* 1–22.

Wetherill, G. W. (1994). Possible consequences of absence of "Jupiters "in planetary systems. In *Planetary systems: Formation, evolution, and detection* (pp. 23–32). Dordrecht: Springer.

White, A. J. R., & Chappell, B. W. (1977). Ultrametamorphism and granitoid genesis. *Tectonophysics, 43,* 7–22.

Woese, C. R., Kandler, O., & Wheelis, M. L. (1990). Towards a natural system of organisms: proposal for the domains Archaea, Bacteria, and Eucarya. *Proceedings of the National Academy of Sciences, 87,* 4576–4579.

Woo, J. M. Y., Brasser, R., Matsumura, S., Mojzsis, S. J., & Ida, S. (2018). The curious case of Mars' formation. *Astronomy & Astrophysics, 617,* A17.

Zeebe, R. E. (2012). History of seawater carbonate chemistry, atmospheric CO_2, and ocean acidification. *Annual Review of Earth and Planetary Sciences, 40,* 141–165.

Zharkov, V. N. (2000). On the history of the lunar orbit. *Solar System Research, 34*, 1–11.

Ziegler, L. B., & Stegman, D. R. (2013). Implications of a long-lived basal magma ocean in generating Earth's ancient magnetic field. *Geochemistry, Geophysics, Geosystems, 14,* 4735–4742.

Zuluaga, J. I., Bustamante, S., Cuartas, P. A., & Hoyos, J. H. (2013). The influence of thermal evolution in the magnetic protection of terrestrial planets. *The Astrophysical Journal, 770*, 23 pp.

Morpho- and Chemo-Fossil Evidence of Early Life

11

Abstract

This chapter summarizes what is known about the timing of the emergence of life on Earth from the morpho- and chemo-fossil (chemical and isotopic signals remaining from the decomposition of living organisms) records. The geologic record back to ca. 3.5 billion years includes low grade sedimentary rocks in which organic residues of microbiota present during deposition have remained substantially intact. As different metabolic mechanisms variably fractionate carbon isotopes toward isotopically light values, a longstanding strategy has been to measure $\delta^{13}C$ in these organic residues, or kerogens, for biologic signatures. When compared to carbon isotopes in inorganic carbonate rocks, a consistent offset is seen throughout the past 3.5 billion years with inorganic carbon averaging $\delta^{13}C$ close to 0‰ and kerogens yielding $\delta^{13}C$ of approximately −25‰. As the latter value is broadly characteristic of oxygenating photosynthesis, this relationship has been seen as evidence of past biologic activity. However, as metamorphic grade increases, kerogens are reacted to simpler hydrocarbons, ultimately yielding graphitic residues. The discovery of isotopically light carbon isotopes in microscopic graphite inclusions in rocks as old as ca. 3.83 billion years and in a 4.1 Ga zircon extends the possible emergence of life on this planet back into the Hadean eon. Although inorganic mechanisms exist that could potentially produce light $\delta^{13}C$ signatures, these isotopic data are consistent with molecular clock calibrations of genomic mutations which suggest a lower bound for the time of life's origin between 4.1 and 4.4 billion years.

11.1 Microfossils and Carbon Isotopes

The opportunities we have to detect when, and in what form, living organisms emerged on Earth are largely controlled by the physical characteristics of those lifeforms (e.g., their preservation potential), the extent and degree of metamorphism

T. M. Harrison, *Hadean Earth*, https://doi.org/10.1007/978-3-030-46687-9_11

of the rock record, and our ability to quantitatively determine the age of a host rock. In contrast to the Phanerozoic fossil record of macroscopic life (i.e., since 0.542 Ga; Amthor et al. 2003) contained in globally correlative strata that can be quantitatively dated (either directly or via cross-cutting relationships; e.g., Bowring et al. 1993), the Precambrian (>0.542 Ga) presents a greater, but potentially still surmountable, challenge. The discovery of prokaryotic microfossils in Proterozoic (e.g., Barghoorn and Tyler 1965) and Archean (Awramik et al. 1983; Schopf and Packer 1987) strata permitted extension of morphofossil[1] identification back to ca. 3.5 Ga—the age of the oldest known sedimentary rocks of sufficiently low grade to preserve fossil forms (the Warrawoona Group, Western Australia; Awramik et al. 1983)—and thus there is broad agreement that life must have arisen prior to 3.5 Ga. However, prokaryotes are physiologically diverse and those with similar appearances can have very different metabolisms. Thus traditional morphology-based identification may be insufficient to classify Precambrian microfossil taxa.

One longstanding supplement to morphologic identification has been to undertake carbon isotopic analyses of kerogens—acid-resistant carbonaceous residues from microfossil-bearing strata—to identify the presence of a biologic, or 'vital', isotopic signature (Schidlowski et al. 1983; Hayes et al. 1992). This is because the different metabolic pathways of autotrophic prokaryotes characteristically fractionate carbon isotopes differently. For example, a kinetic isotope fraction catalyzed by ribulose-l,5-bisphosphate carboxylase oxygenase (RuBisCO), the dominant CO_2-fixing enzyme of the Calvin cycle, produces a $\delta^{13}C_{PDB}$ (i.e., $^{13}C/^{12}C$ relative to the Pee Dee belemnite in per mil, ‰, hereafter designated $\delta^{13}C$; Epstein et al. 1953) depletion of −20 to −30‰ relative to inorganic carbon (Wickman 1952; Schidlowski et al. 1983; Roeske and O'Leary 1984). This reaction is shown in context of carbon fixation in Fig. 11.1. The reductive citric acid cycle (Krebs) cycle, used by all aerobic organisms, yields $\delta^{13}C$ fractionations of about −10‰, the reductive pentose phosphate cycle about −25‰, the reductive acetyl-CoA pathway about −35‰ $\delta^{13}C$, and methanogenesis up to −90‰ $\delta^{13}C$ (Fuchs et al. 1979; Schidlowski et al. 1983; Preuss et al. 1989; Krzycki et al. 1987; House et al. 2000). Thus isotopic signatures of the kerogenous constituents of fossil microorganisms may provide evidence of metabolic and phylogenetic affinities beyond what morphofossil identification alone can do.

Carbon isotopes in carbonate and kerogen (i.e., inorganic vs. organic carbon) from a large database of rocks with ages from the present back to 3.5 Ga consistently show (Fig. 11.2) respective $\delta^{13}C$ averages of approximately 0 and −25‰ (Strauss and Moore 1992; Schidlowski 2001; Schopf 2014). The former value is that of modern inorganic carbon while the latter value, characteristic of oxygenating photosynthesis, is taken as evidence that past biologic activity is robustly preserved in kerogenous materials. But as metamorphic grade increases, the preservation potential of microfossils diminishes greatly. By amphibolite facies, metamorphism

[1]Fossilized remains of a lifeform recognized by their characteristic morphological features.

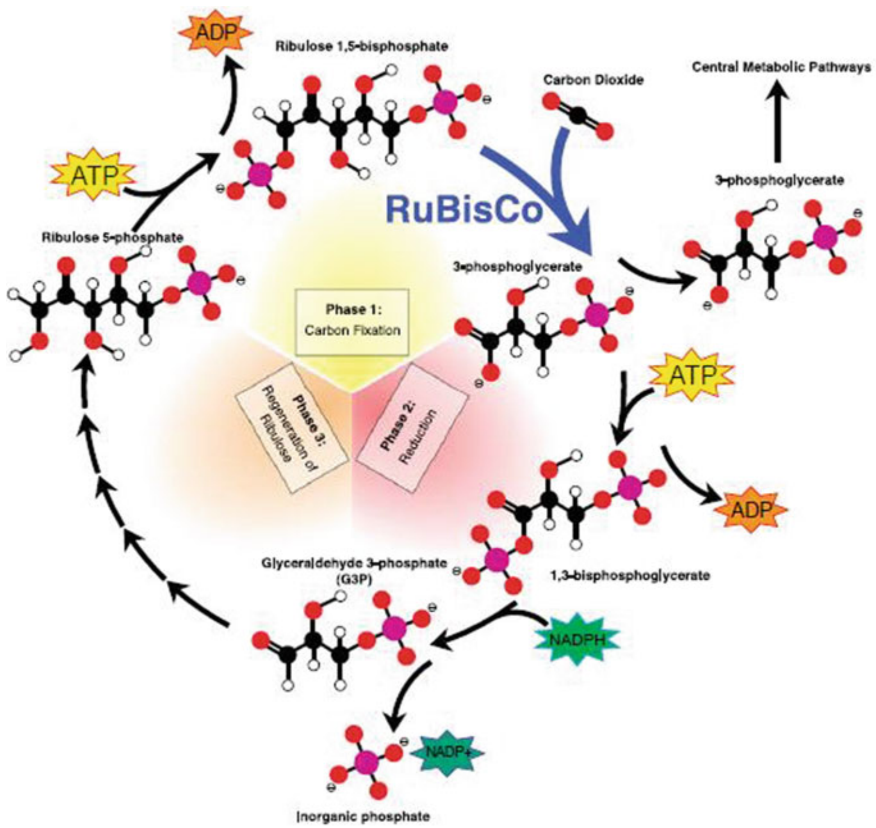

Fig. 11.1 A kinetic fractionation of carbon isotopes occurs in the first step of carbon fixation when the enzyme RuBisCO catalyzes reduction of CO_2 producing two, 3-carbon sugars called 3-phosphoglycerate, one of which is available to drive metabolism and the other catalyzes the cyclic reactions shown that recreate RuBisCo. Adenosine triphosphate (ATP) and adenosine diphosphate (ADP) provide the energy needed for this regeneration and $NADP^+$ (nicotinamide adenine dinucleotide phosphate), and its reduced form NADPH, aid nucleic acid synthesis. Attribution: Mike Jones

is sufficiently intense to effectively obliterate microfossil morphologies and to react any kerogens present to simpler hydrocarbons, ultimately yielding a graphitic residue.

Given broad agreement that life had become established on Earth by at least 3.4 Ga (e.g., Altermann and Kazmierczak 2003; Wacey et al. 2011), this chapter reviews putative evidence for earlier life on Earth. While the lack of a >4.02 Ga rock record largely—but not exclusively—leaves Eoarchean rocks for study, evidence from that source may imply even earlier biologic activity. Knowledge that living organisms had established or colonized our planet by, say, 3.8 Ga, bolsters

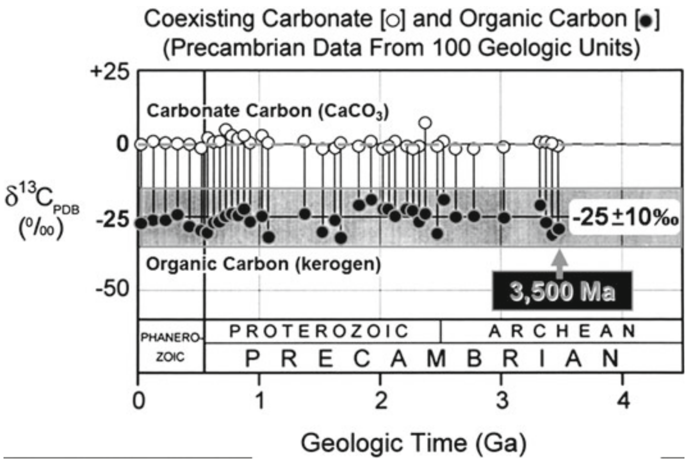

Fig. 11.2 Carbon isotopes in inorganic marine carbonates and bioorganic compounds preserved as kerogen over that past ca. 3.5 Ga. The variations in $\delta^{13}C_{org}$ seen in modern marine sediments are mirrored in the geologic record back to 3.5 Ga. Reproduced with permission from Schopf (2014)

the possibility of a habitable Hadean world, particularly if a case can be made for the existence of relatively sophisticated metabolic mechanisms (say, photosynthesis rather than the acetyl-CoA mechanism).

11.2 Bulk Rock Carbon Isotopes

Carbon isotopic analyses of bulk kerogen samples have proved useful in documenting the biologic origin of organic carbon in low-grade sedimentary rocks as old as Mesoarchean, and possibly even older. Rosing (1999) documented the occurrence of graphite globules in upper-greenschist, marine clastic rocks from the Isua supracrustal belt, West Greenland, for which cross-cutting relationships provide a lower age bound of 3.7 Ga. He interpreted the light carbon isotope composition ($\delta^{13}C \approx -19$) to indicate that the graphite globules are the remains of biogenic detritus of marine microorganisms, possibly plankton, that existed at or prior to 3.7 Ga.

Tashiro et al. (2017) measured total organic carbon content and carbon isotopes of graphite and carbonate in pelitic metasediments from the Saglek Block, northern Labrador. Similar recrystallization temperatures of the graphite and the host pelites suggested to them that the graphite was not introduced as a post-metamorphic contaminant. Kerogen extracted from the pelitic rocks yielded light carbon isotopic values ($\delta^{13}C = -28$) which these authors interpreted as evidence of microbiotic life (possibly utilizing the Calvin cycle) at 3.95 Ga, the age of a tonalite across a fault bounding the two rock units. While a biologic origin for the graphite seems plausible, no dating of any rocks crosscutting the pelites was presented (Whitehouse et al. 2019) and U–Pb dating of detrital zircons in the host pelites yield ~2.6 Ga ages (Tsuyoshi Komiya, pers. comm., October 11, 2017). Thus it appears inescapable that the graphite-bearing pelitic rocks are much more youthful (<2.6 Ga) than supposed by Tashiro et al. (2017) and their report provides no evidence of life at 3.95 Ga.

11.3 Ion Microprobe Analysis of Carbon Isotopes in Microfossils

While useful in assessing biologic origin, bulk rock carbon isotope analyses cannot provide unambiguous information specific to the metabolic processes of, or the phylogenetic relations among, individual microfossils. However, both these limitations can potentially be transcended by utilizing the high spatial selectivity of the ion microprobe.

The ion microprobe (*aka* secondary ion mass spectrometer; see Sect. 12.2) utilizes a primary ion beam that is finely focused (typically 1–20 μm in diameter) onto the sample surface (e.g., a polished petrologic section) causing atoms in the sample to be ejected, some of which are ionized and then accelerated by a strong electric field into a spectrometer that separates these secondary ions into beams of equal mass, the intensity of which are then each measured to determine isotopic composition. A variety of primary ion sources are utilized depending on the application at hand. For analysis of electronegative elements, such as carbon, a Cs^+ source is typically utilized to create C^- ions. The analysis of negative secondary ions from electrically insulating samples (e.g., carbon isotope measurements in silicates or carbonates) requires use of an electron flood gun or similar approach to compensate for the buildup of positive charge carried to the sample surface by the primary Cs^+ beam and left behind by escaping electrons. Ion microprobes such as the CAMECA 1200-series instruments we use at UCLA routinely attain mass resolving powers (MRP) of 5000 or more without significant loss of secondary ion intensity. Given that most isotopic analyses of carbon only require an MRP of ~2000, this generally results in high analytical sensitivity. Using a multicollector ion detection system, precision of carbon isotope ratios can be better that ±0.1‰ in favorable cases, but can be ±1–5‰ in those instances in which fewer than $\sim 10^6$ ions are detected.

The in situ capability and capacity of the ion microprobe to determine accurate isotope ratios of carbon on nanogram-scale quantities make possible analysis of individual Precambrian microfossils. House et al. (2000) pioneered the application of ion microprobe carbon isotope measurements on microorganisms in stromatolitic cherts from the ~850 Ma Bitter Springs Formation ($\delta^{13}C$ from −21 ± 2 to −32 ± 1‰), Australia, and the ~2.1 Ga Gunflint Formation ($\delta^{13}C$ from −32 ± 1 to −45 ± 1‰), Canada. The results were generally consistent with carbon fixation via either the Calvin cycle or the acetyl-CoA pathways, but inconsistent with the fractionations expected from either the 3-hydroxypropionate cycle or the reductive TCA cycle. The level of these carbon isotope fractionations is generally consistent with the microfossil morphologies which resemble cyanobacteria (i.e., Calvin cycle).

Ueno et al. (2001) subsequently undertook ion microprobe analysis of carbonaceous filamentous microstructures inferred to be microfossils from two chert localities in the ca. 3.5 Ga Warrawoona Group in the North Pole region of Western Australia. They documented $\delta^{13}C$ values ranging from −42 to −32‰ that they interpreted to indicate a biologic origin for the filaments, possibly reflecting autotrophs utilizing the acetyl-CoA pathway or the Calvin cycle. A follow up study examining the source of kerogen in these chert dykes allowed for the possibility that an abiotic mechanism could be responsible for the carbon isotope depletions observed (see next section), but argued the likely source was anaerobic chemoautotrophs (Ueno et al. 2004).

Recently, Schopf et al. (2018) examined microfossils from the ~3.5 Ma Apex chert (also part of the Warrawoona Group) near Marble Bar, Western Australia, by ion microprobe and found $\delta^{13}C$ values that appeared to vary systematically between taxa from −31 to −39‰. They inferred that two of the five species studied were primitive photosynthesizers, one was an Archaeal methane producer, and two others were methane consumers. These results appeared to corroborate the putative biogenicity of microfossils from the Apex chert (cf. Brasier et al. 2002, 2015) and correlations between $\delta^{13}C$ compositions and morphological identification bolsters confidence in their taxonomic assignments.

11.4 Ion Microprobe Analysis of Carbon Isotopes in Carbonaceous Inclusions

The lack of distinctive morphofossils and potentially highly exchanged and/or contaminated bulk rock carbon obviates the use of visual identification or bulk carbon isotopic analysis in high grade metamorphic rocks. Biogenic carbon that becomes included in minerals that grow under high grade metamorphic conditions could potentially preserve the original isotopic composition of the microorganism from which it was derived. This is because most silicate minerals have very low solubilities and diffusivities for carbon (e.g., Keppler et al. 2003) and the self-diffusion of carbon in graphite under lithospheric conditions is vanishingly low (Kanter 1957) making isotopic exchange virtually impossible.

11.4.1 Carbon Isotopes in Graphite Inclusions: The Akilia Saga

The southwest coast of Greenland contains some of the oldest rocks known on Earth, including a suite of granulite-grade supracrustal rocks consisting largely of mafic, ultramafic, and Fe-rich lithologies of likely metasedimentary origin.

This suite is called the Akilia association (McGregor and Mason 1977; Griffin et al. 1980) after its type locality at the southern tip of Akilia Island. Among these lithologies found throughout this region of southern West Greenland (Cates and Mojzsis 2006) is a rock largely comprised of quartz and Fe-rich ferromagnesian minerals that has been variously termed banded iron-formation (BIF), metachert, quartz-rich rock, or quartz-pyroxene rock (McGregor and Mason 1977; Nutman et al. 1996; Manning et al. 2006). At its type locality, this rock contains quartz, clinopyroxene, and minor amphibole, garnet, apatite, magnetite and sulfides (Fig. 11.3).

Mojzsis et al. (1996) interpreted this quartz-pyroxene rock to be a metamorphosed chemical sediment (i.e., metachert) that had been later invaded by fluids that precipitated pyroxenite veins (Fig. 11.3). From within the quartzite, they documented the occurrence of apatite crystals containing ca. 5 μm carbonaceous inclusions. As a U–Pb zircon date of 3.83 Ga from a cross-cutting tonalitic sheet had been reported (Nutman et al. 1996), they interpreted the metachert to have been deposited prior to 3.83 Ga. They speculated that the since biologic activity appears to be key to marine phosphate precipitation, the tiny graphite blebs could be the remains of Neoarchean microbiota. At such high metamorphic grade, however, there is no likelihood that fossil microorganisms could retain recognizable form. But, as described in the previous section, the possibility remains that the graphite residium could retain an isotopic signature of biologic activity throughout the degradation of cellular material. Using an ion microprobe, Mojzsis et al. (1996) found isotopically light ($\delta^{13}C = -37 \pm 3$‰; range from −21 to −49‰) carbon isotopes in individual graphite inclusions that they interpreted to reflect the presence

Fig. 11.3 Quartzite containing pyroxenite veins from the outcrop on Akilia Island from which Mojzsis et al. (1996) obtained their sample. Graphite inclusions occur within apatite crystals hosted in the quartzite. Note that the crosscutting nature of the pyroxenite veins precludes their origin as a lit-par-lit metasomatic replacement of a komatiitic protholith as proposed by Fedo and Whitehouse (2002). Scale is in cm. Photo credit T. M. Harrison

of biological activity at the time the chert protolith was sedimented and that subsequent incorporation into apatite had preserved the original carbon isotope composition. They concluded that the simplest explanation of their results is that life had emerged on Earth at least 300 Ma earlier than indicated by ca. 3.5 Ga microfossils in Western Australia (e.g., Schopf 1993).

This discovery was met with both excitement and a remarkable degree of antagonism. Both facets are summed up in this excerpt from Myers and Crowley (2000): "The possibility that any trace of early Archean life that may have existed in SW Akilia surviving these multiple episodes of intense ductile deformation…appears miraculous. Yet such a miracle was claimed by Mojzsis et al. (1996) and received world-wide publicity."

Numerous challenges to the conclusion of Mojzsis et al. (1996) were raised including: (1) crystallization of the host apatite didn't occur until 1.6 Ga (Sano et al. 1999), (2) the cross-cutting granite is significantly younger than 3.83 Ga (Whitehouse et al. 1999), (3) the tonalite doesn't actually crosscut the quartzite (Myers and Crowley 2000), (4) the quartz-magnetite rock is actually a metasomatized ultramafic rock (Fedo and Whitehouse 2002), and, possibly most remarkably, (5) multiple claims that graphite inclusions do not occur in apatite within the Akilia metachert (Lepland et al. 2005; Nutman and Friend 2006). Let's address these five issues in turn.

1. Ion microprobe $^{207}Pb/^{206}Pb$ dating by Sano et al. (1999) of the Akilia apatites that host the graphite inclusions in question yielded an age of ca. 1.5 Ga which they interpreted to be the time of apatite formation. They concluded that the graphite inclusions had been incorporated at that time and thus had no bearing on the presence of life during the Neoarchean. However, given the polymetamorphic nature of the terrane and nearby reset minerals ages of the same age (indicative of when slow cooling through ca. 400–300 °C occurred), Mojzsis et al. (1999) noted that the data of Sano et al. (1999) is the expected result for ca. 20 μm-radius apatite grains due to closure of radiogenic Pb (Cherniak et al. 1991) at ca. 350 °C. That is, the method that Sano et al. (1999) chose is fundamentally incapable of determining the crystallization age of apatite in polymetamorphic, granulite grade terranes.
2. In the course of spot dating U–Pb dating zircons from Akilia metatonalites, Whitehouse et al. (1999) observed igneous grains with ≥ 3.8 Ga cores that were mantled by thin zircons rims at ca. 3.6 and 2.7 Ga zircon overgrowths. They interpreted this data to indicate a minimum age of the Akilia metachert of 3.65 Ga, rather than the 3.85 Ga claimed by Mojzsis et al. (1996), and regarded the ≥ 3.8 Ga cores as inherited zircon. But a typical tonalitic magma intruding into zircon-poor rocks at ca. >900 °C would be highly undersaturated with respect to zircon and thus not expected to preserve widespread inheritance.

By using the ion microprobe in depth profiling mode, as opposed to the spot analysis used by Whitehouse et al. (1999), the spatial resolution of this analysis method can be increased by a factor of about one hundred. Mojzsis and Harrison (2002a) depth profiled into an Akilia metatonalite zircon and revealed three phases of concentric zircon growth at 3.83, ~3.6 and ~2.6 Ga. In addition to U–Pb dating, they simultaneously measured Th/U and found it to be highly correlated with age. Knowing the Th/U zircon/melt partition coefficient to be ~5, they calculated that a zircon crystallizing from the host tonalite (Th/U = 3.8) should be characterized by a Th/U ratio of ~0.8. However, the only portion of that zircon with such a ratio is the 3.83 Ga core. The zircon rims grown at ~3.6 Ga and ca. 2.6 Ga have Th/U ratios orders of magnitude lower—consistent with their precipitation from a U-rich metamorphic fluid and thus unrelated to the age of magmatic intrusion and the timing of the crosscutting relationship. Manning et al. (2006) subsequently used the rare earth element (REE) data of Whitehouse and Kamber (2004) to show that, while the ca. 3.8 Ga cores in Akilia tonalite sheets have the strong LREE/HREE fractionation typical of igneous zircons, the ca. 3.6 Ga zircon rims have flat HREE patterns that are instead consistent with exchange with metamorphic garnet.

3. Fedo and Whitehouse (2002) proposed that the Akilia quartz-pyroxene rocks had originated as ultramafic rocks (cf. Mojzsis and Harrison 2002b) that were subsequently metasomatised to quartzite (i.e., the pyroxene veins are restitic rather than cross-cutting; Fig. 11.3). Manning et al. (2006) undertook the first detailed mapping of the Akilia supracrustal enclave and confirmed it to be comprised of laterally continuous units of mafic amphibolite, ultramafic rocks, and Fe-rich quartz-pyroxene units. This package was then isoclinally folded and tightly refolded about a steep hinge plane resulting in two limbs of contrasting total strain. The outcrop from which the Mojzsis et al. (1996) sample was obtained is located in the lower strain portion of the anticline.

Manning et al. (2006) tested both models of formation of quartz-pyroxene rocks (i.e., metachert vs. metasomatized ultramafic) and found that (i) simple mixing relationships using the geochemical data presented by Fedo and Whitehouse (2002) were fundamentally inconsistent with metasomatism; (ii) the contacts adjacent the quartzite show no evidence of metasomatic zoning (e.g., in SiO_2) at their margins, (iii) the quartzite $\delta^{18}O$ (+13‰) is consistent with an Fe-rich chert or BIF origin whereas the encompassing ultramafic rocks have values consistent with a komatiitic-peridotitic-tholeiitic suite (+7.5‰); (iv) the existence of $\Delta^{33}S$ anomalies in sulphides from within the quartzite almost certainly point to a sedimentary protolith exposed to atmospheric deposition; and (v) rather than representing a restitic component of an originally ultramafic layer, the pyroxenite veins clearly crosscut the quartzite (Fig. 11.3). Manning et al. (2006) concluded that the quartz-pyroxene rocks are a primary part of the supracrustal sequence and thus have the same minimum age as the rest of the package.

4. Myers and Crowley (2000) argued from reconnaissance-scale field observations of Akilia Island that the tonalite gneiss that Mojzsis et al. (1996) assumed crosscut the supracrustal enclave had been tectonically infolded into the volcano-sedimentary section and thus did not provide a lower age bound on the

quartzite. Indeed, there was some reason to be skeptical of claimed crosscutting relationships as Nutman et al. (1997) had a few years earlier published a map showing a large quartz-diorite gneiss dated to 3.87 ± 0.01 Ga that appeared to cross-cut both enclave and adjacent orthogneiss. Myers and Crowley (2000) found that the sketch map of Nutman et al. (1997) had both been drawn in reverse image and the scale misrepresented. They stated that the discordance between this layer and gneissosity seen by Nutman et al. (1997) in the adjacent rocks "does not exist". This putative cross-cutting relationship was also not observed in the 1:250 scale map of Manning et al. (2006). However, in the course of their mapping, Manning et al. (2006) identified an orthogneiss sheet that preserves magmatic crosscutting relations with supracrustal units in the low-strain limb of the enclave. U–Pb zircon dating of this rock yielded and age of 3.82 ± 0.01 Ga. Thus the deposition of the enclave package is greater than 3.82 Ga.

5. About 10 years after the publication of Mojzsis et al. (1996), two papers appeared claiming that graphite inclusions do not occur at all in apatite within the Akilia metachert (Lepland et al. 2005; Nutman and Friend 2006). As an aside, the second of these papers was authored by the couple that had provided the original Akilia sample used in the Mojzsis et al. (1996) study and on that basis, had sought co-authorship of that publication. These were remarkable claims, in essence charging the authors of Mojzsis et al. (1996) with either negligence or outright fraud.

In 2005 Stephen Moorbath wrote a News & Views article for Nature in which he summarized his view of the evolving Akilia controversy (Moorbath 2005). He repeated most of the above claims regarding the Akilia rocks, although as previously noted several had already been refuted, but went further stating "Even more worrying was the proposal (Van Zuilen et al. 2002) that graphite inclusions in apatite grains resulted from thermal dissociation…of iron-rich carbonates in the rock to iron oxide, carbon dioxide and elemental carbon, the latter with a $^{13}C/^{12}C$ ratio overlapping values indicative of a biogenic origin". This was surprising as in their paper, Van Zuilen et al. (2002) had clearly stated that their "study does not include Akilia rocks and our conclusions about the origin of graphite and apatite-graphite association in Isua cannot, without additional petrographic and chemical analyses, be applied to the more extensively metamorphosed rocks from Akilia island". Moorbath (2009) repeated this claim four years later ("…it is now known that low $^{13}C/^{12}C$ ratios in graphite can be produced by thermochemical reactions involving the decomposition of non-biological carbonate rocks").

Moorbath (2005) adopted the assertion of Lepland et al. (2005) that the rock investigated by Mojzsis et al. (1996) was free of graphite and wrote: "This persuasive discovery [i.e., the absence of graphite] seems an almost inevitable, yet highly problematic, consequence to the increasing scientific doubts about the original claim. We may well ask what exactly was the material originally analysed and reported? What was the apatite grain with supposed graphite inclusions that figured on the covers of learned and popular journals soon after the discovery?

These questions must surely be answered and, if necessary, lessons learned for the more effective checking and duplication of spectacular scientific claims from the outset."

Subsequently, McKeegan et al. (2007) used a combined Raman imaging-ion microprobe carbon isotope analysis approach to image graphite included in an apatite crystal within the quartzite from the original sample provided by Nutman and Friend. By careful polishing, they were able to bring that inclusion to within 1 μm of the polished surface and subsequently sputter into it to determine its $\delta^{13}C$ to be −29 ± 4‰. This appeared to incontrovertibly demonstrate the presence and primary nature of graphite inclusions with light carbon isotope compositions in Akilia apatites. They concluded that their results are "consistent with the hypothesis that graphite-containing apatite grains of the older than 3830 Ma Akilia metasediments may represent chemical fossils of early life". Although neither Lepland et al. (2005) or Nutman and Friend (2006) formally retracted their papers, the publication of McKeegan et al. (2007) appears to have abruptly ended this line of criticism.

Indeed, all of the questions that Moorbath (2005) raised have been addressed and, as documented above, answered in the negative, in some cases at the expense of the reputation of those who raised counter claims. Is this a case where the scientific dialectic has, in the fullness of time achieved the desired result? Perhaps. But, as concluded by Barnes et al. (2018), ad hominem attacks falsely implying misconduct have the same negative impact on attitudes towards science claims as direct attacks on the empirical basis of those claims. Certainly it is not the role of 'popular' science journals to aid in erosion of the public's confidence in the pursuit of scholarship. I have chronicled the controversy surrounding evidence for early life recorded in the Akilia quartzite in some level of detail as I agree with the late Prof. Moorbath that lessons can be learned from this episode, but perhaps not those that he may have then had in mind.

11.4.2 Carbon Isotopes in Graphite Inclusions: Hadean Zircons

As discussed more extensively in Sect. 7.8.5, Bell et al. (2015) documented the existence of two graphite inclusions they interpreted to be primary in a 4.1 Ga zircon from the classic Jack Hills locality. Ion microprobe carbon isotopic measurements yielded an average $\delta^{13}C_{PDB}$ of −24 ± 5‰, consistent with a biogenic origin (see Sect. 7.8.5). If the Bell et al. (2015) result does indeed represent an isotopic signal of biologic activity, it would extend our knowledge of the timing of terrestrial life back to at least 4.1 Ga, or ≥ 300 Ma earlier than that suggested by Mojzsis et al. (1996) and coincident with estimates derived from molecular divergence among prokaryotes (e.g., Battistuzzi et al. 2004; Sect. 11.6.3).

In reviewing interpretations of possible organic carbon found as graphitic masses in early Earth environments, Alleon and Summons (2019) briefly discussed the Bell et al. (2015) result. They concluded that these inclusions were "likely derived from secondary processes, possibly during subsequent metamorphism as proposed for other inclusions (Rasmussen et al. 2011) or during polishing as it was the case for putative Hadean diamonds in zircons from Jack Hills (Dobrzhinetskaya et al. 2014). Indeed, even assuming structural disorder induced by polishing artefacts (Beyssac et al. 2003), the reported Raman spectral characteristics of this carbonaceous matter, interpreted by the authors to be "disordered graphite", indicate that it did not experienced peak temperatures above 300 °C".

There is much to unpack here. Let's start with "polishing artefacts". Alleon and Summons (2019) appear to believe that the carbonaceous inclusions documented by Bell et al. (2015) were exposed and abraded by laboratory polishing compound prior to Raman spectroscopic analysis. In this they are mistaken. As described in the analytical methods section in Bell et al. (2015), Raman structural characterization was undertaken prior to the host zircon being removed from its original mount by ion milling. During this phase, the graphitic inclusions were >10 µm below the polished surface and thus not only isolated from such disturbance but from the possibility that they could have been incorporated into the zircon. In the specific case mentioned by Alleon and Summons (2019), Dobrzhinetskaya et al. (2014) found that Menneken et al. (2007) had enmeshed diamond polishing compound into surface crevices, not somehow transported them into the crystalline volume of Jack Hills zircons.

Turning to the matter of a secondary origin, Alleon and Summons (2019) appear to have misunderstood the capacity of the ultra-high resolution imaging method used by Bell et al. (2015) to establish a primary (i.e., included at the time of zircon formation) origin. To be sure, not all inclusions in Hadean Jack Hills zircons are primary (see Hopkins et al. 2008, 2010, 2012; Rasmussen et al. 2011; Bell et al. 2015, 2016, 2017, 2018, 2019; Bell and Harrison 2013). Because of the potential importance in establishing a primary origin for these inclusions, Bell et al. (2015) undertook transmission X-ray nanotomography on the sliver of zircon containing the two encompassed inclusions. The Supplementary Information section of their open access paper includes two movies showing different styles of 3D reconstructions of that sliver. This unprecedented imaging of zircon inclusions revealed no through-going (or otherwise) cracks or defects (such as healed cracks or bubble trains) associated with these inclusions. The inclusions themselves exhibit the crystal habit of graphite. These facts raise a question not directly asked in the Bell et al. (2015) paper but, given the misapprehensions of Alleon and Summons (2019), is worthwhile stating here: How could pure carbon (in a carbon-poor host metasediment) ingress a magmatic zircon, create and fill two hexagonoid caverns, while leaving no physical trace of such activity. The answer is that it is, in the absence of a plausible mechanism, simply not possible.

Finally, Alleon and Summons (2019) inferred that the partially disordered nature of the graphite documented in the Raman imaging of Bell et al. (2015) precludes the two inclusions from originating in a magmatic zircon as the peak temperature they could have experienced must have been less than 300 °C. However, ancient zircons contain a relatively intense integrated source of radiation which can impart structural changes to graphite. The Hadean zircon host of the two inclusions presently contains ~100 ppm U, which translates to an initial concentration at 4.1 Ga of

~200 ppm (recall that the half-lives of ^{238}U and ^{235}U are 4.4 and 0.7 Ga, respectively). Given that each decay of ^{235}U and ^{238}U produces either 7 or 8 alpha (α) particles, the decay of that 100 ppm [U] difference produces $\sim 10^{-3}$ α particles per atom. But the characteristic α recoil distance in zircon is ~25 μm (Hourigan et al. 2005), or about 80,000 graphite unit cells. Thus ~4 Ga of α damage could lead to ~100 atomic displacements per C atom within each graphite inclusion. Since α recoil damage is annealed at temperatures below that of fission track damage (Gleadow 1978), which in zircon is annealed over geologic timescales at a temperature of ~200 °C (Bernet 2009), the host crystal would not become metamict if the host rock remained under only several km of cover. However, the same damage in graphite requires temperatures >2000 °C to heal in laboratory experiments. Even one atomic displacement per C atom yields a measurable volume change in graphite (Simmons 2013) so two orders of magnitude greater damage could be expected to lead to the level of disordering seen in the Raman spectra. Thus the observation of partially disordered primary graphite inclusions within a structurally homogeneous, U-rich, ancient zircon is the expected result from what is known about the zircon hosting the graphite inclusions.

11.5 The Significance of Isotopically Light Carbon in Neoarchean-Hadean Rocks

11.5.1 Mechanisms Producing Isotopically Light Carbon

Isotopically light carbon signatures can be produced in Neoarchean-Hadean rocks and minerals by both biotic and abiotic processes. They include: incorporation of carbonaceous meteorites (Kerridge 1985), Fischer-Tropsch-type catalysis (McCollom 2013), carbon isotopic fractionation by diffusion (Mueller et al. 2014), degassing of mid-ocean ridge basalts (Shilobreeva et al. 2011), high-temperature breakdown of siderite (Van Zuilen et al. 2002), and biogenic processes (Schopf 2014).

Carbon isotope ratios in meteorites range from $\delta^{13}C$ of +80 to −60‰ (Hoefs and Hoefs 1980; Vacher et al. 2017) while carbonaceous chondrites, which contain average of ~3.5 wt% carbon (McDonough and Sun 1995), have a mean $\delta^{13}C$ of −12.5 ± 7.1‰ (n = 101; Boato 1954; Kerridge 1985; Pearson et al. 2006). Although carbonaceous compounds range between +68 and −34‰ (Marty et al. 2013), with refractory organic matter yielding $\delta^{13}C$ values around −20‰ (Sephton et al. 2003), it is unclear to the author how the structural state of carbonaceous compounds in meteorites might help or hinder its incorporation in terrestrial sediments. It seems possible, if highly coincidental, that extraterrestrial carbon in the range of that produced by photosynthetic microorganisms could have been incorporated into the marine sediments preserved at Akilia (Mojzsis et al. 1996) and Isua (Rosing 1999). If further examples of >3.7 Ga marine sediments containing $\delta^{13}C$ in the range of photosynthetic bacteria (i.e., −20 to −30‰) are documented, appeals to an extraterrestrial source would be increasingly untenable. However, the case for an extraplanetary source of light carbon in granitoid zircon inclusions like that reported by Bell et al. (2015), is already more difficult to support. The quantity of extraterrestrial material necessary to dominate the carbon budget of a felsic magma protolith would be enormous and profoundly influence the chemistry of that magma away from its granitoid character unless the constituent carbon had been separated from the host meteorite(s). A possible mechanism to effect this on ancient Earth might be through sedimentary processing and concentration of meteoritic carbon in pelagic sediments. Even if meteoritic carbon could be concentrated in this fashion, the isotopic signal observed by Bell et al. (2015) is uncharacteristic of the likeliest of candidates (i.e., carbonaceous chondrites). Given that virtually all meteorites plot off the terrestrial-lunar oxygen isotope fractionation line (Clayton 1993), extraterrestrial inputs should be detectable through associated $\Delta^{17}O$ anomalies (which have not been documented in Hadean zircons; Marc Chaussidon, pers. comm.).

Laboratory experiments have shown that reduction of oxidized carbon, methane, and other hydrocarbons is possible by Fischer-Tropsch-type (FTT) mechanisms in the presence of NiFe-alloy. However, the latter is an unlikely crustal component and the conversion efficiency is extremely low ($\ll 1\%$), even at high temperatures (McCollom 2013). Schidlowski (2001) pointed out that to invalidate a biological interpretation of the Eoarchean $\delta^{13}C$ record, one would have to "postulate an inorganic process operating on a global scale that was capable of mimicking, both in direction and magnitude, the principal enzymatic isotopic effect of the photosynthetic pathway with a remarkable degree of precision". FTT reactions don't meet this requirement of a "near-perfect isotopic mimicry" as isotopic fractionations between reduced and oxidized carbon greatly exceed (−50 to −100‰; Lancet and Anders 1970) that of photosynthesis.

Serpentinization produces hydrogen- and methane-rich fluids that create highly reducing conditions and light carbon isotopic signatures (McCollom and Seewald 2013). Documented cases of reduced carbon in MORB's with $\delta^{13}C$ around −25‰ (Delacour et al. 2008; Shilobreeva et al. 2011) are generally interpreted as due to a mixture of marine carbonate and organic C. For example, Delacour et al. (2008) concluded that the reduced carbon in MORBs originated from microbial activity. However, Shilobreeva et al. (2011) inferred the deepest organic components to be compatible with FTT reduction involving chromite. Even if correct, a MORB environment is an unlikely location for the formation of low-crystallization temperature zircons of continental affinity.

Diffusion of carbon through metallic Fe causes isotopic fractionation due to the faster diffusivity of ^{12}C relative to ^{13}C, with observed effects ranging to 30–40‰ (Mueller et al. 2014). Although metallic Fe is an unlikely crustal phase, the possibility exists for a similar effect in other media. If so, the production of a light carbon reservoir would occur concurrently with the production of a heavy carbon reservoir in geochemically similar media and it remains unclear why light carbon would be preferentially retained in magmatic systems over heavy carbon.

Van Zuilen et al. (2002) noted that graphite forms from the disproportionation of Fe-bearing carbonates at high temperature via the reaction $6FeCO_3 \Rightarrow 2Fe_3O_4 + 5CO_2 + C$. However, $\delta^{13}C$ values of graphite produced by this mechanism were limited to a narrow range between −12 and −10‰ (an average shift of −6‰ from the siderite). This small isotopic shift precluded this mechanism as a candidate to explain the magnitude of isotopic depletion in carbonaceous inclusions included in both Hadean zircons and, as noted earlier and by Van Zuilen et al. (2002), in graphite included in Akilia Island apatites (see Sect. 11.4.1).

Biogenic organic matter, which averages $\delta^{13}C = -25 \pm 10$‰ over the past 3.5 Ga (Schopf 2014; Fig. 11.2), is incorporated into the vast majority of preserved clastic sediments and can reach 10 wt% (Hunt 1979). Kerogens tend to get isotopically heavier by ~3‰ during thermal maturation (Des Marais 1997) so the production of an artificially *low* carbon isotopic value by this process is not possible. Given the secular trend in $\delta^{13}C$ and the several lines of evidence indicative of sediment involvement in the Jack Hills zircon magmas, the simple interpretation of the observation of Bell et al. (2015), consistent with the geochemistry of the zircon host, is that the carbonaceous inclusions represent graphitized organic carbon present during melting of a pelitic protolith at 4.10 Ga.

The possibility that isotopically light carbon in ancient terrestrial materials is of biogenic origin is consistent with interpretations of light $\delta^{13}C$ in mantle diamonds (e.g., Pearson et al. 2003). Although diamonds with $\delta^{13}C$ values as negative as −10‰ could be accounted for by isotopic fractionation of abiogenic precursors, lighter values, down to −23‰, do not appear to be explicable by such processes but are rather suggestive of an origin from subducted organic matter (Stachel et al. 2009; also see Farquhar et al. 2002).

11.5.2 The Ladder of Life Detection

The paucity of an early Earth rock record and the intense metamorphism of what little is left make definitive detection of preserve signals of life from this period quite challenging. Claims of evidence that push back the established minimum age of life's origin are often met with intense criticism. That such a backlash can range from healthy skepticism to false characterizations (see Sect. 11.4.1) argues for a set of guidelines from which to judge the merit of a claim. Neveu et al. (2018) advocated a set of criteria—the Ladder of Life Detection—to help guide the design of robotic space investigations seeking to detect signs of life, but their system has some application to studies of early terrestrial life. Their seven criteria build toward an increasingly robust interpretation of life detection. They are: Sensitivity (i.e., signal-to-noise be $\gg$1), Contaminant-free signal (i.e., any contamination be discriminated from the signal of biologic activity), Repeatability (measurements of a sample can be replicated), Context (signal is compatible with what is known biologic processes), Detectability (the sample matrix does not prevent detection), Preservation (biologic signal be retained), Definitiveness (the biologic signal be distinguished from background abiotic sources or sinks), and Compatibility (the signal be compatible with what is known about terrestrial life). An eighth criterion, the Last Resort Hypothesis, is the ultimate hurdle: does the signal "compellingly preclude an abiotic origin".

Evaluation of those cases described above in which light carbon isotope ratios were measured in situ on carbonaceous inclusions preserved within an armoring mineral shell appear to meet all Ladder of Life Detection criteria save perhaps Definitiveness and the Last Resort Hypothesis. While the existence of abiotic mechanisms capable of creating light carbon isotope signals precludes an absolute definitive conclusion, Schidlowski's (2001) argument (Sect. 11.5.1) that the lack of those mechanisms to globally mimick (in direction and magnitude) the vital effect of photosynthesis on carbon isotopes bring this approach to the threshold of that state. What's the path forward? The eventual acquisition of a large database of carbon isotope measurements of Hadean carbonaceous materials (see Appendix) might clearly select between a biogenic versus abiogenic origin of these signals.

11.6 Other Approaches

11.6.1 Stromatolites

Stromatolites are conical and domical structures formed by the trapping and cementation of sediments by microbial mats in near-shore environments, and thus have the potential to become a robust part of the geologic record. Modern occurrences are rare but found in hypersaline lakes (Cuatro Ciénegas, Mexico), marine lagoons (e.g., Shark Bay, Western Australia), and open marine environments (Exuma Cays, Bahamas). Stromatolites with compelling morphological characteristics as old as ca. 3.48 Ga (Dresser Formation, Western Australia) have been documented (e.g., Noffke et al. 2013).

Nutman et al. (2016) identified a low strain zone in the $\sim$3.7 Ga Isua supracrustal belt, West Greenland, in which they argued putative conical and domical stromatolites were preserved. However, Allwood et al. (2018) showed that the chevron-like cross-sectional features apparent in 2D outcrops are actually extended 3D structures in metasediments that they interpreted had been axially deformed post-deposition along with addition of non-biogenic, secondary carbonate. Nutman et al. (2019) acknowledged that the rocks in question had been deformed approximately in the fashion noted by Allwood et al. (2018) but that such stretching should be expected in rocks ductilely deformed at high metamorphic grade throughout Earth history. While that's certainly true, it is also an invitation to be additionally cautious in evaluating any interpretation of such highly contorted and recrystallized rocks.

The primary concern equating stromatolite-like structures with the existence of microbiotic life is the degree to which pattern recognition is required. While prokaryotic life is constrained by cellular lengthscales (say, 0.5–50 μm) and the limited number of known metabolic strategies, the nature of habitats created by microorganisms is poorly understood. Grotzinger and Rothman (1996) developed a precipitation-diffusion model of abiotic stromatolite growth that recreated the spectral spatial characteristics of a natural stromatolite, calling into question the assumption that microorganisms necessarily play a role in determining stromatolite morphology. While one might think that stromatolites would be a rich source of microfossils, the paucity of such evidence in Archean occurrences seems difficult to explain if their origin was owed to the presence of large, multigenerational microbial populations.

11.6.2 Microfossils

Dodd et al. (2017) described possible permineralized microorganisms in jaspilite box veinings in a highly-deformed terrane dykes from the Nuvvuagittuq belt, Quebec. The age of this sequence remains in dispute (see Sect. 3.7) with estimates ranging from less than 3.78 Ga (the oldest U–Pb zircon age) to 4.28 Ga (inferred from Sm–Nd data) which likely reflects the mantle separation age of the protolith. Dodd et al. (2017) interpreted micron-scale tubes and filamental features to be similar to filamentous microorganisms found in precipitates at modern hydrothermal vents, and thus inferred their origin in hydrothermal seafloor vents at, or prior to, 3.78 Ga. However, McMahon (2019) was able to abiotically create features similar in both morphology and composition by 'chemical gardening. In any event, others familiar with this region note that the host jasper crosscuts the dated basement rocks (Stephen Mojzsis, Elizabeth Bell and Dustin Trail pers. comm., 2017) thereby constraining the age of their occurrence only to be younger than the 3.8–3.5 Ga Nuvvuagittuq belt.

11.6.3 Molecular Clocks

A wholly different approach to determining when life first appeared is to use the molecular structure of modern microbiota to infer when they diverged from a shared forebearer—the Last Universal Common Ancestor, or LUCA (Zuckerkandl and Pauling 1965; Woese 1998). This assumes that the number of genomic mutations is somehow proportional to the time since they shared that common ancestor (Pisani and Liu 2015). Assuming that all presently living organisms descend from the same progenitor and establishing when their divergence occurred could provide a lower bound on life's emergence. In particular, small subunit ribosomal RNA sequences act as 'molecular clocks'. By calibrating the rate at which a biomolecule (e.g., nucleotides or amino acid sequences) mutates, this approach can in principle provide an absolute time framework given certain assumptions.

Battistuzzi et al. (2004) used a set of amino acids sequences from 32 proteins common to 72 species of primitive life to deconvolve their phylogenetic relationships. From this data, they estimated divergence times for archaebacteria as old as 4.1 Ga, placing the origin of life during the Hadean eon. Based in part on molecular clock data, Hedges (2009) argued that life arose between 4.4 and 4.2 Ga and quickly achieved prokaryote complexity, with the Eubacteria and Archaebacteria

Superkindoms splitting off a common lineage at ~4.2 Ga. The utility of molecular clocks, however, is limited by a number of parameters that are difficult to assess: changing generation times, population size, species-specific differences, changes in protein functionality, and the rate of natural selection (Schwartz and Maresca 2006).

Recently, Betts et al. (2018) used 11 different molecular clock calibrations to constrain a Bayesian analysis of molecular fossils. Independent of assumptions about the linearity of the clocks, they confidently rejected the hypothesis that LUCA emerged subsequent to 3.9 Ga. Their posterior time estimates place the emergence of the common ancestor of Eubacteria and Archaebacteria between about 4.2 and 4.4 Ga.

The nature of earliest life can be examined using similar methods. For example, Weiss et al. (2016) identified 355 proteins shared by archaebacterial and bacterial lineages (~0.1% of all protein clusters). The physiological functionality shared among these proteins suggests LUCA was an anaerobic, CO_2-fixing, H_2-dependent, thermophilic organism. Those 355 phylogenies point to simple metabolisms, such as methanogens who presently inhabit hydrothermal environments rich in H_2, CO_2 and Fe. Weiss et al. (2016) concluded that their data support an autotrophic origin of life involving the acetyl-CoA pathway (see Sect. 11.1) in a hydrothermal setting (e.g., Lane et al. 2010). It is now broadly agreed that eukaryotes arose via lateral gene transfer contributed from both archaebacteria and eubacteria (Fig. 11.4).

Ribosomes, found within all living cells, are the macromolecular factories that link amino acids together in the order specified by messenger RNA to form proteins. Since the molecular structure of ribosomes represents their integrated chemical development, they are in effect chemofossils that preserve a record of

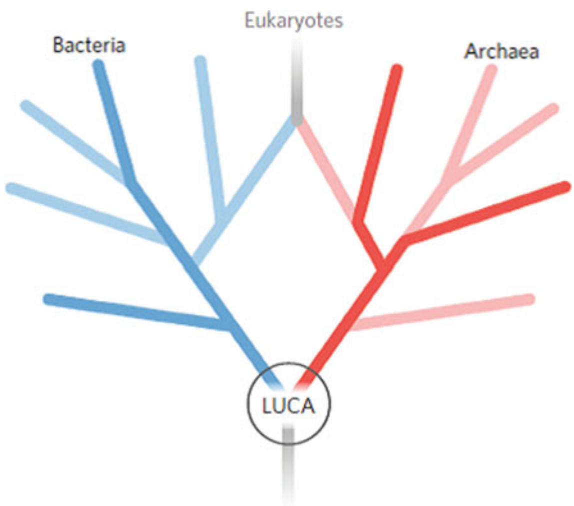

Fig. 11.4 A two-domain tree of life in which eukaryotes stem from both archaea and bacteria. The last universal common ancestor (LUCA) is their shared forebearer. Determining the time of their divergence is tantamount to understanding when life emerged. Reproduced with permission from Weiss et al. (2016)

'life's dark ages'—the pre-LUCA history of biology (Marshall 2019). For example, Petrov et al. (2015) used a comparison of ribosomal structures across the tree of life to constrain a model of how RNA translation originated during the Hadean eon by abiotic chemical accretion.

11.7 Critical Summary

The paucity of Neoarchean metasedimentary rocks below amphibolite facies—and the absence of any known macroscopic Hadean rocks—precludes use of traditional, morphology-based fossil identification. As different metabolic pathways variably fractionate carbon isotopes to isotopically light values (i.e., ^{13}C deficient), a longstanding strategy has been to search for a biologic, or 'vital', isotopic signature in carbonaceous residues. While a variety of inorganic processes could potentially produce light $\delta^{13}C$ signatures, including incorporation of meteoritic materials, Fischer-Tropsch-type catalysis, diffusive fractionation, mid-ocean ridge basalt degassing, and high-temperature breakdown of siderite, none can globally mimick (in direction and magnitude) the vital effect of photosynthesis on carbon isotopes.

The observation of isotopically light carbon in graphite inclusions in a 4.1 Ga zircon doesn't represent smoking gun evidence of Hadean life, but it does offer a pathway through which carbon cycling on earliest Earth could be revealed. Indeed, isotopic analysis of these graphite inclusions constitutes currently the only means of constraining carbon isotope variations prior to 4 Ga, and the identification of isotopically light carbon may suggest a Hadean biosphere. As already noted, there are a number of hypothetical scenarios for the abiotic production of light carbon on the Hadean Earth. To distinguish among these scenarios, a large number of graphite inclusions may be necessary to allow statistical tests for various potential abiotic and biotic origins to be more closely scrutinized.

Lastly, molecular clock calibrations of genomic mutations among modern Eubacteria and Archaebacteria appear to be converging on an interval between 4.1 and 4.4 Ga as the age of their divergence, and thus a lower bound on the time of life's origin.

References

Alleon, J., & Summons, R. E. (2019). Organic geochemical approaches to understanding early life. *Free Radical Biology and Medicine*.

Allwood, A. C., Rosing, M. T., Flannery, D. T., Hurowitz, J. A., & Heirwegh, C. M. (2018). Reassessing evidence of life in 3,700-million-year-old rocks of Greenland. *Nature, 563*, 241–244.

Altermann, W., & Kazmierczak, J. (2003). Archean microfossils: A reappraisal of early life on Earth. *Research in Microbiology, 154,* 611–617.

Amthor, J. E., Grotzinger, J. P., Schröder, S., Bowring, S. A., Ramezani, J., Martin, M. W., et al. (2003). Extinction of Cloudina and Namacalathus at the Precambrian-Cambrian boundary in Oman. *Geology, 31,* 431–434.

Awramik, S. M., Schopf, J. W., & Walter, M. R. (1983). Filamentous fossil bacteria from the Archean of Western Australia. *Precambrian Research, 20,* 357–374.

Barghoorn, E. S., & Tyler, S. A. (1965). Microorganisms from the Gunflint chert. *Science, 147,* 563–577.

Barnes, R. M., Johnston, H. M., MacKenzie, N., Tobin, S. J., & Taglang, C. M. (2018). The effect of ad hominem attacks on the evaluation of claims promoted by scientists. *PLoS ONE, 13,* e0192025.

Battistuzzi, F. U., Feijão, A., & Hedges, S. B. (2004). A genomic timescale of prokaryote evolution: Insights into the origin of methanogenesis, phototrophy, and the colonization of land. *BMC Evolutionary Biology, 4*, 44–51. https://doi.org/10.1186/1471-2148-4-44.

Bell, E. A., Boehnke, P., Barboni, M., & Harrison, T. M. (2019). Tracking chemical alteration in magmatic zircon using REE patterns. *Chemical Geology, 510*, 56–71.

Bell, E. A., Boehnke, P., Harrison, T. M., & Mao, W. (2015). Potentially biogenic carbon preserved in a 4.1 Ga zircon. *Proceedings of The National Academy of Sciences, 112*, 14518–14521.

Bell, E. A., Boehnke, P., & Harrison, T. M. (2016). Recovering the primary geochemistry of Jack Hills zircons through quantitative estimates of chemical alteration. *Geochimica et Cosmochimica Acta, 191,* 187–202.

Bell, E. A., Boehnke, P., & Harrison, T. M. (2017). Applications of biotite inclusion composition to zircon provenance determination. *Earth and Planetary Science Letters, 473,* 237–246.

Bell, E. A., Boehnke, P., Harrison, T. M., & Wielicki, M. M. (2018). Mineral inclusion assemblage and detrital zircon provenance. *Chemical Geology, 477,* 151–160.

Bell, E. A., & Harrison, T. M. (2013). Post-Hadean transitions in Jack Hills zircon provenance: A signal of the Late Heavy Bombardment? *Earth and Planetary Science Letters, 364,* 1–11.

Bernet, M. (2009). A field-based estimate of the zircon fission-track closure temperature. *Chemical Geology, 259,* 181–189.

Betts, H. C., Puttick, M. N., Clark, J. W., Williams, T. A., Donoghue, P. C., & Pisani, D. (2018). Integrated genomic and fossil evidence illuminates life's early evolution and eukaryote origin. *Nature Ecology & Evolution, 2*, 1556–1562.

Beyssac, O., Goffé, B., Petitet, J. P., Froigneux, E., Moreau, M., & Rouzaud, J. N. (2003). On the characterization of disordered and heterogeneous carbonaceous materials by Raman spectroscopy. *Spectrochimica Acta Part A: Molecular and Biomolecular Spectroscopy, 59*(10), 2267–2276.

Boato, G. (1954). The isotopic composition of hydrogen and carbon in the carbonaceous chondrites. *Geochimica et Cosmochimica Acta, 6,* 209–220.

Bowring, S. A., Grotzinger, J. P., Isachsen, C. E., Knoll, A. H., Pelechaty, S. M., & Kolosov, P. (1993). Calibrating rates of Early Cambrian evolution. *Science, 261,* 1293–1298.

Brasier, M. D., Green, O. R., Jephcoat, A. P., Kleppe, A. K., Van Kranendonk, M. J., Lindsay, J. F., et al. (2002). Questioning the evidence for Earth's oldest fossils. *Nature, 416,* 76–81.

Brasier, M. D., Antcliffe, J., Saunders, M., & Wacey, D. (2015). Changing the picture of Earth's earliest fossils (3.5–1.9 Ga) with new approaches and new discoveries. *Proceedings of the National Academy of Sciences, 112,* 4859–4864.

Cates, N. L., & Mojzsis, S. J. (2006). Chemical and isotopic evidence for widespread Eoarchean ($\geq$3750 Ma) metasedimentary enclaves in southern West Greenland. *Geochimica et Cosmochimica Acta, 70,* 4229–4257.

Cherniak, D. J., Lanford, W. A., & Ryerson, F. J. (1991). Lead diffusion in apatite and zircon using ion implantation and Rutherford backscattering techniques. *Geochimica et Cosmochimica Acta, 55,* 1663–1673.

Clayton, R. N. (1993). Oxygen isotopes in meteorites. *Annual Review of Earth and Planetary Sciences, 21,* 115–149.

Delacour, A., Früh-Green, G. L., Bernasconi, S. M., Schaeffer, P., & Kelley, D. S. (2008). Carbon geochemistry of serpentinites in the Lost City Hydrothermal System (30°N, MAR). *Geochimica et Cosmochimica Acta, 72,* 3681–3702.

Des Marais, D. J. (1997). Isotopic evolution of the biogeochemical carbon cycle during the Proterozoic Eon. *Organic Geochemistry, 27,* 185–193.

Dobrzhinetskaya, L., Wirth, R., & Green, H. (2014). Diamonds in Earth's oldest zircons from Jack Hills conglomerate Australia are contamination. *Earth and Planetary Science Letters, 387,* 212–218.

Dodd, M. S., Papineau, D., Grenne, T., Slack, J. F., Rittner, M., Pirajno, F., et al. (2017). Evidence for early life in Earth's oldest hydrothermal vent precipitates. *Nature, 543,* 60–64.

Epstein, S., Buchsbaum, R., Lowenstam, H. A., & Urey, H. C. (1953). Revised carbonate-water isotopic temperature scale. *Geological Society of America Bulletin, 64,* 1315–1326.

Farquhar, J., Wing, B. A., McKeegan, K. D., Harris, J. W., Cartigny, P., & Thiemens, M. H. (2002). Mass-independent sulfur of inclusions in diamond and sulfur recycling on early Earth. *Science, 298,* 2369–2372.

Fedo, C. M., & Whitehouse, M. J. (2002). Metasomatic origin of quartz-pyroxene rock, Akilia, Greenland, and implications for Earth's earliest life. *Science, 296,* 1448–1452.

Fuchs, G., Thauer, R., Ziegler, H., & Stichler, W. (1979). Carbon isotope fractionation by Methanobacterium thermoautotrophicum. *Archives of Microbiology, 120,* 135–139.

Gleadow, A. J. W. (1978). Anisotropic and variable track etching characteristics in natural sphenes. *Nuclear Track Detection, 2,* 105–117.

Griffin, W. L., McGregor, V. R., Nutman, A., Taylor, P. N., & Bridgwater, D. (1980). Early Archaean granulite-facies metamorphism south of Ameralik, West Greenland. *Earth and Planetary Science Letters, 50,* 59–74.

Grotzinger, J. P., & Rothman, D. H. (1996). An abiotic model for stromatolite morphogenesis. *Nature, 383,* 423–425.

Hayes, J. M., Des Marais, I. B., Lambert, H., Strauss, H., & Summons, R. E. (1992). Proterozoic biogeochemistry. In J. W. Schopf & C. Klein (Eds.), *The Proterozoic biosphere* (pp. 81–134). New York: Cambridge University Press.

Hedges, S. B. (2009). Life. In S. B. Hedges & S. Kumar (Eds.), *The timetree of life* (pp. 89–98). Oxford: Oxford University Press.

Hoefs, J., & Hoefs, J. (1980). *Stable isotope geochemistry*. Berlin: Springer.

Hopkins, M., Harrison, T. M., & Manning, C. E. (2008). Low heat flow inferred from >4 Ga zircons suggests Hadean plate boundary interactions. *Nature, 456,* 493–496.

Hopkins, M., Harrison, T. M., & Manning, C. E. (2010). Constraints on Hadean geodynamics from mineral inclusions in >4 Ga zircons. *Earth and Planetary Science Letters, 298,* 367–376.

Hopkins, M., Harrison, T. M., & Manning, C. E. (2012). Comment: Metamorphic replacement of mineral inclusions in detrital zircon from Jack Hills, Australia: Implications for the Hadean Earth. *Geology, 40,* e281–e281.

Hourigan, J. K., Reiners, P. W., & Brandon, M. T. (2005). U-Th zonation-dependent alpha-ejection in (U-Th)/He chronometry. *Geochimica et Cosmochimica Acta, 69,* 3349–3365.

House, C. H., Schopf, J. W., McKeegan, K. D., Coath, C. D., Harrison, T. M., & Stetter, K. O. (2000). Carbon isotopic composition of individual Precambrian microfossils. *Geology, 28,* 707–710.

Hunt, M. J. (1979). *Petroleum geochemistry and geology*. New York: W. H. Freeman and Company.

Kanter, M. A. (1957). Diffusion of carbon atoms in natural graphite crystals. *Physical Review, 107,* 655–663.

Keppler, H., Wiedenbeck, M., & Shcheka, S. S. (2003). Carbon solubility in olivine and the mode of carbon storage in the Earth's mantle. *Nature, 424,* 414–416.

Kerridge, J. F. (1985). Carbon, hydrogen and nitrogen in carbonaceous chondrites: Abundances and isotopic compositions in bulk samples. *Geochimica et Cosmochimica Acta, 49,* 1707–1714.

Krzycki, J. A., Kenealy, W. R., DeNiro, M. J., & Zeikus, J. G. (1987). Stable carbon isotope fractionation by *Methanosarcina barkeri* during methanogenesis from acetate, methanol, or carbon dioxide-hydrogen. *Applied and Environmental Microbiology, 53,* 2597–2599.

Lancet, M. S., & Anders, E. (1970). Carbon isotope fractionation in the Fischer-Tropsch synthesis and in meteorites. *Science, 170,* 980–982.

Lane, N., Allen, J. F., & Martin, W. (2010). How did LUCA make a living? Chemiosmosis in the origin of life. *BioEssays, 32,* 271–280.

Lepland, A., van Zuilen, M. A., Arrhenius, G., Whitehouse, M. J., & Fedo, C. M. (2005). Questioning the evidence for Earth's earliest life—Akilia revisited. *Geology, 33,* 77–79.

Manning, C. E., Mojzsis, S. J., & Harrison, T. M. (2006). Geology, age and origin of supracrustal rocks at Akilia, West Greenland. *American Journal of Science, 306,* 303–366.

Marshall, M. (2019). Life's dark ages. *New Scientist, 241,* 28–32.

Marty, B., Alexander, C. M. D., & Raymond, S. N. (2013). Primordial origins of Earth's carbon. *Reviews in Mineralogy and Geochemistry, 75,* 149–181.

McCollom, T. M. (2013). Laboratory simulations of abiotic hydrocarbon formation in Earth's deep subsurface. *Reviews in Mineralogy and Geochemistry, 75,* 467–494.

McCollom, T. M., & Seewald, J. S. (2013). Serpentinites, hydrogen, and life. *Elements, 9,* 129–134.

McDonough, W. F., & Sun, S. S. (1995). The composition of the Earth. *Chemical Geology, 120,* 223–253.

McGregor, V. R., & Mason, B. (1977). Petrogenesis and geochemistry of metabasaltic and metasedimentary enclaves in the Amıtsoq gneisses, West Greenland. *American Mineralogist, 62,* 887–904.

McKeegan, K. D., Kudryavtsev, A. B., & Schopf, J. W. (2007). Raman and ion microscopic imagery of graphitic inclusions in apatite from older than 3830 Ma Akilia supracrustal rocks, West Greenland. *Geology, 35,* 591–594.

McMahon, S. (2019). Earth's earliest and deepest purported fossils may be iron-mineralized chemical gardens. *Proceedings of the Royal Society B: Biological Sciences, 286*(1916), 20192410.

Menneken, M., Nemchin, A. A., Geisler, T., Pidgeon, R. T., & Wilde, S. A. (2007). Hadean diamonds in zircon from Jack Hills Western Australia. *Nature, 448,* 917–920.

Mojzsis, S. J., & Harrison, T. M. (2002a). Establishment of a 3.83-Ga magmatic age for the Akilia tonalite (southern West Greenland). *Earth and Planetary Science Letters, 202,* 563–576.

Mojzsis, S. J., & Harrison, T. M. (2002b). Origin and significance of Archean quartzose rocks at Akilia, Greenland. *Science, 298,* 917a.

Mojzsis, S. J., Arrhenius, G., McKeegan, K. D., Harrison, T. M., Nutman, A. P., & Friend, C. R. L. (1996). Evidence for life on Earth by 3800 Myr. *Nature, 384,* 55–59.

Mojzsis, S. J., Harrison, T. M., Arrhenius, G., McKeegan, K. D., & Grove, M. (1999). Origin of life from apatite dating? Reply. *Nature, 400,* 127–128.

Moorbath, S. (2005). Palaeobiology: Dating earliest life. *Nature, 434,* 155–156.

Moorbath, S. (2009). The discovery of the Earth's oldest rocks. *Notes and Records of the Royal Society*.

Mueller, T., Watson, E. B., Trail, D., Wiedenbeck, M., Van Orman, J., & Hauri, E. H. (2014). Diffusive fractionation of carbon isotopes in γ-Fe: Experiment, models and implications for early solar system processes. *Geochimica et Cosmochimica Acta, 127,* 57–66.

Myers, J. S., & Crowley, J. L. (2000). Vestiges of life in the oldest Greenland rocks? A review of early Archean geology in the Godthåbsfjord region, and reappraisal of field evidence for >3850 Ma life on Akilia. *Precambrian Research, 103,* 101–124.

Neveu, M., Hays, L. E., Voytek, M. A., New, M. H., & Schulte, M. D. (2018). The ladder of life detection. *Astrobiology, 18,* 1375–1402.

Noffke, N., Christian, D., Wacey, D., & Hazen, R. M. (2013). Microbially induced sedimentary structures recording an ancient ecosystem in the ca. 3.48 billion-year-old Dresser Formation, Pilbara, Western Australia. *Astrobiology, 13,* 1103–1124.

Nutman, A. P., & Friend, C. R. (2006). Petrography and geochemistry of apatites in banded iron formation, Akilia, W. Greenland: Consequences for oldest life evidence. *Precambrian Research, 147,* 100–106.

Nutman, A. P., McGregor, V. R., Friend, C. R. L., Bennett, V. C., & Kinny, P. D. (1996). The Itsaq Gneiss Complex of southern west Greenland; The world's most extensive record of early crustal evolution (3900–3600 Ma). *Precambrian Research, 78,* 1–39.

Nutman, A. P., Mojzsis, S. J., & Friend, C. R. (1997). Recognition of $\geq$3850 Ma water-lain sediments in West Greenland and their significance for the early Archaean Earth. *Geochimica et Cosmochimica Acta, 61,* 2475–2484.

Nutman, A. P., Bennett, V. C., Friend, C. R., Van Kranendonk, M. J., & Chivas, A. R. (2016). Rapid emergence of life shown by discovery of 3,700-million-year-old microbial structures. *Nature, 537,* 535–538.

Nutman, A. P., Bennett, V. C., Friend, C. R., Van Kranendonk, M. J., Rothacker, L., & Chivas, A. R. (2019). Cross-examining Earth's oldest stromatolites: Seeing through the effects of heterogeneous deformation, metamorphism and metasomatism affecting Isua (Greenland) $\sim$3700 Ma sedimentary rocks. *Precambrian Research*. https://doi.org/10.1016/j.precamres.2019.105347.

Pearson, D. G., Canil, D., & Shirey, S. B. (2003). Mantle samples included in volcanic rocks: Xenoliths and diamonds. *Treatise on Geochemistry (Elsevier, Amsterdam), 2,* 171–275.

Pearson, V. K., Sephton, M. A., Franchi, I. A., Gibson, J. M., & Gilmour, I. (2006). Carbon and nitrogen in carbonaceous chondrites: Elemental abundances and stable isotopic compositions. *Meteoritics & Planetary Science, 41,* 1899–1918.

Petrov, A. S., Gulen, B., Norris, A. M., Kovacs, N. A., Bernier, C. R., Lanier, K. A., et al. (2015). History of the ribosome and the origin of translation. *Proceedings of the National Academy of Sciences, 112,* 15396–15401.

Pisani, D., & Liu, A. G. (2015). Animal evolution: Only rocks can set the clock. *Current Biology, 25,* R1079–R1081.

Preuss, A., Schauder, R., Fuchs, G., & Stichler, W. (1989). Carbon isotope fractionation by autotrophic bacteria with three different CO_2 fixation pathways. *Zeitschrift für Naturforschung C, 44,* 397–402.

Rasmussen, B., Fletcher, I. R., Muhling, J. R., Gregory, C. J., & Wilde, S. A. (2011). Metamorphic replacement of mineral inclusions in detrital zircon from Jack Hills Australia: Implications for the Hadean Earth. *Geology, 39,* 1143–1146.

Roeske, C. A., & O'Leary, M. H. (1984). Carbon isotope effects on the enzyme-catalyzed carboxylation of ribulose bisphosphate. *Biochemistry, 23,* 6275–6284.

Rosing, M. T. (1999). ^{13}C-depleted carbon microparticles in >3700-Ma sea-floor sedimentary rocks from West Greenland. *Science, 283,* 674–676.

Sano, Y., Terada, K., Takahashi, Y., & Nutman, A. P. (1999). Origin of life from apatite dating? *Nature, 400,* 127–129.

Schidlowski, M. (2001). Carbon isotopes as biogeochemical recorders of life over 3.8 Ga of Earth history: Evolution of a concept. *Precambrian Research, 106,* 117–134.

Schidlowski, M., Hayes, J. M., & Kaplan, I. R. (1983). Isotopic inferences of ancient biochemistries: Carbon, sulfur, hydrogen, and nitrogen. In J. W. Schopf (Ed.), *The Earth's earliest biosphere* (pp. 149–185). Princeton, New Jersey: Princeton University Press.

Schopf, J. W. (1993). Microfossils of the Early Archean Apex chert: New evidence of the antiquity of life. *Science, 260,* 640–646.

Schopf, J. W. (2014). Geological evidence of oxygenic photosynthesis and the biotic response to the 2400–2200 Ma "great oxidation event". *Biochemistry (Moscow), 79,* 165–177.

Schopf, J. W., Kitajima, K., Spicuzza, M. J., Kudryavtsev, A. B., & Valley, J. W. (2018). SIMS analyses of the oldest known assemblage of microfossils document their taxon-correlated carbon isotope compositions. *Proceedings of the National Academy of Sciences, 115*, 53–58.

Schopf, J. W., & Packer, B. M. (1987). Early Archean (3.3 billion to 3.5 billion-year-old) microfossils from Warrawoona Group, Australia. *Science, 237,* 70–73.

Schwartz, J. H., & Maresca, B. (2006). Do molecular clocks run at all? A critique of molecular systematics. *Biological Theory, 1,* 357–371.

Sephton, M. A., Verchovsky, A. B., Bland, P. A., Gilmour, I., Grady, M. M., & Wright, I. P. (2003). Investigating the variations in carbon and nitrogen isotopes in carbonaceous chondrites. *Geochimica et Cosmochimica Acta, 67,* 2093–2108.

Shilobreeva, S., et al. (2011). Insights into C and H storage in the altered oceanic crust: Results from ODP/IODP Hole 1256D. *Geochimica et Cosmochimica Acta, 75,* 2237–2255.

Simmons, J. H. W. (2013). *Radiation damage in graphite: International series of monographs in nuclear energy* (Vol. 102). Elsevier.

Stachel, T., Harris, J. W., & Muehlenbachs, K. (2009). Sources of carbon in inclusion bearing diamonds. *Lithos, 112,* 625–637.

Strauss, H., & Moore, T. B. (1992). *The Proterozoic biosphere: A multidisciplinary study* (J. W. Schopf & C. Klein, Eds.) (pp. 93–134). New York: Cambridge University Press.

Tashiro, T., Ishida, A., Hori, M., Igisu, M., Koike, M., Méjean, P., et al. (2017). Early trace of life from 3.95 Ga sedimentary rocks in Labrador, Canada. *Nature, 549,* 516–517.

Ueno, Y., Isozaki, Y., Yurimoto, H., & Maruyama, S. (2001). Carbon isotopic signatures of individual Archean microfossils (?) from Western Australia. *International Geology Review, 43,* 196–212.

Ueno, Y., Yoshioka, H., Maruyama, S., & Isozaki, Y. (2004). Carbon isotopes and petrography of kerogens in ~3.5-Ga hydrothermal silica dikes in the North Pole area, Western Australia1. *Geochimica et Cosmochimica Acta, 68,* 573–589.

Vacher, L. G., Marrocchi, Y., Villeneuve, J., Verdier-Paoletti, M. J., & Gounelle, M. (2017). Petrographic and C & O isotopic characteristics of the earliest stages of aqueous alteration of CM chondrites. *Geochimica et Cosmochimica Acta, 213,* 271–290.

Van Zuilen, M. A., Lepland, A., & Arrhenius, G. (2002). Reassessing the evidence for the earliest traces of life. *Nature, 418,* 627–630.

Wacey, D., Kilburn, M. R., Saunders, M., Cliff, J., & Brasier, M. D. (2011). Microfossils of sulphur-metabolizing cells in 3.4-billion-year-old rocks of Western Australia. *Nature Geoscience, 4,* 698–701.

Weiss, M. C., Sousa, F. L., Mrnjavac, N., Neukirchen, S., Roettger, M., Nelson-Sathi, S., et al. (2016). The physiology and habitat of the last universal common ancestor. *Nature Microbiology, 1,* 16116.

Whitehouse, M. J., & Kamber, B. S. (2004). Assigning dates to thin gneissic veins in high-grade metamorphic terranes: A cautionary tale from Akilia, southwest Greenland. *Journal of Petrology, 46,* 291–318.

Whitehouse, M. J., Kamber, B. S., & Moorbath, S. (1999). Age significance of U-Th–Pb zircon data from early Archaean rocks of West Greenland—A reassessment based on combined ion-microprobe and imaging studies. *Chemical Geology, 160,* 201–224.

Whitehouse, M. J., Dunkley, D. J., Kusiak, M. A., & Wilde, S. A. (2019). On the true antiquity of Eoarchean chemofossils—Assessing the claim for Earth's oldest biogenic graphite in the Saglek Block of Labrador. *Precambrian Research, 323*. https://doi.org/10.1016/j.precamres.2019.01.001.

Wickman, F. E. (1952). Variations in the relative abundance of the carbon isotopes in plants. *Geochimica et Cosmochimica Acta, 2,* 243–254.

Woese, C. (1998). The universal ancestor. *Proceedings of the National Academy of Sciences, 95,* 6854–6859.

Zuckerkandl, E., & Pauling, L. (1965). Molecules as documents of evolutionary history. *Journal of Theoretical Biology, 8,* 357–366.

12 Collectanea

Abstract

How the scientific community, in the absence of any observational evidence, came to a consensus that the first many hundreds of millions of years of Earth history saw a desiccated, lifeless, molten wasteland is worthy of analysis. This chapter addresses problematic aspects of our epistemology that led to this paradigm and concludes that the historical sciences can sometimes be influenced by the same existential urges for control that fueled the past four thousand years of ubiquitous creation mythology. On a more tangible level, emerging scientific views in the late 1960s provided heretofore unavailable sources of thermal energy to models of the early solar system. This occurred just prior to the return of lunar highland samples which showed that Moon had almost been globally melted almost immediately upon formation, in stark contrast to the then prevailing paradigm of cold accretion. Arguably overreacting in overthrow of that model, the community quickly adopted the view that the first many hundreds of millions of years of Earth history had been too turbulent to leave any record. Shortly thereafter, the emergence of the large radius ion microprobe provided the tool needed to first discover and then explore Hadean zircons from Western Australia. The seemingly contradictory story these results presented would take a generation to seriously challenge the orthodoxy of a protracted, hellish world. This intellectual inertia partially reflects the inevitability of the Earth and planetary sciences being more tolerant of what amounts to untestable hypotheses relative to other physical sciences. While that is understandable given the challenge that historical sciences face in attempting to understand processes operating many billions of years ago, overly elaborate models invoking speculative mechanisms that lack the basis for falsification tend to crowd out other, possibly better, models from the scientific arena.

T. M. Harrison, *Hadean Earth*, https://doi.org/10.1007/978-3-030-46687-9_12

12.1 Hadean Epistemology

12.1.1 Is Geology Science?

Returning to the opening sentence of this book ("All societies have origin myths"), it's interesting to speculate what compelled the scientific community through the latter third of the twentieth century and into the twenty first (Wetherill 1972; Fyfe 1978; Solomon 1980; Smith 1981; Ernst 1983; Maher and Stevenson 1988; Abe 1993; Hamilton 1998; Lunine 1999; Ward and Brownlee 2000; Gradstein et al. 2004; Moorbath 2005b; Waltham 2014) to promulgate its own origin myth—of a protracted, hellish beginning—in the absence of any direct evidence. One likely reason is the greater premium that geologists place on narrative than most other physical scientists. Tell a geologist after they've given a particularly inspiring seminar that it was "a great story" and she's likely to smile. Tell a physicist the same thing and you might risk a punch in the mouth. The fragmentary nature of the rock record and the extraordinary timescales involved lend themselves to narrative frameworks that embody multiple, untested assumptions. New results introduced into such a framework either support it or require ad hoc adjustments to be made. Although this gives the appearance of hypothesis testing, the underlying assumptions of the narrative have not been challenged. Popper (1957) argued that, "while the theoretical sciences are mainly interested in finding and testing universal laws, the historical sciences take all kinds of universal laws for granted and are mainly interested in finding and testing singular statements". As students of deep time are generally not afforded the luxury of either directly viewing the processes we investigate or performing full-scale, controlled experiments, our field could be viewed in a strict Popperian sense as more of a "metaphysical research programme" (Popper 1976). That is not to say that what we do is by its nature unscientific, but creating our own origin myth surely is. Why did we do it? There are at least two partial answers to that question. The first is that, while science is clearly distinguished from religious mythology by its emphasis on verification (Popper 1962), its practitioners may be as subject to the same existential need to feel that they know where they came from as any primitive society. Without recurrent self-appraisal, the historical sciences can lapse into wells of mistaken belief that momentarily reward the community with an unearned sense of control. The second, as we'll see in the next section, relates to the changing scientific times in the late sixties.

12.1.2 What Was the Appeal of a Hellish Hadean?

Toward the end of his distinguished career, Harold Urey, a Nobel-prize winning chemist, developed an interest in the origin of the solar system (he is credited with coining the term cosmochemistry) and the origin of life. During the 1950s, he drew on chemical reasoning to deduce that the terrestrial planets and their satellites had accreted cold from largely undifferentiated chondritic materials, with only the larger ones eventually growing warm enough to create liquid iron alloy cores after perhaps a billion years or so (Urey 1951; 1952a, b, 1955). These latter bodies would have sufficient gravity to retain atmospheres rich in NH_4, CH_4, and H_2, explaining his longstanding interest in synthesizing organic molecules using electric discharges in mixtures of those gases (e.g. Miller and Urey 1959).

Urey's views were in keeping with the times as the prevailing paradigm in the early 1950s was influenced by Weizsäcker's (1943) hypothesis (popularized by Gamow and Hynek 1945) that planetary solids formed by accretion of cold particles in "whirlpools" between nebular vortices that continuously extracted angular momentum from Sun. Weizsäcker (1943) had resurrected the long disfavored Kant-Laplace hypothesis of stellar nebula collapse by proposing that there had been about one hundred times more mass—in the form of hydrogen and helium—in the primordial planetary envelope than presently manifested in the planets. The subsequent and relatively rapid ($\tau_{½} \approx 10^7$ year) turbulent dissipation of that gas transcended the longstanding problem with Kant-Laplace theory that the total observed planetary mass was insufficient to initiate gravitational collapse. Kuiper (1951) expanded on this scenario by suggesting that the system of turbulent eddies corresponded to the placement of each of the nine planets. The radiant heat that these condensing clouds of dust and gas acquired from the young Sun was assumed to be lost via turbulent convection, keeping the protoplanets cool. Urey (1952a) believed that planetesimals (one of which was assumed to form Moon) formed relatively quickly from capture of material within an eddy at $\sim$1 AU following nebular collapse onto the central plane, but remained cool due to the evaporation of water. As the protoplanets gained mass, their internal temperatures rose but accretion was sufficiently slow that temperatures remained "comparatively low". Indeed, Urey (1952a) supposed it "probable that the earth could and did accumulate below the melting point of silicates throughout its entire growth from a small size to its present one", in part because of very slow core formation (cf., Eucken 1944). Safronov (1958, 1972) estimated that aggregation from protoplanets into planets took about one billion years.

As an aside, it's worth noting that this shift in thinking had both exobiologic significance and provided a stimulus for manned lunar exploration. Early in the twentieth century it was widely believed that solar system formation was a consequence of tidal interactions between a protosun and intruding star (e.g. Chamberlin 1901, 1905, 1916; Moulton 1905; Jeans 1919; Jeffreys 1917, 1918, cf. 1929). If so, planetary formation would likely be comparatively rare and we would likely be alone in the galaxy. However, if planets formed as a direct consequence of stellar formation, then they, and life on them, might abound elsewhere. Urey was influential in persuading post-Sputnik American governments that Moon held the key to the origin of the Solar System and perhaps life (Brush 1982).

Views began to change in the 1960s once it became clear that the solar nebula comprised elements generated in multiple nucleosynthetic events over many billions of years (Burbidge et al. 1957). Although the products of short-lived radionuclides found in meteorites were initially thought to be due to spallation reactions in the primitive solar nebula (Fowler et al. 1962), it was almost immediately thereafter (Cameron 1962) realized that their abundances were better explained due to a supernova shortly before nebular contraction The presence of freshly synthesized isotopes, such as ^{26}Al ($t_{½}$ = 0.72 Ma) whose existence would eventually be confirmed by Gray and Compston (1974), could occur at levels that would quickly heat planetesimals and planets to melting. Simultaneously, planetary formation models moved toward consideration of high velocity collisions between planetesimals and planetary embryos (Cameron 1962), which retain far greater heat than the smaller and slower moving particles (e.g. Safronov 1958) implied in earlier theories. But it was return of lunar highland samples by the Apollo program that cemented this new view of a hot origin. They provided clear evidence that Moon, contrary to Urey's (1952a) view, had not accreted cold and remained forever so but instead had almost immediately been globally fractionated in an accretional-energy-fueled magma ocean and kept considerably warm for some time thereafter by radioactive heating (Wetherill 1972). Wetherill (1972) well-captured the thinking of the time: "Lunar studies carried out in connection with the Apollo program permit considerable understanding of the early history of this planetary body…Application of this same model to the earth implies the entire earth was initially melted and geochemically fractionated. Review of the geological and geochronological evidence for the most ancient rocks indicates that not until 3400 m.y. ago did the earth cool sufficiently to permit the formation of extensive areas of stable crust".

To summarize the above, the shift of thinking to a protracted, hellish Earth model in the 1960s was largely led by physicists in reaction, and now in retrospect perhaps overreaction, to the now problematic cold accretion model developed largely by Urey (1952a) from chemical arguments. It is unclear to me why Wetherill (1972) and others overlooked the implications of earlier Pb isotope evolution studies which then appeared to establish the age of Earth (e.g. Russell and Allan 1955; Patterson et al. 1955) by assuming a much earlier timing of crust generation (cf. Sect. 1.5).

Curiously, geologists in the early part of the twentieth century held a much more benign view of early Earth. For example, in his classic work *Igneous Rocks and Their Origin* (1914), R.A. Daly wrote:

> After aggregation…the resulting rock being igneous in character…the earth's surface was cool enough to support a water ocean…and the surface always thereafter retained temperature of the same order of magnitude…"Speculation as to the primitive differentiation of the earth's silicate mantle…granitic and basaltic materials may have been in fairly uniform solution; and they may have later separated…as the temperature fell…difficulties are avoided if we assume a granitic "crust" for the earth which antedated the eruption of the oldest…Precambrian terranes".

12.2 The Role of the Ion Microprobe in Hadean Exploration

At about the time that Wetherill (1972) inferred a protracted (i.e. billion year), continent-free phase of Earth history from comparative planetology, William Compston, a geochronologist at the Australian National University, was regularly attending the annual Lunar Science Conference in Houston. There he became aware of an emerging analysis method—secondary ion mass spectrometry (SIMS)—that would eventually put paid to Wetherill's contention. The method uses a finely focused ion beam to "sputter" atoms from a polished sample. The fraction of those atoms ionized are accelerated into, and mass separated within, a magnetic sector spectrometer. These isotopically distinct secondary ion beams are then counted in a detector permitting isotope ratios to be determined as precisely as permitted by counting statistics. The in situ analysis capability of the new method held the promise of revolutionizing isotope geochemistry in the same way that the electron probe had recast petrologic analysis during the previous decade (Bence and Albee 1968)). An obvious drawback was the "zoo" of ionized molecules that sputtering produces from the sample matrix that can mass interfere with the isotope of interest. For example, the molecule $^{94}Zr_2^{16}O^+$, a likely product of sputtering zircon ($ZrSiO_4$), requires a mass resolving power (MRP[1]) of nearly 5000 to separate it from $^{206}Pb^+$, the final daughter product of ^{238}U decay. Mass spectrometers of the day used by geochemists typically had MRPs of only about 500 so it was clear that a physically large mass analyzer would be required to attain both high sensitivity and mass resolution. Thus was born the concept of the Sensitive High Resolution Ion Micro Probe, or SHRIMP as it was puckishly referred. The project was largely undertaken (and underwritten) in house and involved significant technical and political challenges. With regard to the latter, Compston later noted[2] "We had to fight against advice that (the Director) got from people who said we would never be able to do it, and the mass spectrometer manufacturers were each busy saying that their machine would produce the high resolution and it ought to work. We had to say, 'Well, for this and that reason we don't accept that. We feel the need to go ahead and do it this way.'" After seven years of design, manufacture and testing, SHRIMP was ready for service.

Prior to 1983, the idea that any rock or mineral older than ca. 3.9 Ga would ever be found on Earth was close to geological heresy. Thus the publication of Froude et al. (1983) stunned the geological community with the report of detrital zircons from a Western Australian quartzite were as old as 4.2 Ga. How could zircon, a mineral largely associated with continental crust, have formed and survived through a period when Earth's surface was surely being ravaged from above and below? Many in the global community initially took a skeptical view of this report. In a

[1]An MRP of 5000 permits a molecule of mass 5001 to be recognized separately from a molecule of mass 5000.

[2]https://www.science.org.au/learning/general-audience/history/interviews-australian-scientists/professor-bill-compston-isotope#6.

News and Views article accompanying the publication of the Froude et al. (1983) report, Moorbath (1983) raised the possibility that the oldest zircons were actually 3.7 Ga, but had experienced episodes of U loss followed by Pb loss that resulted in seemingly ancient, but illusory, ages. Schärer and Allegre (1985) obtained a mineral concentrate from the rock used by Froude et al. (1983) and undertook single zircon U-Pb analyses using the conventional isotope dilution, thermal ionization mass spectrometry (ID-TIMS) approach "To substantiate the existence of these old zircons". They could neither confirm the 4.1 to 4.2 Ga ages nor the particular discordancy pattern seen using the ion microprobe (i.e. ion microprobe data were substantially more concordant than the ID-TIMS results). In retrospect, the Schärer and Allegre (1985) result is unsurprising as the bulk analysis method they used tends to weight the younger, generally higher U rims that almost invariably coat detrital grains over the older, generally U poor cores, thus overpowering the contribution of the latter to the overall U-Pb age signal. It was later learned that the high degree of discordancy seen in ID-TIMS data reflects volumetrically small pockets of partially metamict, high U zircon (Mattinson 2005) whereas the in situ capability of the ion microprobe could target the old cores directly. Although every new analytical method must demonstrate ground truth validity to overcome healthy skepticism, this case might have been an exception as the dual decay mode of U-Pb dating permits age information to be obtained from measurement of Pb isotopes alone. Given that Froude et al. (1983) described their isotope ratio standardization protocol clearly, looking back it's hard to understand how they could possibly have measured $^{207}Pb/^{206}Pb$ ratios corresponding to ages as old as 4.2 Ga if the zircons were, as Schärer and Allegre (1985) contended, only 3.3 to 3.8 Ga.

Subsequent application of the ion microprobe to dating lunar zircons (Compston et al. 1984) cemented its reputation as the tool of choice to obtain spatially resolved U-Pb chronologic information from zircon subdomains. By the early 1990s, a competitor instrument manufactured by CAMECA, then a privately held French firm, was commissioned in my laboratory at UCLA (Chambost 2011). The *ims*1200-series instruments have similar U-Pb geochronologic capabilities to SHRIMP but are also capable of analysis of negative secondary ions from electrically insulating samples (e.g. O isotope measurements in silicates or carbonates). This involves use of a normal incidence electron flood gun that provides compensation for the positive charge introduced by the primary ion beam (typically Cs^+ in this case) or left behind by escaping electrons. This capability made possible in situ, micro-scale analysis of the carbon isotope composition of graphite inclusions in accessory phases that suggest life may have emerged prior to 3.8 Ga (Mojzsis et al. 1996) or 4.1 Ga (Bell et al. 2015a, b) (see Sect. 11.4).

Every significant advance in geochronology has produced a paradigm-shifting breakthrough in our understanding of Earth history (e.g. age of Earth, Boltwood 1907; seafloor spreading from age calibration of geomagnetic reversals, McDougall and Tarling 1964). The same can be argued for the development of the high sensitivity, high mass resolution ion microprobe which single-handedly opened a frontier to Hadean research—a frontier whose existence had not previously been conceived.

12.3 Why Are There no Hadean Rocks?

The title of this sub-section is oxymoronic since earlier I defined the Hadean as the period of Earth history prior to the beginning of the macroscopic terrestrial rock record (i.e. at 4.02 Ga) but subsequent to globally disruptive formation and differentiation events (e.g. Moon-forming impact, core formation, magma ocean), all of which must have ceased by 4.50 Ga (Sects. 1.3 and 1.5). Rather, this question addresses the view of some geologists that, had a continental-like crust mass of a similar order to today existed on the planet prior to 4 Ga, then we should have discovered vestigial rocks from that eon by now. Of course we have found material evidence in the form of Hadean zircons, but that microlithic record does not fit the general view of what constitutes part of the rock record.

Thus there are three responses to the question, why are there no Hadean rock? The first is semantic. If a rock is a naturally occurring aggregate of minerals, then the mineral assemblage in the Hadean zircon inclusion shown in Fig. 7.3 is a micro-rock. If so, the rock record sensu latu extends back to nearly 4.4 Ga. The second arises from the general agreement that the lithosphere today is close to a volumetric balance between the creation of rocks, whether at ridges or arcs, and their loss to the mantle at convergent margins. The recycling model (see Sect. 5.4) extends this observation by positing that continental crust added from Hadean times to the present were similarly compensated by the recycling of coequal amounts of continental material back into the mantle via sediment subduction (Sect. 5.4). If this is true, then the oldest rocks, which have been exposed to these processes the longest, should be either rare or perhaps even extinct. The third is the fact that, as discussed in sect. 6.3.6, we have thus far chronologically characterized a vanishingly small fraction of the continental crust. Depending on how one might associate a radiometric age with an adjacent rock mass, we could have surveyed as much as one part in a billion of the crust or as little as a million times less. Even in the former case, this is a minuscule representation of the present continental crust. As noted in sect. 1.3, the literature is replete with examples since the 1970s of the certainty with which geochronologists believed that the terrestrial crust had, at the moment of publication, revealed the full range of its preserved rock record and past history. Indeed, the discovery of zircons as old at 4.2 Ga was greeted by the geologic community with considerable skepticism—we had implicitly and collectively agreed that they simply couldn't exist (see Sect. 12.2). Should the sort of systematic, mission-scale geochronologic survey proposed in Appendix I come to pass, the reader should be prepared for equally stunning discoveries.

12.4 Final Thoughts

In *The Structure of Scientific Revolutions*, Thomas Kuhn wrote: "Today in the sciences, books are usually either texts or retrospective reflections upon one aspect or another of the scientific life. The scientist who writes one is more likely to find his professional reputation impaired than enhanced" (Kuhn 1962). As the reader has likely come to appreciate, the intent of this book is to straddle both styles of exposition to explore what we know about earliest Earth while highlighting what I've come to see as a form of scientific dysfunction in our community. Whether doing so impairs my professional reputation will become clear in time, but my now 40-year-long career has permitted some insights into problematic aspects of the way we build interpretive models that I think are worth sharing.

The first is that, relative to the other physical sciences, the Earth and planetary science communities are unusually tolerant of what amounts to untestable hypotheses. This is to some degree understandable for reasons already discussed in sect. 12.1.1, but overly elaborate models invoking multiple speculative mechanisms that lack the basis for falsification (e.g. Sect. 9.9) tend to pile up in the literature stoking tribal allegiances while potentially crowding out other key arguments.

A more facile variant of this practice is to justify first-principles speculation on Hadean geo- and biochemistry *because* there are so few physical constraints. For example, Smith and Morowitz (2016) wrote:

> Life appeared on Earth in a period known as the Hadean, the Earth's oldest eon…The Hadean was, however, a time we think of as governed by laws of geophysics and geochemistry, and therefore open to understanding. (Indeed, the absence of memory makes the Hadean, more than later periods with accreted history, a simpler period to study with general laws.)…Thus in geology the complement to historicity is lawfulness. What we cannot infer from preserved memories we seek to deduce by understanding the action of laws. The complement to historicity in its earliest periods was not chaos, but lawfulness.

If I understand the author's viewpoint, it is that in 2016 we held no preserved lithic record of Earth history between 4.4 and 4.0 Ga which in turn simplifies quantitative analysis because the lack of knowledge of then extant conditions empowers theory. The first claim is refuted in Chap. 7 and the second is problematic epistemology. Harkening back to sect. 1.1, if the study of origin myths tells us anything about human societies, it is that the absence of historicity is rarely equated with chaos. Rather, it tends to trigger a compulsion in our species to invent mystic rules of order lest anarchy be glimpsed. True, the premise of this book, laid out in sect. 1.1, is that the first of the four ways to investigate the Hadean eon is the presumption that time invariant physical laws permit some limits to be placed on early Earth history. While this appears superficially consistent with the above statement, it differs in an important way. First order physical mechanisms, such as radioactive decay, can be confidently extrapolated back in time to provide constraints on an era with no preserved record. But mechanisms that require knowledge of system scale or, more problematically, non-linear systems, do not lend themselves to deductive solution in the absence of highly specified constraints. I have made the case earlier that the approach advocated by Smith and Morowitz (2016), well known to Lord Kelvin in the nineteenth century (Sect. 2.1), Harold Urey in the mid-twentieth century (Sect. 12.1.2), and geodynamic modelers in the late twentieth century (Sect. 2.4), actually set back a better understanding of early Earth in those instances. Those efforts were surely "lawful" in that they didn't violate, for example, thermodynamics. But the takeaway from that protracted history lesson should be that applying universal laws without knowledge of the relevant intensive/extensive parameters and boundary conditions invites scientific caricatures of physicochemical systems as complex as Earth and life. While reconceptualizing the Hadean as an eon particularly conducive to thought experiment may temporarily stave off the sense of disorder our ignorance generates, it is that intellectual discomfort which drives innovation. And it is surely preferable to the damage that can result from creating a stultifying, untestable convention—our very own creation myth.

It is not yet possible to confidently ascribe conditions to Hadean Earth from the four avenues of investigation outlined in Chap. 1 (time-invariant physical laws, mantle isotopes, lunar samples, and >4 Ga zircons). But we can certainly rule out certain hypotheses, such as Wetherill's (1972) view that no continental crust formed during the first billion years of Earth history. No scenario as yet proposed is without flaws. Rather, our goal should be to identify parsimonious, internally-consistent models of Earth evolution that explain all robust aspects of these four approaches, and then rigorously test them by seeking further observational constraints (e.g. see Appendix I). As you've seen, I view plate boundary interactions as not only providing a setting that well explains the nature of Hadean zircon geochemistry and the inclusions they host, but is the simplest explanation that invokes a dynamical mode that is clearly plausible for this planet. However, this model could be falsified by, for example, a clear demonstration that the thermal structure inferred from zircon geochemistry is inconsistent with convergent margin processes.

Internal consistency alone is not smoking-gun proof of a hypothesis. Most accumulated evidence is indirect and thus open to alternate interpretations. But overly elaborate scenarios, especially those that stand in contradiction to aspects of the geochemical evidence, don't help advance our understanding of the first five hundred million years of Earth history. Rather, they muddle a discussion which is generally poorly understood by those outside this somewhat arcane field. Multi-stage scenarios that invoke crystallization products of a magma ocean (e.g. Shirey et al. 2008; Kemp et al. 2010) are unfalsifiable as, despite the potential for a largely liquid silicate Earth to have formed upon accretion, there is no observational evidence that requires that such a condition ever prevailed. For example, experimental constraints on partitioning between molten iron and silicate are consistent with a continuum of solutions (Righter 2015). To then use this assumption as the foundational condition on which to build a multi-stage hypothesis begs the question: Is such an activity consistent with the scientific method?

A further concern that merits discussion here is that alternate explanations for the origin of Hadean zircons sometimes selectively ignore entire lines of evidence (see Ottati et al. 2015 for an analysis of this phenomenon). For example, interpretations of the Jack Hills Lu-Hf data that invoke mafic sources (e.g. Rollinson 2008; Kemp et al. 2015) typically do not address or explain the characteristic nature of the Hadean zircon inclusion assemblages or their low temperatures of formation. Lastly, discussions of early Earth are not enhanced by endowing mantle-derived rocks with a facility they can't possibly possess; i.e. knowledge that ancient continental rocks don't exist elsewhere on the planet (e.g. Kamber et al. 2005; Kemp et al. 2015; Reimink et al. 2016). This is the intellectual equivalent of concluding that no ancient cratons exist on Earth today by geochemical analysis of a sole rock from Samoa.

If the various 'retrospective reflections' embodied in this book have a common thread, it is that progress in our field can be impeded by a tendency toward herd instinct—the capacity of the scientific community to prematurely coalesce around a geophysical concept before that mechanism is well understood. During my career I have seen multiple cycles of this phenomenon. We may be at the threshold of doing so yet again. Specifically, I think that our community is on the verge of coalescing around a groupthink that plate tectonics began three billion years ago in much the same way it did 50 years ago when it imagined, without any empirical evidence, that at least the first half billion years of Earth history saw a desiccated, molten, lifeless planet (Sect. 1.1). Or the way it adopted the Late Heavy Bombardment 30 years ago or the Mars-sized impactor origin of Moon 20 years ago. All three of those concepts are currently under serious challenge (see Sects. 1.1, 4.10 and 3.3, respectively) as a result of new thinking which, I believe, was forestalled by decades of conformity to a consensus built upon weak evidentiary foundations.

If we're to raise our game, both in terms of hypothesis building and testing and in resisting the instinct to uncritically adopt appealing models from allied fields whose foundations we might not all be able to digest, it might first be useful to explore how we got here. As already noted, we are a community of storytellers and it can be difficult to know exactly the point in a story being told at which it ceases to be constrained by observational evidence and becomes rank speculation. This issue can be addressed by taking care to examine information that is both contradictory as well as supportive of the hypothesis. Granted, such an approach tends to be discouraged, for example by weekly, international science journals, in favor of provocative or hyperbolic endmember conclusions rather than a balanced analysis of the range of evidence (Collins and Tabak 2014).

During graduate thesis defenses, the first question I ask the candidate is, *What is science?* I don't do this because I think I know the answer, because my view has changed markedly through my career. I do so because we collectively put little effort into directly challenging the next generation to think about the foundation of what we do. Instead, we typically socialize the student to the scientific outlook through their prolonged participation in the research endeavor. Before I became notorious for asking this question, at which point the answers became homogenized, I was inspired by the range of responses. They did, however, generally share the view that science is an enterprise that exists outside the moral sphere and thus was free of qualitative human judgement. I think I once believed that myself but the grizzled veteran I've now become sees science as a very human construct that is strongly influenced by perceptions of social order and subjective selection. While there are multiple reasons why less than half, and often much less than half, of all psychology, cancer, and pharmaceutical research studies can be replicated (Prinz et al. 2011; Begley and Ellis 2012; Aarts et al. 2015; Ioannidis 2005), human fallibility is an important contributing cause (Collins and Tabak 2014; NASEM 2019). My complaint of course isn't that science doesn't work, because it manifestly has led us to an extraordinary understanding of the natural world. My concern is one of efficiency. By not resisting the call to groupthink, we retard progress. How much more would we know about the world today if the community had not rolled over and uncritically adopted, for example, the paradigms described above? How many young scientists would have been inspired to pursue alternate explanations for lunar formation, or the origin of continental crust, or the lunar bombardment history had we not told them that these were solved problems?

Lastly, it's worth pondering how widespread is this issue I raise—a combination of groupthink, resistance to new ideas, reactionary responses, existential angst, and tribalism (Barber 1961; Dawkins 2007; Leeming 2010)—in the Earth and planetary sciences. One might be tempted to imagine that this problem is largely restricted to matters of deepest time as the paucity or absence of a rock record tends to encourage unsupported speculation. But during my career, I think I have achieved expert knowledge of three disciplines—$^{40}Ar/^{39}Ar$ thermochronology (McDougall and Harrison 1999; Chap. 4), Himalayan-Tibetan tectonics (Harrison et al. 1992; Yin and Harrison 2000), and early Earth (Harrison 2009; Harrison et al. 2017; this book). The first of those is skewed to Phanerozoic processes and the second involves a continental collision that is active today. Despite their relatively youthful foci, I have seen many of the same behaviors in $^{40}Ar/^{39}Ar$ thermochronology (e.g. Parsons et al. 1999; cf., Harrison et al. 2010) and Himalayan-Tibetan tectonics (e.g. England and Molnar 1993; cf. Harrison et al. 1997) that I describe above in context of early Earth studies. I cannot have been immune to this disease but will leave it to others to diagnose. Of course we're all victims of our own experience so it's difficult to generalize, but my best guess is that the reader has either already witnessed similar behaviors or will do in the near future.

We can do better. As investigators, mentors, reviewers, editors, publishers and colleagues. And by doing so, we surely draw closer to the day when we truly understand Hadean Earth.

References

Aarts, A. A. et al. (2015). Estimating the reproducibility of psychological science. *Science*, *349*, p. aac4716.

Abe, Y. (1993). Physical state of the very early Earth. *Lithos, 30,* 223–235.

Barber, B. (1961). Resistance by scientists to scientific discovery. *Science, 134,* 596–602.

Begley, C. G., & Ellis, L. M. (2012). Drug development: Raise standards for preclinical cancer research. *Nature, 483,* 531–533.

Bell, E. A., Boehnke, P., Harrison, T. M., & Mao, W. (2015a). Potentially biogenic carbon preserved in a 4.1 Ga zircon. *Proceedings of the National Academy of Sciences, 112,* 14518–14521.

Bell, E. A., Boehnke, P., Hopkins-Wielicki, M. D., & Harrison, T. M. (2015b). Distinguishing primary and secondary inclusion assemblages in Jack Hills zircons. *Lithos, 234,* 15–26.

Bence, A. E., & Albee, A. L. (1968). Empirical correction factors for the electron microanalysis of silicates and oxides. *Journal of Geology, 76,* 382–403.

Boltwood, B. (1907). On the ultimate disintegration products of the radioactive elements. Part II. The disintegration products of uranium. *American Journal of Science, 4,* 77–80.

Brush, S. G. (1982). Nickel for your thoughts: Urey and the origin of the Moon. *Science, 217,* 891–898.

Burbidge, E. M., Burbidge, G. R., Fowler, W. A., & Hoyle, F. (1957). Synthesis of the elements in stars. *Reviews of Modern Physics, 29,* 547–650.

Cameron, A. G. W. (1962). The formation of the sun and planets. *Icarus, 1,* 13–69.

Chamberlin, T. C. (1901). On a possible function of disruptive approach in the formation of meteorites, comets, and nebulae. *Journal of Geology, 9,* 369–392.

Chamberlin, T. C. (1905). *Carnegie inst. Year book no. 3 for 1904*, (p. 195).

Chamberlin, T. C. (1916). *The origin of the earth*. (p. 271). University of Chicago Press.

Collins, F. S., & Tabak, L. A. (2014). NIH plans to enhance reproducibility. *Nature, 505,* 612–613.

Compston, W., Williams, I. S., & Meyer, C. (1984). U-Pb geochronology of zircons from lunar breccia 73217 using a sensitive high mass-resolution ion microprobe. *Journal of Geophysical Research: Solid Earth, 89,* B525–B534.

Daly, R. A. (1914). *Igneous rocks and their origin*. (p. 563). McGraw-Hill.

Dawkins, R. (2007). *The god delusion*. Random House.

de Chambost, E. (2011). A history of CAMECA (1954–2009). *Advances in Imaging and Electron Physics, 167,* 1–119.

England, P., & Molnar, P. (1993). The interpretation of inverted metamorphic isograds using simple physical calculations. *Tectonics, 12,* 145–157.

Ernst, W. G. (1983). The early earth and the archean rock record. In *Earth's earliest biosphere: Its origin and evolution.* (pp. 41–52). Princeton, NJ: Princeton University Press.

Eucken, A. (1944). Über den zustand des erdinnern. *Naturwissenschaften, 32,* 112–121.

Fowler, W. A., Greenstein, J. L., & Hoyle, F. (1962). Nucleosynthesis during the early history of the solar system. *Geophysical Journal International, 6,* 148–220.

Froude, D. O., Ireland, T. R., Kinny, P. D., Williams, I. S., & Compston, W. (1983). Ion microprobe identification of 4100–4200 myr-old terrestrial zircons. *Nature, 304,* 616–618.

Fyfe, W. S. (1978). The evolution of the earth's crust: Modern plate tectonics to ancient hot spot tectonics? *Chemical Geology, 23,* 89–114.

Gamow, G., & Hynek, J. A. (1945). A new theory by C.F. von Weizsäcker of the origin of the planetary systen. *Astrophysical Journal, 101,* 249–254.

Gradstein, F. M., Ogg, J. G., Smith, A. G., Bleeker, W., & Lourens, L. J. (2004). A new geologic time scale, with special reference to precambrian and neogene. *Episodes, 27,* 83–100.

Gray, C., & Compston, W. (1974). Excess ^{26}Mg in the Allende meteorite. *Nature, 251,* 495–497.

Hamilton, W. B. (1998). Archean magmatism and deformation were not products of plate tectonics. *Precambrian Research, 91,* 143–179.

Harrison, T. M. (2009). The hadean crust: Evidence from >4 Ga zircons. *Annual Reviews of Earth and Planetary Sciences, 37,* 479–505.

Harrison, T. M., Bell, E. A., & Boehnke, P. (2017). Hadean zircon petrochronology. *Reviews in Mineralogy and Geochemistry, 83,* 329–363.

Harrison, T. M., Copeland, P., Kidd, W. S. F., & Yin, A. N. (1992). Raising Tibet. *Science, 255,* 1663–1670.

Harrison, T. M., Heizler, M. T., McKeegan, K. D., & Schmitt, A. K. (2010). In situ ^{40}K-^{40}Ca 'double-plus' SIMS dating resolves Klokken feldspar ^{40}K-^{40}Ar paradox. *Earth and Planetary Science Letters, 299,* 426–433.

Harrison, T. M., Ryerson, F. J., Le Fort, P., Yin, A., Lovera, O. M., & Catlos, E. J. (1997). A late Miocene-Pliocene origin for the central Himalayan inverted metamorphism. *Earth and Planetary Science Letters, 146,* E1–E8.

Ioannidis, J. P. (2005). Why most published research findings are false. *PLoS Medicine 2*. https://doi.org/10.1371/journal.pmed.0020124.

Jeans, J. H. (1919). *Problems of cosmogony and stellar dynamics* (p. 292). Adams Prize Essay: Cambridge University Press.

Jeffreys, H. (1917). Theories regarding the origin of the solar system. *Science Progress, 12,* 52–62.

Jeffreys, H. (1918). The early history of the solar system. *Nature, 101*, 447–449.

Jeffreys, H. (1929). The early history of the solar system on the collision theory. *Monthly Notices of the Royal Astronomical Society, 89,* 731–738.

Kamber, B. S., Whitehouse, M. J., Bolhar, R., & Moorbath, S. (2005). Volcanic resurfacing and the early terrestrial crust: Zircon U-Pb and REE constraints from the Isua greenstone belt, southern West Greenland. *Earth Planet Science Letter, 240,* 276–290.

Kemp, A. I. S., Hickman, A. H., Kirkland, C. L., & Vervoort, J. D. (2015). Hf isotopes in detrital and inherited zircons of the pilbara craton provide no evidence for hadean continents. *Precambrian Research, 261,* 112–126.

Kemp, A. I. S., Wilde, S. A., Hawkesworth, C. J., Coath, C. D., Nemchin, A., Pidgeon, R. T., et al. (2010). Hadean crustal evolution revisited: New constraints from Pb-Hf isotope systematics of the Jack Hills zircons. *Earth and Planetary Science Letters, 296,* 45–56.

Kuhn, T. S. (1962). *The structure of scientific revolutions*. (p. 210). University of Chicago Press.

Kuiper, G. P. (1951). On the origin of the solar system. *Proceedings of the National Academy of Sciences, 37,* 1–14.

Leeming, D. A. (2010). *Creation myths of the world: An encyclopedia* (p. 553) (in two volumes). ABC-CLIO Inc.

Lunine, J. I. (1999). *Earth: Evolution of a habitable world*. Cambridge University Press.

Maher, K. A., & Stevenson, D. J. (1988). Impact frustration of the origin of life. *Nature, 331,* 612–614.

Mattinson, J. M. (2005). Zircon U-Pb chemical abrasion ("CA-TIMS") method: Combined annealing and multi-step partial dissolution analysis for improved precision and accuracy of zircon ages. *Chemical Geology, 220,* 47–66.

McDougall, I., & Harrison, T. M. (1999). *Geochronology and thermochronology by the $^{40}Ar/^{39}Ar$ method*. Oxford University Press.

McDougall, I., & Tarling, D. H. (1964). Dating geomagnetic polarity zones. *Nature, 202,* 171–172.

Miller, S. L., & Urey, H. C. (1959). Origin of Life. *Science, 130,* 1622–1624.

Mojzsis, S. J., Arrhenius, G., McKeegan, K. D., Harrison, T. M., Nutman, A. P., & Friend, C. R. L. (1996). Evidence for life on Earth by 3800 Myr. *Nature, 384,* 55–59.

Moorbath, S. (1983). Precambrian geology: The most ancient rocks? *Nature, 304,* 585–586.

Moorbath, S. (2005). Oldest rocks, earliest life, heaviest impacts, and the Hadean-Archaean transition. *Applied Geochemistry, 20,* 819–824.

Moulton, F. R. (1905). On the evolution of the solar system. *Astrophysical Journal, 22,* 165–181.

NASEM (National Academies of Sciences, Engineering, and Medicine). (2019). *Reproducibility and replicability in science*. National Academies Press. https://doi.org/10.17226/25303.

Ottati, V., Price, E. D., Wilson, C., & Sumaktoyo, N. (2015). When self-perceptions of expertise increase closed-minded cognition: The earned dogmatism effect. *Journal of Experimental Social Psychology, 61,* 131–138.

Parsons, I., Brown, W. L., & Smith, J. V. (1999). $^{40}Ar/^{39}Ar$ thermochronology using alkali feldspars: Real thermal history or mathematical mirage of microtexture? *Contributions to Mineralogy and Petrology, 136,* 92–110.

Patterson, C., Tilton, G., & Inghram, M. (1955). Age of the Earth. *Science, 121,* 69–75.

Popper, K. (1957). *The poverty of historicism* (p. 166). Boston: The Beacon Press.

Popper, K. (1962). *Conjectures and Refutations: The growth of scientific knowledge*. Routledge.

Popper, K. (1976). *Unended quest*. Open Court, LaSalle, IL: An Intellectual Autobiography.

Prinz, F., Schlange, T., & Asadullah, K. (2011). Believe it or not: How much can we rely on published data on potential drug targets? *Nature Reviews Drug Discovery, 10,* 712–715.

Reimink, J. R., Davies, J. H. F. L., Chacko, T., Stern, R. A., Heaman, L. M., Sarkar, C., et al. (2016). No evidence for hadean continental crust within earth's oldest evolved rock unit. *Nature Geoscience, 9,* 777–780. https://doi.org/10.1038/ngeo2786.

Righter, K. (2015). Modeling siderophile elements during core formation and accretion, and the role of the deep mantle and volatiles. *American Mineralogist, 100,* 1098–1109.

Rollinson, H. (2008). Ophiolitic trondhjemites: A possible analogue for hadean felsic 'crust'. *Terra Nova, 20,* 364–369.

Russell, R. D., & Allan, D. W. (1955). The age of the earth from lead isotope abundances. *Geophysical Journal International, 7,* 80–101.

Safronov, V. S. (1958). On the growth of terrestrial planets. Vopr. Kosmog., Akad. Nauk S.S.S.R. 6, 63–77.

Safronov, V. S. (1972). Evolution of the protoplanetary cloud and the formation of the Earth and planets. Translated from Russian. Jerusalem (Israel): Israel program for scientific translations. (p. 212). Keter Publishing House.

Schärer, U., & Allegre, C. J. (1985). Determination of the age of the Australian continent by single-grain zircon analysis of Mt. Narryer metaquartzite.*Nature, 315,* 52–55.

Shirey, S. B., Kamber, B. S., Whitehouse, M. J., Mueller, P. A., & Basu, A. R. (2008). A review of the isotopic and trace element evidence for mantle and crustal processes in the hadean and archean: Implications for the onset of plate tectonic subduction. *Geological Society of America Special Paper, 440,* 1–29.

Smith, J. V. (1981). The first 800 million years of earths history. *Philosophical transactions of the royal society London Ser. A 301*, pp. 401–422.

Smith, E., & Morowitz, H. J. (2016). *The origin and nature of life on earth: The emergence of the fourth geosphere*. Cambridge University Press.

Solomon, S. C. (1980). Differentiation of crusts and cores of the terrestrial planets: Lessons for the early earth? *Precambrian Research, 10,* 177–194.

Urey, H. C. (1951). The origin and development of the earth and other terrestrial planets. *Geochimica et Cosmochimica Acta, 1,* 209–277.

Urey, H. C. (1952a). *The planets: Their origin and development* (p. 245). New Haven: Yale Univ. Press.

Urey, H. C. (1952b). The origin of the earth. *Scientific American, 187*(October), 53–61.

Urey, H. C. (1955). The cosmic abundances of potassium, uranium, and thorium and the heat balances of the Earth, the Moon, and Mars. *Processes National Academic Science USA, 41,* 127–144.

Waltham, J. (2014). *Lucky Planet* (p. 198). New York, NY: Basic Books (Perseus).

Ward, P. D., & Brownlee, D. (2000). *Rare earth: Why complex life is uncommon in the universe*. New York: Copernicus Books.

Weizsäcker, C. F. V. (1943). Über die entstehung des planetensystems. *Zeitschrift für Astrophysik 22*, 319–355.

Wetherill, G. W. (1972). The beginning of continental evolution. *Tectonophysics, 13,* 13–45.

Yin, A., & Harrison, T. M. (2000). Geologic evolution of the Himalayan-Tibetan Orogen. *Annual Review Earth Planetary Science, 28,* 211–280.

Appendix: Expanding the Search for Terrestrial Hadean Zircons

A.1 Introduction

As documented in Chap. 8, at least one Hadean (>4.02 Ga) zircon has been documented from fifteen localities across five continents (Fig. 8.1), although no locality outside the Jack Hills has yielded more than a few hundred Hadean zircons compared to the >6000 documented from a single outcrop at the Erawondoo Hills discovery location (Compston and Pidgeon 1986; Holden et al. 2009). A global program of U–Pb age surveying and geochemical characterization could lead to fundamental new information on earliest Earth. Despite the heroic role that the ion microprobe (i.e., SIMS) played in the discovery and exploration of a Hadean lithic record, it is likely to share future discoveries with upstart technologies.

A.2 LA-ICPMS Versus SIMS

The advent of the ion microprobe was pivotal to the discovery of >4 Ga zircons (Sect. 12.2), but its future in Hadean research may be more specialized. While the vast majority of Hadean zircons recognized to date have been documented using ion microprobes, the remarkable analytical development and refinement of the LA-ICPMS over the past 20 years make it the future dating tool of choice for age surveys of large numbers of detrital zircons. Effective ion yields have increased by over an order of magnitude dropping both analytical time and the mass of material needed to attain a specified precision. This in turn has decreased analytical costs dramatically. While the ion microprobe remains the ultimate tool for most in situ isotopic analysis, it no longer makes economic sense to undertake large (i.e., ≥ 5000 U–Pb zircon) age surveys using this approach. Where once zircons were largely evaporated to attain an LA-ICPMS U–Pb age, multicollector instruments can obtain a U–Pb with ±2% precision from a $\sim 1000\ \mu m^3$ volume (Ibanez-Mejia et al. 2014) which begins to compare favorably with the $\sim 150\ \mu m^3$ volume long attainable using the ion microprobe. Even lower cost, quadrupole LA-ICPMS systems can attain similar precision from $\sim 6000\ \mu m^3$ ablation craters, which still represents only a few % of a typical Hadean zircon mass (i.e., 2–5 µg).

T. M. Harrison, *Hadean Earth*, https://doi.org/10.1007/978-3-030-46687-9

A.3 Rapid U–Pb Age Surveying

There are two types of age surveys for Hadean zircons—examination of age populations in rocks from which at least one >4 Ga zircon has been identified (i.e., the 15 global locations documented in Chap. 8) and those in promising candidate rocks which have not yet revealed Hadean grains. Thus the optimal benefit/cost for the latter project is to explore age populations using quadrupole LA-ICPMS. However, even in those rocks in which a Hadean zircon has already been identified, this approach would maximize the return on investment due to the low cost and only marginally greater sample mass consumed.

Archean rocks for which fewer than 100s of zircons have been U–Pb dated without identifying at least one Hadean zircon themselves fall into two categories. Those in which >4 Ga zircons are present at a level of less than $\sim 1\%$ but haven't yet been detected, and those in which they are simply absent. How many zircons should we date in order to ascertain to which category a sample belongs? The probability of detecting at least a single >4 Ga zircon as a function of their abundance is shown in Fig. A.1. A reasonable assumption is that the ca. 2% >4 Ga zircon abundance in the Jack Hills (Holden et al. 2009) is anomalously high for most Archean quartzites and gneisses and thus we examine the detection probabilities where abundances are between one and two orders of magnitude lower (i.e., 0.2–0.02%). From Fig. 12.1, we can see that at the 95% confidence level (bright red band), diminishing returns are achieved following analysis of ~ 5000 zircons, corresponding to an effective abundance limit of $\sim 0.05\%$. Thus identifying which samples contain >0.05% Hadean zircons requires analysis of ca. 5000 zircons.

The developments described above have so reduced the time needed for age analysis that handpicking 20×20 zircon grids, the method used in age surveying the first 200,000 Jack Hills zircons (e.g., Holden et al. 2009), is now the rate limiting step in characterizing an age population (i.e., handpicking a 400 zircon grain mount can take up to 5 h depending on the quality of the concentrate). Simultaneous with developments in LA-ICPMS analysis, the adaptation of automated image acquisition and analysis to geochemistry provides a path forward that enhances efficiency to the point where we could potentially survey nearly as many zircons in the coming three years as we have in the past 15. Specifically, advances in fission track dating automation have the capacity to take polished 1″ diameter "sprinkle" mounts of ≥ 2500 accessory mineral grains, automatically identify and map each grain location, and then create a stacked 3D image (with ~ 1 μm resolution) of each grain from which inclusions can be identified (Gleadow et al. 2015). Using this spatial information, the mount can then be transferred for automatic analysis by quadrupole LA-ICPMS.

Preparing polished zircon sprinkle mounts and undertaking automated surface mapping and grain identification using optical microscopy can be routine. Following characterization, the mounts are then transferred to the automated stage in the LA-ICPMS sample chamber where a ~ 20 μm diameter $\times$ ~ 20 μm deep laser spot targets the center of each grain. Automated U–Pb dating of the

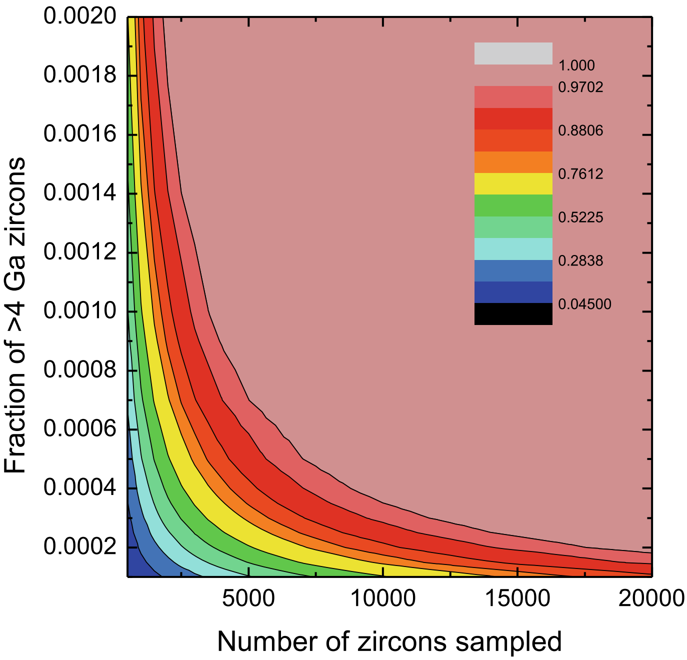

Fig. A.1 Plot showing the probability of identifying at least one Hadean zircon from populations with a range of assumed occurrence rates of >4 Ga grains as a function of number of dated grains. Note that achieving 89–93% confidence in detecting a Hadean zircon from a population in which 1-in-2000 are >4 Ga requires U–Pb dating ~5000 grains. Reproduced from Harrison et al. (2017)

ablated volume takes ~1 min. As the imaging and dating systems can be operated simultaneously, a single mount can be processed in under two days. Once U–Pb dating is complete, the mount is transferred back to the optical microscope and the identified >4 Ga grains scanned in 3D for inclusions that can be later examined for geochemical significance.

The LA-ICPMS approach can lack the capacity to accuracy measure and correct for common ^{204}Pb and thus the possibility exists that single zircon occurrences with apparent ages of >4 Ga could be due to inclusion of non-radiogenic Pb signals. The ion microprobe can then be utilized to screen the grains isolated by the LA-ICPMS survey as well as used for the more instrumentally demanding, post-age survey geochemical characterizations (i.e., δ^{18}O, δ^{13}C, Ti, REE, etc.).

With regard to sampling requirements of the host rocks, the quartzites and orthogneisses that have provided our current archive of Hadean zircons typically contain ≥ 80 ppm Zr and thus a 5 kg sample likely contains at least half a gram of zircon. Given a typical zircon mass of 3–5 µg and separation efficiency of ~20%, experience shows that thousands of zircons should be routinely obtainable from most such rocks.

A.4 Toward a Global Hadean Zircon Archive

How and when life emerged is consistently among the consensus selections of the handful of most important unresolved questions in science (DePaolo et al. 2008) and thus the greatest potential breakthrough that Hadean zircons could facilitate is discovery of a clear signal of biologic activity during that eon. As noted earlier (Sect. 7.8.5, 11.4.2), Bell et al. (2015) documented the existence of two, primary, graphite inclusions in a 4.1 Ga zircon from Jack Hills. Ion microprobe carbon isotopic measurements showed them to be isotopically light and in the range of photosynthetic activity. While consistent with a biogenic origin, these data taken alone could reflect a number of abiotic processes (e.g., meteoritic contamination, Fischer–Tropsch catalysis, diffusive carbon isotopic fractionation). But, for argument sake, what sense could we make of the carbon isotope compositions of one thousand graphite inclusions in Hadean zircons? If the resulting distribution mimics that of extraterrestrial carbon (e.g., Kerridge 1985), that would appear to make a biogenic origin less likely. But what if the spectrum instead shows peaks corresponding to metabolisms (e.g., Preuss et al. 1989) close to the base of the tree of life (Woese and Fox 1977)? Given the relatively limited ways in which reduced carbon could come to be incorporated in a crystallizing granitoid melt, this could be compelling evidence of Hadean biologic activity. Even if you disagree with that opinion, such results represent the only known pathway for understanding carbon isotopic variations over the first 500 million years of Earth history. But restricting analysis to the Jack Hills locality alone limits the implications that could be drawn regarding the global carbon isotope budget. A mix of the more than dozen other localities from which Hadean zircons have been documented (Chap. 8) would enhance confidence in the generality of the results.

The occurrence rate of carbonaceous inclusions in Jack Hills zircons containing opaque inclusions appears to be $\sim 3\%$. As the occurrence rate of >4 Ga grains in the Jack Hills population that contain opaque inclusion is only $\sim 1\%$, then acquiring 1000 candidate inclusions for isotopic analysis will require U–Pb dating and optical imaging of over 3,000,000 zircons. That's about fifteen times more analyses than have been undertaken from that locality over the past 30 years and is of a magnitude I think is beyond the reach of any one investigative group.

Today there are about two dozen large geometry ion microprobes operating in the realm of Earth and planetary sciences, but several hundred LA-ICPMS instruments. In the absence of a planetary-mission-scale initiative, for which we have found little international interest, it is conceivable that the three to five million documented Hadean zircons required to archive 1000 carbonaceous inclusions could be realized, using the methods described in the previous section, in 5–8 years by a network of one to two dozen cooperating laboratories working part time. I believe the potential for scientific breakthrough presented by such a project is comparable with the science goals of recent, ca. half-billion-dollar planetary missions and it could be accomplished at less than ten percent of their cost.

There is of course a chance that we will not find any additional carbon-bearing inclusions in the course of such a megaproject but that is the risk associated with any truly exploratory investigation. In my view, it is balanced by the potentially transformative nature of the research outcomes.

References

Bell, E. A., Boehnke, P., Harrison, T. M., & Mao, W. (2015). Potentially biogenic carbon preserved in a 4.1 Ga zircon. *Proceedings of the National Academy of Sciences, 112*, 14518–14521.

Compston, W., & Pidgeon, R. T. (1986). Jack Hills, evidence of more very old detrital zircons in Western Australia. *Nature, 321*, 766–769.

DePaolo, D. J., et al. (2008). *Origin and evolution of Earth: Research questions for a changing planet*. Washington, DC: National Academies Press.

Gleadow, A., Harrison, M., Kohn, B., Lugo-Zazueta, R., & Phillips, D. (2015). The Fish Canyon Tuff: A new look at an old low-temperature thermochronology standard. *Earth and Planetary Science Letters, 424*, 95–108.

Harrison, T. M., Bell, E. A., & Boehnke, P. (2017). Hadean zircon petrochronology. *Reviews in Mineralogy and Geochemistry, 83*, 329–363.

Holden, P., Lanc, P., Ireland, T. R., Harrison, T. M., Foster, J. J., & Bruce, Z. P. (2009). Mass-spectrometric mining of Hadean zircons by automated SHRIMP multi-collector and single-collector U/Pb zircon age dating: The first 100,000 grains. *International Journal of Mass Spectrometry, 286*, 53–63.

Ibanez-Mejia, M., Gehrels, G. E., Ruiz, J., Vervoort, J. D., Eddy, M. P., & Li, C. (2014). Small-volume baddeleyite (ZrO_2) U-Pb geochronology and Lu-Hf isotope geochemistry by LA-ICP-MS. Techniques and applications. *Chemical Geology, 384*, 149–167.

Kerridge, J. F. (1985). Carbon, hydrogen and nitrogen in carbonaceous chondrites: Abundances and isotopic compositions in bulk samples. *Geochimica et Cosmochimica Acta, 49*, 1707–1714.

Preuss, A., Schauder, R., Fuchs, G., & Stichler, W. (1989). Carbon isotope fractionation by autotrophic bacteria with three different CO_2 fixation pathways. *Zeitschrift für Naturforschung C, 44*, 397–402.

Woese, C. R., & Fox, G. E. (1977). Phylogenetic structure of the prokaryotic domain: The primary kingdoms. *Proceedings of the National Academy of Sciences, 74*, 5088–5090.